2018

High-throughput prediction and analysis of drug-protein interactions in the druggable human proteome

Chen Wang
Virginia Commonwealth University

High-throughput prediction and analysis of drug-protein interactions in the druggable human proteome

A dissertation submitted in partial fulfillment of the requirements for the degree of Doctor of Philosophy at the Virginia Commonwealth University.

by

Chen Wang
Ph.D., Department of Computer Science
May 17, 2018

Supervisor: Lukasz Kurgan
Ph.D., Qimonda Endowed Professor, Department of Computer Science

Virginia Commonwealth University,
Richmond, Virginia
May 2018

Acknowledgment

First, I would like to express my deep gratitude to my supervisor Dr. Lukasz Kurgan for all his continuous motivation, guidance, support, encouragement, enthusiasm, knowledge, and time that have helped me over the last few years to become a better researcher. Dr. Kurgan is the best advisor for directing my development in work and also the best mentor for answering my concerns in life.

I am grateful to the members of my dissertation committee, Dr. Tomasz Arodz, Dr. Michal Brylinski, Dr. Krzysztof Cios, and Dr. Vladimir Uversky. Their constructive suggestions and inspiring comments helped me to clarify my understanding of the project and improve the quality of this work.

I would like to thank other members and visitors of the BioMine lab for their collaboration and support.

Thanks to my friends and all the people who helped me to complete my PhD journey.

Last, but not least, I would like to thank my family for their unconditional love and endless encouragement. Thanks to our parents for taking care of their kids and our kid. Thanks to my marvelous wife Xiao for everything. Also thanks to our son Jonathan for being cute and bringing happiness and surprise to our life.

Dedication

This dissertation is dedicated to my wife, our parents, and our son.

Preface

This dissertation is an original work conducted by Chen Wang. It includes materials and results from the following publications and submitted works.

[1] Wang C, Hu G, Wang K, Brylinski M, Xie L, Kurgan LA. PDID: database of molecular-level putative protein-drug interactions in the structural human proteome. *Bioinformatics*, 32(4): 579-586, 2016

[2] Wang C, Kurgan LA. Survey of similarity-based prediction of drug-protein interactions. Revision submitted to the *Current Medicinal Chemistry* journal on April 15, 2018.

[3] Wang C, Kurgan LA. Review and comparative assessment of similarity-based methods for prediction of drug-protein interactions in the druggable human proteome. Submitted to the *Briefings in Bioinformatics* journal on May 1, 2018.

Chapter 3 of this dissertation is based on Ref [1]. Materials from Chapter 4 and 5 have been submitted for publication as Ref [2] and [3], respectively.

Table of Contents

List of Tables

List of Figures

Abstract

HIGH-THROUGHPUT PREDICTION AND ANALYSIS OF DRUG-PROTEIN INTERACTIONS IN THE DRUGGABLE HUMAN PROTEOME

by Chen Wang, Ph.D.

A dissertation submitted in partial fulfillment of the requirements for the degree of Doctor of Philosophy at the Virginia Commonwealth University.

Virginia Commonwealth University, 2018

Supervisor: Lukasz Kurgan
Ph.D., Qimonda Endowed Professor, Department of Computer Science

Drugs exert their (therapeutic) effects via molecular-level interactions with proteins and other biomolecules. Computational prediction of drug-protein interactions plays a significant role in the effort to improve our current and limited knowledge of these interactions. The use of the putative drug-protein interactions could facilitate the discovery of novel applications of drugs, assist in cataloging their targets, and help to explain the details of medicinal efficacy and side-effects of drugs. We investigate current studies related to the computational prediction of drug-protein interactions and categorize them into protein structure-based and similarity-based methods. We

evaluate three representative structure-based predictors and develop a Protein-Drug Interaction Database (PDID) that includes the putative drug targets generated by these three methods for the entire structural human proteome. To address the fact that only a limited set of proteins has known structures, we study the similarity-based methods that do not require this information. We review a comprehensive set of 35 high-impact similarity-based predictors and develop a novel, high-quality benchmark database. We group these predictors based on three types of similarities and their combinations that they use. We discuss and compare key architectural aspects of these methods including their source databases, internal databases and predictive models. Using our novel benchmark database, we perform comparative empirical analysis of predictive performance of seven types of representative predictors that utilize each type of similarity individually or in all possible combinations. We assess predictive quality at the database-wide drug-protein interaction level and we are the first to also include evaluation across individual drugs. Our comprehensive analysis shows that predictors that use more similarity types outperform methods that employ fewer similarities, and that the model combining all three types of similarities secures AUC of 0.93. We offer a first-of-its-kind analysis of sensitivity of predictive performance to intrinsic and extrinsic characteristics of the considered predictors. We find that predictive performance is sensitive to low levels of similarities between sequences of the drug targets and several extrinsic properties of the input drug structures, drug profiles and drug targets.

Chapter 1 Introduction

Proteins are fundamental components of all organisms. They are essential to virtually all biological processes in cells. At the molecular level, proteins perform their functions by interacting with a wide range of molecules including other proteins, DNA, RNAs, and a variety of other smaller ligands.

Drug is a chemical substance that is used to prevent, treat, or cure a disease. Drugs work through molecular interactions with biological macromolecules, such as proteins and nucleic acids, which are typically referred to as drug targets. Approximately 90% of the existing drugs interact with human genome-encoded proteins [1], and this is why we focus on the druggable human proteome (collection of all the human proteins that are interacting with drugs). The molecular interactions between proteins and drugs typically inhibit or stimulate the cellular functions of proteins where such changes of functional states lead to the therapeutic effects or side effects [2]. Knowledge of the associations between drug compounds and their protein targets is essential for a wide range of pharmaceutical and bioinformatics studies. These studies include screening drug candidates that targets specific disease-associated genes/proteins [3-6], drug repurposing (searching for targets associated with diseases that are not yet known to benefit from the existing drugs) [7-11], discovery and characterization of side-effects that stem from the interactions with non-therapeutic off-targets [12-16], and elucidation of the druggable human proteome, which is

defined as the complement of human proteins that interact with drugs [1, 17-20]. Many databases house information on drug-protein interactions (DPIs) and capture knowledge on drugs and targets to facilitate these studies [21, 22]. However, these databases are relatively incomplete. They cover a small portion (~15%) of human proteins that are already known to be drug targets and for which the three-dimensional (3D) structures are known [23]. The databases are complemented by computational methods that generate putative drug-protein pairs on a large, up to the whole proteome scale. These predictions can be used to facilitate discovery of new DPIs by constraining the scope of expensive and time consuming in vitro and in vivo experiments that are employed to discover and validate the putative DPIs [24-26]. They are also utilized to develop databases of pre-computed putative DPIs [27-29] and were used to facilitate discovery of the therapeutic mechanisms and side-effects of drugs [16, 30, 31].

Computational prediction of DPIs typically incorporates information about drugs and structures or sequences of target proteins. Inspired by recent surveys [32-34], we define two categories of computational methods for DPI predictions: 1) Protein structure-based methods and 2) similarity-based methods that do not use 3D structures of the target proteins. The first group search for binding sites (the locations on the protein surface where binding occurs) from protein 3D structures. This group could be divided into two subgroups: molecular docking and structural alignment. The molecular docking models the physical interactions, including geometric complementarity, between a given drug and protein surface to detect potential binding sites. The structural alignment finds binding sites that are similar to known binding sites based on protein structure alignment. The second group of methods explores similarities between structures and profiles of drugs and non-structural information about their target proteins with known DPIs to predict novel DPIs. The protein structure-based methods use more information, and therefore the

predictive quality of their results is typically higher than the predictive quality of the second group of methods. However, the protein structure-based methods are limited to the proteins that have known 3D structures or for which structures can be accurately predicted. The similarity-based methods rely on protein sequences, drug structures and profiles that are more widely accessible than protein structures. For instance, in March 2017, 5870 protein structures are available in the RCSB Protein Data Bank (PDB [35], a comprehensive repository for three-dimensional structures of proteins and nucleic acids) for 19,077 human protein-coding genes [36], while there are 70,946 gene products (that include isoforms of proteins) in the Universal Protein Resource (UniProt [37]), a comprehensive repository for protein sequences and annotations [38]. In contrast to the protein structure-based methods, the similarity-based methods can be applied to predict potential protein targets. Additionally, in general, the protein structure-based methods, in particular the molecular docking approaches, are computationally more costly than the similarity-based methods. Altogether, the similarity-based methods cover a larger population of target proteins and are less computationally intensive compared to the structure-based methods.

1.1 Goals of the dissertation

The objectives of this dissertation are to review and characterize a comprehensive collection of methods for the prediction of DPIs, assess their predictive performance, and provide access to their predictions. These objectives are addressed with the following three goals:

1) **Evaluation of protein structure-based predictions of DPIs and development and deployment of DPI database.** We empirically assess predictive performance of several protein structure-based DPI predictors for selected representative drugs over the entire

structural human proteome. We develop and deploy a large-scale database of putative and native DPIs for the entire structural human proteome.

2) **Review of the similarity-based DPI predictors.** We provide a comprehensive and in-depth review of a comprehensive collection of high-impact similarity-based methods for DPI predictions. This review substantially improves and expands over the existing reviews on this topic.

3) **Empirical assessment and comparative analysis of similarity-based DPI predictors and their consensuses.** We implement, empirically evaluate, and compare representative similarity-based DPI predictors on a novel and high-quality benchmark database. We include new ways to assess predictive performance, including analysis of the relation between the predictive quality and characteristics of the predictors. We also deploy implementations of the representative methods as a webserver.

In this dissertation, we first introduce background knowledge concerning the biological foundations of drug-protein interactions and basic information about computational predictions in Chapter 2. Then we report empirical findings and provide detailed discussions for each of the three goals stated above in Chapters 3, 4, and 5, respectively. Finally, Chapter 6 presents summary, conclusions, and possible directions for future works.

Chapter 2 Background on drug-protein interactions

In this Chapter we introduce the essential knowledge concerning protein sequences and structures and their importance to characterize the molecular details of the DPIs. We discuss significance of computational prediction of DPIs and briefly review the current structure-based and similarity-based methods for the prediction of DPIs.

2.1 Protein sequence and structure

Proteins are involved in virtually all cellular processes and functions. Examples of these functions include transcription, translation, gene regulation, cell metabolism, and molecular transport. Proteins are built from a sequence of 20 different amino acids that are linearly ordered in a polypeptide chain and connected by peptide bonds. These peptide bonds and α-carbon atoms in the concatenated amino acids constitute of the protein backbone. The sequence of amino acids determines the shape of the corresponding protein and is typically referred to as protein primary structure.

The shape of a protein is formed to a large extent by interactions between amino acids. Protein structure consists of a collection of the local structures (segments in the primary structure). These segments of the local structures are called the protein secondary structures. Typical secondary structures include α helices, β sheets, β strands, turns, coils, loops, etc. Formation of these

structures is mostly detemined by hydrogen bonds that connect the sequence of amino acids in the protein backbone.

The set of secondary structures folds into a specific spatial arrangement, typically forming a compact globular molecule. This arrangement defines the protein tertiary structure. The process of folding the sequence into this three-dimensional molecule relies on hydrophobic interactions with solvent and tertiary interactions between amino acids. An illustration of hierarchical protein structures for an example protein (PDB ID: 4NKX [39]) is shown in Figure 1. The sequence (Figure 1a) is collected from PDB [35]. The secondary structure (Figure 1b) is annotated by Dictionary of Protein Secondary Structure (DSSP) [40, 41]. DSSP is a program that computes secondary structure assignments for PDB entries, which are graphically illustrated in PDB [35]. We use Protein Workshop [42] to visualize the tertiary structure using a ribbon style format (Figure 1c) and with rendering of its molecular surface (Figure 1d).

(a)

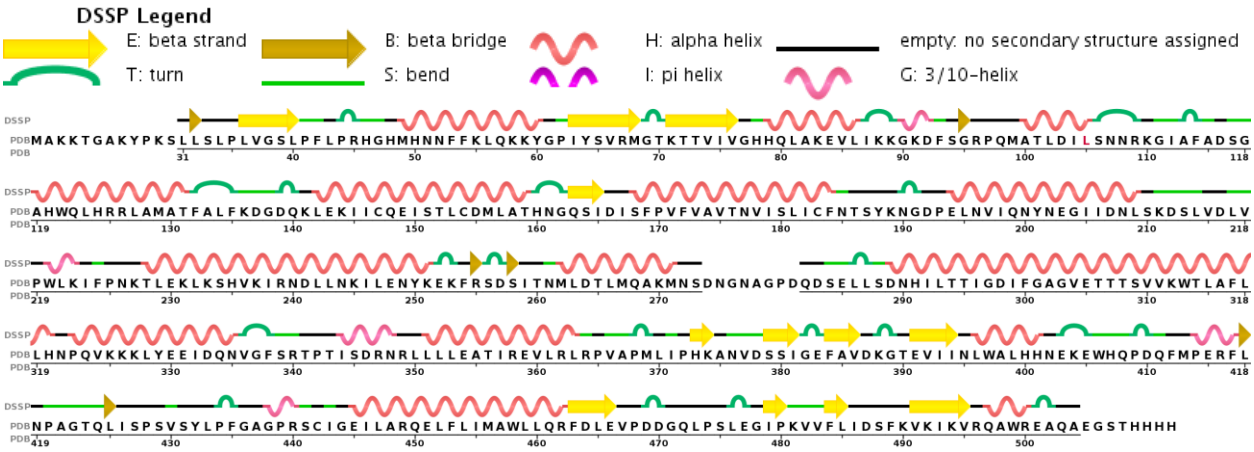

(b)

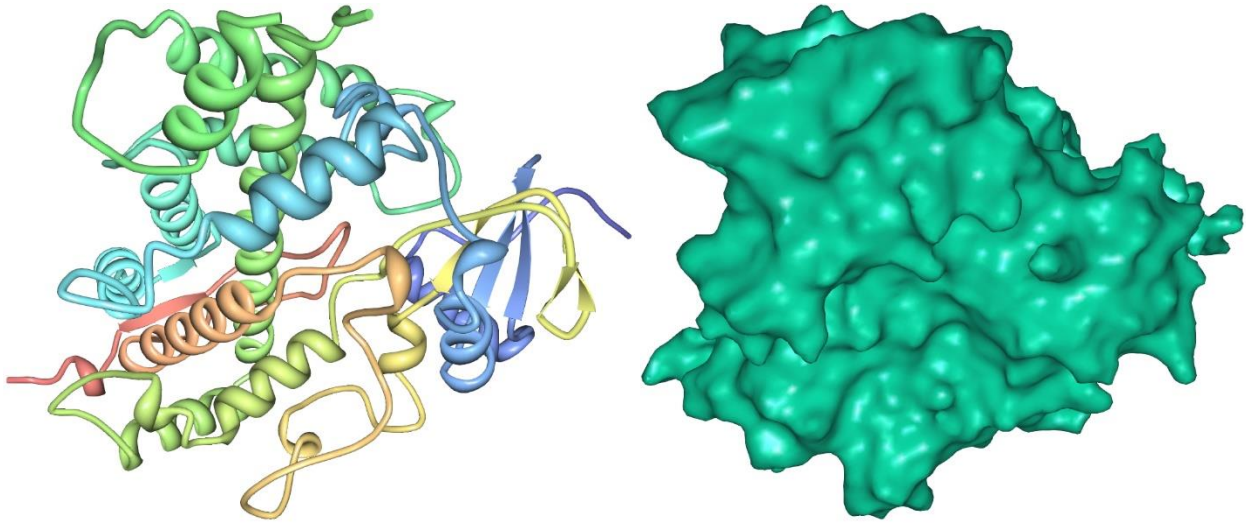

(c) (d)

Figure 1. Protein sequence and structures of an example protein. This protein is collected from PDB ID: 4NKX [39]. (a) Sequence (primary structure) that is represented by single-letter codes for amino acids. (b) Secondary structure that is generated by DSSP [40, 41] and visualized in PDB [35]. (c) Tertiary structure that is visualized by Protein Workshop [42] and represented using ribbons-style format. (d) Molecular surface of the tertiary structure that is rendered with Protein Workshop [42].

2.2 Drug and drug-protein interaction

Drugs are chemical substances that are used to prevent, treat, or cure diseases in human and other living organisms. Drugs exert their therapeutic effects (desired) or side-effects (undesired) through interactions with biological targets including proteins, DNA, RNA, and membrane components such as lipid and carbohydrates [43]. There are significant challenges to accurately and comprehensively define targets, consistently map these targets to specific proteins and genes, and comprehensively compile and update repositories of targets [44]. We are very far from having all-inclusive and consistent repositories that include all existing drug targets and that specify a precise number for different categories of targets, especially for the nucleic acids and other non-protein partners. However, ongoing attempts have provided a consensus on the overall landscape of drug targets. An early and influential study in 2002 conceptualized the druggable genome for the first time and showed that the majority of marketed drug targets are proteins, with DNAs and other miscellaneous biomolecules accounting for only 3% of targets [18]. Recently, researchers estimated that 44% of unique human targets associated with approved drugs were G-protein-coupled receptors, nuclear receptors, protein kinases and ion channels, while 29% were enzymes and 15% were transporter proteins [45]; all of these are proteins. Furthermore, as reflected in their review [45] and a more recent update [1], these protein families make up between 93% and 95% of drug-target interactions. Additionally, a recent comprehensive analysis provided a similar perspective on the characteristics of current drug targets: 96% of 893 mechanistic drug targets were mapped to proteins while the remaining 4% of targets are nucleic acids and other biomolecules. Moreover, the protein targets are responsible for the clinical efficacy of 89% of 1578 FDA-approved drugs and involved in 93% of all identified drug-target interactions [44]. Considering that such predominant fraction of targets are proteins, we focus on the DPIs in this dissertation.

Drug discovery and development requires a large amount of money and time to address identification of the potential targets, to search for drug leads, to analyze massive quantities of data to select promising leads, to validate leads in a wet-lab, and to perform clinical trials [46]. High-quality identification and validation of DPIs is a vital prerequisite to investigate new drugs and determine their targets. This is important since drugs may interact with undesired targets (off-targets) that result in adverse events or side-effects, precluding further drug development and use. The chemical screening with cell assays is used to measure drug-protein binding affinity (how tightly a drug lead compound binds to a selected protein target). However, such experiments are limited in scope as they screen against a relatively small panel of protein targets [47, 48]. For instance, SafetyScreen44 panel screens against 44 targets recommended by four major pharmaceutical companies including AstraZeneca, GlaxoSmithKline, Novartis, and Pfizer [49]. Moreover, Novartis screens against interactions with a panel of 24 targets associated with severe side-effects and high hit rates [50], Pfizer screens against between 15 and 30 targets [51], and Roche uses a panel of 48 targets [52]. Therefore, there is a need to develop high-throughput computational methods for the prediction of DPIs. In particular, to develop methods that can screen a given drug against a comprehensive set of thousands of protein targets that make up the human proteome. The computational methods that identify putative DPIs by exploiting information about both drugs and proteins can be used for that purpose. Depending on whether the three-dimensional structure of a protein is used (known) or not, the prediction methods could be categorized into two groups: protein structure-based methods and similarity-based methods that do not rely on protein structures. Next, we define and discuss these two groups of methods.

2.3 Protein structure-based methods

A binding site is a location on the surface of a protein where the intermolecular interaction occurs. The structure of binding site typically looks like an open pocket or cavity that provides geometrical fit for the structure of the drug. The surface of the pocket not only offers geometric complementarity between protein and drug structures but also has to provide favorable physical characteristics like charge and hydrophobicity. Progesterone is an FDA-approved drug to support and regulate embryo implantation, pregnancy maintenance, and the development of mammary tissue for milk production [53]. Human cytochrome P450 17A1 and progesterone receptor are two representative targets of progesterone that have structures in complex with this molecule. Figure 2a shows the 3D structure of the cytochrome P450 17A1 (PDB ID: 4NKX [39]) and Figure 2c shows a binding site where this protein interacts with progesterone compound. The binding site is a pocket with a specific shape and size that fit the progesterone molecule which is displayed with red balls and sticks. Similar protein structures may have similar cavities/pockets that could interact with the same drug. Figure 2b is the structure of human progesterone receptor (PDB ID: 1A28 [54]) and Figure 2d is its binding site for progesterone. These two protein structures are globally dissimilar with noticeable differences (Root-mean-square deviation of atomic positions = 5.49 Å), which can be observed when comparing Figure 2a and Figure 2b. However, the binding sites, i.e., the pockets in Figure 2c and Figure 2d, are composed of similar spatial arrangement of secondary structures that include three long helices. Significant structural similarity between these two binding sites have been identified in Ref. [55].

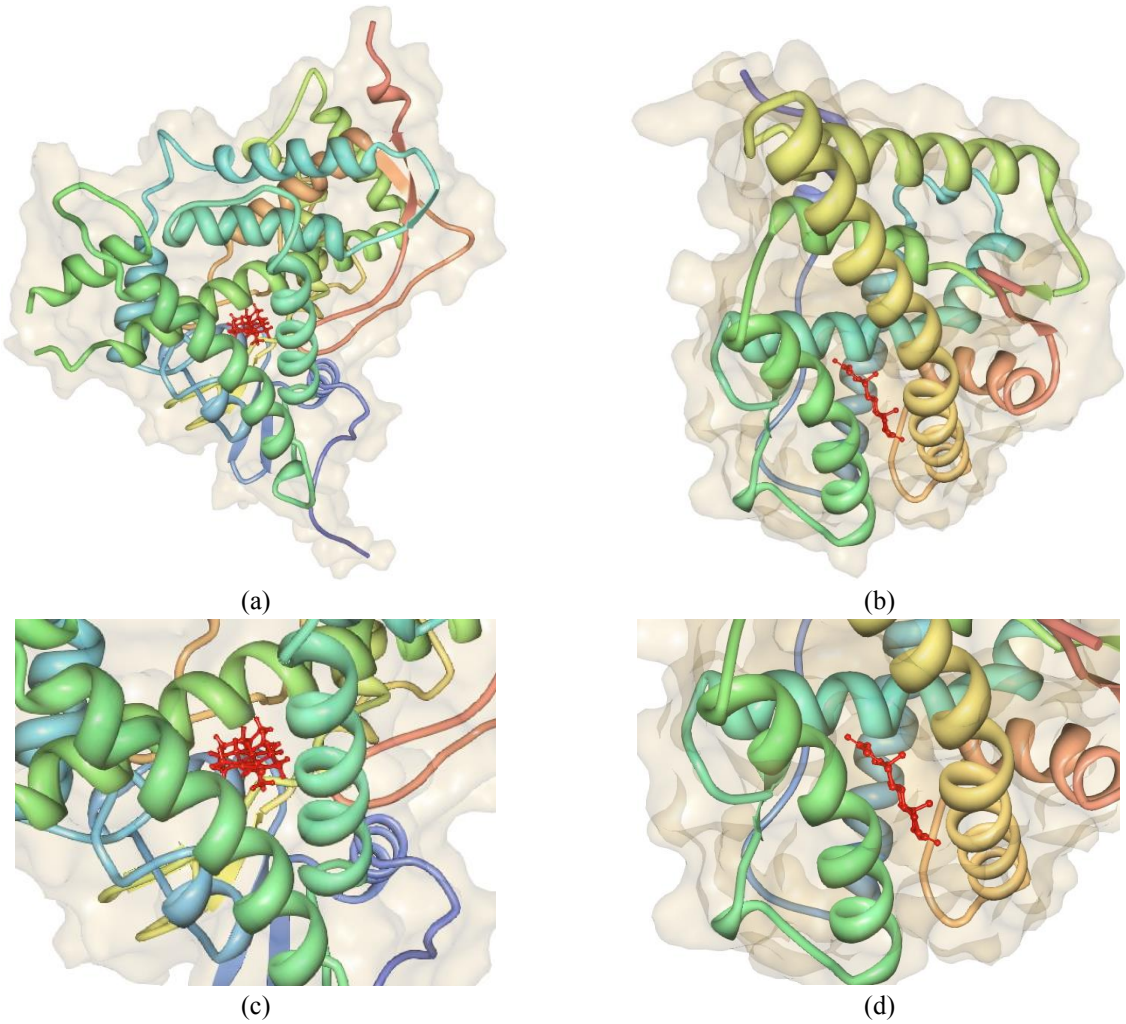

Figure 2. Two structurally dissimilar protein structures and their similar binding sites for progesterone. (a) The structure of human epidermal growth factor receptor inactive tyrosine kinase domain complexed with progesterone (PDB ID: 4NKX [39]). (b) The structure of human epidermal growth factor receptor tyrosine kinase domain complexed with progesterone (PDB ID: 1A28 [54]). (c) Progesterone and its binding site on 4NKX. (d) Progesterone and its binding site on 1A28. Protein molecules are represented by green surfaces. Progesterone molecule is represented by red balls and sticks. We use Protein Workshop [42] to visualize these structures.

The assertion that the same drug may bind to structurally similar proteins with similar binding sites provides an opportunity for prediction of DPIs using proteins structures. Thus, the protein structure-based prediction of DPIs for a given drug could be done by searching for sites that are similar to the known binding sites of this drug.

There are three classes of structure-based prediction methods that implement different trade-offs between accuracy and computational cost. These methods are based on searching for the

similar sites using a reduced representation of protein structure or complete all-atom structure of protein, and by docking the all-atom structure of ligand into the all-atom structure of the target proteins.

The fastest class of methods utilizes the reduced representation, usually in the form of a numeric vector that summarizes geometry and physicochemical properties of binding sites. Representative examples of such methods that find similar binding sites are PatchSurfer [56, 57] and method by Tomii's group [58]. The latter algorithm was recently used to create the PoSSuM database [59, 60] that includes 49 million pairs of similar binding sites computed from the known binding sites of 194 drug-like molecules over all protein structures from PDB. Given the large number of these putative binding sites it is likely that many of them are false positives and would have to be further screened via a more advanced method.

The second class of methods that is characterized by a lower throughput performs docking of a given compound into protein structures to find which proteins harbor binding sites that are complementary to the given ligand. Molecular docking predicts an optimized position and orientation of a drug molecule relative to a target protein molecule so that the drug fits the binding site and forms a stable interaction. Docking method relies on two steps. The first step is searching all possible rotational and translational orientations of the poses of a drug-protein pair. The second step is scoring and ranking the poses by a particular measurement that indicates the strength of binding affinity for each possible pose. An example platform that utilizes such type of docking to find targets of a given ligand, specifically focusing on screening a given drug against a large collection of targets, is INVDOCK [61]. Given the relatively high computational cost of docking, we highlight the availability of the BioDrugScreen database [28]. This database stores results of docking with AutoDock and scores these putative interactions based on several scoring functions,

such as AutoDock, GoldScore, X-Score, ChemScore, PMF, and DFIRE. This docking-based database covers about 1600 drug-like molecules and 2000 cavities on the surfaces of close to 1600 human proteins. However, these results are limited to interactions that are localized in cavities on the protein surface rather than exploring the whole surface. This limitation is motivated by a prohibitively high computational costs of searching the entire surface. BioDrugScreen uses Relibase+ algorithm [62] to identify pockets of interest, while INVDOCK uses an older algorithm by Kuntz and colleagues [63].

The third class of methods is complementary to docking. These methods are not constrained to surface pockets and produce accurate predictions of the drug-protein binding at the molecular level. They implement inverse ligand binding where structure(s) of the known drug-protein complex(es), called template(s), is used to predict other protein targets together with the corresponding binding sites for the same drug. There are two ways to find potential binding sites based on similarity to known binding sites, one based on the similarity of the corresponding protein fold and another based on similarity of binding pockets. The first approach is implemented by the FINDSITE [64, 65] and eFindSite [66, 67] methods and the other approach by the SMAP [68-70] and IsoMIF [71, 72] algorithms. The eFindSite predictor is an improved version of the FINDSITE method that uses meta-threading with the eThread [73, 74] and an advanced clustering algorithm [75] to optimize the selection of the ligand-bound templates for a given query structure. The eFindSite method was empirically shown to outperform FINDSITE and several geometrical methods for detection of pockets [66]. SMAP is designed based on a sequence order-independent profile-profile alignment (SOIPPA) which finds evolutionary and functional relationships across the space of protein structures [68-70]. SMAP utilizes a shape descriptor to characterize the structure of the protein template and the SOIPPA algorithm to detect and align similar pockets

between the query and template proteins. A recent study shows that eFindSite/FINDSITE and SMAP accurately predict targets even when the corresponding structure of the query protein and the template(s) are substantially different, i.e., they are from different SCOP folds [76]. IsoMIF applies GetCleft [77] algorithm to identify pockets on the surfaces of proteins, uses six chemical probes to represent atoms of pockets, and employs subgraph-matching algorithm to compute similarities of binding pockets so that putative binding sites could be predicted by comparison with known binding pockets [71]. A recent large-scale analysis utilizes IsoMIF to identify opportunities to repurpose drugs and to explain side-effects for ~400 drugs and ~8000 proteins and to validate quality of these putative interactions by comparing them with docking simulations [78]. We discuss details of the FINDSITE, eFindSite and SMAP methods in Chapter 3.

2.4 Similarity-based methods

The protein structure-based methods utilize the 3D structure of the target protein(s). However, recent works estimate that only about 20% to 30% of the human proteins have 3D structures [79-81], which means that the protein structure-based methods are limited to a relatively small fraction of the human proteome. Moreover, they cannot be used for proteins with a substantial amount of intrinsically disordered regions [20] while recent works show that as many as 44% of human proteins contain at least one long (30 or more consecutive residues) disordered region [82-84]. Finally, the computational cost of the structure-based predictions for even this small set of proteins is typically high, particularly for the docking [32]. At the same time, the entire human proteome that has a full complement of ~70,000 sequences when including isoforms (source: UniProt reference proteome ID UP000005640) that can be covered by the similarity-based predictions of DPIs. The similarity-based methods are built based on two assertions: 1) similar drugs likely target

the same proteins; and 2) that similar targets tend to interact with the same drugs [32, 85-87]. This is motivated in part by a quote from James W. Black, winner of the 1988 Nobel Prize in Medicine: "the most fruitful basis for the discovery of a new drug is to start with an old drug" [88].

The similarity-based methods for the prediction of DPIs rely on two components: an internal database of known DPIs and a predictive model. They work in three steps. First, a user provides inputs in the form of drug structure, drug profile and/or its target sequence(s), whatever is available. In the second step, similarities between the input drug structure and/or profile and the structures and/or profiles of the drugs in the internal database are computed. If the target(s) of the query drug are known as input or can be retrieved from the internal database (the query drug is already included in the database), then the similarities between the query target and all targets in the database are also computed. In the third step, the predictive model combines the similarities to produce a propensity score that quantifies a likelihood that the query drug interacts with relevant protein targets that are included in the internal database, i.e., the propensity of putative DPI. Novel putative interactions generated by these methods could suggest potential ways to repurpose the existing drugs and also could explain molecular levels details behind side-effects.

Table 1. List of surveys concerning similarity-based DPI predictors. These surveys were published in the past five years. The bottom row corresponds to our review that is described in Chapter 4.

Survey	Year	Number of predictors reviewed	Number of recent predictors reviewed (published since 2013)
Ding et al. [32]	2013	10	2
Pahikkala et al. [89]	2014	2	1
Mousavian et al. [90]	2014	27	16
Chen et al. [21]	2015	17	10
Cichonska et al. [91]	2015	17	9
Lavecchia et al. [92]	2016	11	9
Hart et al. [93]	2016	8	6
Shahreza et al. [94]	2017	17	8
Fang et al. [95]	2017	10	5
Ezzat et al. [96]	2018	28	17
Hao et al. [97]	2018	12	9
Our review	2018	35	22

The similarity-based methods utilize different approaches to express and quantify the similarities. The predictive quality of the similarity-based methods is critically dependent on how the similarities are quantified and whether and how they are combined. Eleven survey articles that were published in the last five years have summarized the development and frontiers of the prediction of DPIs for the similarity-based methods [21, 32, 89-97]. Table 1 chronologically lists these surveys and summarizes the number of prediction methods that are analyzed including the number of recent methods which were published in the past five years. In this dissertation, we present our own review (bottom row in Table 1) of 35 selected similarity-based methods including 22 recent studies that appeared in the past five years. Compared to the existing surveys, our analysis is broader than most of the existing reviews (35 vs between 2 and 28 approaches in total) and more current (22 vs between 1 and 17 recent approaches). Criteria of selection of these approaches are described in Chapter 4. Besides the predictive models, some of these reviews also summarize the databases of DPIs [21, 22, 32, 91, 92, 94, 95] and the assessment of predictive results [32, 89, 96, 97] that are employed in prediction approaches. We present our review and compare it at a greater depth with the other surveys in Chapter 4.

Chapter 3 Evaluation of protein structure-based predictions of drug-protein interactions and development and deployment of protein-drug interaction database

In this chapter we assess the predictive quality of three representative protein structure-based methods for the predictions of DPIs. Using results produced by these methods, we develop and deploy a DPI database that covers interactions between 51 popular, FDA-approved drugs and the proteins from the structural human proteome. This repository provides a query interface to search a comprehensive set of putative DPIs that are generated by the predictors, as well as annotations of native DPIs collected from relevant databases.

3.1 Motivation to develop a novel database

The significant majority of the molecular targets of drugs are proteins and there are several databases of the already characterized DPIs. DrugBank [98-102] provides access to biochemical and pharmacological information about a large set of 7759 drugs, including 1600 FDA-approved compounds, and their known 4104 protein targets. Therapeutic Target Database [43, 103-107] offers a comprehensive coverage of over 20,000 drugs, including close to 15,000 experimental drugs, and their interactions with 2360 protein targets. This database also links targets and drugs

to about 900 diseases. Other databases expand beyond the drug molecules to cover small drug-like ligands. BindingDB [108-112] gives experimentally measured binding affinities between about 7000 known protein targets and a large set of almost half a million of small ligands. ChEMBL [113-116] contains structures, physicochemical properties and bioactivity (e.g. binding constants, pharmacology data) of drug-like small molecules. The current release of ChEMBL incorporates 1.7 million distinct compounds and 13.5 million bioactivity data points which are mapped to over 10 thousand protein targets, where the corresponding binding sites are defined at varying levels of granularity (protein, protein domain, or residue-level). SuperTarget [117, 118] includes about 6200 protein targets from several dozens of species and close to 200,000 drug-like compounds. It integrates drug-related information from BindingDB, DrugBank, and the SuperCyp database of cytochrome-drug interactions [119], adverse drug effects from SIDER [120, 121], drug metabolism, and pathways and Gene Ontology (GO) terms for the target proteins. The PROMISCUOUS database [122] integrates data from DrugBank, SuperTarget, and SuperCyp and covers about 6500 protein targets and over 25 thousands drug-like compounds that are annotated with side-effects. This database also provides facilities that can be used to predict novel targets based on the structural similarity between drugs and between side-effect profiles of drugs. STITCH [123-127] combines information from many sources of experimentally and manually curated interactions between small ligands and proteins including ChEMBL, PDB, DrugBank, Therapeutic Target Database, text mining of articles from MEDLINE and PubMed, and several other resources. It currently houses data on 390,000 chemicals and 3.6 million proteins. The recently released IntSide database [128] links about 1000 drugs with their human protein targets collected from DrugBank and STITCH, and with close to 1200 side-effects and other annotations of associated diseases, pathways, and cellular functions. While most of these resources summarize the

interactions at the protein or residue level, scPDB [129, 130] includes molecular-level (all-atom) information for native binding sites in proteins structures collected from PDB [35] that are suitable for docking of drug-like ligands. It includes molecular-level details of about 9200 binding sites (all-atom annotation of binding sites and list of ligand-binding residues grouped by various types of bonds) and binding modes (all-atom position of ligand inside the site) for 3600 proteins, and a summary of physicochemical properties of approximately 5600 drug-like ligands.

However, many of the established drugs interact not only with the intended therapeutic target protein(s) but also with other protein targets (off-targets). Individual compounds were shown to on average target 6.3 proteins [10, 131]. Given a high degree of incompleteness of this information [131, 132], the number of off-targets is likely substantially higher. To compare, DrugBank includes 15199 DPIs for 7759 drugs with the average number of targets per drug at 1.96, which further substantiates the claim of the incompleteness of the currently available data. This polypharmacology can be both beneficial, when a given drug can be repurposed for a different disease, and harmful, leading to the side-effects [132]. A couple of high-profile examples include imatinib that was repurposed for treatment of gastrointestinal stromal tumors [133] and sorafenib for the kidney and liver cancers [134]. The incompleteness of the data combined with the importance of polypharmacology motivates research towards the elucidation of novel and more comprehensive set of DPIs.

Conventional (non-computational) methods for the identification of novel off-targets rely on an in vitro counter-screen of a given drug against a small set of a few dozens of enzymes and receptors [49-52, 135]. Compared to the experimental screens, computational methods that find novel drug targets are more cost- and time-effective, allow screening of a larger number of targets and provide insights into the molecular-level mechanisms of DPIs [136]. These *in-silico* methods

are successful in the context of drug repositioning and identification of off-targets [137]. A couple of databases that focus on the putative protein-drug and druggable protein-protein interactions were recently released. BioDrugScreen [28] stores results of docking of about 1600 small drug-like molecules against 1589 known proteins targets in human, which were annotated based on DrugBank and HCPIN [138] databases. Docking was run for close to 2000 cavities on the surfaces of these proteins, for the total of about 3 million receptor-ligand complexes. Druggable Protein-protein Interaction Assessment System (Dr. PIAS) [139, 140] is a database of druggable protein-protein interactions (PPIs) predicted by a machine learning method. This database lists druggable interactions predicted from over 83 thousand PPIs in human, mouse, and rat, but they are not associated with specific compounds.

We developed Protein-Drug Interaction Database (PDID) that complements existing repositories and addresses the lack of access to a comprehensive set of putative DPIs [29]. This database relies on predictions generated by three representative protein structure-based methods, eFindSite [66, 67], SMAP [68-70], and ILbind [76]. These methods are complementary and independent of docking that was used in the BioDrugScreen database. They were also shown empirically to provide high-quality predictions of drug targets [76], and their results were already successfully used to predict novel off-targets. Examples include applications to find new off-targets of estrogen receptor modulators [141], cholesteryl ester transfer protein inhibitors [30], comtan [142], inhibitors of Trypanosoma brucei RNA editing ligase 1 [143], nelfinavir [31], raloxifene [144], and cyclosporine A [16]. We describe in detail and re-assess the selected three representative methods to provide a more recent estimate and comparative analysis of their predictive performance before we describe the PDID database.

3.2 Considered protein structure-based predictors

The fundamental principle of protein structure-based predictors is to transfer the binding sites from known drug-protein complexes to a protein that is structurally similar to these known drug-complexed proteins. There are two ways to measure the similarity between the input protein structure and the known drug-protein complexes: one applies the similarity of the corresponding protein fold, such as FINDSITE [64, 65] and eFindSite [66, 67] algorithms, and the other that exploits the similarity of binding sites, such as SMAP [68-70] and IsoMIF [71, 72] methods.

3.2.1 FINDSITE and eFindSite

FINDSITE predicts binding sites for an input protein using template protein(s) which have the structure(s) in complex with a given input drug [64, 65]. These template proteins come from a database of templates (a set of non-redundant high-quality structures of drug-protein complexes curated from the PDB database) that is part of the FINDSITE algorithm. FINDSITE accepts either an experimentally determined structure annotated in PDB or a putative structure modelled computationally with TASSER [145-147], MODELLER [148, 149] or PROSPECTOR_3 [150], three accurate protein structure modelling algorithms. We use experimentally determined structures for the input proteins in our experiments. The protocol of FINDSITE is briefly described as the following four steps:

1) A threading algorithm, PROSPECTOR_3 [150] is utilized to find template proteins for the input protein from the template database. PROSPECTOR_3 threading recognizes template proteins which likely have similar structural folds when compared to the input protein based on sequence alignment and predicted secondary structure, given the sequence of the input

protein. The identified template proteins are supposed to be structurally similar to the input protein, no matter whether or not they have high sequence similarity to the input protein.

2) The template proteins that are known to be in complex with the input drug are selected from the template set which is obtained by the threading alignment. Then the template set is expanded by including homologous proteins of the current templates. Consequently, we get a set of template proteins that interact with the input drug, have known three-dimensional structures of drug-protein complex, are likely structurally similar to the input protein, and are possibly remotely homologous to the input protein.

3) A structural alignment algorithm, TM-align [151], is utilized to superimpose the structures of template proteins (including their drug-complexes) into the structure of the input protein. A set of superimposed atomic coordinates for each template protein is generated in this step.

4) The superimposed coordinates of the center of the input drug in each template structure are clustered based on spatial distance with a threshold distance equal to 8Å. The geometric center of each cluster is a predicted position of the input drug into the input protein structure, which represents a putative binding site for this input drug-protein pair. These predicted binding sites could be ranked by the number of templates from the corresponding cluster where each binding site (cluster center) comes from.

Besides a putative position of the center of the given drug, FINDSITE also outputs other information that allows ranking predictions across different input proteins: (i) TM-score, a structural alignment score generated by TM-align; (ii) root mean square deviation (RMSD) of the Cα atoms in the aligned region between input protein and templates by TM-align; (iii) alignment length which is number of residues aligned with the template protein structure by TM-align; (iv) fraction of templates that share the predicted binding site (cluster center); (v) sequence identity

calculated over the residues aligned by the TM-align; (vi) number of predicted binding sites; and (vii) number of predicted binding residues.

As an improved version of FINDSITE, eFindSite combines multiple threading approaches by machine learning models to select template proteins and employs an advanced clustering algorithm to predict the putative binding sites [66, 67]. More specifically, eThread [73, 74], a meta-threading approach that applies Naïve Bayes classifier to build a consensus threading alignment from ten individual threading algorithms, is utilized to identify template proteins; this concerns the steps 1) and 2) of FINDSITE. Moreover, eFindSite also improves steps 3) and 4) of FINDSITE. This concerns an approach to superimpose template structures to the input protein and to cluster binding sites in the template structures. First, Affinity Propagation [75] is utilized to cluster the structures of template drug-protein complexes based on structural similarities between templates computed with fr-TM-align [152]. Second, the clustered template structures are superimposed into the structure of input protein. Finally, the resulting superimposed locations of drug from each clustered template constitute the predicted position of the input drug, which in turn can be used to annotate putative binding sites in the structures of the input proteins.

3.2.2 SMAP

SMAP works by generating potential binding pockets in the input protein structure and next finding whether these pockets are similar to the known binding pockets in the drug-binding proteins [68-70]. It relies on a geometric representation of protein structure to characterize binding sites [68] and a sequence profile alignment to compare binding sites [69]. The protocol of SMAP algorithm is summarized in the following five steps:

1) SMAP reduces the representation of an input protein structure by using only the coordinates of alpha carbon (Cα) atoms which are the first carbon atoms attached to the carboxyl group

of an amino acid. These Cα atoms are represented as vertices in a graph. A convex hull algorithm, Delaunay tessellation, is applied to partition the Cα atoms into tetrahedra (triangular pyramids) that are defined by the graph edges [68].

2) The Delaunay tessellation is constrained by removing tetrahedra that include edges (atomic distances) longer than 30Å because such distance implies a open binding pocket on the molecular surface, not an enclosed sphere. The outside layer of the remained convex hull defines a environmental boundary which surrounds the input protein and its binding pockets. Next, the tetrahedra larger than 7.5Å are removed. This cut-off length is related to the average radius between two amino acids that are in contact with each other. The remaining tetrahedra on the outside of the structure form a protein boundary. The removed tetrahedra which are the tetrahedra located between the protein boundary and the environmental boundary, make up the possible positions where drugs could be located.

3) The distance and orientation of each Cα atom to the protein boundary and environmental boundary is computed. Based on these values, a geometric potential is computed using specific formulas listed in Ref. [68] for each Cα atom. The geometric potential quantifies the positions of a Cα atom and its neighbor atoms relative to the environmental boundary, and the relative positions between this Cα atom and its neighbor Cα atoms.

4) The possible positions of drugs obtained in step 2) are clustered based on their overlap in circumscribed spheres of the corresponding tetrahedron. The cluster centers represent the predicted potential positions of the drugs that could bind to the given protein. If a Cα atom is located within 10Å from the predicted potential positions and the edge between these two atoms are not cut by other circumscribed spheres, this Cα atom (that represents a drug-binding

amino acid) is predicted as a part of a binding site. This way the amino acids that make up specific binding pockets are defined.

5) The predicted potential positions of drugs generated in step 4) represent a candidate drug-binding position but without specifying for which specific drug. SMAP uses a sequence order independent profile-profile alignment (SOIPPA) method to align the candidate drug-binding sites (the corresponding amino acids) in the input protein to the known binding sites in the template proteins which are found in complex with the input drug in PDB [69]. Next, a candidate binding site is mapped to a known binding site of the specific input drug if the SOIPPA alignment shows that these two sites are similar enough. SOIPPA algorithm is designed to compare and align two subgraphs that are extracted from the geometric representations of the input protein and the template protein. The computation of the alignment uses the geometric potential scores computed in step 3). The binding sites from the template protein are aligned and superimposed as the candidate sites in the input protein. A alignment score is computed based on the position specific score matrix [153] to measure the similarity of these binding sites.

SMAP outputs seven measurements that can be used to rank binding site similarity between the input protein and the template protein: (i) local alignment (pairs of aligned residues) between drug-binding sites in the input and template proteins; (ii) alignment score generated by SOIPPA; (iii) *p*-value that estimates the statistical significance of the alignment score by considering a random set of PDB chains; (iv) volume of overlapping binding pockets between the input protein and the template protein computed in the structure of input protein; (v) the same volume computed in the structure of template protein; (vi) Tanimoto coefficient between the two proteins; (vii) root mean square deviation (RMSD) between the binding sites in the input and template proteins.

3.2.3 ILbind

The inverse ligand binding (ILbind) predictor is an ensemble machine learning predictor of drug-binding sites for a specific input drug. ILbind uses selected outputs (the outputs were chosen based on an empirical feature selection process) generated by FINDSITE and SMAP [76] as its inputs. This meta-approach exploits the fact that FINDSITE and SMAP use complementary approaches for the prediction. FINDSITE's prediction is based on similarity of protein structures while SMAP's prediction is based on similarity of binding pockets. ILbind was designed to provide predictions for a wide range of drugs and nutraceuticals. First, a dataset of ~150 drugs was clustered into three structurally similar clusters. These clusters were represented by three drugs that correspondingly have diverse structures: N-Acetyl-D-glucosamine (NAG), Adenosine-5'-Diphosphate (ADP), and Palmitic Acid (PLM) [76]. Structures of five randomly chosen complexes of proteins with each of these three drugs were used to design ILbind, resulting in total of 15 configurations. Correspondingly, 15 Support Vector Machine (SVM) models were designed using a training dataset. A total of 14 outputs (features) from FINDSITE and SMAP were ranked by their average AUC values on the training set. Next, a wrapper-based best-first search to select features was applied using cross-validation on the training dataset. The search started from including only the top ranked feature, and added next feature from the ranked set of features to the feature set if the inclusion of this feature increased AUC value when compared with the feature set before including this feature. Between the 15 SVM models, the selected feature sets typically contain two or more features which correspond to the outputs from both FINDSITE and SMAP.

Given an input drug and the structure of an input protein, ILbind works in two steps:

1) Compute predictions with the 15 SVM models using the selected outputs of FINDSITE and SMAP as the inputs.

2) Use the consensus (average) of the 15 SVM predictions as the predicted propensity for binding to the input drug.

Since ILbind does not predict the putative position of the center of the input drug, these positions are borrowed from the outputs of FINDSITE and SMAP.

3.3 Assessment of predictive quality

We assessed predictive performance of eFindSite, SMAP, and ILbind to demonstrate that predictions from these methods have practical value. This assessment was performed on a set of 25 representative drugs that are currently included in PDID. These compounds were selected from 25 clusters of chemically similar drug structures (one compound from each cluster) that were generated from the 355 drugs that could be found in complex with proteins in PDB at the time of the experiment. The evaluation follows the protocol from [16]. Briefly, native targets of the 25 drugs were collected from PDB, BindingDB, and DrugBank and we compare predictions from the three methods on the structural human proteome against these native drug targets. We clustered proteins in the structural human proteome at 90% sequence identity using BLASTCLUST [153, 154] and evaluated the results on the corresponding clusters, i.e., a given cluster is considered to be a native target of given drug (predicted to bind the drug) if at least one protein in this cluster shares at least 90% identity with a native target of that drug (at least one protein in this cluster is predicted to bind that drug). The clustering assures that the evaluation is not biased towards targets that are overrepresented with many structures of similar folds.

Empirical results demonstrate that the three methods are characterized by practical levels of predictive quality. The average AUCs over the 25 drugs of eFindSite, SMAP and ILbind equal 0.63, 0.74 and 0.76, respectively (Figure 3a). Although ILbind outperforms the other two methods,

which is expected given that it combines results of these methods and which is consistent with the results in [76], different methods perform better for different drugs. More specifically, eFindSite provides the highest AUC for 5 drugs, SMAP for 6 drugs, and ILbind for the remaining 14 drugs. Figure 3b gives average true positive rates (fractions of correctly predicted native targets) in the function of the fraction of predicted protein targets sorted in the descending order by the propensities for the interaction generated by each of the three predictors. This figure shows that 40% of the native targets (true positive rate = 0.4) are found among the top 4% of predictions from ILbind and SMAP and among the top 14% of predictions from eFindSite.

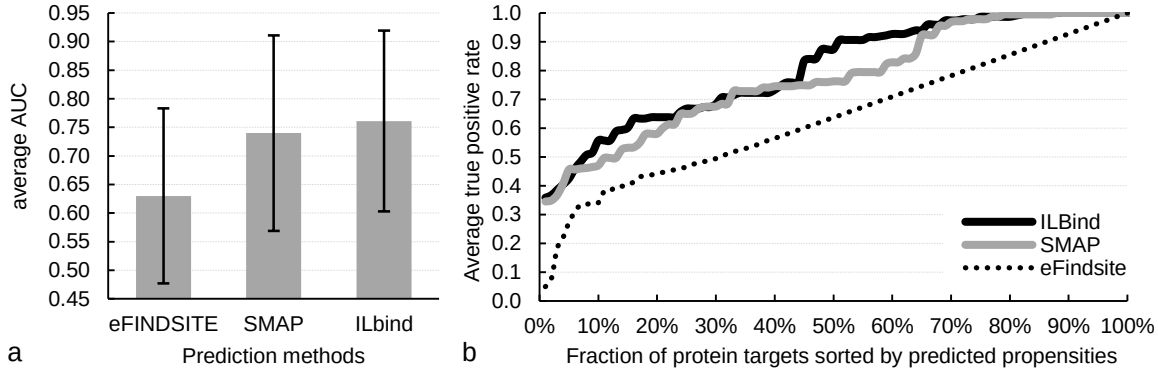

Figure 3. Predictive quality of eFindSite, SMAP, and ILbind for the 25 representative drugs. Panel a shows the average AUC computed over the 25 drugs; error bars give the corresponding standard deviations. Panel b shows average true positive rate (fraction of correctly predicted native targets) computed over the 25 drugs in the function of the ranking of predictions; the *x*-axis shows fraction of predicted protein targets sorted in the descending order by the predicted propensities for the interaction.

We observe that predictive performance of these three methods varies between compounds and depends on their size. Higher AUCs are characteristic for medium sized drugs (with a molecular weight between 200 and 400 g/mol) and lower AUCs for either small (below 200 g/mol) or large (over 400 g/mol) drugs. To compare, the average AUCs for the small/medium/large drugs for eFindSite, SMAP and ILbind are 0.56/0.68/0.58, 0.7/0.83/0.58, and 0.7/0.86/0.59, respectively. Example small and large compounds for which predictive quality is relatively low are salicylic acid (138.1 g/mol; average AUC over the three methods of 0.50), isoflurane (184.5 g/mol; 0.60),

suramin (1297.3 g/mol; 0.55), and cyanocobalamin (1355.4 g/mol; 0.57). Example drugs for which prediction are more accurate are naproxen (230.3 g/mol; 0.88), furosemide (330.7 g/mol; 0.94), and prednisone (358.4 g/mol; 0.87).

3.4 Protein-drug interaction database

3.4.1 Contents and availability

We collected the structural human proteome from PDB by removing low-resolution structures (> 3Å) and following [16, 141] we kept proteins for which sequences were mapped to human proteins in Ensembl [155]. More specifically, structures of chains with at least 90% sequence identity quantified using BLAST [154, 156] with default parameters to any human protein from 68th release of Ensembl were selected. As a result, we include a total of 9652 human and human-like high-resolution structures that correspond to 3746 unique human proteins. Protein chains that correspond to these PDB structures were mapped to UniProt [157] to facilitate mapping of proteins between PDID, PDB, DrugBank and BindingDB.

The PDID database includes drugs which were solved structurally in complex with at least one protein; this is necessary to predict targets. There are 355 such drugs in PDB which we extracted with PDBsum [158]. The current release 1.1 of PDID includes 51 drugs compared to the release 1.0 that had 26 drugs, all of which were selected from the 355 drugs. We clustered structures of the 355 drugs using their structural fingerprint expressed with Tanimoto coefficient and sampled at least one drug from each of the resulting 25 clusters to select the 51 drugs. Thus, the selected drugs comprehensively sample the structural drug space. These drugs are listed in Table 2 and include popular antibiotics, anti-inflammatory, anti-viral and anti-cancers agents,

immunosuppressants, and drugs for the treatment of osteoporosis, diabetes, heart attack, hypertension, edema, angina, glaucoma and other diseases.

Table 2. Drugs included in the current release 1.1 of PDID.

Drug name	Formula	PDB ID	# complexes	Primary use
acetazolamide	$C_4H_6N_4O_3S_2$	AZM	22	treatment of glaucoma, edema and epilepsy
acyclovir	$C_8H_{11}N_5O_3$	AC2	5	anti-viral for herpes, chickenpox, and shingles
adenosine	$C_{10}H_{13}N_5O_4$	ADN	107	treatment of cardiac arrhythmia
alendronate	$C_4H_9NO_7P_2$	AHD	3	treatment of osteoporosis
ampicillin	$C_{16}H_{19}N_3O_4S$	AIC	8	antibiotic
bepridil	$C_{24}H_{34}N_2O$	BEP	2	treatment of angina
caffeine	$C_8H_{10}N_4O_2$	CFF	10	stimulant
captopril	$C_9H_{15}NO_3S$	MCO	5	treatment of hypertension
cerulenin	$C_{12}H_{19}NO_3$	CER	8	antibiotic
chloramphenicol	$C_{11}H_{12}CL_2N_2O_5$	CLM	16	antibiotic
chloroquine	$C_{18}H_{26}CLN_3$	0TX	1	treatment of malaria
clavulanate	$C_8H_9NO_5$	J01	4	antibiotic
cyanocobalamin	$C_{63}H_{88}CON_{14}O_{14}P_1$	CNC	10	vitamin B12 activity
cyclosporin A	$C_{62}H_{111}N_{11}O_{12}$	CSA	30	Immunosuppressant
didanosine	$C_{10}H_{12}N_4O_3$	2DI	1	anti-viral for HIV
dopamine	$C_8H_{11}NO_2$	LDP	9	treatment of hypotension and cardiac arrest
efavirenz	$C_{14}H_9CLF_3NO_2$	EFZ	6	anti-viral for HIV
erlotinib	$C_{22}H_{23}N_3O_4$	AQ4	3	anti-cancer
ertapenem	$C_{22}H_{27}N_3O_7S$	1RG	3	antibiotic
erythromycin	$C_{37}H_{67}NO_{13}$	ERY	9	antibiotic
estradiol	$C_{18}H_{24}O_2$	EST	28	hormonal contraception
exemestane	$C_{20}H_{24}O_2$	EXM	1	anti-cancer
furosemide	$C_{12}H_{11}CLN_2O_5S$	FUN	3	treatment of hypertension and edema
gemcitabine	$C_9H_{11}F_2N_3O_4$	GEO	3	anti-cancer
ibuprofen	$C_{13}H_{18}O_2$	IBP	9	anti-inflammatory
imipenem	$C_{12}H_{19}N_3O_4S$	IM2	12	antibiotic
indomethacin	$C_{19}H_{16}CLNO_4$	IMN	24	anti-inflammatory
isoflurane	$C_3H_2CLF_5O$	ICF	2	anesthetic
kanamycin	$C_{18}H_{36}N_4O_{11}$	KAN	21	antibiotic
l-carnitine	$C_7H_{16}NO_{31}$	152	8	treatment of heart attack and heart failure
mercaptopurine	$C_5H_4N_4S$	PM6	2	immunosuppressant
naproxen	$C_{14}H_{14}O_3$	NPS	4	anti-inflammatory
niflumic acid	$C_{13}H_9F_3N_2O_2$	NFL	2	anti-inflammatory
nitroxoline	$C_9H_6N_2O_3$	HNQ	1	antibiotic
pentamidine	$C_{19}H_{24}N_4O_2$	PNT	7	anti-microbial
pioglitazone	$C_{19}H_{20}N_2O_3S$	P1B	2	treatment of diabetes
ponatinib	$C_{29}H_{27}F_3N_6O$	0LI	3	anti-cancer
prednisone	$C_{21}H_{26}O_5$	PDN	8	immunosuppressant
progesterone	$C_{21}H_{30}O_2$	STR	15	hormone replacement therapy
rifampin	$C_{43}H_{58}N_4O_{12}$	RFP	7	antibiotic
ritonavir	$C_{37}H_{48}N_6O_5S_2$	RIT	12	anti-viral for HIV
salicyclic acid	$C_7H_6O_3$	SAL	36	treatment of acne
saxagliptin	$C_{18}H_{25}N_3O_2$	BJM	1	treatment of diabetes
streptomycin	$C_{21}H_{39}N_7O_{12}$	SRY	14	antibiotic
sulindac	$C_{20}H_{17}FO_3S$	SUZ	7	anti-inflammatory
suramin	$C_{51}H_{40}N_6O_{23}S_6$	SVR	12	anti-microbial
tobramycin	$C_{18}H_{37}N_5O_9$	TOY	6	antibiotic
tretinoin	$C_{20}H_{28}O_2$	REA	30	treatment of acne
vidarabine	$C_{10}H_{13}N_5O_4$	RAB	2	antibiotic
zidovudine	$C_{10}H_{13}N_5O_4$	AZZ	4	anti-viral for HIV
zoledronate	$C_5H_{10}N_2O_7P_2$	ZOL	12	treatment of osteoporosis

The PDID database provides access to pre-computed results of computationally expensive all-atom predictions by eFindSite and SMAP. Their average runtime for a single protein structure and a given drug is about 30 minutes on a single CPU; the runtime of ILbind is negligible since it is based a consensus of results generated by the two predictors. This high computational cost makes *ad hoc* predictions for a given user query (a given drug or a given protein) computationally impractical.

The current version of PDID includes results of about 1.1 million predictions of targets over the 10 thousand structures and 51 drugs, with the corresponding 5172, 7184, and 4444 putative targets of these drugs generated by ILbind, SMAP, and eFindSite. It also includes 730 known targets of the 51 drugs mapped from and linked to the corresponding records in DrugBank, BindingDB, and PDB. Figure 4 shows the number of native and putative targets for each drug. The median number of putative DPIs equals 23, 30, and 31 for SMAP, eFindSite, and ILbind, respectively, compared to the median of 8 based on the known interactions collected from DrugBank, BindingDB and PDB.

PDID is freely available at http://biomine.cs.vcu.edu/servers/PDID/. The backend of this database is implemented with the MySQL relational database and query pages using PHP script. Protein targets are linked to PDB, UniProt, BindingDB and DrugBank. Drugs are linked to the corresponding records in PDB, BindingDB, and DrugBank. Protein and drugs are linked with each other through their known and putative interactions. The interactions are defined at the molecular level, i.e., coordinates of the location of the drug in the protein structure file are included. Besides displaying this information in the browser window, PDID provides access to the source files with the sequence and structure of the target proteins. We also offer download of the parsable raw source datasets in text format under the "Datasets" section on the main page. They include the

current version of the structural human proteome (IDs of all considered protein structures), a list of drugs, and predicted targets for each drug together with scores from each of the three prediction methods and the corresponding coordinates of the putative positions of the center of the drug.

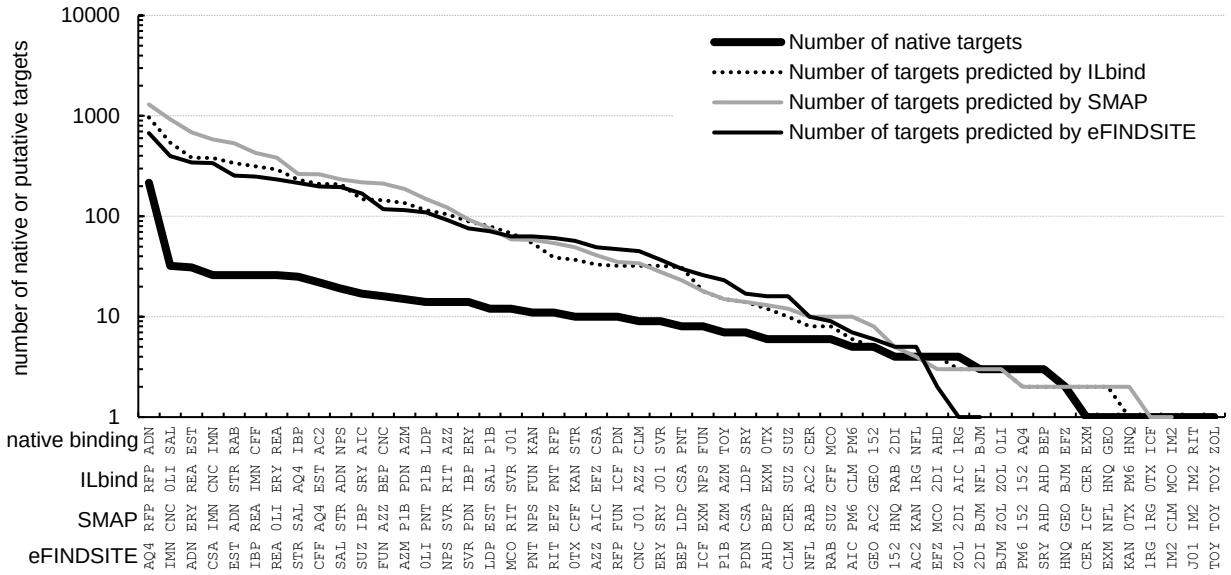

Figure 4. Number of native and putative targets for the considered 51 drugs. The native targets are based on the combined annotations from PDB, DrugBank, and BindingDB. The predictions were generated by ILbind, SMAP and eFindSite. The drugs, which are shown on the *x*-axis, are sorted by their corresponding number of targets in the descending order and separately for each of the four annotations.

3.4.2 User interface

The main page of PDID includes an overview of the contents of the database, provides access to three available search types (by drug name, by ID of the protein target, and by a sequence of the protein target), lists links to the source datasets and related resources, and gives the release date. It also includes link to the "About" page that explains contents of the database and introduces related methods, and to the "Help & Tutorial" page that explains the interface of the main page and the three types of output pages that correspond to the three search types (Figure 5).

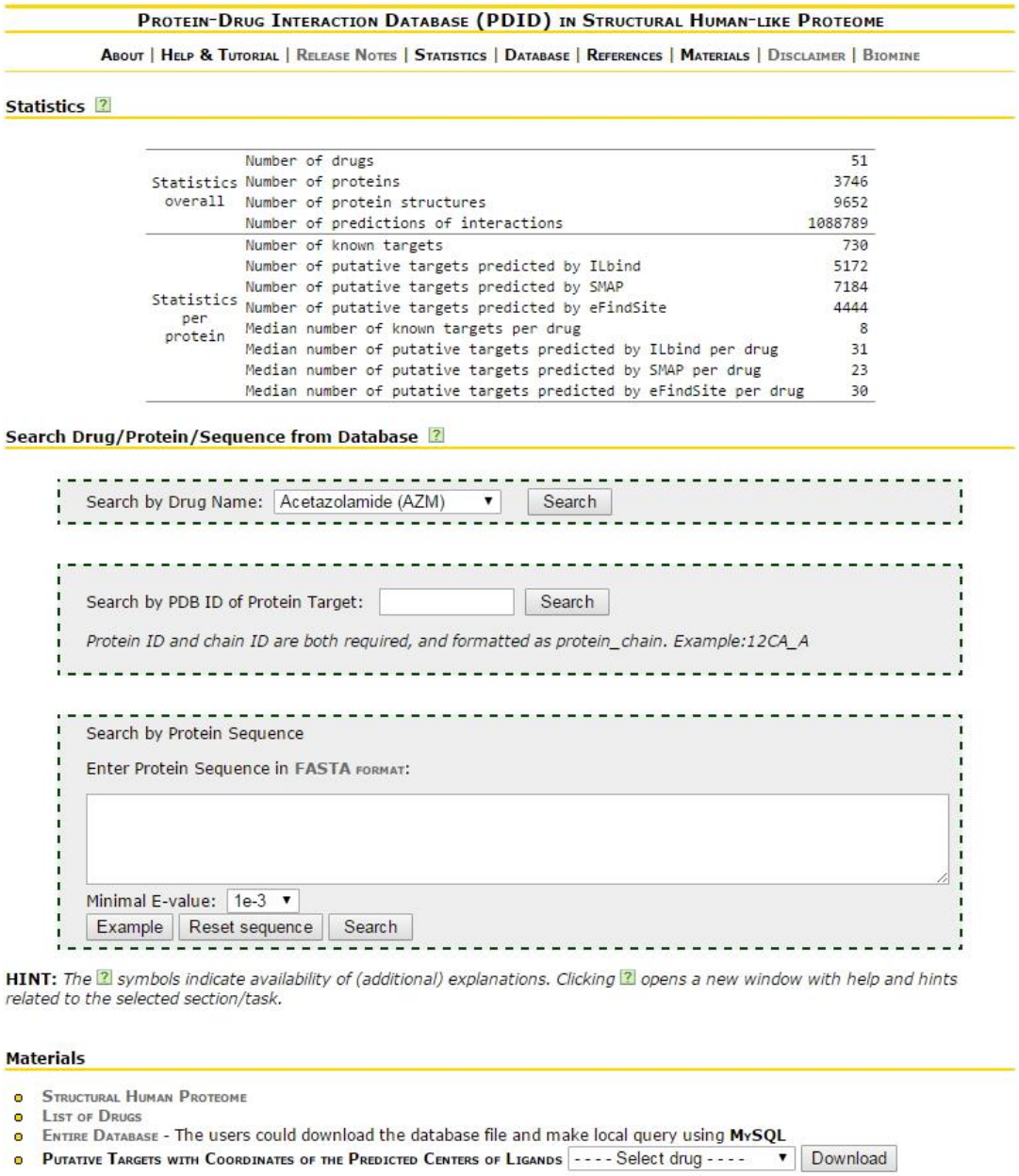

Figure 5. Main page of the PDID database. The main page includes statistics of drugs, proteins and interactions, three types of queries in the database, download links of partial or entire database, and pointers to help and tutorial pages that can be accessed by clicking on the "?" icon.

The search by drug name returns a table with details of known and putative targets including links to the corresponding records in PDB, DrugBank and BindingDB, links to files with structure and sequence of each target, and propensities for binding output by ILbind, SMAP, and eFindSite (Figure 6a). Targets are sorted by the number of methods that predict them as binding (propensities

shown in green font indicate that binding is predicted) and by the scores generated by the most accurate ILbind when the number is the same. A more detailed description of the formatting and contents of this output page can be found at http://biomine.cs.vcu.edu/servers/PDID/help.html#drug_page. Each target protein is available as a link that leads to a web page with the summary of results for this protein.

The search by protein ID returns a web page that maps this ID into corresponding UniProt protein (quality of mapping is annotated using sequence similarity), gives links to the sequence and structure files, and provides customizable visualization of the structure together with the localization of the putative (red dots) and known (blue sticks) ligands. The page also includes a table that summarizes information about drugs that are known and predicted to bind this protein (Figure 6b). This information includes color-coded scores generated by each method that produced the predictions and the corresponding predicted location of the drug in the protein structure. We use JSmol [159] to visualize structures and BLAST to compute sequence similarity. A more detailed description of this web page is available at http://biomine.cs.vcu.edu/servers/PDID/help.html#prot_page.

The search based on protein sequence invokes BLAST that compares the input chain with the target sequences included in the databases. The most similar target is selected given that its similarity quantified with the *e*-value is better than a user-defined cutoff; default *e*-value cutoff equals 0.001. The resulting web page displays the alignment of the query and target proteins and the summary of results for the aligned target protein; the format of the summary is the same as for the query based on the protein ID.

(a)

Protein Targets for Mercaptopurine(PM6)

More information about Mercaptopurine(PM6) could be found at
PDB: http://www.rcsb.org/pdb/ligand/ligandsummary.do?hetid=PM6
DrugBank: http://www.drugbank.ca/drugs/DB01033

The table lists all proteins from the structural human-like proteome that are sorted by the ILbind binding propensity.
For each protein target, the table includes annotations of known binding events from BindingDB, DrugBank, and PDB, and binding predicted by ILbind, SMAP, and eFindSite.
Click protein name to obtain results per selected protein target.

PDB ID	Protein Name {Synonym}	Organism	Sequence File	Structure File	Type of Annotation	Source Database	Sequence Similarity to Known Target [%]	Binding Prediction Score (Unlikely|Possibly|Likely to bind)		
								ILbind binding propensity	SMAP raw score	eFindSite confidence score
2E1Q_A	XANTHINE DEHYDROGENASE/OXIDASE {XANTHINE DEHYDROGENASE; XD; XANTHINE OXIDASE; XO; XANTHINE OXIDOREDUCTASE}	HOMO SAPIENS	Click to Open	Click to Open	Known to Bind	DrugBank	99.9	0.91	123.33	0.28
1WYG_A	XANTHINE DEHYDROGENASE/OXIDASE	RATTUS NORVEGICUS	Click to Open	Click to Open	Known to Bind	DrugBank	90.3	0.91	122.16	0.28
2E3T_A	XANTHINE DEHYDROGENASE/OXIDASE	RATTUS NORVEGICUS	Click to Open	Click to Open	Known to Bind	DrugBank	90.5	0.91	122.34	0.29
3AN1_A	XANTHINE DEHYDROGENASE/OXIDASE {XANTHINE DEHYDROGENASE; XD; XANTHINE OXIDASE; XO; XANTHINE OXIDOREDUCTASE}	RATTUS NORVEGICUS	Click to Open	Click to Open	Known to Bind	DrugBank	90.5	0.91	115.70	0.28
2BZG_A	THIOPURINE S-METHYLTRANSFERASE {THIOPURINE METHYLTRANSFERASE}	HOMO SAPIENS	Click to Open	Click to Open	Known to Bind	DrugBank	100	0.87	135.84	0.41
3TMI_A	ATP-DEPENDENT RNA HELICASE DDX58 {RIG-I; DEAD BOX PROTEIN 58; RETINOIC ACID-INDUCIBLE GENE I PROTEIN}	HOMO SAPIENS	Click to Open	Click to Open	Predicted to Bind			0.77	47.56	
3HHM_A	PHOSPHATIDYLINOSITOL-4;5-BISPHOSPHATE 3-KINASE CATALYTIC SUBUNIT ALPHA ISOFORM {PI3-KINASE P110 SUBUNIT ALPHA; PTDINS-3-KINASE P110; PI3K}	HOMO SAPIENS	Click to Open	Click to Open	Predicted to Bind			0.76	45.65	
3HNC_A	RIBONUCLEOSIDE-DIPHOSPHATE REDUCTASE LARGE SUBUNIT {RIBONUCLEOSIDE-DIPHOSPHATE REDUCTASE SUBUNIT M1; RIBONUCLEOTIDE REDUCTASE LARGE SUBUNIT}	HOMO SAPIENS	Click to Open	Click to Open	Predicted to Bind			0.75	42.31	
3TLM_A	SARCOPLASMIC/ENDOPLASMIC RETICULUM CALCIUM ATPASE 1 {SERCA1; SR CA(2+)-ATPASE 1; CALCIUM PUMP 1; CALCIUM- TRANSPORTING ATPASE SARCOPLASMIC RETICULUM TYPE; FAST TWITCH SKELETAL MUSCLE ISOFORM; ENDOPLASMIC RETICULUM CLASS 1/2 CA(2+) ATPASE}	BOS TAURUS	Click to Open	Click to Open	Predicted to Bind			0.75	41.52	
1HK3_A	SERUM ALBUMIN	HOMO SAPIENS	Click to Open	Click to Open	No Interaction			0.75	45.26	

(b)

Results for MINERALOCORTICOID RECEPTOR {MR}

The structure of MINERALOCORTICOID RECEPTOR {MR} is identified as **2OAX** (chain A) in PDB.

2OAX shares 99.6% similarity with **B0ZBF6** in UniProt.

The protein sequence file could be downloaded **HERE**.

The protein structure file could be downloaded **HERE**.

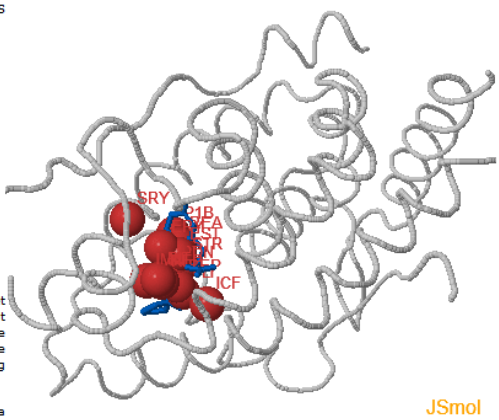

The panel on the right shows structure of the protein target (using gray trace of the backbone), position of ligands that are in complex with this protein (using blue sticks; they are included in the structure file), and the predicted center of the drug molecule (using red balls) as summarized in the 'Binding to drugs' table.

The structure is editable, it can be rotated and zoomed with a mouse.

Binding to drugs

Drug ID	Drug Name	Annotated as Known Target		Predicted as Target (Unlikely|Possibly|Likely to bind)			Predicted Coordinates of the Center of the Drug Molecule [X;Y;Z]	Binding Summary	
		Type of interaction	Source database	ILbind binding propensity	SMAP raw score	eFindSite confidence score		Known target?	# methods predicting the protein as target
PDN	Prednisone	In Complex	PDB	0.87	295.63	0.49	-20.745;59.983;4.164	Yes	2
STR	Progesterone	In Complex	PDB	0.87	297.88	0.4	-19.437;59.756;3.684	Yes	2
EST	Estradiol	Known to Bind	BindingDB	0.86	132.57	0.47	-18.900;59.988;5.307	Yes	2
RIT	Ritonavir	Known to Bind	BindingDB	0.7	62.28		-22.241;59.420;8.579	Yes	1
IMN	Indomethacin			0.82	78.04	0.81	-19.86;67.169;10.877	No	3
RFP	Rifampin			0.81	92.85	0.92	-21.901;59.351;6.597	No	3
REA	Tretinoin			0.82	77.53	0.43	-17.837;61.083;3.980	No	2

Figure 6. Results of queries against the PDID database. Panel a shows results for a query for mercaptopurine. Detailed description of this webpage is given at http://biomine.cs.vcu.edu/servers/PDID/help.html#drug_page. Panel b gives results form a query for mineralocorticoid receptor protein. Detailed explanations of this page are available at http://biomine.cs.vcu.edu/servers/PDID/help.html#prot_page. The "?" icon opens the corresponding help page.

3.5 Conclusions

PDID provides access to all putative targets (between 4444 and 7184, depending on the prediction method used) of several dozens of popular drugs. These data are based on close to 1.1 million of all-atom predictions over the entire structural human proteome (10 thousand structures for over 3700 proteins). Our database offers four unique features:

1) It incorporates accurate predictions generated by three representative protein structure-based methods.
2) It provides predictions for a comprehensively defined structural human proteome. We borrow structures of similar proteins from other organisms and cluster similar proteins to reduce redundancy.
3) It includes molecular level information on localization of the putative position of the center of drugs in the structures of the corresponding protein targets.
4) It includes comprehensive annotations of known drug targets that are linked to their sources: DrugBank, BindingDB, and PDB.

Numerous drugs are highly promiscuous and we do not know many of their targets. PDID addresses this issue by providing access to a complete set of putative DPIs and a set of known DPIs in the structural human proteome. Our database includes data that otherwise would be accessible only to individuals and research groups with significant computational expertise and resources. The putative interactions were generated by three accurate predictors that were shown to produce results that have previously led to finding new drug targets [16, 30, 31, 141-144]. PDID complements the existing BioDrugScreen database that relies on docking. The database integrates annotations of known protein targets collected across DrugBank, BindingDB, and PDB. It also

links proteins to the corresponding records in UniProt and provides coordinates of the location of binding sites in the structures of the putative drug targets.

PDID can be used to systematically catalog DPIs and to facilitate various studies related to polypharmacology of drugs [160], such as explaining side-effects caused by interactions with off-targets and for the drug repurposing. Relevant recent examples include the use of predictions with ILbind to find three novel off-targets of cyclosporine A that explain nephrotoxicity associated with the use of this immunosuppressant [16]. Another example involves repurposing of raloxifene, which is used for prevention and treatment of osteoporosis, as a potential compound to treat *Pseudomonas aeruginosa* infections based on predictions with the SMAP method [144].

However, as discussed in section 2.4, the protein structure-based approaches cover only a relatively small part the entire human proteome. This is due to the fact that most proteins do not have structures. A perhaps extreme example of that are GPCRs, a big family of drug targets composed of mostly membrane proteins, which almost entirely lack structures [161, 162]. This motivates us to investigate the other category of methods for the prediction of DPIs – the similarity-based predictions which do not rely on the knowledge of protein structures.

Chapter 4 Review of the similarity-based predictions of drug-protein interactions

In this chapter, we investigate the current similarity-based methods for the prediction of DPIs. Starting from several recent reviews and a series of selected predictors, we distill the main types of similarities that are used to predict DPIs and categorize the available predictors according to the type(s) of similarities they use and whether they combine these similarities together. We qualitatively compare these approaches in the context of their methodological underpinnings, data that they cover, and how they were assessed. We also analyze their advantages and drawbacks and make a note of missing aspects related to how they were evaluated in the past.

4.1 Overview of recent surveys

A total of 11 surveys that were written in the last five years have focused on the similarity-based methods [21, 32, 89-97]. We also note two other articles that focus on related topics including biological profiles [163] and machine learning tools [164] that are employed in DPI predictions. The 11 surveys summarize relevant databases, review representative methods, and discuss common criteria that are used to evaluate predictive performance. Table 3 assesses scope of these articles with the number of methods they reviewed, coverage of recent predictors,

inclusion of summary of databases used by the considered predictors, and presence of empirical assessment and analysis of sensitivity of predictive quality. The two most comprehensive surveys cover 28 [96] and 27 predictors [90] while the remaining nine articles discuss fewer than 20 methods. In most cases, over half of the methods that were reviewed was published in the past five years. This reflects growing interest in the similarity-based predictors. However, at least eight methods that were published in 2016 and 2017 [165-172] were not included in any of these articles. While most of the surveys provide a brief discussion of the available DPI databases, these are not necessarily the databases that are used by specific predictors to compute the similarity values. In fact, only one article provides a more complete discussion that introduces specific databases which are utilized by a small set of ten predictors that this survey covers [32]. A complete summary of the DPI databases that covers modern methods is still missing, which is why we discuss this topic. We survey 35 predictors and investigate two types of relevant databases: internal databases which are intrinsic to the predictors and source databases that are used to derive the internal databases. Moreover, only four surveys provide empirical assessment of predictive performance of similarity-based DPI predictors [32, 89, 96, 97]. While they provide quantitative and comparative analysis, they focus on a limited set of approaches. In particular, they only consider certain types and combinations of similarities. They also do not perform sensitivity analysis, i.e., they do not analyze whether and how predictive performance changes with intrinsic and extrinsic characteristics of the considered predictors. To summarize, while the previous surveys offer useful insights they also have several drawbacks. In particular, they miss several recent similarity-based DPI predictors, provide shallow treatment of databases used by these predictors, offer incomplete empirical analysis, and do not include sensitivity analysis.

Table 3. Overview of surveys of the similarity-based methods for the DPI prediction. The surveys are sorted chronologically according to their publication year. The check symbol indicates that a given measure (column) is included in a given survey (row) while a blank cell means absence of a given measure. The last row corresponds to this review.

Survey	Year	Number of predictors reviewed	Number of recent predictors reviewed (published since 2013)	Summary of source and internal databases that each predictor uses	Empirical assessment of predictive performance	Comparative analysis of predictors that use different numbers and types of similarities	Sensitivity analysis
Ding et al. [32]	2013	10	2	√	√		
Pahikkala et al. [89]	2014	2	1		√		
Mousavian et al. [90]	2014	27	16				
Chen et al. [21]	2015	17	10				
Cichonska et al. [91]	2015	17	9				
Lavecchia et al. [92]	2016	11	9				
Hart et al. [93]	2016	8	6				
Shahreza et al. [94]	2017	17	8				
Fang et al. [95]	2017	10	5				
Ezzat et al. [96]	2018	28	17		√		
Hao et al. [97]	2018	12	9		√		
This dissertation	2018	35	22	√	√	√	√

In this dissertation, we focus on a comprehensive set of 35 similarity-based DPI predictors that were published in the last decade, including the largest set of recent predictors when compared to previous surveys. The considered predictors comprise of 22 recent tools that were published in the last five years and eight latest methods that were published since 2016. This way our review includes the latest advances in the DPI predictions. We define the three main types of similarities that these 35 methods use to predict compound-protein interactions, describe key architectural details of these tools and comment on their impact. We also offer in-depth summary of the internal and source databases that these predictors use and discuss how these databases are linked. Moreover, under the third goal we also combine multiple sources databases to build a novel benchmark dataset that we use to perform comprehensive empirical evaluation. The empirical evaluation that we perform as part of the third goal (details are given in Chapter 5) encompasses representative approaches that rely on each of three main types of drug and protein similarities and ensemble predictors that combine two and three types of similarities. Besides providing the overall

predictive performance of the considered predictors, we are the first to consider predictive quality across individual drugs. Finally, our first-of-its-kind sensitivity analysis investigates whether and how the predictive performance depends on several intrinsic and extrinsic factors, e.g., the number of targets that are a priori known for a given drug.

The chapter starts with the selection of representative similarity-based predictors. We provide discussion of their source databases to build up the background to survey the selected predictors. These databases include native DPIs that are used to implement predictions by the similarity-based predictors. We summarize their timeline, impact, data contents, and overlap. Next, we investigate the timeline, impact, and availability of the 35 selected predictors. Moreover, we compare the contents of their internal databases and review the types of similarities that they utilize. After that, we provide a timeline that links the chronological record of source databases with the emergence of the 35 predictors. We also analyze how different types of similarities were used and combined over time to develop these methods.

4.2 Selection and overview of similarity-based DPI predictors

To cover a complete landscape of top-tier similarity-based predictors of DPIs, we collected corresponding articles that were published in high-impact venues. We searched the PubMed repository [173] in April 2018 for relevant articles using the following query: (predict* [Title/Abstract] AND ("drug target interaction" [Title/Abstract] OR "drug protein interaction" [Title/Abstract])). The query generated 170 possibly germane articles. We manually processed these results to select articles that describe similarity-based predictors that were published in reputable journals, i.e., journals with impact factor > 3.5. We collected the impact factors from the latest Journal Citation Reports that was released by Clarivate Analytics (formerly Thomson

Reuters) on June 14, 2017 [174]. This version of JCR is based on the citation data in 2016 and reveals the scientific impact of a JCR-indexed journal by quantifying the ratio between the number of 2016 citations to the articles published in this journal in 2014-2015 and the number of articles published in this journal in 2014-2015. The resulting 35 similarity-based DPI predictors are included in this review [165-172, 175-201]. This list is longer than the lists covered in the prior surveys which also include methods published in conference proceedings, lower impact factor journals as well as methods that target ligand/chemical-protein interactions besides DPIs.

The similarity-based predictors of DPIs are implemented based on the assertions that similar drugs may share the same protein targets and that similar proteins may interact with the same drugs. To identify putative interaction between a given drug and protein, a predictive model typically searches its internal database for drugs that are similar to the given drug and their known targets that are similar to the given target protein. Therefore, the core aspect that defines these predictions is how to measure the drug-drug and protein-protein similarities. Analysis of the 35 similarity-based DPI predictors reveals that the similarities are typically quantified using information about the chemical structures of drugs, side-effect profiles of drugs, and sequences of their protein targets. In other words, the predictors rely on three main types of similarities: chemical similarity of drugs (DCS), drug profile similarity (DPS), and protein sequence similarity (PSS). Some predictors employ one type of similarity to infer putative DPIs. Other methods combine multiple types of similarities motivated by an assumption that this may improve predictive quality when compared to using just a single type of similarity.

The similarity-based predictive methods are composed of two components: an internal database of known DPIs and a predictive model. Prediction of DPIs is performed in three steps. First, a user provides inputs in the form of drug structure, drug profile, and/or protein sequence(s)

of known target(s) for an input drug, whatever is necessary for the selected similarity-based approach. In the second step, similarities between the input drug structure (profile) and the structures (profiles) of the drugs in the internal database are computed. If target(s) of the query drug are known or can be collected from the internal database (the query drug is already included in the database), then similarity between the known target of the query drug and all proteins targets in the database is also quantified. In the third step, the predictive model combines the similarities to produce a propensity which quantifies likelihood that the query drug interacts with relevant protein targets which are included in the internal database.

The architectures of these predictive models are designed and tuned for their corresponding internal databases. Thus, data quality of the internal database largely determines the predictive performance of similarity-based DPI predictors. The internal databases typically consist of a set of native DPIs that are aggregated and collated from multiple source databases which store curated annotations of DPIs. Next, we review the source databases that are used to derive the internal databases of the 35 selected methods.

4.3 Source databases

We investigate the 35 predictors to come up with a list of all source databases that they use to derive the corresponding internal databases. In total, we found 12 publicly accessible source databases that these methods utilize. They include, in chronological order of publication: PDSP Ki [202], BRENDA [203-211], BindingDB [108-112], TTD [43, 103-107], KEGG BRITE [212-218], DrugBank [98-102], GLIDA [219, 220], KEGG DRUG [212-218], SuperTarget [117, 118], Matador [117], STITCH [123-127], and ChEMBL [113-116]. One of the selected predictors, SEA (Similarity Ensemble Approach) [175, 221], utilizes a collection of drugs and associated targets

from a commercial MDL Drug Data Report (MDDR) [222, 223]. This database is not available publicly and thus it is excluded from our analysis. Next, we summarize the contents, timeline, impact, and relationships between these 12 publicly available source databases.

4.3.1 Timeline and impact

Besides storing the data and providing facilities to conveniently query and access the data, databases must be maintained and regularly updated. They also should be periodically disseminated to inform the users about their contents and the available features. One way to measure the impact of these databases is to tally the citation counts for the scientific articles that introduce these databases and their updated versions.

Table 4. Timeline and impact of the source databases of drug-protein interactions. The source databases were used to derive the internal databases of the 35 selected similarity-based predictors. The timeline is a chronological summary of publications and releases for these source databases. The impact measures citation counts for the publications of databases. This table is sorted chronologically according to the date of the first publication. The data of this table was collected on April 1, 2018.

Source database	Date of the first publication[1]	Date of the first release[2]	Date of the latest publication[3]	Date of the latest release[4]	Date of the first predictor[5]	All citations[6]	Annual citations[7]
PDSP Ki [202]	8/1/2000	11/1/1999	N/A	4/1/2018	7/11/2008	231	13
BRENDA [203-211]	10/1/2000	10/1/2000	10/19/2016	1/1/2018	7/1/2008	2557	146
BindingDB [108-112]	12/1/2001	11/1/2000	10/19/2015	4/1/2018	3/4/2016	1398	86
TTD [43, 103-107]	1/1/2002	1/1/2002	11/13/2017	10/4/2017	3/25/2013	961	59
KEGG BRITE [212-218]	1/1/2006	4/1/2005	11/29/2016	4/1/2018	7/1/2008	*13974	*1140
DrugBank [98-102]	1/1/2006	1/1/2006	11/8/2017	4/2/2018	7/1/2008	5822	475
GLIDA [219, 220]	1/1/2006	1/1/2006	11/5/2007	10/10/2010	3/1/2011	194	16
KEGG DRUG [212-218]	1/1/2006	7/1/2005	11/29/2016	3/29/2018	9/3/2012	*13974	*1140
SuperTarget [117, 118]	10/16/2007	10/16/2007	11/8/2011	11/8/2011	7/1/2008	410	39
Matador [117]	10/16/2007	10/16/2007	N/A	10/16/2007	7/11/2008	316	30
STITCH [123-127]	12/15/2007	8/9/2007	11/20/2015	6/30/2016	6/10/2015	1068	104
ChEMBL [113-116]	9/23/2011	10/27/2009	11/28/2016	5/1/2017	7/8/2013	2434	373

[1] The date when a given source database was originally published in a scientific article. It corresponds to the publication date of early access, if available. Otherwise, the date of the journal issue where the first publication appeared is used.
[2] The date when a given database was first made available, which typically is before the database was originally published. We collect these dates from the release notes or time stamps recorded on the database websites, if available, and we use the date of the first publication, otherwise.
[3] The date of the most recent republished article that introduced an updated version of a given database after the database was originally published.
[4] The date of the most recent release of a given database, which typically is after the latest republishing.
[5] The date when a given source database was first to be utilized to derive the internal database of a predictor.
[6] The "All citations" column is the total number of citations that include citations to the first publication and all republished articles for a given source database. The citation counts were collected from Google Scholar.
[7] The "Annual citations" column is the average citation counts per one calendar year (365 days) over the period from the first publication date until April 1, 2018, rounded to the nearest integer.
* KEGG BRITE and KEGG DRUG are a part of the Kyoto Encyclopedia of Genes and Genomes (KEGG) project. They were published together with the KEGG database and all of its affiliated databases. The citation data for these two databases include the citations to the entire KEGG database, and they cannot be distributed to each affiliated database of KEGG. These counts are relatively high because they reflect the citations to all 23 databases affiliated with KEGG by now.

Table 4 provides a summary of the 12 source databases. It includes information about publications that introduce the original and the updated versions of these databases as well as the corresponding citation data. The source databases are sorted chronologically according to the date of their first publication. Specifically, we use the date of the early access online publication when it was available. Otherwise, we use the date of the journal issue in which the first publication has appeared. Apart from the date of the first publication, we also list the date when the database was first made available, which typically is before the database was published. We collect these first release dates from the release notes or time stamps recorded on the database websites, if available,

and we use the first publication date otherwise. In this chronological order, the four earliest source databases debuted between August 2000 and January 2002. The next seven databases were published several years later, between 2006 and 2007. The last source database was published in 2011. Eleven out of the twelve sources were published within about one year after their first public release. The one exception, the ChEMBL database was first published two years after its initial release. ChEMBL was originally a commercial database called StARlite that was launched before 2005, acquired by EMBL-EBI in 2008, released to the public in 2009, and finally published in 2011 [224-226]. Given that all these databases were originally released by 2007 or built based on an earlier database, the data stored in these 12 source databases are being accumulated for at least ten years.

Most of the source databases have been regularly updated and republished. Besides just the addition of new data, these updates typically include new features and improved user interface. We list the publication date of the latest republished article and the most recent release date for each source database as of April 1, 2018. These two dates together with the first release and the first publication dates provide interesting insights into the progress of the database development. Considering the latest republishing and release dates, GLIDA, SuperTarget, and Matador have not been republished or updated in the last six years. This suggests that they are no longer actively maintained. The PDSP Ki database is actively and frequently updated, but it has never been republished since it was originally published 17 years ago. Meanwhile, the other eight source databases are being updated and republished regularly. Frequent dissemination informs the users about new contents and features and also may help to attract additional users. In general, these frequently updated sources are relatively more mature since they gradually accumulate DPIs, include more recent data, and typically offer a more refined interface and a longer list of features.

Another relevant aspect is to mark when the source databases were de facto used to build the similarity-based predictors of DPIs. Thus, Table 4 shows the date when the earliest predictor has utilized a given source database to derive its internal database of known DPIs. The list of the source databases that were first used to develop the predictors includes PDSP Ki, BRENDA, KEGG BRITE, DrugBank, SuperTarget, and Matador. The earlier adoption of these source databases reflects to a certain degree their popularity and impact. Moreover, these source databases were also used for other purposes including protein structure-based prediction of DPIs [78, 227, 228] and development of various cheminformatics and bioinformatics methods and datasets [229-233].

Table 4 summarizes citations for the 12 source databases. The citations are one way to quantify the impact of these resources. The citation counts were collected from Google Scholar (http://scholar.google.com/) on April 1, 2018. We list the total number of citations that include citations to the first publication and all subsequent publications of a given database. Every source database has received at least about two hundred citations. BRENDA, BindingDB, DrugBank, ChEMBL, KEGG BRITE, KEGG DRUG, and STITCH have accumulated over one thousand citations. A notable exception is the KEGG BRITE and KEGG DRUG databases, which are part of the Kyoto Encyclopedia of Genes and Genomes (KEGG) project since 2005. They were published together with the KEGG database and all of its other affiliated databases in 2006 [212]. Currently, KEGG includes 23 individual databases including, for example, KEGG PATHWAY that provides pathway maps of molecular interaction, reaction and relation networks. The citation data for KEGG BRITE and KEGG DRUG includes the citations to the entire KEGG database; these citations cannot be attributed to individual KEGG resources. The citation counts to KEGG BRITE and KEGG DRUG are so high because they reflect the citations to all 23 databases affiliated with KEGG.

An arguably more robust measure to quantify impact are the annual citation counts. The annual counts are defined as the average citation frequency per one calendar year (365 days) computed over the period from the date of the first publication until the date when we acquired the citation data (April 1, 2018). These counts accommodate for the differences in the age of the source databases. PDSP Ki, GLIDA, SuperTarget, and Matador received moderate (<50) numbers of annual citations. These relatively low citation counts could be a result of a lack of effort to update GLIDA, SuperTarget, and Matador which were last updated in 2011 or earlier. PDSP Ki is frequently updated but it was last published in 2000. On the other hand, BRENDA, BindingDB, TTD, and STITCH have received relatively high (50-150) annual citations. This is likely because these are mature resources that have ten years of history of regular republishing and updates. Noticeably, DrugBank and ChEMBL attract over 300 citations per year. They were also regularly updated and republished. Their success can be attributed to the high-quality of their data contents, a broad range of functional features, and a user-friendly web interface. Next, we review the data contents for the 12 source databases.

4.3.2 Data contents

Typically, multiple source databases are used to derive an internal database of a given predictor. They are used as a source for information about drugs, their protein targets, and native DPIs. Table 5 summarizes information about the number of relevant drugs or drug-like compounds that are known to interact with protein targets, the number of these targets, and the number of annotated drug- and compound-protein interactions for the 12 source databases. These data were collected from the latest release of each database on April 1, 2018. We captured the numbers from the release notes or statistics page if they were available. Otherwise, we tallied the numbers from

the data dumps. BRENDA, a database dedicated to enzyme functions, does not provide specific statistics and data downloads. Thus, we could not calculate the quantities for this database.

Table 5. Data contents of the source databases of drug-protein interactions. These source databases were used to derive the internal databases of the 35 selected similarity-based predictors. The data of this table correspond to the latest release of each database as of April 2018. The numerical data were captured from the release notes or statistics page if they were available. Otherwise, we counted the numbers from the data dumps of each database.

Type	Database	Abbr.[1]	Drugs[2]	Proteins[3]	DPIs[4]	DPIs/drug[5]	URL
Drug	Matador	MA	801	2,901	15,843	19.8	http://matador.embl.de
	KEGG BRITE	KB	5,045	1,061	14,222	2.8	http://www.genome.jp/kegg/brite.html
	KEGG DRUG	KD	5,045	1,061	14,222	2.8	http://www.genome.jp/kegg/drug/
	DrugBank	DR	10,562	5,020	23,380	2.2	http://www.drugbank.ca
	PDSP Ki	PK	11,569	1,673	63,619	5.5	http://kidbdev.med.unc.edu/databases/kidb.php
	TTD	TT	23,486	3,036	33,467	1.4	http://bidd.nus.edu.sg/BIDD-Databases/TTD/TTD.asp
Bioactive compound	GLIDA	GL	23,214	410	30,410	1.3	http://pharminfo.pharm.kyoto-u.ac.jp/services/glida/
	STITCH	ST	*156,686	*3,908,233	*148,826,348	*949.8	http://stitch.embl.de
	SuperTarget	SU	195,770	6,219	332,828	1.7	http://bioinformatics.charite.de/supertarget/
	BindingDB	BI	644,978	7,042	1,439,799	2.2	http://www.bindingdb.org/bind/index.jsp
	ChEMBL	CH	2,101,843	11,538	14,675,320	7.0	http://www.ebi.ac.uk/chembl/
	BRENDA	BR	Unavailable	Unavailable	Unavailable	Unavailable	http://www.brenda-enzymes.org/index.php

[1] Abbreviated name of a given source database. The abbreviations are used to denote the source databases of predictors in Table 8.
[2] The number of drugs and drug-like compounds that are known to interact with protein targets in a given source database.
[3] The number of proteins that are targeted by drugs and drug-like compounds in a given source database.
[4] The "DPIs" column is the number of known DPIs that are stored in a given database.
[5] The "DPIs/drug" column is the average number of DPIs per drug, which is calculated by dividing the "DPIs" column to the "Drugs" column for a given database. Unavailable means that these numbers are missing because BRENDA does not provide specific statistics and downloads for the entire collection of DPIs that it store.
* The numerical data for the STITCH database includes both direct and indirect DPIs, while data for other databases include only the direct interactions. The indirect interactions are based on effects of signaling pathways where effects of drugs are propagated onto proteins that interact with other proteins that directly interact with these drugs. The indirect interactions in this database cannot be separated from the direct interactions, and thus the corresponding numbers are higher than expected.

Table 5 categorizes the source databases into two types depending on if they are dedicated to drugs or a more generic set of bioactive compounds. The first type of six databases including PDSP Ki, TTD, DrugBank, Matador, KEGG BRITE, and KEGG DRUG focus on approved, under a clinical trial, and experimental drugs. The other six source databases include both drugs and other bioactive compounds that typically are small molecules with drug-like properties. Consequently, the first type of databases has fewer compounds, between 8 hundred and 23 thousand, compared to the second group that includes between 23 thousand and over 2 million compounds. Table 5 is sorted by the number of compounds within each of the two categories. Except for BRENDA for which data are not available and GLIDA that is dedicated solely to the G protein-coupled receptors

(GPCR), the bioactive compound-centric databases have more DPIs and protein targets than the drug-centric databases. Specifically, the six smaller databases include between 15 and 60 thousand interactions, compared to the group of larger sources that features up to 148 million interactions. The largest compound repository, ChEMBL, stores a comprehensive set of two million bioactive compounds. This number is 90 times higher than the total number of the drugs in the largest repository that focuses exclusively on drugs, TTD. Unsurprisingly, the number of compound-protein interactions in ChEMBL is 440 times larger than the number of DPIs in TTD.

The main focus of these databases is typically on the human protein targets. The druggable human proteome, which is defined as all human proteins that interact with current drugs, is estimated to comprise of between 1000 and 3000 proteins [1, 18-20]. The numbers of protein targets in the source databases typically vary between about 1000 and 12,000, with a median value of 3036. Half of these databases are larger than the druggable proteome because they cover proteins from other organisms. For example, BindingDB contains targets from over 400 organisms. There are two exceptions that include GLIDA and STITCH. The GLIDA database focuses on the GPCRs, and thus, it is limited to the corresponding 410 GPCR proteins. STITCH covers over nine million proteins from 2031 organisms, which include a substantial number of putative and low-quality annotations of targets. We excluded these predicted and low-confidence interactions (using their confidence score < 0.7) when calculating the numbers for Table 5. This resulted in a set of about 4 million targets and 149 million interactions. The reason why this database is so large is that STITCH includes both direct and indirect DPIs, while data in the other databases include only the direct interactions. The indirect interactions are derived based on signaling pathways where effects of drugs are propagated onto downstream proteins.

In each of the 12 source databases, the number of DPIs is greater than the number of drugs. This is a result of promiscuity of drugs that typically interact with multiple targets. The field of polypharmacology [234-236] and efforts in drug repurposing [7, 8, 10] depend on this promiscuity. However, drug promiscuity may also lead to undesired side-effects and unintended toxicities [12, 15, 16]. We measure the drug promiscuity in these source databases by calculating the average number of DPIs per drug (see DPIs/drug in Table 5). The median degrees of drug promiscuity for the 12 source databases is 2.8, which is close to the promiscuity measured using assays that ranges between 2.6 and 3.4 [237]. Ten databases have between 1.3 and 19.8 DPIs per drug. The STITCH database is again an exception. It includes a relatively dense mapping between proteins and drugs due to the inclusion of a considerable number of indirect interactions. The drug promiscuity has inspired the development of the similarity-based predictive models, where the similarity between targets is used to predict DPIs. It also provides an opportunity to use the currently known targets of a given drug to build models that predict other targets of the same drug.

Besides the interactions, these source databases also encompass rich annotations of the structures, functions, and properties of the drugs and targets, together with the corresponding references. For example, DrugBank provides over 200 such annotations. The native DPIs and the additional knowledge are accessible through the web interfaces of these sources. The corresponding URLs for the 12 source databases are listed in Table 5.

4.3.3 Relationships between source databases

Each of the 12 source databases includes a different collection of DPIs. However, these source databases also overlap with each other. This is because different source databases collect the interactions from some of the same sources, and because some of them also directly import annotations from the other source database. Table 6 summarizes inputs that are used to derive data

stored in a given source database. The inputs include data coming from the 12 source databases, directly from literature, and from other resources. The first 12 inputs in the table indicate whether a given source database directly imports DPIs from another source databases. Seven source databases draw DPIs from between one and nine (for STITCH) other source databases. Moreover, some of the inputs are more popular than the others. Six of the nine input databases provide data for at least three source databases. For example, TTD is used as an input to four source databases including DrugBank, SuperTarget, Matador, and STITCH, compared to BRENDA, SuperTarget, and STITCH that are never used as inputs. The direct inclusion of source databases as inputs results in a substantial overlap between databases. For example, Matador shares a substantial overlap with SuperTarget since they both draw data from the same four source databases while SuperTarget also imports data from one more source. Interestingly, ChEMBL and BindingDB exchange data reciprocally. BindingDB obtains data on compound-protein binding affinities from ChEMBL and exports binding data that were extracted from patents to ChEMBL. Noticeably, STITCH includes the interactions taken from nine other source databases, which explains why Table 5 shows that it hosts the largest collection of interactions. Only the BRENDA database neither imports interactions directly from other source databases nor is used as an input.

Table 6. Relationships between source databases. Each row lists a source database, and each column specifies an input where the data of a given source database come from. The inputs include data coming from other source databases, literature, and other types of inputs. The "Literature" column denotes that the data are manually curated from scientific articles, patents, and annual reports of pharmaceutical companies. The "Other inputs" column includes predictions, experimental data, and other databases that are not named in the table. "x" indicates that a given source database draws data from a given input.

	Inputs													
Source database	**PDSP Ki**	**BRENDA**	**BindingDB**	**TTD**	**KEGG BRITE**	**DrugBank**	**GLIDA**	**KEGG DRUG**	**SuperTarget**	**Matador**	**STITCH**	**ChEMBL**	**Literature**	**Other inputs**
PDSP Ki													x	x
BRENDA													x	x
BindingDB	x											x	x	x
TTD													x	x
KEGG BRITE													x	x
DrugBank				x									x	x
GLIDA	x					x							x	x
KEGG DRUG													x	x
SuperTarget			x	x	x	x		x					x	x
Matador				x	x	x		x					x	x
STITCH	x		x	x	x	x	x	x		x		x	x	x
ChEMBL			x										x	x

Moreover, we list two additional types of inputs: literature and other inputs. The literature includes scientific articles, patents, and annual reports of pharmaceutical companies. The other inputs incorporate predictions, experimental data, and other input databases that exclude the 12 source databases. Table 6 shows that all 12 source databases include data coming directly from the literature. This is yet another factor that contributes to the overlap in the contents of the 12 source databases. The data coming from the literature typically includes information about experiments and assays that were used to validate bioactivity and measure affinities of interactions. This information provides context for the interactions. Every source database also acquires data from other inputs that include predictions, other databases such as the Comparative Toxicogenomics Database [238] and PubChem BioAssay [239], and experimental data that were not stored in a dedicated database, such as the data from Refs. [240, 241].

Our analysis reveals that each of the 12 source databases overlaps with at least one other source database. Table 6 qualitatively summarizes this overlap. A quantitative estimate would be extremely challenging. This is because these databases lack a uniform definition of drugs and targets and a consistent way to name and identify compounds and biomolecules. Even if the same literature is used to extract DPIs the resulting data could be different. For example, when the interaction is annotated at the gene level, the same gene could be mapped to different proteins and different types of protein identifiers, depending on which software and databases were used to perform the mapping. The assignments of information from literature to a precisely and uniquely defined set of drugs and protein targets is still an open challenge [44]. The bottom line that that different databases adopt different nomenclatures and identifiers to represent the drugs and proteins, which makes it virtually impossible to quantify the degree of overlap between the 12 databases. A few works have analyzed the overlap of drugs and targets for a small subset of these source databases [23, 177]. A study over a set of 502 approved drugs shows that 49% and 20% of the DPIs in DrugBank were included in Matador and PDSP Ki, respectively [177]. The data that are unique to DrugBank account for only 46% of its DPIs. Moreover, PDSP Ki shares 42% of its known interactions with Matador. As concluded by another investigation, DrugBank had 52% and 21% of drugs in common with ChEMBL and TTD, respectively [23]. The 74% and 55% of the protein targets stored in DrugBank were also included in ChEMBL and TTD, respectively. Moreover, ChEMBL covered 91% and 55% of the drugs and targets that were housed in TTD, respectively. These numeric analyses support our observation about the relatively large extend of overlap and also reflect the fact that source databases have their unique data.

We show that the 12 source databases were developed using some of the same data sources and some of them even swap the data with each other. These relationships lead to a certain amount

of overlap of information that they store. However, each source database also houses its own unique data, and therefore, they should be combined together to collect the most complete set of known DPIs. This is in fact the case for 22 out of the 35 methods that we survey. They use at least two source databases to develop their internal databases. Moreover, 17 methods, including KRM [176], BLM [179], Yamanishi et al. [180], GIP [182], NBI [183], KBMF2K [184], Cao et al. [186], BLM-NII [187], DT-Hybrid [189], DINIES [191], Shi et al. [192], RLS-KF [196], NRLMF [197], DASPfind [199], PUDTI [168], DVM [169], and iDTI-ESBoost [172] have utilized at least four source databases to create their internal DPI databases.

4.3.4 Other drug-target interaction databases

Besides the 12 source databases, we discuss another 19 databases that have not been adopted to develop the selected similarity-based predictors. These databases house the drug-target interactions accompanied by other information, such as details of mechanisms of DPIs [242], unstudied/dark targets [243], interactions at the gene level [244-250], structures of protein targets [29, 35, 251, 252], information about protein-protein and drug-drug interactions [253-261], side-effects of drugs [128], and information focused on specific diseases, such as cancer [262-266]. Some databases are constrained to a particular group of drugs [267] or a specific family of proteins [268]. Next, we discuss these 19 databases in greater depth.

DrugCentral (http://drugcentral.org) is a comprehensive knowledgebase that integrates information about drug actions and pharmacological indications, which can be used to elucidate therapeutic mechanisms mediated through DPIs [242]. The Pharos database (http://pharos.nih.gov) incorporates drug action data taken from DrugCentral to define druggable levels of protein targets and define unstudied/dark protein targets. These dark targets are not yet known to be involved in small molecule activities, but they are potentially druggable [243].

Some resources aggregate biological annotations and disease-related knowledge for the druggable genome, which is defined as a collection of genes that encode druggable proteins. These resources include the PharmGKB database (http://www.pharmgkb.org) [244], DGIdb (http://dgidb.genome.wustl.edu) [245, 246], the Drug2Gene database (http://www.drug2gene.com) [247], IUPHAR/BPS GtPdb (http://www.guidetopharmacology.org) [248, 249], and Open Targets (http://www.targetvalidation.org) [250].

The next three databases rely on the 3D structures of protein targets. The PDB database (http://www.rcsb.org) provides access to an extensive collection of 3D structures of drug-protein complexes [35, 251]. The BioLip database (http://zhanglab.ccmb.med.umich.edu/BioLiP) provides access to residue-level annotations of ligand-binding sites, binding affinity data, and biological functions for a comprehensive collection of proteins that have 3D structures [252]. The PDID (http://biomine.cs.vcu.edu/servers/PDID) is a structural human genome-wide repository of putative and native DPIs that are mapped into the 3D structures of protein targets [29]. It currently stores data about over one million interactions for 51 drugs.

A typical database focuses on DPIs. However, some drugs target protein-protein interactions and targets that are relevant to the same disease or condition can be modulated by multiple drugs. Several databases address these aspects. For example, three databases that focus on the druggability of protein-protein interactions include TIMBAL (http://mordred.bioc.cam.ac.uk/timbal) [253, 254], 2P2Idb (http://2p2idb.cnrs-mrs.fr) [255-257], and iPPI-DB (http://www.ippidb.cdithem.fr) [258, 259]. On the other hand, DCDB (http://www.cls.zju.edu.cn/dcdb) is a resource that centers on the therapeutic effects of multi drug combinations [260, 261].

The IntSide database (http://intside.irbbarcelona.org) focuses on drug side-effects. This database includes data about both therapeutic and off-targets, relevant pathways, biological functions, and chemical traits of drugs [128]. This information is particularly useful to explain and understand undesired responses to drug treatments.

The CancerResource (http://data-analysis.charite.de/care) [262, 263] and canSAR (http://cansar.icr.ac.uk) [264-266] databases aim to bridge cancer research with drug discovery. These two resources provide underlying information about drug-target interactions that are relevant to cancer treatment, such as data of gene expression, mutations in cancer-related genes, drug sensitivity in cancer cell lines, and pathways of drug targets.

Finally, some resources are dedicated to a particular collection of drugs or a specific family of protein targets. For example, the WITHDRAWN database (http://cheminfo.charite.de/withdrawn) includes data on targets and pathways of drugs that were recalled from the market due to toxicity or inefficacy [267]. The GLASS database (http://zhanglab.ccmb.med.umich.edu/GLASS) is exclusively focused on the ligand-protein interactions for the G protein-coupled receptors [268]. About 33% of currently used drugs target this family of proteins [44].

The additional information that can be extracted from these databases complements the information about drug-target interactions that can be obtained from the 12 source databases. We suppose that it would be beneficial for the future similarity-based predictors of DPIs to include these databases as sources.

4.4 Similarity-based predictors

We review several key aspects of the 35 selected high-impact similarity-based DPI predictors. We classify these methods into different categories according to the types and numbers of similarities that they use. We summarize the timeline, impact, and availability of these predictors. We link their internal databases to the specific source databases that we discussed in section 4.3. We also discuss architectural details of these methods. Finally, we comment on the assessment of predictive performance that was adopted by the previous approaches.

4.4.1 Categorization of predictors

The three types of similarities can be combined to formulate an ensemble predictor with the underlining goal to improve predictive quality when compared to using single similarity. Many of the predictors proposed in recent years rely on the ensembles that include two or three similarity types. Consequently, we categorize the 35 considered predictors into three groups: the methods that apply one type of similarity (1S), ensemble models that combine two types of similarities (2S), and ensembles of all three similarities (3S); see "Type of predictor" column in Table 8 and Table 9.

4.4.2 Timeline, impact, and availability

The 35 similarity-based predictors were developed in the past decade. Table 7 lists these predictors in chronological order by their first publication dates. The first five predictors were published between 2007 and 2009. We note a steady pace of the development of methods between 2010 and 2015. Specifically, eight methods were released between 2010 and 2012, and another eight between 2013 and 2015. The pace has picked up recently and already 14 methods were

published between 2016 and the first quarter of 2018. These data reveal an increasing interest in the development of the similarity-based approaches.

Table 7. Timeline, impact, and availability of the 35 selected similarity-based DPI predictors. This table is sorted chronologically according to the date of publication. The data of this table was collected on April 1, 2018.

Predictor[1]	Date[2]	JIF[3]	Citations[4]	Annual citations[5]	Availability[6]	URL
SEA [175, 221]	2/7/2007	41.7	922	83	WS	http://sea.bkslab.org
KRM [176]	7/1/2008	7.3	446	46	None	N/A
Campillos et al. [177]	7/11/2008	37.2	892	92	None	N/A
COPICAT [178, 269]	6/5/2009	4.5	41	5	WS	http://copicat.dna.bio.keio.ac.jp
BLM [179]	7/15/2009	7.3	265	30	SS	http://members.cbio.mines-paristech.fr/~yyamanishi/bipartitelocal/
Yamanishi et al. [180]	6/1/2010	7.3	249	32	None	N/A
Yabuuchi et al. [181]	3/1/2011	9.8	102	14	None	N/A
GIP [182]	9/4/2011	7.3	195	30	SS	http://cs.ru.nl/~tvanlaarhoven/drugtarget2011/
NBI [183]	5/10/2012	4.5	339	57	None	N/A
KBMF2K [184]	6/23/2012	7.3	125	22	SS	http://github.com/mehmetgonen/kbmf/
PKR [185]	9/3/2012	7.3	71	13	None	N/A
Cao et al. [186]	9/24/2012	5.0	33	6	None	N/A
BLM-NII [187]	11/17/2012	7.3	109	20	None	N/A
Cheng et al. [188]	3/25/2013	3.8	49	10	None	N/A
DT-Hybrid [189]	5/29/2013	7.3	73	15	WS & SS	http://alpha.dmi.unict.it/dtweb/index.php
PRW & NB [190]	7/8/2013	3.8	69	15	SS	http://pubs.acs.org/doi/suppl/10.1021/ci300435j
DINIES [191]	5/16/2014	10.2	44	11	WS	http://genome.jp/tools/dinies/
Shi et al. [192]	5/6/2015	3.8	24	8	SS	http://web.hku.hk/~liym1018/projects/drug/drug.html
Liu et al. [193]	6/10/2015	7.3	24	9	None	N/A
RWR [194]	8/19/2015	4.2	11	4	None	N/A
SLP & RLS [195]	9/9/2015	4.3	6	2	SS	http://pan.baidu.com/s/1dDqDLuD
RLS-KF [196]	1/14/2016	5.0	7	3	SS	http://github.com/minghao2016/RLS-KF/
DrugMiner [165]	1/25/2016	6.4	14	6	WS	http://www.drugminer.org
NRLMF [197]	2/12/2016	4.5	34	16	SS	http://github.com/stephenliu0423/PyDTI/
SDTNBI [198]	3/4/2016	5.1	20	10	SS	http://lmmd.ecust.edu.cn/methods/sdtnbi/
DASPfind [199]	3/16/2016	4.2	14	7	WS	http://cbrc.kaust.edu.sa/daspfind/
DrugE-Rank [200]	6/11/2016	7.3	23	13	WS	http://datamining-iip.fudan.edu.cn/service/DrugE-Rank/
DBN [166]	3/6/2017	4.3	10	9	SS	http://github.com/Bjoux2/DeepDTIs_DBN/
EnsemDT/KRR [201]	5/24/2017	3.8	4	5	None	N/A
Peón et al [167]	6/19/2017	4.3	3	4	None	N/A
PUDTI [168]	8/14/2017	4.3	0	0	None	N/A
DVM [169]	9/11/2017	4.3	1	2	None	N/A
DTINet [170]	9/18/2017	12.1	4	7	SS	http://github.com/luoyunan/DTINet/
bSDTNBI [171, 270]	9/28/2017	3.8	2	4	SS	http://lmmd.ecust.edu.cn/methods/bsdtnbi/
iDTI-ESBoost [172]	12/18/2017	4.3	1	4	WS & SS	http://farshidrayhan.pythonanywhere.com/iDTI-ESBoost/

[1] The name of each predictor is either provided in relevant publications or otherwise, named using the last name of its first author.
[2] The date of early access online publication or the date of journal issue where a given predictor was originally published.
[3] The "JIF" column is the journal impact factor of the journal where a given predictor appeared. The data were collected from the 2017 Journal Citation Reports that was released by Clarivate Analytics (formerly Thomson Reuters) on June 14, 2017.
[4] The "Citations" column is the number of citations to the article(s) of a predictor, which were collected from Google Scholar.
[5] The "Annual citations" column is the average citation counts per one calendar year (365 days) over the period from the publication date until April 1, 2018, rounded to the nearest integer.
[6] The type of publicly availability of implementations, where WS stands for webserver and SS for standalone software including either compiled or source code. None means the implementation is not offered and thus the corresponding URL is not applicable (N/A).

One way to measure the impact is to consider the impact factors of venues where these methods were published. The 35 predictors were published in high-impact venues with impact factors > 3.5. Table 7 lists the impact factors for these reputable journals, which are based on the 2017 Journal Citation Reports [174]. The impact factor values for a significant majority of these methods, 33 out of 35, range between 3.8 and 12.1. Two pioneering predictors were published in 2007 and 2008 in journals with the impact factors around 40 [175, 177]. Another way to measure the scientific impact of these methods is based on the citation counts for the articles that introduce these methods. Table 7 lists the corresponding total citation counts, which were collected from the Google Scholar on April 1, 2018. The median total of citations over the 35 methods equals 33. Noticeably, the three earliest predictors [175-177] have accumulated over 400 citations each over the last decade. Their combined number of citations (2260) is greater than the combined count of citations of the remaining 32 methods (1966). These three highly cited predictors have defined and used for the first time the three types of similarities. The SEA method is based on DCS [175]. The chronologically second method, KRM, was the first to use PSS, which was combined with DCS [176]. The third method by Campillos et al. has introduced DPS and used it together with DCS to make predictions [177]. There are also three other method that secured at least 200 citations. They include BLM [179], the predictor by Yamanishi et al. [180], and NBI [183]. The low citation counts for the recent methods that were published since 2016 should be dismissed because there was not enough time yet to accumulate citations. We also analyze a more robust number of annual citations. This number is defined as the total number of citations divided by the number of years (365-day periods), measured between the date of publication and April 1, 2018. The median annual citation number equals ten. The three highest cited predictors attract over 40 citations per year. Moreover, most of the 35 considered methods enjoy high levels of annual citations (median = 10),

in many cases exceeding the corresponding journal impact factors (median = 5). This result suggests that the similarity-based DPI predictors elicit strong interest of the scientific community.

Table 7 also summarizes availability of implementations for these predictors. The authors of eight methods [165, 172, 175, 178, 189, 191, 199, 200] have developed webservers that are geared towards less computer savvy users. The webservers are convenient to use because calculations are done on the server side and consequently the end users only need an internet connection and a web browser to process predictions. Fourteen predictors [166, 170-172, 179, 182, 184, 189, 190, 192, 195-198] are available as standalone software. In this case, the end users must install and use them on their own hardware. This requires more skill and effort but it also facilitates inclusion of these methods in other computational pipelines. Two methods [172, 189] are available as both standalone software and webserver. The URLs of these 20 publicly available approaches are listed in Table 7. The other 15 methods are not available publicly.

4.4.3 Internal databases

Every similarity-based predictor is implemented based an internal database that includes known DPIs and relevant information about these drugs and proteins. The contents of internal databases are derived from the data that were collected from one or more of the 12 source databases that we reviewed in section 4.3. Table 8 lists the source databases that are used to generate the internal database of each predictor. Individual predictors utilize between one and six source databases, with a median of three. Specifically, 13 predictors collect data from a single source database, five from two or three sources, 16 from four sources, and one from six sources. The authors of KRM predictor [176] have released their internal database. This database combines DPIs collected from BRENDA (BR), KEGG BRITE (KB), DrugBank (DR), and SuperTarget (SU). This internal database was later reused by another 15 predictors that we review [168, 169, 172,

179, 180, 182-184, 186, 187, 189, 192, 196, 197, 199]. It was also used by a different set of 18 methods which we did not include in our analysis because of the relatively low impact factor of the venues where they were published [271-288]. The frequent reuse of this database explains to some extent why this predictor enjoys high citation counts in Table 7.

We observe that only up to 6 out of 12 source databases are used to develop an internal database. This is in spite of the fact that each of the 12 source databases includes data that are unique to that source, and that many other source databases are available, including the databases listed in section 4.3.4. We recommend that future predictors should rely on more comprehensive internal databases that integrate more source databases. However, this would require a significant effort to map and curate data across the sources that utilize different ways to define, name, and identify the drugs and protein targets.

Except for the 15 methods that reuse the internal database of KRM [176], the other predictors employ unique internal databases by combining data coming from different sets of source databases. Some predictors, such as NBI [183], SDTNBI [198], and DASPfind [199], use more than one internal database. In our analysis, we combine the contents of these internal databases for these three methods. Table 8 summarizes the main characteristics of the internal databases including the numbers of drugs, protein targets, DPIs, and average number of DPIs per drug. Table 8 shows that most of the internal databases cover between 276 and 7,739 drugs. Some of the internal databases also include other drug-like molecules, and correspondingly their sizes are larger and they span between 22,839 and 105,946 bioactive molecules. The number of protein targets in the internal databases ranges between 246 and 6,662. These are typically human proteins, except for nine methods that do not explicitly specify organism information of the proteins that they use (see “Focus on human proteins” column in Table 8). These numbers are comparable to an expected

scale of druggable human proteome, which is estimated to include between 1,000 and 3,000 proteins [1, 18-20]. Another important measure that quantifies coverage of the internal databases is the number of DPIs. This number varies between 1,731 and 155,208. While some databases include a large number of drugs or targets (e.g., databases for SEA, SDTNBI and EnsemDT/KRR predictors), they cover a relatively low number of DPIs per drug. The density of DPIs, which is calculated as the average number of DPIs per drug, varies widely between 1.1 and 11.5 (see "DPIs/drug" column in Table 8). Databases with low densities might be missing a substantial number of DPIs and consequently the corresponding predictors might provide inaccurate values of similarities. Moreover, higher density of interactions is likely associated with a more complete coverage of interactions for individual drugs. The corresponding internal databases can be used to provide a more reliable estimation of predictive quality at the drug level.

The medians of the main four characteristics of the internal databases over the 35 predictors are 932 drugs, 989 proteins, 5127 DPIs, and 5.1 DPIs per drug. The first three medians correspond to the frequently reused internal database of KRM predictor [176]. The corresponding medians for the latest releases of the 12 source databases in Table 5 are 23124 drugs, 3036 proteins, 33467 DPIs, and 2.8 DPIs per drug. Interestingly, the first three numbers are much higher while the last number is lower when compared to the sizes of the internal databases. This is in spite of the fact that individual predictors combine multiple source databases to derive their internal databases. One of the reasons why internal databases are relatively small is that they focus on particular collections of drugs and proteins. For example, the internal database of COPICAT [178, 269] includes only the 964 FDA-approved drugs, while its source database, DrugBank, also stores five thousand experimental drugs. The method developed by Liu et al. [193] focuses on *H. sapiens* and *C. elegans*, while its source databases also cover other organisms such as mouse and *E. coli*.

Another reason is that the internal databases are not being updated in contrast to the source databases that are frequently updated and grow in size [23]. In other words, some internal databases are based on outdated version(s) of the source database(s). For example, 16 predictors [168, 169, 172, 176, 179, 180, 182-184, 186, 187, 189, 192, 196, 197, 199], including some recent methods that were developed in 2017, utilize the same internal database [176] which has not been updated since it was published in 2008.

Although the internal databases include fewer drugs, proteins, and DPIs than the source databases, their median drug promiscuity at 5.1 DPIs per drug is 80% larger than the median promiscuity of the source databases, which equals 2.8. This increase is due to the aggregation of different DPIs for the same drugs that are coming from different source databases. The higher promiscuity suggests that the information about the interactions in the internal databases is more complete when compared to the individual source databases. This may benefit the similarity-based predictive models. For example, knowledge of a larger number of native targets would likely result in a larger set of candidate protein targets that could be explored to predict novel targets for a given drug. Also, a higher promiscuity increases the chances to identify proteins that are targeted by different drugs.

Table 8. Overview of the source and internal databases of the 35 similarity-based DPI predictors that were published in high impact venues. We group these methods into three categories: predictors using single type of similarity (1S), ensemble predictors employing two types of similarities (2S) and ensembles of three types of similarities (3S). We summarize the source databases that these predictors use to derive their internal databases. We provide information about the internal databases including number of drugs, proteins and DPIs, number of DPIs per drug, and number of data sources contained in the internal databases. We denote whether or not these methods focus on human proteins only. We also indicate whether a given predictor includes only interacting drug-protein pairs or both interacting and non-interacting pairs to evaluate predictive performance.

Type of predictor	Predictor	Year	Sources databases[1]	Number of sources	Drugs	Proteins	DPIs	DPIs/ drug	Focus on human proteins	Scope of evaluation
1S	SEA [175]	2007	MD	1	65,241	246	71,094	1.1		complete
	PRW & NB [190]	2013	CH	1	105,946	894	155,208	1.5	√	interacting
	DrugMiner [165]	2016	DR	1	1,396	1,224	4,729	3.4	√	complete
	SDTNBI [198]	2016	BI DR CH	3	22,839	1,541	57,726	2.5	√	complete
	Peón et al. [167]	2017	CH	1	745	1,427	8,535	11.5		complete
	bSDTNBI [171]	2017	BI CH	2	276	453	1,796	6.5	√	complete
2S	KRM [176]	2008	BR KB DR SU	4	932	989	5,127	5.5	√	complete
	Campillos et al. [177]	2008	PK DR MA	3	502	N/A	4,857	9.7	√	interacting
	COPICAT [178]	2009	DR	1	964	456	1,731	1.8		complete
	BLM [179]	2009	BR KB DR SU	4	932	989	5,127	5.5	√	complete
	Yabuuchi et al. [181]	2011	GL	1	866	317	5,207	6.0		complete
	GIP [182]	2011	BR KB DR SU	4	932	989	5,127	5.5	√	complete
	NBI [183]	2012	BR KB DR SU	4	5,330	4,785	17,610	3.3	√	complete
	KBMF2K [184]	2012	BR KB DR SU	4	932	989	5,127	5.5	√	complete
	Cao et al. [186]	2012	BR KB DR SU	4	932	989	5,127	5.5	√	complete
	BLM-NII [187]	2012	BR KB DR SU	4	932	989	5,127	5.5	√	complete
	Cheng et al. [188]	2013	TT DR	2	621	893	3,195	5.1		complete
	DT-Hybrid [189]	2013	BR KB DR SU	4	5,330	4,773	17,573	3.3	√	complete
	RWR [194]	2015	DR	1	684	627	2,557	3.7		complete
	SLP & RLS [195]	2015	DR	1	786	809	3,681	4.7		complete
	RLS-KF [196]	2016	BR KB DR SU	4	932	989	5,127	5.5	√	complete
	NRLMF [197]	2016	BR KB DR SU	4	932	989	5,127	5.5	√	complete
	DASPfind [199]	2016	BR KB DR SU	4	3,897	6,662	12,919	3.3	√	complete
	DrugE-Rank [200]	2016	DR	1	1,242	1,324	5,701	4.6	√	complete
	DBN [166]	2017	DR	1	1,412	1,520	6,262	4.4		complete
	EnsemDT/KRR [201]	2017	DR	1	7,739	4,902	17,483	2.3		complete
	PUDTI [168]	2017	BR KB DR SU	4	932	989	5,127	5.5	√	complete
	DVM [169]	2017	BR KB DR SU	4	932	989	5,127	5.5	√	complete
	iDTI-ESBoost [172]	2017	BR KB DR SU	4	932	989	5,127	5.5	√	complete
3S	Yamanishi et al. [180]	2010	BR KB DR SU	4	443	989	2,649	6.0	√	complete
	PKR [185]	2012	KD	1	2,423	436	6,769	2.8	√	complete
	DINIES [191]	2014	PK TT DR KD MA CH	6	678	277	1,804	2.7	√	complete
	Shi et al. [192]	2015	BR KB DR SU	4	932	989	5,127	5.5	√	complete
	Liu et al. [193]	2015	DR MA ST	3	2,486	3,356	7,369	3.0	√	complete
	DTINet [170]	2017	DR	1	708	1,512	1,923	2.7	√	complete
	This article	2018	PK TT DR CH + 15	19	449	1,469	34,456	76.7	√	complete

[1]The source databases include MDDR (MD), PDSP Ki (PK), BRENDA (BR), BindingDB (BI), TTD (TT), KEGG BRITE (KB), DrugBank (DR), GLIDA (GL), KEGG DRUG (KD), SuperTarget (SU), Matador (MA), STITCH (ST), and ChEMBL (CH). This review relies primarily on the Drug2Gene resource where the data are derived from 19 source databases: PK TT DR CH + 15 other databases: CGDCP, ChEBI, CTD, HGNC, IUPHAR, Ligand Expo, MICAD, NCBI Gene, Pathway Commons DB, PDBsum, PharmGKB, PubChem Bioassay, PubChem Compound, PubChem Substance, and UniProt.

4.4.4 Predictive models

The considered 35 predictors rely on three main types of similarities: chemical similarity (DCS), drug profile similarity (DPS), and protein sequence similarity (PSS). The three types of similarities can be combined to formulate an ensemble predictor with the underlining goal to improve predictive quality when compared to using a single similarity. Many of the predictors proposed in recent years rely on the ensembles that include two or three similarity types. Consequently, we categorize the 35 considered predictors into three groups: the methods that apply one type of similarity (1S), ensemble models that combine two types of similarities (2S), and ensembles of all three similarities (3S).

Table 9 includes six 1S predictors. Four methods [167, 171, 190, 198] measure DCS based on Tanimoto coefficient [289] that quantifies similarity between drug structures which are represented using molecular fingerprints [290, 291]. One predictor applies a statistical test over a set of DCSs based on Tanimoto coefficients between an input drug and a group of drugs in its internal database which are known to bind the input protein target [175]. The other method, DrugMiner, converts protein sequences into numeric feature vectors that represent physicochemical properties and amino acid compositions. Subsequently, it quantifies PSS for these feature vectors using machine learning algorithms and estimates druggability of a given protein based on its PSS to the known drug targets [165].

There are twenty three 2S models that utilize two types of similarities. Besides listing the similarity types we also define how they are combined together to generate predictions. Almost all of the 2S methods (21 out of 23) integrate DCS and PSS. Eleven predictors [176, 179, 182-184, 187, 189, 195-197, 199] quantify DCS using the SIMCOP algorithm [292, 293] while two other predictors [194, 200] utilize Tanimoto coefficient; these 13 methods rely on sequence alignment

algorithms such as BLAST [153] and Smith-Waterman [294] to measure PSS. A set of eight other methods represents drug structures and protein sequences using feature vectors that quantify DCS and PSS and they apply machine learning algorithms to generate predictions. These algorithms include kernel functions [168, 169, 178, 181, 186, 201], neural networks [166], and decision trees [172]. DPS is adopted rarely. Only two 2S predictors combine DPS with DCS [177, 188]. They define drug side-effect profile as a vector of binary values that indicate the presence or absence of specific side-effect terms. They quantify DPS based on weighted Tanimoto coefficients that measure similarities between side-effect profiles. The predictive models applied in these methods reveal that DPS could be used to infer DPIs in a similar way to DCS. This approach assumes that drugs that have similar side-effects are likely to target the same proteins. The drug profiles that were used in Ref. [177] have motivated the development of the SIDER database which stores drug side-effect information [120, 121]. This resource was later used in other works that we review including another 2S model [188] and three 3S methods [170, 185, 193]. However, SIDER focuses on marketed drugs and so the information about drug side-effects it provides is narrower when compared to drug structures that encompass a wider spectrum of drugs and protein sequences that span the entire human proteome. This is likely the reason why DPS is less frequently employed. Moreover, none of the 23 2S methods combines DPS with PSS. There are two ways in which the predictors combine two similarities. Five predictors apply a simple summation and weighted summation of two similarities [177, 187-189, 200]. The other predictors employ a more complex approach that typically involves operations such as maximum, multiplication, and geometric mean of multiple similarities.

There are six 3S methods that combine all three similarities. They utilize the same approaches to quantify DCS and PSS as the 1S and 2S models. Three of the six methods compute DPS based

on the cosine correlation coefficients between side-effect profiles [180, 185, 191] while two other models use Tanimoto coefficients [170, 193]. The sixth predictor [295] defines drug profiles using the ATC codes, which represent hierarchical classification of drugs and measure semantic similarity between ATC codes [192]. Like for the 2S methods, the 3S models utilize either a simple summation [191, 193] or a more complex approach to combine similarities [170, 180, 185, 192].

Table 9. Comparison of similarity-based DPI predictors. We review 35 methods that were published in high impact venues. We group these predictors into three categories (separated by horizontal line): predictors using one similarity (1S), predictors combining two types of similarities (2S), and predictors integrating three type of similarities (3S). Methods are sorted chronologically within each group. We summarize approaches that are used to quantify similarities and to compute ensembles of similarities for each predictor. We also summarize availability of empirical evaluation. This denotes inclusion of assessment of predictive quality, assessment of benefits of use of ensembles, assessment at per DPI and per drug levels, and analysis of sensitivity of predictive performance to intrinsic characteristics (similarity of inputs to the database) and extrinsic characteristics (information about the inputs) of predictors. The check symbol √ means a given assessment is included in a given method (row) while a blank cell means it is not included. DCS: chemical similarity; DPS: drug profile similarity; PSS: protein sequence similarity; SE: SEA algorithm that measures DCS [175]; SI: SIMCOMP tool that quantifies DCS [292, 293]; TC: Tanimoto coefficient or other similarity score which measures similarity between binary or numeric vectors [289]; KF: kernel function that measures similarity between feature vectors used by machine learning algorithms; NN: neural networks; CO: correlation; SS: semantic similarity of drug profiles represented by the ATC codes [192]; AL: sequence alignment using PSI-BLAST [153] or Smith-Waterman algorithms [294]; and ML: machine learning tools that measure similarity between feature vectors.

Type of predictor	Predictor	Year	Similarities and their ensembles				Predictive quality		Benefit of ensemble		Sensitivity analysis	
			DCS	DPS	PSS	Ensemble	per DPI	per drug	per DPI	per drug	Intrinsic	Extrinsic
1S	SEA [175]	2007	SE			N/A	√		N/A	N/A		
	PRW & NB [190]	2013	TC			N/A	√		N/A	N/A		
	DrugMiner [165]	2016			ML	N/A	√		N/A	N/A		
	SDTNBI [198]	2016	TC			N/A	√		N/A	N/A		
	Peón et al. [167]	2017	TC			N/A	√		N/A	N/A		
	bSDTNBI [171]	2017	TC			N/A	√		N/A	N/A		
2S	KRM [176]	2008	SI		AL	C	√					
	Campillos et al. [177]	2008	TC	TC		S	√		√			
	COPICAT [178]	2009	KF		KF	C	√					
	BLM [179]	2009	SI		AL	C	√		√			
	Yabuuchi et al. [181]	2011	KF		KF	C	√		√			
	GIP [182]	2011	SI		AL	C	√					
	NBI [183]	2012	SI		AL	C	√		√			
	KBMF2K [184]	2012	SI		AL	C	√					
	Cao et al. [186]	2012	KF		KF	C	√					
	BLM-NII [187]	2012	SI		AL	S	√					
	Cheng et al. [188]	2013	TC	TC		S & C	√		√			
	DT-Hybrid [189]	2013	SI		AL	S	√					
	RWR [194]	2015	TC		AL	C	√					
	SLP & RLS [195]	2015	SI		AL	C	√					
	RLS-KF [196]	2016	SI		AL	C	√					
	NRLMF [197]	2016	SI		AL	C	√					
	DASPfind [199]	2016	SI		AL	C	√					
	DrugE-Rank [200]	2016	TC		AL	S	√		√			
	DBN [166]	2017	NN		NN	C	√					
	EnsemDT/KRR [201]	2017	KF		KF	C	√					
	PUDTI [168]	2017	KF		KF	C	√					
	DVM [169]	2017	KF		KF	C	√					
	iDTI-ESBoost [172]	2017	ML		ML	C	√					
3S	Yamanishi et al. [180]	2010	SI	CO	AL	C	√		√			
	PKR [185]	2012	KF	CO	KF	C	√		√			
	DINIES [191]	2014	SI	CO	AL	S	√		√			
	Shi et al. [192]	2015	TC	SS	AL	C	√					
	Liu et al. [193]	2015	TC	TC	AL	S	√					
	DTINet [170]	2017	TC	TC	AL	C	√					
	This dissertation	N/A	TC	TC	AL	S	√	√	√	√	√	√

4.4.5 Timeline of the use of similarities and their ensembles

There are seven potential types of predictive models including three 1S, three 2S, and one 3S models. Figure 7 provides a timeline of the use of these seven types of predictive models for the 35 considered methods. In general, the ensemble-based models are much more widely utilized than the single similarity-based methods. The most frequently developed ensemble includes DCS and PSS. At least one of these methods was published every year except only for 2007, 2010, and 2014. The second most commonly used type of methods combines the three types of similarities. These methods were shown to outperform ensembles that are based on specific pairs of similarities, such as ensemble of DCS and PSS and ensemble of DPS and PSS [185]. However, a significant majority of current predictors combines only two similarities: DCS and PSS, without DPS. This is likely because the information on side-effects is not available in most of the source databases and this information used to be difficult to collect, especially before databases such as SIDER [120, 121] and MetaADEDB [296] were developed. Also, the mapping of drugs from the side-effect databases into the drugs in the internal databases is non-trivial. Another reason why DPS is not an attractive option is the fact that the side-effect information is limited to the marketed drugs. Consequently, this limits the internal databases to this group of drugs. Unlike the two broadly adopted types of models mentioned above, the other types of models are published less frequently. These models rely on DCS, PSS, and the ensemble of DCS and DPS. Some designs, such as methods that use DPS and the ensemble of DPS and PSS, have not been employed among the 35 considered methods. In summary, the most popular configuration is the ensemble that combines DCS with another type(s) of similarity.

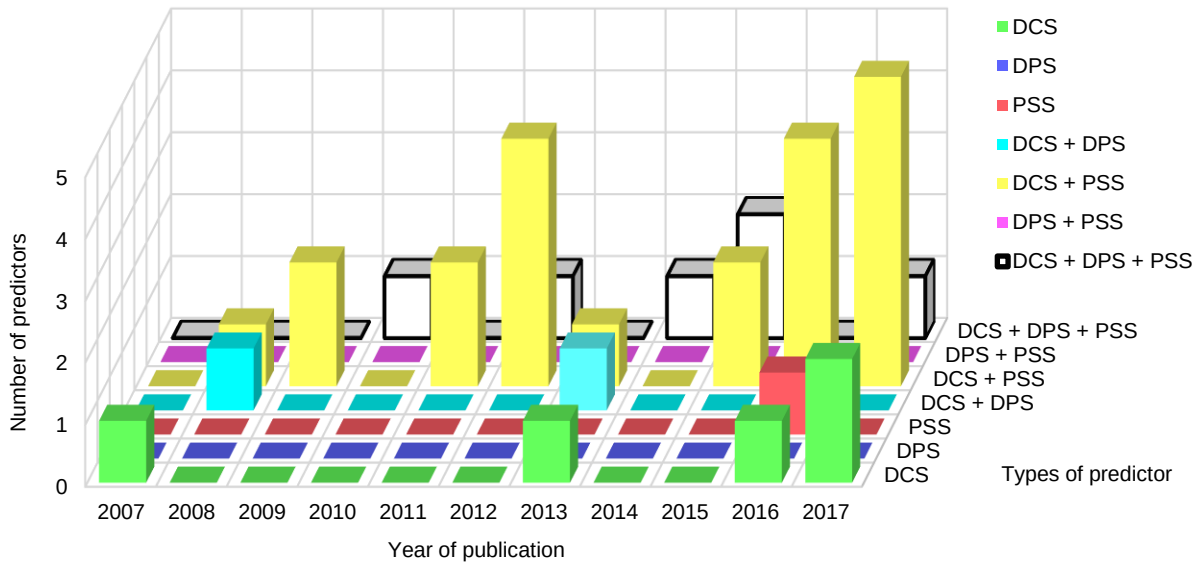

Figure 7. Timeline of similarity-based predictors of drug-protein interactions. The x-axis (width) denotes when the similarity-based predictors were published. The y-axis (depth) denotes the type of predictors. The z-axis (height) shows the number of a given predictors that were published in a given year. Green, blue, and red cubes represent drug chemical similarity (DCS), drug profile similarity (DPS), and protein sequence similarity-based predictors (PSS), respectively. The corresponding ensembles are color-coded according to the mixture of these three base colors shown in the figure legend.

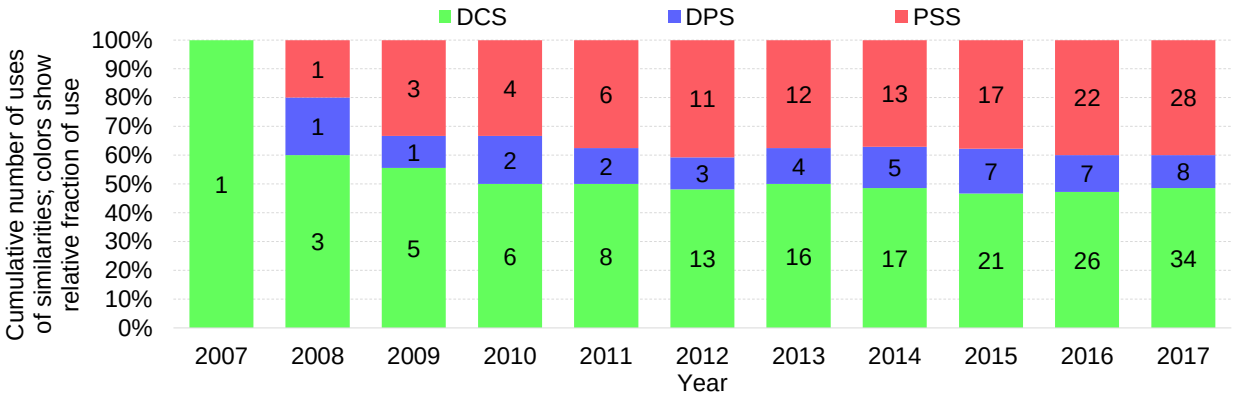

Figure 8. Use of individual similarities in predictors of drug-protein interactions. The x-axis denotes the year. The y-axis shows the fractions of cumulated numbers of uses of drug structure (green bars), drug profile (blue), and protein sequence (red) similarities up to a given year. Numbers inside the bars indicate the cumulative count of uses of each similarity. The similarity is counted when it is used individually by a single similarity-based predictor, and in tandem with other similarities by ensemble-based predictors.

Figure 8 shows how often an individual type of similarity was used over the last decade. We include their use individually and also as part of ensembles. Each bar in Figure 8 shows a cumulative number of times these similarities were used up to a given year. The colors inside the

bars reflect relative fraction of use of specific types of similarities. The first bar reveals that the first predictor that was published in 2007 was based on DCS [175]. The relative rate of use of DCS has gradually decreased between 2008 and 2010 when compared to the other two types of similarities. After 2010, the relative rate of use of the three types of similarities has stabilized; this is reflected by similar proportions of the three colors. The last bar reveals that in total the similarities were used 70 times by the considered set of 35 methods, which correspond to two similarities per method on average. DCS was used 49% of the time, while PSS and DPS were used 40% and 11% of the time, respectively. These fractions are consistent with the observation that the ensemble of DCS and PSS is the most frequently utilized type of predictive model. The relatively infrequent use of DPS is likely due to low drug coverage and difficulty to collect the information on drug side-effects. We believe that with the release and improvements to the databases that provide access to drug profiles, including SIDER and MetaADEDB, this type of similarity will play a more prominent role in the development of future predictors.

4.4.6 Critique of the current assessments of predictive performance

Another important aspect of the considered DPI predictors is the assessment of their predictive performance. The predictions are provided at an interaction level, which means that the predictive models identify whether a given drug-protein pair interacts. Two early predictors were assessed solely using the interacting drug-protein pairs (see "Scope of evaluation" column in Table 8) [177, 190]. While such assessment evaluates true positive rate (TPR), which is defined as fraction of interactions that are correctly identified, it lacks the ability to assess specificity, which measures the fraction of correctly predicted non-interactions. The other 33 methods provide assessment for both interacting and non-interacting drug-protein pairs. This type of assessment is more complete as it measures not only TPR but also the capability to correctly identify the non-

interacting pairs that constitute majority of all possible drug-protein pairs. Moreover, the considered 35 predictors report their predictive performance over all drug-protein pairs that span multiple drugs. This means that they did not assess and compare predictive quality for individual drugs (see "Predictive quality" column in Table 9). However, drugs differ in their structures, profiles, and the number and type of protein partners that they bind to, and these factors likely impact the predictive performance.

Besides quantifying predictive performance, it is also essential to justify the use of ensembles. Since the ensembles require more computations and are more complex to implement than the 1S models, they must offer some benefits to balance these drawbacks. In particular, these benefits typically boil down to higher predictive performance when compared to the 1S methods. Only six out of 23 2S methods compare 2S model with 1S to quantify the corresponding improvement in the predictive quality evaluated per interaction (see "Benefit of ensemble" column in Table 9) [177, 179, 181, 183, 188, 200]. Additionally, three 3S methods provide empirical evidence that the ensemble of three similarities boosts the predictive quality at interaction level when compared to the 2S ensembles [180, 185, 191]. While this suggests that ensemble models may provide more accurate results than the 1S models, follow up studies are needed to explore the benefits of ensembles using both per interaction and per drug evaluation. Moreover, none of these methods has comprehensively compared all three 1S, three 2S, and one 3S models. Such analysis would provide important insights on the use of the similarity-based predictors.

Another interesting aspect is sensitivity of predictive performance to certain characteristics of predictors. For example, in a scenario where the query drug is dissimilar to the drugs in the internal database of a given predictor, DCS and DPS are likely to be ineffective. On the other hand, if the query drug has sufficient levels of similarity to some of the drugs in the internal database

then we can use these similar drugs to likely accurately predict the protein targets. Similarity between the user-provided inputs and the contents of the internal database of a given predictor relies on an intrinsic property of this predictor (i.e., its database). On the other hand, predictive performance could be also affected by extrinsic to the predictor and known a priori properties of the query drug and targets, such as the drug promiscuity. For instance, it might be easier to identify DPIs for a drug that target numerous proteins because this increases a chance to find many other similar targets in the internal database. Analysis of sensitivity of performance to these characteristics would help to calibrate the expectations of predictive quality and optimize the design of predictors for specific use cases. However, this type of sensitivity analysis was never addressed in the past studies (see "Sensitivity analysis" column in Table 9).

Besides quantifying predictive performance in silico, some of these predictive tools were also assessed experimentally. In that case, the correctness of the putative DPIs that they generate was additionally verified by *in vitro* binding assays and cell assays. This type of validation was done for the earliest predictor [175], the method that first defined DPS [177], and in one recent study [170].

4.5 Conclusions

We have discussed the timeline, impact, availability, contents, and architectures for the 35 high-impact similarity-based DPI predictors and the related 12 source databases.

The source databases store curated annotations of DPIs that are used to derive the internal databases of the predictors. Their contents were obtained from relevant literature, experiments, and other data repositories. Most of the 12 source databases also directly import the annotations of DPIs from the other source databases. Consequently, each source database stores its unique data

and also a certain amount of data that overlap with the other source databases. Moreover, some source databases focus on the interaction data for the approved and experimental drug compounds, while the others include the protein targets for a more generic collection of bioactive compounds that includes drugs and drug-like molecules. This contributes to the diversity of contents of the source databases, in terms of the number and type of compounds, protein targets, and DPIs. Drugs that are included in the source databases typically target multiple proteins. This drug promiscuity defines the field of polypharmacology and benefits the development of the similarity-based predictors. The source databases have accumulated data for over ten years and have been frequently used by the scientific community. This is reflected by the fact that they were cited at least 190 times each. Most of the databases are continually updated and periodical republished. Our analysis shows that the source databases that are more frequently updated and republished are also more often cited.

The similarity-based predictors have been developed at a steady pace over the past decade. These methods rely on the internal databases that typically include data derived from multiple source databases. We found that recent methods have used a larger number of source databases than the older methods, although this number is still relatively low compared to the number of available source databases. The internal databases generally include lower numbers of drugs, proteins, and interactions but higher degrees of drug promiscuity when contrasted with the corresponding source databases. A higher drug promiscuity allows the similarity-based predictors to screen a more complete set of candidate protein targets and increases likelihood of identifying targets shared by multiple drugs. Given these advantages, the future predictive models should exploit an even more comprehensive set of DPIs that would be collected from a larger number of source databases.

Most of the predictors have received a relatively high annual citation counts when compared to the corresponding impact factors of the journals where they were published. This points to the substantial impact of the similarity-based methods. These methods incorporate predictive models that quantify similarities between the input drugs and proteins and the drugs and their known targets in the internal databases. We show that they rely on a variety of approaches to quantify DCS, DPS, and PSS. Most of these predictors utilize ensembles that combine two or three types of similarities, were published in high impact venues and are highly cited. The three earliest predictors are the most cited. They were the first to use DCS and the ensemble of DCS and PSS/DPS. These pioneering works resulted in the DCS-centric trend for the development of the similarity-based models. The vast majority of the 35 methods applies DCS or ensemble models that combine DCS with DPS and/or PSS. The ensemble of DCS and PSS is the most commonly utilized type of predictive model. Our analysis of the frequencies of use of similarities has found that DCS and PSS have been utilized about 90% of the time, while DPS is relatively underutilized. The infrequent use of DPS likely results from the incompleteness and difficulty to use and collect the drug profiles. This motivates the need to further develop the drug side-effect profile databases, thereby facilitating a new generation of methods that would more heavily rely on DPS.

These studies assess predictive performance at the interaction level and some of them have demonstrated that the use of certain ensembles leads to improved predictive performance when compared to the use of a single similarity. However, a comprehensive empirical comparison of all types of similarities and their ensembles is missing. Although the current works perform empirical assessments over a large number of drug-protein pairs, primarily in the druggable human proteome, the density of DPIs in the databases that were utilized in these assessments is rather low. Moreover, per drug assessment of the predictive quality was not yet performed. Similarly, sensitivity of

predictive performance to characteristics of predictors was not yet studied. To this end, we provide comprehensive and in-depth empirical comparative analysis for a representative set of similarity-based predictors. First, we build a novel database that includes drugs characterized by high density of DPIs. Next, we comprehensively evaluate a representative set of predictors that are based on each of the three main types of similarities and the corresponding four possible ensembles. Besides evaluating predictive performance at the interaction level, we are the first to perform the drug level assessment and to analyze sensitivity of predictive quality to the intrinsic and extrinsic characteristics of predictors. This work is described in Chapter 5.

Chapter 5 Empirical assessment and comparative analysis of similarity-based methods for prediction of drug-protein interactions

We empirically evaluate seven representative similarity-based DPI predictors. These seven predictors rely on each of the three individually used similarities (DCS, DPS, and PSS) plus four ensembles that combine each pair and all three similarities. We delineate the setup for the assessment by describing the seven predictors and defining measures and a novel high-quality benchmark database of DPIs that we use to assess the predictive performance. Like in the previous studies, we analyze predictive performance at the interaction level. Moreover, we are the first to compare all seven representative methods, to measure and compare predictive performance at the drug level, and to analyze sensitivity of predictive performance to characteristics of input drugs and proteins. We also release a webserver that provides access to the server-size implementations of the seven predictors.

5.1 Experimental setup

5.1.1 Computation of similarities

The key underpinning concepts that define similarity-based predictors of DPIs is how they quantify and combine the three similarities. We selected one representative approach drawn from previous works to measure each type of similarity. The Tanimoto similarity of chemical structures has been widely applied to quantify DCS [289]. Recent comparative studies have demonstrated that the Tanimoto similarity is one of the best DCS measures [291, 297, 298]. Eleven selected predictors have used the Tanimoto coefficient to quantify DCS [167, 170, 171, 177, 188, 190, 192-194, 198, 200]. The above reasons motivate our choice of this measure to quantify DCS. Tanimoto coefficient is computed based on molecular fingerprint that converts a chemical structure of a given drug into a bit vector of fixed size. For a given compound, the fingerprint represents presence of certain substructures with a bit value of 1 and their absence with a bit value of 0. Similarity of two drug fingerprints is represented by the similarity between their corresponding bit vectors A and B:

$$DCS\ (A, B) = a_1 b_1 / (a_1 + b_1 - a_1 b_1)$$

where $a_1 b_1$ is a count of corresponding positions where both vectors A and B have values 1, and a_1 and b_1 are the counts of positions with value 1 in vectors A and B, respectively. Higher value of the Tanimoto similarity means the two molecules are more structurally similar since they have a higher fraction of similar substructures in common. We use the Chemistry Development Kit software [299-302] to generate 1024-bit molecular fingerprints of drug structures and to compute the Tanimoto similarity between drugs.

We quantify DPS based on a drug side-effect profile similarity introduced in one of the pioneering predictors that utilized this type of similarity for the first time [177]. A given drug is

represented by a profile vector that denotes presence/absence of certain side-effect term with a bit value of 1/0. The profile similarity is computed using the weighted Tanimoto coefficient between the side-effect profiles of a given pair of drugs. Each side-effect term has its own weight. The weight is derived based on an abundance of the corresponding term in a large collection of drugs (all drugs included in the internal database) and a correlation of this term with the other terms. Higher weights are associated with terms that are less frequent (specific to a small number of drugs) and that are dissimilar to other terms (they are infrequently used together with other terms for the same drugs). Consequently, higher value of DPS means that a given pair of drugs share a high fraction of side-effect terms with high values of weights. This approach to quantify DPS is arguably more accurate than the approaches taken by some other methods that use a simpler definition of weights [193] or unweighted Tanimoto coefficients [188].

We use sequence alignment to estimate PSS. This is the most popular approach that was adopted by 18 predictors [170, 176, 179, 180, 182-184, 187, 189, 191-197, 199, 200]. First, we run BLAST [154, 156] with default parameters to perform sequence alignment between a sequence of a protein target of the input drug provided by user and each protein target in the database of known DPIs. BLAST finds the closest protein from the database based on a distance defined as the fraction of identical and similar residues in the pairwise alignment. Therefore, proteins from the database that have high value of sequence similarity are arguably likely to also interact with the input drug by the virtue of being similar to the known target of this drug.

We create the four ensemble models using a linear combination of multiple types of similarities. This approach is in line with a number of published ensemble methods [177, 187-189, 200]. We consider the 3S model that combines the three types of similarities and three 2S ensembles that combine each pair of the three similarities, which we denote as DCS+DPS,

DCS+PSS, and DPS+PSS. Some of the past methods combine similarities using more sophisticates approaches, such as machine learning models and drug-protein networks. A typical machine learning-based predictor uses an algorithm such as SVM to combine multiple kernel functions/matrices derived from two or three similarities [191]. However, SVM requires computationally costly parameterization and this is a black-box method, which means that the model is so complex that is impossible to understand how predictions are performed. Network-based predictors rely on a linear combination of similarities to quantify weights associated with edges in the network [187]. These predictors require knowledge of drug-drug or drug-target connections (network edges) for an input drug. Consequently, they cannot be utilized to predict DPIs for drugs that are not already integrated in the network [32]. We opt to use the linear combination of similarities which is computationally efficient, white-box (linear function explicitly defines how similarities are combined), and works with novel drugs.

5.1.2 Prediction of drug-protein interactions

To perform the prediction, we screen the query drug against all candidate proteins from the internal database of known DPIs to evaluate how likely they may interact with this drug. Given the three types of similarities, the input information for the query drug may include drug structure, drug profile and/or protein sequences of its known targets. The procedure to perform predictions depends on which inputs are available. If the drug structure is available then for every candidate protein in the database we compute DCS between the query drug and every single drug that is known to bind to that candidate protein (excluding the query structure itself if the candidate protein is already known as a binding partner of this drug). The maximal value among these DCS values is used as the propensity of DPI between the query drug and the candidate protein. A higher propensity indicates that the candidate protein is more likely to bind to the query drug because this

protein is known to be a target of a drug which is structurally similar to the query drug. This is consistent with an observation that similar drug structures share the same protein target [32, 85-87]. A similar procedure is used when the drug profile is available. The propensity of DPI for the input drug and a given candidate protein is computed as the maximal DPS between this drug and all drugs that are known to bind to this candidate protein in the database of known DPIs. Such prediction relies on the assertion that drugs with similar side-effect profiles likely target the same protein [177]. If the protein targets of the input drug are known and their sequences are available then we compute pairwise PSS between each candidate protein and all known targets of this drug (excluding the candidate protein itself if this protein is already known to interact with the query drug in the database). The maximal PSS among all known targets is used as the propensity of DPI for the query drug and the candidate protein. The sequence similarity-based prediction is motivated by an observation that similar proteins tend to interact with the same drug [32, 85-87]. If multiple inputs are available then they are combined together. We assess whether such ensembles of two or three similarities would provide improved quality of predictions when compared to using these similarities individually.

5.1.3 Benchmark database of drug-protein interactions

The DPI predictors rely on the internal database that contains native DPIs. We develop a novel benchmark database that we use as the internal database to evaluate these predictors. The benchmark database integrate three resources: Drug2Gene [247], Therapeutic Target Database (TTD) [43, 103-107], and IUPHAR/BPS Guide to Pharmacology database (GtP) [248, 249, 303-306]. Our database is primarily derived from Drug2Gene that integrates 19 source databases. These sources include four databases, PDSP Ki [202], TTD [43, 103-107], DrugBank [98-102], and ChEMBL [113-116], which are used by the 35 considered predictors to derive their internal

databases. However, we also include 15 other sources: CGDCP [307], ChEBI [308], CTD [238], HGNC [309], GtP [248, 249, 303-306], Ligand Expo [310], MICAD [311], NCBI Gene [312], Pathway Commons DB [313], PDBsum [314], PharmGKB [315], Pubchem Bioassay [239], PubChem Compound [316], PubChem Substance [316], and UniProt [37]. Considering that the 35 predictors adopt no more than six source databases, Drug2Gene provides us with a more complete information about DPIs. Another survey also highlights Drug2Gene as the most comprehensive DPI database [22]. In particular, use of Drug2Gene helps us to acquire high density of DPIs in the benchmark database. However, Drug2Gene (version 5) incorporates older versions of the TTD database (release 2011) and GtP database (release 2012) when compared its other sources. Thus, we combined Drug2Gene with newer versions of TTD (release 2015) and GtP (release 2015). These three resources altogether cover 10,515 compounds, 16,880 proteins, and 161,736 interactions. The density of DPIs for this database is 15 DPIs/drug, before removal of duplicates across these sources (see first row in Table 10).

The seven predictors that we assess rely on quantification of the three types of similarities. Thus, drug structures, drug profiles, and protein sequences are required for every drug/protein entry in the benchmark database. Drug fingerprints were collected from PubChem [316] by querying their compound identifiers (CIDs) that are available in three sources databases. Drug profiles were obtained from SIDER 2 [120, 121], a database of drug side-effects for marketed drugs, by matching PubChem CIDs. Protein sequences were retrieved from UniProt [37] using their UniProt accession numbers (UniProt IDs) which are available in TTD and GtP, and with the Entrez Gene [312] identifiers which are available in Drug2Gene. Consequently, drugs and proteins are respectively indexed by PubChem CIDs and UniProt IDs along with drug structures from PubChem, drug profiles from SIDER, and protein sequences from UniProt in the benchmark

database. We found redundant drug/protein entries because older versions of TTD and GtP have already been imported into Drug2Gene. We removed the duplicate drugs and proteins by comparing PubChem CID and UniProt ID, respectively. SIDER 2 provides side-effects for 996 drugs, which limits the number of drugs in our benchmark database. After collecting information for computing similarities and cleaning the duplicates, the resulting benchmark database contains 965 drugs, 7,565 proteins, 93,015 interactions, and 96 DPIs/drug (see second row in Table 10). Like most of studies in this area [165, 168-172, 176, 177, 179, 180, 182-187, 189-193, 196-200], we focus on the human protein targets. Thus, we eliminated non-human proteins based on their taxonomic identifiers from UniProt. Consequently, 563 drugs, 1,537 proteins, 35,352 interactions, and 63 DPIs/drug are left in the benchmark database (see third row in Table 10). Next, to ensure that sufficient amount of information about drug structure and protein sequence similarities is available to perform empirical assessment and sensitivity analysis, we removed small compounds that have fewer than 10 atoms and drugs that have fewer than five known protein targets, respectively. The final version of the benchmark database is composed of 449 drugs, 1,469 proteins, 34,456 interactions, and includes 76 DPIs/drug (see the last row in Table 10). When compared to the internal databases of the considered 35 predictors, this benchmark database is among the top 11% with respect to the number of DPIs shown in Table 8. Moreover, an arguably key indicator of a high-quality benchmark DPI database is the density of DPIs. High density of interactions facilitates reliable estimates for per-drug assessment of predictive performance. The benchmark database has the highest value of average per-drug density of DPIs at 76 DPIs/drug (median density = 95 DPIs/drug). Moreover, the median per-target density of DPIs is 4 DPIs/protein. This is a direct result of merging the largest number of sources of the DPI data and the fact that we only consider drugs that have at least five protein targets. Figure 9 shows the per-drug and per-target

density of DPIs for the drugs and proteins in the benchmark database, respectively. The top ten drugs that have the highest number of known targets include Imatinib (PubChem: 5291, 485 DPIs), Sorafenib (PubChem: 216239, 388 DPIs), Erlotinib (PubChem: 176870, 385 DPIs), Nilotinib (PubChem: 644241, 385 DPIs), Dasatinib (PubChem: 3062316, 384 DPIs), Gefitinib (PubChem: 123631, 343 DPIs), Chlorpromazine (PubChem: 2726, 168 DPIs), Mitoxantrone (PubChem: 4212, 166 DPIs), Nifedipine (PubChem: 4485, 162 DPIs), and Verapamil (PubChem: 2520, 158 DPIs). The top ten proteins that interact with the largest number of drugs include Cytochrome P450 3A4 (UniProt: P08684, 350 DPIs), Cytochrome P450 2D6 (UniProt: C1ID52, 329 DPIs), Cytochrome P450 2C9 (UniProt: P11712, 307 DPIs), Potassium voltage-gated channel, subfamily H (UniProt: A0A090N7W1, 298 DPIs), Cytochrome P450 1A2 (UniProt: P05177, 296 DPIs), Mitogen-activated protein kinase 1 (UniProt: P28482, 288 DPIs), Dopamine receptor D2, isoform CRA_c (UniProt: A0A024R3C5, 283 DPIs), Muscarinic acetylcholine receptor (UniProt: A0A024R3S2, 280 DPIs), Muscarinic acetylcholine receptor M1 (UniProt: P11229, 280 DPIs), and Muscarinic acetylcholine receptor (UniProt: A4D1Q0, 279 DPIs). The list of drugs, protein targets, and DPIs of the benchmark database are shown in the Appendixes 1, 2 and 3, respectively.

Table 10. Summary of the benchmark DPI database. The numbers were counted after each major step of the procedure that that lead to the completion of the benchmark database. The density of DPIs (DPIs/drug) is calculated by the average number of DPIs per drug.

Procedure of data processing	**Drugs**	**Proteins**	**DPIs**	**DPIs/drug**
Total counts in original sources databases	10,515	16,880	161,736	15
Filtered by availability of necessary information to compute similarities	965	7,565	93,015	96
Filtered by to include human proteins	563	1,537	35,352	63
Filtered by drug size (> 10 atoms) and number of known targets per drug (> 5 DPIs/drug)	449	1,469	34,456	76

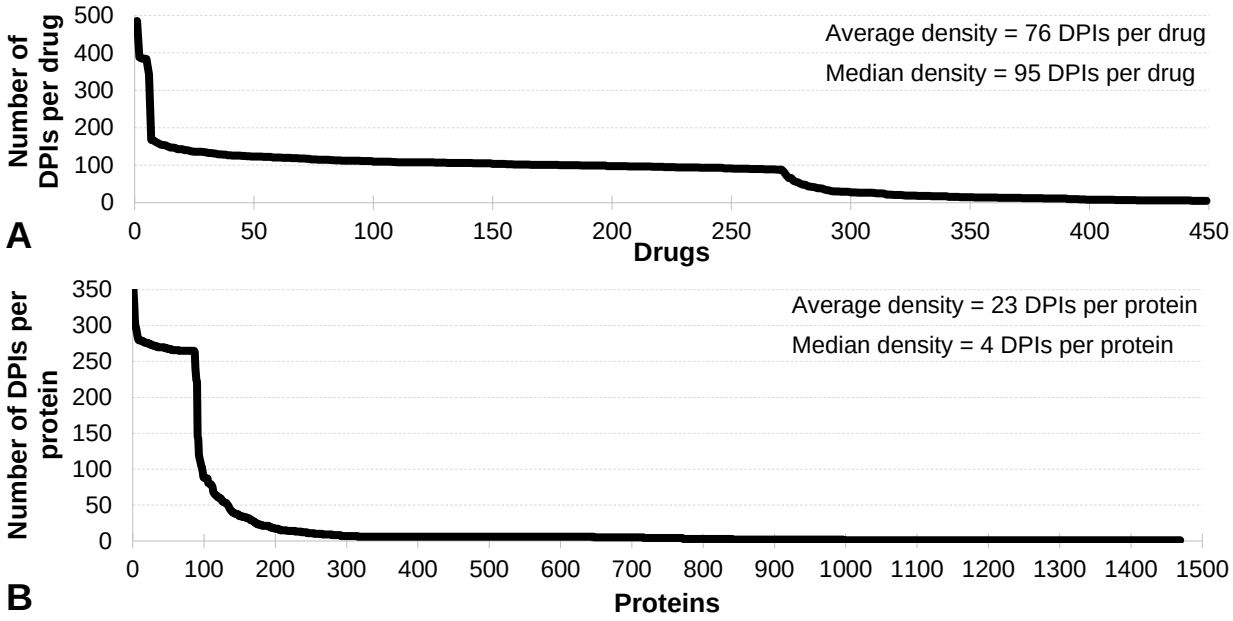

Figure 9. Density of DPIs for the drugs and protein targets in the benchmark database. Panel A shows the numbers of DPIs per drug and sorts the drugs in the decending order by these numbers. Panel B shows the numbers of DPIs per protein and sorts the proteins in the decending order by these numbers.

The source DPI databases include annotations of native interacting drug-protein pairs but they lack the annotations of non-interacting pairs. In the past, these databases were used to assess predictors of DPIs in several ways. A few early studies have assessed predictive performance using only the native interacting pairs [177, 190]. These assessments are incomplete since they measured only the rate of correctly predicted native DPIs while they did not evaluate the predictive performance for the non-interacting pairs, i.e., they did not evaluate the number of false positives. More recent works have assessed predictions using both interacting and non-interacting drug-protein pairs. Most of these studies assume that the drug-protein pairs that are not annotated as interacting are non-interacting. This assumption may result in mislabeling some of the native interacting pairs as non-interacting; in particular, those that were not yet discovered. This commonly applied approach to annotate the non-interacting pairs relies on an assertion that the number of such mislabeled pairs is much smaller than the number of correctly assumed non-

interacting pairs. We are the first to study this assumption empirically. We annotate weak binders among the native drug-protein binding pairs and we compare similarity between the assumed non-interacting drug-protein pairs and the similarity among the weakly binding pairs. We hypothesize that the assumed non-interacting drug-protein pairs can be used to represent the native non-interacting pairs if the difference between similarity of the non-interacting drug-protein pairs and similarity among the native interacting pairs is significantly higher than the difference between similarity of weak interactors and the similarity of the native interacting pairs.

We map the drug-protein pairs from the benchmark database into the PDSP Ki database that provides binding affinities [202]. A high binding affinity (affinity constant Ki < 10 μM) is typically considered to indicate an interacting drug-protein pair [177, 234]. Consequently, we divide the mapped drug-protein pairs into three subsets: the native interacting pairs with Ki < 10 μM, weak native interacting pairs with Ki > 10 μM, and the non-interacting pairs that include all pairs that are not annotated as DPIs. We compute DCS, DPS, and PSS for the drug-protein pairs in each subset. Figure 10 compares distributions of the values of three similarities for the native interacting pairs, weak native interacting pairs (borderline pairs), and non-interacting pairs. The distributions are represented by the 5th, 20th, 50th (median), 80th, and 95th percentiles. The results are consistent across the three similarities. The similarity values for the non-interacting drug-protein pairs are significantly lower when compared to the similarities for the weak native interactors (p-value < 0.01). They are also significantly lower when compared to the similarities for the native interacting pairs (p-value < 0.01). In other words, Figure 10 reveals that only a small portion of the non-interacting pairs has DCS, DPS and PSS values that are comparable to the DCS values of the native DPIs. We also observe that the distributions for DPS and PSS for the weak native interactors are similar to the distributions for the native interactors (p-value = 0.11 and 0.65,

respectively). While the difference between weak native interactors and native interactors for DCS is significant, the median DCS are 0.65, 0.41, and 0.28 for the native interacting pairs, weak native interacting pairs and non-interacting pairs, respectively. Over 95% / 80% of the native interacting pairs have higher DCS values than at least 50% / 80% of the non-interacting pairs. In agreement with previous studies, these results suggest that the assumed non-interacting pairs can be used to represent non-interacting pairs since their similarity is significantly lower than the similarity of the weak native interactors and the native interactors, while the differences between the latter two sets of drug-protein pairs are substantially smaller. We also observe that the number of non-interacting pairs that have relatively high PSS is greater than those that have relatively high DCS and PSS. This implies that predictions using PSS might be less accurate than the predictions with DCS or DPS.

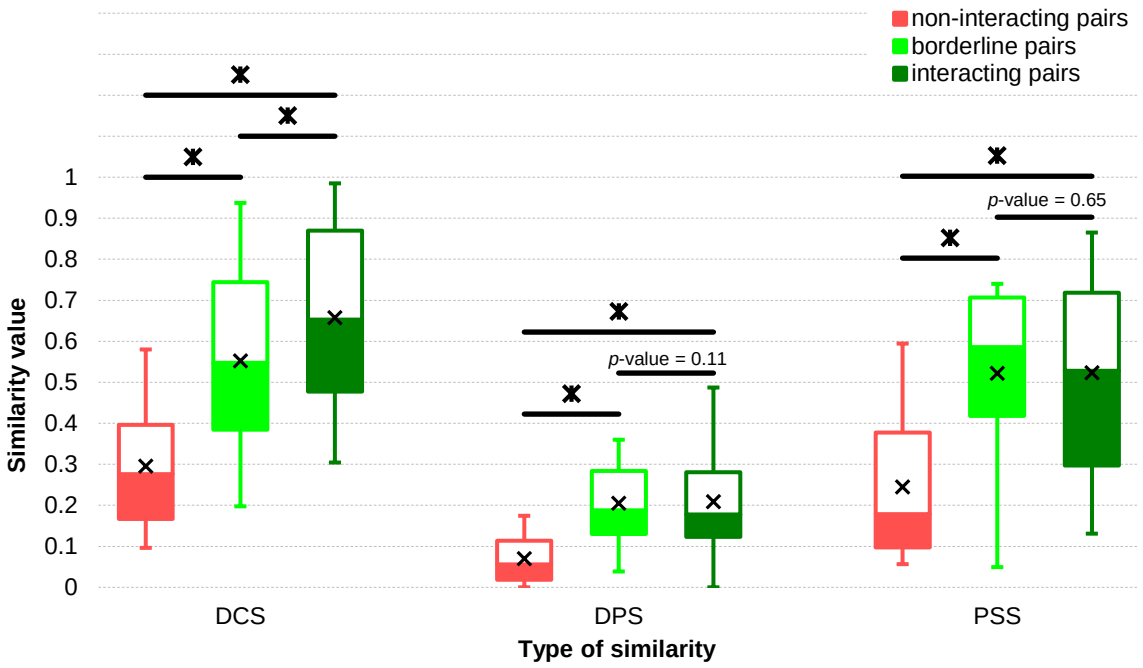

Figure 10. Distributions of values of the three types of similarities for native interacting drug-protein pairs (Ki < 10 μM; dark green), weak native interactors (Ki > 10 μM; borderline pairs in light green), and non-interacting drug-protein pairs (in red). Boxes and whiskers represent the 5th, 20th, 50th, 80th, and 95th percentiles of the similarity values. Marker × represents average similarity value for a given set of drug-protein pairs. We assess significance of differences between the similarity values for each pair of drug-protein pair sets using the Wilcoxon rank sum test [317]; we use the non-parametric test since these data are not normal according to the Anderson-Darling test at 0.01 significance. * indicates that the difference is statistically significant (p-value < 0.01); otherwise the actual p-value is shown.

5.1.4 Assessment of predictive performance

Using the benchmark database, we empirically test predictions for each of the 449 drugs by comparing the putative targets generated by a given method with the known native interactors for this drug. When testing predictions for a given drug, we remove information about its known targets from the database. We analyze the results across all drugs and separately for each drug. Like virtually all considered in this review methods we use the receiver operating characteristic (ROC) curve and the area under the ROC curve (AUC) to assess quality of DPI predictions [165, 166, 168-172, 175, 176, 178-189, 191-201]. ROC curve is a plot of True Positive Rates (TPRs) against False Positive Rates (FPRs): TPR = TP / (TP + FN) and FPR = FP / (FP + TN), where the

TP (True Positive) and the TN (True Negative) are the numbers of native interacting pairs and native non-interacting pairs that are predicted correctly, respectively; the FN (False Negative) is the number of native interacting pairs predicted as non-interacting; and the FP (False Positive) corresponds to the number of native non-interacting pairs predicted as interacting. The predicted propensities are transformed into binary predictions (positive vs. negative) using threshold values, which are next used to compute the TPR and FPR. Drug-protein pairs with propensity above the threshold are assumed to bind (positive), otherwise they are assumed to be non-binding (negative). The thresholds are set to be equal to all unique values of the predicted propensities of DPIs in order to derive the most accurate ROC curve. Higher AUC values denote better predictive performance, i.e., they correspond to predictions that offer higher TPRs (more correct predictions of DPIs) for lower FPRs (fewer incorrect predictions of non-interactions as DPIs).

The fraction of the native interacting drug-protein pairs among all drug-protein pairs in the benchmark database is at about 5%. Thus, for example, if FPR = 10% then the number of predicted putative DPIs is about twice the number of actual native interacting pairs. This corresponds to a substantial over-prediction of putative DPIs. Moreover, the AUC values are determined primarily by the part of the curve where FPR is high, focusing on the over-prediction, i.e., area under the curve for the low FPR values is much smaller than for high FPR values. Thus, motivated by recent works [318-321] we focus the lower part of ROC with FPR less than 5% (ROC_{low}) where the number of incorrectly predicted DPIs is not larger than the number of native DPIs. Accordingly, we calculate the corresponding area under ROC_{low} curve (AUC_{low}). Moreover, to ease interpretation of this index, we report $Ratio_{AUClow} = AUC_{low} / AUC_{low\text{-}random}$, where $AUC_{low\text{-}random}$ is AUC_{low} for a random predictor. A random predictor generates TPRs that are equal to FPRs, resulting in a diagonal line in the TPR-FPR space. $Ratio_{AUClow}$ measures to what degree a given

predictor is better than a random predictor. $Ratio_{AUClow} > 1$ means the method is better than random. An alternative to measuring the ROC for dataset with low numbers of positive samples is to use Precision-Recall curves. However, we opt to use ROC_{low} because this is the most frequently used measure in this area [165, 166, 168-172, 175, 176, 178-189, 191-201].

5.2 Empirical analysis of predictive performance

We perform evaluation of the predictive quality of the three 1S predictors as well as their 2S and 3S ensembles. We assess predictive performance for each drug by removing it from the benchmark database, predicting its interactions with each proteins target in that database, and evaluating these predictions against the removed native interactions of this drug. We aggregate these results over all the drugs and 659,581 drug-protein pairs. A query drug might be dissimilar to the drugs in the benchmark database in terms of its structure and side-effect profile. To simulate a practical scenario, we limit the similarity between the query drug and the drugs in database. Specifically, given a query drug, we not only remove this drug but we also remove the drugs with above median DCS and DPS from the benchmark database when performing the evaluations. Use of the median represents an average case. Note that the protein sequences are easy to collect and all of them are available for every prediction. The complete set of sequences for human proteins can be obtained from UniProt. Thus, the predictions for a given query drug are generated based on the drugs with the below-median DCS and DPS, and the complete set of protein sequences.

5.2.1 Assessment of predictive performance at the drug-protein interaction level

Figure 11 shows the ROCs and $ROCs_{low}$ that measure the predictive quality at the interaction level over all drug-protein pairs in the benchmark database for the three 1S, three 2S, and one 3S predictors. The 3S model has the highest AUC, AUC_{low} and $Ratio_{AUClow}$ values, which are given

in the legend for Figure 11. The 1S models register a modest drop in predictive quality when compared to the 2S models. Specifically, the relative difference in AUC (in AUC_{low}) between 3S and the best 2S model equals [0.926–0.913]/0.913 = 1.4% ([0.0285–0.0274]/0.0274 = 4.0%) (Figure 11A). The corresponding relative difference when comparing 3S and 1S models are at least [0.926-0.883]/0.883 = 4.9% for AUC and [0.0285-0.0231]/0.0231 = 23.4% for AUC_{low}. These results consistently demonstrate that the use of ensembles results in improvement in predictive quality. Moreover, our results show that adoption of the 3S, the three 2S, and DCS and DPS models provides high-quality predictions. The only relatively low results for PSS could be perhaps explained by the larger overlap of similarities between the native DPIs and non-DPIs observed in Figure 10. Although DCS provides more accurate predictions in terms of AUC when compared to DPS and PSS, the ensemble of DPS+PSS outperforms the two 2S predictors that rely on DCS. Combing DPS and PSS provides the largest improvement over these similarities used individually. Specifically, the relative difference in AUC (in AUC_{low}) is 4.8% (13.7%) and 20.4% (130%) when comparing DPS+PSS with DPS and PSS, respectively. The corresponding improvements for the other two 2S models are more modest. DCS+PSS provides a relative increase in AUC (in AUC_{low}) when compared to DCS and PSS by 2.6% (9.5%) and 19.5% (143%), respectively. Similarly, the value of AUC (AUC_{low}) for DCS+DPS is better by 1.9% (18.6%) and 3.3% (29.9%) than the values for DCS and DPS, respectively. One possible explanation for these differences is that each of the three similarities offers good predictive performance while DPS and PSS are lack any correlation (Spearman correlation coefficient [SCC] = 0.05), DCS and PSS are weakly correlated (SCC = 0.14), and DCS and DPS are modestly correlated (SCC = 0.30). Therefore, PSS and DPS complement each other the most which results in the largest improvement in the quality of predictions.

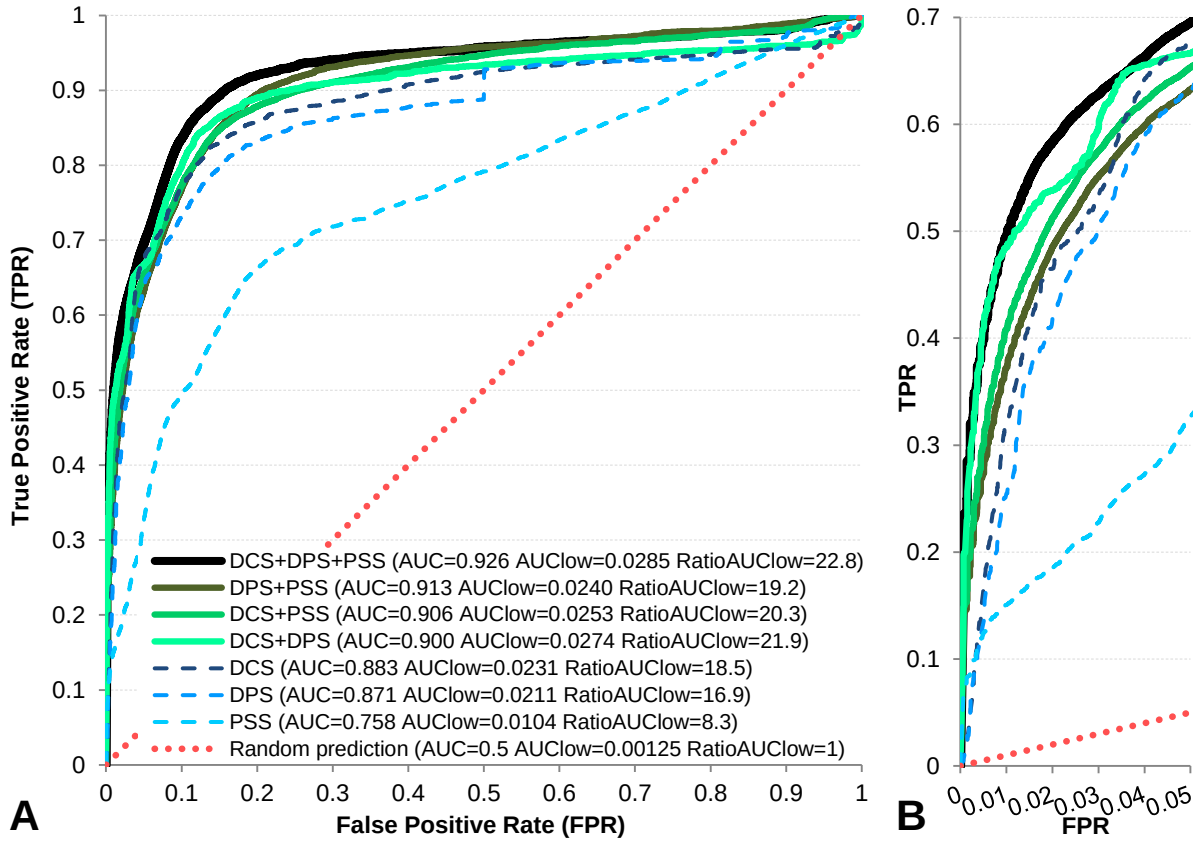

Figure 11. Comparison of predictive performance for the 1S, 2S, and 3S DPI predictors measured at the interaction level. Panel A shows ROC curves and panel B shows ROC_{low} for which FPRs ≤ 0.05. Diagonal dotted line denotes the ROC curve for a random predictor for which TPR = FPR. Values of AUC, AUC_{low} and $Ratio_{AUClow}$ are shown in the legend for panel A.

When FPR is greater than 0.05, the number of native non-DPIs that are incorrectly predicted as DPIs is larger than the total number of native DPIs. In other words, we over-predict DPIs. Therefore, we utilize AUC_{low} that considers the ROC curve for FPR < 0.05. The advantages of using multiple similarities, i.e., 3S vs 2S and 2S vs 1S, are maintained for AUC_{low} (Figure 11B). The $Ratio_{AUClow}$ reveals that 3S model is about 23 times more accurate than random predictions while 2S and 1S models are up to 22 and 19 times more accurate when compared to the random predictions. In particular, 3S predictor identifies 70% and the best 2S model finds 67% of native DPIs while they incorrectly recognize 5% of non-DPIs as DPIs (FPR = 0.05). Almost all predictors

successfully detect over 63% of native DPIs (TPR > 0.6) at 5% level of FPR, except PSS which finds 33% of native DPIs. Similar to the evaluations based on the overall AUC, predictor based on DCS is the most accurate 1S model in terms of AUC_{low}. Therefore, DCS drives the predictive quality of the ensembles. Moreover, PSS has the lowest performance of the three similarities, which is still eight times better than the random predictions. Moreover, PSS is helpful for the ensemble models given its lack of correlation with the other two similarities. The AUC_{low} for the 2S ensembles that include PSS register relative improvement by 9.5% and 13.7% when contrasted with DCS and DPS, respectively.

We also evaluate statistical significance of the differences in predictive quality between the 3S model, the three 2S models, and the three 1S models. To do that, we evaluate the differences over a diverse collection of 100 datasets drawn from the benchmark database. Each dataset includes 10% of randomly selected (without replacement) drugs from the benchmark database. Therefore, overlap between these datasets is minimal resulting in a large and diverse sampling of subsets of the benchmark datasets. We measure the AUC, AUC_{low}, and $Ratio_{AUClow}$ for each dataset. The corresponding averages and standard deviations quantified over the 100 datasets are given in Table 11. These averages are consistent with the results on the entire benchmark database that we give in Figure 11A. The *p*-values that measure significance of differences between all pairs of the considered seven methods are below 0.01, which mean that the differences in the predictive quality are statistically significant. This reveals that the benefits brought by the use of multiple similarities and the higher predictive performance of DCS compared to other 1S models are consistent over a diverse sampling of datasets. Overall, we show that 3S is the most accurate and significantly more accurate than the 2S predictors, while the 2S predictors are significantly better than the 1S models.

DCS is significantly more accurate when compared to DPS and PSS. These observations provide useful hints for future users and designers of the DPI predictors.

Table 11. Significance of differences in the predictive performance of DPI predictors measured at interaction level. The distribution of AUC, AUC_{low}, and $Ratio_{AUClow}$ values quantified over 100 different datasets (randomly selected 10% of drugs from the benchmark database) are represented by average ± standard deviation. The *italic* and underlined fonts represent results of tests of significance of difference in AUC and in AUC_{low}, respectively, for each pair of predictors. We quantify the corresponding *p*-values by running *t*-test (for measurement with normal distribution) or Wilcoxon signed-rank test (for non-normal data) between each pair of predictors. We test the normality with the Anderson-Darling test at 0.01 significance.

Method	Predictive quality (average ± standard deviation)			Statistical significance (p-value) of the differences between all pairs of predictors						
	AUC	AUC_{low}	$Ratio_{AUClow}$	3S	DPS+PSS	DCS+PSS	DCS+DPS	DCS	DPS	PSS
3S	0.925±0.005	0.0284±0.0005	22.7±0.4		*5.4E-26*	*4.0E-77*	*2.3E-46*	*3.7E-59*	*1.6E-54*	*8.5E-104*
DPS+PSS	0.912±0.004	0.0240±0.0005	19.2±0.4	1.0E-69		*3.3E-10*	*1.9E-12*	*1.0E-30*	*5.5E-51*	*5.8E-105*
DCS+PSS	0.905±0.005	0.0252±0.0005	20.2±0.4	4.7E-64	3.9E-14		*7.4E-07*	*4.1E-37*	*5.8E-34*	*4.8E-98*
DCS+DPS	0.899±0.006	0.0273±0.0007	21.9±0.6	1.3E-08	1.3E-30	1.7E-18		*8.2E-45*	*8.4E-32*	*5.5E-81*
DCS	0.882±0.006	0.0230±0.0006	18.4±0.5	2.0E-56	3.0E-05	3.2E-22	5.2E-58		*3.3E-08*	*5.1E-74*
DPS	0.869±0.008	0.0210±0.0007	16.8±0.6	2.9E-69	3.7E-34	7.9E-39	5.7E-78	8.2E-23		*1.5E-66*
PSS	0.759±0.012	0.0100±0.0029	8.0±2.3	3.2E-92	9.2E-87	2.0E-88	2.1E-72	1.6E-65	1.2E-57	

We study relationship between the predictive performance and similarity values by comparing predictions between the 3S and 1S models to understand how the predictive performance benefits from combining multiple similarities. We divide values of DCS, DPS, and PSS into 20 equally sized intervals and utilize these intervals to partition the benchmark database into subsets in which the drug-protein pairs have comparable similarity values. Figure 12 deconstructs the 3S model into two dimensional plots of two similarities, each divided into 20 intervals for the total of 400 data points. This figure compares the predictive quality of the 3S model (shown inside of the first quadrant) with the three 1S models (left most vertical set of points and bottom most horizontal set of points, which are outside of the quadrant). The predictive quality is measured with accuracy defined as a fraction of correctly identified DPIs and non-DPIs to total number of drug-protein pairs in a given data point; we denote that by the bubble size in Figure 12. We could not use AUC because some of these data points may not have either native DPIs or native non-DPIs. We use colors to denote relative enrichment of native DPIs and non-DPIs for

each data point where dark red denotes enrichment in non-DPIs and dark green is for enrichment in DPIs. The enrichment is defined as the difference between the fractions of DPIs and non-DPIs, which are computed by dividing the number of native DPIs (non-DPIs) in a given data point by the total number of DPIs (non-DPIs) in the benchmark database. For instance, a light red point for DCS $\in$ [0.25, 0.3] and PSS $\in$ [0, 0.05] in Figure 12B. shows that a modest majority of drug-protein pairs with these values of the two similarities are non-DPIs (which is denoted by the light red color) and accuracy of the 3S model for this data point is 100% (which is denoted by the large size of the bubble).

Figure 12A shows that the predictive accuracy for 3S model is separated into two distinct regions. The first region includes red data points for DCS $\in$ [0.05, 0.45] and DPS $\in$ [0, 0.15]. This region is enriched in native non-DPIs (red color) and has high predictive accuracy (large bubble). The second region includes green data points for DCS $\in$ [0.45, 1] and DPS $\in$ [0.1, 0.3]. This region is enriched in native DPIs (green color) and has lower predictive accuracy (smaller bubble) when compared to the red region. As expected, the colors reveal that the native non-DPIs are concentrated in the drug-protein pairs with low values of DCS and DPS while the native DPIs are more enriched in the drug-protein pairs with high similarities. This demonstrates that similarities could be used to discriminate DPIs from non-DPIs. The bubble sizes reveal that it is easier to provide high predictive performance for non-DPIs because they contain many drug-protein pairs and most of them include drugs which are very dissimilar to drugs which are known to bind the same protein. Such dissimilar drugs are easy to be correctly predicted as the non-interacting pairs. On the other hand, the predictions are less accurate for the green bubbles. This is because they cover drug-protein pairs for which drug structures are similar to the drugs that interact with the same proteins. Moreover, some of the pairs in these bubbles are still non-DPIs and they are difficult

to differentiate from the native DPIs. Most importantly, Figure 12A explains why 3S model is better than the corresponding two 1S models that rely on DCS and DPS. DCS values can be used to reliably separate non-DPIs (dark red bubbles in the bottom horizontal line where DCS <0.4) from DPIs (dark green bubbles where DCS > 0.5). However, drug-protein pairs for DCS between 0.4 and 0.5 cannot be easily separated. The separation of these drug-protein pairs into DPIs and non-DPIs can be improved by adding the values of DPS. Specifically, drug-protein pairs with DCS $\in$ [0.4, 0.5] and DPS $\in$ [0, 0.1] are mostly non-DPIs (red bubbles) while the drug-protein pairs with DCS $\in$ [0.4, 0.5] and DPS > 0.1 are mostly DPIs (green bubbles). Moreover, the bubble sizes also suggest that the accuracy of the 3S model is better than DCS model. The bubble for DCS $\in$ [0.45, 0. 5] has moderate accuracy = 78%. The corresponding column for the 3S model at DCS $\in$ [0.45, 0.5] has includes much larger bubbles that correspond to higher accuracies. The accuracy for the 3S model is high (between 89% and 98%) when DPS < 0.2 and DCS $\in$ [0.45, 0.5]. On average, accuracy of the 3S model for DCS $\in$ [0.45, 0.5] equals 84% when compared to 78% when DCS is employed alone. Similar observations can be made for Figure 12B. Overall, the 3S model improves over the 1S models in the interface between the red and green regions.

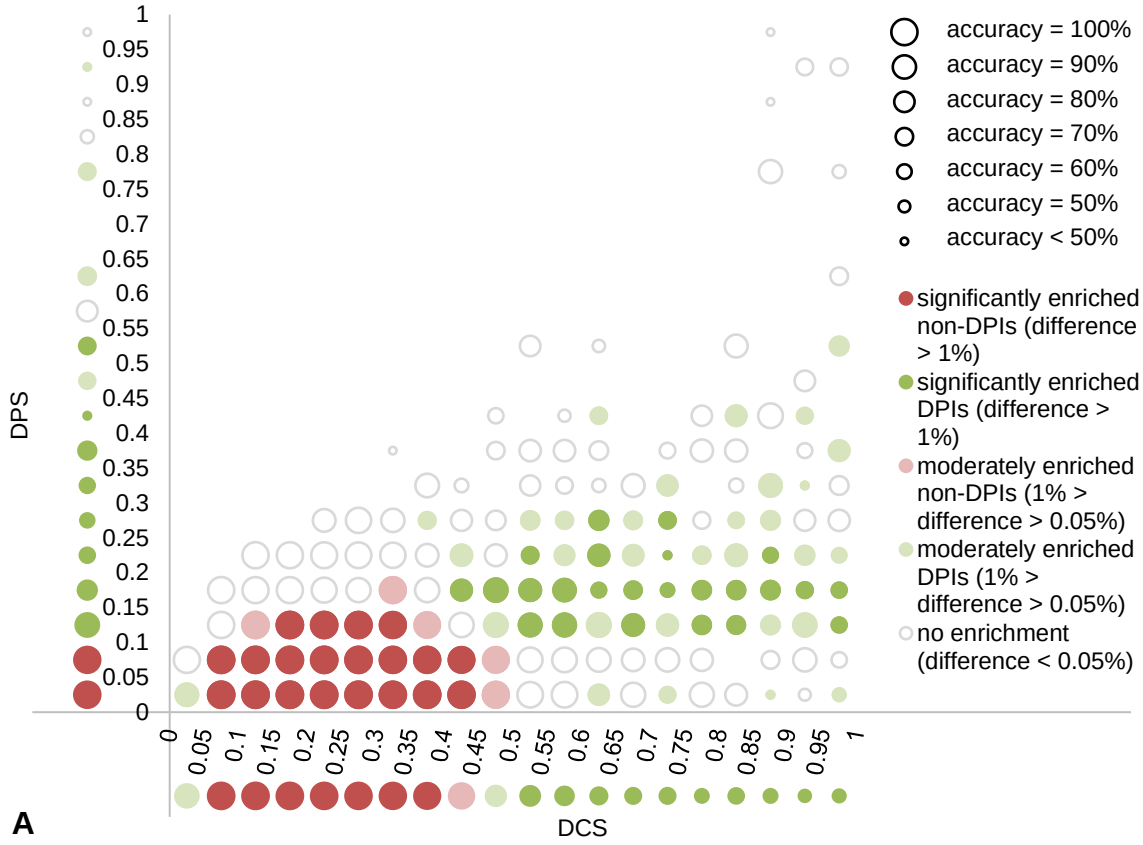
DPS
DCS
accuracy = 100%
accuracy = 90%
accuracy = 80%
accuracy = 70%
accuracy = 60%
accuracy = 50%
accuracy < 50%
significantly enriched non-DPIs (difference > 1%)
significantly enriched DPIs (difference > 1%)
moderately enriched non-DPIs (1% > difference > 0.05%)
moderately enriched DPIs (1% > difference > 0.05%)
no enrichment (difference < 0.05%)

A

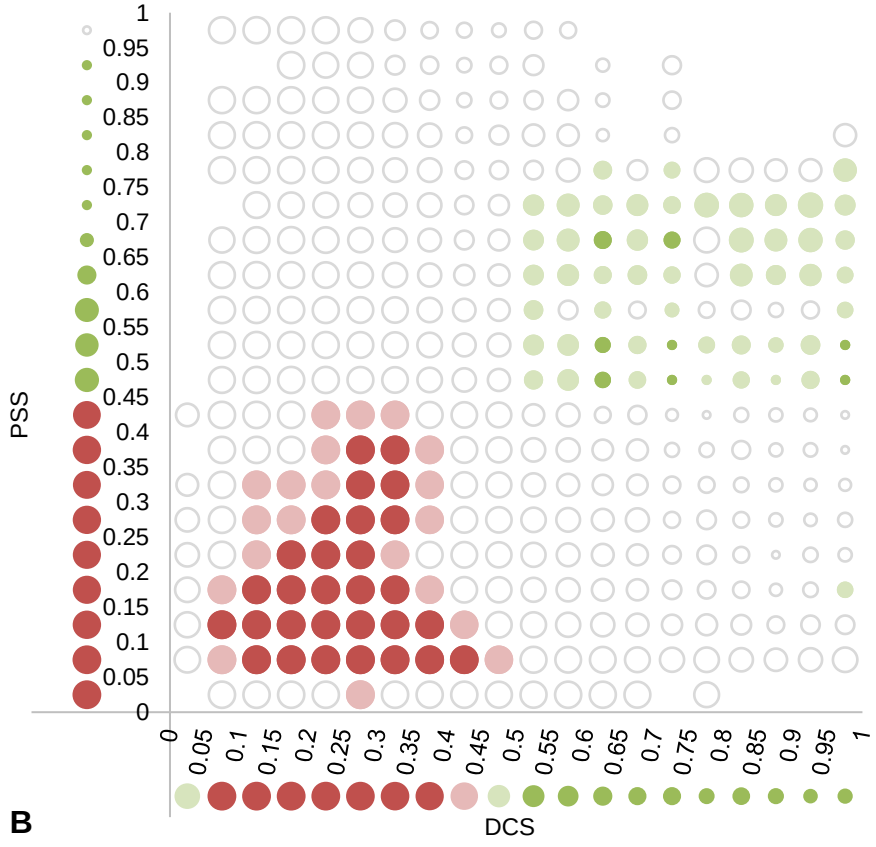
PSS
DCS

B

Figure 12. Comparison of predictive performance between 3S and 1S models in the function of values of the three similarities. The values of the three similarities are divided into 20 equally sized intervals. The comparison of the 3S vs the three 1S models is divided into two panels that compare the 3S model vs. two sets of 1S models each. Panel A shows the comparison of 3S vs. DCS and DPS. Panel B shows the comparison of 3S vs. DCS and PSS. Accuracy for the 3S model is shown inside the first quadrant while 1S models are given as a horizontal line below x-axis and a vertical line to left from the y-axis. Each bubble represents the drug-protein pairs in a given interval. Bubble sizes denote accuracy, which is defined as the fraction of correctly identified DPIs and non-DPIs to total number of drug-protein pairs in that bubble. Color denotes enrichment in native DPIs/non-DPIs, which is defined as the difference between the fractions of native DPIs and non-DPIs. These are computed by dividing the number of DPIs (non-DPIs) in a given bubble by the total number of DPIs (non-DPIs) in the benchmark database. We discretize the enrichment into five levels: dark green (dark red) bubble denotes significant enrichment in DPIs (non-DPIs) if the difference ≥1%; light green (light red) bubble indicates moderate enrichment in DPIs (non-DPIs) if the difference ≥0.5%; and white hollow bubble means no enrichment for which the difference <0.5%. White space in the figure denotes bubbles that we removed because they contain fewer than 100 drug-protein pairs; this is to ensure that statistics are robust.

5.2.2 Assessment of predictive performance at drug level

All previous studies evaluate predictive performance at the interaction level, which measures accuracy of the DPI predictions over drug-protein pairs that span across multiple drugs. Considering the fact that different drugs may share different levels of similarity to the benchmark database, it would be useful to evaluate these drugs individually. We provide first-of-its-kind assessment of predictive performance for DPI predictions at the drug level. The drug-level assessment provides further insight into complementarity and differences between various 1S, 2S, and 3S predictors. We measure the AUC over the DPI predictions for each individual drug (AUC_{drug}), which evaluates the quality of associations that are predicted between a given drug and all of the 1469 druggable proteins. We ensure that each drug in the benchmark database has at least five protein targets, which allows us to provide relatively robust estimates of the AUC_{drug} values.

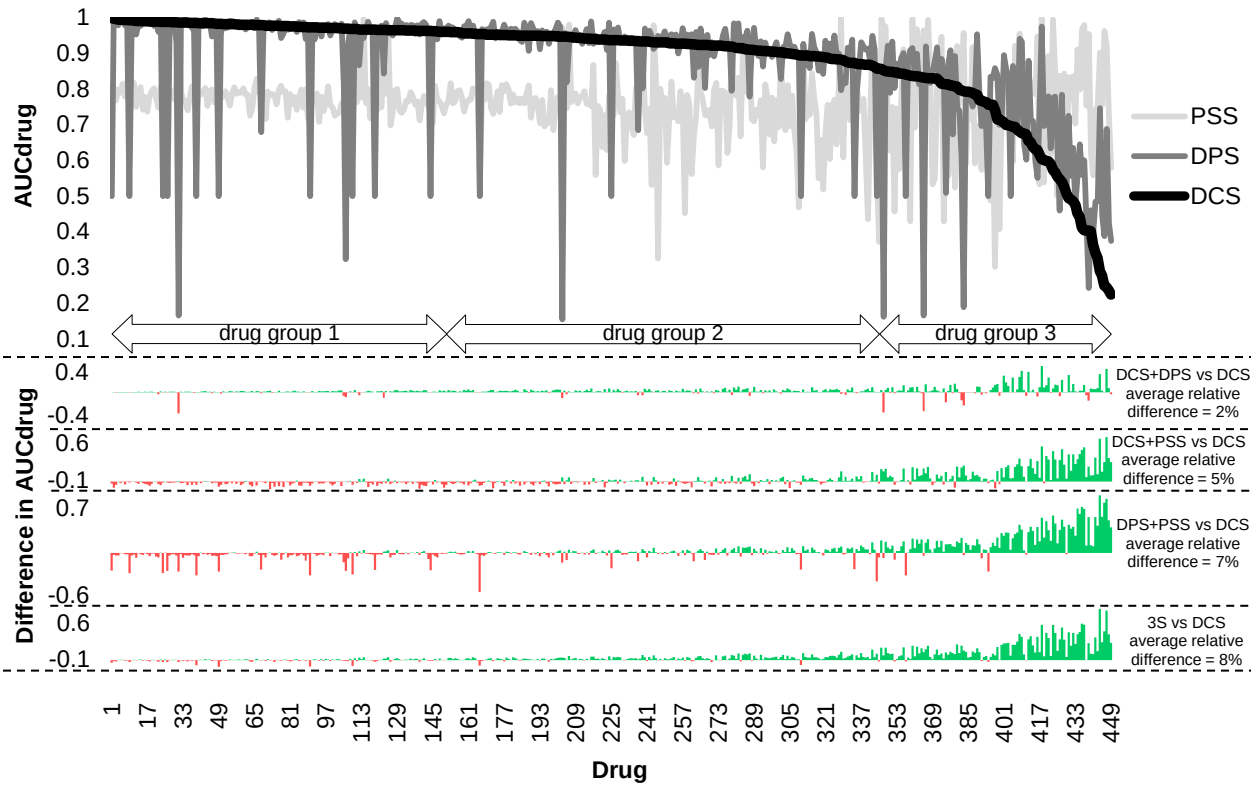

Figure 13. Comparison of predictive performance for the considered DPI predictors at the drug level. Black and gray lines at the top of the figure show the AUC measured per drug (AUC_{drug}) for each of the three 1S models. Drugs are sorted by their AUC produced by the most accurate DCS model. The four sets of bar charts at the bottom of the figure show the difference in drug-level AUC between each ensemble model and DCS. Green bar (red bar) means improvement (decline) in the AUC_{drug} values.

The upper half of Figure 13 shows the AUC_{drug} for the three 1S predictors over each of the 449 drugs. The drugs are sorted by the corresponding AUC_{drug} values of DCS, which is the most accurate 1S model when measured at the interaction level (Figure 11). We divide the drugs into three groups. The *first group* of 150 drugs has AUC_{drug} for DCS > 0.96. The AUC_{drug} for DPS and PSS is virtually always lower than AUC_{drug} for DCS for this group. The *second group* of 195 drugs has AUC_{drug} for DCS between 0.96 and 0.86. The values of AUC_{drug} for PSS are almost always lower than DCS while AUC_{drug} for DPS and DCS are similar for these 195 drugs. The *third group* of the remaining 104 drugs has AUC_{drug} values for DCS that are on average lower than DPS and PSS. Although DCS and DPS are much better than PSS for the first two drug groups, the AUC_{drug}

for PSS (0.752) for the *third group* of drugs is on average higher than the AUC_{drug} for DCS and DPS (0.674 and 0.709). This reveals that although overall PSS provides lower predictive performance, it outperforms the other two measures of similarity for 60/449 = 13% of drugs. The lists of drugs for each of the three groups are shown as three separate columns in the Appendix 1.

The interaction-level AUC of DCS across the 449 drugs is 0.883 (Figure 11). DCS achieves $AUC_{drug} > 0.883$ for 324/449 = 72% of drugs. Moreover, AUC_{drug} for either DPS or PSS > AUC_{drug} for DCS for 100 out of the 125 drugs for which AUC_{drug} for DCS < 0.883. These drugs should be of particular focus for the designers of future DPI predictors since they should be predicted with the help of the DPS and PSS rather than the most accurate at the interaction level DCS. This reflects trade-offs between the three measures of similarity and motivates the development of predictors that use consensus of multiple similarities.

We also compare the drug-level performance for the three 2S and the one 3S predictor with the most accurate 1S predictor, DCS. The lower half of Figure 13 shows the difference in AUC_{drug} between DCS and each of the four ensemble predictors. Overall, the ensemble models are more accurate than DCS for most of the drugs (green bars in Figure 13). Specifically, DCS is outperformed by DCS+DPS, DCS+PSS, DPS+PSS, and 3S model for 370, 222, 244, and 349 drugs, respectively. We measure relative difference in AUC_{drug}, which is defined as the absolute difference in AUC_{drug} divided by the AUC_{drug} for DCS. The average relative differences in AUC_{drug} over the 449 drugs between DCS and the four ensembles are 2% (when compared to DCS+DPS), 5% (DCS+PSS), 7% (DPS+PSS), and 8% (3S). Thus, as expected based on the interaction-level results, the 3S model is also the most accurate predictor at the drug level. The drug-level results for the 2S models are also consistent with the evaluations at the interaction level. DPS+PSS is the most accurate 2S predictor that secures 7% improvement over the DCS model. In particular, it

benefits from PSS for the drugs in the third drug group. AUC_{drug} for DCS and DPS are correlated for the third drug group (SCC = 0.58). On the other hand, AUC_{drug} for PSS is not correlated with either DCS or DPS (SCC = 0.07 and 0.05) and it secures relatively high AUC_{drug} values. This implies that PSS is a strong predictive input that compliments the other two similarities, which explains why the ensemble predictors outperform DCS for the third group of drugs.

Our novel drug-level assessment of predictive performance shows that no single similarity could provide accurate DPI predictions across all drugs. DCS is the most accurate 1S model and the primary driver of the ensemble-based predictors for the first two group of drugs. For 23% of drugs (the third drug group) for which DCS does not provide higher predictive quality, the use of the other two similarities substantially increases the predictive performance. The 1S models are strongly dependent on the assumption that similar drugs share the same targets and similar proteins tend to interact with the same drug. The complementarity between PSS and DCS/DPS allows us to accurately cover a wider range of drugs for which only some of these similarities work individually.

5.3 Sensitivity of predictive performance to characteristics of predictors

The predictive performance can be influenced by two factors: 1) intrinsic characteristics of the similarity-based predictors of DPIs, which are defined based on similarity of the query drug or its known targets to the benchmark database; and 2) extrinsic characteristics that are defined solely based on properties of the query drug and its known targets. For instance, if the query drug is similar to many of the drugs from the benchmark database then we anticipate it might be more likely to accurately find its protein targets when compared to a drug that is dissimilar to the drugs in the database. Also, a query drug that has a large number of known targets might be easier to

predict, irrespective of the predictive system used. This is because its targets can be exploited to find more potential new targets from the database when compared to a query drug with no or few known targets. We are the first to assess the sensitivity of predictive quality to a set of practical intrinsic and extrinsic characteristics of predictors.

5.3.1 Sensitivity to intrinsic characteristics

Similarity-based DPI predictors rely on finding drugs that are similar to a query drug and proteins that are similar to the known targets of the query drug. The quality of DPI predictions depends on the values of the similarities between query drug/protein and the benchmark database, which in turn are dependent on the size and coverage of the database. In principle, the benchmark database is incomplete as it only covers the currently known drug structures, drug profiles, and druggable human sequences. In a typical practical scenario, a query drug might be dissimilar to all the drugs in the benchmark database. This reduces the chance that a DCS- or DPS-based predictor successfully identifies potential DPIs for the query drug, even if the query drug actually shares targets with the drugs in the benchmark database. We simulate such scenarios by excluding drugs (proteins) that share certain levels of similarity to the query drug (target) from the benchmark database when making predictions for the query drug (target). We partition the drugs and proteins from the benchmark databases into clusters using average-linkage hierarchical clustering [322]. As a result, the average similarity of drugs or proteins between any two clusters is lower than a predefined similarity threshold used for the clustering. In other words, the drugs (proteins) from one cluster are dissimilar to drugs (proteins) from another cluster. Subsequently, given a query drug (protein), we exclude the drugs (proteins) that belong to its cluster and use the only remaining drugs (proteins) to compute DCS/DPS/PSS for prediction. Thus, the predictions are based on drugs and proteins that are dissimilar to the inputs. Specifically, we use the 80^{th}, 50^{th} (median), and 20^{th}

percentile of similarity values over all the drug-protein pairs in the benchmark database as the clustering thresholds. We also consider a scenario where all drugs and proteins are utilized for the predictions except for the query drug or protein itself. This scenario is equivalent to the clustering using the 100th (maximal) percentile of similarity values. Additionally, random predictions that correspond to the 0th percentile are also considered. We use these five scenarios to study the sensitivity of the predictive performance to the similarities between the query drug (protein) and the benchmark database. The predictive performance is quantified with the interaction-level AUCs.

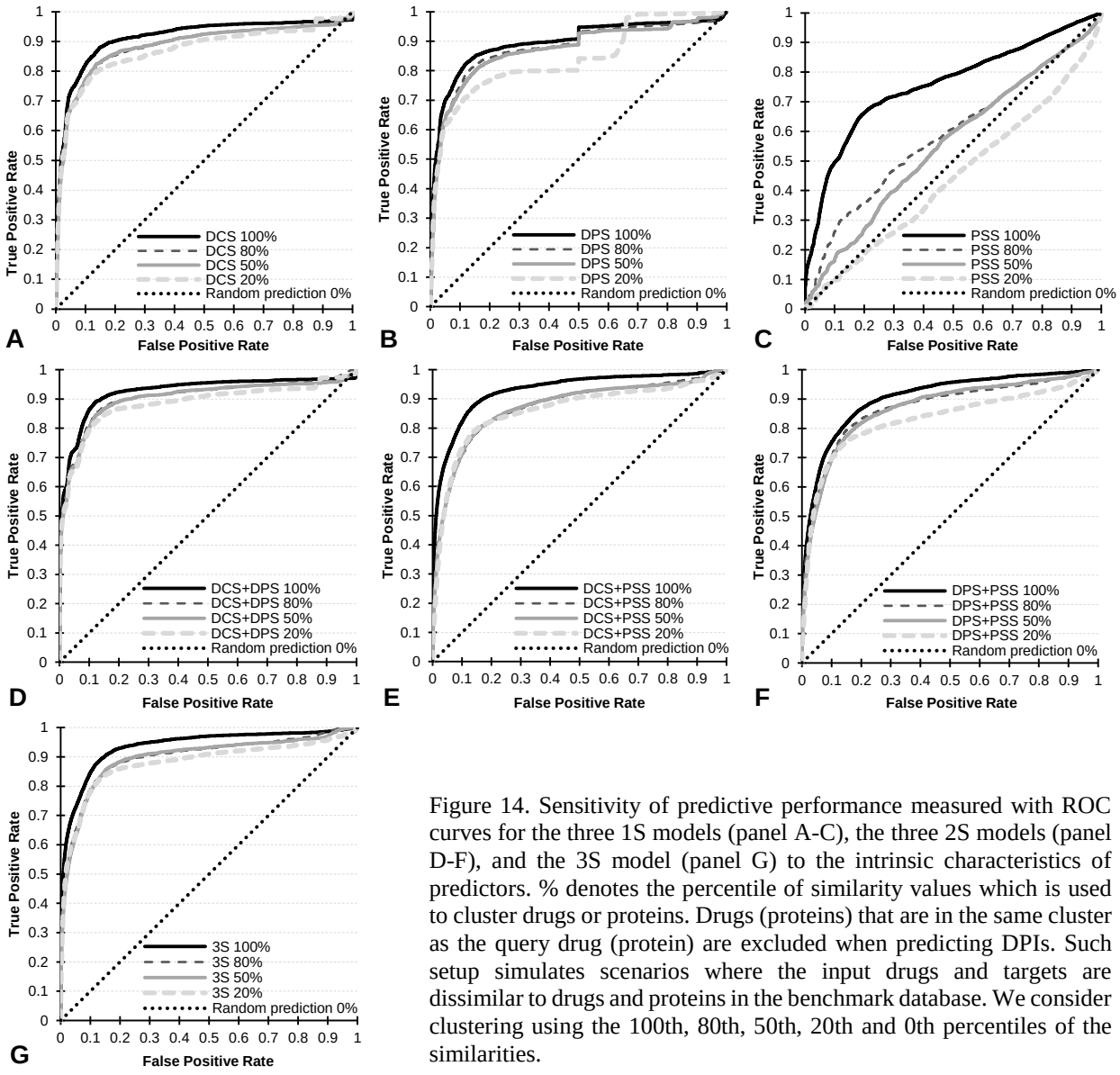

Figure 14. Sensitivity of predictive performance measured with ROC curves for the three 1S models (panel A-C), the three 2S models (panel D-F), and the 3S model (panel G) to the intrinsic characteristics of predictors. % denotes the percentile of similarity values which is used to cluster drugs or proteins. Drugs (proteins) that are in the same cluster as the query drug (protein) are excluded when predicting DPIs. Such setup simulates scenarios where the input drugs and targets are dissimilar to drugs and proteins in the benchmark database. We consider clustering using the 100th, 80th, 50th, 20th and 0th percentiles of the similarities.

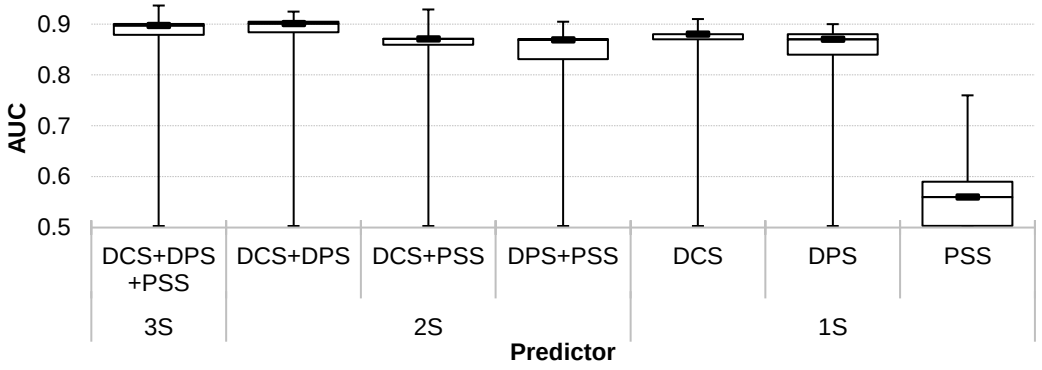

Figure 15. Sensitivity of predictive performance to the intrinsic characteristics of predictors. The box-plots denotes the AUC values for the scenarios where drugs (proteins) similar to the query drug (protein) are excluded from predictions based on clustering using the 100^{th}, 80^{th}, 50^{th}, and 20^{th} percentile of the similarities. The bottom bar denotes random predictions that corresponds to the 0^{th} percentile (AUC = 0.5).

Figure 14 shows the ROC curves for the five scenarios and the three 1S, three 2S, and one 3S model. Figure 15 summarizes the corresponding AUC values. In general, all but one model are not sensitive to the three intrinsic characteristics. The range of AUC values between 100^{th} and 20^{th} percentiles of similarities for the 3S, the three 2S, DCS, and DPS models is narrow. This means that predictive quality drops by only between 0.04 (DCS+DPS and DCS) and 0.07 (DCS+PSS and DPS+PSS) with the decrease in similarities by 80%. Consequently, the six models offer high predictive quality even when dealing with the input drugs that have low similarity to the benchmark database. The one exception is the PSS model for which the predictive performance is sensitive to the degree of similarity to the targets in the database. Its AUC value substantially drops from 0.76 (100^{th} percentile; clustering threshold for PSS = 0.4 which corresponds to 40% pairwise sequence similarity) to 0.56 (50^{th} percentile; threshold = 19% pairwise sequence similarity). The results for the 20^{th} percentile of PSS (threshold = 10% pairwise sequence similarity) are equivalent to random predictions. This is consistent with previous studies which unveiled that protein sequences with identity < 0.25 are likely to have different functions and structures [323, 324]. This is also related to our observations in the Figure 10 where the distributions of the PSS values overlap

between interacting and non-interacting drug-protein pairs, in particular when compared to DCS and DPS.

This analysis also confirms that use of a larger set of similarities in general results in an improved predictive performance. In particular, for the 100^{th} percentile scenario, the AUC of the best 1S model is 0.91, the best 2S model is 0.93, and the 3S model is 0.94. Because the adoption of low PSS similarities results in lower predictive performance, combining it with DCS or DPS into a 2S model does not enhance predictive performance (compare DCS+PSS vs DCS, and DPS+PSS vs DPS plots in Figure 15).

The results of analysis of sensitivity to the intrinsic characteristics of predictors reveal that the predictive performance is not sensitive to the values of DCS and DPS, while it is sensitive to the values of PSS. Moreover, combining PSS with DCS and/or DPS makes the predictors robust to the low values of PSS. We conclude that use of PSS only model is risky when the known targets of query drug are dissimilar to the targets in the benchmark database.

5.3.2 Sensitivity to extrinsic characteristics

Predictive performance could also be sensitive to extrinsic characteristics that describe known a priori input drug structure, drug profile, and protein target. We are the first to investigate several extrinsic characteristics for each of the three types of similarities. They include surface area, charge, shape, weight, size, lipophilicity, number of similar drugs, number of similar drugs sharing targets, and similarity to the most similar drugs which are computed from the drug structure. We also considered three markers of drug profiles: number of side-effects, similarity of the profile to the most similar profile, and number of similar profiles. Finally, we investigated three markers of the input drug targets: number of known targets, number of known targets that interact with similar drugs, and known targets that interact with the most similar drug. We discuss one “best” marker

for each type of similarity, which we selected based on the fact that it significantly affects the predictive performance and is easy to quantify. These markers include the number of similar drug structures that share targets with the input drug, the number of side-effects, and the number of known targets.

We study sensitivity of predictive quality to these extrinsic markers by partitioning the considered drugs into two groups for which we observe large differences in predictive performance. For the best DCS marker, we compare 177 drugs that share targets with < 50 similar drugs (which corresponds to the median level of DCS) vs the remaining drugs that share targets with a larger number of similar drugs. Similarly, for the best DPS characteristic, we contrast 55 drugs that have relatively small side-effects profile (<40) vs the remaining drugs that have a larger profile. Finally, for the best PSS marker, we compare 128 drugs with < 20 native targets vs the remaining more promiscuous drugs. Figure 16 compares distributions of AUC_{drug} values between these groups of drugs when considering the corresponding 1S models and the 3S model.

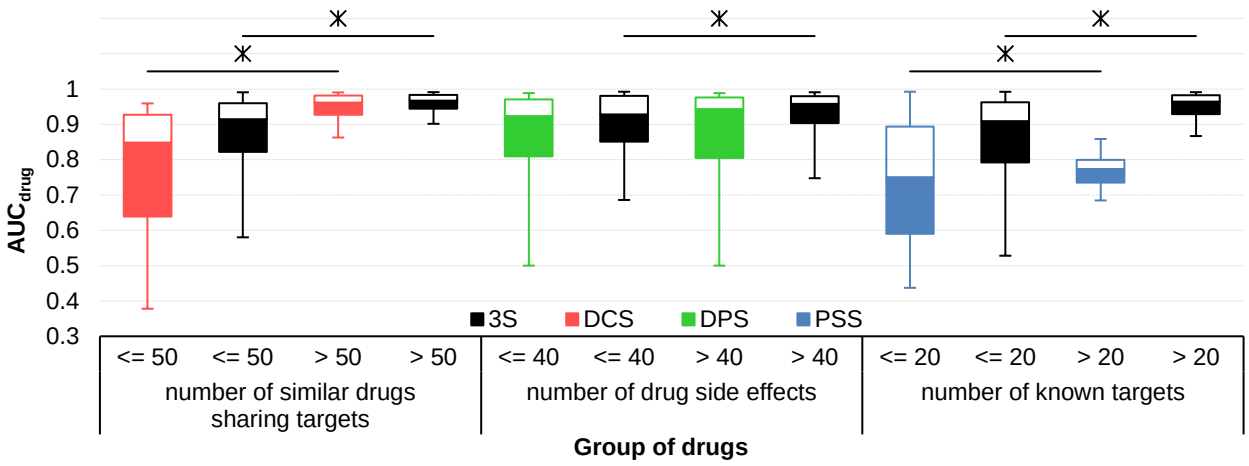

Figure 16. Sensitivity of predictive quality to extrinsic characteristics of predictors. The boxplots denote the 5th, 20th, 50th, 80th, and 95th percentiles of AUC_{drug} values for the 1S and 3S model over the corresponding two groups of drugs separated with help of a given marker that characterizes the input drug/targets. The asterisk indicates that the difference in the AUC_{drug} is significant (p-value < 0.05) between drug groups. We assess significance of differences between the corresponding two groups of drugs using the Wilcoxon rank sum test [317]; we use the non-parametric test since these data are not normal according to the Anderson-Darling test at 0.01 significance.

Figure 16 shows that the AUC_{drug} for DCS varies substantially between 0.38 and 0.96 with a median = 0.85 for the drugs that share targets with fewer similar drugs. For the remaining drugs that share targets with the larger number of similar drugs, the AUC_{drug} for DCS is always > 0.86 with a median = 0.96. These drugs have lower variation and significantly higher values for AUC_{drug} (p-value < 0.05) when compared to the drug that share targets with fewer similar drugs. Similarly, the 3S model also has significantly higher AUC_{drug} values with narrower spread for the drugs with larger number of similar drugs sharing targets. These observations reveal that the predictive quality is significantly higher when working with drugs that share targets with a larger number of similar drugs in the benchmark database. Based on the assertion that similar drugs tend to target the same proteins, that makes it easier to accurately identify targets for such drugs when using DCS. In contrast, the drugs that share targets with a low number of similar drugs are harder to accurately predict.

The AUC_{drug} for DPS is lower for the drugs that have a smaller profile (median AUC_{drug} = 0.92) than for the drugs that have larger profile (median AUC_{drug} = 0.94), but this difference is not statistically significant (*p*-value = 0.17). The corresponding difference for the 3S model is slightly higher and statistically significant (*p*-value < 0.05): median AUC_{drug} = 0.93 vs 0.96, respectively. The sensitivity to the size of the drug profile is expected since a larger profile offers more information that in turn result in a more accurate quantification of DPS.

The differences in AUC_{drug} between the less vs more promiscuous drugs are significant for the PSS and 3S models (*p*-value < 0.05). The median AUC_{drug} for the 3S model is 0.91 for the less promiscuous drugs while it equals 0.96 for the more promiscuous drugs. Similarly, for the 1S model that relies on PSS the median AUC_{drug} = 0.75 vs 0.77. This trend could be explained by an observation that the drugs which interact with many targets are more likely to have targets that are highly similar to the proteins in the benchmark database. This is supported by the assertion that similar proteins tend to interact with the same drugs.

The results of the analysis of sensitivity to the extrinsic characteristics reveal that the predictive performance is sensitive to several easy to estimate characteristics of the input drug structures, drug profiles, and drug targets. As expected, we find that it is more likely to secure higher predictive quality when a more comprehensive information is available for the input drugs, such as a larger number of similar drugs sharing targets, a larger drug profile, and a higher number of known targets.

5.4 CONNECTOR webserver

CONNECTOR (prediCtOr of compouNd-proteiN intEraCTiOn based on ensemble of similaRities) is a webserver that implements the seven predictors that we evaluate in this review.

The webserver and the benchmark database are freely available at http://biomine.cs.vcu.edu/servers/CONNECTOR/. Figure 17 shows the interface of the webserver.

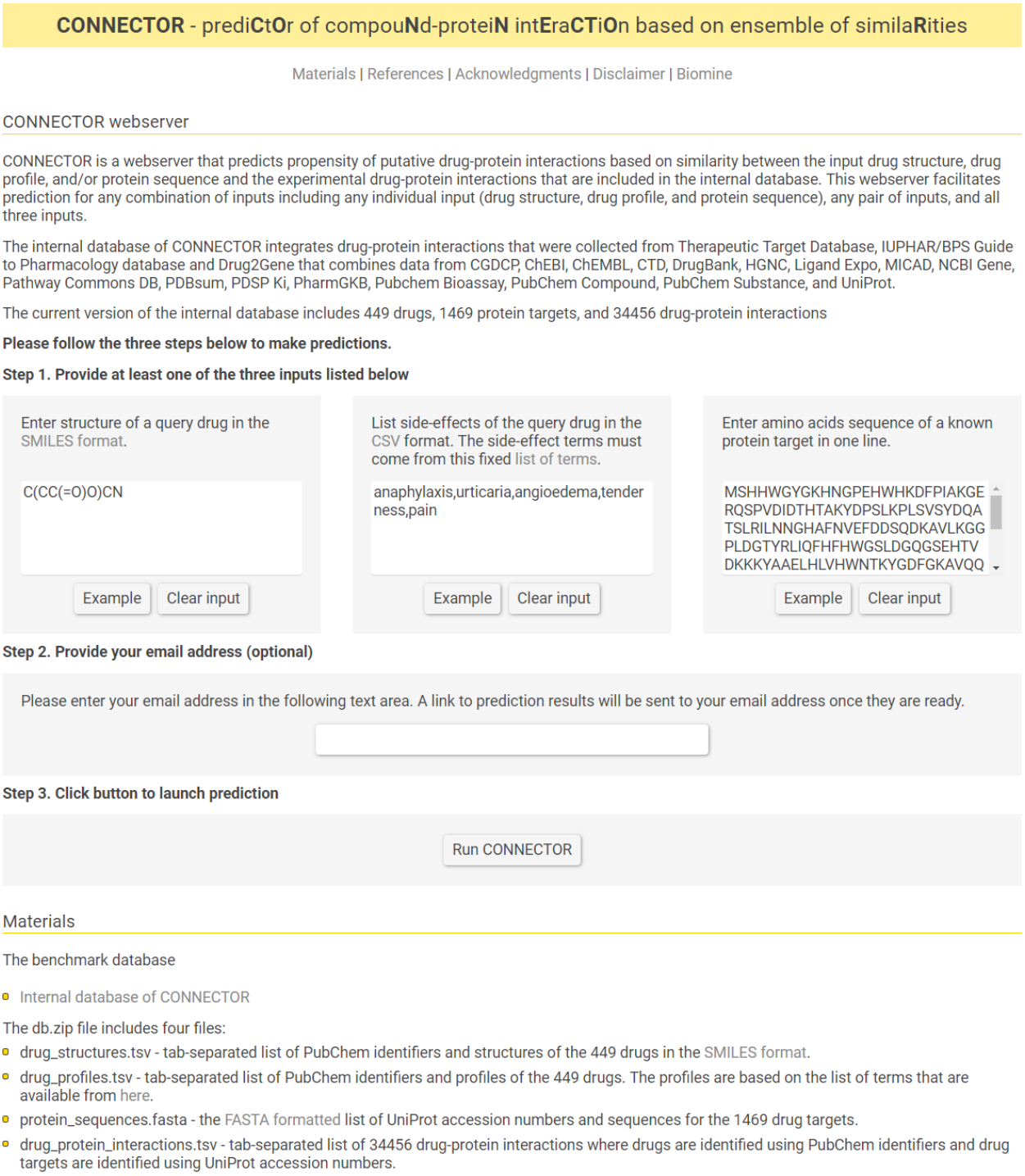

Figure 17. The interface of the CONNECTOR webserver.

CONNECTOR facilitates prediction for any combination of the three inputs including any individual input (drug structure, drug profile, and protein sequence), any pair of inputs, and all three inputs. CONNECTOR uses the benchmark dataset as its internal database. The computations are performed on the server side and thus the end user only needs to access the webserver page via any major web browser and provide the inputs. The prediction is performed in three steps: 1) provide any combination of the three inputs including drug structure in the SMILES format, comma separated list of side effects (drug profile), and/or protein sequences in the FASTA format; 2) provide email address where a unique link to the results will be sent once the predictions are ready; and 3) click "Run CONNECTOR" (see Figure 17). Each submitted job is entered into a FIFO queue of jobs on the server. User is notified via the browser window about the current placement in the queue and when the job reaches the front of the queue. The results are displayed in the browser window and the unique link to the page with the results is sent to the user-identified email address. We provide four views of the results:

- All DPIs, which shows all putative drug-protein pairs that include query drug and target(s) and similar compounds and proteins.
- DPIs that include the query drug structure, which cover interactions between the query drug structure and its putative protein targets (if drug structure was provided as one of the inputs)
- DPIs that include the query drug profile, which include interactions between the query drug represented by its profile and its putative protein targets (if drug profile was provided as one of the inputs)
- DPIs that include the query protein sequence, which gives interactions between the query target sequence and the drugs that are predicted to interact with this target (if target sequence was provided as one of the inputs)

Each putative interaction is coupled with the corresponding value of similarity. Drugs are linked to their entries in the PubChem databases and target sequences are linked to their UniProt entries. For user's convenience, similarities between query drug/target and the drug/target used to make prediction and the propensities of putative drug-protein interactions are color-coded. Dark green/green/light green/pale green/red denotes that the corresponding drug-protein pair is very likely/likely/moderately likely/unlikely/very unlikely to interact. We annotate these five colors based on the values of the similarity that belong to the top 20%, 20 to 40%, 40 to 60%, 60 to 80%, and the bottom 20% of the distribution of these values. We also provide a text-based version of the results for download. We will store the page with the results for at least three months.

5.5 Conclusions

We have developed a novel benchmark database that includes drugs characterized by high density of interactions and we use it to evaluate a representative set of 1S, 2S, and 3S predictors. This database integrates data coming from three resources (19 source databases) and includes 449 drugs, 1469 druggable human proteins, and 34456 native DPIs, resulting in high density of native DPIs per drug that equals 76. We observe that most of the surveyed methods have evaluated predictive performance on both DPIs and non-DPIs, which allowed for computation of TPR, FPR, and the resulting AUC values. However, these methods accessed predictive performance only at the interaction level that spans multiple drugs which may differ in structure, profile, and the number and type of protein partners that they bind to. We are the first to perform both interaction- and drug-level assessments and to comprehensively and side-by-side compare all 1S, 2S, and 3S models.

At the interaction level, we reveal that the use of ensembles results in improved predictive quality. Specifically, the 3S model significantly outperforms the 1S and 2S models, while the 2S models are significantly more accurate than the 1S models. We empirically analyze reasons for these improvements and we show that they stem from an improved handling of interactions characterized by modest levels of similarities. Among the three 1S models, DCS and DPS are more accurate than PSS. We also find a modest level of correlation between DCS and DPS while correlations between PSS and DCS as well as PSS and DPS are low. The modest or low levels of correlations further explain why the ensembles benefit from the integration of multiple similarities and why the majority of current predictors are ensembles.

At the drug level, we demonstrate that the predictive quality varies widely between drugs and these differences depend on the type of similarity used. We show that no single 1S model could provide accurate DPI predictions across all the drugs. Moreover, we demonstrate that ensembles improve over the 1S models. The average relative improvements in AUC_{drug} over the 449 drugs between the best 1S model, DCS, and the four ensembles are: 2% (compared to DCS+DPS), 5% (DCS+PSS), 7% (DPS+PSS), and 8% (3S). We divide drugs into three groups: group one includes 150 drugs with high AUC_{drug} for DCS; group two includes 195 drugs with moderate AUC_{drug} for DCS; and group three with 104 drugs for which AUC_{drug} for DCS is on average lower than DPS and PSS. We found that the use of 3S ensemble provides particularly large improvements by on average 29% in AUC_{drug} over the use of DCS for the 23% of drugs which constitute the third group. Our empirical analysis also reveals that although per-interaction PSS provides the lowest predictive performance, it outperforms the other two 1S models for 13% of drugs when assessed at the drug level. These drugs should be of particular focus for the development of future DPI predictors because more accurate predictions could be obtained with the help of the DPS and PSS

rather than with the overall most accurate at the interaction-level DCS that dominates the current methods.

DPI prediction relies on accurate values of similarities between the query drug (its known target) and the drugs (proteins) in the benchmark database. The quality of these values is likely affected by the intrinsic characteristics of predictors, such as the similarity between inputs and the benchmark database. We provide the first-of-its-kind sensitivity analysis of predictive quality for each of the three similarities. We find that the predictive quality is not sensitive to the values of DCS and DPS, which means that the predictive performance of the methods that utilize DCS/DPS does not substantially change when the input drug structures or profiles are dissimilar to the structures and profiles in the internal database. In contrast, the predictive quality for PSS drops significantly when the input protein sequences are dissimilar to the sequences in the database. However, such sensitivity to low values of PSS is mitigated when using methods that combine PSS with other similarities. These observations demonstrate that the ensembles are not only accurate at the interaction and drug levels but they are also robust to low values of similarities.

We are also the first to investigate sensitivity of predictive quality to extrinsic characteristics of the predictive models. These extrinsic characteristics are intrinsic to the inputs and include information extracted directly from drug structures, drug profiles, and drug targets. We find that the 3S model and the corresponding three 1S models are more likely to provide accurate predictions when the input drugs share targets with a larger number of similar drugs in the benchmark database, when the input drugs have larger side-effect profiles, and when the input drugs are more promiscuous. This suggest that a larger amount of available data (number of known targets and/or side-effects) leads to calculations of higher quality and higher values of similarities, which in turn results in higher predictive performance.

Chapter 6 Summary and conclusions

This dissertation has three goals that focus on the prediction and analysis of the DPIs in the druggable human proteome. In Chapter 2 we provide a brief introduction to the related background to explain and motivate our goals. This chapter includes information about protein and drug-protein complex structures that define molecular-level details of the therapeutic and off-target effects of drugs, as well as a summary and classification of current publications related to the computational predictions of DPIs. This is followed by the subsequent three chapters which detail methods and results for each of the three goals. My original contributions in this dissertation that are organized under each of the three goals include:

Goal 1: Evaluation of protein structure-based DPI predictors and development of DPI database.

- We provide empirical comparative analysis of the protein structure-based DPI predictors: eFindSite, SMAP and ILbind.
- We develop and deploy the PDID database that stores 1.1 million predictions and 17 thousand high-confidence putative DPIs for the entire structure human proteome and provides interface for drug-based, protein-based, and target sequence-based data queries.

Goal 2: Review of the similarity-based DPI predictors.

- We review a comprehensive set of 35 high-impact similarity-based DPI predictors spanning from the three pioneering methods in this area which were published a decade ago to eight most recent approaches which have never been covered by other surveys.
- We define the categorization of similarity-based DPI predictors based on the types and numbers of similarities that they use.
- We review the 12 source databases that are used to derive the internal databases of predictors and we comprehensively explain connections between the internal and source databases.
- We investigate impact and describe internal databases of the 35 considered methods including the recent approaches.
- We analyze the use of similarities and ensembles in the considered set of 35 predictors.
- We critically analyze drawbacks of current reviews and methods in this area.

Goal 3: Empirical assessment and comparative analysis of similarity-based DPI predictors.

- We develop and release a novel benchmark database that covers large-scale drug-protein data and high-density DPIs. This database is particularly suitable for comparative empirical assessment of DPI predictors.
- We are the first to compare all seven representative predictors including three individual predictors that rely on each of the three main types of similarities and four ensemble predictors that combine two or three similarities.
- We are the first to assess predictive quality at the drug level. This novel drug-level assessment of predictive performance provides additional insights.

- We provide a first-of-its-kind sensitivity analysis of predictive performance to the intrinsic characteristics of DPI predictors which describe the similarities between the inputs and the benchmark database.
- We are also the first to analyze the sensitivity of predictive performance to the extrinsic characteristics that are the priori known properties of the input drug structures, drug profiles, and protein targets.
- We develop and release at http://biomine.cs.vcu.edu/servers/CONNECTOR/ the CONNECTOR webserver that implements seven similarity-based DPI predictors that we assessed.

Following, we summarize the work done and list major conclusions for each of the three goals. In the context of the *first goal*, we empirically assess the predictive quality of three representative protein structure-based approaches for the prediction of the DPIs. This is done for dozens of representative drugs over the structural human proteome. Out tests show that these three methods provide relatively accurate predictions. Relying on the putative DPIs that were accurately predicted by these approaches and the native DPIs collected from PDB, DrugBank and BindingDB, we develop and deploy a large-scale database of putative and native DPIs. This PDID database stores 1.1 million predictions that cover 51 popular and representative drugs and the entire structural human proteome, which includes 9652 protein structures. PDID maps the drugs to their target proteins, where these interactions may correspond to therapeutic effects and/or adverse events. The database helps to comprehensively catalogs drug targets, facilitates repurposing and repositioning of existing drugs, and unveils an opportunity to systematically analyze molecular-level DPIs at a proteome scale. The research related to this goal was published in Ref. [29].

For the *second goal*, we completed a comprehensive review for 35 selected high-impact similarity-based DPI predictors. These similarity-based methods offer the opportunity to perform prediction when protein structures are unavailable, complementing the protein-structure based methods that are studied in our first goal. We systematically summarize the key aspects of these similarity-based predictors including their methodological underpinnings, volume and coverage of their internal databases, information about source databases, inclusion of empirical analysis, timeline of development, and their impact. Majority of them were published in high-impact journals and are highly cited, suggesting that they are of substantial value to the community. Our review shows that combining more source databases would likely further increase the completeness of information about drug promiscuity in the internal databases. This would benefit predictive quality of the similarity-based predictors and would also enable the development of higher-quality benchmark databases. Additionally, we note that regular update and dissemination would help to increase the effectiveness, completeness, and impact of the source databases. Periodic publications and peer review will also boost quality of underlying data and features. Given the fact that three main types of similarities are used by these methods, we categorize the 35 tools based on the number of similarities that they apply and combine together. We find that most of these methods ensemble two or three similarities. Recently, DCS and PSS are frequently employed and combined to constitute ensemble predictors while DPS is infrequently utilized due to the incompleteness and difficulty in acquiring side-effect profiles of drugs. Moreover, we unveil drawbacks of current reviews and methods: lack of a systematic empirical analysis of predictive quality for individual drugs; lack of an in-depth analysis of sensitivity of predictive performance to intrinsic and extrinsic characteristics of predictors is missing; and lack of a comprehensive

comparative analysis that includes the three single-similarity-based predictors and the four ensembles.

The *third goal* was motivated by the drawbacks of the current reviews and similarity-based methods which we uncovered in our second goal. To overcome these drawbacks, we implement, empirically evaluate, and compare all seven representative similarity-based DPI predictors. We develop a novel benchmark database that stores a comprehensive collection of high-quality DPIs which we harvested from 19 data sources. The benchmark database also encompasses essential information for the development of similarity-based methods, including chemical structures and side-effect profiles of drugs and protein sequences of drug targets. Like in the previous studies we assess the predictive performance of the seven representative predictors at the interaction level. We also provide the first-of-its-kind assessment of predictive quality at the drug level. This drug-level analysis shows that different combination of similarities should be used for different drugs to obtain more accurate predictions. Moreover, we reveal that ensembles of multiple similarities offer higher predictive quality than models that rely on single or fewer similarities. This result is consistent for evaluations at both interaction and drug levels. We are the first to analyze the sensitivity of predictive quality to the intrinsic and extrinsic characteristics of predictors. Our analysis reveals sensitivity to lower values of PSS while the predictive quality is not sensitive to values of DCS and DPS. This suggests that the approach using PSS only would not provide accurate predictions when the input proteins are dissimilar to the proteins in the internal database. However, ensemble models are robust to low values of similarities. The sensitivity analysis also demonstrates that the predictive quality could benefit from a larger amount of information for the inputs, including a larger a larger number of similar drugs sharing targets in the internal database,

a larger side-effect profile, and a larger number of known targets. These conclusions arguably offer a useful guidance for the selection of similarity-based predictors for specific drugs and protein targets.

The studies and conclusions summarized above inspire several possible directions for future works. Combining a larger and more diverse set of source databases would likely further improve quality of the internal databases, which in turn would further boosts the predictive quality. Authors of future predictors should consider to integrate recent and comprehensive resources, such as the DGIdb database [245, 246] and Pharos database [243], to expand our benchmark database and/or the internal databases of their algorithms. Additionally, since the size of the benchmark database is primarily limited by the availability of drug profiles in the SIDER database, we recommend that future works should also consider combining related information about drug side-effects from the MetaADEDB [296] and IntSide database [128]. Moreover, most of the current development efforts focuses on protein targets that are structured [20]. However, about 30% of eukaryotic proteins are either fully disordered or have long regions of intrinsic disorder [83, 325]. These disordered proteins are implicated in a wide range of diseases [326-333]. Moreover, certain protein families are enriched in the intrinsic disorder, such as nuclear receptors, kinases, and various enzymes [20, 83, 84, 334-336]. These protein families include important therapeutic drug targets and druggable proteins [1, 2, 18, 19, 44]. This prompts our recommendation that future works should invest into the development of disorder-specific DPI databases and methods, which by definition cannot rely on the protein structure-based computations.

Bibliography

1. Rask-Andersen M, Masuram S, Schioth HB. The druggable genome: Evaluation of drug targets in clinical trials suggests major shifts in molecular class and indication, Annu Rev Pharmacol Toxicol 2014;54:9-26.
2. Imming P, Sinning C, Meyer A. Drugs, their targets and the nature and number of drug targets, Nat Rev Drug Discov 2006;5:821-834.
3. Schneider G. Virtual screening: an endless staircase?, Nat Rev Drug Discov 2010;9:273-276.
4. Núñez S, Venhorst J, Kruse CG. Target–drug interactions: first principles and their application to drug discovery, Drug Discov Today 2012;17:10-22.
5. Dalkas GA, Vlachakis D, Tsagkrasoulis D et al. State-of-the-art technology in modern computer-aided drug design, Brief Bioinform 2013;14:745-752.
6. Tseng CY, Tuszynski J. A unified approach to computational drug discovery, Drug Discov Today 2015;20:1328-1336.
7. Chong CR, Sullivan DJ. New uses for old drugs, Nature 2007;448:645-646.
8. Haupt VJ, Schroeder M. Old friends in new guise: repositioning of known drugs with structural bioinformatics, Brief Bioinform 2011;12:312-326.
9. Oprea TI, Mestres J. Drug repurposing: far beyond new targets for old drugs, AAPS J 2012;14:759-763.
10. Hu Y, Bajorath J. Compound promiscuity: what can we learn from current data?, Drug Discov Today 2013;18:644-650.
11. Li J, Zheng S, Chen B et al. A survey of current trends in computational drug repositioning, Brief Bioinform 2016;17:2-12.
12. Lounkine E, Keiser MJ, Whitebread S et al. Large-scale prediction and testing of drug activity on side-effect targets, Nature 2012;486:361-367.
13. Wang J, Li Z-x, Qiu C-x et al. The relationship between rational drug design and drug side effects, Brief Bioinform 2012;13:377-382.
14. Kuhn M, Al Banchaabouchi M, Campillos M et al. Systematic identification of proteins that elicit drug side effects, Mol Syst Biol 2013;9:663.
15. Tarcsay Á, Keserű GM. Contributions of Molecular Properties to Drug Promiscuity, J Med Chem 2013;56:1789-1795.
16. Hu G, Wang K, Groenendyk J et al. Human structural proteome-wide characterization of Cyclosporine A targets, Bioinformatics 2014;30:3561-3566.

17. Cimermancic P, Weinkam P, Rettenmaier TJ et al. CryptoSite: Expanding the Druggable Proteome by Characterization and Prediction of Cryptic Binding Sites, J Mol Biol 2016;428:709-719.
18. Hopkins AL, Groom CR. The druggable genome, Nat Rev Drug Discov 2002;1:727-730.
19. Russ AP, Lampel S. The druggable genome: an update, Drug Discov Today 2005;10:1607-1610.
20. Hu G, Wu Z, Wang K et al. Untapped Potential of Disordered Proteins in Current Druggable Human Proteome, Curr Drug Targets 2016;17:1198-1205.
21. Chen X, Yan CC, Zhang X et al. Drug-target interaction prediction: databases, web servers and computational models, Brief Bioinform 2016;17:696-712.
22. Glaab E. Building a virtual ligand screening pipeline using free software: a survey, Brief Bioinform 2016;17:352-366.
23. Southan C, Sitzmann M, Muresan S. Comparing the Chemical Structure and Protein Content of ChEMBL, DrugBank, Human Metabolome Database and the Therapeutic Target Database, Mol Inform 2013;32:881-897.
24. Hughes JP, Rees S, Kalindjian SB et al. Principles of early drug discovery, Br J Pharmacol 2011;162:1239-1249.
25. Chen B, Butte AJ. Leveraging big data to transform target selection and drug discovery, Clin Pharmacol Ther 2016;99:285-297.
26. Pessetto ZY, Chen B, Alturkmani H et al. In silico and in vitro drug screening identifies new therapeutic approaches for Ewing sarcoma, Oncotarget 2017;8:4079-4095.
27. Gao Z, Li H, Zhang H et al. PDTD: a web-accessible protein database for drug target identification, BMC Bioinformatics 2008;9:104.
28. Li L, Bum-Erdene K, Baenziger PH et al. BioDrugScreen: a computational drug design resource for ranking molecules docked to the human proteome, Nucleic Acids Res 2010;38:D765-773.
29. Wang C, Hu G, Wang K et al. PDID: database of molecular-level putative protein-drug interactions in the structural human proteome, Bioinformatics 2016;32:579-586.
30. Xie L, Li J, Xie L et al. Drug Discovery Using Chemical Systems Biology: Identification of the Protein-Ligand Binding Network To Explain the Side Effects of CETP Inhibitors, PLoS Comput Biol 2009;5:e1000387.
31. Xie L, Evangelidis T, Xie L et al. Drug Discovery Using Chemical Systems Biology: Weak Inhibition of Multiple Kinases May Contribute to the Anti-Cancer Effect of Nelfinavir, PLoS Comput Biol 2011;7:e1002037.
32. Ding H, Takigawa I, Mamitsuka H et al. Similarity-based machine learning methods for predicting drug-target interactions: a brief review, Brief Bioinform 2014;15:734-747.
33. Schomburg KT, Rarey M. What is the potential of structure-based target prediction methods?, Future Med Chem 2014;6:1987-1989.
34. Somody JC, MacKinnon SS, Windemuth A. Structural coverage of the proteome for pharmaceutical applications, Drug Discov Today 2017.
35. Berman HM, Westbrook J, Feng Z et al. The Protein Data Bank, Nucleic Acids Res 2000;28:235-242.
36. RCSB PDB - Browse Human Genes. http://www.rcsb.org/pdb/browse/homo_sapiens.do (April 13 2017, date last accessed).
37. Consortium TU. UniProt: the universal protein knowledgebase, Nucleic Acids Res 2017;45:D158-D169.

38. Proteomes - Homo sapiens (Human). http://www.uniprot.org/proteomes/UP000005640 (April 13 2017, date last accessed).
39. Petrunak EM, DeVore NM, Porubsky PR et al. Structures of Human Steroidogenic Cytochrome P450 17A1 with Substrates, J Biol Chem 2014;289:32952-32964.
40. Kabsch W, Sander C. Dictionary of protein secondary structure: Pattern recognition of hydrogen-bonded and geometrical features, Biopolymers 1983;22:2577-2637.
41. Touw WG, Baakman C, Black J et al. A series of PDB-related databanks for everyday needs, Nucleic Acids Res 2015;43:D364-D368.
42. Moreland JL, Gramada A, Buzko OV et al. The Molecular Biology Toolkit (MBT): a modular platform for developing molecular visualization applications, BMC Bioinformatics 2005;6:21.
43. Yang H, Qin C, Li YH et al. Therapeutic target database update 2016: enriched resource for bench to clinical drug target and targeted pathway information, Nucleic Acids Res 2016;44:D1069-D1074.
44. Santos R, Ursu O, Gaulton A et al. A comprehensive map of molecular drug targets, Nat Rev Drug Discov 2017;16:19-34.
45. Rask-Andersen M, Almén MS, Schiöth HB. Trends in the exploitation of novel drug targets, Nat Rev Drug Discov 2011;10:579-590.
46. Paul SM, Mytelka DS, Dunwiddie CT et al. How to improve R&D productivity: the pharmaceutical industry's grand challenge, Nat Rev Drug Discov 2010;9:203-214.
47. Mestres J, Gregori-Puigjane E, Valverde S et al. Data completeness—the Achilles heel of drug-target networks, Nat Biotech 2008;26:983-984.
48. Lavecchia A, Giovanni CD. Virtual Screening Strategies in Drug Discovery: A Critical Review, Curr Med Chem 2013;20:2839-2860.
49. Bowes J, Brown AJ, Hamon J et al. Reducing safety-related drug attrition: the use of in vitro pharmacological profiling, Nat Rev Drug Discov 2012;11:909-922.
50. Urban L. Translational value of early target-based safety assessment and associated risk mitigation. In: 4th Annual Predictive Toxicology Summit. London, UK, 2012.
51. Wang XY, Greene N. Comparing Measures of Promiscuity and Exploring Their Relationship to Toxicity, Molecular Informatics 2012;31:145-159.
52. Bendels S BC, Fasching B, Fischer H, Gerebtzoff G, Guba W, Hert J, Kansy M, Migeon J, Peters J, et al. Safety screening in early drug discovery: An improved assay profile. In: Gordon Research Conference on Computer Aided Drug Design. Mount Snow (VT), USA, 2013.
53. Progesterone - Drugbank. http://www.drugbank.ca/drugs/DB00396 (May 14 2018, date last accessed).
54. Williams SP, Sigler PB. Atomic structure of progesterone complexed with its receptor, Nature 1998;393:392.
55. Skolnick J, Gao M, Roy A et al. Implications of the small number of distinct ligand binding pockets in proteins for drug discovery, evolution and biochemical function, Bioorg Med Chem Lett 2015;25:1163-1170.
56. Zhu X, Xiong Y, Kihara D. Large-scale binding ligand prediction by improved patch-based method Patch-Surfer2.0, Bioinformatics 2015;31:707-713.
57. Hu B, Zhu X, Monroe L et al. PL-PatchSurfer: a novel molecular local surface-based method for exploring protein-ligand interactions, Int J Mol Sci 2014;15:15122-15145.
58. Ito J, Tabei Y, Shimizu K et al. PDB-scale analysis of known and putative ligand-binding sites with structural sketches, Proteins 2012;80:747-763.

59. Ito J, Tabei Y, Shimizu K et al. PoSSuM: a database of similar protein-ligand binding and putative pockets, Nucleic Acids Res 2012;40:D541-548.
60. Ito J, Ikeda K, Yamada K et al. PoSSuM v.2.0: data update and a new function for investigating ligand analogs and target proteins of small-molecule drugs, Nucleic Acids Res 2015;43:D392-398.
61. Ji ZL, Wang Y, Yu L et al. In silico search of putative adverse drug reaction related proteins as a potential tool for facilitating drug adverse effect prediction, Toxicol Lett 2006;164:104-112.
62. Hendlich M, Bergner A, Gunther J et al. Relibase: design and development of a database for comprehensive analysis of protein-ligand interactions, J Mol Biol 2003;326:607-620.
63. Kuntz ID, Blaney JM, Oatley SJ et al. A geometric approach to macromolecule-ligand interactions, J Mol Biol 1982;161:269-288.
64. Brylinski M, Skolnick J. A threading-based method (FINDSITE) for ligand-binding site prediction and functional annotation, Proceedings of the National Academy of Sciences 2008;105:129-134.
65. Skolnick J, Brylinski M. FINDSITE: a combined evolution/structure-based approach to protein function prediction, Brief Bioinform 2009;10:378-391.
66. Brylinski M, Feinstein WP. eFindSite: Improved prediction of ligand binding sites in protein models using meta-threading, machine learning and auxiliary ligands, J Comput-Aided Mol Des 2013;27:551-567.
67. Feinstein WP, Brylinski M. eFindSite: Enhanced Fingerprint-Based Virtual Screening Against Predicted Ligand Binding Sites in Protein Models, Molecular Informatics 2014;33:135-150.
68. Xie L, Bourne PE. A robust and efficient algorithm for the shape description of protein structures and its application in predicting ligand binding sites, BMC Bioinformatics 2007;8 Suppl 4:S9.
69. Xie L, Bourne PE. Detecting evolutionary relationships across existing fold space, using sequence order-independent profile-profile alignments, Proc Natl Acad Sci U S A 2008;105:5441-5446.
70. Xie L, Xie L, Bourne PE. A unified statistical model to support local sequence order independent similarity searching for ligand-binding sites and its application to genome-based drug discovery, Bioinformatics 2009;25:i305-312.
71. Chartier M, Najmanovich R. Detection of Binding Site Molecular Interaction Field Similarities, J Chem Inf Model 2015;55:1600-1615.
72. Chartier M, Adriansen E, Najmanovich R. IsoMIF Finder: online detection of binding site molecular interaction field similarities, Bioinformatics 2016;32:621-623.
73. Brylinski M, Lingam D. eThread: a highly optimized machine learning-based approach to meta-threading and the modeling of protein tertiary structures, PLoS One 2012;7:e50200.
74. Brylinski M, Feinstein W. Setting up a meta-threading pipeline for high-throughput structural bioinformatics: eThread software distribution, walkthrough and resource profiling, J Comput Sci Syst Biol 2012;6:001-010.
75. Frey BJ, Dueck D. Clustering by passing messages between data points, Science 2007;315:972-976.
76. Hu G, Gao J, Wang K et al. Finding protein targets for small biologically relevant ligands across fold space using inverse ligand binding predictions, Structure 2012;20:1815-1822.
77. Gaudreault F, Morency L-P, Najmanovich RJ. NRGsuite: a PyMOL plugin to perform docking simulations in real time using FlexAID, Bioinformatics 2015;31:3856-3858.

78. Chartier M, Morency L-P, Zylber MI et al. Large-scale detection of drug off-targets: hypotheses for drug repurposing and understanding side-effects, BMC Pharmacology and Toxicology 2017;18:18.
79. Mizianty MJ, Fan X, Yan J et al. Covering complete proteomes with X-ray structures: a current snapshot, Acta Crystallogr D Biol Crystallogr 2014;70:2781-2793.
80. Liu T, Altman RB. Relating Essential Proteins to Drug Side-Effects Using Canonical Component Analysis: A Structure-Based Approach, J Chem Inf Model 2015;55:1483-1494.
81. Zhang QC, Petrey D, Deng L et al. Structure-based prediction of protein–protein interactions on a genome-wide scale, Nature 2012;490:556.
82. Pentony MM, Jones DT. Modularity of intrinsic disorder in the human proteome, Proteins: Structure, Function, and Bioinformatics 2010;78:212-221.
83. Peng Z, Yan J, Fan X et al. Exceptionally abundant exceptions: comprehensive characterization of intrinsic disorder in all domains of life, Cell Mol Life Sci 2015;72:137-151.
84. Wang C, Uversky VN, Kurgan L. Disordered nucleiome: Abundance of intrinsic disorder in the DNA- and RNA-binding proteins in 1121 species from Eukaryota, Bacteria and Archaea, Proteomics 2016;16:1486-1498.
85. Mitchell JB. The relationship between the sequence identities of alpha helical proteins in the PDB and the molecular similarities of their ligands, J Chem Inf Comput Sci 2001;41:1617-1622.
86. Schuffenhauer A, Floersheim P, Acklin P et al. Similarity metrics for ligands reflecting the similarity of the target proteins, J Chem Inf Comput Sci 2003;43:391-405.
87. Klabunde T. Chemogenomic approaches to drug discovery: similar receptors bind similar ligands, Br J Pharmacol 2007;152:5-7.
88. Raju TNK. The Nobel Chronicles, The Lancet 2000;355:1022.
89. Pahikkala T, Airola A, Pietila S et al. Toward more realistic drug-target interaction predictions, Brief Bioinform 2015;16:325-337.
90. Mousavian Z, Masoudi-Nejad A. Drug-target interaction prediction via chemogenomic space: learning-based methods, Expert Opin Drug Metab Toxicol 2014;10:1273-1287.
91. Cichonska A, Rousu J, Aittokallio T. Identification of drug candidates and repurposing opportunities through compound-target interaction networks, Expert Opin Drug Discov 2015;10:1333-1345.
92. Lavecchia A, Cerchia C. In silico methods to address polypharmacology: current status, applications and future perspectives, Drug Discov Today 2016;21:288-298.
93. Hart T, Xie L. Providing data science support for systems pharmacology and its implications to drug discovery, Expert Opin Drug Discov 2016;11:241-256.
94. Lotfi Shahreza M, Ghadiri N, Mousavi SR et al. A review of network-based approaches to drug repositioning, Brief Bioinform 2017:bbx017-bbx017.
95. Fang J, Liu C, Wang Q et al. In silico polypharmacology of natural products, Brief Bioinform 2017:bbx045-bbx045.
96. Ezzat A, Wu M, Li X-L et al. Computational prediction of drug–target interactions using chemogenomic approaches: an empirical survey, Brief Bioinform 2018:bby002-bby002.
97. Hao M, Bryant SH, Wang Y. Open-source chemogenomic data-driven algorithms for predicting drug–target interactions, Brief Bioinform 2018:bby010-bby010.
98. Wishart DS, Knox C, Guo AC et al. DrugBank: a comprehensive resource for in silico drug discovery and exploration, Nucleic Acids Res 2006;34:D668-D672.

99. Wishart DS, Knox C, Guo AC et al. DrugBank: a knowledgebase for drugs, drug actions and drug targets, Nucleic Acids Res 2008;36:D901-D906.
100. Knox C, Law V, Jewison T et al. DrugBank 3.0: a comprehensive resource for 'Omics' research on drugs, Nucleic Acids Res 2011;39:D1035-D1041.
101. Law V, Knox C, Djoumbou Y et al. DrugBank 4.0: shedding new light on drug metabolism, Nucleic Acids Res 2014;42:D1091-1097.
102. Wishart DS, Feunang YD, Guo AC et al. DrugBank 5.0: a major update to the DrugBank database for 2018, Nucleic Acids Res 2018;46:D1074-D1082.
103. Chen X, Ji ZL, Chen YZ. TTD: therapeutic target database, Nucleic Acids Res 2002;30:412-415.
104. Zhu F, Han B, Kumar P et al. Update of TTD: Therapeutic Target Database, Nucleic Acids Res 2010;38:D787-791.
105. Zhu F, Shi Z, Qin C et al. Therapeutic target database update 2012: a resource for facilitating target-oriented drug discovery, Nucleic Acids Res 2012;40:D1128-1136.
106. Qin C, Zhang C, Zhu F et al. Therapeutic target database update 2014: a resource for targeted therapeutics, Nucleic Acids Res 2013;42:D1118-D1123.
107. Li YH, Yu CY, Li XX et al. Therapeutic target database update 2018: enriched resource for facilitating bench-to-clinic research of targeted therapeutics, Nucleic Acids Res 2018;46:D1121-D1127.
108. Chen X, Liu M, Gilson MK. BindingDB: a web-accessible molecular recognition database, Combinatorial Chem High Throughput Screening 2001;4:719-725.
109. Chen X, Lin Y, Liu M et al. The Binding Database: data management and interface design, Bioinformatics 2002;18:130-139.
110. Chen X, Lin Y, Gilson MK. The binding database: overview and user's guide, Biopolymers 2002;61:127-141.
111. Liu T, Lin Y, Wen X et al. BindingDB: a web-accessible database of experimentally determined protein-ligand binding affinities, Nucleic Acids Res 2007;35:D198-201.
112. Gilson MK, Liu T, Baitaluk M et al. BindingDB in 2015: A public database for medicinal chemistry, computational chemistry and systems pharmacology, Nucleic Acids Res 2016;44:D1045-D1053.
113. Gaulton A, Bellis LJ, Bento AP et al. ChEMBL: a large-scale bioactivity database for drug discovery, Nucleic Acids Res 2012;40:D1100-1107.
114. Bento AP, Gaulton A, Hersey A et al. The ChEMBL bioactivity database: an update, Nucleic Acids Res 2014;42:D1083-1090.
115. Davies M, Nowotka M, Papadatos G et al. ChEMBL web services: streamlining access to drug discovery data and utilities, Nucleic Acids Res 2015;43:W612-W620.
116. Gaulton A, Hersey A, Nowotka M et al. The ChEMBL database in 2017, Nucleic Acids Res 2017;45:D945-D954.
117. Günther S, Kuhn M, Dunkel M et al. SuperTarget and Matador: resources for exploring drug-target relationships, Nucleic Acids Res 2008;36:D919-D922.
118. Hecker N, Ahmed J, von Eichborn J et al. SuperTarget goes quantitative: update on drug-target interactions, Nucleic Acids Res 2012;40:D1113-1117.
119. Preissner S, Kroll K, Dunkel M et al. SuperCYP: a comprehensive database on Cytochrome P450 enzymes including a tool for analysis of CYP-drug interactions, Nucleic Acids Res 2010;38:D237-243.

120. Kuhn M, Campillos M, Letunic I et al. A side effect resource to capture phenotypic effects of drugs, Mol Syst Biol 2010;6:343.
121. Kuhn M, Letunic I, Jensen LJ et al. The SIDER database of drugs and side effects, Nucleic Acids Res 2016;44:D1075-1079.
122. von Eichborn J, Murgueitio MS, Dunkel M et al. PROMISCUOUS: a database for network-based drug-repositioning, Nucleic Acids Res 2011;39:D1060-1066.
123. Kuhn M, von Mering C, Campillos M et al. STITCH: interaction networks of chemicals and proteins, Nucleic Acids Res 2008;36:D684-D688.
124. Kuhn M, Szklarczyk D, Franceschini A et al. STITCH 2: an interaction network database for small molecules and proteins, Nucleic Acids Res 2010;38:D552-556.
125. Kuhn M, Szklarczyk D, Franceschini A et al. STITCH 3: zooming in on protein–chemical interactions, Nucleic Acids Res 2012;40:D876-D880.
126. Kuhn M, Szklarczyk D, Pletscher-Frankild S et al. STITCH 4: integration of protein-chemical interactions with user data, Nucleic Acids Res 2014;42:D401-407.
127. Szklarczyk D, Santos A, von Mering C et al. STITCH 5: augmenting protein–chemical interaction networks with tissue and affinity data, Nucleic Acids Res 2016;44:D380-D384.
128. Juan-Blanco T, Duran-Frigola M, Aloy P. IntSide: a web server for the chemical and biological examination of drug side effects, Bioinformatics 2015;31:612-613.
129. Desaphy J, Bret G, Rognan D et al. sc-PDB: a 3D-database of ligandable binding sites--10 years on, Nucleic Acids Res 2015;43:D399-404.
130. Meslamani J, Rognan D, Kellenberger E. sc-PDB: a database for identifying variations and multiplicity of 'druggable' binding sites in proteins, Bioinformatics 2011;27:1324-1326.
131. Mestres J, Gregori-Puigjane E, Valverde S et al. Data completeness - the Achilles heel of drug-target networks, Nat Biotechnol 2008;26:983-984.
132. Peters JU. Polypharmacology - foe or friend?, J Med Chem 2013;56:8955-8971.
133. Hirota S, Isozaki K, Moriyama Y et al. Gain-of-function mutations of c-kit in human gastrointestinal stromal tumors, Science 1998;279:577-580.
134. Wilhelm S, Carter C, Lynch M et al. Discovery and development of sorafenib: a multikinase inhibitor for treating cancer, Nat Rev Drug Discov 2006;5:835-844.
135. Bass A, Kinter L, Williams P. Origins, practices and future of safety pharmacology, J Pharmacol Toxicol Methods 2004;49:145-151.
136. MacDonald ML, Lamerdin J, Owens S et al. Identifying off-target effects and hidden phenotypes of drugs in human cells, Nat Chem Biol 2006;2:329-337.
137. Liu X, Zhu F, Ma XH et al. Predicting targeted polypharmacology for drug repositioning and multi- target drug discovery, Curr Med Chem 2013;20:1646-1661.
138. Huang YJ, Hang D, Lu LJ et al. Targeting the human cancer pathway protein interaction network by structural genomics, Mol Cell Proteomics 2008;7:2048-2060.
139. Sugaya N, Furuya T. Dr. PIAS: an integrative system for assessing the druggability of protein-protein interactions, BMC Bioinformatics 2011;12:50.
140. Sugaya N, Kanai S, Furuya T. Dr. PIAS 2.0: an update of a database of predicted druggable protein-protein interactions, Database (Oxford) 2012;2012:bas034.
141. Xie L, Wang J, Bourne PE. In silico elucidation of the molecular mechanism defining the adverse effect of selective estrogen receptor modulators, PLoS Comput Biol 2007;3:e217.
142. Kinnings SL, Liu N, Buchmeier N et al. Drug Discovery Using Chemical Systems Biology: Repositioning the Safe Medicine Comtan to Treat Multi-Drug and Extensively Drug Resistant Tuberculosis, PLoS Comput Biol 2009;5.

143. Durrant JD, Amaro RE, Xie L et al. A multidimensional strategy to detect polypharmacological targets in the absence of structural and sequence homology, PLoS Comput Biol 2010;6:e1000648.
144. Sui SJH, Lo R, Fernandes AR et al. Raloxifene attenuates Pseudomonas aeruginosa pyocyanin production and virulence, Int J Antimicrob Agents 2012;40:246-251.
145. Zhang Y, Skolnick J. Tertiary Structure Predictions on a Comprehensive Benchmark of Medium to Large Size Proteins, Biophys J 2004;87:2647-2655.
146. Zhang Y, Skolnick J. Automated structure prediction of weakly homologous proteins on a genomic scale, Proc Natl Acad Sci U S A 2004;101:7594-7599.
147. Zhang Y, Arakaki AK, Skolnick J. TASSER: An automated method for the prediction of protein tertiary structures in CASP6, Proteins: Structure, Function, and Bioinformatics 2005;61:91-98.
148. Šali A, Blundell TL. Comparative protein modelling by satisfaction of spatial restraints, J Mol Biol 1993;234:779-815.
149. Martí-Renom MA, Stuart AC, Fiser A et al. Comparative protein structure modeling of genes and genomes, Annu Rev Biophys Biomol Struct 2000;29:291-325.
150. Skolnick J, Kihara D, Zhang Y. Development and large scale benchmark testing of the PROSPECTOR_3 threading algorithm, Proteins: Structure, Function, and Bioinformatics 2004;56:502-518.
151. Zhang Y, Skolnick J. TM-align: a protein structure alignment algorithm based on the TM-score, Nucleic Acids Res 2005;33:2302-2309.
152. Pandit SB, Skolnick J. Fr-TM-align: a new protein structural alignment method based on fragment alignments and the TM-score, BMC Bioinformatics 2008;9:531.
153. Altschul SF, Madden TL, Schäffer AA et al. Gapped BLAST and PSI-BLAST: a new generation of protein database search programs, Nucleic Acids Res 1997;25:3389-3402.
154. Camacho C, Coulouris G, Avagyan V et al. BLAST+: architecture and applications, BMC Bioinformatics 2009;10:421.
155. Hubbard T, Barker D, Birney E et al. The Ensembl genome database project, Nucleic Acids Res 2002;30:38-41.
156. Altschul SF, Gish W, Miller W et al. Basic local alignment search tool, J Mol Biol 1990;215:403-410.
157. Consortium U. Reorganizing the protein space at the Universal Protein Resource (UniProt), Nucleic Acids Res 2012;40:D71-D75.
158. de Beer TA, Berka K, Thornton JM et al. PDBsum additions, Nucleic Acids Res 2014;42:D292-296.
159. Hanson RM, Prilusky J, Renjian Z et al. JSmol and the Next-Generation Web-Based Representation of 3D Molecular Structure as Applied to Proteopedia, Isr J Chem 2013;53:207-216.
160. Xie L KS, Xie L, Bourne PE. Predicting the polypharmacology of drugs: identifying new uses through chemoinformatics, structural informatics, and molecular modeling-based approaches. In: DE B. M. a. F. (ed) Drug Repositioning: Bringing New Life to Shelved Assets and Existing Drugs. John Wiley & Sons, 2012.
161. Kolb P, Ferreira RS, Irwin JJ et al. Docking and chemoinformatic screens for new ligands and targets, Curr Opin Biotechnol 2009;20:429-436.
162. De Smet F, Christopoulos A, Carmeliet P. Allosteric targeting of receptor tyrosine kinases, Nat Biotech 2014;32:1113-1120.

163. Vilar S, Hripcsak G. The role of drug profiles as similarity metrics: applications to repurposing, adverse effects detection and drug-drug interactions, Brief Bioinform 2016.
164. Lavecchia A. Machine-learning approaches in drug discovery: methods and applications, Drug Discov Today 2015;20:318-331.
165. Jamali AA, Ferdousi R, Razzaghi S et al. DrugMiner: comparative analysis of machine learning algorithms for prediction of potential druggable proteins, Drug Discov Today 2016;21:718-724.
166. Wen M, Zhang Z, Niu S et al. Deep-Learning-Based Drug–Target Interaction Prediction, J Proteome Res 2017;16:1401-1409.
167. Peón A, Naulaerts S, Ballester PJ. Predicting the Reliability of Drug-target Interaction Predictions with Maximum Coverage of Target Space, Sci Rep 2017;7:3820.
168. Peng L, Zhu W, Liao B et al. Screening drug-target interactions with positive-unlabeled learning, Sci Rep 2017;7:8087.
169. Li Z, Han P, You Z-H et al. In silico prediction of drug-target interaction networks based on drug chemical structure and protein sequences, Sci Rep 2017;7:11174.
170. Luo Y, Zhao X, Zhou J et al. A network integration approach for drug-target interaction prediction and computational drug repositioning from heterogeneous information, Nature Communications 2017;8:573.
171. Fang J, Wu Z, Cai C et al. Quantitative and Systems Pharmacology. 1. In Silico Prediction of Drug–Target Interactions of Natural Products Enables New Targeted Cancer Therapy, J Chem Inf Model 2017;57:2657-2671.
172. Rayhan F, Ahmed S, Shatabda S et al. iDTI-ESBoost: Identification of Drug Target Interaction Using Evolutionary and Structural Features with Boosting, Sci Rep 2017;7:17731.
173. Coordinators NR. Database Resources of the National Center for Biotechnology Information, Nucleic Acids Res 2017;45:D12-D17.
174. 2017 Journal Citation Reports®. Clarivate Analytics, 2017.
175. Keiser MJ, Roth BL, Armbruster BN et al. Relating protein pharmacology by ligand chemistry, Nat Biotechnol 2007;25:197-206.
176. Yamanishi Y, Araki M, Gutteridge A et al. Prediction of drug-target interaction networks from the integration of chemical and genomic spaces, Bioinformatics 2008;24:i232-240.
177. Campillos M, Kuhn M, Gavin AC et al. Drug target identification using side-effect similarity, Science 2008;321:263-266.
178. Nagamine N, Shirakawa T, Minato Y et al. Integrating statistical predictions and experimental verifications for enhancing protein-chemical interaction predictions in virtual screening, PLoS Comput Biol 2009;5:e1000397.
179. Bleakley K, Yamanishi Y. Supervised prediction of drug–target interactions using bipartite local models, Bioinformatics 2009;25:2397-2403.
180. Yamanishi Y, Kotera M, Kanehisa M et al. Drug-target interaction prediction from chemical, genomic and pharmacological data in an integrated framework, Bioinformatics 2010;26:i246-254.
181. Yabuuchi H, Niijima S, Takematsu H et al. Analysis of multiple compound-protein interactions reveals novel bioactive molecules, Mol Syst Biol 2011;7:472.
182. van Laarhoven T, Nabuurs SB, Marchiori E. Gaussian interaction profile kernels for predicting drug-target interaction, Bioinformatics 2011;27:3036-3043.
183. Cheng F, Liu C, Jiang J et al. Prediction of drug-target interactions and drug repositioning via network-based inference, PLoS Comput Biol 2012;8:e1002503.

184. Gonen M. Predicting drug-target interactions from chemical and genomic kernels using Bayesian matrix factorization, Bioinformatics 2012;28:2304-2310.
185. Takarabe M, Kotera M, Nishimura Y et al. Drug target prediction using adverse event report systems: a pharmacogenomic approach, Bioinformatics 2012;28:i611-i618.
186. Cao D-S, Liu S, Xu Q-S et al. Large-scale prediction of drug–target interactions using protein sequences and drug topological structures, Anal Chim Acta 2012;752:1-10.
187. Mei JP, Kwoh CK, Yang P et al. Drug-target interaction prediction by learning from local information and neighbors, Bioinformatics 2013;29:238-245.
188. Cheng F, Li W, Wu Z et al. Prediction of polypharmacological profiles of drugs by the integration of chemical, side effect, and therapeutic space, J Chem Inf Model 2013;53:753-762.
189. Alaimo S, Pulvirenti A, Giugno R et al. Drug-target interaction prediction through domain-tuned network-based inference, Bioinformatics 2013;29:2004-2008.
190. Koutsoukas A, Lowe R, Kalantarmotamedi Y et al. In silico target predictions: defining a benchmarking data set and comparison of performance of the multiclass Naive Bayes and Parzen-Rosenblatt window, J Chem Inf Model 2013;53:1957-1966.
191. Yamanishi Y, Kotera M, Moriya Y et al. DINIES: drug-target interaction network inference engine based on supervised analysis, Nucleic Acids Res 2014;42:W39-45.
192. Shi J-Y, Yiu S-M, Li Y et al. Predicting drug–target interaction for new drugs using enhanced similarity measures and super-target clustering, Methods 2015;83:98-104.
193. Liu H, Sun J, Guan J et al. Improving compound-protein interaction prediction by building up highly credible negative samples, Bioinformatics 2015;31:i221-229.
194. Seal A, Ahn YY, Wild DJ. Optimizing drug-target interaction prediction based on random walk on heterogeneous networks, J Cheminform 2015;7:40.
195. Kuang Q, Xu X, Li R et al. An eigenvalue transformation technique for predicting drug-target interaction, Sci Rep 2015;5:13867.
196. Hao M, Wang Y, Bryant SH. Improved prediction of drug-target interactions using regularized least squares integrating with kernel fusion technique, Anal Chim Acta 2016;909:41-50.
197. Liu Y, Wu M, Miao C et al. Neighborhood Regularized Logistic Matrix Factorization for Drug-Target Interaction Prediction, PLoS Comput Biol 2016;12:e1004760.
198. Wu Z, Cheng F, Li J et al. SDTNBI: an integrated network and chemoinformatics tool for systematic prediction of drug-target interactions and drug repositioning, Brief Bioinform 2016.
199. Ba-Alawi W, Soufan O, Essack M et al. DASPfind: new efficient method to predict drug-target interactions, J Cheminform 2016;8:15.
200. Yuan Q, Gao J, Wu D et al. DrugE-Rank: improving drug-target interaction prediction of new candidate drugs or targets by ensemble learning to rank, Bioinformatics 2016;32:i18-i27.
201. Ezzat A, Wu M, Li X-L et al. Drug-target interaction prediction using ensemble learning and dimensionality reduction, Methods 2017.
202. Roth BL, Lopez E, Patel S et al. The multiplicity of serotonin receptors: uselessly diverse molecules or an embarrassment of riches?, Neuroscientist 2000;6:252-262.
203. Schomburg I, Hofmann O, Baensch C et al. Enzyme data and metabolic information: BRENDA, a resource for research in biology, biochemistry, and medicine, Gene Funct Dis 2000;1:109-118.
204. Schomburg I, Chang A, Schomburg D. BRENDA, enzyme data and metabolic information, Nucleic Acids Res 2002;30:47-49.

205. Schomburg I, Chang A, Ebeling C et al. BRENDA, the enzyme database: updates and major new developments, Nucleic Acids Res 2004;32:D431-D433.
206. Barthelmes J, Ebeling C, Chang A et al. BRENDA, AMENDA and FRENDA: the enzyme information system in 2007, Nucleic Acids Res 2007;35:D511-D514.
207. Chang A, Scheer M, Grote A et al. BRENDA, AMENDA and FRENDA the enzyme information system: new content and tools in 2009, Nucleic Acids Res 2008;37:D588-D592.
208. Scheer M, Grote A, Chang A et al. BRENDA, the enzyme information system in 2011, Nucleic Acids Res 2010;39:D670-D676.
209. Schomburg I, Chang A, Placzek S et al. BRENDA in 2013: integrated reactions, kinetic data, enzyme function data, improved disease classification: new options and contents in BRENDA, Nucleic Acids Res 2012;41:D764-D772.
210. Chang A, Schomburg I, Placzek S et al. BRENDA in 2015: exciting developments in its 25th year of existence, Nucleic Acids Res 2014;43:D439-D446.
211. Placzek S, Schomburg I, Chang A et al. BRENDA in 2017: new perspectives and new tools in BRENDA, Nucleic Acids Res 2017;45:D380-D388.
212. Kanehisa M, Goto S, Hattori M et al. From genomics to chemical genomics: new developments in KEGG, Nucleic Acids Res 2006;34:D354-D357.
213. Kanehisa M, Araki M, Goto S et al. KEGG for linking genomes to life and the environment, Nucleic Acids Res 2008;36:D480-D484.
214. Kanehisa M, Goto S, Furumichi M et al. KEGG for representation and analysis of molecular networks involving diseases and drugs, Nucleic Acids Res 2009;38:D355-D360.
215. Kanehisa M, Goto S, Sato Y et al. KEGG for integration and interpretation of large-scale molecular data sets, Nucleic Acids Res 2011;40:D109-D114.
216. Kanehisa M, Goto S, Sato Y et al. Data, information, knowledge and principle: back to metabolism in KEGG, Nucleic Acids Res 2013;42:D199-D205.
217. Kanehisa M, Sato Y, Kawashima M et al. KEGG as a reference resource for gene and protein annotation, Nucleic Acids Res 2016;44:D457-D462.
218. Kanehisa M, Furumichi M, Tanabe M et al. KEGG: new perspectives on genomes, pathways, diseases and drugs, Nucleic Acids Res 2017;45:D353-D361.
219. Okuno Y, Yang J, Taneishi K et al. GLIDA: GPCR-ligand database for chemical genomic drug discovery, Nucleic Acids Res 2006;34:D673-D677.
220. Okuno Y, Tamon A, Yabuuchi H et al. GLIDA: GPCR—ligand database for chemical genomics drug discovery—database and tools update, Nucleic Acids Res 2008;36:D907-D912.
221. Keiser MJ, Setola V, Irwin JJ et al. Predicting new molecular targets for known drugs, Nature 2009;462:175-181.
222. Schuffenhauer A, Zimmermann J, Stoop R et al. An Ontology for Pharmaceutical Ligands and Its Application for in Silico Screening and Library Design, J Chem Inf Comput Sci 2002;42:947-955.
223. Southan C, Várkonyi P, Muresan S. Quantitative assessment of the expanding complementarity between public and commercial databases of bioactive compounds, J Cheminform 2009;1:10.
224. Euskirchen G. Integrative approaches in molecular medicine, Pharmacogenomics 2004;5:357-360.
225. Warr WA. ChEMBL. An interview with John Overington, team leader, chemogenomics at the European Bioinformatics Institute Outstation of the European Molecular Biology Laboratory (EMBL-EBI), J Comput-Aided Mol Des 2009;23:195-198.

226. Bender A. Databases: Compound bioactivities go public, Nat Chem Biol 2010;6:309-309.
227. Zhou H, Gao M, Skolnick J. Comprehensive prediction of drug-protein interactions and side effects for the human proteome, Sci Rep 2015;5:11090.
228. Brylinski M. Aromatic interactions at the ligand–protein interface: Implications for the development of docking scoring functions, Chem Biol Drug Des 2017:1-11.
229. Tatonetti NP, Ye PP, Daneshjou R et al. Data-Driven Prediction of Drug Effects and Interactions, Sci Transl Med 2012;4:125ra131-125ra131.
230. Schomburg KT, Rarey M. Benchmark Data Sets for Structure-Based Computational Target Prediction, J Chem Inf Model 2014;54:2261-2274.
231. Wishart D, Arndt D, Pon A et al. T3DB: the toxic exposome database, Nucleic Acids Res 2015;43:D928-D934.
232. Legehar A, Xhaard H, Ghemtio L. IDAAPM: integrated database of ADMET and adverse effects of predictive modeling based on FDA approved drug data, J Cheminform 2016;8:33.
233. Shameer K, Glicksberg BS, Hodos R et al. Systematic analyses of drugs and disease indications in RepurposeDB reveal pharmacological, biological and epidemiological factors influencing drug repositioning, Brief Bioinform 2017:bbw136-bbw136.
234. Paolini GV, Shapland RHB, van Hoorn WP et al. Global mapping of pharmacological space, Nat Biotech 2006;24:805-815.
235. Hopkins AL. Drug discovery: Predicting promiscuity, Nature 2009;462:167-168.
236. Anighoro A, Bajorath J, Rastelli G. Polypharmacology: Challenges and Opportunities in Drug Discovery, J Med Chem 2014;57:7874-7887.
237. Jasial S, Hu Y, Bajorath J. Determining the Degree of Promiscuity of Extensively Assayed Compounds, PLoS One 2016;11:e0153873.
238. Davis AP, Grondin CJ, Johnson RJ et al. The Comparative Toxicogenomics Database: update 2017, Nucleic Acids Res 2017;45:D972-D978.
239. Wang Y, Bryant SH, Cheng T et al. PubChem BioAssay: 2017 update, Nucleic Acids Res 2017;45:D955-D963.
240. Anastassiadis T, Deacon SW, Devarajan K et al. Comprehensive assay of kinase catalytic activity reveals features of kinase inhibitor selectivity, Nat Biotech 2011;29:1039-1045.
241. Davis MI, Hunt JP, Herrgard S et al. Comprehensive analysis of kinase inhibitor selectivity, Nat Biotech 2011;29:1046-1051.
242. Ursu O, Holmes J, Knockel J et al. DrugCentral: online drug compendium, Nucleic Acids Res 2017;45:D932-D939.
243. Nguyen D-T, Mathias S, Bologa C et al. Pharos: Collating protein information to shed light on the druggable genome, Nucleic Acids Res 2017;45:D995-D1002.
244. Whirl-Carrillo M, McDonagh EM, Hebert JM et al. Pharmacogenomics Knowledge for Personalized Medicine, Clin Pharmacol Ther 2012;92:414-417.
245. Griffith M, Griffith OL, Coffman AC et al. DGIdb: mining the druggable genome, Nat Meth 2013;10:1209-1210.
246. Wagner AH, Coffman AC, Ainscough BJ et al. DGIdb 2.0: mining clinically relevant drug–gene interactions, Nucleic Acids Res 2016;44:D1036-D1044.
247. Roider HG, Pavlova N, Kirov I et al. Drug2Gene: an exhaustive resource to explore effectively the drug-target relation network, BMC Bioinformatics 2014;15:68.
248. Pawson AJ, Sharman JL, Benson HE et al. The IUPHAR/BPS Guide to PHARMACOLOGY: an expert-driven knowledgebase of drug targets and their ligands, Nucleic Acids Res 2014;42:D1098-D1106.

249. Southan C, Sharman JL, Benson HE et al. The IUPHAR/BPS Guide to PHARMACOLOGY in 2016: towards curated quantitative interactions between 1300 protein targets and 6000 ligands, Nucleic Acids Res 2016;44:D1054-D1068.
250. Koscielny G, An P, Carvalho-Silva D et al. Open Targets: a platform for therapeutic target identification and validation, Nucleic Acids Res 2017;45:D985-D994.
251. Rose PW, Prlić A, Altunkaya A et al. The RCSB protein data bank: integrative view of protein, gene and 3D structural information, Nucleic Acids Res 2017;45:D271-D281.
252. Yang J, Roy A, Zhang Y. BioLiP: a semi-manually curated database for biologically relevant ligand–protein interactions, Nucleic Acids Res 2013;41:D1096-D1103.
253. Higueruelo AP, Schreyer A, Bickerton GRJ et al. Atomic Interactions and Profile of Small Molecules Disrupting Protein–Protein Interfaces: the TIMBAL Database, Chem Biol Drug Des 2009;74:457-467.
254. Higueruelo AP, Jubb H, Blundell TL. TIMBAL v2: update of a database holding small molecules modulating protein–protein interactions, Database 2013;2013:bat039-bat039.
255. Bourgeas R, Basse M-J, Morelli X et al. Atomic Analysis of Protein-Protein Interfaces with Known Inhibitors: The 2P2I Database, PLoS One 2010;5:e9598.
256. Basse MJ, Betzi S, Bourgeas R et al. 2P2Idb: a structural database dedicated to orthosteric modulation of protein–protein interactions, Nucleic Acids Res 2013;41:D824-D827.
257. Basse M-J, Betzi S, Morelli X et al. 2P2Idb v2: update of a structural database dedicated to orthosteric modulation of protein–protein interactions, Database 2016;2016:baw007-baw007.
258. Labbé CM, Laconde G, Kuenemann MA et al. iPPI-DB: a manually curated and interactive database of small non-peptide inhibitors of protein–protein interactions, Drug Discov Today 2013;18:958-968.
259. Labbé CM, Kuenemann MA, Zarzycka B et al. iPPI-DB: an online database of modulators of protein–protein interactions, Nucleic Acids Res 2016;44:D542-D547.
260. Liu Y, Hu B, Fu C et al. DCDB: Drug combination database, Bioinformatics 2010;26:587-588.
261. Liu Y, Wei Q, Yu G et al. DCDB 2.0: a major update of the drug combination database, Database 2014;2014:bau124-bau124.
262. Ahmed J, Meinel T, Dunkel M et al. CancerResource: a comprehensive database of cancer-relevant proteins and compound interactions supported by experimental knowledge, Nucleic Acids Res 2011;39:D960-D967.
263. Gohlke B-O, Nickel J, Otto R et al. CancerResource—updated database of cancer-relevant proteins, mutations and interacting drugs, Nucleic Acids Res 2016;44:D932-D937.
264. Halling-Brown MD, Bulusu KC, Patel M et al. canSAR: an integrated cancer public translational research and drug discovery resource, Nucleic Acids Res 2012;40:D947-D956.
265. Bulusu KC, Tym JE, Coker EA et al. canSAR: updated cancer research and drug discovery knowledgebase, Nucleic Acids Res 2014;42:D1040-D1047.
266. Tym JE, Mitsopoulos C, Coker EA et al. canSAR: an updated cancer research and drug discovery knowledgebase, Nucleic Acids Res 2016;44:D938-D943.
267. Siramshetty VB, Nickel J, Omieczynski C et al. WITHDRAWN—a resource for withdrawn and discontinued drugs, Nucleic Acids Res 2016;44:D1080-D1086.
268. Chan WKB, Zhang H, Yang J et al. GLASS: a comprehensive database for experimentally validated GPCR-ligand associations, Bioinformatics 2015;31:3035-3042.
269. Sakakibara Y, Hachiya T, Uchida M et al. COPICAT: a software system for predicting interactions between proteins and chemical compounds, Bioinformatics 2012;28:745-746.

270. Wu Z, Lu W, Yu W et al. Quantitative and systems pharmacology 2. In silico polypharmacology of G protein-coupled receptor ligands via network-based approaches, Pharmacol Res 2018;129:400-413.
271. He Z, Zhang J, Shi X-H et al. Predicting Drug-Target Interaction Networks Based on Functional Groups and Biological Features, PLoS One 2010;5:e9603.
272. Xia Z, Wu L-Y, Zhou X et al. Semi-supervised drug-protein interaction prediction from heterogeneous biological spaces, BMC Syst Biol 2010;4:S6.
273. Yu W, Jiang Z, Wang J et al. Using feature selection technique for drug-target interaction networks prediction, Curr Med Chem 2011;18:5687-5693.
274. Chen X, Liu M-X, Yan G-Y. Drug-target interaction prediction by random walk on the heterogeneous network, Molecular BioSystems 2012;8:1970-1978.
275. Chen H, Zhang Z. A Semi-Supervised Method for Drug-Target Interaction Prediction with Consistency in Networks, PLoS One 2013;8:e62975.
276. van Laarhoven T, Marchiori E. Predicting Drug-Target Interactions for New Drug Compounds Using a Weighted Nearest Neighbor Profile, PLoS One 2013;8:e66952.
277. Yu W, Yan Y, Liu Q et al. Predicting drug–target interaction networks of human diseases based on multiple feature information, Pharmacogenomics 2013;14:1701-1707.
278. Cao D-S, Zhang L-X, Tan G-S et al. Computational Prediction of Drug□Target Interactions Using Chemical, Biological, and Network Features, Molecular Informatics 2014;33:669-681.
279. Huang Y-A, You Z-H, Chen X. A systematic prediction of drug-target interactions using molecular fingerprints and protein sequences, Curr Protein Peptide Sci 2016.
280. Nascimento ACA, Prudêncio RBC, Costa IG. A multiple kernel learning algorithm for drug-target interaction prediction, BMC Bioinformatics 2016;17:46.
281. Shi J-Y, Li J-X, Lu H-M. Predicting existing targets for new drugs base on strategies for missing interactions, BMC Bioinformatics 2016;17:282.
282. Wang L, You Z-H, Chen X et al. RFDT: A Rotation Forest-based Predictor for Predicting Drug-Target Interactions using Drug Structure and Protein Sequence Information, Curr Protein Peptide Sci 2016.
283. Yan X-Y, Zhang S-W, Zhang S-Y. Prediction of drug-target interaction by label propagation with mutual interaction information derived from heterogeneous network, Molecular BioSystems 2016;12:520-531.
284. Buza K, Peška L. Drug–target interaction prediction with Bipartite Local Models and hubness-aware regression, Neurocomputing 2017;260:284-293.
285. Keum J, Nam H. SELF-BLM: Prediction of drug-target interactions via self-training SVM, PLoS One 2017;12:e0171839.
286. Meng F-R, You Z-H, Chen X et al. Prediction of Drug–Target Interaction Networks from the Integration of Protein Sequences and Drug Chemical Structures, Molecules 2017;22:1119.
287. Shen C, Ding Y, Tang J et al. An Ameliorated Prediction of Drug–Target Interactions Based on Multi-Scale Discrete Wavelet Transform and Network Features, International Journal of Molecular Sciences 2017;18:1781.
288. Zhang J, Zhu M, Chen P et al. DrugRPE: Random projection ensemble approach to drug-target interaction prediction, Neurocomputing 2017;228:256-262.
289. Willett P, Barnard JM, Downs GM. Chemical Similarity Searching, J Chem Inf Comput Sci 1998;38:983-996.

290. Bender A, Jenkins JL, Scheiber J et al. How similar are similarity searching methods?: a principal component analysis of molecular descriptor space, J Chem Inf Model 2009;49.
291. Cereto-Massagué A, Ojeda MJ, Valls C et al. Molecular fingerprint similarity search in virtual screening, Methods 2015;71:58-63.
292. Hattori M, Okuno Y, Goto S et al. Development of a Chemical Structure Comparison Method for Integrated Analysis of Chemical and Genomic Information in the Metabolic Pathways, J Am Chem Soc 2003;125:11853-11865.
293. Hattori M, Tanaka N, Kanehisa M et al. SIMCOMP/SUBCOMP: chemical structure search servers for network analyses, Nucleic Acids Res 2010;38:W652-W656.
294. Smith TF, Waterman MS. Identification of common molecular subsequences, J Mol Biol 1981;147:195-197.
295. ATC classification index with DDDs. Oslo, Norway: WHO Collaborating Centre for Drug Statistics Methodology, 2017.
296. Cheng F, Li W, Wang X et al. Adverse Drug Events: Database Construction and in Silico Prediction, J Chem Inf Model 2013;53:744-752.
297. Todeschini R, Consonni V, Xiang H et al. Similarity coefficients for binary chemoinformatics data: overview and extended comparison using simulated and real data sets, J Chem Inf Model 2012;52.
298. Bajusz D, Rácz A, Héberger K. Why is Tanimoto index an appropriate choice for fingerprint-based similarity calculations?, J Cheminform 2015;7:20.
299. Steinbeck C, Han Y, Kuhn S et al. The Chemistry Development Kit (CDK): An Open-Source Java Library for Chemo- and Bioinformatics, J Chem Inf Comput Sci 2003;43:493-500.
300. Steinbeck C, Hoppe C, Kuhn S et al. Recent developments of the chemistry development kit (CDK) - an open-source java library for chemo- and bioinformatics, Curr Pharm Des 2006;12:2111-2120.
301. May JW, Steinbeck C. Efficient ring perception for the Chemistry Development Kit, J Cheminform 2014;6:3-3.
302. Willighagen EL, Mayfield JW, Alvarsson J et al. The Chemistry Development Kit (CDK) v2.0: atom typing, depiction, molecular formulas, and substructure searching, J Cheminform 2017;9:33.
303. Harmar AJ, Hills RA, Rosser EM et al. IUPHAR-DB: the IUPHAR database of G protein-coupled receptors and ion channels, Nucleic Acids Res 2009;37:D680-D685.
304. Sharman JL, Mpamhanga CP, Spedding M et al. IUPHAR-DB: new receptors and tools for easy searching and visualization of pharmacological data, Nucleic Acids Res 2011;39:D534-D538.
305. Sharman JL, Benson HE, Pawson AJ et al. IUPHAR-DB: updated database content and new features, Nucleic Acids Res 2013;41:D1083-D1088.
306. Harding SD, Sharman JL, Faccenda E et al. The IUPHAR/BPS Guide to PHARMACOLOGY in 2018: updates and expansion to encompass the new guide to IMMUNOPHARMACOLOGY, Nucleic Acids Res 2018;46:D1091-D1106.
307. The NCI Cancer Gene Data Curation Pilot. https://wiki.nci.nih.gov/display/caBIO/caBIO+Data+Sources#caBIODataSources-CancerGeneIndexProject.
308. Hastings J, Owen G, Dekker A et al. ChEBI in 2016: Improved services and an expanding collection of metabolites, Nucleic Acids Res 2016;44:D1214-D1219.
309. Yates B, Braschi B, Gray KA et al. Genenames.org: the HGNC and VGNC resources in 2017, Nucleic Acids Res 2017;45:D619-D625.

310. Feng Z, Chen L, Maddula H et al. Ligand Depot: a data warehouse for ligands bound to macromolecules, Bioinformatics 2004;20:2153-2155.
311. Chopra A, Shan L, Eckelman WC et al. Molecular Imaging and Contrast Agent Database (MICAD): Evolution and Progress, Mol Imaging Biol 2012;14:4-13.
312. Brown GR, Hem V, Katz KS et al. Gene: a gene-centered information resource at NCBI, Nucleic Acids Res 2015;43:D36-D42.
313. Cerami EG, Gross BE, Demir E et al. Pathway Commons, a web resource for biological pathway data, Nucleic Acids Res 2011;39:D685-D690.
314. de Beer TAP, Berka K, Thornton JM et al. PDBsum additions, Nucleic Acids Res 2014;42:D292-D296.
315. Whirl‐Carrillo M, McDonagh EM, Hebert JM et al. Pharmacogenomics Knowledge for Personalized Medicine, Clin Pharmacol Ther 2012;92:414-417.
316. Kim S, Thiessen PA, Bolton EE et al. PubChem Substance and Compound databases, Nucleic Acids Res 2016;44:D1202-D1213.
317. Gibbons JD, Chakraborti S. Nonparametric statistical inference. International encyclopedia of statistical science. Springer, 2011, 977-979.
318. Meng F, Kurgan L. DFLpred: High-throughput prediction of disordered flexible linker regions in protein sequences, Bioinformatics 2016;32:i341-i350.
319. Yan J, Kurgan L. DRNApred, fast sequence-based method that accurately predicts and discriminates DNA- and RNA-binding residues, Nucleic Acids Res 2017;45:e84-e84.
320. Zhang J, Kurgan L. Review and comparative assessment of sequence-based predictors of protein-binding residues, Brief Bioinform 2017:bbx022-bbx022.
321. Zhang J, Ma Z, Kurgan L. Comprehensive review and empirical analysis of hallmarks of DNA-, RNA- and protein-binding residues in protein chains, Brief Bioinform 2017:bbx168-bbx168.
322. Cios KJ, Pedrycz W, Swiniarski RW et al. Data mining: a knowledge discovery approach. Springer Science & Business Media, 2007.
323. Rost B. Twilight zone of protein sequence alignments, Protein Eng 1999;12:85-94.
324. Todd AE, Orengo CA, Thornton JM. Evolution of function in protein superfamilies, from a structural perspective1, J Mol Biol 2001;307:1113-1143.
325. Peng Z, Mizianty MJ, Kurgan L. Genome-scale prediction of proteins with long intrinsically disordered regions, Proteins: Structure, Function, and Bioinformatics 2014;82:145-158.
326. Mark W-Y, Liao JCC, Lu Y et al. Characterization of Segments from the Central Region of BRCA1: An Intrinsically Disordered Scaffold for Multiple Protein–Protein and Protein–DNA Interactions?, J Mol Biol 2005;345:275-287.
327. Cheng Y, LeGall T, Oldfield CJ et al. Abundance of Intrinsic Disorder in Protein Associated with Cardiovascular Disease, Biochemistry 2006;45:10448-10460.
328. Uversky VN, Oldfield CJ, Dunker AK. Intrinsically Disordered Proteins in Human Diseases: Introducing the D2 Concept, Annual Review of Biophysics 2008;37:215-246.
329. Uros M, Christopher JO, Dunker AK et al. Unfoldomics of Human Genetic Diseases: Illustrative Examples of Ordered and Intrinsically Disordered Members of the Human Diseasome, Protein Peptide Lett 2009;16:1533-1547.
330. Uversky VN, Oldfield CJ, Midic U et al. Unfoldomics of human diseases: linking protein intrinsic disorder with diseases, BMC Genomics 2009;10:S7.

331. Rajagopalan K, Mooney SM, Parekh N et al. A majority of the cancer/testis antigens are intrinsically disordered proteins, J Cell Biochem 2011;112:3256-3267.
332. Casu F, Duggan Brendan M, Hennig M. The Arginine-Rich RNA-Binding Motif of HIV-1 Rev Is Intrinsically Disordered and Folds upon RRE Binding, Biophys J 2013;105:1004-1017.
333. Uversky VN, Davé V, Iakoucheva LM et al. Pathological Unfoldomics of Uncontrolled Chaos: Intrinsically Disordered Proteins and Human Diseases, Chem Rev 2014;114:6844-6879.
334. Ward JJ, Sodhi JS, McGuffin LJ et al. Prediction and Functional Analysis of Native Disorder in Proteins from the Three Kingdoms of Life, J Mol Biol 2004;337:635-645.
335. Kathiriya JJ, Pathak RR, Clayman E et al. Presence and utility of intrinsically disordered regions in kinases, Molecular BioSystems 2014;10:2876-2888.
336. DeForte S, Uversky VN. Not an exception to the rule: the functional significance of intrinsically disordered protein regions in enzymes, Molecular BioSystems 2017;13:463-469.

Vita

Chen Wang was born on July 21, 1986, in Baoding, Hebei, China. He received the M.Sc. degree in Information and Communication Engineering and the B.Sc. degree in Electronics and Information Engineering from the Harbin Institute of Technology, China, in 2011 and 2009, respectively. He is currently a Ph.D. Candidate and Research Assistant in the Computer Science Department at the Virginia Commonwealth University. Before joining Virginia Commonwealth University, he was a Research Assistant at the University of Alberta and the Harbin Institute of Technology between 2012 and 2015.

Appendix 1 List of drugs included in the benchmark database for Goal 3

The list of PubChem CIDs and names for the 449 drugs that are included in the benchmark database from Chapter 5.

Drug group 1		Drug group 2		Drug group 3	
CID	Drug name	CID	Drug name	CID	Drug name
3366	5-fluorocytosine	5419	Tetrahydrozoline	3080	2,3-dimercaptopropanol
3385	5-fluorouracil	3406	4-methylpyrazole	4075	5-aminosalicylic acid
4114	8-methoxypsoralen	667490	6-mercaptopurine	71158	Acamprosate
1978	Acebutolol	2723601	6-thioguanine	60164	Adapalene
71771	Aceclofenac	1983	Acetaminophen	5493444	Aliskiren
2094	Allopurinol	1986	Acetazolamide	3007	Amphetamine
2099	Alosetron	2022	Acyclovir	2179	Amsacrine
3125	Alpha-methyl-p-tyrosine	2082	Albendazole	2182	Anagrelide
2118	Alprazolam	2088	Alendronate	166548	Anidulafungin
2130	Amantadine	51263	Alfentanil	60795	Aripiprazole
2145	Aminoglutethimide	2092	Alfuzosin	2266	Azelaic acid
2170	Amoxapine	123606	Almotriptan	82146	Bexarotene
3698	Amrinone	2141	Amifostine	104865	Bosentan
2187	Anastrozole	2160	Amitriptyline	2441	Bromazepam
2249	Atenolol	2162	Amlodipine	2471	Bumetanide
2284	Baclofen	2216	Apraclonidine	60953	Capecitabine
2337	Benzocaine	2244	Aspirin	2551	Carbachol
2366	Betahistine	148192	Atazanavir	2678	Cetirizine
2375	Bicalutamide	2265	Azathioprine	2713	Chlorhexidine
2391	Bisacodyl	2267	Azelastine	8612	Chloroprocaine
444	Bupropion	2578	BCNU	2719	Chloroquine
2477	Buspirone	7699	Benzonatate	2789	Clobazam
2478	Busulfan	12555	Benzydamine	25419	Clodronate
2484	Butenafine	2369	Betaxolol	119182	Clofarabine
2541	Candesartan	2370	Bethanechol	151171	Conivaptan
2708	Chlorambucil	39042	Bezafibrate	5625	Delavirdine
2725	Chlorpheniramine	2381	Biperiden	137	Delta-aminolevulinic acid
2749	Ciclopirox	2405	Bisoprolol	2973	Desferrioxamine
2764	Ciprofloxacin	2435	Brimonidine	42113	Desflurane
2802	Clonazepam	68844	Brinzolamide	125017	Desvenlafaxine
2907	Cyclophosphamide	60726	Bromfenac	3009	DFMO
2913	Cyproheptadine	6834	Brompheniramine	3117	Disulfiram
2972	Deferiprone	2474	Bupivacaine	71329	Dofetilide
124087	Desloratadine	2519	Caffeine	681	Dopamine
2140	Diatrizoate	2554	Carbamazepine	4510	DWP-401
3042	Dicyclomine	2576	Carisoprodol	60877	Emtricitabine
3059	Diflunisal	2583	Carteolol	3226	Enflurane
3100	Diphenhydramine	2585	Carvedilol	176870	Erlotinib
36811	Dobutamine	2662	Celecoxib	60198	Exemestane
3151	Domperidone	2726	Chlorpromazine	150311	Ezetimibe
3158	Doxepin	2727	Chlorpropamide	3331	Felbamate
3168	Droperidol	2732	Chlorthalidone	3345	Fentanyl
3198	Econazole	2733	Chlorzoxazone	119	Gamma-aminobutyric acid

3241	Epinastine
564	Aminocaproic acid
59768	Esmolol
3261	Estazolam
3291	Ethosuximide
3305	Etidronate
3308	Etodolac
3324	Famciclovir
3325	Famotidine
3339	Fenofibrate
3342	Fenoprofen
6918558	Fesoterodine
3354	Flavoxate
3365	Fluconazole
3373	Flumazenil
3372	Fluphenazine
3393	Flurazepam
3410	Formoterol
3446	Gabapentin
3478	Glipizide
3510	Granisetron
3516	Guaifenesin
2123	Hexamethylmelamine
3637	Hydralazine
3652	Hydroxychloroquine
3690	Ifosfamide
5291	Imatinib
57469	Imiquimod
3767	Isoniazid
3825	Ketoprofen
3826	Ketorolac
3869	Labetalol
3883	Lansoprazole
3914	Levobunolol
3948	Lomefloxacin
3950	Lomustine
3957	Loratadine
3961	Losartan
453	Mannitol
4053	Melphalan
8271	Mephobarbital
4062	Mepivacaine
598	Mesna
1349907	Methimazole
4107	Methocarbamol
4171	Metoprolol
4173	Metronidazole
4174	Metyrapone
4197	Milrinone
5746	Mitomycin C
4211	Mitotane
4236	Modafinil
7638	Monobenzone
4409	Nabumetone
4456	Neostigmine
644241	Nilotinib
4539	Norfloxacin
4543	Nortriptyline
4595	Ondansetron
4601	Orphenadrine
4614	Oxaprozin
4634	Oxybutynin
4678	Panthenol
4723	Pemoline
4725	Penciclovir
4748	Perphenazine
4763	Phenobarbital
4828	Pindolol
4891	Praziquantel
4906	Prilocaine
4909	Primidone
4915	Procarbazine
4917	Prochlorperazine
4927	Promethazine
4932	Propafenone
4935	Proparacaine
657298	Propylthiouracil
1046	Pyrazinamide
5002	Quetiapine
5029	Rabeprazole
5039	Ranitidine
2756	Cimetidine
2762	Cinoxacin
2771	Citalopram
2801	Clomipramine
2803	Clonidine
2812	Clotrimazole
2895	Cyclobenzaprine
2955	Dapsone
3062316	Dasatinib
2995	Desipramine
30623	Dexrazoxane
3016	Diazepam
3019	Diazoxide
679	Dimethyl sulphoxide
3105	Dipivefrin
3108	Dipyridamole
3114	Disopyramide
3152	Donepezil
3156	Doxapram
3157	Doxazosin
3182	Dyphylline
77993	Eletriptan
838	Epinephrine
3278	Ethacrynic acid
2761171	Ethionamide
3292	Ethotoin
6049	Edetic Acid
3333	Felodipine
3348	Fexofenadine
3386	Fluoxetine
3394	Flurbiprofen
3397	Flutamide
3440	Furosemide
3454	Ganciclovir
5379	Gatifloxacin
3463	Gemfibrozil
3488	Glibenclamide
3475	Gliclazide
3494	Glycopyrrolate
3519	Guanfacine
3559	Haloperidol
3598	Hexachlorophene
3639	Hydrochlorothiazide
785	Hydroquinone
3658	Hydroxyzine
3672	Ibuprofen
3696	Imipramine
3702	Indapamide
3715	Indomethacin
3739	Iodipamide
3749	Irbesartan
3759	Isocarboxazid
3779	Isoproterenol
3783	Isoxsuprine
3821	Ketamine
3827	Ketotifen
3878	Lamotrigine
3899	Leflunomide
3902	Letrozole
59708	Levetiracetam
3676	Lidocaine
3958	Lorazepam
3964	Loxapine
3998	Mafenide acetate
4032	Mecamylamine
4044	Mefenamic acid
4046	Mefloquine
4054	Memantine
4060	Mephenytoin
4078	Mesoridazine
4086	Metaproterenol
4091	Metformin
4095	Methadone
4158	Methylphenidate
4168	Metoclopramide
4170	Metolazone
4178	Mexiletine
4192	Midazolam
4195	Midodrine
4205	Mirtazapine
4212	Mitoxantrone
10413	Gamma-hydroxybutyrate
123631	Gefitinib
774	Histamine
3647	Hydroflumethiazide
60852	Ibandronate
60753	Ibutilide
104741	ICI 182,780
5311181	Iloprost
3763	Isoflurane
27661	Isosorbide-5-mononitrate
219078	Lacosamide
612	Lactate
216326	Lenalidomide
3915	Levocabastine
4004	Malathion
4057	Mepenzolate methylbromide
4058	Meperidine
4064	Meprobamate
6476	Methsuximide
4139	Methylene blue solution
4189	Miconazole
51634	Miglustat
47641	Naftifine
4421	Nalidixic acid
4436	Naphazoline
50294	Nedocromil sodium
4493	Nilutamide
4499	Nisoldipine
41684	Nitazoxanide
4616	Oxazepam
60843	Pemetrexed
4768	Phenoxybenzamine
750	Polyglycine
4993	Pyrimethamine
104758	Raltitrexed
56959	Ranolazine
449193	Roflumilast
446157	Rosuvastatin
129228	Rufinamide
5206	Sevoflurane
5312125	Silodosin
4369359	Sitagliptin
216239	Sorafenib
5314	Succinylcholine
41693	Sufentanil
110635	Tadalafil
5381	Tazarotene
5391	Temazepam
6018	Tetrabenazine
1130	Thiamine
2720	Thiazide
853	Thyroxine
216237	Tolvaptan
110634	Vardenafil
170361	Varenicline
2520	Verapamil
5665	Vigabatrin
1054	Vitamin B6
68740	Zoledronic acid
5734	Zonisamide
5735	Zopiclone

5071	Rimantadine
5245	Risedronate
2083	Salbutamol
5152	Salmeterol
5161	Salsalate
5193	Secobarbital
5210	Sibutramine
5253	Sotalol
5318	Sulconazole
5215	Sulfadiazine
5344	Sulfisoxazole
5401	Terazosin
5403	Terbutaline
5426	Thalidomide
5430	Thiabendazole
5452	Thioridazine
5479	Tinidazole
41781	Torasemide
5523	Tramadol
5533	Trazodone
5556	Triazolam
5572	Trihexyphenidyl
5593	Tropicamide
119607	Valdecoxib
5656	Venlafaxine
5719	Zaleplon
23897	Molindone
4034	Monamine
4440	Naratriptan
4449	Nefazodone
4463	Nevirapine
4485	Nifedipine
4497	Nimodipine
4506	Nitrazepam
4033	Nitrogen mustard
4583	Ofloxacin
130881	Olmesartan medoxomil
4594	Omeprazole
34312	Oxcarbazepine
115237	Paliperidone
4679	Pantoprazole
4680	Papaverine
4649	Para-aminosalicylic acid
4737	Pentobarbital
4740	Pentoxifylline
3675	Phenelzine
4771	Phentermine
5775	Phentolamine
1775	Phenytoin
16362	Pimozide
4829	Pioglitazone
27400	Pizotifen
4893	Prazosin
4908	Primaquine
4911	Probenecid
4913	Procainamide
4914	Procaine
4934	Propantheline
4943	Propofol
10100	Propoxyphene
4946	Propranolol
4976	Protriptyline
4991	Pyridostigmine
5035	Raloxifene
5070	Riluzole
5073	Risperidone
5078	Rizatriptan
5090	Rofecoxib
5095	Ropinirole
77999	Rosiglitazone
338	Salicylic acid
65863	Sertaconazole
5212	Sildenafil
54454	Simvastatin
5320	Sulfacetamide
5358	Sumatriptan
5359	Suprofen
1935	Tacrine
65999	Telmisartan
5411	Tetracaine
2153	Theophylline
5453	Thiotepa
5472	Ticlopidine
5487	Tizanidine
5503	Tolazamide
5546	Triamterene
5566	Trifluoperazine
6256	Trifluorothymidine
861	Triiodothyronine
5578	Trimethoprim
6503	Tris-HCl
5591	Troglitazone
3121	Valproic acid
5978	Vincristine
71616	Voriconazole
5717	Zafirlukast
5732	Zolpidem

Appendix 2 Druggable human proteome included in the benchmark database for Goal 3

The list of UniProt accession numbers for the 1469 druggable human proteins that are included in the benchmark database from Chapter 5.

A0N0Q1 A0N0X8 A0PJA6 A0PJF5 A0PJF8 A0ZT98 A1A4V4 A1A5A9 A1E5M1 A1L4K2 A2A3U5 A2RUF7 A2RUS0 A2VDG3
A3QNQ0 A4D0V9 A4D0X1 A4D1D0 A4D1D2 A4D1Q0 A4D2J9 A4D2N2 A4D2P0 A4QPA9 A5X2V1 A6NGA6 A6NMQ1 A6NNF7
A6PW57 A7E2E0 A7E2E5 A7LFK2 A8K161 A8K177 A8K1F6 A8K1U5 A8K228 A8K249 A8K2J1 A8K2Q2 A8K2S4 A8K341
A8K379 A8K3B6 A8K3H3 A8K3J4 A8K3M3 A8K496 A8K4G3 A8K4H7 A8K4S9 A8K5M4 A8K5P7 A8K5W4 A8K5Z0 A8K602
A8K7I0 A8K7N8 A8K7T1 A8K840 A8K858 A8K8D3 A8K987 A8K996 A8K9L2 A8KAE3 A8KAE4 A8KAF4 A8KAG8 A8MPY1
A8MWW6 A9ZM15 B0AZM9 B0FWH2 B0LPE5 B0YIY3 B0YJ76 B0YJ89 B0YJ93 B0ZBD3 B0ZBE0 B0ZBE2 B0ZBF6 B1ALM3
B2CQT6 B2KJ49 B2R7Y7 B2R807 B2R812 B2R9N9 B2RA41 B2RAH7 B2RAP9 B2RAZ5 B2RBL3 B2RC52 B2RCU6 B2RCW8
B2RDS2 B2RUU2 B2RXH2 B2ZGL7 B3KN77 B3KNJ3 B3KP53 B3KP78 B3KPX6 B3KQH9 B3KQV3 B3KRI8 B3KRP1 B3KRT8
B3KRV2 B3KRZ3 B3KS07 B3KS12 B3KS39 B3KT70 B3KTT5 B3KU60 B3KUB4 B3KVM3 B3KWC4 B3KXJ4 B4DDG2 B4DER4
B4DER9 B4DEW2 B4DF27 B4DF30 B4DG22 B4DG79 B4DHI4 B4DII1 B4DIW2 B4DK59 B4DK78 B4DKC0 B4DKH4 B4DLF9
B4DLR2 B4DM55 B4DM56 B4DMJ5 B4DN15 B4DN83 B4DNF7 B4DNQ5 B4DPF4 B4DR80 B4DS37 B4DT73 B4DTF4 B4DTP4
B4DTW8 B4DUB1 B4DUC2 B4DUH8 B4DV95 B4DVP5 B4DW50 B4DWC1 B4DX41 B4DXF8 B4DXM8 B4DZW8 B4E000 B4E058
B4E0R1 B4E0R9 B4E0X2 B4E0Y5 B4E1E9 B4E292 B4E295 B4E398 B4E3E9 B5BNW5 B6D4Y2 B6ZGS9 B7Z1F5 B7Z1F9
B7Z1G6 B7Z1L9 B7Z1W5 B7Z226 B7Z242 B7Z274 B7Z2G8 B7Z2S5 B7Z325 B7Z3P6 B7Z3P7 B7Z3V5 B7Z3W8 B7Z5E9
B7Z5K4 B7Z7J5 B7Z9H7 B7ZKJ3 B7ZKN7 B7ZLY6 B7ZM24 B7ZM71 B7ZW53 B7ZW66 B8K2Q5 C1ID52 C4IXS7 C8C060
C9J1J0 C9J5X1 C9JE82 C9JEV6 C9JXA2 D0VY79 D2CGD1 D2KUA6 D3DNN4 D3DPA4 D3DX95 D3YTB5 D4Q8H0 D6RFW5
D9YZU5 E5KQF5 E5KS60 E7DBM8 E7ERK3 E7ESA6 E7ETZ0 E7EVN3 E9KL36 E9KL48 E9PER6 E9PG18 E9PJX5 F1D8N3
F1D8N5 F1D8N7 F1D8P4 F1D8P6 F1D8P8 F1D8P9 F1D8Q5 F1D8S4 F1D8S6 F1DAL4 F1T0G6 F2Z2J1 F2Z2Y4 F5CTF3
F5GWI4 F5H1T4 F5H2B5 F6U4U2 F7VJQ1 F8VBW7 F8VQZ7 F8W6L1 F8WBA3 F8WCM8 G3V5Q5 G5E9C5 H6UYS5 H6VQ59
H7BYT1 H9NIL8 H9NIM1 I6L9H2 J3KMW1 J3KNB8 J3KNE8 J3KNN3 J3KRN4 J3QSS1 K9J958 K9JA46 L7RSL3 L7RTI5
L7RXH5 L8B082 M0R0W6 M0R1I2 O00167 O00325 O00408 O00444 O00459 O00519 O00763 O08562 O14521 O14578
O14649 O14684 O14727 O14746 O14788 O14842 O14920 O14936 O14939 O14965 O15111 O15118 O15244 O15245
O15296 O15303 O15374 O15375 O15379 O15399 O15438 O15440 O15460 O15554 O43283 O43318 O43353 O43497
O43526 O43570 O43704 O43741 O43781 O43849 O54898 O60240 O60331 O60341 O60391 O60568 O60656 O60658
O60674 O60760 O60840 O60885 O60909 O60939 O70507 O75116 O75164 O75311 O75385 O75460 O75469 O75582
O75604 O75751 O75762 O75795 O75874 O75899 O75936 O76039 O76068 O76074 O76082 O76083 O88703 O88704
O88871 O94759 O94768 O94782 O94804 O94806 O94925 O94956 O95069 O95255 O95259 O95263 O95264 O95342
O95382 O95467 O95665 O95835 O95907 O96017 P00156 P00325 P00326 P00352 P00374 P00390 P00403 P00491
P00492 P00519 P00533 P00734 P00747 P00750 P00797 P00813 P00915 P00918 P01258 P01275 P01375 P01579
P01584 P02144 P02545 P02585 P02593 P02708 P02741 P02751 P02763 P02768 P02788 P03372 P03886 P04035
P04040 P04054 P04083 P04629 P04775 P04818 P05023 P05091 P05093 P05108 P05141 P05164 P05177 P05181
P05362 P05369 P05412 P05543 P06133 P06213 P06239 P06241 P06276 P06280 P06401 P06858 P07101 P07202
P07204 P07327 P07339 P07437 P07451 P07550 P07607 P07741 P07947 P07949 P08104 P08172 P08173 P08185
P08235 P08236 P08246 P08254 P08311 P08482 P08483 P08588 P08684 P08697 P08729 P08842 P08908 P08909
P08912 P08913 P08922 P09172 P09211 P09619 P09769 P09871 P09917 P0C1S8 P0C264 P10109 P10253 P10275
P10276 P10696 P10721 P10826 P10827 P10980 P11021 P11142 P11177 P11229 P11362 P11387 P11388 P11413
P11474 P11509 P11511 P11712 P11884 P11926 P12004 P12104 P12235 P12236 P12268 P12657 P12931 P13196
P13500 P13569 P13612 P13631 P13674 P13716 P13726 P13945 P14091 P14207 P14324 P14416 P14550 P14616
P14679 P14780 P14842 P14867 P14902 P15056 P15291 P15388 P15389 P15390 P15428 P15538 P16050 P16066
P16234 P16388 P16435 P16591 P16662 P16860 P17252 P17302 P17405 P17516 P17948 P18054 P18089 P18505
P18507 P18545 P18825 P19020 P19099 P19224 P19320 P19327 P19525 P19652 P19784 P19793 P20309 P20594
P20648 P20813 P20839 P21266 P21397 P21439 P21451 P21452 P21462 P21549 P21554 P21589 P21709 P21728
P21731 P21817 P21860 P21912 P21917 P21918 P21964 P22002 P22102 P22303 P22309 P22310 P22413 P22460
P22462 P22557 P22607 P22748 P22888 P22894 P23141 P23219 P23378 P23415 P23416 P23434 P23443 P23458
P23469 P23921 P23944 P23975 P23977 P24046 P24298 P24530 P24666 P24723 P25021 P25024 P25025 P25099

P25100 P25101 P25102 P25103 P25122 P25929 P25962 P25963 P26255 P26447 P26599 P26684 P27037 P27338
P27487 P27695 P27732 P27815 P27986 P28221 P28222 P28223 P28335 P28476 P28482 P28566 P28647 P28702
P28845 P29274 P29275 P29276 P29322 P29323 P29350 P29401 P30049 P30291 P30411 P30518 P30542 P30543
P30556 P30560 P30613 P30711 P30729 P30872 P30874 P30939 P30966 P31213 P31350 P31388 P31391 P31644
P31645 P31652 P31930 P31939 P31947 P32238 P32239 P32245 P32297 P32298 P32304 P32305 P32320 P32745
P33032 P33151 P33402 P33527 P33535 P33765 P33981 P34896 P34903 P34913 P34949 P34969 P34995 P35218
P35219 P35228 P35318 P35346 P35348 P35354 P35367 P35368 P35372 P35462 P35498 P35499 P35610 P35790
P35916 P36021 P36507 P36537 P36544 P36888 P36894 P36896 P36897 P37023 P37088 P37231 P37288 P39748
P39900 P40763 P41143 P41145 P41250 P41440 P41595 P41743 P41968 P42261 P42262 P42336 P42345 P42574
P42681 P42684 P42685 P42858 P42898 P43088 P43116 P43119 P43140 P43166 P43220 P43403 P43681 P45954
P45984 P45985 P46098 P46734 P47712 P47869 P47870 P47898 P47901 P47989 P48039 P48167 P48169 P48443
P48542 P48544 P48545 P48637 P49019 P49137 P49146 P49327 P49336 P49419 P49585 P49759 P49841 P49895
P50052 P50225 P50281 P50406 P50440 P50613 P51160 P51164 P51168 P51170 P51570 P51606 P51639 P51649
P51681 P51692 P51787 P51788 P51813 P51857 P51956 P51957 P52209 P52895 P53350 P53582 P53597 P53667
P54219 P54284 P54646 P54753 P54760 P54762 P54802 P55011 P55017 P55072 P55926 P56373 P56524 P57058
P57789 P58406 P61088 P61168 P61169 P63142 P63316 P68366 P68371 P68400 P70604 P70605 P70673 P78334
P78348 P78356 P78368 P78508 P78527 P80365 P80404 P83916 P97288 P97717 P97794 P98073 Q00526 Q00788
Q00975 Q01098 Q01453 Q01538 Q01650 Q01668 Q01717 Q01815 Q01959 Q02108 Q02127 Q02153 Q02156 Q02485
Q02641 Q02763 Q02769 Q02779 Q02790 Q02880 Q03164 Q04759 Q04760 Q04828 Q05329 Q05513 Q05586 Q05932
Q05940 Q06187 Q06203 Q06278 Q06418 Q06432 Q06643 Q07343 Q07699 Q07869 Q08209 Q08289 Q08499 Q08881
Q09428 Q09470 Q0IJ49 Q12791 Q12809 Q12866 Q12879 Q12882 Q13043 Q13126 Q13131 Q13183 Q13224 Q13233
Q13255 Q13258 Q13332 Q13370 Q13393 Q13464 Q13470 Q13526 Q13547 Q13563 Q13621 Q13627 Q13639 Q13698
Q13705 Q13873 Q13882 Q13936 Q13946 Q13956 Q13976 Q14032 Q14191 Q14289 Q14376 Q14432 Q14500 Q14524
Q14534 Q14643 Q14654 Q14749 Q14894 Q14973 Q14994 Q15303 Q15375 Q15413 Q15418 Q15569 Q15722 Q15746
Q15759 Q15822 Q15825 Q15831 Q15835 Q15842 Q15858 Q16236 Q16288 Q16322 Q16348 Q16445 Q16512 Q16513
Q16558 Q16566 Q16568 Q16659 Q16696 Q16739 Q16790 Q16832 Q16850 Q16853 Q17RV3 Q17ST2 Q2M2I8 Q32MC3
Q32MK0 Q32P28 Q38Q88 Q3V008 Q3V050 Q4LE27 Q4U2R8 Q4VAM5 Q4VBY6 Q52WX2 Q53EW6 Q53GD3 Q56UN5 Q5DSZ6
Q5DSZ7 Q5DT02 Q5JXL9 Q5KU17 Q5QD15 Q5SQQ7 Q5SUJ9 Q5T6X5 Q5TAT6 Q5VT25 Q5XXA6 Q60614 Q61743 Q62897
Q62968 Q64737 Q68DU8 Q6DT37 Q6IB77 Q6P3R8 Q6PKF2 Q6RI86 Q6XUX3 Q6ZN16 Q6ZQN7 Q6ZWB6 Q71U36 Q7RTT9
Q7Z2W7 Q86TI2 Q86TP1 Q86UX6 Q86V86 Q86VL8 Q86W47 Q86YV6 Q8IUX4 Q8IVL5 Q8IVL6 Q8IW41 Q8IYT8 Q8IZF0
Q8IZS8 Q8N1C3 Q8N1Q1 Q8N4C8 Q8N568 Q8N5S9 Q8N695 Q8N752 Q8N8N7 Q8NDX3 Q8NE62 Q8NE63 Q8NER1 Q8NEV4
Q8NFD2 Q8TCT1 Q8TCU5 Q8TD08 Q8TD43 Q8TDC3 Q8TDR2 Q8TDS4 Q8TE04 Q8WTQ7 Q8WUI4 Q91ZY1 Q91ZY2 Q923Y7
Q92630 Q92731 Q92736 Q92769 Q92830 Q92887 Q92918 Q92952 Q92959 Q96BD0 Q96CX2 Q96FI4 Q96FL8 Q96GD4
Q96L34 Q96LB2 Q96NT5 Q96NX5 Q96Q40 Q96QE3 Q96RJ0 Q96RP8 Q96SB4 Q99246 Q99250 Q99418 Q99527 Q99549
Q99571 Q99643 Q99683 Q99700 Q99714 Q99808 Q99816 Q99928 Q9BPW9 Q9BR01 Q9BRL5 Q9BRS2 Q9BVS4 Q9BX84
Q9BXA5 Q9BXC0 Q9BY41 Q9BY49 Q9BY64 Q9BYC2 Q9BYV1 Q9BZL6 Q9C007 Q9D6N1 Q9EQ60 Q9ERZ4 Q9GZV3 Q9H015
Q9H1D0 Q9H1R3 Q9H221 Q9H222 Q9H244 Q9H2G2 Q9H2K8 Q9H2S1 Q9H2X6 Q9H2X9 Q9H3N8 Q9H3Y6 Q9H4B4 Q9H598
Q9HAB3 Q9HAZ1 Q9HB55 Q9HBH1 Q9HC16 Q9HC97 Q9HCF6 Q9HCG7 Q9HCR9 Q9JIS7 Q9NP56 Q9NPA1 Q9NPA2 Q9NPD5
Q9NQA5 Q9NR96 Q9NR97 Q9NRP7 Q9NS40 Q9NS75 Q9NS85 Q9NSA0 Q9NSY1 Q9NTF0 Q9NTN3 Q9NVH6 Q9NY47 Q9NY57
Q9NYB5 Q9NYG8 Q9NYK1 Q9NYX4 Q9NZK7 Q9NZQ8 Q9P0X4 Q9P0Z9 Q9P289 Q9P2K8 Q9QYN8 Q9UBC3 Q9UBF8 Q9UBS5
Q9UEE5 Q9UEW8 Q9UHC3 Q9UHC9 Q9UHD2 Q9UHL4 Q9UI33 Q9UIF8 Q9UIG8 Q9UK23 Q9UK32 Q9UKE5 Q9UL54 Q9UL62
Q9ULX7 Q9UM07 Q9UN88 Q9UNA4 Q9UPE1 Q9UPY5 Q9UQB9 Q9UQD0 Q9UQL6 Q9WUD2 Q9Y233 Q9Y251 Q9Y271 Q9Y2H1
Q9Y2H9 Q9Y2I1 Q9Y468 Q9Y5K3 Q9Y5N1 Q9Y5Y4 Q9Y5Y9 Q9Y616 Q9Y666 Q9Y694 Q9Y6L6 Q9Y6M4 Q9Z0U4 Q9Z0V1
Q9Z2J6 V9GXZ4 A0A024QYT5 A0A024QYW7 A0A024QYX0 A0A024QZ12 A0A024QZ15 A0A024QZ20 A0A024QZ26
A0A024QZ30 A0A024QZ70 A0A024QZA8 A0A024QZM9 A0A024QZS4 A0A024QZU0 A0A024QZU1 A0A024QZV1 A0A024QZW0
A0A024QZY5 A0A024QZY7 A0A024R040 A0A024R049 A0A024R0C0 A0A024R0C6 A0A024R0H1 A0A024R0H9 A0A024R0I0
A0A024R0J1 A0A024R0L5 A0A024R0Q9 A0A024R125 A0A024R136 A0A024R151 A0A024R157 A0A024R183 A0A024R1H6
A0A024R1I3 A0A024R1V0 A0A024R222 A0A024R230 A0A024R244 A0A024R276 A0A024R2B3 A0A024R2H8 A0A024R2M7
A0A024R2N2 A0A024R2Q0 A0A024R2W7 A0A024R2Y6 A0A024R324 A0A024R325 A0A024R328 A0A024R374 A0A024R397
A0A024R3C5 A0A024R3C7 A0A024R3D5 A0A024R3G7 A0A024R3H7 A0A024R3K6 A0A024R3S2 A0A024R3S3 A0A024R3T2
A0A024R3W4 A0A024R3Z2 A0A024R426 A0A024R440 A0A024R452 A0A024R4B2 A0A024R4E2 A0A024R4H0 A0A024R4X4
A0A024R4X8 A0A024R4Z5 A0A024R567 A0A024R5B6 A0A024R5C5 A0A024R5E6 A0A024R5H1 A0A024R5I4 A0A024R5K6
A0A024R5P0 A0A024R5S8 A0A024R5W3 A0A024R5X5 A0A024R5Z3 A0A024R5Z6 A0A024R5Z9 A0A024R603 A0A024R638
A0A024R6L5 A0A024R6N2 A0A024R6Q6 A0A024R6R2 A0A024R6R4 A0A024R6T9 A0A024R704 A0A024R718 A0A024R720
A0A024R728 A0A024R730 A0A024R7C0 A0A024R7E4 A0A024R7J0 A0A024R7M7 A0A024R7T2 A0A024R880 A0A024R8A6
A0A024R8E2 A0A024R8J3 A0A024R8K3 A0A024R8S3 A0A024R8U1 A0A024R8U8 A0A024R906 A0A024R909 A0A024R913
A0A024R928 A0A024R964 A0A024R980 A0A024R9A7 A0A024R9C1 A0A024R9H3 A0A024R9I2 A0A024R9I5 A0A024R9Q4
A0A024R9Q5 A0A024R9X6 A0A024R9X9 A0A024R9Y0 A0A024R9Z8 A0A024RA31 A0A024RA66 A0A024RA96 A0A024RAE8
A0A024RAG0 A0A024RAH0 A0A024RAH7 A0A024RAP2 A0A024RAP4 A0A024RAP7 A0A024RAT5 A0A024RAU7 A0A024RAV0
A0A024RAV2 A0A024RAV7 A0A024RAY5 A0A024RB10 A0A024RB43 A0A024RB59 A0A024RB99 A0A024RBB2 A0A024RBB6
A0A024RBG4 A0A024RBG6 A0A024RBH0 A0A024RBL3 A0A024RBN1 A0A024RBP6 A0A024RBU5 A0A024RBV5 A0A024RBW9
A0A024RC53 A0A024RC61 A0A024RC92 A0A024RCE9 A0A024RCJ0 A0A024RCN9 A0A024RCW6 A0A024RD04 A0A024RD15
A0A024RD18 A0A024RD21 A0A024RD25 A0A024RD33 A0A024RD58 A0A024RD59 A0A024RD62 A0A024RD88 A0A024RDA0
A0A024RDA5 A0A024RDD4 A0A024RDH4 A0A024RDJ4 A0A024RDK3 A0A024RDL4 A0A024RDM3 A0A024RE05 A0A068F658
A0A075B7B4 A0A087WSY1 A0A087WT22 A0A087WT64 A0A087WTS4 A0A087WU84 A0A087WV24 A0A087WVC4 A0A087WW63
A0A087WW79 A0A087WWV0 A0A087WXV4 A0A087WYJ0 A0A087WYZ4 A0A087WZ06 A0A087WZ88 A0A087WZL8 A0A087X090
A0A087X0I6 A0A087X0W8 A0A087X1B1 A0A088AWN0 A0A088QCU6 A0A090N7W1 A0A090N7W4 A0A090N7X8 A0A090N8Q6
A0A090N8Y0 A0A090N8Z1 A0A0A0MQR8 A0A0A0MQX8 A0A0A0MR48 A0A0A0MR60 A0A0A0MR67 A0A0A0MRG0 A0A0A0MRG2
A0A0A0MRL7 A0A0A0MRV2 A0A0A0MS52 A0A0A0MSE3 A0A0A0MSK3 A0A0A0MSK8 A0A0A0MSS8 A0A0A0MT22 A0A0A0MTA6
A0A0A0MTJ0 A0A0A0N0L2 A0A0A6YYA8

Appendix 3 Benchmark database of drug-protein interactions for Goal 3

The list of 34456 drug-protein interactions that are included in the benchmark database from Chapter 5. We provide PubChem CIDs and names for drugs (highlighted in gray color) and UniProt accession numbers for protein targets for each drug.

CID 119: gamma-aminobutyric acid
A0A024QZY7 A0A024R4E2 A0A024R909 A0A024R9X6 A0A024RCN9 A0A090N8Z1 A0A0A0MTJ0 A0A0A6YYA8 A8K177 B4DN83 B4E398 B7ZKN7 F1D8N7 O75899
O88871 P02545 P13612 P21728 P23415 P24046 P31644 P34903 P50440 Q03164 Q16445 Q68DU8 Q6ZWB6 Q92830 Q96CX2 Q96QE3 Q9UBS5 Q9UIF8 Q9Z0U4
CID 137: delta-aminolevulinic acid
A0A024QZY7 B2CQT6 P02545 P13716 P24046 Q16348 Q9UIF8
CID 338: salicylic acid
A0A024QZY7 A0A024R2N2 A0A024R2Q0 A0A024R3C5 A0A024R3S2 A0A024R5I4 A0A024R6R4 A0A024R6T9 A0A024R9I2 A0A024RAP2 A0A024RBW9 A0A024RD15
A0A087WU84 A0A090N7W1 A0A090N7X8 A0A0A0MRG0 A0A0A0MSK3 A0A0A0MT22 A0N0Q1 A1A4V4 A2A3U5 A2RUS0 A4D1D2 A4D1Q0 A8K1F6 A8K249 A8K3J4
A8K7N8 A8KAF4 A8KAG8 B0ZBE0 B2R7Y7 B2R807 B2RXH2 B3KUB4 B4DN15 B4DUH8 B7Z1L9 B8K2Q5 C1ID52 E5KQF5 F1D8N3 F5H1T4 G5E9C5 H6VQ59 K9J958
L7RSL3 L7RXH5 O60656 P00352 P00533 P00915 P00918 P02768 P05177 P05181 P06133 P06239 P06241 P07451 P07550 P08173 P08236 P08246 P08254
P08311 P08588 P08684 P08913 P09917 P11229 P11509 P11712 P14780 P14902 P15428 P17252 P18825 P21397 P21452 P21554 P21728 P21917 P22303
P22748 P22894 P23219 P25021 P25024 P25025 P25101 P25103 P25929 P28223 P28482 P30411 P30872 P30874 P31391 P32238 P32245 P32745 P33032
P35218 P35346 P35354 P35367 P36537 P37288 P41143 P41595 P41968 P43166 P49146 P50052 P50406 P51681 Q01959 Q04828 Q08209 Q16790 Q38Q88
Q4U2R8 Q92830 Q9NSA0 Q9UHC3
CID 444: bupropion
A0A024QZY7 A0A024R2N2 A0A024R2Q0 A0A024R3C5 A0A024R3S2 A0A024R5I4 A0A024R6T9 A0A024R9I2 A0A024RAP2 A0A024RAU7 A0A024RCN9 A0A024RD15
A0A087WU84 A0A090N7W1 A0A0A0MQX8 A0A0A0MRG0 A0A0A0MSK3 A0A0A0MT22 A0A0A0MTJ0 A0N0Q1 A1A4V4 A2A3U5 A2RUS0 A4D1Q0 A8K1F6 A8K249 A8K5W4
A8K7N8 A8KAF4 A8KAG8 B0ZBD3 B0ZBE0 B2R7Y7 B3KP78 B4DN15 B7Z1L9 B7Z242 B7ZKN7 B8K2Q5 C1ID52 E5KQF5 F1D8N3 F5H1T4 G5E9C5 H6VQ59 K9J958
L7RSL3 L7RXH5 O94782 P00352 P00533 P00918 P05177 P05181 P06239 P06241 P07550 P08173 P08246 P08311 P08588 P08684 P08913 P11229 P11509
P11712 P14780 P17252 P17405 P18825 P20813 P21397 P21452 P21554 P21728 P21917 P22303 P23975 P25021 P25024 P25025 P25101 P25103 P25929
P28223 P28482 P30411 P32238 P32245 P32297 P33032 P35354 P35367 P37288 P41143 P41595 P41968 P49146 P50052 P50406 P51681 P83916 Q01959
Q08209 Q38Q88 Q92830 Q92887 Q9UIF8
CID 453: mannitol
A0A024QZY7 A0A024R2N2 A0A024R2Q0 A0A024R3C5 A0A024R3S2 A0A024R4E2 A0A024R6T9 A0A024R9I2 A0A024RAP2 A0A024RD15 A0A087WU84 A0A090N7W1
A0A0A0MRG0 A0A0A0MSK3 A0A0A0MT22 A0N0Q1 A1A4V4 A2A3U5 A2RUS0 A4D1D2 A4D1Q0 A8K1F6 A8K249 A8K7N8 A8KAF4 A8KAG8 B0ZBE0 B2R7Y7 B4DN15
B7Z1L9 B7Z242 B8K2Q5 C1ID52 E5KQF5 F1D8N3 F5H1T4 G5E9C5 H6VQ59 K9J958 L7RSL3 L7RXH5 O15245 P00533 P00918 P02545 P05177 P05181 P06239
P06241 P07550 P08173 P08246 P08311 P08588 P08684 P08913 P11229 P11509 P11712 P14780 P17252 P18825 P21397 P21452 P21554 P21728 P21917
P22303 P25021 P25024 P25025 P25101 P25103 P25929 P28223 P28482 P30411 P32238 P32245 P33032 P35354 P35367 P37288 P39748 P41143 P41595
P41968 P49146 P50052 P50406 P51681 P83916 Q01959 Q08209 Q16236 Q38Q88 Q92830 Q9Y468
CID 564: epsilon-aminocaproic acid
A0A024QZY7 A0A024R2N2 A0A024R2Q0 A0A024R3C5 A0A024R3S2 A0A024R6T9 A0A024R909 A0A024R9I2 A0A024RAP2 A0A024RAV2 A0A024RCN9 A0A024RD15
A0A087WU84 A0A090N7W1 A0A0A0MRG0 A0A0A0MSK3 A0A0A0MT22 A0N0Q1 A1A4V4 A2A3U5 A2RUS0 A4D1Q0 A8K1F6 A8K249 A8K7N8 A8KAF4 A8KAG8 B0ZBE0
B2R7Y7 B4DN15 B7Z1L9 B8K2Q5 C1ID52 E5KQF5 F1D8N3 F1D8N7 F5H1T4 G5E9C5 H6VQ59 K9J958 L7RSL3 L7RXH5 P00352 P00533 P00747 P00750 P00918
P02545 P05177 P05181 P06239 P06241 P07550 P08173 P08246 P08311 P08588 P08684 P08913 P11229 P11509 P11712 P14780 P16050 P17252 P18825
P21397 P21452 P21554 P21728 P21917 P22303 P25021 P25024 P25025 P25101 P25103 P25929 P28223 P28482 P30411 P32238 P32245 P33032 P35354
P35367 P37288 P41143 P41595 P41968 P49146 P50052 P50406 P51681 P83916 Q01959 Q08209 Q13526 Q38Q88 Q92830 Q96QE3
CID 598: mesna
A0A024R2N2 A0A024R2Q0 A0A024R3C5 A0A024R3S2 A0A024R6T9 A0A024R9I2 A0A024R9Y0 A0A024RAP2 A0A024RD15 A0A087WU84 A0A090N7W1 A0A0A0MRG0
A0A0A0MSK3 A0A0A0MT22 A0N0Q1 A1A4V4 A2A3U5 A2RUS0 A4D1Q0 A8K1F6 A8K249 A8K7N8 A8KAF4 A8KAG8 B0ZBE0 B2R7Y7 B2RXH2 B4DN15 B7Z1L9
B8K2Q5 C1ID52 E5KQF5 F1D8N3 F5H1T4 G5E9C5 H6VQ59 K9J958 L7RSL3 L7RXH5 P00533 P00918 P05177 P05181 P06239 P06241 P07550 P08173 P08246
P08311 P08588 P08684 P08913 P11229 P11509 P11712 P14780 P16050 P17252 P18825 P21397 P21452 P21554 P21728 P21917 P22303 P25021 P25024
P25025 P25101 P25103 P25929 P28223 P28482 P30411 P32238 P32245 P33032 P35354 P35367 P37288 P41143 P41595 P41968 P49146 P50052 P50406
P51681 Q01959 Q08209 Q38Q88
CID 612: lactate
A0A024R0H1 A0A024R2N2 A0A024R2Q0 A0A024R3C5 A0A024R3S2 A0A024R5C5 A0A024R5I4 A0A024R5Z9 A0A024R6T9 A0A024R8J3 A0A024R8U1 A0A024R9I2
A0A024R9I5 A0A024RAP2 A0A024RBB2 A0A024RD15 A0A087WT22 A0A087WU84 A0A090N7W1 A0A0A0MRG0 A0A0A0MSK3 A0A0A0MT22 A0N0Q1 A1A4V4 A2A3U5
A2RUS0 A4D1Q0 A8K1F6 A8K249 A8K7N8 A8KAF4 A8KAG8 B0ZBE0 B2R7Y7 B3KU60 B4DF30 B4DN15 B4DPF4 B7Z1L9 B7ZM24 B8K2Q5 C1ID52 E5KQF5 F1D8N3
F5H1T4 G5E9C5 H6VQ59 K9J958 L7RSL3 L7RXH5 O15374 O15375 O95907 P00533 P00915 P00918 P05177 P05181 P06239 P06241 P07550 P08173 P08246
P08311 P08588 P08684 P08913 P11177 P11229 P11509 P11712 P14780 P17252 P18825 P21397 P21452 P21554 P21728 P21917 P22303 P22748 P25021
P25024 P25025 P25101 P25103 P25929 P28223 P28482 P30411 P30613 P32238 P32245 P33032 P35218 P35354 P35367 P36021 P37288 P41143 P41595
P41968 P49146 P50052 P50406 P51681 P80404 Q01959 Q08209 Q16790 Q38Q88 Q92959 Q9BYV1 Q9H2X9 Q9Y666
CID 679: dimethyl sulphoxide
A0A024QYT5 A0A024QZS4 A0A024R2N2 A0A024R2Q0 A0A024R3C5 A0A024R3S2 A0A024R6T9 A0A024R9I2 A0A024RAP2 A0A024RD15 A0A087WU84 A0A090N7W1
A0A0A0MRG0 A0A0A0MSK3 A0A0A0MSS8 A0A0A0MT22 A0N0Q1 A1A4V4 A2A3U5 A2RUS0 A4D1Q0 A8K1F6 A8K249 A8K7N8 A8KAF4 A8KAG8 B0YJ76 B0ZBE0
B2R7Y7 B4DN15 B7Z1L9 B8K2Q5 C1ID52 E5KQF5 E9KL36 F1D8N3 F1D8Q5 F5H1T4 G5E9C5 H6VQ59 K9J958 L7RSL3 L7RXH5 O60885 P00533 P00918 P05177
P05181 P06239 P06241 P07550 P08173 P08185 P08246 P08311 P08588 P08684 P08913 P11229 P11509 P11712 P14780 P17252 P18825 P21397 P21452

P21554 P21728 P21917 P22303 P25021 P25024 P25025 P25101 P25103 P25929 P28223 P28482 P30411 P32238 P32245 P33032 P35354 P35367 P37288
P41143 P41595 P41968 P47712 P49146 P50052 P50406 P51681 Q01959 Q02790 Q08209 Q38Q88
CID 681: dopamine
A0A024QZY7 A0A024R276 A0A024R3C5 A0A024R6L5 A0A024R6T9 A0A024R9Y0 A0A024RAP4 A0A024RAV2 A0A024RBW9 A0A024RCN9 A0A087WT22 A1A4V4
A8K3J4 A8K5W4 B2R7Y7 B2RXH2 B3KUB4 B4DUH8 B4E398 B7Z242 B7ZKN7 B7ZW53 C1ID52 D0VY79 F8W6L1 L8B082 O15244 O15245 O43704 O75164 O94925
P00352 P00915 P00918 P02545 P07451 P07550 P08588 P09172 P10253 P16050 P16662 P21397 P21728 P21917 P21918 P21964 P22309 P22310 P22748
P27695 P28482 P30729 P35218 P35462 P39748 P42345 P43166 P43220 P50225 P61169 P83916 Q01453 Q01959 Q16790 Q16853 Q5DSZ7 Q5DT02 Q99549
Q99700 Q99714 Q9UIF8 Q9UNA4
CID 750: polyglycine
A0A024R2N2 A0A024R2Q0 A0A024R3C5 A0A024R3S2 A0A024R4Z5 A0A024R6T9 A0A024R9I2 A0A024RAP2 A0A024RB99 A0A024RD15 A0A087WU84 A0A090N7W1
A0A0A0MRG0 A0A0A0MSK3 A0A0A0MT22 A0A0A6YYA8 A0N0Q1 A1A4V4 A2A3U5 A2RUS0 A4D1Q0 A8K1F6 A8K228 A8K249 A8K7N8 A8KAF4 A8KAG8 A9ZM15
B0ZBE0 B2CQT6 B2R7Y7 B4DN15 B4E398 B7Z1L9 B7Z3W8 B8K2Q5 C1ID52 E5KQF5 F1D8N3 F5H1T4 G5E9C5 H6VQ59 H9NIM1 K9J958 L7RSL3 L7RXH5 O15399
O60391 O75311 P00533 P00918 P05177 P05181 P06239 P06241 P07550 P07741 P08173 P08246 P08311 P08588 P08684 P08913 P11229 P11509 P11712
P13196 P14780 P17252 P18825 P21397 P21452 P21549 P21554 P21728 P21917 P22303 P22309 P22557 P23378 P23415 P23416 P23434 P25021 P25024
P25025 P25101 P25103 P25929 P28223 P28482 P30411 P32238 P32245 P33032 P34896 P35354 P35367 P37288 P41143 P41250 P41595 P41968 P48167
P48637 P49146 P50052 P50406 P50440 P51681 Q01098 Q01959 Q05586 Q08209 Q12879 Q13126 Q13224 Q14032 Q14749 Q38Q88 Q4VAM5 Q5T6X5 Q6IB77
Q9BY49 Q9BYV1 Q9H598 Q9P0Z9
CID 774: histamine
A0A024QZY7 A0A024R909 A0A024RBW9 A0A024RCN9 A0A0A0MR48 A0A0A0MTJ0 A8K3J4 B2KJ49 B3KUB4 B4DUH8 B4DWC1 B4E398 B7ZKN7 O15244 O15245
O75751 O94782 P00915 P00918 P02545 P07451 P22748 P25021 P25102 P27695 P28223 P34969 P35218 P35367 P43166 P58406 Q16790 Q91ZY1 Q91ZY2
Q9H3N8 Q9QYN8 Q9UIF8 Q9UNA4 Q9Y5N1
CID 785: hydroquinone
A0A024QZY7 A0A024R909 A0A024R9Y0 A0A024R9Z8 A0A024RAV2 A0A024RBV5 A0A024RBW9 A0A024RCN9 A0A024RCW6 A0A024RDA5 A0A024RDJ4 A8K3J4
A8KAF4 B2RXH2 B3KUB4 B4DUH8 B6ZGS9 B7ZKN7 D0VY79 D9YZU5 E5KQF5 F1D8N5 F1D8N7 F1D8P6 F1D8Q5 F8W6L1 O15118 O94925 P00352 P00915 P00918
P02545 P07451 P08684 P15428 P16050 P22748 P35218 P39748 P42345 P43166 P83916 Q01453 Q13526 Q16790 Q5DSZ7 Q5DT02 Q96QE3 Q99549 Q99700
Q99714
CID 838: epinephrine
A0A024QZY7 A0A024R2N2 A0A024R2Q0 A0A024R3C5 A0A024R3S2 A0A024R6L5 A0A024R6T9 A0A024R9I2 A0A024R9Y0 A0A024RAP2 A0A024RAP4 A0A024RAV2
A0A024RBG4 A0A024RBW9 A0A024RCN9 A0A024RD15 A0A087WU84 A0A090N7W1 A0A090N8Z1 A0A0A0MRG0 A0A0A0MSK3 A0A0A0MT22 A0A0A0MTJ0 A0N0Q1
A1A4V4 A2A3U5 A2RUS0 A4D1Q0 A8K1F6 A8K249 A8K3J4 A8K7N8 A8KAF4 A8KAG8 B0ZBD3 B0ZBE0 B2R7Y7 B2RXH2 B3KUB4 B4DN15 B4DUH8 B7Z1L9 B7ZKN7
B8K2Q5 C1ID52 D0VY79 E5KQF5 E9PG18 F1D8N3 F1D8P4 F1D8P8 F5H1T4 G5E9C5 H6VQ59 K9J958 L7RSL3 L7RXH5 O15245 O15296 O75164 O94782 P00352
P00533 P00915 P00918 P05177 P05181 P06239 P06241 P07451 P07550 P08173 P08246 P08311 P08588 P08684 P08913 P11229 P11509 P11712 P13945
P14780 P17252 P18054 P18089 P18825 P21397 P21452 P21554 P21728 P21917 P22303 P22748 P25021 P25024 P25025 P25101 P25103 P25929 P25962
P26255 P27695 P28223 P28482 P30411 P32238 P32245 P33032 P34969 P35218 P35354 P35367 P35368 P37288 P39748 P41143 P41595 P41968 P42345
P43166 P43220 P49146 P50052 P50406 P51681 Q01453 Q01959 Q03164 Q08209 Q13526 Q15858 Q16790 Q38Q88 Q99549 Q99700 Q99714 Q9Y5Y9
CID 853: thyroxine
A0A024R5I4 A0A024R9X6 A0A024R9Y0 A0A024R9Z8 A0A024RAP4 A0A024RAT5 A0A024RAU7 A0A024RCN9 A0A024RCW6 A0A024RD62 A4D1D2 A8K177 A8K1F6
B3KP78 B6ZGS9 B7Z1L9 B7ZW53 D2KUA6 E9KL36 F1D8N7 F1D8P8 F1D8P9 H6VQ59 O15245 O43704 O60656 O75604 O94782 P00352 P02545 P02768 P05543
P07202 P08684 P10827 P11712 P12004 P16050 P19224 P22309 P22310 P29275 P31644 P34903 Q01650 Q13526 Q14894 Q16445 Q6ZQN7 Q92830 Q96BD0
Q99714 Q9BR01 Q9NYB5
CID 861: triiodothyronine
A0A024QZY7 A0A024R2N2 A0A024R2Q0 A0A024R3C5 A0A024R3S2 A0A024R6T9 A0A024R9I2 A0A024R9Y0 A0A024R9Z8 A0A024RAP2 A0A024RAP4 A0A024RAT5
A0A024RAU7 A0A024RCN9 A0A024RD15 A0A024RD62 A0A068F658 A0A087WT64 A0A087WU84 A0A090N7W1 A0A090N8Z1 A0A0A0MQX8 A0A0A0MRG0 A0A0A0MSK3
A0A0A0MT22 A0A0A0MTJ0 A0N0Q1 A1A4V4 A2A3U5 A2RUS0 A4D1D2 A4D1Q0 A8K1F6 A8K249 A8K7N8 A8KAF4 A8KAG8 B0ZBE0 B2R7Y7 B3KP78 B4DN15
B6ZGS9 B7Z1L9 B7Z1W5 B7ZKN7 B7ZW53 B8K2Q5 C1ID52 D0VY79 E5KQF5 E9KL36 F1D8N3 F1D8N5 F1D8N7 F1D8P8 F5H1T4 G5E9C5 H6VQ59 K9J958 L7RSL3
L7RXH5 O43704 O60656 O75164 O75604 O75874 O94782 O94925 P00352 P00533 P00918 P02545 P02768 P05177 P05181 P05543 P06239 P06241 P07550
P08173 P08246 P08311 P08588 P08684 P08913 P10827 P11229 P11509 P11712 P12004 P14780 P15428 P17252 P18054 P18825 P19224 P21397 P21452
P21554 P21728 P21917 P22303 P22309 P22310 P25021 P25024 P25025 P25101 P25103 P25929 P27695 P28223 P28482 P30411 P32238 P32245 P33032
P35354 P35367 P37288 P39748 P41143 P41595 P41968 P43220 P49146 P50052 P50225 P50406 P51681 P83916 Q01650 Q01959 Q08209 Q13526 Q14191
Q16236 Q38Q88 Q6ZQN7 Q92830 Q96BD0 Q99714 Q9BR01 Q9NYB5 Q9UIF8 Q9UNA4 Q9Y468
CID 1046: pyrazinamide
A0A024R2N2 A0A024R2Q0 A0A024R3C5 A0A024R3S2 A0A024R6T9 A0A024R9I2 A0A024RAP2 A0A024RCN9 A0A024RCW6 A0A024RD15 A0A087WU84 A0A090N7W1
A0A0A0MRG0 A0A0A0MSK3 A0A0A0MT22 A0A0A0MTJ0 A0N0Q1 A1A4V4 A2A3U5 A2RUS0 A4D1Q0 A8K1F6 A8K249 A8K7N8 A8KAF4 A8KAG8 B0ZBE0 B2R7Y7
B4DN15 B7Z1L9 B8K2Q5 C1ID52 E5KQF5 F1D8N3 F1D8N7 F1D8P8 F5H1T4 G5E9C5 H6VQ59 K9J958 L7RSL3 L7RXH5 O94782 P00533 P00918 P05177 P05181
P06239 P06241 P07550 P08173 P08246 P08311 P08588 P08684 P08913 P11229 P11509 P11712 P14780 P17252 P18825 P21397 P21452 P21554 P21728
P21917 P22303 P25021 P25024 P25025 P25101 P25103 P25929 P27695 P28223 P28482 P30411 P32238 P32245 P33032 P35354 P35367 P37288 P41143
P41595 P41968 P47989 P49146 P49327 P50052 P50406 P51681 P83916 Q01959 Q08209 Q38Q88 Q96QE3
CID 1054: vitamin B6
A0A024QZY7 A0A024R1I3 A0A024R222 A0A087WT22 B2RXH2 F1D8N5 F2Z2Y4 P00352 P02768 P15428 P42898 P49419 Q99714 Q9NTF0 Q9UNA4
CID 1130: thiamine
A0A024QZY7 A0A024R4E2 A0A024R928 A0A090N8Y0 G3V5Q5 K9JA46 O15244 O15245 O94782 P29401 P83916 Q92830
CID 1775: phenytoin
A0A024QZY7 A0A024R2N2 A0A024R2Q0 A0A024R3C5 A0A024R3S2 A0A024R5I4 A0A024R6T9 A0A024R909 A0A024R9I2 A0A024R9X6 A0A024R9Y0 A0A024RAH7
A0A024RAP2 A0A024RAU7 A0A024RCN9 A0A024RD15 A0A087WU84 A0A090N7W1 A0A0A0MRG0 A0A0A0MSK3 A0A0A0MT22 A0N0Q1 A1A4V4 A2A3U5 A2RUS0
A4D1D2 A4D1Q0 A8K177 A8K1F6 A8K249 A8K7N8 A8KAF4 A8KAG8 B0ZBE0 B2R7Y7 B3KP78 B4DKH4 B4DN15 B4DN83 B7Z1F5 B7Z1L9 B7Z3P6 B7ZKN7 B8K2Q5
C1ID52 E5KQF5 E9PG18 F1D8N3 F1D8N7 F1DAL4 F5H1T4 G5E9C5 H6VQ59 K9J958 L7RSL3 L7RXH5 O00519 O15245 P00352 P00533 P00918 P02545 P02768
P04775 P05177 P05181 P06239 P06241 P06280 P07550 P08173 P08246 P08311 P08588 P08684 P08913 P11229 P11509 P11712 P14780 P17252 P18825
P20813 P21397 P21452 P21554 P21728 P21917 P22303 P25021 P25024 P25025 P25101 P25103 P25929 P28223 P28482 P29275 P30411 P31644 P32238
P32245 P33032 P34903 P35354 P35367 P35498 P37288 P39748 P41143 P41595 P41968 P42898 P49146 P50052 P50406 P51681 P83916 Q01453 Q01959
Q03164 Q08209 Q15858 Q16236 Q16445 Q38Q88 Q92830 Q92887 Q99250
CID 1935: tacrine
A0A024QZY7 A0A024R2N2 A0A024R2Q0 A0A024R3C5 A0A024R3D5 A0A024R3S2 A0A024R4E2 A0A024R6T9 A0A024R909 A0A024R9I2 A0A024RAH7 A0A024RAP2
A0A024RCN9 A0A024RD15 A0A024RDA5 A0A024RDJ4 A0A087WU84 A0A090N7W1 A0A0A0MR48 A0A0A0MRG0 A0A0A0MSK3 A0A0A0MT22 A0A0A0MTJ0 A0N0Q1
A1A4V4 A2A3U5 A2RUS0 A4D1D2 A4D1Q0 A8K1F6 A8K249 A8K7N8 A8KAF4 A8KAG8 B0ZBE0 B2R7Y7 B2RXH2 B4DN15 B7Z1L9 B7Z242 B8K2Q5 C1ID52 D3DNN4
E5KQF5 F1D8N3 F1D8N5 F1D8N7 F1D8Q5 F5H1T4 G5E9C5 H6VQ59 K9J958 L7RSL3 L7RXH5 O15244 O15245 O15296 P00352 P00533 P00918 P02545 P05177
P05181 P06239 P06241 P06276 P07550 P08173 P08246 P08311 P08588 P08684 P08913 P11229 P11509 P11712 P12657 P14780 P16050 P17252 P18825
P21397 P21452 P21554 P21728 P21917 P22303 P25021 P25024 P25025 P25101 P25103 P25929 P27695 P28223 P28482 P30411 P32238 P32245 P33032
P35354 P35367 P37288 P39748 P41143 P41595 P41968 P49146 P50052 P50406 P51681 Q01959 Q08209 Q13526 Q13627 Q16236 Q38Q88 Q86VL8 Q92630
Q96FL8 Q96QE3 Q99700 Q99714 Q9ERZ4 Q9UNA4
CID 1978: acebutolol
A0A024QZY7 A0A024R2N2 A0A024R2Q0 A0A024R3C5 A0A024R3S2 A0A024R6T9 A0A024R9I2 A0A024RAP2 A0A024RCN9 A0A024RD15 A0A087WU84 A0A090N7W1
A0A0A0MRG0 A0A0A0MSK3 A0A0A0MT22 A0N0Q1 A1A4V4 A2A3U5 A2RUS0 A4D1D2 A4D1Q0 A8K1F6 A8K249 A8K7N8 A8KAF4 A8KAG8 B0ZBE0 B2R7Y7 B2RXH2
B4DN15 B7Z1L9 B8K2Q5 C1ID52 D0VY79 E5KQF5 F1D8N3 F5H1T4 G5E9C5 H6VQ59 K9J958 L7RSL3 L7RXH5 O15245 P00533 P00918 P02545 P05177 P05181
P06239 P06241 P07550 P08173 P08246 P08311 P08588 P08684 P08913 P11229 P11509 P11712 P14780 P17252 P18825 P21397 P21452 P21554 P21728
P21917 P22303 P25021 P25024 P25025 P25101 P25103 P25929 P28223 P28482 P30411 P32238 P32245 P35367 P37288 P41143 P41595
P41968 P49146 P50052 P50406 P51681 Q01959 Q08209 Q38Q88
CID 1983: acetaminophen
A0A024R2N2 A0A024R2Q0 A0A024R3C5 A0A024R3S2 A0A024R5Z3 A0A024R6T9 A0A024R9I2 A0A024R9Y0 A0A024RAH7 A0A024RAP2 A0A024RBW9 A0A024RD15
A0A087WU84 A0A090N7W1 A0A0A0MRG0 A0A0A0MSK3 A0A0A0MSS8 A0A0A0MT22 A0A0A0MTJ0 A0N0Q1 A0N0X8 A1A4V4 A2A3U5 A2RUS0 A4D1D2 A4D1Q0 A8K177
A8K1F6 A8K249 A8K3J4 A8K7N8 A8KAF4 A8KAG8 B0ZBE0 B2R7Y7 B2ZGL7 B3KUB4 B4DN15 B4DUH8 B7Z1L9 B7ZW53 B8K2Q5 C1ID52 E5KQF5 F1D8N3 F1D8P6
F5H1T4 G5E9C5 H6VQ59 K9J958 L7RSL3 L7RXH5 O15245 O60656 O94925 P00352 P00533 P00915 P00918 P02144 P05177 P05181 P06133 P06239 P06241
P07451 P07550 P08173 P08246 P08311 P08588 P08684 P08913 P11229 P11509 P11712 P14780 P16662 P17252 P18825 P19224 P20813 P21397 P21452
P21554 P21728 P21917 P22303 P22309 P22310 P22748 P23219 P25021 P25024 P25025 P25101 P25103 P25929 P28223 P28482 P30411 P32238 P32245
P33032 P35218 P35354 P35367 P36537 P37288 P41143 P41595 P41968 P43166 P49146 P50052 P50225 P50406 P51681 P83916 Q01959 Q08209 Q16790
Q38Q88 Q5DSZ6 Q5DSZ7 Q5DT02 Q96QE3
CID 1986: acetazolamide
A0A024QZY7 A0A024R2N2 A0A024R2Q0 A0A024R3C5 A0A024R3S2 A0A024R6L5 A0A024R6R4 A0A024R6T9 A0A024R9I2 A0A024RA31 A0A024RAP2 A0A024RBW9
A0A024RCN9 A0A024RD15 A0A087WU84 A0A090N7W1 A0A0A0MQX8 A0A0A0MRG0 A0A0A0MSK3 A0A0A0MT22 A0N0Q1 A0PJA6 A1A4V4 A2A3U5 A2RUS0 A4D1Q0
A8K1F6 A8K249 A8K3J4 A8K7N8 A8KAF4 A8KAG8 B0ZBE0 B2R7Y7 B3KUB4 B4DN15 B4DUH8 B7Z1L9 B7Z242 B7ZKN7 B8K2Q5 C1ID52 E5KQF5 F1D8N3 F1D8N7
F5H1T4 G5E9C5 H6VQ59 K9J958 L7RSL3 L7RXH5 O43570 P00533 P00915 P05177 P05181 P06239 P06241 P07451 P07550 P08173 P08246 P08311 P08588
P08684 P08913 P11229 P11509 P11712 P14780 P17252 P18825 P21397 P21452 P21554 P21728 P21917 P22303 P22748 P25021 P25024 P25025 P25101
P25103 P25929 P28223 P28482 P30411 P32238 P32245 P33032 P35218 P35354 P35367 P37288 P39900 P41143 P41595 P41968 P43166 P49146 P50052
P50406 P51681 Q01959 Q08209 Q16790 Q38Q88 Q8N1Q1 Q92769 Q9D6N1 Q9ULX7
CID 2022: acyclovir
A0A024R2N2 A0A024R2Q0 A0A024R3C5 A0A024R3S2 A0A024R5I4 A0A024R5Z3 A0A024R6T9 A0A024R9I2 A0A024RAP2 A0A024RAU7 A0A024RAV2 A0A024RCN9
A0A024RD15 A0A087WU84 A0A090N7W1 A0A0A0MRG0 A0A0A0MSK3 A0A0A0MT22 A0A0A0MTJ0 A0N0Q1 A1A4V4 A2A3U5 A2RUS0 A4D1Q0 A8K1F6 A8K249 A8K7N8
A8KAF4 A8KAG8 B0ZBE0 B2R7Y7 B2R807 B3KP78 B4DN15 B7Z1L9 B7ZKN7 B8K2Q5 C1ID52 D9YZU5 E5KQF5 F1D8N3 F5H1T4 G5E9C5 H6VQ59 K9J958 L7RSL3
L7RXH5 O15245 O75604 P00491 P00533 P00918 P02545 P05177 P05181 P06239 P06241 P07550 P08173 P08246 P08311 P08588 P08684 P08913 P11229

P11509 P11712 P14780 P17252 P18825 P21397 P21452 P21554 P21728 P21917 P22303 P25021 P25024 P25025 P25101 P25103 P25929 P28223 P28482
P30411 P32238 P32245 P33032 P35354 P35367 P37288 P41143 P41595 P41968 P49146 P50052 P50406 P51681 Q01959 Q08209 Q38Q88 Q4U2R8 Q99714
CID 2082: albendazole
A0A024QZY7 A0A024R2N2 A0A024R2Q0 A0A024R3C5 A0A024R3S2 A0A024R6T9 A0A024R9I2 A0A024RAP2 A0A024RCN9 A0A024RD15 A0A087WT22 A0A087WU84
A0A090N7W1 A0A090N8Z1 A0A0A0MQX8 A0A0A0MRG0 A0A0A0MSK3 A0A0A0MT22 A0N0Q1 A1A4V4 A2A3U5 A2RUS0 A4D1D2 A4D1Q0 A8K1F6 A8K249 A8K7N8
A8KAF4 A8KAG8 B0ZBE0 B2R7Y7 B4DN15 B4DN83 B7Z1L9 B8K2Q5 C1ID52 E5KQF5 F1D8N3 F5H1T4 F8VQZ7 G5E9C5 H6VQ59 K9J958 L7RSL3 L7RXH5 O75874
P00533 P00918 P02545 P05177 P05181 P06239 P06241 P07437 P07550 P08173 P08246 P08311 P08588 P08684 P08913 P11229 P11509 P11712 P14780
P15428 P17252 P18825 P21397 P21452 P21554 P21728 P21917 P22303 P25021 P25024 P25025 P25101 P25103 P25929 P28223 P28482 P30411 P32238
P32245 P33032 P35354 P35367 P37288 P41143 P41595 P41968 P43220 P49146 P50052 P50406 P51681 P53582 P68371 P83916 Q01959 Q08209 Q16236
Q38Q88 Q71U36 Q96QE3 Q9HC16
CID 2083: salbutamol
A0A024R2N2 A0A024R2Q0 A0A024R3C5 A0A024R3S2 A0A024R6L5 A0A024R6T9 A0A024R909 A0A024R9I2 A0A024RAP2 A0A024RCN9 A0A024RD15 A0A024RDA5
A0A024RDJ4 A0A087WU84 A0A090N7W1 A0A0A0MRG0 A0A0A0MSK3 A0A0A0MT22 A0A0A0MTJ0 A0N0Q1 A1A4V4 A2A3U5 A2RUS0 A4D1Q0 A8K1F6 A8K249 A8K7N8
A8KAF4 A8KAG8 B0ZBE0 B2R7Y7 B4DN15 B7Z1L9 B8K2Q5 C1ID52 D0VY79 E5KQF5 F1D8N3 F5H1T4 G5E9C5 H6VQ59 K9J958 L7RSL3 L7RXH5 O15244 O15245
O94925 P00533 P00918 P01375 P01584 P02768 P05177 P05181 P06239 P06241 P07550 P08173 P08246 P08311 P08588 P08684 P08913 P11229 P11509
P11712 P14780 P17252 P18825 P21397 P21452 P21554 P21728 P21917 P22303 P25021 P25024 P25025 P25101 P25103 P25929 P27695 P28223 P28482
P30411 P32238 P32245 P33032 P35354 P35367 P37288 P39748 P41143 P41595 P41968 P49146 P50052 P50406 P51681 Q01959 Q08209 Q38Q88
CID 2088: alendronate
A0A024R2N2 A0A024R2Q0 A0A024R3C5 A0A024R3S2 A0A024R3W4 A0A024R6T9 A0A024R9I2 A0A024RAE8 A0A024RAP2 A0A024RD15 A0A087WU84 A0A087X090
A0A090N7W1 A0A0A0MR60 A0A0A0MRG0 A0A0A0MSK3 A0A0A0MT22 A0N0Q1 A1A4V4 A2A3U5 A2RUS0 A4D1Q0 A8K1F6 A8K249 A8K3M3 A8K7N8 A8KAF4 A8KAG8
B0ZBE0 B2R7Y7 B4DN15 B7Z1L9 B8K2Q5 C1ID52 E5KQF5 F1D8N3 F5H1T4 G5E9C5 H6VQ59 K9J958 L7RSL3 L7RXH5 P00533 P00918 P05177 P05181 P06239
P06241 P07550 P08173 P08246 P08311 P08588 P08684 P08913 P11229 P11509 P11712 P14324 P14780 P17252 P18825 P21397 P21452 P21554 P21728
P21917 P22303 P23469 P25021 P25024 P25025 P25101 P25103 P25929 P28223 P28482 P30411 P32238 P32245 P33032 P35354 P35367 P37288 P41143
P41595 P41968 P49146 P50052 P50406 P51681 Q01959 Q08209 Q13332 Q38Q88
CID 2092: alfuzosin
A0A024RCN9 A0A068F658 A0A090N7W1 B0ZBD3 B0ZBE0 B2RXH2 O94782 P00352 P02545 P06280 P08684 P10253 P15428 P25100 P35348 P35368 P39748
Q99714
CID 2094: allopurinol
A0A024QZY7 A0A024R2N2 A0A024R2Q0 A0A024R3C5 A0A024R3S2 A0A024R4E2 A0A024R5I4 A0A024R6T9 A0A024R9I2 A0A024RAP2 A0A024RAU7 A0A024RBV5
A0A024RCN9 A0A024RD15 A0A024RDA5 A0A087WT22 A0A087WU84 A0A090N7W1 A0A0A0MRG0 A0A0A0MSK3 A0A0A0MT22 A0A0A0MTJ0 A0N0Q1 A1A4V4 A2A3U5
A2RUS0 A4D1Q0 A8K1F6 A8K249 A8K7N8 A8KAF4 A8KAG8 B0ZBE0 B2R7Y7 B3KP78 B4DN15 B4DN83 B7Z1L9 B7ZKN7 B8K2Q5 C1ID52 E5KQF5 F1D8N3 F5H1T4
G5E9C5 H6VQ59 K9J958 L7RSL3 L7RXH5 O15245 O75874 P00492 P00533 P00918 P02545 P05177 P05181 P06239 P06241 P07550 P08173 P08246 P08311
P08588 P08684 P08913 P11229 P11509 P11712 P14780 P17252 P18825 P21397 P21452 P21554 P21728 P21917 P22303 P23469 P25021 P25024 P25025
P25103 P25929 P28223 P28482 P30411 P32238 P32245 P33032 P35354 P35367 P37288 P41143 P41595 P41968 P47989 P49146 P50052 P50406 P51681
Q01959 Q08209 Q16236 Q38Q88
CID 2099: alosetron
A0A024QZY7 A0A024R2N2 A0A024R2Q0 A0A024R3C5 A0A024R3S2 A0A024R6T9 A0A024R9I2 A0A024RAP2 A0A024RD15 A0A087WU84 A0A090N7W1 A0A0A0MRG0
A0A0A0MSK3 A0A0A0MT22 A0N0Q1 A1A4V4 A2A3U5 A2RUS0 A4D1Q0 A8K1F6 A8K249 A8K7N8 A8K8D3 A8KAF4 A8KAG8 B0ZBE0 B2R7Y7 B4DN15 B4DN83
B4E398 B7Z1L9 B8K2Q5 C1ID52 E5KQF5 F1D8N3 F5H1T4 G5E9C5 H6VQ59 K9J958 L7RSL3 L7RXH5 P00533 P00918 P05177 P05181 P06239 P06241 P07550
P08173 P08246 P08311 P08588 P08684 P08913 P11229 P11509 P11712 P14780 P17252 P18825 P20813 P21397 P21452 P21554 P21728 P21917 P22303
P25021 P25024 P25025 P25101 P25103 P25929 P28223 P28482 P30411 P32238 P32245 P33032 P35354 P35367 P37288 P39748 P41143 P41595 P41968
P46098 P49146 P50052 P50406 P51681 Q01959 Q08209 Q38Q88 Q9GZV3
CID 2118: alprazolam
A0A024R2N2 A0A024R2Q0 A0A024R3C5 A0A024R3S2 A0A024R6T9 A0A024R9I2 A0A024R9X6 A0A024RAP2 A0A024RD15 A0A087WU84 A0A090N7W1 A0A0A0MRG0
A0A0A0MSK3 A0A0A0MT22 A0N0Q1 A1A4V4 A2A3U5 A2RUS0 A4D1Q0 A8K177 A8K1F6 A8K249 A8K496 A8K7N8 A8KAF4 A8KAG8 B0ZBE0 B2R7Y7 B2RCW8
B4DN15 B4DTP4 B7Z1L9 B8K2Q5 C1ID52 E5KQF5 F1D8N3 F5H1T4 G5E9C5 H6VQ59 K9J958 L7RSL3 L7RXH5 O76068 P00533 P00918 P02545 P05177 P05181
P06239 P06241 P07550 P08173 P08246 P08311 P08588 P08684 P08913 P11229 P11509 P11712 P14780 P14867 P15428 P17252 P18505 P18507 P18825
P21397 P21452 P21554 P21728 P21917 P22303 P25021 P25024 P25025 P25101 P25103 P25929 P28223 P28482 P30411 P31644 P32238 P32245 P33032
P34903 P35354 P37288 P41143 P41595 P41968 P47869 P47870 P48169 P49146 P50052 P50406 P51681 P78334 Q01959 Q08209 Q16445 Q38Q88 Q8N1C3
Q99928 Q9UN88
CID 2123: hexamethylmelamine
A0A024R2N2 A0A024R2Q0 A0A024R3C5 A0A024R3S2 A0A024R6T9 A0A024R909 A0A024R9I2 A0A024RAP2 A0A024RCN9 A0A024RD15 A0A087WU84 A0A090N7W1
A0A0A0MRG0 A0A0A0MSK3 A0A0A0MT22 A0N0Q1 A1A4V4 A2A3U5 A2RUS0 A4D1Q0 A8K1F6 A8K249 A8K7N8 A8KAF4 A8KAG8 B0ZBE0 B2R7Y7 B4DN15 B7Z1L9
B7ZKN7 B8K2Q5 C1ID52 E5KQF5 F1D8N3 F1D8N7 F5H1T4 G5E9C5 H6VQ59 K9J958 L7RSL3 L7RXH5 P00533 P00918 P02545 P05177 P05181 P06239 P06241
P06280 P07550 P08173 P08246 P08311 P08588 P08684 P08913 P11229 P11509 P11712 P14780 P17252 P18825 P21397 P21452 P21554 P21728 P21917
P22303 P25021 P25024 P25025 P25101 P25103 P25929 P28223 P28482 P30411 P32238 P32245 P33032 P35354 P35367 P37288 P41143 P41595 P41968
P49146 P50052 P50406 P51681 Q01959 Q08209 Q38Q88 Q92830 Q99714
CID 2130: amantadine
A0A024QZY7 A0A024R2N2 A0A024R2Q0 A0A024R3C5 A0A024R3S2 A0A024R5I4 A0A024R6T9 A0A024R909 A0A024R9I2 A0A024RAP2 A0A024RAU7 A0A024RCN9
A0A024RD15 A0A024RDJ4 A0A087WU84 A0A087WV24 A0A090N7W1 A0A0A0MRG0 A0A0A0MSK3 A0A0A0MT22 A0A0A0MTJ0 A0N0Q1 A1A4V4 A2A3U5 A2RUS0
A4D1D2 A4D1Q0 A8K1F6 A8K249 A8K4S9 A8K7N8 A8KAF4 A8KAG8 B0ZBE0 B2R7Y7 B3KP78 B4DN15 B4DN83 B7Z1L9 B7Z1W5 B7Z242 B7ZKN7 B8K2Q5 C1ID52
E5KQF5 F1D8N3 F1D8N7 F5H1T4 G5E9C5 H6VQ59 K9J958 L7RSL3 L7RXH5 O15244 O15245 O15399 P00533 P00918 P02545 P05177 P05181 P06239 P06241
P07550 P08173 P08246 P08311 P08588 P08684 P08913 P11229 P11509 P11712 P14780 P17252 P18825 P21397 P21452 P21554 P21728 P21917 P22303
P25021 P25024 P25025 P25101 P25103 P25929 P28223 P28482 P30411 P32238 P32245 P33032 P35354 P35367 P37288 P41143 P41595 P41968 P49146
P50052 P50406 P51681 P83916 Q01098 Q01453 Q01959 Q08209 Q12879 Q13224 Q16236 Q38Q88 Q8TCU5 Q92830 Q92887 Q96FL8
CID 2140: diatrizoate
A0A024R2N2 A0A024R2Q0 A0A024R3C5 A0A024R3S2 A0A024R6T9 A0A024R9I2 A0A024RAP2 A0A024RCN9 A0A024RD15 A0A087WU84 A0A090N7W1 A0A0A0MRG0
A0A0A0MSK3 A0A0A0MT22 A0N0Q1 A1A4V4 A2A3U5 A2RUS0 A4D1Q0 A8K1F6 A8K249 A8K7N8 A8KAF4 A8KAG8 B0ZBE0 B2R7Y7 B4DN15 B7Z1L9 B8K2Q5
C1ID52 E5KQF5 F1D8N3 F5H1T4 G5E9C5 H6VQ59 K9J958 L7RSL3 L7RXH5 P00533 P00918 P02545 P05177 P05181 P06239 P06241 P07550 P08173 P08246
P08311 P08588 P08684 P08913 P11229 P11509 P11712 P14780 P17252 P18825 P21397 P21452 P21554 P21728 P21917 P22303 P25021 P25024 P25025
P25101 P25103 P25929 P28223 P28482 P30411 P32238 P32245 P33032 P35354 P35367 P37288 P41143 P41595 P41968 P49146 P50052 P50406 P51681
Q01959 Q08209 Q38Q88
CID 2141: amifostine
A0A024R2N2 A0A024R2Q0 A0A024R3C5 A0A024R3S2 A0A024R6T9 A0A024R909 A0A024R9I2 A0A024RAG0 A0A024RAP2 A0A024RCN9 A0A024RD15 A0A087WU84
A0A090N7W1 A0A0A0MRG0 A0A0A0MSK3 A0A0A0MT22 A0N0Q1 A1A4V4 A2A3U5 A2RUS0 A4D1Q0 A8K1F6 A8K249 A8K7N8 A8KAF4 A8KAG8 B0ZBE0 B2R7Y7
B4DN15 B7Z1L9 B7ZKN7 B8K2Q5 C1ID52 E5KQF5 F1D8N3 F5H1T4 G5E9C5 H6VQ59 K9J958 L7RSL3 L7RXH5 P00533 P00918 P05177 P05181 P06239 P06241
P07550 P08173 P08246 P08311 P08588 P08684 P08913 P10696 P11229 P11509 P11712 P14780 P17252 P18825 P21397 P21452 P21554 P21728 P21917
P22303 P22413 P25021 P25024 P25025 P25101 P25103 P25929 P28223 P28482 P30411 P32238 P32245 P33032 P35354 P35367 P37288 P41143 P41595
P41968 P49146 P50052 P50406 P51681 Q01959 Q08209 Q38Q88
CID 2145: aminoglutethimide
A0A024QZY7 A0A024R2N2 A0A024R2Q0 A0A024R3C5 A0A024R3S2 A0A024R5S8 A0A024R6T9 A0A024R9I2 A0A024RAP2 A0A024RD15 A0A024RDJ4 A0A087WU84
A0A090N7W1 A0A0A0MRG0 A0A0A0MSK3 A0A0A0MT22 A0N0Q1 A1A4V4 A2A3U5 A2RUS0 A4D1Q0 A8K1F6 A8K249 A8K7N8 A8KAF4 A8KAG8 B0ZBE0 B2R7Y7
B4DN15 B4DN83 B7Z1L9 B8K2Q5 C1ID52 E5KQF5 F1D8N3 F5H1T4 G5E9C5 H6VQ59 K9J958 L7RSL3 L7RXH5 O75874 P00533 P00918 P05108 P05177 P05181
P06239 P06241 P07550 P08173 P08246 P08311 P08588 P08684 P08913 P11229 P11509 P11511 P11712 P14780 P17252 P18825 P21397 P21452 P21554
P21728 P21917 P22303 P23141 P25021 P25024 P25025 P25101 P25103 P25929 P28223 P28482 P30411 P32238 P32245 P33032 P35354 P35367 P37288
P41143 P41595 P41968 P49146 P50052 P50406 P51681 Q01453 Q01959 Q08209 Q13526 Q38Q88
CID 2153: theophylline
A0A024QZY7 A0A024R2N2 A0A024R2Q0 A0A024R3C5 A0A024R3S2 A0A024R4E2 A0A024R5I4 A0A024R6T9 A0A024R9I2 A0A024RAP2 A0A024RAU7 A0A024RCN9
A0A024RD15 A0A087WU84 A0A090N7W1 A0A0A0MRG0 A0A0A0MSK3 A0A0A0MT22 A0N0Q1 A1A4V4 A2A3U5 A2RUS0 A4D1Q0 A8K1F6 A8K249 A8K7N8 A8KAF4
A8KAG8 B0ZBE0 B2R7Y7 B3KP78 B4DN15 B4DN83 B7Z1L9 B8K2Q5 C1ID52 C9J1J0 D0VY79 E5KQF5 F1D8N3 F1D8P6 F5GWI4 F5H1T4 G5E9C5 H6VQ59 K9J958
L7RSL3 L7RXH5 O15245 O75874 O94782 O95467 P00533 P00918 P05177 P05181 P06239 P06241 P07550 P08173 P08246 P08311 P08588 P08684 P08913
P11229 P11509 P11712 P14780 P17252 P18825 P21397 P21452 P21554 P21728 P21917 P22303 P25021 P25024 P25025 P25099 P25101 P25103 P25929
P27815 P28223 P28482 P28647 P29274 P29275 P30411 P30542 P30543 P32238 P32245 P33032 P33765 P35354 P35367 P37288 P41143 P41595 P41968
P49146 P50052 P50406 P51681 Q01959 Q07343 Q08209 Q14432 Q38Q88 Q60614 Q92769 Q9UIF8 Q9Y694
CID 2160: amitriptyline
A0A024QZY7 A0A024R0C6 A0A024R230 A0A024R2N2 A0A024R2Q0 A0A024R3C5 A0A024R3C7 A0A024R3S2 A0A024R5I4 A0A024R5Z3 A0A024R6T9 A0A024R9I2
A0A024R9Y0 A0A024RAP2 A0A024RAU7 A0A024RCN9 A0A024RCW6 A0A024RD15 A0A024RDJ4 A0A087WT22 A0A087WU84 A0A090N7W1 A0A0A0MQX8 A0A0A0MR48
A0A0A0MRG0 A0A0A0MSK3 A0A0A0MT22 A0N0Q1 A1A4V4 A2A3U5 A2RUS0 A4D0V9 A4D1D2 A4D1Q0 A8K1F6 A8K249 A8K5W4 A8K7N8 A8KAF4 A8KAG8 B0ZBD3
B0ZBE0 B2KJ49 B2R7Y7 B2RXH2 B3KP78 B4DN15 B6ZGS9 B7Z1L9 B8K2Q5 C1ID52 D2KUA6 E5KQF5 E9PG18 F1D8N3 F1D8N7 F1D8P6 F1D8Q5 F5H1T4 G5E9C5
H6VQ59 K9J958 L7RSL3 L7RXH5 O15245 O15296 O43526 O60656 O75874 O94782 O95467 P00352 P00533 P00918 P02545 P04629 P05177 P05181 P06239
P06241 P07550 P08172 P08173 P08246 P08311 P08588 P08684 P08909 P08912 P08913 P11229 P11509 P11712 P14842 P17252 P17405 P18825
P19224 P20309 P21397 P21452 P21554 P21728 P21917 P21918 P22303 P22309 P22310 P23975 P25021 P25024 P25025 P25101 P25103 P25929 P28223
P28482 P30411 P31388 P31645 P32238 P32245 P32304 P32305 P33032 P35354 P35367 P37288 P41143 P41595 P41968 P42345 P43220 P48542 P48545
P49146 P50052 P50406 P51681 P83916 Q01453 Q01959 Q08209 Q09470 Q15858 Q38Q88 Q5DSZ7 Q5DT02 Q8NER1 Q92887 Q99250 Q99549 Q99700 Q99714
CID 2162: amlodipine
A0A024R2N2 A0A024R2Q0 A0A024R3C5 A0A024R3S2 A0A024R5Z3 A0A024R6T9 A0A024R9I2 A0A024RAP2 A0A024RD15 A0A087WU84 A0A090N7W1 A0A0A0MR67
A0A0A0MRG0 A0A0A0MSK3 A0A0A0MT22 A0N0Q1 A1A4V4 A2A3U5 A2RUS0 A4D1D2 A4D1Q0 A8K1F6 A8K249 A8K7N8 A8KAF4 A8KAG8 B0ZBE0 B1ALM3 B2R7Y7
B4DN15 B7Z1L9 B8K2Q5 C1ID52 E5KQF5 E7ERK3 F1D8N3 F5H1T4 G5E9C5 H6VQ59 K9J958 L7RSL3 L7RXH5 O95069 P00533 P00915 P00918 P05177 P05181

P06239 P06241 P07550 P08173 P08246 P08311 P08588 P08684 P08913 P11229 P11509 P11712 P14780 P17252 P17405 P18825 P21397 P21452 P21554
P21728 P21917 P22303 P25021 P25024 P25025 P25101 P25103 P25929 P28223 P28482 P30411 P32238 P32245 P33032 P35354 P35367 P37288 P41143
P41595 P41968 P49146 P50052 P50406 P51681 Q00975 Q01668 Q01959 Q06432 Q08209 Q08289 Q38Q88 Q8IZS8 Q92830

CID 2170: amoxapine

A0A024QZY7 A0A024R2N2 A0A024R2Q0 A0A024R3C5 A0A024R3S2 A0A024R4E2 A0A024R6L5 A0A024R6T9 A0A024R9I2 A0A024R9X6 A0A024RAP2 A0A024RCN9
A0A024RD15 A0A024RDJ4 A0A087WT22 A0A087WU84 A0A090N7W1 A0A090N8Z1 A0A0A0MRG0 A0A0A0MSK3 A0A0A0MT22 A0A0A0MTJ0 A0N0Q1 A1A4V4 A2A3U5
A2RUS0 A4D1Q0 A8K177 A8K1F6 A8K249 A8K496 A8K5W4 A8K7N8 A8KAF4 A8KAG8 B0ZBD3 B0ZBE0 B2KJ49 B2R7Y7 B2RCW8 B2RXH2 B4DN15 B4DTP4 B4E398
B7Z1L9 B8K2Q5 C1ID52 D0VY79 E5KQF5 F1D8N3 F1D8N7 F1D8P8 F5H1T4 F8W6L1 G5E9C5 H6VQ59 K9J958 L7RSL3 L7RXH5 O15296 O75604 O75874 O94782
P00352 P00533 P00918 P02545 P05177 P05181 P06239 P06241 P07550 P08173 P08246 P08311 P08588 P08684 P08909 P08913 P11229 P11509 P11712
P14780 P14842 P17252 P18505 P18507 P18825 P21397 P21452 P21554 P21728 P21917 P22303 P23975 P25021 P25024 P25025 P25101 P25103 P25929
P28222 P28223 P28482 P30411 P31388 P31644 P31645 P32238 P32245 P32305 P33032 P34903 P34969 P35354 P35367 P35368 P37288 P41143 P41595
P41968 P42345 P47870 P48169 P49146 P50052 P50406 P51681 P78334 P83916 Q01453 Q01959 Q08209 Q16236 Q16445 Q38Q88 Q8N1C3 Q8NER1 Q92830
Q99549 Q99700 Q99928 Q9UN88

CID 2179: amsacrine

A0A024QZY7 A0A024R4E2 A0A024R5Z3 A0A024R9Y0 A0A024RAV2 A0A024RCN9 A0A024RD62 A0A068F658 A0A087WT22 A0A090N7W1 A0A090N8Z1 A0A0A0MQX8
A0A0A0MRL7 A0A0A0MTJ0 A4D1D2 A8K249 A8K4S9 A8K987 A8K996 B2RXH2 B4DN83 B7Z1F9 B7Z2G8 B7ZKN7 C1ID52 D0VY79 F1D8P8 F8W6L1 O15245
O75164 O75874 O94782 O94925 O95467 P00352 P02545 P05177 P06280 P08684 P11387 P11388 P11712 P15428 P17405 P27695 P39748 P43220 Q01453
Q02880 Q03164 Q06278 Q16236 Q96QE3 Q99549 Q99700 Q99714 Q9UIF8 Q9UNA4

CID 2182: anagrelide

A0A024QZY7 A0A024RCN9 O75164 P05177 P27695 Q14432

CID 2187: anastrozole

A0A024R2N2 A0A024R2Q0 A0A024R3C5 A0A024R3S2 A0A024R5S8 A0A024R6T9 A0A024R913 A0A024R9I2 A0A024RAP2 A0A024RD15 A0A087WU84 A0A090N7W1
A0A0A0MRG0 A0A0A0MSK3 A0A0A0MT22 A0N0Q1 A1A4V4 A2A3U5 A2RUS0 A4D1Q0 A8K1F6 A8K249 A8K7N8 A8KAF4 A8KAG8 B0ZBE0 B2R7Y7 B4DN15 B7Z1L9
B8K2Q5 C1ID52 E5KQF5 F1D8N3 F5H1T4 G5E9C5 H6VQ59 K9J958 L7RSL3 L7RXH5 P00533 P00918 P05177 P05181 P06239 P06241 P07550 P08173 P08246
P08311 P08588 P08684 P08842 P08913 P11229 P11509 P11511 P11712 P14780 P17252 P18825 P21397 P21452 P21554 P21728 P21917 P22303 P25021
P25024 P25025 P25101 P25103 P25929 P28223 P28482 P30411 P32238 P32245 P33032 P35354 P35367 P37288 P41143 P41595 P41968 P49146 P50052
P50406 P51681 Q01959 Q08209 Q38Q88

CID 2216: apraclonidine

A0A024R909 A0A024RCN9 A0A024RDJ4 A0A068F658 A0A090N7W1 A0A0A0MTJ0 B0ZBD3 B7ZKN7 O94925 P08913 P18825 Q99714

CID 2244: aspirin

A0A024R125 A0A024R2N2 A0A024R2Q0 A0A024R3C5 A0A024R3S2 A0A024R426 A0A024R6L5 A0A024R6T9 A0A024R9I2 A0A024RAH7 A0A024RAP2 A0A024RAP4
A0A024RBN1 A0A024RCN9 A0A024RD15 A0A024RDA5 A0A068F658 A0A087WU84 A0A090N7W1 A0A090N7X8 A0A090N8Q6 A0A0A0MRG0 A0A0A0MSK3 A0A0A0MSS8
A0A0A0MT22 A0A0A0MTJ0 A0N0Q1 A1A4V4 A2A3U5 A2RUS0 A4D1D2 A4D1Q0 A4D2N2 A8K1F6 A8K249 A8K5W4 A8K7N8 A8KAF4 A8KAG8 B0ZBD3 B0ZBE0
B2R7Y7 B2RXH2 B4DN15 B4E398 B7Z1L9 B7ZKN7 B8K2Q5 C1ID52 D2KUA6 D3DNN4 E5KQF5 F1D8N3 F1D8N5 F1D8P6 F5H1T4 G5E9C5 H6VQ59 K9J958 L7RSL3
L7RXH5 O15245 O43741 O60656 O75874 P00352 P00533 P00915 P00918 P04035 P05177 P05181 P06239 P06241 P07550 P08173 P08246 P08311 P08588
P08684 P11229 P11509 P11712 P14780 P15428 P17252 P19224 P21397 P21452 P21554 P22303 P22309 P23219 P25024 P25025 P25101 P25103 P25929
P25963 P28482 P30411 P32238 P32245 P33032 P35354 P37288 P41143 P41968 P49146 P50052 P51681 Q01959 Q04828 Q08209 Q38Q88 Q4U2R8 Q99714
Q9UHC3 Q9UNA4

CID 2249: atenolol

A0A024QZY7 A0A024R2N2 A0A024R2Q0 A0A024R3C5 A0A024R3S2 A0A024R4E2 A0A024R5I4 A0A024R6L5 A0A024R6T9 A0A024R909 A0A024R9I2 A0A024RAP2
A0A024RAU7 A0A024RCN9 A0A024RD15 A0A024RDJ4 A0A087WU84 A0A090N7W1 A0A0A0MRG0 A0A0A0MSK3 A0A0A0MT22 A0A0A0MTJ0 A0N0Q1 A1A4V4 A2A3U5
A2RUS0 A4D1D2 A4D1Q0 A8K1F6 A8K249 A8K7N8 A8KAF4 A8KAG8 B0ZBE0 B2R7Y7 B2RXH2 B3KP78 B4DN15 B7Z1L9 B7ZKN7 B8K2Q5 C1ID52 E5KQF5 F1D8N3
F5H1T4 F8W6L1 G5E9C5 H6VQ59 K9J958 L7RSL3 L7RXH5 O15245 O94782 P00533 P00918 P02545 P02788 P05177 P05181 P06239 P06241 P06280 P07550
P08173 P08246 P08311 P08588 P08684 P08913 P11229 P11509 P11712 P14780 P17252 P18825 P21397 P21452 P21554 P21728 P21917 P22303 P25021
P25024 P25025 P25101 P25103 P25929 P27695 P28482 P30411 P32238 P32245 P33032 P35354 P35367 P37288 P39748 P41143 P41595 P41968 P43220
P49146 P50052 P50406 P51681 P83916 Q01453 Q01959 Q08209 Q38Q88 Q9NZK7 Q9UNA4

CID 2265: azathioprine

A0A024QZY7 A0A024R2N2 A0A024R2Q0 A0A024R3C5 A0A024R3S2 A0A024R6L5 A0A024R6T9 A0A024R9I2 A0A024R9Y0 A0A024RAP2 A0A024RCN9 A0A024RCW6
A0A024RD15 A0A024RDA5 A0A087WT22 A0A087WU84 A0A090N7W1 A0A0A0MQX8 A0A0A0MRG0 A0A0A0MSK3 A0A0A0MT22 A0N0Q1 A1A4V4 A2A3U5 A2RUS0
A4D1Q0 A8K1F6 A8K249 A8K7N8 A8KAF4 A8KAG8 B0ZBE0 B2R7Y7 B4DN15 B7Z1L9 B7ZKN7 B8K2Q5 C1ID52 D9YZU5 E5KQF5 F1D8N3 F1D8N5 F1D8P6 F5H1T4
G5E9C5 H6VQ59 K9J958 L7RSL3 L7RXH5 O15245 O75874 P00492 P00533 P00918 P02545 P05177 P05181 P06239 P06241 P07550 P08173 P08246 P08311
P08588 P08684 P08913 P11229 P11509 P11712 P14780 P17252 P18825 P20839 P21397 P21452 P21554 P21728 P21917 P22303 P25021 P25024 P25025
P25101 P25103 P25929 P28223 P28482 P30411 P32238 P32245 P33032 P35354 P35367 P37288 P41143 P41595 P41968 P49146 P50052 P50406 P51681
P56373 Q01453 Q01959 Q06203 Q08209 Q32MC3 Q38Q88 Q96QE3 Q99549 Q99700 Q9UNA4

CID 2266: azelaic acid

A0A024QZY7 A0A024R4E2 A0A024RCN9 A0A024RDJ4 A0A0A0MQX8 A0A0A0MTJ0 L8B082 P02545 P27695 P31213 P51857 Q01453 Q9UIF8

CID 2267: azelastine

A0A090N7W1 A0A0A0MR48 A4D1D2 B0ZBD3 B4DN83 C1ID52 H6UYS5 O15296 O75874 P02545 P05177 P08684 P35367 P35368 P43220 Q99700 Q9UNA4

CID 2284: baclofen

A0A024R2N2 A0A024R2Q0 A0A024R3C5 A0A024R3S2 A0A024R6T9 A0A024R909 A0A024R9I2 A0A024RAP2 A0A024RCN9 A0A024RD15 A0A024RDJ4 A0A087WU84
A0A090N7W1 A0A0A0MRG0 A0A0A0MSK3 A0A0A0MT22 A0A0A0MTJ0 A0N0Q1 A1A4V4 A2A3U5 A2RUS0 A4D1Q0 A8K1F6 A8K249 A8K7N8 A8KAF4 A8KAG8 B0ZBE0
B2R7Y7 B4DN15 B7Z1L9 B7ZKN7 B8K2Q5 C1ID52 E5KQF5 F1D8N3 F1D8N7 F5H1T4 G5E9C5 H6VQ59 H9NIL8 K9J958 L7RSL3 L7RXH5 O15245 O75899 O94782
O95467 P00533 P00918 P02545 P05177 P05181 P06239 P06241 P07550 P08173 P08246 P08311 P08588 P08684 P08913 P11229 P11509 P11712 P14780
P17252 P18825 P21397 P21452 P21554 P21728 P21917 P22303 P25021 P25024 P25025 P25101 P25103 P25929 P28223 P28482 P30411 P32238 P32245
P33032 P35354 P35367 P37288 P41143 P41595 P41968 P49146 P50052 P50406 P51681 Q01959 Q08209 Q16236 Q38Q88 Q5SUJ9 Q68DU8 Q6ZWB6 Q92830
Q96CX2 Q96QE3 Q9UBS5

CID 2337: benzocaine

A0A024QZY7 A0A024R2N2 A0A024R2Q0 A0A024R3C5 A0A024R3S2 A0A024R4E2 A0A024R6T9 A0A024R9I2 A0A024RAP2 A0A024RD15 A0A087WU84 A0A090N7W1
A0A0A0MRG0 A0A0A0MSK3 A0A0A0MT22 A0N0Q1 A1A4V4 A2A3U5 A2RUS0 A4D1D2 A4D1Q0 A8K1F6 A8K249 A8K7N8 A8KAF4 A8KAG8 B0ZBE0 B2R7Y7 B4DN15
B7Z1L9 B8K2Q5 C1ID52 E5KQF5 F1D8N3 F5H1T4 G5E9C5 H6VQ59 K9J958 L7RSL3 L7RXH5 O94782 P00533 P00918 P02545 P05177 P05181 P06239 P06241
P07550 P08173 P08246 P08311 P08588 P08684 P08913 P11229 P11509 P11712 P14780 P17252 P18825 P21397 P21452 P21554 P21728 P21917 P22303
P25021 P25024 P25025 P25101 P25103 P25929 P28223 P28482 P30411 P32238 P32245 P33032 P35354 P35367 P37288 P41143 P41595 P41968 P43220
P49146 P50052 P50406 P51681 Q01959 Q08209 Q38Q88 Q96QE3 Q9Y5Y9

CID 2366: betahistine

A0A024QZY7 A0A024R2N2 A0A024R2Q0 A0A024R3C5 A0A024R3S2 A0A024R4E2 A0A024R6T9 A0A024R9I2 A0A024RAP2 A0A024RCN9 A0A024RD15 A0A087WU84
A0A090N7W1 A0A0A0MR48 A0A0A0MRG0 A0A0A0MSK3 A0A0A0MT22 A0N0Q1 A1A4V4 A2A3U5 A2RUS0 A4D1Q0 A8K1F6 A8K249 A8K7N8 A8KAF4 A8KAG8 B0ZBE0
B2R7Y7 B4DN15 B7Z1L9 B8K2Q5 C1ID52 E5KQF5 F1D8N3 F5H1T4 G5E9C5 H6VQ59 K9J958 L7RSL3 L7RXH5 O75164 O75874 O94782 P00352 P00533 P00918
P02545 P05177 P05181 P06239 P06241 P07550 P08173 P08246 P08311 P08588 P08684 P08913 P11229 P11509 P11712 P14780 P16050 P17252 P18825
P21397 P21452 P21554 P21728 P21917 P22303 P25021 P25024 P25025 P25101 P25103 P25929 P28223 P28482 P30411 P32238 P32245 P33032 P35354
P35367 P37288 P41143 P41595 P41968 P49146 P50052 P50406 P51681 P83916 Q01959 Q08209 Q15822 Q38Q88 Q8TCU5 Q96RJ0 Q9UIF8

CID 2369: betaxolol

A0A024QZY7 A0A024R4E2 A0A024R5Z3 A0A024RCN9 A0A090N7W1 B7ZKN7 C1ID52 P02545 P07550 P08588 P10253 P11712 P27695 Q9UNA4

CID 2370: bethanechol

A0A024R909 A0A024RCN9 A0A0A0MTJ0 A0A0A6YYA8 A4D1Q0 O94782 P02545 P08172 P08173 P08482 P11229 P11712 P20309 P39748 P83916

CID 2375: bicalutamide

A0A024R2N2 A0A024R2Q0 A0A024R3C5 A0A024R3S2 A0A024R6T9 A0A024R9I2 A0A024RAP2 A0A024RD15 A0A087WU84 A0A090N7W1 A0A0A0MRG0 A0A0A0MSK3
A0A0A0MT22 A0N0Q1 A1A4V4 A2A3U5 A2RUS0 A4D1Q0 A8K1F6 A8K249 A8K7N8 A8KAF4 A8KAG8 B0ZBE0 B2R7Y7 B4DN15 B4DNQ5 B7Z1L9 B8K2Q5 C1ID52
E5KQF5 F1D8N3 F1D8N5 F5H1T4 G5E9C5 H6VQ59 K9J958 L7RSL3 L7RXH5 P00533 P00918 P05177 P05181 P06239 P06241 P07550 P08173 P08246 P08311
P08588 P08684 P08913 P10275 P11229 P11509 P11712 P14780 P17252 P18825 P21397 P21452 P21554 P21728 P21917 P22303 P25021 P25024 P25025
P25101 P25103 P25929 P28223 P28482 P30411 P32238 P32245 P33032 P35354 P35367 P37288 P41143 P41595 P41968 P49146 P50052 P50406 P51681
Q01959 Q08209 Q38Q88

CID 2381: biperiden

A0A024QZY7 A0A024R3S2 A0A024R9I2 A0A024RCN9 A0A068F658 A4D1D2 A4D1Q0 C1ID52 D0VY79 P02545 P08172 P08173 P08684 P08912 P11229 P20309
P35367 P39748 P83916 Q15822 Q99700

CID 2391: bisacodyl

A0A024QZY7 A0A024R2N2 A0A024R2Q0 A0A024R3C5 A0A024R3S2 A0A024R6T9 A0A024R9I2 A0A024RAP2 A0A024RD15 A0A068F658 A0A087WU84 A0A090N7W1
A0A0A0MRG0 A0A0A0MSK3 A0A0A0MT22 A0A0A0MTJ0 A0N0Q1 A1A4V4 A2A3U5 A2RUS0 A4D1Q0 A8K1F6 A8K249 A8K2J1 A8K4S9 A8K7N8 A8K858 A8KAF4
A8KAG8 B0ZBE0 B2R7Y7 B2RXH2 B4DN15 B6ZGS9 B7Z1L9 B8K2Q5 C1ID52 D0VY79 D2KUA6 E5KQF5 F1D8N3 F1D8N5 F1D8N7 F1D8P6 F1D8Q5 F5H1T4 G5E9C5
H6VQ59 K9J958 L7RSL3 L7RXH5 O75874 P00533 P00918 P02545 P05177 P05181 P06239 P06241 P07550 P08173 P08246 P08311 P08588 P08684 P08913
P11229 P11509 P11712 P14780 P17252 P18825 P21397 P21452 P21554 P21728 P21917 P22303 P25021 P25024 P25025 P25101 P25103 P25929 P28223
P28482 P30411 P32238 P32245 P33032 P35354 P35367 P37288 P41143 P41595 P41968 P49146 P50052 P50406 P51681 Q01959 Q08209 Q38Q88

CID 2405: bisoprolol

A0A024RAP4 A8KAG8 C1ID52 F1D8N7 P07550 P08588 P83916 Q96QE3

CID 2435: brimonidine

A0A024R2N2 A0A024R2Q0 A0A024R3C5 A0A024R3S2 A0A024R6T9 A0A024R909 A0A024R9I2 A0A024R9Y0 A0A024RAP2 A0A024RCN9 A0A024RD15 A0A024RD62
A0A087WU84 A0A090N7W1 A0A0A0MQX8 A0A0A0MRG0 A0A0A0MSK3 A0A0A0MT22 A0N0Q1 A1A4V4 A2A3U5 A2RUS0 A4D1Q0 A8K1F6 A8K249 A8K7N8 A8KAF4
A8KAG8 B0ZBD3 B0ZBE0 B2R7Y7 B2RXH2 B4DN15 B4DW50 B7Z1L9 B7ZKN7 B8K2Q5 C1ID52 E5KQF5 F1D8N3 F1D8P8 F5H1T4 G5E9C5 H6VQ59 K9J958 L7RSL3
L7RXH5 P00352 P00533 P00918 P02545 P05177 P05181 P06239 P06241 P07550 P08173 P08246 P08311 P08588 P08684 P08913 P11229 P11509 P11712

P14780 P15428 P16050 P17252 P18089 P18825 P21397 P21452 P21554 P21728 P21917 P22303 P25021 P25024 P25025 P25101 P25103 P25929 P28223 P28482 P30411 P32238 P32245 P33032 P35354 P35367 P35368 P37288 P39748 P41143 P41595 P41968 P49146 P50052 P50406 P51681 P83916 Q01959 Q06278 Q08209 Q38Q88 Q8NER1 Q96QE3 Q99714 Q9UNA4

CID 2441: bromazepam

A0A024R9X6 A8K177 A8K496 A8MPY1 B2RCW8 B4DTP4 P18505 P18507 P24046 P28476 P31644 P34903 P47870 P48169 P78334 Q16445 Q8N1C3 Q99928 Q9UN88

CID 2471: bumetanide

A0A024QZY7 A0A024R730 A0A024RBW9 A0A024RCN9 A0A090N8Z1 A0A0A0MQX8 A0A0A0MTJ0 A8K3J4 B2R807 B2RA41 B2RXH2 B3KUB4 B4DF30 B4DPF4 B4DUH8 B7ZKN7 B7ZM24 B7ZW53 D0VY79 O60656 O75604 O75874 P00352 P00915 P00918 P02545 P07451 P15428 P22309 P22310 P22748 P35218 P43166 P55011 P83916 Q13621 Q16790 Q4U2R8 Q92830 Q99714 Q9H2X9 Q9HC97 Q9NSA0

CID 2474: bupivacaine

A0A024R2N2 A0A024R2Q0 A0A024R3C5 A0A024R3S2 A0A024R6T9 A0A024R9I2 A0A024RAP2 A0A024RD15 A0A087WU84 A0A090N7W1 A0A0A0MRG0 A0A0A0MSK3 A0A0A0MT22 A0A0A0MTJ0 A0N0Q1 A1A4V4 A2A3U5 A2RUS0 A4D1Q0 A8K1F6 A8K249 A8K7N8 A8KAF4 A8KAG8 B0ZBE0 B2R7Y7 B4DN15 B7Z1L9 B8K2Q5 C1ID52 E5KQF5 F1D8N3 F1D8P8 F5H1T4 G5E9C5 H6VQ59 K9J958 L7RSL3 L7RXH5 P00533 P00918 P05177 P05181 P06239 P06241 P07550 P08173 P08246 P08311 P08588 P08684 P08913 P11229 P11509 P11712 P14780 P17252 P18825 P21397 P21452 P21554 P21728 P21917 P22303 P22460 P25021 P25024 P25025 P25101 P25103 P25929 P28223 P28482 P30411 P32238 P32245 P33032 P34995 P35354 P35367 P37288 P41143 P41595 P41968 P49146 P50052 P50406 P51681 Q01959 Q08209 Q38Q88 Q92830 Q9Y5Y9 Q9Z0V1

CID 2477: buspirone

A0A024QZY7 A0A024R2N2 A0A024R2Q0 A0A024R3C5 A0A024R3S2 A0A024R5I4 A0A024R6T9 A0A024R909 A0A024R9I2 A0A024RAP2 A0A024RAU7 A0A024RCN9 A0A024RD15 A0A087WU84 A0A090N7W1 A0A0A0MQX8 A0A0A0MRG0 A0A0A0MSK3 A0A0A0MT22 A0N0Q1 A1A4V4 A2A3U5 A2RUS0 A4D1D2 A4D1Q0 A8K1F6 A8K249 A8K5W4 A8K7N8 A8KAF4 A8KAG8 B0ZBE0 B2R7Y7 B2RXH2 B3KP78 B4DN15 B4E398 B7Z1L9 B8K2Q5 C1ID52 D0VY79 E5KQF5 F1D8N3 F5H1T4 G5E9C5 H6VQ59 K9J958 L7RSL3 L7RXH5 O00519 O15244 O15245 O75874 O95467 P00352 P00533 P00918 P05177 P05181 P06239 P06241 P07550 P08173 P08246 P08311 P08588 P08684 P08908 P08913 P11229 P11509 P11712 P14780 P17252 P18825 P21397 P21452 P21554 P21728 P21917 P22303 P25021 P25024 P25025 P25101 P25103 P25929 P27695 P28223 P28482 P30411 P32238 P32245 P32304 P32305 P33032 P35354 P35367 P37288 P41143 P41595 P41968 P49146 P50052 P50406 P51681 P83916 Q01453 Q01959 Q08209 Q16236 Q38Q88 Q86VL8 Q96FL8

CID 2478: busulfan

A0A024QZY7 A0A024R2N2 A0A024R2Q0 A0A024R3C5 A0A024R3S2 A0A024R6T9 A0A024R9I2 A0A024RAP2 A0A024RD15 A0A087WU84 A0A090N7W1 A0A0A0MRG0 A0A0A0MSK3 A0A0A0MT22 A0A0A0MTJ0 A0N0Q1 A1A4V4 A2A3U5 A2RUS0 A4D1Q0 A8K1F6 A8K249 A8K7N8 A8K987 A8KAF4 A8KAG8 B0ZBE0 B2R7Y7 B2RXH2 B4DN15 B7Z1F9 B7Z1L9 B8K2Q5 C1ID52 E5KQF5 F1D8N3 F5H1T4 G5E9C5 H6VQ59 K9J958 L7RSL3 L7RXH5 O75164 O75604 P00352 P00533 P00918 P02545 P05177 P05181 P06239 P06241 P07550 P08173 P08246 P08311 P08588 P08684 P08913 P11229 P11509 P11712 P14780 P16050 P17252 P18825 P21397 P21452 P21554 P21728 P21917 P22303 P25021 P25024 P25025 P25101 P25103 P25929 P28223 P28482 P30411 P32238 P32245 P33032 P35354 P35367 P37288 P41143 P41595 P41968 P49146 P50052 P50406 P51681 Q01959 Q08209 Q16236 Q38Q88

CID 2484: butenafine

A0A024QZY7 A0A024R2N2 A0A024R2Q0 A0A024R3C5 A0A024R3S2 A0A024R6T9 A0A024R9I2 A0A024RAP2 A0A024RAP4 A0A024RCN9 A0A024RD15 A0A087WU84 A0A090N7W1 A0A0A0MRG0 A0A0A0MSK3 A0A0A0MT22 A0N0Q1 A1A4V4 A2A3U5 A2RUS0 A4D1Q0 A8K1F6 A8K249 A8K7N8 A8KAF4 A8KAG8 B0ZBE0 B2R7Y7 B4DN15 B7Z1L9 B8K2Q5 C1ID52 E5KQF5 F1D8N3 F5H1T4 G5E9C5 H6VQ59 K9J958 L7RXH5 O94782 P00533 P00918 P02545 P05177 P05181 P06239 P06241 P07550 P08173 P08246 P08311 P08588 P08684 P08913 P11229 P11509 P11712 P14780 P17252 P18825 P21397 P21452 P21554 P21728 P21917 P22303 P25021 P25024 P25025 P25101 P25103 P25929 P28223 P28482 P30411 P32238 P32245 P33032 P35354 P35367 P37288 P41143 P41595 P41968 P49146 P50052 P50406 P51681 Q01959 Q08209 Q14534 Q38Q88

CID 2519: caffeine

A0A024QZY7 A0A024R2N2 A0A024R2Q0 A0A024R3C5 A0A024R3S2 A0A024R5I4 A0A024R6T9 A0A024R9I2 A0A024RAP2 A0A024RAP4 A0A024RAU7 A0A024RCN9 A0A024RD15 A0A087WU84 A0A090N7W1 A0A0A0MRG0 A0A0A0MSK3 A0A0A0MT22 A0N0Q1 A1A4V4 A2A3U5 A2RUS0 A4D1D2 A4D1Q0 A8K1F6 A8K249 A8K7N8 A8KAF4 A8KAG8 B0ZBE0 B2R7Y7 B3KP78 B4DN15 B7Z1L9 B7Z1W5 B7Z242 B8K2Q5 C1ID52 C9J1J0 D3DNN4 E5KQF5 F1D8N3 F1D8N5 F1D8N7 F5H1T4 F7VJQ1 G5E9C5 H6VQ59 K9J958 L7RSL3 L7RXH5 O15245 P00533 P00918 P02768 P05177 P05181 P06239 P06241 P07550 P08173 P08246 P08311 P08588 P08684 P08913 P11229 P11509 P11712 P14780 P17252 P18825 P21397 P21452 P21554 P21728 P21817 P21917 P22303 P25021 P25024 P25025 P25099 P25101 P25103 P25929 P28223 P28482 P28647 P29276 P30411 P30543 P32238 P32245 P33032 P33765 P35354 P35367 P37288 P41143 P41595 P41968 P49146 P50052 P50406 P51681 P83916 Q01959 Q07343 Q08209 Q14643 Q15413 Q38Q88 Q60614 Q92736

CID 2520: verapamil

A0A024QZY7 A0A024R2N2 A0A024R2Q0 A0A024R3C5 A0A024R3S2 A0A024R5I4 A0A024R6T9 A0A024R909 A0A024R9I2 A0A024R9Y0 A0A024RAP2 A0A024RAT5 A0A024RAU7 A0A024RAV2 A0A024RCN9 A0A024RCW6 A0A024RD15 A0A024RD21 A0A024RDD4 A0A024RE05 A0A068F658 A0A087WU84 A0A087WW63 A0A090N7W1 A0A090N8Z1 A0A0A0MR67 A0A0A0MRG0 A0A0A0MSK3 A0A0A0MT22 A0A0A0MTJ0 A0N0Q1 A1A4V4 A2A3U5 A2RUS0 A4D1D2 A4D1Q0 A8K1F6 A8K249 A8K2Q2 A8K7N8 A8KAF4 A8KAG8 B0ZBE0 B1ALM3 B2R7Y7 B2RC52 B3KP78 B4DN15 B6ZGS9 B7Z1F5 B7Z1L9 B7Z3P6 B8K2Q5 C1ID52 D2KUA6 E5KQF5 E7DBM8 E9PG18 F1D8N3 F1D8P8 F1D8Q5 F5H1T4 F7VJQ1 G5E9C5 H6VQ59 K9J958 L7RSL3 L7RXH5 O15245 O15296 O43497 O60840 O75604 O75874 O76082 O94782 O95342 P00533 P00915 P00918 P02545 P02768 P05177 P05181 P06239 P06241 P07550 P08173 P08246 P08311 P08588 P08684 P08913 P10253 P11229 P11509 P11712 P14780 P17252 P18825 P21397 P21439 P21452 P21554 P21728 P21917 P22002 P22303 P22462 P25021 P25024 P25025 P25101 P25103 P25929 P28223 P28482 P30411 P32238 P32245 P33032 P33527 P35354 P35367 P37288 P41143 P41595 P41968 P42345 P42858 P43220 P48542 P49146 P50052 P50406 P51681 P54284 Q00975 Q01453 Q01668 Q01959 Q02641 Q06432 Q08209 Q08289 Q13698 Q13936 Q16322 Q38Q88 Q7RTT9 Q8IZF0 Q92887 Q96RP8 Q99549 Q99700 Q9H015 Q9JIS7 Q9P0X4

CID 2541: candesartan

A0A024QZY7 A0A024R2N2 A0A024R2Q0 A0A024R3C5 A0A024R3S2 A0A024R5I4 A0A024R6T9 A0A024R9I2 A0A024RAP2 A0A024RAU7 A0A024RD15 A0A087WU84 A0A090N7W1 A0A0A0MRG0 A0A0A0MSE3 A0A0A0MSK3 A0A0A0MT22 A0N0Q1 A1A4V4 A2A3U5 A2RUS0 A4D1D2 A4D1Q0 A8K1F6 A8K249 A8K7N8 A8KAF4 A8KAG8 B0ZBE0 B2R7Y7 B3KP78 B4DN15 B7Z1L9 B8K2Q5 C1ID52 E5KQF5 F1D8N3 F5H1T4 G5E9C5 H6VQ59 K9J958 L7RSL3 L7RXH5 O15245 O94782 P00533 P00918 P05177 P05181 P06239 P06241 P07550 P08173 P08246 P08311 P08588 P08684 P08913 P11229 P11509 P11712 P14780 P17252 P18825 P19099 P21397 P21452 P21554 P21728 P21917 P22303 P25021 P25024 P25025 P25101 P25103 P25929 P28223 P28482 P30411 P30556 P32238 P32245 P33032 P35354 P35367 P37288 P41143 P41595 P41968 P49146 P50052 P50406 P51681 Q01959 Q08209 Q38Q88

CID 2551: carbachol

A0A024R0C0 A0A024R151 A0A024R3S2 A0A024R4X4 A0A024R909 A0A024R9I2 A0A024RDH4 A0A088QCU6 A0A0A0MTJ0 A0A0A6YYA8 A4D1Q0 B4DK78 B4DTF4 D3DNN4 D3DX95 F5H2B5 O14939 P02545 P08172 P08173 P08482 P08483 P08912 P10980 P11229 P20309 P22303 P28223 P35790 P49585 Q13393 Q15822 Q53GD3 Q8NE62 Q8TCT1 Q92830 Q9GZV3 Q9Y5K3

CID 2554: carbamazepine

A0A024QZY7 A0A024R2N2 A0A024R2Q0 A0A024R3C5 A0A024R3S2 A0A024R5I4 A0A024R6T9 A0A024R9I2 A0A024RAP2 A0A024RAU7 A0A024RCN9 A0A024RD15 A0A087WT22 A0A087WU84 A0A090N7W1 A0A0A0MRG0 A0A0A0MSK3 A0A0A0MT22 A0A0A0MTJ0 A0N0Q1 A1A4V4 A2A3U5 A2RUS0 A4D1D2 A4D1Q0 A8K1F6 A8K249 A8K5W4 A8K7N8 A8KAF4 A8KAG8 B0ZBE0 B2R7Y7 B3KP78 B4DN15 B4E398 B7Z1F5 B7Z1L9 B8K2Q5 C1ID52 E5KQF5 E9PG18 F1D8N3 F1D8N5 F1D8N7 F5H1T4 G5E9C5 H6VQ59 K9J958 L7RSL3 L7RXH5 O15245 O60656 O75874 P00533 P00918 P02545 P05177 P05181 P06239 P06241 P07550 P08173 P08246 P08311 P08588 P08684 P08913 P11229 P11509 P11712 P14780 P16662 P17252 P18825 P19224 P20813 P21397 P21452 P21554 P21917 P22303 P22309 P22310 P25021 P25024 P25025 P25101 P25103 P25929 P28223 P28482 P30411 P32238 P32245 P33032 P35354 P37288 P41143 P41595 P41968 P42858 P49146 P50052 P50406 P51681 Q01453 Q01959 Q08209 Q38Q88 Q96QE3

CID 2576: carisoprodol

A0A024QZY7 A0A024R6L5 A0A024R9X6 A0A024RAP4 A0A024RBV5 A0A024RCN9 A0A024RDJ4 A0A0A0MTJ0 A8K177 A8KAF4 O00519 O15245 O94782 P02545 P08684 P31644 P34903 P39748 P48169 P83916 Q16445 Q9UNA4

CID 2578: BCNU

A0A024R2N2 A0A024R2Q0 A0A024R3C5 A0A024R3S2 A0A024R6T9 A0A024R9I2 A0A024RAP2 A0A024RCN9 A0A024RD15 A0A087WU84 A0A090N7W1 A0A0A0MRG0 A0A0A0MSK3 A0A0A0MT22 A0A0A0MTJ0 A0N0Q1 A1A4V4 A2A3U5 A2RUS0 A4D1Q0 A8K1F6 A8K249 A8K7N8 A8KAF4 A8KAG8 B0ZBE0 B2R7Y7 B4DN15 B7Z1L9 B7ZKN7 B8K2Q5 C1ID52 D2KUA6 E5KQF5 F1D8N3 F1D8N7 F5H1T4 G5E9C5 H6UYS5 H6VQ59 K9J958 L7RSL3 L7RXH5 P00352 P00390 P00533 P00918 P05177 P05181 P06239 P06241 P07550 P08173 P08246 P08311 P08588 P08684 P08913 P11229 P11509 P11712 P14780 P17252 P18825 P21266 P21397 P21452 P21554 P21728 P21917 P22303 P25021 P25024 P25025 P25101 P25103 P25929 P28223 P28482 P30411 P30711 P32238 P32245 P33032 P35354 P35367 P37288 P41143 P41595 P41968 P42858 P49146 P50052 P50406 P51681 Q01453 Q01959 Q08209 Q38Q88 Q96QE3

CID 2583: carteolol

A0A024RAP4 B4DN83 C1ID52 P07550 P08588 P08684

CID 2585: carvedilol

A0A024R2N2 A0A024R2Q0 A0A024R3C5 A0A024R3S2 A0A024R5K6 A0A024R6L5 A0A024R6T9 A0A024R9I2 A0A024R9Y0 A0A024RAP2 A0A024RCN9 A0A024RD15 A0A024RD33 A0A087WU84 A0A090N7W1 A0A0A0MRG0 A0A0A0MSK3 A0A0A0MT22 A0N0Q1 A1A4V4 A2A3U5 A2RUS0 A4D1D2 A4D1Q0 A8K1F6 A8K249 A8K7N8 A8KAF4 A8KAG8 B0ZBD3 B0ZBE0 B2R7Y7 B2RXH2 B4DN15 B7Z1L9 B8K2Q5 C1ID52 E5KQF5 F1D8N3 F5H1T4 G5E9C5 H6VQ59 K9J958 L7RSL3 L7RXH5 O15244 P00533 P00918 P05177 P05181 P06133 P06239 P06241 P07550 P08173 P08246 P08311 P08588 P08684 P08913 P10253 P11229 P11509 P11712 P13945 P14780 P16662 P16860 P17252 P17302 P18825 P19320 P21397 P21452 P21554 P21728 P21917 P22303 P22309 P25021 P25024 P25025 P25101 P25103 P25929 P28223 P28482 P30411 P32238 P32245 P33032 P35354 P35367 P37288 P41143 P41595 P41968 P42345 P47989 P49146 P50052 P50406 P51681 P83916 Q01959 Q03164 Q08209 Q38Q88 Q86VL8 Q96FL8 Q96QE3 Q99700 Q9UIF8

CID 2662: celecoxib

A0A024QZY7 A0A024R2N2 A0A024R2Q0 A0A024R3C5 A0A024R3S2 A0A024R5I4 A0A024R5Z3 A0A024R6T9 A0A024R9I2 A0A024RAH7 A0A024RAP2 A0A024RAU7 A0A024RBW9 A0A024RCW6 A0A024RD15 A0A087WU84 A0A090N7W1 A0A0A0MRG0 A0A0A0MSK3 A0A0A0MT22 A0A0A0MTJ0 A0N0Q1 A1A4V4 A2A3U5 A2RUS0 A4D1Q0 A8K1F6 A8K249 A8K2Q2 A8K3J4 A8K5W4 A8K7N8 A8KAF4 A8KAG8 B0ZBD3 B0ZBE0 B2R7Y7 B3KP78 B3KUB4 B4DN15 B4DUH8 B4E398 B7Z1L9 B8K2Q5 C1ID52 D2KUA6 E5KQF5 E9PER6 F1D8N3 F1D8N5 F1D8N7 F1D8P6 F1D8Q5 F5H1T4 G5E9C5 H6VQ59 K9J958 L7RSL3 L7RXH5 O14684 O15245 O43570 O75874 O94782 P00403 P00533 P00915 P00918 P02545 P05177 P05181 P06239 P06241 P07451 P07550 P08173 P08246 P08311 P08588 P08684 P09917 P11229 P11509 P11712 P14780 P16050 P17252 P18054 P21397 P21452 P21554 P22303 P22748 P25024 P25025 P25101 P25103 P25929 P28482 P30411 P32238 P32245 P33032 P34913 P35218 P35354 P37288 P40763 P41143 P41968 P43166 P43220 P49146 P50052 P51681 Q01959 Q08209 Q16236 Q16790 Q38Q88 Q8N1Q1 Q92887

CID 2678: cetirizine

A0A024QZY7 A0A024R5I4 A0A024R6L5 A0A024RAU7 A0A024RCN9 A0A090N7W1 B3KP78 B4DN83 B7Z242 O15244 O15245 O75164 O75604 O95467 P07550
P08684 P09917 P20813 P21397 P35367 Q02763 Q96FL8 Q9HB55 Q9UIF8 Q9UNA4
CID 2708: chlorambucil
A0A024QZY7 A0A024R2N2 A0A024R2Q0 A0A024R3C5 A0A024R3S2 A0A024R6T9 A0A024R9I2 A0A024R9Y0 A0A024RAP2 A0A024RCN9 A0A024RCW6 A0A024RD15
A0A024RDA5 A0A024RDJ4 A0A087WT22 A0A087WU84 A0A090N7W1 A0A0A0MQX8 A0A0A0MRG0 A0A0A0MSK3 A0A0A0MT22 A0A0A0MTJ0 A0N0Q1 A1A4V4 A2A3U5
A2RUS0 A4D1Q0 A8K1F6 A8K249 A8K7N8 A8K987 A8KAF4 A8KAG8 B0ZBE0 B2R7Y7 B4DN15 B7Z1F9 B7Z1L9 B7ZKN7 B8K2Q5 C1ID52 D0VY79 E5KQF5 F1D8N3
F1D8N5 F1D8P6 F1D8P8 F5H1T4 F8W6L1 G5E9C5 H6VQ59 K9J958 L7RSL3 L7RXH5 O94925 P00352 P00533 P00918 P02545 P05177 P05181 P06239 P06241
P07550 P08173 P08246 P08311 P08588 P08684 P08913 P09211 P11229 P11509 P11712 P14780 P17252 P18825 P21397 P21452 P21554 P21728 P21917
P22303 P25021 P25024 P25025 P25101 P25103 P25929 P28223 P28482 P30411 P32238 P32245 P33032 P35354 P35367 P37288 P41143 P41595 P41968
P49146 P50052 P50406 P51681 P83916 Q01453 Q01959 Q08209 Q38Q88 Q9UIF8
CID 2713: chlorhexidine
A0A024QZY7 A0A024R136 A0A024R4E2 A0A024R5B6 A0A024R5Z3 A0A024R6R4 A0A024R9Y0 A0A024RAP4 A0A024RCN9 A0A024RCW6 A0A024RDA5 A0A024RDJ4
A0A068F658 A0A087WT22 A0A087WXV4 A0A090N7W1 A0A0A0MTJ0 A8KAF4 B3KT70 B4DN83 B6ZGS9 B7Z2G8 B7ZKN7 C1ID52 D0VY79 E5KQF5 F1D8N5 F1D8N7
F1D8P6 F1D8P8 F1D8Q5 H6UYS5 O00167 O15244 O15245 O15296 O60240 O75164 O75604 O75751 O75874 O94782 O94925 P00390 P02545 P08684 P11021
P11712 P14780 P15428 P16050 P17405 P25101 P25929 P28482 P32245 P39748 P42858 P43220 P61088 Q03164 Q14191 Q86VL8 Q96FL8 Q96QE3 Q99700
CID 2719: chloroquine
A0A024R5I4 A0A024R6L5 A0A024RAU7 A0A024RCN9 A0A090N7W1 A4D1D2 A8K987 B2R9N9 B3KP78 B3KPX6 C1ID52 K9J958 O15245 O94782 P01375 P02768
P05177 P07339 P08684 P11712 P20813 P39748 Q92887 Q96LB2 Q99700 Q9NR96
CID 2720: thiazide
A0A024RDJ4 A0A087WZL8 A0A0A0MTJ0 B4DN83 B7ZKN7 J3QSS1 P00915 P00918 P02545 P02768 P08684 P22748 P55017
CID 2725: chlorpheniramine
A0A024R2N2 A0A024R2Q0 A0A024R3C5 A0A024R3S2 A0A024R6T9 A0A024R9I2 A0A024RAP2 A0A024RAP4 A0A024RD15 A0A024RDJ4 A0A087WU84 A0A090N7W1
A0A0A0MRG0 A0A0A0MSK3 A0A0A0MT22 A0A0A0MTJ0 A0N0Q1 A1A4V4 A2A3U5 A2RUS0 A4D1D2 A4D1Q0 A8K1F6 A8K249 A8K7N8 A8KAF4 A8KAG8 B0ZBE0
B2KJ49 B2R7Y7 B4DN15 B7Z1L9 B8K2Q5 C1ID52 E5KQF5 F1D8N3 F5H1T4 F8W6L1 G5E9C5 H6VQ59 K9J958 L7RSL3 L7RXH5 O60656 P00533 P00918 P02768
P05177 P05181 P06239 P06241 P07550 P08173 P08246 P08311 P08588 P08684 P08913 P11229 P11509 P11712 P14780 P17252 P18825 P19224 P21397
P21452 P21554 P21728 P21917 P22303 P22310 P25021 P25024 P25025 P25101 P25103 P25929 P27695 P28482 P30411 P32238 P32245 P33032 P35354
P35367 P37288 P39748 P41143 P41595 P41968 P49146 P50052 P50406 P51681 Q01959 Q08209 Q38Q88 Q99700
CID 2726: chlorpromazine
A0A024QZY7 A0A024R2N2 A0A024R2Q0 A0A024R3C5 A0A024R3S2 A0A024R4E2 A0A024R5I4 A0A024R5Z3 A0A024R6L5 A0A024R6T9 A0A024R9I2 A0A024R9Y0
A0A024RAP2 A0A024RAP4 A0A024RAU7 A0A024RBV5 A0A024RCN9 A0A024RD15 A0A024RD62 A0A024RDJ4 A0A068F658 A0A087WT22 A0A087WU84 A0A090N7W1
A0A090N8Z1 A0A0A0MR48 A0A0A0MRG0 A0A0A0MSK3 A0A0A0MT22 A0N0Q1 A0PJF5 A1A4V4 A2A3U5 A2RUS0 A4D1D2 A4D1Q0 A4D2N2 A6NGA6 A8K1F6 A8K249
A8K5W4 A8K7N8 A8KAF4 A8KAG8 B0ZBD3 B0ZBE0 B2KJ49 B2R7Y7 B2RXH2 B3KP78 B4DN15 B4E398 B6ZGS9 B7Z1L9 B7Z1W5 B7Z2G8 B8K2Q5 C1ID52 D3DNN4
E5KQF5 E7ETZ0 F1D8N3 F1D8P8 F1DAL4 F5H1T4 F8W6L1 G5E9C5 H6VQ59 K9J958 L7RSL3 L7RXH5 O00325 O15245 O15296 O75164 O75874 O94782 O94925
O95342 P00533 P00918 P02545 P02763 P02768 P05177 P05181 P06239 P06241 P08173 P08246 P08311 P08684 P08908 P08913 P10253 P11229 P11509
P11712 P14416 P14780 P14842 P17252 P17405 P18089 P18825 P19020 P19652 P21397 P21452 P21554 P21728 P21917 P21918 P22303 P22310 P25021
P25024 P25025 P25101 P25103 P25929 P28221 P28222 P28223 P28335 P28482 P28566 P30411 P30939 P31388 P32238 P32245 P32297 P32304 P32305
P33032 P34969 P35354 P35367 P35368 P35462 P37288 P39748 P41143 P41595 P41968 P42345 P43220 P49146 P50052 P50406 P51681 P61169 P83916
Q01453 Q06278 Q08209 Q13526 Q15822 Q38Q88 Q92830 Q92887 Q96QE3 Q99549 Q99700 Q9BRL5 Q9UIF8 Q9UL62
CID 2727: chlorpropamide
A0A024R2N2 A0A024R2Q0 A0A024R3C5 A0A024R3K6 A0A024R3S2 A0A024R6T9 A0A024R9I2 A0A024RAP2 A0A024RCN9 A0A024RD15 A0A024RDJ4 A0A087WU84
A0A090N7W1 A0A090N8Z1 A0A0A0MRG0 A0A0A0MSK3 A0A0A0MT22 A0A0A0MTJ0 A0N0Q1 A1A4V4 A2A3U5 A2RUS0 A4D1D2 A4D1Q0 A8K1F6 A8K249 A8K7N8
A8KAF4 A8KAG8 B0ZBE0 B2R7Y7 B2RA41 B4DN15 B4DN83 B7Z1L9 B8K2Q5 C1ID52 E5KQF5 F1D8N3 F1D8N7 F5H1T4 G5E9C5 H6VQ59 K9J958 L7RSL3 L7RXH5
P00352 P00533 P00918 P02545 P02768 P05177 P05181 P06239 P06241 P07550 P08173 P08246 P08288 P08684 P08908 P08913 P11229 P11509 P11712
P14780 P17252 P18825 P21397 P21452 P21554 P21728 P21917 P22303 P25021 P25024 P25025 P25101 P25103 P25929 P28223 P28482 P30411 P32238
P32245 P33032 P35354 P35367 P37288 P39748 P41143 P41595 P41968 P49146 P50052 P50406 P51681 P78508 P83916 Q01959 Q08209 Q09428 Q16850
Q38Q88
CID 2732: chlorthalidone
A0A024QZY7 A0A024R2N2 A0A024R2Q0 A0A024R3C5 A0A024R3S2 A0A024R5Z3 A0A024R6T9 A0A024R9I2 A0A024R9Y0 A0A024RAP2 A0A024RBW9 A0A024RD15
A0A087WU84 A0A090N7W1 A0A0A0MRG0 A0A0A0MSK3 A0A0A0MT22 A0N0Q1 A1A4V4 A2A3U5 A2RUS0 A4D1Q0 A8K1F6 A8K249 A8K3J4 A8K7N8 A8KAF4 A8KAG8
B0ZBE0 B2R7Y7 B3KUB4 B4DN15 B4DPF4 B4DUH8 B7Z1L9 B8K2Q5 C1ID52 E5KQF5 F1D8N3 F5H1T4 G5E9C5 H6VQ59 K9J958 L7RSL3 L7RXH5 O43570 P00533
P00915 P00918 P05177 P05181 P06239 P06241 P07451 P07550 P08173 P08246 P08311 P08588 P08684 P08913 P11229 P11509 P11712 P14780 P17252
P18825 P21397 P21452 P21554 P21728 P21917 P22303 P22748 P25021 P25024 P25025 P25101 P25103 P25929 P28223 P28482 P30411 P32238 P32245
P33032 P35218 P35354 P35367 P37288 P41143 P41595 P41968 P43166 P49146 P50052 P50406 P51681 Q01959 Q08209 Q13621 Q16790 Q38Q88 Q9ULX7
CID 2733: chlorzoxazone
A0A024QZY7 A0A024R2N2 A0A024R2Q0 A0A024R3C5 A0A024R3S2 A0A024R5I4 A0A024R6T9 A0A024R9I2 A0A024RAP2 A0A024RAU7 A0A024RCN9 A0A024RD15
A0A087WU84 A0A087WZL8 A0A090N7W1 A0A090N8Z1 A0A0A0MQX8 A0A0A0MRG0 A0A0A0MSK3 A0A0A0MT22 A0A0A0MTJ0 A0N0Q1 A0N0X8 A1A4V4 A2A3U5
A2RUS0 A4D1D2 A4D1Q0 A8K1F6 A8K249 A8K7N8 A8KAF4 A8KAG8 B0ZBE0 B2R7Y7 B3KP78 B4DN15 B7Z1L9 B7ZKN7 B8K2Q5 C1ID52 E5KQF5 F1D8N3 F5H1T4
F8W6L1 G5E9C5 H6VQ59 K9J958 L7RSL3 L7RXH5 O00519 O15245 O15554 P00533 P00918 P02545 P05177 P05181 P06239 P06241 P07550 P08173 P08246
P08311 P08588 P08684 P08913 P11229 P11509 P11712 P14780 P17252 P18825 P21397 P21554 P21728 P21917 P22303 P25021 P25024 P25025
P25101 P25103 P25929 P28223 P28482 P30411 P32238 P32245 P33032 P35354 P35367 P37288 P41143 P41595 P41968 P49146 P50052 P50406 P51681
P70604 P83916 Q01959 Q08209 Q12791 Q38Q88 Q92830 Q92887 Q9UIF8
CID 2749: ciclopirox
A0A024R2N2 A0A024R2Q0 A0A024R3C5 A0A024R3S2 A0A024R6T9 A0A024R9I2 A0A024RAP2 A0A024RD15 A0A087WU84 A0A090N7W1 A0A0A0MRG0 A0A0A0MSK3
A0A0A0MT22 A0N0Q1 A1A4V4 A2A3U5 A2RUS0 A4D1Q0 A8K1F6 A8K249 A8K7N8 A8KAF4 A8KAG8 B0ZBE0 B2R7Y7 B4DN15 B7Z1L9 B8K2Q5 C1ID52 E5KQF5
F1D8N3 F5H1T4 G5E9C5 H6VQ59 K9J958 L7RSL3 L7RXH5 P00533 P00918 P05023 P05177 P05181 P06239 P06241 P07550 P08173 P08246 P08311 P08588
P08684 P08913 P11229 P11509 P11712 P14780 P16050 P17252 P18825 P21397 P21452 P21554 P21728 P21917 P22303 P25021 P25024 P25025 P25101
P25103 P25929 P28223 P28482 P30411 P32238 P32245 P33032 P35354 P35367 P37288 P41143 P41595 P41968 P49146 P50052 P50406 P51681 Q01959
Q08209 Q38Q88 Q96FL8
CID 2756: cimetidine
A0A024QZY7 A0A024R2N2 A0A024R2Q0 A0A024R3C5 A0A024R3S2 A0A024R5I4 A0A024R6T9 A0A024R9I2 A0A024RAP2 A0A024RAP4 A0A024RAU7 A0A024RCN9
A0A024RD15 A0A024RDA5 A0A087WU84 A0A090N7W1 A0A0A0MR48 A0A0A0MRG0 A0A0A0MSK3 A0A0A0MT22 A0A0A0MTJ0 A0N0Q1 A1A4V4 A2A3U5 A2RUS0
A4D1D2 A4D1Q0 A8K1F6 A8K249 A8K7N8 A8KAF4 A8KAG8 B0ZBE0 B2KJ49 B2R7Y7 B2R807 B3KP78 B4DN15 B7Z1L9 B8K2Q5 C1ID52 E5KQF5 F1D8N3 F5H1T4
G5E9C5 H6VQ59 K9J958 L7RSL3 L7RXH5 O15244 O15245 O75751 O76082 O95342 P00533 P00918 P02545 P05108 P05177 P05181 P06239 P06241 P06280
P07550 P08173 P08246 P08311 P08588 P08684 P08913 P11229 P11509 P11712 P14780 P17252 P18825 P21397 P21452 P21554 P21728 P21917 P22303
P25021 P25024 P25025 P25101 P25102 P25103 P25929 P27695 P28223 P28482 P30411 P32238 P32245 P33032 P35354 P37288 P41143 P41595 P41968
P49146 P50052 P50406 P51681 Q01959 Q06278 Q08209 Q16236 Q38Q88 Q4U2R8 Q7RTT9 Q86VL8 Q92887 Q96FL8 Q99549 Q9H015 Q9NSA0 Q9UM07
CID 2762: cinoxacin
A0A024RCN9 A0A0A0MQX8 A0A0A0MTJ0 B2RXH2 B7ZKN7 O00519 O75164 P00352 P02545 P43220 Q01453 Q02880 Q9UNA4
CID 2764: ciprofloxacin
A0A024R2N2 A0A024R2Q0 A0A024R3C5 A0A024R3S2 A0A024R6T9 A0A024R9I2 A0A024RAP2 A0A024RD15 A0A087WU84 A0A090N7W1 A0A0A0MRG0 A0A0A0MSK3
A0A0A0MT22 A0N0Q1 A1A4V4 A2A3U5 A2RUS0 A4D1D2 A4D1Q0 A8K1F6 A8K249 A8K7N8 A8KAF4 A8KAG8 B0ZBD3 B0ZBE0 B2R7Y7 B2RXH2 B4DN15 B7Z1L9
B8K2Q5 C1ID52 E5KQF5 F1D8N3 F5H1T4 G5E9C5 H6VQ59 K9J958 L7RSL3 L7RXH5 P00352 P00533 P00918 P02545 P02768 P05177 P05181 P06239 P06241
P07550 P08173 P08246 P08311 P08588 P08684 P08913 P11229 P11388 P11509 P11712 P14780 P15428 P17252 P18825 P21397 P21452 P21554 P21728
P21917 P22303 P25021 P25024 P25025 P25101 P25103 P25929 P27695 P28223 P28482 P30411 P32238 P32245 P33032 P35354 P35367 P35368 P37288
P41143 P41595 P41968 P49146 P50052 P50406 P51681 Q01959 Q02880 Q08209 Q38Q88 Q4U2R8 Q99714
CID 2771: citalopram
A0A024QZY7 A0A024R2N2 A0A024R2Q0 A0A024R3C5 A0A024R3S2 A0A024R6T9 A0A024R9I2 A0A024RAP2 A0A024RAP4 A0A024RCN9 A0A024RD15 A0A024RDJ4
A0A087WU84 A0A090N7W1 A0A090N8Z1 A0A0A0MRG0 A0A0A0MSK3 A0A0A0MT22 A0N0Q1 A1A4V4 A2A3U5 A2RUS0 A4D1D2 A4D1Q0 A8K1F6 A8K249 A8K5W4
A8K7N8 A8KAF4 A8KAG8 B0ZBD3 B0ZBE0 B2R7Y7 B4DN15 B4E398 B7Z1L9 B7Z242 B7ZKN7 B8K2Q5 C1ID52 E5KQF5 F1D8N3 F5H1T4 G5E9C5 H6VQ59 K9J958
L7RSL3 L7RXH5 O15118 O15245 O15296 O75874 P00352 P00533 P00918 P05177 P05181 P06239 P06241 P07550 P08173 P08246 P08311 P08588 P08684
P11229 P11509 P11712 P14780 P16050 P17252 P18825 P21397 P21452 P21554 P21728 P21917 P22303 P23975 P25021 P25024 P25025 P25101 P25103
P25929 P28482 P30411 P31645 P32238 P32245 P33032 P35354 P35367 P37288 P41143 P41595 P41968 P43220 P49146 P50052 P50406 P51681 Q01453
Q08209 Q38Q88 Q8NER1 Q99700 Q9UNA4
CID 2789: clobazam
A0A024R9X6 A4D1D2 A8K177 A8K496 B2RCW8 B4DTP4 P14867 P18505 P18507 P31644 P34903 P47870 P48169 P78334 Q16445 Q8N1C3 Q99928 Q9UN88
CID 2801: clomipramine
A0A024QZY7 A0A024R2N2 A0A024R2Q0 A0A024R3C5 A0A024R3S2 A0A024R6T9 A0A024R9I2 A0A024R9Y0 A0A024RAP2 A0A024RCN9 A0A024RD15 A0A068F658
A0A087WT22 A0A087WU84 A0A090N7W1 A0A090N8Z1 A0A0A0MRG0 A0A0A0MSK3 A0A0A0MT22 A0A0A0MTJ0 A0N0Q1 A1A4V4 A2A3U5 A2RUS0 A4D1D2 A4D1Q0
A8K1F6 A8K249 A8K5W4 A8K7N8 A8KAF4 A8KAG8 B0ZBD3 B0ZBE0 B2R7Y7 B2RXH2 B4DN15 B7Z1L9 B8K2Q5 C1ID52 E5KQF5 F1D8N3 F1D8N7 F5H1T4 F8W6L1
G5E9C5 H6VQ59 K9J958 L7RSL3 L7RXH5 O15245 O15296 O75874 O94782 P00533 P00918 P02545 P02768 P05177 P05181 P06239 P06241 P07550 P08173
P08246 P08311 P08588 P08684 P08913 P09211 P11229 P11509 P11712 P14780 P17252 P18054 P18825 P21397 P21452 P21554 P21728 P21917 P22303
P23975 P25021 P25024 P25025 P25101 P25103 P25929 P27695 P28221 P28222 P28223 P28482 P30411 P31645 P32238 P32245 P33032 P35354 P35367
P37288 P41143 P41595 P41968 P42345 P43220 P48542 P48545 P49146 P50052 P50406 P51681 P83916 Q01453 Q01959 Q08209 Q16696 Q38Q88 Q96QE3
Q99700 Q9UIF8
CID 2802: clonazepam
A0A024R2N2 A0A024R2Q0 A0A024R3C5 A0A024R3S2 A0A024R6T9 A0A024R9I2 A0A024R9X6 A0A024RAP2 A0A024RD15 A0A087WU84 A0A090N7W1 A0A0A0MRG0
A0A0A0MSK3 A0A0A0MT22 A0N0Q1 A1A4V4 A2A3U5 A2RUS0 A4D1Q0 A8K177 A8K1F6 A8K249 A8K496 A8K7N8 A8KAF4 A8KAG8 B0ZBE0 B2R7Y7 B2RCW8
B4DN15 B4DTP4 B7Z1L9 B8K2Q5 C1ID52 E5KQF5 F1D8N3 F5H1T4 G5E9C5 H6VQ59 K9J958 L7RSL3 L7RXH5 O76068 P00533 P00918 P02768 P05177 P05181

P06239 P06241 P07550 P08173 P08246 P08311 P08588 P08684 P08913 P11229 P11509 P11712 P14780 P14867 P17252 P18505 P18507 P18825 P21397
P21452 P21554 P21728 P21917 P22303 P25021 P25024 P25025 P25101 P25103 P25929 P28223 P28482 P30411 P31644 P32238 P32245 P33032 P34903
P35354 P35367 P37288 P41143 P41595 P41968 P47869 P47870 P48169 P49146 P50052 P50406 P51681 P78334 Q01959 Q08209 Q16445 Q38Q88 Q8N1C3
Q99928 Q9UN88
CID 2803: clonidine
A0A024R2N2 A0A024R2Q0 A0A024R3C5 A0A024R3S2 A0A024R6T9 A0A024R909 A0A024R9I2 A0A024RAP2 A0A024RCN9 A0A024RD15 A0A087WU84 A0A090N7W1
A0A090N8Z1 A0A0A0MRG0 A0A0A0MSK3 A0A0A0MT22 A0N0Q1 A1A4V4 A2A3U5 A2RUS0 A4D1D2 A4D1Q0 A8K1F6 A8K249 A8K5W4 A8K7N8 A8KAF4 A8KAG8
B0ZBD3 B0ZBE0 B2R7Y7 B4DN15 B7Z1L9 B7ZKN7 B8K2Q5 C1ID52 D0VY79 E5KQF5 F1D8N3 F5H1T4 G5E9C5 H6VQ59 K9J958 L7RSL3 L7RXH5 O00519 O15245
O70507 O75751 O76082 O88703 O88704 P00533 P00918 P02545 P05177 P05181 P06239 P06241 P07550 P08173 P08246 P08311 P08588 P08684 P08913
P11229 P11509 P11712 P14780 P17252 P18089 P18825 P21397 P21452 P21554 P21728 P21917 P22303 P23944 P25021 P25024 P25025 P25101 P25103
P25929 P28221 P28222 P28482 P30411 P32238 P32245 P33032 P35354 P35367 P35368 P37288 P41143 P41595 P41968 P49146 P50052 P50406 P51681
Q01959 Q08209 Q38Q88 Q96FL8 Q9H015 Q9Y2I1
CID 2812: clotrimazole
A0A024QZY7 A0A024R2N2 A0A024R2Q0 A0A024R3C5 A0A024R3S2 A0A024R4E2 A0A024R5I4 A0A024R5S8 A0A024R5Z3 A0A024R6L5 A0A024R6T9 A0A024R909
A0A024R9I2 A0A024R9Y0 A0A024RAP2 A0A024RAU7 A0A024RBV5 A0A024RCN9 A0A024RD15 A0A024RDJ4 A0A087WT22 A0A087WU84 A0A090N7W1 A0A090N8Z1
A0A0A0MRG0 A0A0A0MSK3 A0A0A0MT22 A0A0A0MTJ0 A0N0Q1 A1A4V4 A2A3U5 A2RUS0 A4D1D2 A4D1Q0 A8K1F6 A8K249 A8K7N8 A8KAF4 A8KAG8 B0ZBE0
B2R7Y7 B3KP78 B4DN15 B6ZGS9 B7Z1L9 B7ZKN7 B8K2Q5 C1ID52 D0VY79 E5KQF5 F1D8N3 F1D8P8 F1D8P9 F1DAL4 F5H1T4 F8W6L1 G5E9C5 H6UYS5 H6VQ59
K9J958 K9JA46 L7RSL3 L7RXH5 O15245 O15296 O15438 O15554 O75164 O75469 O75604 O75874 O94759 O94782 O95467 P00533 P00918 P02545 P05093
P05108 P05177 P05181 P06239 P06241 P06280 P07550 P08173 P08246 P08311 P08588 P08684 P08913 P11021 P11229 P11509 P11712 P14780 P16050
P17252 P18825 P21397 P21452 P21554 P21728 P21917 P22303 P25021 P25024 P25025 P25101 P25103 P25929 P28223 P28482 P30411 P30518 P32238
P32245 P33032 P35354 P35367 P37288 P39748 P41143 P41595 P41968 P42858 P43220 P49146 P50052 P50406 P51681 P83916 Q01453 Q01959 Q08209
Q14994 Q16850 Q38Q88 Q7Z2W7 Q8TD43 Q92887 Q96QE3 Q99418 Q99549 Q99700 Q9UIF8 Q9Y468
CID 2895: cyclobenzaprine
A0A024QZY7 A0A024R3C5 A0A024RCN9 A0A087WT22 A0A090N7W1 A0A0A0MTJ0 C1ID52 F8W6L1 O15296 O75874 O94782 P02545 P05177 P16050 P17405
P21728 P22310 P27695 P28223 P42345 P43220 P83916 Q01453 Q8NER1 Q96QE3 Q99549 Q99700
CID 2907: cyclophosphamide
A0A024QZY7 A0A024R2N2 A0A024R2Q0 A0A024R3C5 A0A024R3S2 A0A024R4E2 A0A024R5Z3 A0A024R6T9 A0A024R909 A0A024R9I2 A0A024RAP2 A0A024RCN9
A0A024RD15 A0A087WU84 A0A090N7W1 A0A090N8Z1 A0A0A0MRG0 A0A0A0MSK3 A0A0A0MT22 A0N0Q1 A1A4V4 A2A3U5 A2RUS0 A4D1D2 A4D1Q0 A8K1F6 A8K249
A8K7N8 A8KAF4 A8KAG8 B0ZBE0 B2R7Y7 B2RXH2 B4DN15 B7Z1L9 B8K2Q5 C1ID52 E5KQF5 F1D8N3 F5H1T4 G5E9C5 H6VQ59 K9J958 L7RSL3 L7RXH5 O15245
P00533 P00918 P05177 P05181 P06239 P06241 P07550 P08173 P08246 P08311 P08588 P08684 P08913 P11229 P11509 P11712 P14780 P16050 P17252
P18825 P20813 P21397 P21452 P21554 P21728 P21917 P22303 P25021 P25024 P25025 P25101 P25103 P25929 P27695 P28223 P28482 P29275 P30411
P32238 P32245 P33032 P35354 P35367 P37288 P41143 P41595 P41968 P49146 P50052 P50406 P51681 P83916 Q01959 Q08209 Q16236 Q38Q88
CID 2913: cyproheptadine
A0A024QZY7 A0A024R2N2 A0A024R2Q0 A0A024R3C5 A0A024R3S2 A0A024R6T9 A0A024R909 A0A024R9I2 A0A024R9Y0 A0A024RAP2 A0A024RCN9 A0A024RD15
A0A087WT22 A0A087WU84 A0A090N7W1 A0A0A0MR48 A0A0A0MRG0 A0A0A0MSK3 A0A0A0MT22 A0A0A0MTJ0 A0N0Q1 A1A4V4 A2A3U5 A2RUS0 A4D1Q0 A8K1F6
A8K249 A8K5W4 A8K7N8 A8KAF4 A8KAG8 B0ZBE0 B2KJ49 B2R7Y7 B4DN15 B7Z1L9 B7ZW53 B8K2Q5 C1ID52 E5KQF5 F1D8N3 F5H1T4 G5E9C5 H6VQ59 K9J958
L7RSL3 L7RXH5 O15296 O60656 O75874 P00352 P00533 P00918 P02545 P05177 P05181 P06239 P06241 P07550 P08173 P08246 P08311 P08588 P08684
P08913 P11229 P11509 P11712 P14780 P17252 P17405 P18825 P19224 P21397 P21452 P21554 P21728 P21917 P22303 P22309 P22310 P25021 P25024
P25025 P25100 P25101 P25103 P25929 P28221 P28223 P28482 P30411 P31388 P32238 P32245 P32305 P33032 P34969 P35348 P35354 P35367 P35368
P37288 P41143 P41595 P41968 P42345 P42858 P49146 P50052 P50406 P51681 P83916 Q01453 Q01959 Q08209 Q16236 Q38Q88 Q8NER1 Q92830 Q96QE3
Q99549 Q99700 Q99714
CID 2955: dapsone
A0A024QZY7 A0A024R5Z3 A0A024RDA5 A0A0A0MQX8 A0A0A0MTJ0 B0YJ76 C1ID52 F1D8P6 O60656 P02545 P05177 P05181 P08684 P11712 P22309 P22310
P50406 Q9UIF8
CID 2972: deferiprone
A0A024QZY7 A0A024R2N2 A0A024R2Q0 A0A024R3C5 A0A024R3S2 A0A024R6T9 A0A024R9I2 A0A024RAP2 A0A024RCN9 A0A024RD15 A0A087WU84 A0A090N7W1
A0A0A0MRG0 A0A0A0MSK3 A0A0A0MT22 A0N0Q1 A0PJA6 A1A4V4 A2A3U5 A2RUS0 A4D1Q0 A8K1F6 A8K249 A8K7N8 A8KAF4 A8KAG8 B0ZBE0 B2R7Y7 B2RXH2
B4DN15 B7Z1L9 B8K2Q5 C1ID52 E5KQF5 F1D8N3 F5H1T4 G5E9C5 H6VQ59 K9J958 L7RSL3 L7RXH5 O75164 P00533 P00918 P05177 P05181 P06239 P06241
P07550 P08173 P08246 P08311 P08588 P08684 P08913 P11229 P11509 P11712 P14780 P17252 P18825 P21397 P21452 P21554 P21728 P21917 P22303
P25021 P25024 P25025 P25101 P25103 P25929 P28223 P28482 P30411 P32238 P32245 P33032 P35354 P35367 P37288 P41143 P41595 P41968 P49146
P50052 P50406 P51681 P83916 Q01959 Q08209 Q38Q88 Q9UIF8
CID 2973: desferrioxamine
A0A024QZY7 A0A024R6R4 A0PJA6 D0VY79 O75874 O95467 P00918 P11388 P39900 P47989 Q92769 Q9UNA4
CID 2995: desipramine
A0A024QZY7 A0A024R2N2 A0A024R2Q0 A0A024R3C5 A0A024R3S2 A0A024R5I4 A0A024R6T9 A0A024R9I2 A0A024RAP2 A0A024RAU7 A0A024RCN9 A0A024RD15
A0A024RDJ4 A0A087WU84 A0A090N7W1 A0A090N8Z1 A0A0A0MR48 A0A0A0MRG0 A0A0A0MSK3 A0A0A0MT22 A0N0Q1 A1A4V4 A2A3U5 A2RUS0 A4D1D2 A4D1Q0
A8K1F6 A8K249 A8K5W4 A8K7N8 A8KAF4 A8KAG8 B0ZBD3 B0ZBE0 B2R7Y7 B3KP78 B4DN15 B4E398 B7Z1L9 B8K2Q5 C1ID52 E5KQF5 F1D8N3 F5H1T4 F8W6L1
G5E9C5 H6VQ59 K9J958 L7RSL3 L7RXH5 O15244 O15245 O15296 O75751 O75874 O76082 O94925 P00533 P00918 P02768 P05177 P05181 P06239 P06241
P07550 P08173 P08246 P08311 P08588 P08684 P08913 P11229 P11509 P11712 P14780 P17252 P17405 P18825 P21397 P21452 P21554 P21728 P21917
P22303 P22310 P23975 P25021 P25024 P25025 P25101 P25103 P25929 P28223 P28482 P30411 P31645 P31652 P32238 P32245 P33032 P35354 P35367
P35368 P37288 P41143 P41595 P41968 P42345 P42858 P43220 P48542 P48545 P49146 P50052 P50406 P51681 Q01453 Q08209 Q38Q88 Q5DSZ7 Q5DT02
Q8NER1 Q92887 Q99700 Q9UIF8
CID 3007: amphetamine
A0A024R3C5 A0A024R6T9 A1A4V4 A8K5W4 B0ZBD3 B2R7Y7 B7Z242 C1ID52 O76082 P07550 P08913 P21397 P21728 P35368 Q01959 Q05940 Q16568
Q96RJ0
CID 3009: DFMO
A0A024QZY7 A0A024R374 A0A024R909 A0A024R9Y0 A0A024RBV5 A0A024RCN9 A0A0A0MQX8 B2RXH2 B4DXF8 B7ZKN7 O15245 P02545 P11926 P83916 Q01453
Q16236 Q9UIF8
CID 3016: diazepam
A0A024R2N2 A0A024R2Q0 A0A024R3C5 A0A024R3S2 A0A024R5I4 A0A024R6T9 A0A024R9I2 A0A024R9X6 A0A024RAP2 A0A024RAP7 A0A024RAU7 A0A024RD15
A0A087WU84 A0A090N7W1 A0A0A0MRG0 A0A0A0MSK3 A0A0A0MT22 A0N0Q1 A1A4V4 A2A3U5 A2RUS0 A4D1D2 A4D1Q0 A8K177 A8K1F6 A8K249 A8K496 A8K7N8
A8KAF4 A8KAG8 A8MPY1 B0ZBE0 B2R7Y7 B2RCW8 B3KP78 B4DN15 B4DTP4 B7Z1L9 B8K2Q5 C1ID52 E5KQF5 F1D8N3 F5H1T4 G5E9C5 H6VQ59 K9J958 L7RSL3
L7RXH5 M0R1I2 O15245 O76068 P00533 P00747 P00918 P02763 P02768 P05177 P05181 P06239 P06241 P07550 P08173 P08246 P08311 P08588 P08684
P08697 P08913 P11229 P11509 P11712 P14780 P14867 P17252 P18505 P18507 P18825 P21397 P21452 P21554 P21728 P21917 P22303 P24046 P25021
P25024 P25025 P25101 P25103 P25929 P28223 P28476 P28482 P30411 P31644 P32238 P32245 P33032 P34903 P35348 P35354 P35367 P37288 P41143
P41595 P41968 P43220 P47869 P47870 P48169 P49146 P50052 P50406 P51681 P78334 Q01717 Q01959 Q08209 Q16445 Q38Q88 Q8N1C3 Q99928 Q9UN88
CID 3019: diazoxide
A0A024QZY7 A0A024R2N2 A0A024R2Q0 A0A024R3C5 A0A024R3S2 A0A024R6T9 A0A024R718 A0A024R9I2 A0A024RAP2 A0A024RCN9 A0A024RD15 A0A087WU84
A0A087WZL8 A0A090N7W1 A0A0A0MRG0 A0A0A0MSK3 A0A0A0MT22 A0A0A0MTJ0 A0N0Q1 A1A4V4 A2A3U5 A2RUS0 A4D1Q0 A8K1F6 A8K249 A8K7N8 A8KAF4
A8KAG8 B0ZBE0 B2R7Y7 B2RC52 B4DN15 B7Z1L9 B8K2Q5 C1ID52 E5KQF5 F1D8N3 F1D8N7 F5H1T4 G5E9C5 H6VQ59 J3QSS1 K9J958 L7RSL3 L7RXH5 P00352
P00533 P00915 P00918 P02545 P05023 P05177 P05181 P06239 P06241 P07550 P08173 P08246 P08311 P08588 P08684 P08913 P11229 P11509 P11712
P14780 P17252 P18825 P21397 P21452 P21554 P21728 P21917 P22303 P22748 P25021 P25024 P25025 P25101 P25103 P25929 P27986 P28223 P28482
P30411 P32238 P32245 P33032 P35354 P35367 P37288 P41143 P41595 P41968 P49146 P50052 P50406 P51681 P70673 P97794 Q01959 Q08209 Q38Q88
Q61743
CID 3042: dicyclomine
A0A024QZY7 A0A024R2N2 A0A024R2Q0 A0A024R3C5 A0A024R3S2 A0A024R6L5 A0A024R6T9 A0A024R9I2 A0A024RAP2 A0A024RCN9 A0A024RD15 A0A087WU84
A0A090N7W1 A0A090N8Z1 A0A0A0MRG0 A0A0A0MSK3 A0A0A0MT22 A0A0A0MTJ0 A0N0Q1 A1A4V4 A2A3U5 A2RUS0 A4D1Q0 A8K1F6 A8K249 A8K7N8 A8KAF4
A8KAG8 B0ZBE0 B2R7Y7 B4DN15 B7Z1L9 B8K2Q5 C1ID52 E5KQF5 F1D8N3 F5H1T4 F8W6L1 G5E9C5 H6VQ59 K9J958 L7RSL3 L7RXH5 O15296 P00533 P00918
P02545 P05177 P05181 P06239 P06241 P07550 P08172 P08173 P08246 P08311 P08588 P08684 P08913 P11229 P11509 P11712 P14780 P17252 P17405
P18825 P20309 P21397 P21452 P21554 P21728 P21917 P22303 P25021 P25024 P25025 P25101 P25103 P25929 P28223 P28482 P30411 P32238 P32245
P33032 P35354 P35367 P37288 P41143 P41595 P41968 P49146 P50052 P50406 P51681 Q01453 Q01959 Q08209 Q38Q88 Q96QE3 Q99549 Q99700 Q99714
Q9UIF8
CID 3059: diflunisal
A0A024R2N2 A0A024R2Q0 A0A024R3C5 A0A024R3S2 A0A024R6T9 A0A024R9I2 A0A024RAP2 A0A024RD15 A0A087WU84 A0A090N7W1 A0A0A0MRG0 A0A0A0MSK3
A0A0A0MT22 A0N0Q1 A1A4V4 A2A3U5 A2RUS0 A4D1Q0 A8K1F6 A8K249 A8K7N8 A8KAF4 A8KAG8 B0ZBE0 B2R7Y7 B2RXH2 B4DN15 B7Z1L9 B8K2Q5 C1ID52
D0VY79 E5KQF5 E9KL36 F1D8N3 F5H1T4 G5E9C5 H6VQ59 K9J958 L7RSL3 L7RXH5 O60656 O75604 P00352 P00533 P00915 P00918 P02545 P02768 P05177
P05181 P06133 P06239 P06241 P07550 P08173 P08246 P08311 P08588 P08684 P08913 P11229 P11509 P11712 P14780 P15428 P16662 P17252 P18825
P21397 P21452 P21554 P21728 P21917 P22303 P22310 P25021 P25024 P25025 P25101 P25103 P25929 P28223 P28482 P30411 P32238 P32245 P33032
P35354 P35367 P36537 P37288 P41143 P41595 P41968 P49146 P50052 P50406 P51681 Q01959 Q08209 Q38Q88 Q4U2R8 Q5DSZ6 Q5DT02 Q99714
CID 3080: 2,3-dimercaptopropanol
A0A024QZY7 A0A024R5Z3 A0A024R6L5 A0A024RCN9 F1D8P8 O15296 O94925 P00352 P02545 P39748 P42858 Q92830 Q99714
CID 3100: diphenhydramine
A0A024QZY7 A0A024R2N2 A0A024R2Q0 A0A024R3C5 A0A024R3S2 A0A024R4E2 A0A024R6T9 A0A024R909 A0A024R9I2 A0A024RAP2 A0A024RCN9 A0A024RCW6
A0A024RD15 A0A087WU84 A0A090N7W1 A0A0A0MR48 A0A0A0MRG0 A0A0A0MSK3 A0A0A0MT22 A0A0A0MTJ0 A0N0Q1 A1A4V4 A2A3U5 A2RUS0 A4D1Q0 A8K1F6
A8K249 A8K7N8 A8KAF4 A8KAG8 B0ZBE0 B2KJ49 B2R7Y7 B2RXH2 B4DN15 B7Z1L9 B8K2Q5 C1ID52 E5KQF5 F1D8N3 F1D8N7 F1D8P8 F1D8Q5 F5H1T4 F8W6L1
G5E9C5 H6UYS5 H6VQ59 K9J958 L7RSL3 L7RXH5 O00167 O94782 P00533 P00918 P02545 P05177 P05181 P06239 P06241 P07550 P08173 P08246 P08311
P08588 P08684 P08913 P11229 P11509 P11712 P14780 P17252 P18825 P21397 P21452 P21554 P21728 P21917 P22303 P22310 P25021 P25024 P25025

P25101 P25103 P25929 P28223 P28482 P30411 P32238 P32245 P33032 P35354 P35367 P37288 P41143 P41595 P41968 P42858 P49146 P50052 P50406 P51681 P83916 Q01453 Q01959 Q08209 Q38Q88 Q5DSZ7 Q5DT02 Q99700 Q9H1D0 Q9UNA4

CID 3105: dipivefrin

B0ZBD3 D0VY79 D3DNN4 O94782 P00352 P02545 P07550 P08684 P08913 P22303 P43220 Q92830 Q9UNA4

CID 3108: dipyridamole

A0A024QZY7 A0A024R1V0 A0A024R2N2 A0A024R2Q0 A0A024R3C5 A0A024R3C7 A0A024R3S2 A0A024R4E2 A0A024R5I4 A0A024R5Z3 A0A024R6L5 A0A024R6T9 A0A024R7C0 A0A024R909 A0A024R9I2 A0A024R9Y0 A0A024RAP2 A0A024RAU7 A0A024RC53 A0A024RCN9 A0A024RD15 A0A024RDJ4 A0A087WU84 A0A090N7W1 A0A090N8Z1 A0A0A0MQX8 A0A0A0MRG0 A0A0A0MRL7 A0A0A0MSK3 A0A0A0MT22 A0A0A0MTJ0 A0N0Q1 A1A4V4 A1E5M1 A2A3U5 A2RUS0 A4D1D2 A4D1Q0 A8K1F6 A8K249 A8K2Q2 A8K7N8 A8KAF4 A8KAG8 B0ZBE0 B2R7Y7 B2RXH2 B3KN77 B3KP78 B4DN15 B7Z1L9 B7ZKN7 B8K2Q5 C1ID52 D0VY79 D3DNN4 E5KQF5 F1D8N3 F1D8N7 F5GWI4 F5H1T4 F8W6L1 G5E9C5 H6VQ59 K9J958 L7RSL3 L7RXH5 O00167 O15244 O15245 O15296 O15440 O60658 O75604 O75874 O94782 O95263 P00352 P00533 P00813 P00918 P02545 P02768 P05177 P05181 P06239 P06241 P07550 P08173 P08246 P08311 P08588 P08684 P08913 P10253 P11229 P11509 P11712 P14780 P15428 P17252 P17405 P18825 P21397 P21452 P21554 P21728 P21917 P22303 P25021 P25024 P25025 P25101 P25103 P25929 P27695 P27815 P28223 P28482 P30411 P32238 P32245 P33032 P35354 P35367 P37288 P41143 P41595 P41968 P49146 P50052 P50406 P51681 Q01453 Q01959 Q03164 Q06278 Q08209 Q13526 Q38Q88 Q86TP1 Q86VL8 Q8IUX4 Q92830 Q92887 Q96FL8 Q96QE3 Q99700 Q99714 Q99808 Q99816 Q9NP56 Q9UIF8 Q9Y233

CID 3114: disopyramide

A0A024QZY7 A0A024R0C6 A0A024R3S2 A0A024R5I4 A0A024R6L5 A0A024R909 A0A024RAP4 A0A024RAU7 A0A024RCN9 A0A090N7W1 A0A0A0MTJ0 A4D0V9 A4D1Q0 B3KP78 B7ZKN7 E9PG18 F1D8N7 O15244 O15245 P02763 P08684 P11229 P16050 Q01453 Q12809 Q13526 Q14524 Q86VL8 Q92830 Q92887 Q96FL8

CID 3117: disulfiram

A0A024QZY7 A0A024R2N2 A0A024R2Q0 A0A024R3C5 A0A024R3S2 A0A024R4E2 A0A024R5I4 A0A024R5Z3 A0A024R5Z9 A0A024R6T9 A0A024R909 A0A024R9I2 A0A024R9Y0 A0A024R9Z8 A0A024RAP2 A0A024RAU7 A0A024RCN9 A0A024RD15 A0A024RDJ4 A0A087WT22 A0A087WU84 A0A090N7W1 A0A090N8Z1 A0A0A0MQX8 A0A0A0MRG0 A0A0A0MSE3 A0A0A0MSK3 A0A0A0MT22 A0A0A0MTJ0 A0N0Q1 A1A4V4 A2A3U5 A2RUS0 A4D1Q0 A8K1F6 A8K249 A8K7N8 A8KAF4 A8KAG8 B0ZBE0 B2R7Y7 B2ZGL7 B3KP78 B4DN15 B7Z1L9 B8K2Q5 C1ID52 E5KQF5 F1D8N3 F1D8P8 F1D8Q5 F5H1T4 F8W6L1 G5E9C5 H6UYS5 H6VQ59 K9J958 K9JA46 L7RSL3 L7RXH5 O00519 O15296 O75164 O75762 O75874 O76068 O94782 O94925 P00352 P00533 P00918 P02545 P05091 P05177 P05181 P06239 P06241 P07550 P08173 P08246 P08311 P08588 P08684 P08913 P09172 P11229 P11413 P11509 P11712 P11884 P14780 P15428 P16050 P17252 P18054 P18825 P21397 P21452 P21554 P21728 P21917 P22303 P25021 P25024 P25025 P25101 P25103 P25929 P26599 P28223 P28482 P30411 P32238 P32245 P33032 P35354 P35367 P37288 P39748 P41143 P41595 P41968 P42345 P42858 P49146 P50052 P50406 P51681 P83916 Q01453 Q01959 Q03164 Q08209 Q38Q88 Q92830 Q96QE3 Q99549 Q99700 Q99714 Q9UNA4

CID 3121: valproic acid

A0A024QZ26 A0A024R2N2 A0A024R2Q0 A0A024R3C5 A0A024R3S2 A0A024R5I4 A0A024R6L5 A0A024R6T9 A0A024R909 A0A024R9I2 A0A024RAP2 A0A024RAP4 A0A024RAU7 A0A024RD15 A0A024RDJ4 A0A087WU84 A0A090N7W1 A0A090N8Z1 A0A0A0MRG0 A0A0A0MSK3 A0A0A0MT22 A0A0A0MTJ0 A0N0Q1 A1A4V4 A2A3U5 A2RUS0 A4D1Q0 A8K1F6 A8K249 A8K7N8 A8KAF4 A8KAG8 B0ZBE0 B2R7Y7 B2R807 B3KP78 B4DN15 B4E3E9 B7Z1L9 B7Z3P7 B7ZKN7 B7ZW53 B8K2Q5 C1ID52 D2KUA6 D6RFW5 E5KQF5 F1D8N3 F1D8N7 F1D8P6 F5H1T4 G5E9C5 H6VQ59 K9J958 L7RSL3 L7RXH5 O15245 O15379 O60656 O76082 P00533 P00918 P05177 P05181 P06133 P06239 P06241 P07550 P08173 P08246 P08311 P08588 P08684 P08913 P11229 P11509 P11712 P13726 P14780 P16662 P17252 P18825 P19224 P21397 P21452 P21554 P21728 P21917 P22303 P22310 P25021 P25024 P25025 P25101 P25103 P25929 P28223 P28482 P30411 P32238 P32245 P33032 P35354 P35367 P36537 P37288 P41143 P41595 P41968 P45954 P49146 P50052 P50406 P51649 P51681 P56524 P80404 Q01959 Q08209 Q13547 Q16236 Q38Q88 Q5DSZ6 Q5DT02 Q8WUI4 Q92769 Q92830 Q92887 Q96QE3 Q9BY41 Q9UQL6

CID 3125: alpha-methyl-p-tyrosine

A0A024R2N2 A0A024R2Q0 A0A024R3C5 A0A024R3S2 A0A024R6T9 A0A024R909 A0A024R9I2 A0A024R9Y0 A0A024RAP2 A0A024RAV2 A0A024RCN9 A0A024RD15 A0A024RDJ4 A0A087WU84 A0A090N7W1 A0A090N8Z1 A0A0A0MRG0 A0A0A0MSK3 A0A0A0MT22 A0N0Q1 A1A4V4 A2A3U5 A2RUS0 A4D1Q0 A8K1F6 A8K249 A8K7N8 A8KAF4 A8KAG8 B0ZBE0 B2R7Y7 B4DN15 B7Z1L9 B7ZKN7 B8K2Q5 C1ID52 E5KQF5 F1D8N3 F1D8N7 F5H1T4 G5E9C5 H6VQ59 K9J958 L7RSL3 L7RXH5 P00533 P00918 P05177 P05181 P06239 P06241 P07101 P07550 P08173 P08246 P08311 P08588 P08684 P08913 P11229 P11509 P11712 P14780 P16050 P17252 P18825 P21397 P21452 P21554 P21728 P21917 P22303 P25021 P25024 P25025 P25101 P25103 P25929 P28223 P28482 P30411 P32238 P32245 P33032 P35354 P35367 P37288 P39748 P41143 P41595 P41968 P49146 P50052 P50406 P51681 Q01959 Q08209 Q13526 Q38Q88 Q99549 Q9UNA4

CID 3151: domperidone

A0A024QZY7 A0A024R2N2 A0A024R2Q0 A0A024R3C5 A0A024R3S2 A0A024R5Z3 A0A024R6T9 A0A024R909 A0A024R9I2 A0A024RAP2 A0A024RCN9 A0A024RD15 A0A024RDJ4 A0A087WU84 A0A090N7W1 A0A0A0MRG0 A0A0A0MSK3 A0A0A0MT22 A0N0Q1 A1A4V4 A2A3U5 A2RUS0 A4D1D2 A4D1Q0 A8K1F6 A8K249 A8K7N8 A8KAF4 A8KAG8 B0ZBE0 B2R7Y7 B4DN15 B7Z1F5 B7Z1L9 B8K2Q5 C1ID52 D0VY79 E5KQF5 F1D8N3 F5H1T4 G5E9C5 H6VQ59 K9J958 L7RSL3 L7RXH5 O15244 O15296 O75604 P00533 P00918 P02545 P05177 P05181 P06239 P06241 P06280 P07550 P08173 P08246 P08311 P08588 P08684 P08913 P11229 P11509 P11712 P14416 P14780 P17252 P17405 P18825 P19020 P20813 P21397 P21452 P21554 P21728 P21917 P22303 P25021 P25024 P25025 P25101 P25103 P25929 P27695 P28223 P28482 P30411 P32238 P32245 P33032 P35318 P35354 P35367 P35462 P37288 P41143 P41595 P41968 P42345 P49146 P50052 P50406 P51681 P61169 P83916 Q01453 Q01959 Q08209 Q38Q88 Q86VL8 Q96FL8 Q96QE3 Q99549 Q99700 Q9UNA4

CID 3152: donepezil

A0A024QZY7 A0A024R3D5 A0A024RCN9 A0A090N7W1 A2A3U5 B2RXH2 B7Z242 C1ID52 D3DNN4 P05177 P08684 P11712 P17405 P21397 P22303 P28223 Q13627 Q92630

CID 3156: doxapram

A0A024R2N2 A0A024R2Q0 A0A024R3C5 A0A024R3S2 A0A024R6T9 A0A024R9H3 A0A024R9I2 A0A024RAP2 A0A024RD15 A0A087WU84 A0A090N7W1 A0A0A0MRG0 A0A0A0MSK3 A0A0A0MT22 A0N0Q1 A1A4V4 A2A3U5 A2RUS0 A4D1Q0 A8K1F6 A8K249 A8K7N8 A8KAF4 A8KAG8 B0ZBE0 B2R7Y7 B4DN15 B7Z1L9 B8K2Q5 C1ID52 E5KQF5 F1D8N3 F5H1T4 G5E9C5 H6VQ59 K9J958 L7RSL3 L7RXH5 O14649 P00533 P00918 P05177 P05181 P06239 P06241 P07550 P08173 P08246 P08311 P08588 P08684 P08913 P11229 P11509 P11712 P14780 P17252 P18825 P21397 P21452 P21554 P21728 P21917 P22303 P25021 P25024 P25025 P25101 P25103 P25929 P28223 P28482 P30411 P32238 P32245 P33032 P35354 P35367 P37288 P41143 P41595 P41968 P49146 P50052 P50406 P51681 Q01959 Q08209 Q38Q88

CID 3157: doxazosin

A0A024R2N2 A0A024R2Q0 A0A024R3C5 A0A024R3S2 A0A024R5I4 A0A024R6T9 A0A024R9I2 A0A024RAP2 A0A024RAU7 A0A024RCN9 A0A024RD15 A0A068F658 A0A087WU84 A0A090N7W1 A0A0A0MRG0 A0A0A0MSK3 A0A0A0MT22 A0N0Q1 A1A4V4 A2A3U5 A2RUS0 A4D1D2 A4D1Q0 A8K1F6 A8K249 A8K5W4 A8K7N8 A8KAF4 A8KAG8 B0ZBD3 B0ZBE0 B2R7Y7 B3KP78 B4DKC0 B4DN15 B7Z1L9 B8K2Q5 C1ID52 E5KQF5 F1D8N3 F5H1T4 G5E9C5 H6UYS5 H6VQ59 K9J958 L7RSL3 L7RXH5 O15245 O75874 O94782 P00533 P00918 P05177 P05181 P06239 P06241 P07550 P08173 P08246 P08311 P08588 P08684 P08913 P11229 P11509 P11712 P14780 P17252 P17405 P18825 P21397 P21452 P21554 P21728 P21917 P22303 P25021 P25024 P25025 P25100 P25101 P25103 P25929 P28223 P28482 P30411 P32238 P32245 P33032 P35348 P35354 P35367 P35368 P37288 P39748 P41143 P41595 P41968 P42345 P49146 P50052 P50406 P51681 P83916 Q01959 Q03164 Q08209 Q38Q88 Q96QE3 Q99700 Q9NS40 Q9UIF8

CID 3158: doxepin

A0A024QZY7 A0A024R2N2 A0A024R2Q0 A0A024R3C5 A0A024R3S2 A0A024R6T9 A0A024R9I2 A0A024RAP2 A0A024RAV2 A0A024RCN9 A0A024RD15 A0A024RDJ4 A0A087WU84 A0A090N7W1 A0A0A0MRG0 A0A0A0MSK3 A0A0A0MT22 A0A0A0MTJ0 A0N0Q1 A1A4V4 A2A3U5 A2RUS0 A4D1D2 A4D1Q0 A8K1F6 A8K249 A8K5W4 A8K7N8 A8KAF4 A8KAG8 B0ZBD3 B0ZBE0 B2KJ49 B2R7Y7 B2RXH2 B4DN15 B7Z1L9 B8K2Q5 C1ID52 E5KQF5 F1D8N3 F1D8P8 F5H1T4 G5E9C5 H6VQ59 K9J958 L7RSL3 L7RXH5 O15296 P00352 P00533 P00918 P02545 P05177 P05181 P06239 P06241 P07550 P08173 P08246 P08311 P08588 P08684 P08913 P11229 P11509 P11712 P14780 P17252 P17405 P18825 P21397 P21452 P21554 P21728 P21917 P22303 P22310 P25021 P25024 P25025 P25101 P25103 P25929 P28223 P28482 P30411 P32238 P32245 P33032 P35354 P35367 P35368 P37288 P41143 P41595 P41968 P43220 P49146 P50052 P50406 P51681 P83916 Q01959 Q08209 Q38Q88 Q96QE3 Q99700 Q9NER1 Q99700

CID 3168: droperidol

A0A024R2N2 A0A024R2Q0 A0A024R3C5 A0A024R3S2 A0A024R6T9 A0A024R9I2 A0A024R9Y0 A0A024RAP2 A0A024RD15 A0A087WU84 A0A090N7W1 A0A0A0MRG0 A0A0A0MSK3 A0A0A0MT22 A0N0Q1 A1A4V4 A2A3U5 A2RUS0 A4D1Q0 A8K1F6 A8K249 A8K7N8 A8KAF4 A8KAG8 B0ZBD3 B0ZBE0 B2R7Y7 B2RXH2 B4DN15 B7Z1L9 B7Z1W5 B8K2Q5 C1ID52 D0VY79 E5KQF5 F1D8N3 F5H1T4 G5E9C5 H6VQ59 K9J958 L7RSL3 L7RXH5 O00519 P00533 P00918 P02545 P05177 P05181 P06239 P06241 P07550 P08173 P08246 P08311 P08588 P08684 P08913 P11229 P11509 P11712 P14780 P17252 P17405 P18825 P21397 P21452 P21554 P21728 P21917 P22303 P25021 P25024 P25025 P25101 P25103 P25929 P28223 P28482 P30411 P32238 P32245 P33032 P35354 P35367 P37288 P41143 P41595 P41968 P43220 P49146 P50052 P50406 P51681 P83916 Q01959 Q08209 Q38Q88 Q96QE3 Q99700

CID 3182: dyphylline

A0A024QZY7 A0A024R2N2 A0A024R2Q0 A0A024R3C5 A0A024R3S2 A0A024R6T9 A0A024R9I2 A0A024RAP2 A0A024RD15 A0A087WU84 A0A090N7W1 A0A0A0MRG0 A0A0A0MSK3 A0A0A0MT22 A0N0Q1 A1A4V4 A1E5M1 A2A3U5 A2RUS0 A4D1Q0 A8K1F6 A8K249 A8K7N8 A8KAF4 A8KAG8 B0ZBE0 B2R7Y7 B4DN15 B7Z1L9 B7Z1W5 B8K2Q5 C1ID52 E5KQF5 F1D8N3 F5H1T4 G5E9C5 H6VQ59 K9J958 L7RSL3 L7RXH5 O43849 P00533 P00918 P02545 P05177 P05181 P06239 P06241 P07550 P08173 P08246 P08311 P08588 P08684 P08913 P11229 P11509 P11712 P14780 P17252 P18825 P21397 P21452 P21554 P21728 P21917 P22303 P25021 P25024 P25025 P25101 P25103 P25929 P27815 P28223 P28482 P30411 P32238 P32245 P33032 P35354 P35367 P37288 P41143 P41595 P41968 P49146 P50052 P50406 P51681 Q01959 Q07343 Q08209 Q08499 Q13946 Q38Q88

CID 3198: econazole

A0A024QZY7 A0A024R2N2 A0A024R2Q0 A0A024R3C5 A0A024R3S2 A0A024R6L5 A0A024R6T9 A0A024R9I2 A0A024RAP2 A0A024RCN9 A0A024RD15 A0A087WU84 A0A090N7W1 A0A0A0MRG0 A0A0A0MSK3 A0A0A0MT22 A0A0A0MTJ0 A0N0Q1 A1A4V4 A2A3U5 A2RUS0 A4D1Q0 A8K1F6 A8K249 A8K7N8 A8KAF4 A8KAG8 B0ZBE0 B2R7Y7 B4DN15 B7Z1L9 B8K2Q5 C1ID52 E5KQF5 F1D8N3 F1D8P8 F5H1T4 G5E9C5 H6VQ59 K9J958 L7RSL3 L7RXH5 O15296 O94759 O94782 P00533 P00918 P02545 P05093 P05177 P05181 P06239 P06241 P07550 P08173 P08246 P08311 P08588 P08684 P08913 P11229 P11509 P11712 P14780 P16050 P17252 P18825 P21397 P21452 P21554 P21728 P21917 P22303 P25021 P25024 P25025 P25101 P25103 P25929 P28223 P28482 P30411 P32238 P32245 P33032 P35354 P35367 P37288 P41143 P41595 P41968 P49146 P50052 P50406 P51681 Q01959 Q08209 Q16850 Q38Q88 Q99700 Q9NQA5

CID 3226: enflurane

A0A024R9X6 A0A087WZL8 A8K177 A8K496 B2RCW8 B4DTP4 B4E295 O15554 P02768 P03886 P05181 P18505 P18507 P23415 P30049 P31644 P34903 P42261 P47870 P48167 P48169 P78334 Q09470 Q16445 Q8N1C3 Q99928 Q9UN88

CID 3241: epinastine

A0A024R3C5 A0A024R909 A0A024RCN9 A0A090N7W1 A4D1D2 B0ZBD3 O15244 P08913 P21728 P25021 P28223 P34969 P35367 Q86VL8 Q96FL8 Q96QE3

CID 3261: estazolam

A0A024R9X6 A8K177 A8K496 A8MPY1 B2RCW8 B4DTP4 O76068 P08684 P18505 P18507 P24046 P28476 P31644 P34903 P47870 P48169 P78334 Q16445 Q8N1C3 Q99928 Q9UN88

CID 3278: ethacrynic acid

A0A024QZY7 A0A024R2N2 A0A024R2Q0 A0A024R3C5 A0A024R3C7 A0A024R3S2 A0A024R5Z3 A0A024R6T9 A0A024R909 A0A024R9I2 A0A024R9Y0 A0A024RAP2
A0A024RAV2 A0A024RCN9 A0A024RCW6 A0A024RD15 A0A024RD58 A0A024RD62 A0A024RDA5 A0A024RDJ4 A0A087WT22 A0A087WU84 A0A090N7W1 A0A090N8Z1
A0A0A0MQX8 A0A0A0MRG0 A0A0A0MSK3 A0A0A0MT22 A0A0A0MTJ0 A0N0Q1 A1A4V4 A2A3U5 A2RUS0 A4D1Q0 A8K1F6 A8K249 A8K7N8 A8K987 A8KAF4 A8KAG8
B0ZBE0 B2R7Y7 B4DN15 B4DPF4 B6ZGS9 B7Z1F9 B7Z1L9 B8K2Q5 C1ID52 D0VY79 D2KUA6 E5KQF5 F1D8N3 F1D8N5 F1D8N7 F1D8P6 F1D8P8 F1D8Q5 F5H1T4
G5E9C5 H6VQ59 K9J958 L7RSL3 L7RXH5 O60656 O60760 O75874 O95467 P00352 P00533 P00918 P02545 P02768 P05023 P05177 P05181 P06239 P06241
P07550 P08173 P08246 P08311 P08588 P08684 P08913 P09211 P11021 P11229 P11509 P11712 P14780 P17252 P18825 P19224 P21397 P21452 P21554
P21728 P21917 P22303 P22309 P25021 P25024 P25025 P25101 P25103 P25929 P28223 P28482 P30411 P32238 P32245 P33032 P35354 P35367 P37288
P41143 P41595 P41968 P42858 P49146 P50052 P50406 P51681 Q01959 Q08209 Q13526 Q13621 Q14191 Q14376 Q38Q88 Q92830 Q96QE3 Q99700 Q9HC16
Q9UNA4

CID 3291: ethosuximide

A0A024R2N2 A0A024R2Q0 A0A024R3C5 A0A024R3S2 A0A024R6T9 A0A024R9I2 A0A024RAP2 A0A024RCN9 A0A024RD15 A0A087WU84 A0A090N7W1 A0A090N8Z1
A0A0A0MRG0 A0A0A0MSK3 A0A0A0MT22 A0A0A0MTJ0 A0N0Q1 A1A4V4 A2A3U5 A2RUS0 A4D1Q0 A8K1F6 A8K249 A8K7N8 A8KAF4 A8KAG8 B0ZBE0 B2R7Y7
B4DN15 B7Z1L9 B7Z242 B8K2Q5 C1ID52 E5KQF5 F1D8N3 F5H1T4 G5E9C5 H6VQ59 K9J958 L7RSL3 L7RXH5 O43497 P00533 P00918 P05177 P05181 P06239
P06241 P07550 P08173 P08246 P08311 P08588 P08684 P08913 P11229 P11509 P11712 P14780 P17252 P18825 P21397 P21452 P21554 P21728 P21917
P22303 P25021 P25024 P25025 P25101 P25103 P25929 P28223 P28482 P30411 P32238 P32245 P33032 P35354 P37288 P41143 P41595 P41968 P49146
P50052 P50406 P51681 Q01959 Q08209 Q38Q88 Q9P0X4

CID 3292: ethotoin

A0A024QZY7 E9PG18 O75874 P02545 Q14524 Q92830

CID 3305: etidronate

A0A024R2N2 A0A024R2Q0 A0A024R3C5 A0A024R3S2 A0A024R6T9 A0A024R9I2 A0A024RAP2 A0A024RCN9 A0A024RD15 A0A087WU84 A0A090N7W1 A0A0A0MR60
A0A0A0MRG0 A0A0A0MSK3 A0A0A0MT22 A0N0Q1 A1A4V4 A2A3U5 A2RUS0 A4D1Q0 A8K1F6 A8K249 A8K7N8 A8KAF4 A8KAG8 B0ZBE0 B2R7Y7 B4DN15 B6ZGS9
B7Z1L9 B8K2Q5 C1ID52 E5KQF5 F1D8N3 F5H1T4 G5E9C5 H6VQ59 K9J958 L7RSL3 L7RXH5 O75164 O75874 P00533 P00918 P02545 P05177 P05181 P06239
P06241 P07550 P08173 P08246 P08311 P08588 P08684 P08913 P11229 P11509 P11712 P14780 P17252 P17405 P18825 P21397 P21452 P21554 P21728
P21917 P22303 P25021 P25024 P25025 P25101 P25103 P25929 P28223 P28482 P30411 P32238 P32245 P33032 P35354 P35367 P37288 P41143 P41595
P41968 P49146 P50052 P50406 P51681 Q01959 Q08209 Q13332 Q38Q88 Q92830 Q9UNA4

CID 3308: etodolac

A0A024QZY7 A0A024R2N2 A0A024R2Q0 A0A024R3C5 A0A024R3S2 A0A024R6T9 A0A024R9I2 A0A024RAP2 A0A024RCN9 A0A024RD15 A0A024RDJ4 A0A087WU84
A0A090N7W1 A0A0A0MRG0 A0A0A0MSK3 A0A0A0MSS8 A0A0A0MT22 A0A0A0MTJ0 A0N0Q1 A1A4V4 A2A3U5 A2RUS0 A4D1Q0 A8K1F6 A8K249 A8K7N8 A8KAF4
A8KAG8 B0ZBE0 B2R7Y7 B4DN15 B7Z1L9 B7ZKN7 B8K2Q5 C1ID52 E5KQF5 F1D8N3 F1D8P8 F1D8Q5 F5H1T4 G5E9C5 H6VQ59 K9J958 L7RSL3 L7RXH5 O60656
O94782 P00352 P00533 P00918 P02768 P05177 P05181 P06239 P06241 P07550 P08173 P08246 P08311 P08588 P08684 P08913 P11229 P11509 P11712
P14780 P16050 P17252 P18825 P21397 P21452 P21554 P21728 P21917 P22303 P25021 P25024 P25025 P25101 P25103 P25929 P28223 P28482 P30411
P32238 P32245 P33032 P35354 P35367 P37288 P39748 P41143 P41595 P41968 P49146 P50052 P50406 P51681 P83916 Q01453 Q01959 Q08209 Q38Q88
Q4U2R8 Q92830

CID 3324: famciclovir

A0A024R2N2 A0A024R2Q0 A0A024R3C5 A0A024R3S2 A0A024R6T9 A0A024R9I2 A0A024RAP2 A0A024RD15 A0A087WU84 A0A087WWV0 A0A090N7W1 A0A0A0MRG0
A0A0A0MSK3 A0A0A0MT22 A0N0Q1 A1A4V4 A2A3U5 A2RUS0 A4D1Q0 A8K1F6 A8K249 A8K7N8 A8KAF4 A8KAG8 B0ZBE0 B2R7Y7 B2RXH2 B4DN15 B7Z1L9
B8K2Q5 C1ID52 E5KQF5 F1D8N3 F5H1T4 G5E9C5 H6VQ59 K9J958 L7RSL3 L7RXH5 P00352 P00533 P00918 P05177 P05181 P06239 P06241 P07550 P08173
P08246 P08311 P08588 P08684 P08913 P11229 P11509 P11712 P14780 P15428 P17252 P18825 P21397 P21452 P21554 P21728 P21917 P22303 P25021
P25024 P25025 P25101 P25103 P25929 P28223 P28482 P30411 P32238 P32245 P33032 P35354 P35367 P37288 P41143 P41595 P41968 P49146 P50052
P50406 P51681 Q01959 Q06278 Q08209 Q38Q88 Q99714

CID 3325: famotidine

A0A024QZY7 A0A024R2N2 A0A024R2Q0 A0A024R3C5 A0A024R3S2 A0A024R6T9 A0A024R9I2 A0A024RAP2 A0A024RCN9 A0A024RD15 A0A087WU84 A0A090N7W1
A0A0A0MRG0 A0A0A0MSK3 A0A0A0MT22 A0A0A0MTJ0 A0N0Q1 A1A4V4 A2A3U5 A2RUS0 A4D1Q0 A8K1F6 A8K249 A8K7N8 A8KAF4 A8KAG8 B0ZBE0 B2R7Y7
B2R807 B4DN15 B7Z1L9 B7ZKN7 B8K2Q5 C1ID52 E5KQF5 F1D8N3 F1D8P8 F5H1T4 G5E9C5 H6VQ59 K9J958 L7RSL3 L7RXH5 O15244 O15245 O75164 O75751
P00533 P00918 P02545 P05177 P05181 P06239 P06241 P07550 P08173 P08246 P08311 P08588 P08684 P08913 P11229 P11509 P11712 P14780 P17252
P18825 P21397 P21452 P21554 P21728 P21917 P22303 P25021 P25024 P25025 P25101 P25103 P25929 P28223 P28482 P30411 P32238 P32245 P33032
P35354 P35367 P37288 P41143 P41595 P41968 P49146 P50052 P50406 P51681 Q01453 Q01959 Q08209 Q38Q88 Q86VL8 Q96FL8 Q9UNA4

CID 3331: felbamate

A0A024QZY7 A0A024R5Z9 A0A024RCN9 A0A090N7W1 A0A090N8Z1 C1ID52 P05177 P08684 P11712 Q12879 Q13224 Q16236 Q8TCU5

CID 3333: felodipine

A0A024QZY7 A0A024R2N2 A0A024R2Q0 A0A024R3C5 A0A024R3S2 A0A024R5I4 A0A024R5Z3 A0A024R6T9 A0A024R9I2 A0A024RAP2 A0A024RAP4 A0A024RAU7
A0A024RB59 A0A024RCN9 A0A024RD15 A0A024RDJ4 A0A087WT22 A0A087WU84 A0A090N7W1 A0A090N8Z1 A0A0A0MR67 A0A0A0MRG0 A0A0A0MSK3 A0A0A0MT22
A0A0A0MTJ0 A0N0Q1 A1A4V4 A2A3U5 A2RUS0 A4D1D2 A4D1Q0 A8K1F6 A8K249 A8K7N8 A8KAF4 A8KAG8 B0ZBE0 B0ZBF6 B1ALM3 B2R7Y7 B2RXH2 B3KP78
B3KQH9 B4DN15 B6ZGS9 B7Z1L9 B7Z226 B7ZKN7 B8K2Q5 C1ID52 C9JE82 D0VY79 E5KQF5 E7ERK3 E7ETZ0 F1D8N3 F1D8P9 F5H1T4 F8W6L1 G5E9C5 H6UYS5
H6VQ59 K9J958 L7RSL3 L7RXH5 O15245 O94782 P00352 P00533 P00918 P02545 P02585 P05177 P05181 P06239 P06241 P07550 P08173 P08246 P08311
P08588 P08684 P08913 P11229 P11509 P11712 P13569 P14780 P15428 P17252 P18825 P21397 P21452 P21554 P21728 P21917 P22303 P25021 P25024
P25025 P25101 P25103 P25929 P28223 P28482 P30411 P32238 P32245 P33032 P35354 P35367 P37288 P39748 P41143 P41595 P41968 P42345 P43220
P49146 P50052 P50406 P51681 P63316 P83916 Q01453 Q01668 Q01959 Q08209 Q08289 Q38Q88 Q92887 Q96QE3 Q99549 Q99700 Q99714 Q9BRL5

CID 3339: fenofibrate

A0A024R2N2 A0A024R2Q0 A0A024R3C5 A0A024R3C7 A0A024R3S2 A0A024R5I4 A0A024R6L5 A0A024R6T9 A0A024R9I2 A0A024R9Y0 A0A024RAP2 A0A024RAU7
A0A024RCN9 A0A024RCW6 A0A024RD15 A0A087WU84 A0A090N7W1 A0A090N8Z1 A0A0A0MRG0 A0A0A0MSK3 A0A0A0MT22 A0A0A0MTJ0 A0N0Q1 A1A4V4 A2A3U5
A2RUS0 A4D1Q0 A8K1F6 A8K249 A8K7N8 A8KAF4 A8KAG8 B0ZBE0 B2R7Y7 B3KP78 B4DN15 B7Z1L9 B7ZKN7 B8K2Q5 C1ID52 D2KUA6 E5KQF5 F1D8N3 F1D8S4
F5H1T4 G5E9C5 H6VQ59 K9J958 L7RSL3 L7RXH5 O00519 O15245 O60656 O75164 O75604 O94782 P00533 P00918 P02545 P05177 P05181 P06239 P06241
P07550 P08173 P08246 P08311 P08588 P08684 P08913 P11229 P11509 P11712 P14780 P15428 P17252 P18825 P21397 P21452 P21554 P21728 P21917
P22303 P25021 P25024 P25025 P25101 P25103 P25929 P28223 P28482 P30411 P32238 P32245 P33032 P35354 P35367 P37288 P41143 P41595 P41968
P42345 P49146 P50052 P50406 P51681 P83916 Q01453 Q01959 Q07869 Q08209 Q16236 Q38Q88 Q92830 Q92887 Q96QE3 Q99549 Q9NPA2 Q9UIF8

CID 3342: fenoprofen

A0A024R2N2 A0A024R2Q0 A0A024R3C5 A0A024R3S2 A0A024R6T9 A0A024R9I2 A0A024RAP2 A0A024RD15 A0A087WU84 A0A090N7W1 A0A0A0MRG0 A0A0A0MSK3
A0A0A0MT22 A0N0Q1 A1A4V4 A2A3U5 A2RUS0 A4D1Q0 A8K1F6 A8K249 A8K7N8 A8KAF4 A8KAG8 B0ZBE0 B2R7Y7 B4DN15 B7Z1L9 B8K2Q5 C1ID52 E5KQF5
F1D8N3 F5H1T4 G5E9C5 H6VQ59 K9J958 L7RSL3 L7RXH5 O60656 P00533 P00918 P02768 P05177 P05181 P06133 P06239 P06241 P07550 P08173 P08246
P08311 P08588 P08684 P08913 P11229 P11509 P11712 P14780 P16662 P17252 P18825 P21397 P21452 P21554 P21728 P21917 P22303 P22309 P22310
P23219 P25021 P25024 P25025 P25101 P25103 P25929 P28223 P28482 P30411 P32238 P32245 P33032 P35354 P35367 P36537 P37288 P41143 P41595
P41968 P49146 P50052 P50406 P51681 Q01959 Q04760 Q08209 Q13526 Q38Q88 Q8N695 Q9UNA4

CID 3345: fentanyl

A0A024R5I4 A0A024RAU7 A0A024RCN9 A0A087WU84 A4D1D2 B3KP78 B8K2Q5 C1ID52 O15245 P08684 P33535 P35367 P35372 P41143 P41145

CID 3348: fexofenadine

A0A024QZY7 A0A024R2N2 A0A024R2Q0 A0A024R3C5 A0A024R3S2 A0A024R5I4 A0A024R6T9 A0A024R9I2 A0A024RAP2 A0A024RAT5 A0A024RAU7 A0A024RD15
A0A087WU84 A0A090N7W1 A0A0A0MRG0 A0A0A0MSK3 A0A0A0MT22 A0N0Q1 A1A4V4 A2A3U5 A2RUS0 A4D1D2 A4D1Q0 A8K1F6 A8K249 A8K7N8 A8KAF4 A8KAG8
B0ZBE0 B2R7Y7 B3KP78 B4DN15 B7Z1L9 B7ZKN7 B8K2Q5 C1ID52 E5KQF5 F1D8N3 F5H1T4 G5E9C5 H6VQ59 K9J958 L7RSL3 L7RXH5 O15438 P00533 P00918
P02545 P05177 P05181 P06239 P06241 P07550 P08173 P08246 P08311 P08588 P08684 P08913 P11229 P11509 P11712 P14780 P16050 P17252 P18825
P21397 P21452 P21554 P21728 P21917 P22303 P25021 P25024 P25025 P25101 P25103 P25929 P27695 P28223 P28482 P30411 P32238 P32245 P33032
P35354 P35367 P37288 P41143 P41595 P41968 P49146 P50052 P50406 P51681 Q01959 Q08209 Q13526 Q38Q88 Q92830 Q92887 Q99714 Q9UIF8 Q9UNA4

CID 3354: flavoxate

A0A024R2N2 A0A024R2Q0 A0A024R3C5 A0A024R3S2 A0A024R6T9 A0A024R9I2 A0A024RAP2 A0A024RD15 A0A087WU84 A0A090N7W1 A0A0A0MRG0 A0A0A0MSK3
A0A0A0MT22 A0N0Q1 A1A4V4 A2A3U5 A2RUS0 A4D1Q0 A8K1F6 A8K249 A8K7N8 A8KAF4 A8KAG8 B0ZBE0 B2R7Y7 B2RXH2 B4DN15 B7Z1L9 B8K2Q5 C1ID52
E5KQF5 F1D8N3 F5H1T4 G5E9C5 H6VQ59 K9J958 L7RSL3 L7RXH5 P00533 P00918 P02545 P05177 P05181 P06239 P06241 P07550 P08173 P08246 P08311
P08588 P08684 P08913 P11229 P11509 P11712 P14780 P17252 P17405 P18825 P21397 P21452 P21554 P21728 P21917 P22303 P25021 P25024 P25025
P25101 P25103 P25929 P28223 P28482 P30411 P32238 P32245 P33032 P35354 P35367 P37288 P41143 P41595 P41968 P49146 P50052 P50406 P51681
Q01959 Q08209 Q38Q88

CID 3365: fluconazole

A0A024QZY7 A0A024R2N2 A0A024R2Q0 A0A024R3C5 A0A024R3S2 A0A024R4E2 A0A024R5I4 A0A024R6T9 A0A024R9I2 A0A024RAP2 A0A024RAU7 A0A024RD15
A0A087WU84 A0A090N7W1 A0A0A0MRG0 A0A0A0MSK3 A0A0A0MT22 A0N0Q1 A1A4V4 A2A3U5 A2RUS0 A4D1D2 A4D1Q0 A8K1F6 A8K249 A8K7N8 A8KAF4 A8KAG8
B0ZBE0 B2R7Y7 B3KP78 B4DN15 B4DN83 B7Z1L9 B8K2Q5 C1ID52 E5KQF5 F1D8N3 F5H1T4 G5E9C5 H6VQ59 K9J958 K9JA46 L7RSL3 L7RXH5 P00533 P00918
P02545 P05177 P05181 P06239 P06241 P07550 P08173 P08246 P08311 P08588 P08684 P08913 P11229 P11509 P11712 P14780 P17252 P18825 P21397
P21452 P21554 P21728 P21917 P22303 P25021 P25024 P25025 P25101 P25103 P25929 P28223 P28482 P30411 P32238 P32245 P33032 P35354 P35367
P37288 P41143 P41595 P41968 P49146 P50052 P50406 P51681 P83916 Q01959 Q08209 Q16850 Q38Q88 Q9UNA4

CID 3366: 5-fluorocytosine

A0A024QZY7 A0A024R2N2 A0A024R2Q0 A0A024R3C5 A0A024R3S2 A0A024R6T9 A0A024R9I2 A0A024RAP2 A0A024RD15 A0A087WU84 A0A090N7W1 A0A0A0MRG0
A0A0A0MSK3 A0A0A0MT22 A0N0Q1 A1A4V4 A2A3U5 A2RUS0 A4D1Q0 A8K1F6 A8K249 A8K7N8 A8KAF4 A8KAG8 B0ZBE0 B2R7Y7 B4DN15 B7Z1L9 B8K2Q5
C1ID52 E5KQF5 F1D8N3 F5H1T4 G5E9C5 H6VQ59 I6L9H2 K9J958 L7RSL3 L7RXH5 P00533 P00918 P02545 P05177 P05181 P06239 P06241 P07550 P08173
P08246 P08311 P08588 P08684 P08913 P11229 P11509 P11712 P14780 P17252 P18825 P21397 P21452 P21554 P21728 P21917 P22303 P25021 P25024
P25025 P25101 P25103 P25929 P28223 P28482 P30411 P32238 P32245 P33032 P35354 P35367 P37288 P41143 P41595 P41968 P49146 P50052 P50406
P51681 Q01959 Q08209 Q38Q88 Q9UNA4

CID 3372: fluphenazine

A0A024QZY7 A0A024R2N2 A0A024R2Q0 A0A024R3C5 A0A024R3S2 A0A024R5Z3 A0A024R6L5 A0A024R6T9 A0A024R909 A0A024R9I2 A0A024R9X6 A0A024R9Y0
A0A024RAP2 A0A024RAV2 A0A024RCN9 A0A024RD15 A0A024RDJ4 A0A068F658 A0A087WT22 A0A087WU84 A0A090N7W1 A0A090N8Z1 A0A0A0MR48 A0A0A0MRG0
A0A0A0MSK3 A0A0A0MT22 A0N0Q1 A1A4V4 A2A3U5 A2RUS0 A4D1D2 A4D1Q0 A6NGA6 A8K177 A8K1F6 A8K249 A8K7N8 A8KAF4 A8KAG8 B0ZBE0 B2R7Y7
B2RCW8 B4DN15 B7Z1L9 B7Z2G8 B8K2Q5 C1ID52 E5KQF5 E7ETZ0 F1D8N3 F5H1T4 F8W6L1 G5E9C5 H6VQ59 K9J958 L7RSL3 L7RXH5 O15245 O15296 O75164

O75604 O75874 O94782 O94925 P00533 P00918 P02545 P05177 P05181 P06239 P06241 P06280 P08173 P08246 P08311 P08684 P08908 P08913 P10253
P11229 P11509 P11712 P14416 P14780 P17252 P18505 P18825 P21397 P21452 P21554 P21728 P21917 P21918 P22303 P22310 P25021 P25024 P25025
P25101 P25103 P25929 P28223 P28482 P30411 P31388 P31644 P32238 P32245 P32305 P33032 P34903 P34969 P35354 P35367 P37288 P41143 P41595
P41968 P42345 P43220 P47870 P48169 P49146 P50052 P50406 P51681 P61088 P83916 Q01453 Q08209 Q16445 Q38Q88 Q99549 Q99700 Q9BRL5 Q9UIF8
CID 3373: flumazenil
A0A024QZY7 A0A024R2N2 A0A024R2Q0 A0A024R3C5 A0A024R3S2 A0A024R4E2 A0A024R6T9 A0A024R909 A0A024R9I2 A0A024R9X6 A0A024RAP2 A0A024RCN9
A0A024RD15 A0A087WU84 A0A090N7W1 A0A0A0MQX8 A0A0A0MRG0 A0A0A0MSK3 A0A0A0MT22 A0A0A0MTJ0 A0N0Q1 A1A4V4 A2A3U5 A2RUS0 A4D1D2 A4D1Q0
A8K177 A8K1F6 A8K249 A8K7N8 A8KAF4 A8KAG8 B0ZBE0 B2R7Y7 B4DN15 B7Z1L9 B7ZKN7 B8K2Q5 C1ID52 E5KQF5 F1D8N3 F5H1T4 G5E9C5 H6VQ59 K9J958
L7RSL3 L7RXH5 P00352 P00533 P00918 P05177 P05181 P06239 P06241 P07550 P08173 P08246 P08311 P08588 P08684 P08913 P11229 P11509 P11712
P14780 P14867 P17252 P18507 P18825 P21397 P21452 P21554 P21728 P21917 P22303 P25021 P25024 P25025 P25101 P25103 P25929 P28223 P28482
P30411 P31644 P32238 P32245 P33032 P34903 P35354 P35367 P37288 P39748 P41143 P41595 P41968 P47869 P48169 P49146 P50052 P50406 P51681
Q01959 Q08209 Q16445 Q38Q88
CID 3385: 5-fluorouracil
A0A024QZY7 A0A024R2N2 A0A024R2Q0 A0A024R3C5 A0A024R3S2 A0A024R6T9 A0A024R9I2 A0A024R9Y0 A0A024RAP2 A0A024RCN9 A0A024RD15 A0A024RDA5
A0A087WT22 A0A087WU84 A0A090N7W1 A0A0A0MQX8 A0A0A0MRG0 A0A0A0MSK3 A0A0A0MT22 A0A0A0MTJ0 A0N0Q1 A1A4V4 A2A3U5 A2RUS0 A4D1Q0 A8K1F6
A8K249 A8K7N8 A8KAF4 A8KAG8 B0ZBE0 B2R7Y7 B2RBL3 B4DN15 B6ZGS9 B7Z1L9 B8K2Q5 C1ID52 D9YZU5 E5KQF5 F1D8N3 F5H1T4 F8W6L1 G5E9C5 H6VQ59
K9J958 L7RSL3 L7RXH5 O15245 O15440 O75874 P00352 P00533 P00918 P02545 P04818 P05177 P05181 P06239 P06241 P07550 P08173 P08246 P08311
P08588 P08684 P08913 P11229 P11509 P11712 P14780 P17252 P18825 P21397 P21452 P21554 P21728 P21917 P22303 P25021 P25024 P25025 P25101
P25103 P25929 P28223 P28482 P30411 P32238 P32245 P33032 P35354 P35367 P37288 P39748 P41143 P41595 P41968 P42345 P42858 P43220 P49146
P50052 P50406 P51681 P83916 Q01453 Q01959 Q08209 Q16236 Q38Q88 Q96QE3 Q99700
CID 3386: fluoxetine
A0A024QZY7 A0A024R2N2 A0A024R2Q0 A0A024R3C5 A0A024R3S2 A0A024R4E2 A0A024R5I4 A0A024R5Z3 A0A024R6T9 A0A024R909 A0A024R9I2 A0A024RAP2
A0A024RAU7 A0A024RBV5 A0A024RCN9 A0A024RD15 A0A024RDJ4 A0A068F658 A0A087WT22 A0A087WU84 A0A090N7W1 A0A0A0MQX8 A0A0A0MR48 A0A0A0MRG0
A0A0A0MSK3 A0A0A0MT22 A0A0A0MTJ0 A0N0Q1 A1A4V4 A2A3U5 A2RUS0 A4D1Q0 A8K1F6 A8K249 A8K5W4 A8K7N8 A8KAF4 A8KAG8 B0ZBD3 B0ZBE0
B2R7Y7 B2RXH2 B3KP78 B4DN15 B4E398 B7Z1F5 B7Z1L9 B7ZKN7 B8K2Q5 C1ID52 E5KQF5 F1D8N3 F5H1T4 F8W6L1 G5E9C5 H6VQ59 K9J958 L7RSL3 L7RXH5
O15118 O15296 O75874 P00352 P00533 P00918 P02545 P05177 P05181 P06239 P06241 P07550 P08173 P08246 P08311 P08588 P08684 P08909 P08913
P11229 P11509 P11712 P14780 P14842 P15428 P16050 P17252 P18825 P21397 P21452 P21554 P21728 P21917 P22303 P25021 P25024 P25025 P25101
P25103 P25122 P25929 P27695 P28223 P28482 P30411 P31388 P31645 P32238 P32245 P33032 P34969 P35354 P35367 P37288 P41143 P41968 P42345
P42858 P43220 P48542 P49146 P50052 P50406 P51681 P61088 P83916 Q01453 Q01959 Q03164 Q08209 Q13526 Q38Q88 Q5XXA6 Q92830 Q99700 Q9UNA4
CID 3393: flurazepam
A0A024R9X6 A4D1D2 A8K177 A8K496 A8MPY1 B2RCW8 B4DTP4 F1D8P8 P02768 P18505 P18507 P24046 P28476 P31644 P34903 P47870 P48169 P78334
Q16445 Q8N1C3 Q99928 Q9UN88
CID 3394: flurbiprofen
A0A024R2N2 A0A024R2Q0 A0A024R3C5 A0A024R3S2 A0A024R4E2 A0A024R6T9 A0A024R9I2 A0A024R9Y0 A0A024RAP2 A0A024RD15 A0A087WU84 A0A087X1B1
A0A090N7W1 A0A0A0MRG0 A0A0A0MRG2 A0A0A0MSK3 A0A0A0MSS8 A0A0A0MT22 A0A0A0MTJ0 A0N0Q1 A1A4V4 A2A3U5 A2RUS0 A4D1Q0 A8K1F6 A8K1U5 A8K249
A8K2Q2 A8K7N8 A8KAF4 A8KAG8 B0ZBE0 B2R7Y7 B4DN15 B7Z1L9 B8K2Q5 C1ID52 D0VY79 E5KQF5 E9KL36 F1D8N3 F5H1T4 G5E9C5 H6VQ59 K9J958 L7RSL3
L7RXH5 P00533 P00918 P02545 P02768 P05177 P05181 P06239 P06241 P07550 P08173 P08246 P08311 P08588 P08684 P08913 P11229 P11509 P11712
P14780 P15428 P16662 P17252 P17516 P18825 P21397 P21452 P21554 P21728 P21917 P22303 P22310 P23219 P25021 P25024 P25025 P25101 P25103
P25929 P28223 P28482 P30411 P32238 P32245 P33032 P35354 P35367 P37288 P41143 P41595 P41968 P43220 P49146 P50052 P50406 P51681 P52895
P55926 P83916 Q01959 Q04828 Q08209 Q38Q88 Q4U2R8 Q92887
CID 3397: flutamide
A0A024QZY7 A0A024R2N2 A0A024R2Q0 A0A024R3C5 A0A024R3S2 A0A024R5I4 A0A024R6T9 A0A024R913 A0A024R9I2 A0A024R9Z8 A0A024RAP2 A0A024RAU7
A0A024RCN9 A0A024RCW6 A0A024RD15 A0A024RDA5 A0A087WU84 A0A090N7W1 A0A0A0MQX8 A0A0A0MRG0 A0A0A0MSK3 A0A0A0MT22 A0A0A0MTJ0 A0N0Q1
A1A4V4 A2A3U5 A2RUS0 A4D1Q0 A8K1F6 A8K249 A8K7N8 A8KAF4 A8KAG8 B0ZBE0 B2R7Y7 B3KP78 B4DN15 B7Z1L9 B8K2Q5 C1ID52 E5KQF5 F1D8N3 F1D8N5
F1D8P6 F5H1T4 G5E9C5 H6UYS5 H6VQ59 K9J958 L7RSL3 L7RXH5 O15245 P00352 P00533 P00918 P02545 P02768 P05177 P05181 P06239 P06241 P06280
P07550 P08173 P08246 P08311 P08588 P08684 P08913 P10275 P11229 P11509 P11712 P14780 P16050 P17252 P18825 P21397 P21452 P21554 P21728
P21917 P22303 P25021 P25024 P25025 P25101 P25103 P25929 P28223 P28482 P30411 P32238 P32245 P33032 P35354 P35367 P37288 P41143 P41595
P41968 P42858 P49146 P50052 P50406 P51681 P83916 Q01453 Q01959 Q08209 Q38Q88 Q92887 Q96QE3 Q99549 Q99700 Q9UNA4
CID 3406: 4-methylpyrazole
A0A024R2N2 A0A024R2Q0 A0A024R3C5 A0A024R3S2 A0A024R6T9 A0A024R9I2 A0A024RAP2 A0A024RCN9 A0A024RD15 A0A087WU84 A0A090N7W1 A0A0A0MRG0
A0A0A0MSK3 A0A0A0MT22 A0N0Q1 A1A4V4 A2A3U5 A2RUS0 A4D1Q0 A8K1F6 A8K249 A8K7N8 A8KAF4 A8KAG8 B0ZBE0 B2R7Y7 B4DN15 B7Z1L9 B8K2Q5
C1ID52 E5KQF5 F1D8N3 F5H1T4 G5E9C5 H6UYS5 H6VQ59 K9J958 L7RSL3 L7RXH5 O75164 P00325 P00326 P00533 P00918 P02545 P04040 P05177 P05181
P06239 P06241 P07327 P07550 P08173 P08246 P08311 P08588 P08684 P08913 P11229 P11509 P11712 P14550 P14780 P17252 P18825 P21397 P21452
P21554 P21728 P21917 P22303 P25021 P25024 P25025 P25101 P25103 P25929 P27695 P28223 P28482 P30411 P32238 P32245 P33032 P35354 P35367
P37288 P41143 P41595 P41968 P49146 P50052 P50406 P51681 Q01453 Q01959 Q08209 Q38Q88 Q92830 Q9UNA4
CID 3410: formoterol
A0A0A0MTJ0 A8KAG8 C1ID52 O94925 P02768 P07550 P08588 P08684 P11509 P11712 P28482
CID 3440: furosemide
A0A024QZY7 A0A024R2N2 A0A024R2Q0 A0A024R3C5 A0A024R3S2 A0A024R5I4 A0A024R6T9 A0A024R9I2 A0A024RAP2 A0A024RAU7 A0A024RBW9 A0A024RD15
A0A087WU84 A0A087WZL8 A0A090N7W1 A0A0A0MRG0 A0A0A0MSK3 A0A0A0MT22 A0N0Q1 A1A4V4 A2A3U5 A2RUS0 A4D1Q0 A8K1F6 A8K249 A8K2J1 A8K2Q2
A8K3J4 A8K7N8 A8KAF4 A8KAG8 B0ZBE0 B2R7Y7 B2R807 B2RA41 B3KP78 B3KUB4 B4DN15 B4DPF4 B4DUH8 B6ZGS9 B7Z1L9 B8K2Q5 C1ID52 E5KQF5 F1D8N3
F5H1T4 G5E9C5 H6VQ59 K9J958 L7RSL3 L7RXH5 O15245 O60656 O76082 P00352 P00533 P00915 P00918 P02768 P05023 P05177 P05181 P06239 P06241
P07451 P07550 P08173 P08246 P08311 P08588 P08684 P08913 P11229 P11509 P11712 P14780 P17252 P18825 P21397 P21452 P21554 P21728 P21917
P22303 P22309 P22748 P25021 P25024 P25025 P25101 P25103 P25929 P28223 P28482 P28845 P30411 P32238 P32245 P33032 P35218 P35354 P35367
P37288 P41143 P41595 P41968 P43166 P49146 P50052 P50406 P51681 P55011 P80365 Q01959 Q08209 Q13621 Q16790 Q38Q88 Q4U2R8 Q5DSZ6 Q5DT02
Q92887 Q96FL8 Q9HC97 Q9NSA0
CID 3446: gabapentin
A0A024R2N2 A0A024R2Q0 A0A024R3C5 A0A024R3S2 A0A024R6T9 A0A024R909 A0A024R9I2 A0A024RAP2 A0A024RAV0 A0A024RCN9 A0A024RD15 A0A087WU84
A0A090N7W1 A0A0A0MRG0 A0A0A0MSK3 A0A0A0MT22 A0A0A0MTJ0 A0N0Q1 A1A4V4 A2A3U5 A2RUS0 A4D1Q0 A8K1F6 A8K249 A8K7N8 A8KAF4 A8KAG8 B0ZBE0
B2R7Y7 B4DN15 B7Z1L9 B7ZKN7 B8K2Q5 C1ID52 C9JE82 E5KQF5 E7ERK3 F1D8N3 F5H1T4 G5E9C5 H6VQ59 K9J958 L7RSL3 L7RXH5 O15245 O75604 O94782
P00352 P00533 P00918 P02545 P05177 P05181 P06239 P06241 P07550 P08173 P08246 P08311 P08588 P08684 P08913 P11229 P11509 P11712 P14780
P17252 P18825 P21397 P21452 P21554 P21728 P21917 P22303 P25021 P25024 P25025 P25101 P25103 P25929 P28223 P28482 P30411 P32238 P32245
P33032 P35354 P35367 P37288 P41143 P41595 P41968 P49146 P50052 P50406 P51681 Q00975 Q01959 Q08209 Q38Q88 Q9NY47
CID 3454: ganciclovir
A0A024QZY7 A0A024R2N2 A0A024R2Q0 A0A024R3C5 A0A024R3S2 A0A024R6T9 A0A024R9I2 A0A024RAP2 A0A024RCN9 A0A024RD15 A0A024RDJ4 A0A087WU84
A0A090N7W1 A0A0A0MRG0 A0A0A0MSK3 A0A0A0MT22 A0N0Q1 A1A4V4 A2A3U5 A2RUS0 A4D1Q0 A8K1F6 A8K249 A8K5P7 A8K7N8 A8KAF4 A8KAG8 B0ZBE0
B2R7Y7 B2R807 B4DN15 B7Z1L9 B7ZKN7 B8K2Q5 C1ID52 D0VY79 E5KQF5 F1D8N3 F5H1T4 G5E9C5 H6VQ59 K9J958 L7RSL3 L7RXH5 O15245 P00352 P00533
P00918 P02545 P05177 P05181 P06239 P06241 P07550 P08173 P08246 P08311 P08588 P08684 P08913 P11229 P11509 P11712 P14780 P17252 P18825
P21397 P21452 P21554 P21728 P21917 P22303 P25021 P25024 P25025 P25101 P25103 P25929 P28223 P28482 P30411 P32238 P32245 P33032 P35354
P35367 P37288 P41143 P41595 P41968 P49146 P50052 P50406 P51681 Q01959 Q08209 Q13255 Q38Q88 Q4U2R8 Q9UNA4 Q9Y694
CID 3463: gemfibrozil
A0A024QZY7 A0A024R2N2 A0A024R2Q0 A0A024R3C5 A0A024R3S2 A0A024R4E2 A0A024R5I4 A0A024R5Z3 A0A024R6L5 A0A024R6T9 A0A024R9I2 A0A024RAP2
A0A024RAU7 A0A024RD15 A0A024RDA5 A0A087WU84 A0A090N7W1 A0A0A0MQX8 A0A0A0MRG0 A0A0A0MSK3 A0A0A0MT22 A0A0A0MTJ0 A0N0Q1 A1A4V4 A2A3U5
A2RUS0 A4D1Q0 A8K1F6 A8K249 A8K7N8 A8KAF4 A8KAG8 B0ZBE0 B2R7Y7 B3KP78 B4DN15 B7Z1F5 B7Z1L9 B8K2Q5 C1ID52 D2KUA6 E5KQF5 F1D8N3 F1D8S4
F5H1T4 G5E9C5 H6VQ59 K9J958 L7RSL3 L7RXH5 O94956 P00533 P00918 P05177 P05181 P06239 P06241 P06858 P07550 P08173 P08246 P08311 P08588
P08684 P08913 P11229 P11509 P11712 P14780 P17252 P18825 P21397 P21452 P21554 P21728 P21917 P22303 P25021 P25024 P25025 P25101 P25103
P25929 P28223 P28482 P30411 P32238 P32245 P33032 P35354 P35367 P37288 P41143 P41595 P41968 P49146 P50052 P50406 P51681 Q01959 Q07869
Q08209 Q38Q88 Q92830 Q9NPD5 Q9Y6L6
CID 3475: gliclazide
A0A024R2N2 A0A024R2Q0 A0A024R3C5 A0A024R3K6 A0A024R3S2 A0A024R6T9 A0A024R9I2 A0A024RAP2 A0A024RD15 A0A024RD33 A0A087WU84 A0A090N7W1
A0A0A0MRG0 A0A0A0MSK3 A0A0A0MT22 A0N0Q1 A1A4V4 A2A3U5 A2RUS0 A4D1Q0 A8K1F6 A8K249 A8K7N8 A8KAF4 A8KAG8 B0ZBE0 B2R7Y7 B4DN15 B7Z1L9
B8K2Q5 C1ID52 E5KQF5 F1D8N3 F5H1T4 G5E9C5 H6VQ59 K9J958 L7RSL3 L7RXH5 O75164 O94782 O94925 P00352 P00533 P00918 P02545 P02768 P05177
P05181 P06239 P06241 P07550 P08173 P08246 P08311 P08588 P08684 P08913 P11229 P11509 P11712 P14780 P17252 P18825 P21397 P21452 P21554
P21728 P21917 P22303 P25021 P25024 P25025 P25101 P25103 P25929 P27695 P28223 P28482 P30411 P32238 P32245 P33032 P35354 P35367 P37288
P41143 P41595 P41968 P49146 P50052 P50406 P51681 Q01959 Q08209 Q09428 Q38Q88 Q92887 Q9UIF8
CID 3478: glipizide
A0A024QZY7 A0A024R2N2 A0A024R2Q0 A0A024R3C5 A0A024R3K6 A0A024R3S2 A0A024R5I4 A0A024R6T9 A0A024R9I2 A0A024R9Y0 A0A024RAP2 A0A024RAU7
A0A024RCN9 A0A024RD15 A0A024RDJ4 A0A068F658 A0A087WU84 A0A090N7W1 A0A0A0MRG0 A0A0A0MSK3 A0A0A0MT22 A0A0A0MTJ0 A0N0Q1 A1A4V4 A2A3U5
A2RUS0 A4D1Q0 A8K1F6 A8K249 A8K7N8 A8KAF4 A8KAG8 B0ZBE0 B2R7Y7 B3KP78 B4DN15 B7Z1L9 B7ZKN7 B8K2Q5 C1ID52 D2KUA6 E5KQF5 F1D8N3 F5H1T4
G5E9C5 H6VQ59 K9J958 L7RSL3 L7RXH5 O00519 O15245 P00533 P00918 P02545 P05177 P05181 P06239 P06241 P07550 P08173 P08246 P08311 P08588
P08684 P08913 P11229 P11509 P11712 P14780 P17252 P18825 P21397 P21452 P21554 P21728 P21917 P22303 P25021 P25024 P25025 P25101 P25103
P25929 P28223 P28482 P30411 P32238 P32245 P33032 P35354 P35367 P37288 P41143 P41595 P41968 P49146 P50052 P50406 P51681 P78508 Q01959
Q08209 Q09428 Q38Q88 Q92887 Q9UNA4
CID 3488: glibenclamide
A0A024R2N2 A0A024R2Q0 A0A024R3C5 A0A024R3K6 A0A024R3S2 A0A024R5I4 A0A024R6T9 A0A024R730 A0A024R9I2 A0A024RAP2 A0A024RAU7 A0A024RAV7
A0A024RCN9 A0A024RCW6 A0A024RD15 A0A024RDD4 A0A087WU84 A0A090N7W1 A0A0A0MRG0 A0A0A0MSK3 A0A0A0MT22 A0A0A0MTJ0 A0N0Q1 A1A4V4 A2A3U5
A2RUS0 A4D1D2 A4D1Q0 A8K1F6 A8K249 A8K7N8 A8KAF4 A8KAG8 B0ZBE0 B2R7Y7 B2RC52 B2RUU2 B3KP78 B4DN15 B7Z1L9 B7Z242 B7ZKN7 B8K2Q5 C1ID52
D0VY79 E5KQF5 F1D8N3 F1D8Q5 F5H1T4 G5E9C5 H6VQ59 K9J958 L7RSL3 L7RXH5 O15245 O15438 O94956 O95342 O95467 P00352 P00533 P00918 P02545

P02768 P05177 P05181 P06239 P06241 P07550 P08173 P08246 P08311 P08588 P08684 P08913 P11229 P11509 P11712 P13569 P14780 P17252 P18825
P21397 P21452 P21554 P21728 P21917 P22303 P25021 P25024 P25025 P25101 P25103 P25929 P28223 P28482 P30411 P32238 P32245 P33032 P33527
P35354 P35367 P37288 P41143 P41595 P41968 P48544 P49146 P50052 P50406 P51681 P70673 P83916 Q01453 Q01959 Q08209 Q09428 Q14654 Q15842
Q38Q88 Q61743 Q92887

CID 3494: glycopyrrolate

A0A024R3S2 A0A024R9I2 A4D1Q0 F1D8P8 O15244 O15245 P08172 P08173 P08912 P11229 P20309

CID 3510: granisetron

A0A024R2N2 A0A024R2Q0 A0A024R3C5 A0A024R3S2 A0A024R6T9 A0A024R9I2 A0A024RAP2 A0A024RCN9 A0A024RD15 A0A087WU84 A0A090N7W1 A0A0A0MRG0
A0A0A0MSK3 A0A0A0MT22 A0N0Q1 A0N0X8 A1A4V4 A2A3U5 A2RUS0 A4D1Q0 A8K1F6 A8K249 A8K7N8 A8KAF4 A8KAG8 B0ZBE0 B2R7Y7 B4DN15 B4E398
B7Z1L9 B8K2Q5 C1ID52 E5KQF5 F1D8N3 F5H1T4 G5E9C5 H6UYS5 H6VQ59 K9J958 L7RSL3 L7RXH5 O15244 O95264 P00533 P00918 P05177 P05181 P06239
P06241 P07550 P08173 P08246 P08311 P08588 P08684 P08913 P11229 P11509 P11712 P14780 P17252 P18825 P21397 P21452 P21554 P21728 P21917
P22303 P25021 P25024 P25025 P25101 P25103 P25929 P28223 P28482 P30411 P32238 P32245 P33032 P35354 P35367 P37288 P41143 P41595 P41968
P46098 P49146 P50052 P50406 P51681 P83916 Q01959 Q08209 Q38Q88 Q86VL8 Q96FL8 Q9UNA4

CID 3516: guaifenesin

A0A024QZY7 A0A024R2N2 A0A024R2Q0 A0A024R3C5 A0A024R3S2 A0A024R6T9 A0A024R9I2 A0A024RAP2 A0A024RD15 A0A087WU84 A0A090N7W1 A0A0A0MRG0
A0A0A0MSK3 A0A0A0MT22 A0N0Q1 A1A4V4 A2A3U5 A2RUS0 A4D1Q0 A8K1F6 A8K249 A8K7N8 A8KAF4 A8KAG8 B0ZBE0 B2R7Y7 B4DN15 B7Z1L9 B8K2Q5
C1ID52 E5KQF5 F1D8N3 F5H1T4 G5E9C5 H6VQ59 K9J958 L7RSL3 L7RXH5 P00533 P00918 P02545 P05177 P05181 P06239 P06241 P07550 P08173 P08246
P08311 P08588 P08684 P08913 P11229 P11509 P11712 P14780 P17252 P18825 P21397 P21452 P21554 P21728 P21917 P22303 P25021 P25024 P25025
P25101 P25103 P25929 P28223 P28482 P30411 P32238 P32245 P33032 P35354 P35367 P37288 P39748 P41143 P41595 P41968 P49146 P50052 P50406
P51681 Q01959 Q08209 Q38Q88

CID 3519: guanfacine

A0A024QZY7 A0A024R2N2 A0A024R2Q0 A0A024R3C5 A0A024R3S2 A0A024R6T9 A0A024R9I2 A0A024R9Y0 A0A024RAP2 A0A024RCN9 A0A024RD15 A0A087WU84
A0A090N7W1 A0A0A0MRG0 A0A0A0MSK3 A0A0A0MT22 A0N0Q1 A1A4V4 A2A3U5 A2RUS0 A4D1Q0 A8K1F6 A8K249 A8K7N8 A8KAF4 A8KAG8 B0ZBE0 B2R7Y7
B4DN15 B4DN83 B7Z1L9 B7ZKN7 B8K2Q5 C1ID52 D0VY79 E5KQF5 F1D8N3 F5H1T4 G5E9C5 H6VQ59 K9J958 L7RSL3 L7RXH5 O75874 P00533 P00918 P02545
P05177 P05181 P06239 P06241 P07550 P08173 P08246 P08311 P08588 P08684 P08913 P11229 P11509 P11712 P14780 P17252 P18089 P18825 P21397
P21452 P21554 P21728 P21917 P22303 P25021 P25024 P25025 P25101 P25103 P25929 P28223 P28482 P30411 P32238 P32245 P33032 P35354 P35367
P35368 P37288 P41143 P41595 P41968 P49146 P50052 P50406 P51681 Q01453 Q01959 Q08209 Q38Q88 Q99714 Q9UNA4 Q9Y2I1

CID 3559: haloperidol

A0A024QYX0 A0A024QZY7 A0A024R2N2 A0A024R2Q0 A0A024R3C5 A0A024R3S2 A0A024R4E2 A0A024R6T9 A0A024R909 A0A024R9I2 A0A024RAP2 A0A024RCN9
A0A024RD15 A0A024RDJ4 A0A068F658 A0A087WU84 A0A090N7W1 A0A0A0MRG0 A0A0A0MSK3 A0A0A0MT22 A0A0A0MTJ0 A0N0Q1 A0PJF5 A1A4V4 A2A3U5
A2RUS0 A4D1D2 A4D1Q0 A4D2N2 A8K1F6 A8K249 A8K5W4 A8K7N8 A8KAF4 A8KAG8 B0ZBD3 B0ZBE0 B2KJ49 B2R7Y7 B4DN15 B4E398 B7Z1L9 B8K2Q5 C1ID52
E5KQF5 F1D8N3 F1D8P8 F5H1T4 F8W6L1 G5E9C5 H6VQ59 K9J958 L7RSL3 L7RXH5 O00325 O15245 O15296 O95259 P00533 P00918 P02768 P05177 P05181
P06239 P06241 P08246 P08311 P08684 P08908 P08913 P11509 P11712 P14416 P14780 P14842 P16050 P17252 P17405 P18825 P19020 P21397 P21452
P21554 P21728 P21731 P21917 P21918 P22303 P25021 P25024 P25025 P25101 P25103 P25929 P28222 P28223 P28482 P30411 P30939 P32238 P32245
P32297 P32304 P32305 P33032 P34969 P35354 P35367 P35368 P35462 P37288 P41143 P41595 P41968 P42345 P43220 P48542 P49146 P50052 P50406
P51681 P61169 Q01453 Q08209 Q13224 Q15822 Q16236 Q38Q88 Q8NER1 Q92887 Q96QE3 Q99700

CID 3598: hexachlorophene

A0A024QZY7 A0A024R2N2 A0A024R2Q0 A0A024R3C5 A0A024R3S2 A0A024R3Z2 A0A024R4E2 A0A024R4X8 A0A024R5Z3 A0A024R6T9 A0A024R8S3 A0A024R9I2
A0A024R9Y0 A0A024RAP2 A0A024RAV2 A0A024RCN9 A0A024RCW6 A0A024RD15 A0A024RD62 A0A024RDJ4 A0A087WT22 A0A087WT64 A0A087WU84 A0A090N7W1
A0A0A0MRG0 A0A0A0MRL7 A0A0A0MSK3 A0A0A0MT22 A0A0A0MTJ0 A0N0Q1 A1A4V4 A2A3U5 A2RUS0 A4D1Q0 A8K1F6 A8K249 A8K7N8 A8KAF4 A8KAG8 B0ZBE0
B2R7Y7 B3KTT5 B4DN15 B6ZGS9 B7Z1L9 B7Z1W5 B7ZKN7 B8K2Q5 C1ID52 D0VY79 D2KUA6 E5KQF5 E9KL48 F1D8N3 F1D8N5 F1D8N7 F1D8P6 F1D8P8 F1D8Q5
F5H1T4 G5E9C5 H6UYS5 H6VQ59 K9J958 K9JA46 L7RSL3 L7RXH5 O14521 O15118 O15296 O75164 O75604 O75874 O94782 P00533 P00918 P01375 P02545
P05177 P05181 P06239 P06241 P07550 P08173 P08246 P08311 P08588 P08684 P08913 P11142 P11229 P11509 P11712 P14780 P15428 P16050 P17252
P18054 P18825 P21397 P21452 P21554 P21728 P21917 P22303 P25021 P25024 P25025 P25101 P25103 P25929 P28223 P28482 P30411 P32238 P32245
P33032 P35354 P35367 P37288 P39748 P41143 P41595 P41968 P42858 P43220 P49146 P49327 P50052 P50406 P51570 P51681 P55072 P98073 Q01959
Q08209 Q38Q88 Q92830 Q96QE3 Q99700 Q99714 Q9UIF8 Q9UNA4

CID 3637: hydralazine

A0A024R2N2 A0A024R2Q0 A0A024R3C5 A0A024R3S2 A0A024R5Z9 A0A024R6L5 A0A024R6T9 A0A024R9I2 A0A024R9Y0 A0A024RAP2 A0A024RBV5 A0A024RCN9
A0A024RD15 A0A087WT22 A0A087WU84 A0A090N7W1 A0A0A0MRG0 A0A0A0MSK3 A0A0A0MT22 A0N0Q1 A1A4V4 A2A3U5 A2RUS0 A4D1Q0 A8K1F6 A8K249 A8K7N8
A8KAF4 A8KAG8 B0ZBE0 B2R7Y7 B2RXH2 B4DN15 B7Z1L9 B7ZKN7 B8K2Q5 C1ID52 E5KQF5 F1D8N3 F5H1T4 F8W6L1 G5E9C5 H6VQ59 I6L9H2 K9J958 L7RSL3
L7RXH5 O15118 O15245 P00352 P00533 P00918 P02545 P05177 P05181 P06239 P06241 P07550 P08173 P08246 P08311 P08588 P08684 P08913 P11229
P11509 P11712 P13674 P14780 P17252 P18825 P21397 P21452 P21554 P21728 P21917 P22303 P25021 P25024 P25025 P25101 P25103 P25929 P28223
P28482 P30411 P32238 P32245 P33032 P35354 P35367 P37288 P41143 P41595 P41968 P49146 P50052 P50406 P51681 P55017 P83916 Q01453 Q01959 Q08209 Q16236
Q16853 Q38Q88 Q96QE3 Q99700 Q9UBC3

CID 3639: hydrochlorothiazide

A0A024QZY7 A0A024R2N2 A0A024R2Q0 A0A024R3C5 A0A024R3S2 A0A024R6T9 A0A024R9I2 A0A024RAP2 A0A024RCN9 A0A024RD15 A0A087WU84 A0A087WZL8
A0A090N7W1 A0A0A0MRG0 A0A0A0MSK3 A0A0A0MT22 A0N0Q1 A1A4V4 A2A3U5 A2RUS0 A4D1Q0 A8K1F6 A8K249 A8K7N8 A8KAF4 A8KAG8 B0ZBE0 B2R7Y7
B3KUB4 B4DN15 B7Z1L9 B8K2Q5 C1ID52 E5KQF5 F1D8N3 F1D8N7 F5H1T4 G5E9C5 H6VQ59 J3QSS1 K9J958 L7RSL3 L7RXH5 O15245 O95467 P00533 P00915
P00918 P02545 P02768 P05177 P05181 P06239 P06241 P07550 P08173 P08246 P08311 P08588 P08684 P08913 P11229 P11509 P11712 P14780 P17252
P18825 P21397 P21452 P21554 P21728 P21917 P22303 P22748 P25021 P25024 P25025 P25101 P25103 P25929 P27695 P28223 P28482 P30411 P32238
P32245 P33032 P35354 P35367 P37288 P41143 P41595 P41968 P49146 P50052 P50406 P51681 P55017 P83916 Q01453 Q01959 Q08209 Q16790 Q38Q88
Q4U2R8 Q92887

CID 3647: hydroflumethiazide

A0A024QZY7 A0A024R9A7 A0A024RCN9 A0A087WZL8 B2RXH2 B3KUB4 B4DPF4 P00352 P00915 P00918 P02545 P05023 P11712 P22748 Q13621 Q16790

CID 3652: hydroxychloroquine

A0A024R2N2 A0A024R2Q0 A0A024R3C5 A0A024R3S2 A0A024R6T9 A0A024R9I2 A0A024RAP2 A0A024RD15 A0A087WU84 A0A090N7W1 A0A0A0MRG0 A0A0A0MSK3
A0A0A0MT22 A0N0Q1 A1A4V4 A2A3U5 A2RUS0 A4D1Q0 A8K1F6 A8K249 A8K7N8 A8KAF4 A8KAG8 B0ZBE0 B2R7Y7 B2R9N9 B4DN15 B7Z1L9 B8K2Q5 C1ID52
E5KQF5 F1D8N3 F5H1T4 G5E9C5 H6VQ59 K9J958 L7RSL3 L7RXH5 P00533 P00918 P02545 P05177 P05181 P06239 P06241 P07550 P08173 P08246 P08311
P08588 P08684 P08913 P11229 P11509 P11712 P14780 P17252 P18825 P21397 P21452 P21554 P21728 P21917 P22303 P25021 P25024 P25025 P25101
P25103 P25929 P28223 P28482 P30411 P32238 P32245 P33032 P35354 P35367 P37288 P41143 P41595 P41968 P49146 P50052 P50406 P51681 Q01959
Q08209 Q38Q88 Q9NR96 Q9NYK1

CID 3658: hydroxyzine

A0A024RCN9 C1ID52 O00167 O75164 O75604 P05177 P08684 P11712 P35367 P43220

CID 3672: ibuprofen

A0A024QZY7 A0A024R2B3 A0A024R2N2 A0A024R2Q0 A0A024R3C5 A0A024R3S2 A0A024R4E2 A0A024R5I4 A0A024R6T9 A0A024R730 A0A024R909 A0A024R9I2
A0A024RAH7 A0A024RAP2 A0A024RAP4 A0A024RAU7 A0A024RCN9 A0A024RD15 A0A024RDA5 A0A024RDJ4 A0A087WU84 A0A090N7W1 A0A0A0MQX8 A0A0A0MRG0
A0A0A0MSK3 A0A0A0MSS8 A0A0A0MT22 A0A0A0MTJ0 A0N0Q1 A1A4V4 A2A3U5 A2RUS0 A4D1D2 A4D1Q0 A8K1F6 A8K1U5 A8K249 A8K2Q2 A8K5W4 A8K7N8
A8KAF4 A8KAG8 B0ZBD3 B0ZBE0 B2R7Y7 B2R807 B2ZGL7 B3KP78 B4DN15 B4DN83 B4E398 B7Z1L9 B7Z242 B7ZKN7 B8K2Q5 C1ID52 D2KUA6 D6RFW5 E5KQF5
F1D8N3 F5H1T4 G5E9C5 H6VQ59 K9J958 L7RSL3 L7RXH5 O00519 O14684 O15245 O60656 O75795 O75874 P00533 P00750 P00918 P02545 P02768 P05177
P05181 P06133 P06239 P06241 P07204 P07550 P08173 P08246 P08311 P08588 P08684 P09917 P11229 P11509 P11712 P12104 P14780 P16662 P17252
P17516 P19224 P21397 P21452 P21554 P22303 P22309 P22310 P23219 P25024 P25025 P25101 P25103 P25929 P28482 P30411 P32238 P32245 P33032
P33527 P35354 P36537 P37288 P41143 P41968 P49146 P50052 P51681 P52895 P78348 P83916 Q01453 Q04828 Q08209 Q38Q88 Q4U2R8 Q5DSZ6 Q5DSZ7
Q5DT02 Q8N695 Q92887 Q9NSA0

CID 3675: phenelzine

A0A024R2N2 A0A024R2Q0 A0A024R3C5 A0A024R3S2 A0A024R6R2 A0A024R6T9 A0A024R909 A0A024R9I2 A0A024RAP2 A0A024RBV5 A0A024RCN9 A0A024RD15
A0A024RDJ4 A0A087WU84 A0A090N7W1 A0A0A0MRG0 A0A0A0MSK3 A0A0A0MT22 A0A0A0MTJ0 A0N0Q1 A1A4V4 A2A3U5 A2RUS0 A4D1Q0 A8K1F6 A8K249 A8K7N8
A8KAF4 A8KAG8 B0ZBE0 B2R7Y7 B4DN15 B7Z1F5 B7Z1L9 B7Z242 B8K2Q5 C1ID52 E5KQF5 F1D8N3 F5H1T4 G5E9C5 H6VQ59 K9J958 L7RSL3 L7RXH5 O15118
P00352 P00533 P00918 P02545 P05177 P05181 P06239 P06241 P07550 P08173 P08246 P08311 P08588 P08684 P08913 P11229 P11509 P11712 P14780
P17252 P18825 P21397 P21452 P21554 P21728 P21917 P22303 P23975 P24298 P25021 P25024 P25025 P25101 P25103 P25929 P27338 P28223 P28482
P30411 P32238 P32245 P33032 P35354 P35367 P37288 P41143 P41595 P41968 P49146 P50052 P50406 P51681 P80404 Q01959 Q05329 Q08209 Q16236
Q16853 Q38Q88 Q96QE3 Q99549 Q99700

CID 3676: lidocaine

A0A024QZY7 A0A024R2N2 A0A024R2Q0 A0A024R3C5 A0A024R3S2 A0A024R6T9 A0A024R9I2 A0A024R9Y0 A0A024RAP2 A0A024RCN9 A0A024RD15 A0A087WU84
A0A090N7W1 A0A0A0MRG0 A0A0A0MSK3 A0A0A0MT22 A0N0Q1 A1A4V4 A2A3U5 A2RUS0 A4D1D2 A4D1Q0 A8K1F6 A8K249 A8K7N8 A8KAF4 A8KAG8 B0ZBE0
B2R7Y7 B4DN15 B7Z1L9 B7Z242 B7ZKN7 B8K2Q5 C1ID52 E5KQF5 E9PG18 F1D8N3 F5H1T4 G5E9C5 H6VQ59 K9J958 L7RSL3 L7RXH5 O08562 O15245 O75874
O95069 P00352 P00533 P00918 P02545 P04775 P05177 P05181 P06239 P06241 P07550 P08173 P08246 P08311 P08588 P08684 P08913 P10253 P11229
P11509 P11712 P14780 P15389 P15390 P17252 P17405 P18825 P21397 P21452 P21554 P21728 P21917 P22303 P22460 P25021 P25024 P25025 P25101
P25103 P25929 P28223 P28482 P30411 P32238 P32245 P33032 P35354 P35367 P35499 P37288 P39748 P41143 P41595 P41968 P49146 P50052 P50406
P51681 P83916 Q01959 Q08209 Q14524 Q15858 Q38Q88 Q62968 Q8NDX3 Q96FL8 Q9C007 Q9Y5Y9

CID 3690: ifosfamide

A0A024R2N2 A0A024R2Q0 A0A024R3C5 A0A024R3S2 A0A024R6T9 A0A024R9I2 A0A024RAP2 A0A024RD15 A0A087WU84 A0A090N7W1 A0A0A0MRG0 A0A0A0MSK3
A0A0A0MT22 A0N0Q1 A1A4V4 A2A3U5 A2RUS0 A4D1Q0 A8K1F6 A8K249 A8K7N8 A8KAF4 A8KAG8 B0ZBE0 B2R7Y7 B4DN15 B7Z1L9 B8K2Q5 C1ID52 E5KQF5
F1D8N3 F5H1T4 G5E9C5 H6VQ59 I6L9H2 K9J958 L7RSL3 L7RXH5 P00533 P00918 P02545 P05177 P05181 P06239 P06241 P07550 P08173 P08246 P08311
P08588 P08684 P08913 P11229 P11509 P11712 P14780 P17252 P18825 P20813 P21397 P21452 P21554 P21728 P21917 P22303 P25021 P25024 P25025
P25101 P25103 P25929 P28223 P28482 P30411 P32238 P32245 P33032 P35354 P35367 P37288 P41143 P41595 P41968 P49146 P50052 P50406 P51681
P83916 Q01959 Q08209 Q38Q88

CID 3696: imipramine

A0A024QZY7 A0A024R0C6 A0A024R3C5 A0A024R3S2 A0A024R5I4 A0A024R6T9 A0A024R909 A0A024R9I2 A0A024R9Y0 A0A024RAU7 A0A024RCN9 A0A024RDJ4
A0A068F658 A0A090N7W1 A1A4V4 A4D0V9 A4D1D2 A4D1Q0 A8K5W4 A8KAF4 B0ZBD3 B0ZBE0 B2R7Y7 B2RXH2 B3KP78 B4E398 B6ZGS9 B7Z1L9 B7Z242
B7ZW53 C1ID52 F1D8N7 F1D8Q5 H6VQ59 K9J958 O15244 O15245 O15296 O60656 O75751 O75795 O94782 O95259 P00352 P02545 P05177 P06133 P07550
P08172 P08173 P08684 P08913 P11229 P11712 P19224 P21397 P21918 P22309 P22310 P23975 P27695 P28223 P31645 P34969 P35367 P35368 P36537
P42345 P43220 P48542 P48545 P50406 Q01453 Q13526 Q5DSZ6 Q5DSZ7 Q5DT02 Q86VL8 Q8NER1 Q96FL8 Q99549 Q99700
CID 3698: amrinone
A0A024QZY7 A0A024R2N2 A0A024R2Q0 A0A024R3C5 A0A024R3S2 A0A024R6T9 A0A024R909 A0A024R9I2 A0A024R9Y0 A0A024RAP2 A0A024RAV2 A0A024RCN9
A0A024RD15 A0A024RD62 A0A087WU84 A0A090N7W1 A0A0A0MQX8 A0A0A0MRG0 A0A0A0MSK3 A0A0A0MT22 A0N0Q1 A1A4V4 A2A3U5 A2RUS0 A4D1Q0 A8K1F6
A8K249 A8K7N8 A8KAF4 A8KAG8 B0ZBD3 B0ZBE0 B2R7Y7 B2RXH2 B4DN15 B4DW50 B7Z1F5 B7Z1L9 B7ZKN7 B8K2Q5 C1ID52 D0VY79 E5KQF5 F1D8N3 F1D8N7
F1D8P8 F5H1T4 G5E9C5 H6VQ59 K9J958 L7RSL3 L7RXH5 O94782 O94925 P00352 P00533 P00918 P01375 P02545 P05177 P05181 P06239 P06241 P06280
P07550 P08173 P08246 P08311 P08588 P08684 P08913 P11229 P11509 P11712 P14780 P15428 P16050 P17252 P18054 P18825 P21397 P21452 P21554
P21728 P21917 P22303 P25021 P25024 P25025 P25101 P25103 P25929 P27695 P28223 P28482 P30411 P32238 P32245 P33032 P35354 P35367 P37288
P41143 P41595 P41968 P42858 P49146 P50052 P50406 P51681 Q01959 Q07343 Q08209 Q13370 Q13526 Q14432 Q38Q88 Q96QE3 Q99714 Q9UNA4
CID 3702: indapamide
A0A024QZY7 A0A024R2N2 A0A024R2Q0 A0A024R3C5 A0A024R3S2 A0A024R5Z3 A0A024R6T9 A0A024R9I2 A0A024RAP2 A0A024RAP4 A0A024RBW9 A0A024RD15
A0A087WU84 A0A090N7W1 A0A0A0MRG0 A0A0A0MSK3 A0A0A0MT22 A0N0Q1 A1A4V4 A2A3U5 A2RUS0 A4D1Q0 A7LFK2 A8K1F6 A8K249 A8K3J4 A8K7N8 A8KAF4
A8KAG8 B0ZBE0 B2R7Y7 B3KUB4 B4DN15 B4DUH8 B7Z1L9 B8K2Q5 C1ID52 E5KQF5 F1D8N3 F5H1T4 G5E9C5 H6VQ59 K9J958 L7RSL3 L7RXH5 P00352 P00533
P00915 P00918 P05177 P05181 P06239 P06241 P07451 P07550 P08173 P08246 P08311 P08588 P08684 P08913 P10253 P11229 P11509 P11712 P14780
P17252 P18825 P21397 P21452 P21554 P21728 P21917 P22303 P22748 P25021 P25024 P25025 P25101 P25103 P25929 P27695 P28223 P28482 P30411
P32238 P32245 P33032 P35218 P35354 P35367 P37288 P41143 P41595 P41968 P43166 P49146 P50052 P50406 P51681 P51787 Q01959 Q08209 Q13526
Q16790 Q38Q88 Q8N1Q1 Q9UNA4
CID 3715: indomethacin
A0A024R2N2 A0A024R2Q0 A0A024R3C5 A0A024R3S2 A0A024R5I4 A0A024R6Q6 A0A024R6T9 A0A024R9I2 A0A024R9Y0 A0A024RA96 A0A024RAP2 A0A024RAP4
A0A024RAU7 A0A024RBV5 A0A024RCN9 A0A024RCW6 A0A024RD15 A0A024RDA5 A0A068F658 A0A087WU84 A0A090N7W1 A0A090N8Z1 A0A0A0MRG0 A0A0A0MSK3
A0A0A0MSS8 A0A0A0MT22 A0N0Q1 A1A4V4 A2A3U5 A2RUS0 A4D1D2 A4D1Q0 A8K1F6 A8K249 A8K2Q2 A8K7N8 A8KAF4 A8KAG8 B0ZBE0 B2R7Y7 B2R807
B2RXH2 B2ZGL7 B3KP78 B4DN15 B6ZGS9 B7Z1L9 B8K2Q5 C1ID52 D0VY79 D2KUA6 E5KQF5 F1D8N3 F1D8N5 F1D8N7 F1D8P6 F1D8P8 F1D8Q5 F5H1T4 G5E9C5
H6VQ59 K9J958 L7RSL3 L7RXH5 O14684 O60656 O60760 O95255 O95467 P00533 P00918 P02545 P02768 P05177 P05181 P06133 P06239 P06241 P07550
P08173 P08246 P08311 P08588 P08684 P08913 P09917 P11021 P11229 P11509 P11712 P14780 P16662 P17252 P17516 P18825 P21397 P21452 P21554
P21728 P21731 P21917 P22303 P25021 P25024 P25025 P25101 P25103 P25929 P28223 P28482 P30411 P32238 P32245 P33032 P33527 P34913 P35354
P35367 P36537 P37231 P37288 P41143 P41595 P41968 P42345 P43116 P43119 P49146 P50052 P50406 P51681 P52895 Q01453 Q01959 Q04760 Q04828
Q08209 Q38Q88 Q4U2R8 Q8N8N7 Q92887 Q96FL8 Q96NT5 Q99549 Q9BPW9 Q9NSA0 Q9UIF8 Q9UNA4 Q9Y5Y4 Q9Z2J6
CID 3739: iodipamide
A0A024R9X6 A0A0A0MTJ0 A8K177 A8K1F6 B7Z1L9 H6VQ59 P02768 P28482 P31644 P34903 P83916 Q16445
CID 3749: irbesartan
A0A024R2N2 A0A024R2Q0 A0A024R3C5 A0A024R3S2 A0A024R6T9 A0A024R9I2 A0A024RAP2 A0A024RD15 A0A087WU84 A0A090N7W1 A0A0A0MRG0 A0A0A0MSE3
A0A0A0MSK3 A0A0A0MT22 A0N0Q1 A1A4V4 A2A3U5 A2RUS0 A4D1Q0 A8K1F6 A8K249 A8K7N8 A8KAF4 A8KAG8 B0ZBE0 B2R7Y7 B4DN15 B7Z1L9
B8K2Q5 C1ID52 E5KQF5 F1D8N3 F5H1T4 G5E9C5 H6VQ59 K9J958 L7RSL3 L7RXH5 P00533 P00918 P02545 P05177 P05181 P05412 P06239 P06241 P07550
P08173 P08246 P08311 P08588 P08684 P08913 P10253 P11229 P11509 P11712 P14780 P17252 P18825 P21397 P21452 P21554 P21728 P21917 P22303
P25021 P25024 P25025 P25101 P25103 P25929 P28223 P28482 P30411 P30556 P32238 P32245 P33032 P35354 P35367 P37288 P41143 P41595 P41968
P49146 P50052 P50406 P51681 Q01959 Q08209 Q14973 Q38Q88 Q96FL8
CID 3759: isocarboxazid
A0A024RCN9 B7Z242 O94782 P02545 P21397 P83916
CID 3763: isoflurane
A0A024R9X6 A8K177 A8K496 B2RCW8 B4DTP4 B4E295 E7ETZ0 P02768 P03886 P05181 P18505 P18507 P23415 P30049 P31644 P34903 P42261 P47870
P48169 P78334 Q09470 Q16445 Q6RI86 Q8N1C3 Q99928 Q9BRL5 Q9UN88
CID 3767: isoniazid
A0A024QZY7 A0A024R2N2 A0A024R2Q0 A0A024R3C5 A0A024R3S2 A0A024R5I4 A0A024R6T9 A0A024R9I2 A0A024RAP2 A0A024RAU7 A0A024RCN9 A0A024RD15
A0A087WU84 A0A090N7W1 A0A0A0MRG0 A0A0A0MSK3 A0A0A0MT22 A0N0Q1 A1A4V4 A2A3U5 A2RUS0 A4D1Q0 A8K1F6 A8K249 A8K7N8 A8KAF4 A8KAG8 B0ZBE0
B2R7Y7 B2RXH2 B3KP78 B4DN15 B7Z1F5 B7Z1L9 B8K2Q5 C1ID52 E5KQF5 F1D8N3 F5H1T4 G5E9C5 H6VQ59 K9J958 L7RSL3 L7RXH5 O94925 P00533 P00918
P05177 P05181 P06239 P06241 P07550 P08173 P08246 P08311 P08588 P08684 P08913 P11229 P11712 P14780 P17252 P18825 P21397 P21452
P21554 P21728 P21917 P22303 P25021 P25024 P25025 P25101 P25103 P25929 P28223 P28482 P30411 P32238 P32245 P33032 P35354 P35367 P37288
P41143 P41595 P41968 P49146 P50052 P50406 P51681 P80404 Q01959 Q08209 Q38Q88 Q92830 Q92887 Q9UIF8
CID 3779: isoproterenol
A0A024QZY7 A0A024R2N2 A0A024R2Q0 A0A024R3C5 A0A024R3S2 A0A024R6L5 A0A024R6T9 A0A024R909 A0A024R9I2 A0A024R9Y0 A0A024RAP2 A0A024RCN9
A0A024RD15 A0A024RDA5 A0A024RDJ4 A0A087WU84 A0A087WWV0 A0A090N7W1 A0A0A0MRG0 A0A0A0MSK3 A0A0A0MT22 A0A0A0MTJ0 A0N0Q1 A1A4V4 A2A3U5
A2RUS0 A4D1Q0 A8K1F6 A8K249 A8K7N8 A8KAF4 A8KAG8 B0ZBE0 B2R7Y7 B2RXH2 B4DN15 B4DXM8 B7Z1L9 B7Z1W5 B7ZKN7 B8K2Q5 C1ID52 D0VY79 D3DNN4
E5KQF5 F1D8N3 F1D8P8 F5H1T4 G5E9C5 H6VQ59 K9J958 L7RSL3 L7RXH5 O00459 O15296 O94782 O94925 P00352 P00533 P00918 P02545 P02751 P05177
P05181 P06239 P06241 P07550 P08173 P08246 P08311 P08588 P08684 P08913 P10253 P11229 P11509 P11712 P13945 P14780 P15428 P17252 P18825
P21397 P21452 P21554 P21728 P21917 P22303 P25021 P25024 P25025 P25101 P25103 P25929 P25962 P26255 P27695 P27986 P28482 P30411 P32238
P32245 P33032 P35354 P35367 P37288 P41143 P41595 P41968 P42345 P43220 P49146 P50052 P50406 P51681 P83916 Q01453 Q01959 Q08209 Q13526
Q38Q88 Q99549 Q99700 Q99714 Q9GZV3 Q9UNA4
CID 3783: isoxsuprine
A0A024QZY7 C1ID52 D0VY79 H6UYS5 P28482 P83916
CID 3821: ketamine
A0A024QZY7 A0A024R2N2 A0A024R2Q0 A0A024R3C5 A0A024R3S2 A0A024R6T9 A0A024R9I2 A0A024RAP2 A0A024RD15 A0A087WU84 A0A090N7W1 A0A0A0MRG0
A0A0A0MSK3 A0A0A0MT22 A0N0Q1 A1A4V4 A2A3U5 A2RUS0 A4D1D2 A4D1Q0 A8K1F6 A8K249 A8K5W4 A8K7N8 A8KAF4 A8KAG8 B0ZBE0 B2R7Y7 B4DN15
B7Z1L9 B8K2Q5 C1ID52 E5KQF5 F1D8N3 F5H1T4 G5E9C5 H6VQ59 K9J958 L7RSL3 L7RXH5 O15399 P00533 P00918 P02545 P05177 P05181 P06239 P06241
P07550 P08173 P08246 P08311 P08588 P08684 P08913 P11229 P11509 P11712 P14780 P17252 P18825 P20813 P21397 P21452 P21554 P21728 P21917
P22303 P25021 P25024 P25025 P25101 P25103 P25929 P28221 P28222 P28223 P28482 P28566 P30411 P30939 P32238 P32245 P33032 P35354 P35367
P37288 P41143 P41595 P41968 P49146 P50052 P50406 P51681 P83916 Q01098 Q01959 Q08209 Q12879 Q13224 Q38Q88 Q8TCU5
CID 3825: ketoprofen
A0A024QZY7 A0A024R2N2 A0A024R2Q0 A0A024R3C5 A0A024R3S2 A0A024R6T9 A0A024R909 A0A024R9I2 A0A024R9Y0 A0A024RAP2 A0A024RAP4 A0A024RAV2
A0A024RCN9 A0A024RD15 A0A024RDA5 A0A087WU84 A0A090N7W1 A0A0A0MRG0 A0A0A0MSK3 A0A0A0MSS8 A0A0A0MT22 A0N0Q1 A1A4V4 A2A3U5 A2RUS0
A4D1Q0 A8K1F6 A8K249 A8K2Q2 A8K7N8 A8KAF4 A8KAG8 B0ZBE0 B2R7Y7 B2R807 B2RXH2 B4DN15 B4DNF7 B7Z1L9 B8K2Q5 C1ID52 D0VY79 E5KQF5 F1D8N3
F5H1T4 F8W6L1 G5E9C5 H6VQ59 K9J958 L7RSL3 L7RXH5 O14684 O15245 O60656 O75874 O95467 P00352 P00533 P00918 P02545 P02768 P05177 P05181
P06133 P06239 P06241 P07550 P08173 P08246 P08311 P08588 P08684 P08913 P09917 P11229 P11509 P11712 P14780 P15428 P16662 P17252 P18825
P21397 P21452 P21554 P21728 P21917 P22303 P22309 P22310 P23219 P25021 P25024 P25025 P25101 P25103 P25929 P28223 P28482 P30411 P32238
P32245 P33032 P35354 P35367 P36537 P37288 P39748 P41143 P41595 P41968 P49146 P50052 P50406 P51681 P83916 Q01453 Q01959 Q04760 Q08209
Q38Q88 Q4U2R8 Q5DSZ6 Q8N695 Q92887 Q96QE3 Q99714 Q9NSA0
CID 3826: ketorolac
A0A024R2N2 A0A024R2Q0 A0A024R3C5 A0A024R3S2 A0A024R6T9 A0A024R9I2 A0A024RAP2 A0A024RBV5 A0A024RCN9 A0A024RD15 A0A087WU84 A0A090N7W1
A0A0A0MRG0 A0A0A0MSK3 A0A0A0MT22 A0N0Q1 A1A4V4 A2A3U5 A2RUS0 A4D1Q0 A8K1F6 A8K249 A8K7N8 A8KAF4 A8KAG8 B0ZBE0 B2R7Y7 B4DN15 B7Z1L9
B8K2Q5 C1ID52 E5KQF5 F1D8N3 F5H1T4 G5E9C5 H6VQ59 K9J958 L7RSL3 L7RXH5 O15118 P00533 P00918 P02768 P05177 P05181 P06239 P06241 P07550
P08173 P08246 P08311 P08588 P08684 P08913 P11229 P11509 P11712 P14780 P17252 P18825 P21397 P21452 P21554 P21728 P21917 P22303 P23219
P25021 P25024 P25025 P25101 P25103 P25929 P28223 P28482 P30411 P32238 P32245 P33032 P35354 P35367 P37288 P41143 P41595 P41968 P49146
P50052 P50406 P51681 P83916 Q01959 Q08209 Q38Q88 Q99700
CID 3827: ketotifen
A0A024R2N2 A0A024R2Q0 A0A024R3C5 A0A024R3S2 A0A024R6T9 A0A024R909 A0A024R9I2 A0A024RAP2 A0A024RC53 A0A024RCN9 A0A024RD15 A0A087WU84
A0A090N7W1 A0A0A0MRG0 A0A0A0MSK3 A0A0A0MT22 A0A0A0MTJ0 A0N0Q1 A1A4V4 A1E5M1 A2A3U5 A2RUS0 A4D1Q0 A8K1F6 A8K249 A8K7N8 A8KAF4 A8KAG8
B0ZBE0 B2R7Y7 B3KN77 B4DN15 B7Z1L9 B8K2Q5 C1ID52 E5KQF5 F1D8N3 F5H1T4 G5E9C5 H6VQ59 K9J958 L7RSL3 L7RXH5 O15296 O43849 O60656 P00533
P00918 P02545 P05177 P05181 P06239 P06241 P07550 P08173 P08246 P08311 P08588 P08684 P08913 P11229 P11509 P11712 P14780 P17252 P17405
P18825 P19224 P21397 P21452 P21554 P21728 P21917 P22303 P22310 P25021 P25024 P25025 P25101 P25103 P25929 P27815 P28223 P28482 P30411
P32238 P32245 P33032 P35354 P35367 P37288 P41143 P41595 P41968 P49146 P50052 P50406 P51681 P52209 P83916 Q01959 Q07343 Q08209 Q08499
Q13946 Q38Q88 Q99700
CID 3869: labetalol
A0A024R2N2 A0A024R2Q0 A0A024R3C5 A0A024R3S2 A0A024R6T9 A0A024R9I2 A0A024RAP2 A0A024RD15 A0A024RDJ4 A0A087WU84 A0A090N7W1 A0A0A0MRG0
A0A0A0MSK3 A0A0A0MT22 A0N0Q1 A1A4V4 A2A3U5 A2RUS0 A4D1Q0 A8K1F6 A8K249 A8K7N8 A8KAF4 A8KAG8 B0ZBD3 B0ZBE0 B2R7Y7 B2RXH2 B4DN15
B7Z1L9 B7Z242 B8K2Q5 C1ID52 D0VY79 E5KQF5 F1D8N3 F5H1T4 F8W6L1 G5E9C5 H6VQ59 K9J958 L7RSL3 L7RXH5 O60656 P00352 P00533 P00918 P02545
P05177 P05181 P06239 P06241 P07550 P08173 P08246 P08311 P08588 P08684 P08913 P10253 P11229 P11509 P11712 P14780 P15428 P17252 P18825
P21397 P21452 P21554 P21728 P21917 P22303 P22309 P25021 P25024 P25025 P25100 P25101 P25103 P25929 P28223 P28482 P30411 P32238 P32245
P33032 P35354 P35367 P35368 P37288 P41143 P41595 P41968 P49146 P50052 P50406 P51681 Q01959 Q08209 Q38Q88 Q96QE3 Q99700 Q99714 Q9UNA4
Q9Y251
CID 3878: lamotrigine
A0A024QZY7 A0A024R2N2 A0A024R2Q0 A0A024R3C5 A0A024R3S2 A0A024R5I4 A0A024R6T9 A0A024R9I2 A0A024RAP2 A0A024RAU7 A0A024RCN9 A0A024RD15
A0A087WU84 A0A090N7W1 A0A0A0MRG0 A0A0A0MSK3 A0A0A0MT22 A0N0Q1 A1A4V4 A2A3U5 A2RUS0 A4D1Q0 A8K1F6 A8K249 A8K7N8 A8KAF4 A8KAG8 B0YJ76
B0ZBE0 B2R7Y7 B3KP78 B4DN15 B7Z1L9 B7ZKN7 B8K2Q5 C1ID52 E5KQF5 E9PG18 F1D8N3 F5H1T4 G5E9C5 H6VQ59 K9J958 L7RSL3 L7RXH5 P00533 P00918
P04775 P05177 P05181 P06239 P06241 P07550 P08173 P08246 P08311 P08588 P08684 P08913 P11229 P11509 P11712 P14780 P17252 P18825 P21397
P21452 P21554 P21728 P21917 P22303 P22310 P25021 P25024 P25025 P25101 P25103 P25929 P28223 P28482 P30411 P32238 P32245 P33032 P35354

P35367 P35498 P35499 P37288 P41143 P41595 P41968 P49146 P50052 P50406 P51681 Q01453 Q01959 Q08209 Q15858 Q38Q88 Q8NDX3 Q99250 Q9C007 Q9UQD0 Q9Y5Y9

CID 3883: lansoprazole

A0A024QZY7 A0A024R2N2 A0A024R2Q0 A0A024R3C5 A0A024R3S2 A0A024R5I4 A0A024R6L5 A0A024R6T9 A0A024R909 A0A024R9I2 A0A024R9Y0 A0A024RAP2 A0A024RAU7 A0A024RBV5 A0A024RCN9 A0A024RD15 A0A087WU84 A0A090N7W1 A0A0A0MRG0 A0A0A0MSK3 A0A0A0MT22 A0A0A0MTJ0 A0N0Q1 A1A4V4 A2A3U5 A2RUS0 A4D1D2 A4D1Q0 A8K1F6 A8K249 A8K7N8 A8KAF4 A8KAG8 B0ZBE0 B2R7Y7 B2RXH2 B3KP78 B4DN15 B7Z1L9 B8K2Q5 C1ID52 D0VY79 E5KQF5 F1D8N3 F1D8P8 F5H1T4 G5E9C5 H6UYS5 H6VQ59 K9J958 L7RSL3 L7RXH5 O15118 O15296 O75164 P00352 P00533 P00918 P02545 P05177 P05181 P06239 P06241 P06280 P07550 P08173 P08246 P08311 P08588 P08684 P08913 P10253 P11229 P11509 P11712 P14780 P15428 P16050 P17252 P18825 P20648 P21397 P21452 P21554 P21728 P21917 P22303 P25021 P25024 P25025 P25101 P25103 P25929 P28223 P28482 P30411 P32238 P32245 P33032 P35354 P35367 P37288 P41143 P41595 P41968 P49146 P50052 P50406 P51681 P83916 Q01453 Q01959 Q08209 Q38Q88 Q8TCT1 Q92887 Q96QE3 Q99549 Q99700 Q99714 Q9UIF8

CID 3899: leflunomide

A0A024QZY7 A0A024R2N2 A0A024R2Q0 A0A024R3C5 A0A024R3S2 A0A024R6T9 A0A024R9I2 A0A024R9Z8 A0A024RAP2 A0A024RBV5 A0A024RD15 A0A087WT22 A0A087WU84 A0A090N7W1 A0A090N8Z1 A0A0A0MRG0 A0A0A0MSK3 A0A0A0MT22 A0N0Q1 A1A4V4 A2A3U5 A2RUS0 A4D1Q0 A8K1F6 A8K249 A8K7N8 A8KAF4 A8KAG8 B0ZBE0 B2R7Y7 B4DN15 B7Z1L9 B7ZKN7 B8K2Q5 C1ID52 E5KQF5 F1D8N3 F1D8N7 F5H1T4 F8W6L1 G5E9C5 H6VQ59 K9J958 L7RSL3 L7RXH5 O00519 O15118 O75874 O94782 P00533 P00918 P02545 P05177 P05181 P06239 P06241 P07550 P08173 P08246 P08311 P08588 P08684 P08913 P09917 P11229 P11509 P11712 P14780 P17252 P18825 P21397 P21452 P21554 P21728 P21917 P22303 P25021 P25024 P25025 P25101 P25103 P25929 P28223 P28482 P30411 P32238 P32245 P33032 P35354 P35367 P37288 P41143 P41595 P41968 P42858 P43220 P49146 P50052 P50406 P51681 Q01453 Q01959 Q02127 Q08209 Q14289 Q16236 Q38Q88 Q92830 Q96QE3 Q9UNA4

CID 3902: letrozole

A0A024R2N2 A0A024R2Q0 A0A024R3C5 A0A024R3S2 A0A024R5S8 A0A024R6T9 A0A024R9I2 A0A024RAP2 A0A024RD15 A0A087WU84 A0A090N7W1 A0A0A0MRG0 A0A0A0MSK3 A0A0A0MT22 A0A0A0MTJ0 A0N0Q1 A1A4V4 A2A3U5 A2RUS0 A4D1Q0 A8K1F6 A8K249 A8K7N8 A8KAF4 A8KAG8 B0ZBE0 B2R7Y7 B4DN15 B7Z1L9 B8K2Q5 C1ID52 E5KQF5 F1D8N3 F1D8P8 F5H1T4 G5E9C5 H6VQ59 K9J958 L7RSL3 L7RXH5 O94782 P00533 P00918 P05093 P05177 P05181 P06239 P06241 P07550 P08173 P08246 P08311 P08588 P08684 P08842 P08913 P11229 P11509 P11511 P11712 P14780 P15538 P17252 P18825 P19099 P21397 P21452 P21554 P21728 P21917 P22303 P25021 P25024 P25025 P25101 P25103 P25929 P28223 P28482 P30411 P32238 P32245 P33032 P35354 P35367 P37288 P41143 P41595 P41968 P49146 P50052 P50406 P51681 Q01959 Q08209 Q38Q88

CID 3914: levobunolol

A0A024QZY7 A0A024R2N2 A0A024R2Q0 A0A024R3C5 A0A024R3S2 A0A024R4E2 A0A024R6T9 A0A024R9I2 A0A024RAP2 A0A024RCN9 A0A024RD15 A0A087WU84 A0A090N7W1 A0A0A0MRG0 A0A0A0MSK3 A0A0A0MT22 A0A0A0MTJ0 A0N0Q1 A1A4V4 A2A3U5 A2RUS0 A4D1Q0 A8K1F6 A8K249 A8K7N8 A8KAF4 A8KAG8 B0ZBE0 B2R7Y7 B4DN15 B7Z1L9 B8K2Q5 C1ID52 E5KQF5 F1D8N3 F1D8P8 F5H1T4 G5E9C5 H6VQ59 K9J958 L7RSL3 L7RXH5 O95467 P00533 P00918 P05177 P05181 P06239 P06241 P07550 P08173 P08246 P08311 P08588 P08684 P08913 P11229 P11509 P11712 P14780 P17252 P18825 P21397 P21452 P21554 P21728 P21917 P22303 P25021 P25024 P25025 P25101 P25103 P25929 P28223 P28482 P30411 P32238 P32245 P33032 P35354 P35367 P37288 P41143 P41595 P41968 P49146 P50052 P50406 P51681 Q01959 Q08209 Q38Q88

CID 3915: levocabastine

A0A024R4E2 C1ID52 O94782 O95665 P35367

CID 3948: lomefloxacin

A0A024R2N2 A0A024R2Q0 A0A024R3C5 A0A024R3S2 A0A024R6T9 A0A024R9I2 A0A024RAP2 A0A024RCN9 A0A024RD15 A0A087WU84 A0A090N7W1 A0A0A0MRG0 A0A0A0MSK3 A0A0A0MT22 A0N0Q1 A1A4V4 A2A3U5 A2RUS0 A4D1Q0 A8K1F6 A8K249 A8K7N8 A8KAF4 A8KAG8 B0ZBE0 B2R7Y7 B2RXH2 B4DN15 B7Z1L9 B8K2Q5 C1ID52 E5KQF5 F1D8N3 F5H1T4 G5E9C5 H6VQ59 K9J958 L7RSL3 L7RXH5 O76082 P00352 P00533 P00918 P05177 P05181 P06239 P06241 P07550 P08173 P08246 P08311 P08588 P08684 P08913 P11229 P11388 P11509 P11712 P14780 P15428 P17252 P18825 P21397 P21452 P21554 P21728 P21917 P22303 P25021 P25024 P25025 P25101 P25103 P25929 P28223 P28482 P30411 P32238 P32245 P33032 P35354 P35367 P37288 P39748 P41143 P41595 P41968 P49146 P50052 P50406 P51681 Q01453 Q01959 Q02880 Q08209 Q13526 Q38Q88 Q99714

CID 3950: lomustine

A0A024R2N2 A0A024R2Q0 A0A024R3C5 A0A024R3S2 A0A024R6T9 A0A024R9I2 A0A024RAP2 A0A024RD15 A0A087WU84 A0A090N7W1 A0A0A0MRG0 A0A0A0MSK3 A0A0A0MT22 A0N0Q1 A1A4V4 A2A3U5 A2RUS0 A4D1Q0 A8K1F6 A8K249 A8K7N8 A8KAF4 A8KAG8 B0ZBE0 B2R7Y7 B4DN15 B7Z1L9 B7Z242 B8K2Q5 C1ID52 E5KQF5 E7EVN3 F1D8N3 F5H1T4 G5E9C5 H6VQ59 K9J958 L7RSL3 L7RXH5 P00533 P00918 P05177 P05181 P06239 P06241 P07550 P08173 P08246 P08311 P08588 P08684 P08913 P11021 P11229 P11509 P11712 P14780 P17252 P18825 P21397 P21452 P21554 P21728 P21917 P22303 P25021 P25024 P25025 P25101 P25103 P25929 P28223 P28482 P30411 P32238 P32245 P33032 P35354 P35367 P37288 P41143 P41595 P41968 P49146 P50052 P50406 P51681 Q01959 Q08209 Q38Q88

CID 3957: loratadine

A0A024QZY7 A0A024R2N2 A0A024R2Q0 A0A024R3C5 A0A024R3S2 A0A024R5I4 A0A024R6T9 A0A024R9I2 A0A024R9Y0 A0A024RAP2 A0A024RAU7 A0A024RBV5 A0A024RCN9 A0A024RD15 A0A087WT22 A0A087WU84 A0A087WV24 A0A090N7W1 A0A090N8Z1 A0A0A0MRG0 A0A0A0MSK3 A0A0A0MT22 A0A0A0MTJ0 A0N0Q1 A1A4V4 A2A3U5 A2RUS0 A4D1D2 A4D1Q0 A8K1F6 A8K249 A8K7N8 A8KAF4 A8KAG8 B0ZBE0 B2R7Y7 B3KP78 B4DN15 B6ZGS9 B7Z1L9 B7Z242 B7ZKN7 B8K2Q5 C1ID52 D0VY79 E5KQF5 F1D8N3 F1D8P8 F1D8P9 F5H1T4 F8W6L1 G5E9C5 H6VQ59 K9J958 L7RSL3 L7RXH5 O15118 O15245 O15296 O75604 O75874 O94782 O94925 O95467 P00533 P00918 P02545 P05177 P05181 P06239 P06241 P06280 P07550 P08173 P08246 P08311 P08588 P08684 P08913 P09917 P11229 P11509 P11712 P14780 P16050 P17252 P17405 P18825 P21397 P21452 P21554 P21728 P21917 P22303 P25021 P25024 P25025 P25101 P25103 P25929 P28223 P28482 P30411 P32238 P32245 P33032 P35354 P35367 P37288 P41143 P41595 P41968 P42345 P43220 P49146 P50052 P50406 P51681 P83916 Q01453 Q01959 Q08209 Q13526 Q38Q88 Q92887 Q96QE3 Q99549 Q99700 Q9UIF8

CID 3958: lorazepam

A0A024R2N2 A0A024R2Q0 A0A024R3C5 A0A024R3S2 A0A024R6T9 A0A024R9I2 A0A024R9X6 A0A024RAP2 A0A024RD15 A0A087WU84 A0A090N7W1 A0A0A0MRG0 A0A0A0MSK3 A0A0A0MT22 A0N0Q1 A1A4V4 A2A3U5 A2RUS0 A4D1Q0 A8K177 A8K1F6 A8K249 A8K7N8 A8KAF4 A8KAG8 B0ZBE0 B2R7Y7 B2RCW8 B4DN15 B7Z1L9 B8K2Q5 C1ID52 E5KQF5 F1D8N3 F5H1T4 G5E9C5 H6VQ59 K9J958 L7RSL3 L7RXH5 O60656 O76068 P00533 P00918 P02545 P05177 P05181 P06133 P06239 P06241 P07550 P08173 P08246 P08311 P08588 P08684 P08913 P11229 P11509 P11712 P14780 P17252 P18505 P18825 P19224 P21397 P21452 P21554 P21728 P21917 P22303 P22309 P25021 P25024 P25025 P25101 P25103 P25929 P28223 P28482 P30411 P31644 P32238 P32245 P33032 P34903 P35354 P35367 P36537 P37288 P41143 P41595 P41968 P47870 P48169 P49146 P50052 P50406 P51681 P97717 Q01959 Q08209 Q16445 Q38Q88 Q9NTN3

CID 3961: losartan

A0A024R2N2 A0A024R2Q0 A0A024R3C5 A0A024R3S2 A0A024R6T9 A0A024R9I2 A0A024RAP2 A0A024RD15 A0A087WU84 A0A090N7W1 A0A0A0MRG0 A0A0A0MSE3 A0A0A0MSK3 A0A0A0MT22 A0N0Q1 A1A4V4 A2A3U5 A2RUS0 A4D1D2 A4D1Q0 A8K1F6 A8K249 A8K7N8 A8KAF4 A8KAG8 B0ZBE0 B2R7Y7 B4DN15 B7Z1L9 B8K2Q5 C1ID52 E5KQF5 F1D8N3 F5H1T4 G5E9C5 H6VQ59 K9J958 L7RSL3 L7RXH5 P00533 P00918 P05177 P05181 P06239 P06241 P07550 P08173 P08246 P08311 P08588 P08684 P08913 P11229 P11509 P11712 P14780 P17252 P18825 P21397 P21452 P21554 P21728 P21917 P22303 P22310 P25021 P25024 P25025 P25101 P25103 P25929 P28223 P28482 P30411 P30556 P32238 P32245 P33032 P35354 P35367 P37288 P41143 P41595 P41968 P49146 P50052 P50406 P51681 Q01959 Q08209 Q38Q88 Q4U2R8 Q92830 Q96FL8

CID 3964: loxapine

A0A024R3C5 A0A024R3S2 A0A024R6T9 A0A024R9I2 A0A024RCN9 A0PJF5 A1A4V4 A2RUS0 A4D1Q0 A4D2N2 A8K5W4 B0ZBD3 B2KJ49 B2R7Y7 B4E398 K9J958 O00325 P07550 P08173 P08588 P08913 P11229 P14416 P18825 P21728 P21917 P21918 P22310 P25021 P28221 P28222 P28223 P28335 P28566 P30939 P31388 P32297 P32305 P34969 P35367 P35368 P35462 P39748 P50406 P83916 Q01959 Q15822 Q99700

CID 3998: mafenide acetate

A0A024QZY7 A0A024R9Y0 A0A024RBW9 A8K3J4 B3KUB4 B4DUH8 P00915 P00918 P07451 P22748 P35218 P43166 Q16790

CID 4004: malathion

A0A024RCN9 A0A024RDA5 A0A024RDJ4 B6ZGS9 D2KUA6 D3DNN4 F1D8N7 F1D8P6 F1D8P8 P00352 P08684 P16050 P22303 P48039 Q16236 Q92830 Q99714

CID 4032: mecamylamine

A0A024R5Z9 A0A024R909 A0A024R9X6 A0A024RDJ4 A0A0A6YYA8 A8K177 A8K1F6 B4DK78 B7Z1L9 C1ID52 F8W6L1 H6VQ59 O94782 P02545 P02708 P05177 P08684 P11712 P17405 P31644 P32297 P34903 P36544 P43681 Q15822 Q15825 Q16445 Q96QE3 Q9UNA4

CID 4033: nitrogen mustard

A0A024QZY7 A0A024R9Y0 A0A024RCW6 A0A024RDA5 A0A087WT22 A0A0A0MTJ0 A8K987 B6ZGS9 D9YZU5 E5KQF5 F1D8N5 F1D8N7 F1D8P6 F1D8Q5 P02545 P42858

CID 4034: monamine

A0A024QZY7 A0A024RCN9 A0A068F658 A0A0A0MQX8 B4DN83 B7Z242 C1ID52 D0VY79 F1D8P8 F1DAL4 O15245 O15296 O75164 O75604 O75874 O94782 P02545 P05177 P08684 P10253 P11712 P16050 P28482 P35367 P43220 P83916 Q14994 Q3V008 Q92830 Q9UIF8

CID 4044: mefenamic acid

A0A024QZY7 A0A024R2N2 A0A024R2Q0 A0A024R3C5 A0A024R3S2 A0A024R6L5 A0A024R6T9 A0A024R9I2 A0A024RAP2 A0A024RCW6 A0A024RD15 A0A087WU84 A0A090N7W1 A0A0A0MRG0 A0A0A0MSK3 A0A0A0MSS8 A0A0A0MT22 A0N0Q1 A1A4V4 A2A3U5 A2RUS0 A4D1Q0 A8K1F6 A8K249 A8K7N8 A8KAF4 A8KAG8 B0ZBE0 B2R7Y7 B4DN15 B6ZGS9 B7Z1L9 B8K2Q5 C1ID52 D0VY79 D2KUA6 E5KQF5 E9KL36 F1D8N3 F1D8N5 F1D8P8 F1D8Q5 F1D8S4 F5H1T4 G5E9C5 H6VQ59 K9J958 L7RSL3 L7RXH5 O94759 O94925 P00533 P00918 P02545 P02768 P05177 P05181 P06239 P06241 P07550 P08173 P08246 P08311 P08588 P08684 P08913 P11229 P11509 P11712 P14780 P17252 P17516 P18825 P21397 P21452 P21554 P21728 P21917 P22303 P23219 P25021 P25024 P25025 P25101 P25103 P25929 P27695 P28223 P28482 P30411 P32238 P32245 P33032 P35354 P35367 P37288 P41143 P41595 P41968 P49146 P50052 P50406 P51681 P51787 P52895 P83916 Q01959 Q04828 Q08209 Q16236 Q38Q88 Q9HCF6

CID 4046: mefloquine

A0A024QZY7 A0A024R3C5 A0A024R5Z3 A0A068F658 A0A087WT22 A0A090N7W1 A0A0A0MTJ0 A4D1D2 A8K1F6 B2RXH2 B4DN83 B7Z1L9 C1ID52 D3DNN4 F1D8P8 O15296 O75874 P02545 P02768 P08684 P21728 P39748 P42858 P43220 P61088 P83916 Q92830 Q96QE3 Q99700

CID 4053: melphalan

A0A024QZY7 A0A024R2N2 A0A024R2Q0 A0A024R3C5 A0A024R3S2 A0A024R4E2 A0A024R5Z3 A0A024R6L5 A0A024R6T9 A0A024R909 A0A024R9I2 A0A024R9Y0 A0A024RAP2 A0A024RCN9 A0A024RCW6 A0A024RD15 A0A024RDJ4 A0A068F658 A0A087WT22 A0A087WU84 A0A090N7W1 A0A0A0MRG0 A0A0A0MSK3 A0A0A0MT22 A0N0Q1 A1A4V4 A2A3U5 A2RUS0 A4D1Q0 A8K1F6 A8K249 A8K7N8 A8KAF4 A8KAG8 B0ZBE0 B2R7Y7 B2RXH2 B4DN15 B6ZGS9 B7Z1L9 B8K2Q5 C1ID52 D0VY79 D2KUA6 E5KQF5 F1D8N3 F1D8N5 F1D8P6 F1D8P8 F1D8Q5 F5H1T4 F8W6L1 G5E9C5 H6VQ59 K9J958 L7RSL3 L7RXH5 O75874 O94782 O94925 P00352 P00533 P00918 P02545 P05177 P05181 P06239 P06241 P07550 P08173 P08246 P08311 P08588 P08684 P08913 P11229 P11509 P11712 P14780 P16050 P17252 P18825 P21397 P21452 P21554 P21728 P21917 P22303 P25021 P25024 P25025 P25101 P25103 P25929 P28223 P28482 P30411 P32238 P32245 P33032

P35354 P35367 P37288 P39748 P41143 P41595 P41968 P43220 P49146 P50052 P50406 P51681 P83916 Q01453 Q01650 Q01959 Q08209 Q38Q88 Q96QE3 Q99549 Q99700

CID 4054: memantine

A0A024QZY7 A0A024RCN9 A0A024RDJ4 A0A090N8Z1 A0A0A6YYA8 B4E398 C1ID52 O15244 O15245 O75874 P02545 P11712 P20813 P42345 P42858 P83916 Q01453 Q12879 Q13224 Q13627 Q16236 Q8NER1 Q8TCU5 Q92630

CID 4057: mepenzolate methylbromide

A0A024R3S2 A0A024R4E2 C1ID52 O15245 P02545 P11229 P49019 Q8TDS4

CID 4058: meperidine

A0A087WU84 A0A090N7W1 B8K2Q5 C1ID52 O15399 P05177 P08684 P11712 P20813 P22310 P23141 P35372 P41143 P41145 Q05586 Q12879 Q13224 Q8TCU5

CID 4060: mephenytoin

A0A024R5I4 A0A024RAU7 A0A0A0MTJ0 A4D1D2 B3KP78 B7Z3P6 C1ID52 E9PG18 P02768 P05177 P05181 P11712 P20813 Q14524

CID 4062: mepivacaine

A0A024QZY7 A0A024R2N2 A0A024R2Q0 A0A024R3C5 A0A024R3S2 A0A024R4E2 A0A024R6T9 A0A024R9I2 A0A024RAP2 A0A024RAP4 A0A024RD15 A0A024RD62 A0A087WU84 A0A090N7W1 A0A0A0MRG0 A0A0A0MSK3 A0A0A0MT22 A0N0Q1 A1A4V4 A2A3U5 A2RUS0 A4D1Q0 A8K1F6 A8K249 A8K7N8 A8KAF4 A8KAG8 B0ZBE0 B2R7Y7 B4DN15 B7Z1L9 B7Z242 B8K2Q5 C1ID52 E5KQF5 F1D8N3 F5H1T4 G5E9C5 H6VQ59 K9J958 L7RSL3 L7RXH5 O94925 P00533 P00918 P05177 P05181 P06239 P06241 P07550 P08173 P08246 P08311 P08588 P08684 P08913 P11229 P11509 P11712 P14780 P17252 P18825 P21397 P21452 P21554 P21728 P21917 P22303 P25021 P25024 P25025 P25101 P25103 P25929 P28223 P28482 P30411 P32238 P32245 P33032 P35354 P35367 P37288 P41143 P41595 P41968 P49146 P50052 P50406 P51681 P83916 Q01959 Q08209 Q16236 Q38Q88 Q9UNA4 Q9Y5Y9

CID 4064: meprobamate

A0A024R9X6 A4D1D2 A8K177 B7Z242 F1D8Q5 L7RTI5 O00519 P00156 P02545 P14867 P31644 P31930 P34903 P48169 Q02127 Q02156 Q16445 Q99714 Q9HBH1

CID 4075: 5-aminosalicylic acid

A0A024R1V0 A0A024R6L5 A0A024RAP4 A0A024RAV2 A0A024RCN9 A0A0A0MRL7 A8K249 B2RXH2 D0VY79 D2KUA6 F1D8N7 F1D8P8 O14920 O15111 O60656 O94782 O94925 P00352 P05164 P08684 P09917 P11712 P15428 P16050 P19224 P23219 P27695 P35354 P37231 Q92830 Q92887 Q99700 Q99714 Q9UPY5

CID 4078: mesoridazine

A0A024R3C5 A0A024R3S2 A0A024R9I2 A0A024R9Y0 A0A024RCN9 A0A090N7W1 A1A4V4 A4D1Q0 A8K5W4 B0ZBD3 C1ID52 F1D8P8 K9J958 P00352 P08173 P08913 P11229 P14416 P15428 P16050 P21728 P21917 P28223 P30939 P35367 P50406 Q99714

CID 4086: metaproterenol

A0A024R909 A0A0A0MTJ0 D0VY79 D3DNN4 F1D8P8 O15245 P07550 P22303

CID 4091: metformin

A0A024QZY7 A0A024R2N2 A0A024R2Q0 A0A024R3C5 A0A024R3K6 A0A024R3S2 A0A024R4E2 A0A024R5I4 A0A024R6T9 A0A024R9I2 A0A024RAP2 A0A024RAU7 A0A024RBN1 A0A024RD15 A0A087WU84 A0A090N7W1 A0A0A0MRG0 A0A0A0MSK3 A0A0A0MT22 A0N0Q1 A1A4V4 A2A3U5 A2RUS0 A4D1Q0 A8K1F6 A8K249 A8K7N8 A8KAF4 A8KAG8 B0ZBE0 B2R7Y7 B3KP78 B4DN15 B7Z1F5 B7Z1L9 B8K2Q5 C1ID52 E5KQF5 F1D8N3 F5H1T4 G5E9C5 H6VQ59 K9J958 L7RSL3 L7RXH5 O00763 O15244 O15245 P00533 P00918 P02545 P05177 P05181 P06239 P06241 P07550 P08173 P08246 P08311 P08588 P08684 P08913 P11229 P11509 P11712 P14780 P17252 P18825 P21397 P21452 P21554 P21728 P21917 P22303 P25021 P25024 P25025 P25101 P25103 P25929 P28223 P28482 P30411 P31939 P32238 P32245 P33032 P35354 P35367 P37288 P41143 P41595 P41968 P42345 P42858 P49146 P50052 P50406 P51681 P54646 Q01959 Q08209 Q38Q88 Q86VL8 Q92830 Q96FL8

CID 4095: methadone

A0A087WU84 A4D1D2 B8K2Q5 C1ID52 C4IXS7 P08684 P20813 P35372 P41143 Q8TCU5

CID 4107: methocarbamol

A0A024R2N2 A0A024R2Q0 A0A024R3C5 A0A024R3S2 A0A024R4E2 A0A024R6T9 A0A024R9I2 A0A024RAP2 A0A024RD15 A0A087WU84 A0A090N7W1 A0A0A0MRG0 A0A0A0MSK3 A0A0A0MT22 A0N0Q1 A1A4V4 A2A3U5 A2RUS0 A4D1Q0 A8K1F6 A8K249 A8K7N8 A8KAF4 A8KAG8 B0ZBE0 B2R7Y7 B2RXH2 B4DN15 B7Z1L9 B8K2Q5 C1ID52 E5KQF5 F1D8N3 F5H1T4 G5E9C5 H6VQ59 K9J958 L7RSL3 L7RXH5 P00533 P00915 P00918 P02545 P05177 P05181 P06239 P06241 P07550 P08173 P08246 P08311 P08588 P08684 P08913 P11229 P11509 P11712 P14780 P17252 P18825 P21397 P21452 P21554 P21728 P21917 P22303 P25021 P25024 P25025 P25101 P25103 P25929 P28223 P28482 P30411 P32238 P32245 P33032 P35354 P35367 P37288 P41143 P41595 P41968 P49146 P50052 P50406 P51681 P83916 Q01959 Q08209 Q38Q88

CID 4114: 8-methoxypsoralen

A0A024R2N2 A0A024R2Q0 A0A024R3C5 A0A024R3D5 A0A024R3S2 A0A024R4E2 A0A024R5I4 A0A024R6T9 A0A024R9I2 A0A024RAP2 A0A024RAU7 A0A024RD15 A0A087WU84 A0A090N7W1 A0A0A0MRG0 A0A0A0MSK3 A0A0A0MT22 A0A0A0MTJ0 A0N0Q1 A1A4V4 A2A3U5 A2RUS0 A4D1Q0 A8K1F6 A8K249 A8K7N8 A8KAF4 A8KAG8 B0ZBE0 B2R7Y7 B3KP78 B4DN15 B7Z1L9 B8K2Q5 C1ID52 E5KQF5 F1D8N3 F1D8N5 F1D8P6 F1D8P8 F5H1T4 G5E9C5 H6VQ59 K9J958 L7RSL3 L7RXH5 O95467 P00533 P00918 P05177 P05181 P06239 P06241 P07550 P08173 P08246 P08311 P08588 P08684 P08913 P11229 P11509 P11712 P14780 P17252 P18825 P20813 P21397 P21452 P21554 P21728 P21917 P22303 P25021 P25024 P25025 P25101 P25103 P25929 P28223 P28482 P30411 P32238 P32245 P33032 P35354 P35367 P37288 P41143 P41595 P41968 P43220 P49146 P50052 P50406 P51681 P83916 Q01959 Q08209 Q38Q88

CID 4139: methylene blue solution

A0A024QZY7 A0A024R3C7 A0A024R4E2 A0A024R5Z3 A0A024R5Z9 A0A024R6L5 A0A024R9Y0 A0A024RAP4 A0A024RAV2 A0A024RCN9 A0A024RCW6 A0A024RD62 A0A024RDA5 A0A087WT22 A0A087WYZ4 A0A090N8Z1 A0A0A0MQX8 A0A0A0MTJ0 A8KAF4 B2RXH2 B6ZGS9 B7Z1W5 B7Z2G8 B7Z2S5 B7ZKN7 D0VY79 D2KUA6 E5KQF5 F1D8N7 F1D8P6 H6UYS5 O14727 O75164 O75874 O94782 O95467 P00352 P00390 P01375 P08684 P15428 P16050 P22303 P22888 P27695 P28482 P39748 P42858 P43220 Q03164 Q13526 Q96QE3 Q99700 Q99714 Q9UIF8 Q9UNA4

CID 4158: methylphenidate

A0A024R3C5 A0A024R3S2 A0A024R6L5 A0A024R6T9 A0A024R9I2 A0A024RCW6 A0A0A0MTJ0 A2RUS0 A4D1Q0 A4D2N2 A8K5W4 B0ZBD3 B0ZBE0 B2R7Y7 B4DK78 B4E398 C1ID52 P00352 P02545 P08913 P18825 P23141 P23975 P32297 P39748 P83916 Q01959 Q15822 Q16236 Q92830

CID 4168: metoclopramide

A0A024R2N2 A0A024R2Q0 A0A024R3C5 A0A024R3S2 A0A024R6T9 A0A024R9I2 A0A024RAP2 A0A024RBV5 A0A024RCN9 A0A024RD15 A0A087WU84 A0A090N7W1 A0A0A0MRG0 A0A0A0MSK3 A0A0A0MT22 A0N0Q1 A1A4V4 A2A3U5 A2RUS0 A4D1Q0 A8K1F6 A8K249 A8K5W4 A8K7N8 A8KAF4 A8KAG8 B0ZBE0 B2R7Y7 B4DN15 B4DN83 B4E398 B7Z1L9 B8K2Q5 C1ID52 E5KQF5 F1D8N3 F5H1T4 G5E9C5 H6VQ59 K9J958 L7RSL3 L7RXH5 O15245 O95264 P00352 P00533 P00918 P02545 P05177 P05181 P06239 P06241 P07550 P08173 P08246 P08311 P08588 P08684 P08913 P11229 P11509 P11712 P14416 P14780 P17252 P18825 P21397 P21452 P21554 P21917 P22303 P25021 P25024 P25025 P25101 P25103 P25929 P28223 P28482 P30411 P32238 P32245 P35354 P35367 P37288 P41143 P41595 P41968 P46098 P49146 P50052 P50406 P51681 P61168 P83916 P97288 Q01959 Q08209 Q13639 Q38Q88 Q99549

CID 4170: metolazone

A0A024R2N2 A0A024R2Q0 A0A024R3C5 A0A024R3S2 A0A024R6T9 A0A024R9I2 A0A024RAP2 A0A024RBW9 A0A024RCN9 A0A024RD15 A0A024RDJ4 A0A087WU84 A0A090N7W1 A0A0A0MRG0 A0A0A0MSK3 A0A0A0MT22 A0N0Q1 A1A4V4 A2A3U5 A2RUS0 A4D1Q0 A8K1F6 A8K249 A8K3J4 A8K7N8 A8KAF4 A8KAG8 B0ZBE0 B2R7Y7 B2RXH2 B3KUB4 B4DN15 B4DPF4 B4DUH8 B7Z1L9 B7ZKN7 B8K2Q5 C1ID52 E5KQF5 F1D8N3 F5H1T4 G5E9C5 H6VQ59 J3QSS1 K9J958 L7RSL3 L7RXH5 P00352 P00533 P00915 P00918 P02545 P05177 P05181 P06239 P06241 P07451 P07550 P08173 P08246 P08311 P08588 P08684 P08913 P11229 P11509 P11712 P14780 P15428 P17252 P17405 P18825 P21397 P21452 P21554 P21728 P21917 P22303 P22748 P25021 P25024 P25025 P25101 P25103 P25929 P28223 P28482 P30411 P32238 P32245 P33032 P35218 P35354 P35367 P37288 P41143 P41595 P41968 P43166 P49146 P50052 P50406 P51681 P55017 Q01453 Q01959 Q08209 Q16790 Q38Q88 Q99714

CID 4171: metoprolol

A0A024R2N2 A0A024R2Q0 A0A024R3C5 A0A024R3S2 A0A024R5I4 A0A024R6T9 A0A024R9I2 A0A024RAP2 A0A024RAU7 A0A024RD15 A0A087WU84 A0A090N7W1 A0A0A0MRG0 A0A0A0MSK3 A0A0A0MT22 A0N0Q1 A1A4V4 A2A3U5 A2RUS0 A4D1D2 A4D1Q0 A8K1F6 A8K249 A8K7N8 A8KAF4 A8KAG8 B0ZBD3 B0ZBE0 B2R7Y7 B3KP78 B4DN15 B7Z1L9 B8K2Q5 C1ID52 E5KQF5 F1D8N3 F5H1T4 G5E9C5 H6VQ59 K9J958 L7RSL3 L7RXH5 O15244 O15245 P00533 P00918 P05177 P05181 P06239 P06241 P07550 P08173 P08246 P08311 P08588 P08684 P08913 P11229 P11509 P11712 P14780 P17252 P18825 P21397 P21452 P21554 P21728 P21917 P22303 P25021 P25024 P25025 P25101 P25103 P25929 P28223 P28482 P30411 P32238 P32245 P33032 P35354 P35367 P35368 P37288 P41143 P41595 P41968 P49146 P50052 P50406 P51681 Q01959 Q08209 Q38Q88 Q92887

CID 4173: metronidazole

A0A024QZY7 A0A024R2N2 A0A024R2Q0 A0A024R3C5 A0A024R3S2 A0A024R4E2 A0A024R6T9 A0A024R9I2 A0A024RAP2 A0A024RD15 A0A087WU84 A0A090N7W1 A0A0A0MQX8 A0A0A0MRG0 A0A0A0MSK3 A0A0A0MT22 A0A0A0MTJ0 A0N0Q1 A1A4V4 A2A3U5 A2RUS0 A4D1Q0 A8K1F6 A8K249 A8K7N8 A8KAF4 A8KAG8 B0ZBE0 B2R7Y7 B4DN15 B7Z1L9 B7Z242 B8K2Q5 C1ID52 E5KQF5 F1D8N3 F1D8N7 F1D8P8 F5H1T4 G5E9C5 H6VQ59 K9J958 L7RSL3 L7RXH5 P00352 P00533 P00918 P02545 P05177 P05181 P06239 P06241 P07202 P07550 P08173 P08246 P08311 P08588 P08684 P08913 P11229 P11509 P11712 P14780 P17252 P18825 P21397 P21452 P21554 P21728 P21917 P22303 P25021 P25024 P25025 P25101 P25103 P25929 P28223 P28482 P30411 P32238 P32245 P33032 P35354 P35367 P37288 P41143 P41595 P41968 P49146 P50052 P50406 P51681 P52895 Q01959 Q08209 Q16850 Q38Q88

CID 4174: metyrapone

A0A024R2N2 A0A024R2Q0 A0A024R3C5 A0A024R3S2 A0A024R5S8 A0A024R6L5 A0A024R6T9 A0A024R9I2 A0A024RAP2 A0A024RD15 A0A087WU84 A0A090N7W1 A0A0A0MRG0 A0A0A0MSK3 A0A0A0MT22 A0N0Q1 A1A4V4 A2A3U5 A2RUS0 A4D1Q0 A8K1F6 A8K249 A8K7N8 A8KAF4 A8KAG8 B0ZBE0 B2R7Y7 B4DN15 B7Z1L9 B8K2Q5 C1ID52 E5KQF5 F1D8N3 F5H1T4 G5E9C5 H6VQ59 K9J958 L7RSL3 L7RXH5 P00533 P00918 P02545 P05093 P05177 P05181 P06239 P06241 P07550 P08173 P08246 P08311 P08588 P08684 P08913 P11229 P11509 P11712 P14780 P17252 P18825 P21397 P21452 P21554 P21728 P21917 P22303 P25021 P25024 P25025 P25101 P25103 P25929 P28223 P28482 P30411 P32238 P32245 P33032 P35354 P35367 P37288 P41143 P41595 P41968 P49146 P50052 P50406 P51681 P83916 Q01959 Q08209 Q38Q88

CID 4178: mexiletine

A0A024QZM9 A0A024R2N2 A0A024R2Q0 A0A024R3C5 A0A024R3S2 A0A024R6T9 A0A024R9I2 A0A024R9Z8 A0A024RAP2 A0A024RCN9 A0A024RD15 A0A024RDJ4 A0A087WU84 A0A090N7W1 A0A0A0MRG0 A0A0A0MSK3 A0A0A0MT22 A0A0A0MTJ0 A0N0Q1 A1A4V4 A2A3U5 A2RUS0 A4D1Q0 A8K1F6 A8K249 A8K7N8 A8KAF4 A8KAG8 B0ZBE0 B2R7Y7 B4DN15 B7Z1L9 B8K2Q5 C1ID52 E5KQF5 E9PG18 F1D8N3 F5H1T4 G5E9C5 H6VQ59 K9J958 L7RSL3 L7RXH5 P00533 P00918 P02545 P05177 P05181 P06133 P06239 P06241 P07550 P08173 P08246 P08311 P08588 P08684 P08913 P11229 P11509 P11712 P14780 P17252 P18825 P21397 P21452 P21554 P21728 P21917 P22303 P25021 P25024 P25025 P25101 P25103 P25929 P28223 P28482 P30411 P32238 P32245 P33032 P35354 P35367 P35499 P36537 P37288 P41143 P41595 P41968 P49146 P50052 P50406 P51681 P83916 Q01959 Q08209 Q13526 Q14524 Q15858 Q38Q88 Q92830 Q99250 Q99549 Q9Y5Y9

CID 4189: miconazole

A0A024QZY7 A0A024R2N2 A0A024R2Q0 A0A024R3C5 A0A024R3S2 A0A024R5S8 A0A024R5Z3 A0A024R6T9 A0A024R909 A0A024R9I2 A0A024RAP2 A0A024RCN9
A0A024RD15 A0A087WU84 A0A087WYJ0 A0A087WZL8 A0A090N7W1 A0A0A0MRG0 A0A0A0MSK3 A0A0A0MT22 A0A0A0MTA6 A0N0Q1 A1A4V4 A2A3U5 A2RUS0
A4D1D2 A4D1Q0 A8K1F6 A8K249 A8K7N8 A8KAF4 A8KAG8 B0ZBE0 B2R7Y7 B4DKC0 B4DN15 B4E295 B5BNW5 B7Z1L9 B8K2Q5 C1ID52 E5KQF5 E7ETZ0 F1D8N3
F1D8P8 F5H1T4 G5E9C5 H6VQ59 K9J958 K9JA46 L7RSL3 L7RXH5 O15296 O15303 O15554 O75164 O75874 O94759 O94782 P00533 P00918 P02545 P05093
P05177 P05181 P06239 P06241 P07550 P08173 P08246 P08311 P08588 P08684 P08913 P11229 P11509 P11712 P14780 P17252 P18825 P21397 P21452
P21554 P21728 P21917 P22303 P25021 P25024 P25025 P25101 P25103 P25929 P28223 P28482 P30411 P32238 P32245 P33032 P35228 P35354 P35367
P37288 P41143 P41595 P41968 P43220 P49146 P50052 P50406 P51681 Q01959 Q08209 Q16558 Q16850 Q38Q88 Q86W47 Q92952 Q99700 Q9BRL5 Q9H2S1
Q9NPA1 Q9NQA5 Q9NS40 Q9UNA4

CID 4192: midazolam

A0A024QZY7 A0A024R5I4 A0A024R9X6 A0A024RAU7 A0A024RCN9 A4D1D2 A8K177 A8K496 A8MPY1 B2RCW8 B3KP78 B4DTP4 B7Z1F5 B7Z3P6 C1ID52 O15245
O75164 O75874 O76068 P05181 P08684 P11712 P18505 P18507 P20813 P24046 P28476 P31644 P34903 P47870 P48169 P78334 P97717 Q01717 Q16236
Q16445 Q8N1C3 Q96QE3 Q99928 Q9BY64 Q9UN88

CID 4195: midodrine

A0A024QZY7 A0A024R5Z3 A0A0A0MTJ0 B0ZBD3 C1ID52 P02545 P05177 P08684 P11712 P35368 Q92830

CID 4197: milrinone

A0A024QZY7 A0A024R2N2 A0A024R2Q0 A0A024R3C5 A0A024R3S2 A0A024R6T9 A0A024R909 A0A024R9I2 A0A024RAP2 A0A024RCW6 A0A024RD15 A0A087WU84
A0A090N7W1 A0A0A0MRG0 A0A0A0MSK3 A0A0A0MT22 A0A0A0MTJ0 A0N0Q1 A1A4V4 A2A3U5 A2RUS0 A4D1Q0 A7E2E5 A8K1F6 A8K249 A8K7N8 A8KAF4 A8KAG8
B0ZBE0 B2R7Y7 B2RXH2 B4DN15 B7Z1L9 B7ZKN7 B8K2Q5 C1ID52 D2KUA6 E5KQF5 F1D8N3 F1D8Q5 F5H1T4 G5E9C5 H6VQ59 K9J958 L7RSL3 L7RXH5 O00408
O76074 P00533 P00918 P02545 P05177 P05181 P06239 P06241 P07550 P08173 P08246 P08311 P08588 P08684 P08913 P11229 P11509 P11712 P14780
P15428 P17252 P18825 P21397 P21452 P21554 P21728 P21917 P22303 P25021 P25024 P25025 P25101 P25103 P25929 P27815 P28223 P28482 P30411
P32238 P32245 P33032 P35354 P35367 P37288 P41143 P41595 P41968 P43220 P49146 P50052 P50406 P51681 Q01959 Q08209 Q13370 Q13526 Q14432
Q38Q88

CID 4205: mirtazapine

A0A024QZY7 A0A024R3C5 A0A024R4E2 A0A024R6T9 A0A087WU84 A0A0A0MTJ0 A1A4V4 A8K5W4 B2R7Y7 B4E398 C1ID52 K9J958 O94925 P05177 P08684
P08913 P11712 P18089 P18825 P21728 P21917 P28223 P28335 P34969 P35367 P43220 P83916 Q96QE3

CID 4211: mitotane

A0A024QZY7 A0A024R2N2 A0A024R2Q0 A0A024R3C5 A0A024R3C7 A0A024R3S2 A0A024R6L5 A0A024R6T9 A0A024R9I2 A0A024R9Y0 A0A024RAP2 A0A024RCN9
A0A024RCW6 A0A024RD15 A0A024RDJ4 A0A087WT22 A0A087WU84 A0A090N7W1 A0A0A0MRG0 A0A0A0MSK3 A0A0A0MT22 A0A0A0MTJ0 A0N0Q1 A1A4V4 A2A3U5
A2RUS0 A4D1Q0 A8K1F6 A8K249 A8K7N8 A8KAF4 A8KAG8 B0FWH2 B0ZBE0 B2R7Y7 B2RXH2 B4DN15 B6ZGS9 B7Z1L9 B7ZKN7 B8K2Q5 C1ID52 D0VY79 D2KUA6
E5KQF5 F1D8N3 F1D8N5 F1D8N7 F1D8P6 F1D8P8 F1D8Q5 F1D8S4 F5H1T4 G5E9C5 H6VQ59 K9J958 L7RSL3 L7RXH5 O75164 P00533 P00918 P02545 P05108
P05177 P05181 P06239 P06241 P07550 P08173 P08185 P08246 P08311 P08588 P08684 P08913 P10109 P11229 P11509 P11712 P14780 P15538 P17252
P18825 P21397 P21452 P21554 P21728 P21917 P22303 P25021 P25024 P25025 P25101 P25103 P25929 P28223 P28482 P30411 P32238 P32245 P33032
P35354 P35367 P37288 P41143 P41595 P41968 P43220 P49146 P50052 P50406 P51681 P83916 Q01959 Q08209 Q13526 Q16236 Q38Q88 Q99549 Q9UIF8
Q9Y468

CID 4212: mitoxantrone

A0A024QZY7 A0A024R136 A0A024R2N2 A0A024R2Q0 A0A024R3C5 A0A024R3S2 A0A024R4X8 A0A024R5I4 A0A024R5Z3 A0A024R5Z9 A0A024R6L5 A0A024R6T9
A0A024R909 A0A024R9I2 A0A024R9Y0 A0A024RAP2 A0A024RAP4 A0A024RAU7 A0A024RAV2 A0A024RBV5 A0A024RCN9 A0A024RD15 A0A024RD25 A0A024RD62
A0A024RDD4 A0A024RDJ4 A0A087WT22 A0A087WU84 A0A087WYZ4 A0A090N7W1 A0A090N8Z1 A0A0A0MQX8 A0A0A0MRG0 A0A0A0MSK3 A0A0A0MT22 A0N0Q1
A1A4V4 A2A3U5 A2RUS0 A4D1D2 A4D1Q0 A8K1F6 A8K249 A8K7N8 A8K7T1 A8KAF4 A8KAG8 B0LPE5 B0ZBE0 B2R7Y7 B2RXH2 B3KP78 B4DN15 B7Z1L9 B7Z1W5
B7Z2G8 B7ZKN7 B8K2Q5 C1ID52 D0VY79 E5KQF5 F1D8N3 F1D8P8 F5H1T4 F8W6L1 G5E9C5 H6UYS5 H6VQ59 K9J958 L7RSL3 L7RXH5 O14746 O15118 O15244
O15245 O15296 O60656 O75164 O75604 O75751 O75874 O94782 O94925 O95467 O96017 P00352 P00533 P00918 P02545 P05177 P05181 P06239 P06241
P07550 P08173 P08246 P08311 P08588 P08684 P08913 P11021 P11229 P11388 P11509 P11712 P14780 P16050 P17252 P18825 P19224 P19784 P21397
P21452 P21554 P21728 P21917 P22303 P22309 P25021 P25024 P25025 P25101 P25103 P25929 P27695 P28223 P28482 P30411 P32238 P32245 P33032
P33527 P35354 P35367 P37288 P39748 P41143 P41595 P41968 P42345 P42858 P43220 P49146 P50052 P50406 P51681 P83916 Q01453 Q01959 Q02880
Q03164 Q06187 Q08209 Q13526 Q14191 Q38Q88 Q86VL8 Q92830 Q92887 Q96FL8 Q96QE3 Q99549 Q99700 Q9UIF8 Q9UNA4 Q9Y468

CID 4236: modafinil

A0A024QZY7 A0A024R2N2 A0A024R2Q0 A0A024R3C5 A0A024R3S2 A0A024R6T9 A0A024R9I2 A0A024RAP2 A0A024RCN9 A0A024RD15 A0A087WU84 A0A090N7W1
A0A0A0MRG0 A0A0A0MSK3 A0A0A0MT22 A0N0Q1 A1A4V4 A2A3U5 A2RUS0 A4D1Q0 A8K1F6 A8K249 A8K7N8 A8KAF4 A8KAG8 B0ZBE0 B2R7Y7 B4DN15 B7Z1L9
B8K2Q5 C1ID52 E5KQF5 F1D8N3 F5H1T4 G5E9C5 H6VQ59 K9J958 L7RSL3 L7RXH5 O00519 P00533 P00918 P02545 P05177 P05181 P06239 P06241 P07550
P08173 P08246 P08311 P08588 P08684 P08913 P11229 P11509 P11712 P14780 P17252 P18825 P21397 P21452 P21554 P21728 P21917 P22303 P25021
P23977 P25021 P25024 P25025 P25101 P25103 P25929 P28223 P28482 P30411 P32238 P32245 P33032 P35354 P35367 P35368 P37288 P41143 P41595
P41968 P49146 P50052 P50406 P51681 Q01959 Q08209 Q38Q88

CID 4409: nabumetone

A0A024QZY7 A0A024R1V0 A0A024R2N2 A0A024R2Q0 A0A024R3C5 A0A024R3S2 A0A024R6T9 A0A024R9I2 A0A024R9Y0 A0A024RAP2 A0A024RBV5 A0A024RD15
A0A068F658 A0A087WT22 A0A087WU84 A0A090N7W1 A0A0A0MRG0 A0A0A0MSK3 A0A0A0MT22 A0N0Q1 A1A4V4 A2A3U5 A2RUS0 A4D1Q0 A8K1F6 A8K249 A8K7N8
A8KAF4 A8KAG8 B0ZBE0 B2R7Y7 B2RXH2 B4DN15 B7Z1L9 B8K2Q5 C1ID52 E5KQF5 F1D8N3 F5H1T4 G5E9C5 H6VQ59 K9J958 L7RSL3 L7RXH5 O15118 P00533
P00918 P02545 P05177 P05181 P06239 P06241 P07550 P08173 P08246 P08311 P08588 P08684 P08913 P11229 P11509 P11712 P14780 P17252 P18825
P21397 P21452 P21554 P21728 P21917 P22303 P25021 P25024 P25025 P25101 P25103 P25929 P28223 P28482 P30411 P32238 P32245 P33032 P35354
P35367 P37288 P41143 P41595 P41968 P49146 P50052 P50406 P51681 P83916 Q01959 Q08209 Q38Q88 Q9UNA4

CID 4421: nalidixic acid

A0A024RCN9 A0A024RCW6 A0A024RDA5 A0A024RDJ4 A0A0A0MQX8 A8KAF4 B2RXH2 B7ZKN7 F1D8Q5 P02545 P35354 Q02880 Q99714 Q9UIF8

CID 4436: naphazoline

A0A024QZY7 A0A024R9Y0 A0A0A0MQX8 A2RUS0 B0ZBD3 C1ID52 P02545 P08913 P18825 P28482 Q5QD15 Q923Y7 Q96RJ0 Q9Y2I1

CID 4440: naratriptan

A8K5W4 P08908 P28221 P28222 P28566 P30939

CID 4449: nefazodone

A0A024QZY7 A0A024R3C5 A0A024R5I4 A0A024R5Z3 A0A024R6T9 A0A024R9Y0 A0A024RAU7 A0A090N8Z1 A4D1D2 A8K5W4 B0ZBD3 B2R7Y7 B3KP78 C1ID52
F1D8P8 K9J958 O75164 O75874 P02545 P05177 P08684 P08913 P11229 P11712 P23975 P28223 P28335 P31645 P35368 P43220 Q01959 Q13526 Q96QE3
Q99700 Q9UIF8

CID 4456: neostigmine

A0A024R2N2 A0A024R2Q0 A0A024R3C5 A0A024R3S2 A0A024R6T9 A0A024R909 A0A024R9I2 A0A024RAP2 A0A024RCN9 A0A024RD15 A0A087WU84 A0A090N7W1
A0A090N8Z1 A0A0A0MQX8 A0A0A0MRG0 A0A0A0MSK3 A0A0A0MT22 A0N0Q1 A1A4V4 A2A3U5 A2RUS0 A4D1D2 A4D1Q0 A8K1F6 A8K249 A8K7N8 A8KAF4 A8KAG8
B0ZBE0 B2R7Y7 B4DN15 B7Z1L9 B8K2Q5 C1ID52 D3DNN4 E5KQF5 F1D8N3 F5H1T4 G5E9C5 H6VQ59 K9J958 L7RSL3 L7RXH5 O00519 O15245 P00533 P00918
P02545 P05177 P05181 P06239 P06241 P07550 P08173 P08246 P08311 P08588 P08684 P08913 P11229 P11509 P11712 P14780 P17252 P18825 P21397
P21452 P21554 P21728 P21917 P22303 P25021 P25024 P25025 P25101 P25103 P25929 P28223 P28482 P30411 P32238 P32245 P33032 P35354 P35367
P37288 P41143 P41595 P41968 P49146 P50052 P50406 P51681 P83916 Q01959 Q08209 Q38Q88

CID 4463: nevirapine

A0A024QZY7 A0A024R2N2 A0A024R2Q0 A0A024R3C5 A0A024R3S2 A0A024R6T9 A0A024R9I2 A0A024RAP2 A0A024RD15 A0A087WU84 A0A090N7W1 A0A0A0MRG0
A0A0A0MSK3 A0A0A0MT22 A0N0Q1 A1A4V4 A2A3U5 A2RUS0 A4D1Q0 A8K1F6 A8K249 A8K7N8 A8KAF4 A8KAG8 B0ZBE0 B2R7Y7 B4DN15 B7Z1L9 B7Z1W5
B8K2Q5 C1ID52 D2KUA6 E5KQF5 F1D8N3 F5H1T4 G5E9C5 H6VQ59 K9J958 L7RSL3 L7RXH5 O15438 P00352 P00533 P00918 P02545 P05177 P05181 P06239
P06241 P07550 P08173 P08246 P08311 P08588 P08684 P08913 P11229 P11509 P11712 P14780 P17252 P18825 P20813 P21397 P21452 P21554 P21728
P21917 P22303 P25021 P25024 P25025 P25101 P25103 P25929 P27695 P28223 P28482 P30411 P32238 P32245 P33032 P33527 P35354 P35367 P37288
P41143 P41595 P41968 P49146 P50052 P50406 P51681 Q01959 Q08209 Q38Q88 Q92887

CID 4485: nifedipine

A0A024QZY7 A0A024R2N2 A0A024R2Q0 A0A024R3C5 A0A024R3S2 A0A024R5I4 A0A024R5Z3 A0A024R6L5 A0A024R6T9 A0A024R909 A0A024R9I2 A0A024R9Y0
A0A024RAP2 A0A024RAU7 A0A024RCN9 A0A024RCW6 A0A024RD15 A0A024RDJ4 A0A087WT22 A0A087WU84 A0A090N7W1 A0A0A0MQX8 A0A0A0MR67 A0A0A0MRG0
A0A0A0MSK3 A0A0A0MT22 A0A0A0MTJ0 A0N0Q1 A1A4V4 A2A3U5 A2RUS0 A4D1D2 A4D1Q0 A8K1F6 A8K249 A8K7N8 A8KAF4 A8KAG8 B0ZBE0 B1ALM3 B2R7Y7
B2RXH2 B3KP78 B3KQH9 B4DN15 B6ZGS9 B7Z1L9 B7ZKN7 B8K2Q5 C1ID52 D0VY79 D2KUA6 E5KQF5 E7ERK3 E7ETZ0 F1D8N3 F1D8N5 F1D8P6 F1D8P8 F1D8P9
F1D8Q5 F5H1T4 F8W6L1 G5E9C5 H6VQ59 K9J958 L7RSL3 L7RXH5 O15296 O60840 O75164 O75311 O75469 O75874 O94782 P00352 P00390 P00533 P00918
P01375 P02545 P05177 P05181 P06239 P06241 P07550 P08173 P08246 P08311 P08588 P08684 P08913 P11021 P11229 P11509 P11712 P14780 P15388
P15428 P16066 P16388 P17252 P18054 P18825 P20594 P21397 P21452 P21554 P21728 P21917 P22002 P22303 P22460 P23415 P25021 P25024 P25025
P25101 P25103 P25929 P28223 P28482 P30411 P32238 P32245 P33032 P35354 P35367 P37288 P41143 P41595 P41968 P42345 P48167 P49146 P50052
P50406 P51681 P63142 P83916 Q01453 Q01668 Q01959 Q02485 Q03164 Q06432 Q08209 Q08289 Q09470 Q13698 Q13936 Q16236 Q17ST2 Q38Q88 Q96QE3
Q99549 Q99700 Q99714 Q9BRL5 Q9HCF6 Q9UIF8 Q9UNA4

CID 4493: nilutamide

A0A024RBV5 A0A024RCN9 A0A024RDJ4 A0A087WT22 A0A090N8Z1 A0A0A0MQX8 A0A0A0MTJ0 B0ZBD3 C1ID52 F1D8N5 F1D8N7 P02545 P05177 P08684 P10275
P11712 P16435 P18054 P35354 P83916 Q96QE3 Q99549

CID 4497: nimodipine

A0A024QZY7 A0A024R2N2 A0A024R2Q0 A0A024R3C5 A0A024R3S2 A0A024R6T9 A0A024R909 A0A024R9I2 A0A024R9Z8 A0A024RAP2 A0A024RCN9 A0A024RD15
A0A024RDJ4 A0A087WU84 A0A090N7W1 A0A090N8Z1 A0A0A0MR67 A0A0A0MRG0 A0A0A0MSK3 A0A0A0MT22 A0A0A0MTJ0 A0N0Q1 A1A4V4 A2A3U5 A2RUS0
A4D1Q0 A8K1F6 A8K249 A8K7N8 A8KAF4 A8KAG8 B0ZBE0 B0ZBF6 B1ALM3 B2R7Y7 B4DN15 B6ZGS9 B7Z1L9 B7ZKN7 B8K2Q5 C1ID52 E5KQF5 E7DBM8 F1D8N3
F1D8P8 F1D8P9 F5H1T4 F8W6L1 G5E9C5 H6VQ59 K9J958 L7RSL3 L7RXH5 O60840 O94782 P00533 P00918 P02545 P05177 P05181 P06239 P06241 P07550
P08173 P08235 P08246 P08311 P08588 P08684 P08913 P11229 P11509 P11712 P13569 P14780 P17252 P18825 P21397 P21452 P21554 P21728 P21917
P22002 P22303 P25021 P25024 P25025 P25101 P25103 P25929 P27695 P27732 P28223 P28482 P30411 P32238 P32245 P33032 P35354 P35367 P37288
P41143 P41595 P41968 P49146 P50052 P50406 P51681 P54284 P83916 Q01453 Q01668 Q01959 Q02641 Q06432 Q08209 Q08289 Q38Q88 Q96QE3 Q99549
Q99700 Q9UNA4

CID 4499: nisoldipine

A0A087WW63 A0A0A0MR67 A4D1D2 B1ALM3 E7ERK3 P08684 Q01668 Q01815 Q08289 Q13936 Q99246

CID 4506: nitrazepam
A0A024QZY7 A0A024R2N2 A0A024R2Q0 A0A024R3C5 A0A024R3S2 A0A024R6T9 A0A024R9I2 A0A024R9X6 A0A024RAP2 A0A024RD15 A0A087WU84 A0A090N7W1 A0A0A0MRG0 A0A0A0MSK3 A0A0A0MT22 A0N0Q1 A1A4V4 A2A3U5 A2RUS0 A4D1D2 A4D1Q0 A8K177 A8K1F6 A8K249 A8K496 A8K7N8 A8KAF4 A8KAG8 A8MPY1 B0ZBE0 B2R7Y7 B2RCW8 B4DN15 B4DTP4 B7Z1F5 B7Z1L9 B7Z3P6 B8K2Q5 C1ID52 E5KQF5 F1D8N3 F5H1T4 G5E9C5 H6VQ59 K9J958 L7RSL3 L7RXH5 P00533 P00918 P02545 P04083 P05177 P05181 P06239 P06241 P07550 P08173 P08185 P08246 P08311 P08588 P08684 P08913 P11229 P11509 P11712 P14780 P14867 P15428 P17252 P18505 P18507 P18825 P20813 P21397 P21452 P21554 P21728 P21917 P22303 P24046 P25021 P25024 P25025 P25101 P25103 P25929 P28223 P28476 P28482 P30411 P31644 P32238 P32239 P32245 P33032 P34903 P35354 P35498 P37288 P41143 P41595 P41968 P47870 P48169 P49146 P50052 P50406 P51681 P78334 P83916 Q01959 Q08209 Q16445 Q38Q88 Q8N1C3 Q92830 Q99928 Q9UN88 Q9UNA4
CID 4510: nitroglycerin
P00533 P05091 P16066 Q02108 Q02153
CID 4539: norfloxacin
A0A024R2N2 A0A024R2Q0 A0A024R3C5 A0A024R3S2 A0A024R6T9 A0A024R9I2 A0A024RAP2 A0A024RCN9 A0A024RD15 A0A087WU84 A0A090N7W1 A0A090N8Z1 A0A0A0MRG0 A0A0A0MSK3 A0A0A0MT22 A0A0A0MTJ0 A0N0Q1 A1A4V4 A2A3U5 A2RUS0 A4D1Q0 A8K1F6 A8K249 A8K7N8 A8KAF4 A8KAG8 B0ZBE0 B2R7Y7 B2RXH2 B4DN15 B7Z1L9 B8K2Q5 C1ID52 E5KQF5 F1D8N3 F5H1T4 G5E9C5 H6VQ59 K9J958 L7RSL3 L7RXH5 O76082 O94782 P00352 P00533 P00918 P02545 P05177 P05181 P06239 P06241 P07550 P08173 P08246 P08311 P08588 P08684 P08913 P11229 P11712 P14780 P15428 P17252 P18825 P21397 P21452 P21554 P21728 P21917 P22303 P25021 P25024 P25025 P25101 P25103 P25929 P28223 P28482 P30411 P32238 P32245 P33032 P35354 P35367 P37288 P41143 P41595 P41968 P42858 P49146 P50052 P50406 P51681 Q01959 Q02880 Q08209 Q38Q88 Q92830 Q99714
CID 4543: nortriptyline
A0A024QZY7 A0A024R2N2 A0A024R2Q0 A0A024R3C5 A0A024R3S2 A0A024R5Z3 A0A024R6T9 A0A024R9I2 A0A024R9Y0 A0A024RAP2 A0A024RBV5 A0A024RCN9 A0A024RD15 A0A087WT22 A0A087WU84 A0A090N7W1 A0A090N8Z1 A0A0A0MRG0 A0A0A0MSK3 A0A0A0MT22 A0A0A0MTJ0 A0N0Q1 A1A4V4 A2A3U5 A2RUS0 A4D1Q0 A8K1F6 A8K249 A8K5W4 A8K7N8 A8KAF4 A8KAG8 B0ZBD3 B0ZBE0 B2R7Y7 B4DN15 B7Z1F5 B7Z1L9 B8K2Q5 C1ID52 E5KQF5 F1D8N3 F1D8P8 F5H1T4 F8W6L1 G5E9C5 H6VQ59 K9J958 L7RSL3 L7RXH5 O15118 O15296 O75874 P00533 P00918 P02545 P02768 P05177 P05181 P06239 P06241 P07550 P08173 P08246 P08311 P08588 P08684 P08913 P11021 P11229 P11509 P11712 P14780 P17252 P18825 P21397 P21452 P21554 P21728 P21917 P22303 P22310 P23975 P25021 P25024 P25025 P25101 P25103 P25929 P28223 P28482 P30411 P31645 P32238 P32245 P33032 P35354 P35367 P37288 P39748 P41143 P41595 P41968 P42345 P42858 P43220 P48542 P48545 P49146 P50052 P50406 P51681 P78508 Q01453 Q01959 Q08209 Q38Q88 Q96QE3 Q99549 Q99700
CID 4583: ofloxacin
A0A024QZY7 A0A024R2N2 A0A024R2Q0 A0A024R3C5 A0A024R3S2 A0A024R5B6 A0A024R5I4 A0A024R6T9 A0A024R9I2 A0A024RAP2 A0A024RAT5 A0A024RAU7 A0A024RCN9 A0A024RD15 A0A087WU84 A0A090N7W1 A0A0A0MRG0 A0A0A0MSK3 A0A0A0MT22 A0N0Q1 A1A4V4 A2A3U5 A2RUS0 A4D1D2 A4D1Q0 A8K1F6 A8K249 A8K7N8 A8KAF4 A8KAG8 B0ZBE0 B2R7Y7 B2RXH2 B3KP78 B4DN15 B7Z1L9 B8K2Q5 C1ID52 E5KQF5 F1D8N3 F5H1T4 G5E9C5 H6VQ59 K9J958 L7RSL3 L7RXH5 O15244 O15245 O75761 O94782 O95264 P00533 P00918 P05177 P05181 P06239 P06241 P07550 P08173 P08246 P08311 P08588 P08684 P08913 P11229 P11509 P11712 P14780 P17252 P18825 P21397 P21452 P21554 P21728 P21917 P22303 P25021 P25024 P25025 P25101 P25103 P25929 P28222 P28223 P28482 P30411 P32238 P32245 P33032 P35354 P35367 P37288 P41143 P41595 P41968 P43220 P46098 P49146 P50052 P50406 P51681 Q01959 Q08209 Q13639 Q38Q88 Q86VL8 Q96FL8 Q9GZV3 Q9UIF8 Q9UNA4
CID 4595: ondansetron
A0A024QZY7 A0A024R2N2 A0A024R2Q0 A0A024R3C5 A0A024R3S2 A0A024R5I4 A0A024R6T9 A0A024R9I2 A0A024RAP2 A0A024RAU7 A0A024RD15 A0A087WU84 A0A090N7W1 A0A0A0MRG0 A0A0A0MSK3 A0A0A0MT22 A0N0Q1 A1A4V4 A2A3U5 A2RUS0 A4D1Q0 A8K1F6 A8K249 A8K5W4 A8K7N8 A8KAF4 A8KAG8 B0ZBE0 B2R7Y7 B3KP78 B4DN15 B4DN83 B4E398 B7Z1L9 B8K2Q5 C1ID52 E5KQF5 F1D8N3 F5H1T4 G5E9C5 H6VQ59 K9J958 L7RSL3 L7RXH5 O15244 O15245 O75751 O94782 O95264 P00533 P00918 P05177 P05181 P06239 P06241 P07550 P08173 P08246 P08311 P08588 P08684 P08913 P11229 P11509 P11712 P14780 P17252 P18825 P21397 P21452 P21554 P21728 P21917 P22303 P25021 P25024 P25025 P25101 P25103 P25929 P28222 P28223 P28482 P30411 P32238 P32245 P33032 P35354 P35367 P37288 P41143 P41595 P41968 P43220 P46098 P49146 P50052 P50406 P51681 Q01959 Q08209 Q13639 Q38Q88 Q86VL8 Q96FL8 Q9GZV3 Q9UIF8 Q9UNA4
CID 4601: orphenadrine
A0A024QZY7 A0A024R2N2 A0A024R2Q0 A0A024R3C5 A0A024R3S2 A0A024R5Z3 A0A024R6T9 A0A024R9I2 A0A024RAP2 A0A024RCN9 A0A024RD15 A0A087WU84 A0A090N7W1 A0A090N8Z1 A0A0A0MRG0 A0A0A0MSK3 A0A0A0MT22 A0N0Q1 A1A4V4 A2A3U5 A2RUS0 A4D1Q0 A8K1F6 A8K249 A8K7N8 A8KAF4 A8KAG8 B0ZBE0 B2R7Y7 B4DN15 B7Z1L9 B7ZKN7 B8K2Q5 C1ID52 E5KQF5 F1D8N3 F1D8N7 F5H1T4 G5E9C5 H6VQ59 K9J958 L7RSL3 L7RXH5 O15244 O15245 O15399 O60391 O94782 P00533 P00918 P02545 P05177 P05181 P06239 P06241 P07550 P08173 P08246 P08311 P08588 P08684 P08913 P11229 P11509 P11712 P14780 P17252 P18825 P20813 P21397 P21452 P21554 P21728 P21917 P22303 P25021 P25024 P25025 P25101 P25103 P25929 P27695 P28223 P28482 P30411 P32238 P32245 P33032 P35354 P35367 P37288 P41143 P41595 P41968 P49146 P50052 P50406 P51681 Q01453 Q01959 Q05586 Q08209 Q38Q88 Q86VL8 Q8TCU5 Q96FL8 Q99700 Q9Y5Y9
CID 4614: oxaprozin
A0A024QZY7 A0A024R2N2 A0A024R2Q0 A0A024R3C5 A0A024R3S2 A0A024R6T9 A0A024R9I2 A0A024RAP2 A0A024RCN9 A0A024RD15 A0A087WU84 A0A090N7W1 A0A0A0MRG0 A0A0A0MSK3 A0A0A0MT22 A0A0A0MTJ0 A0N0Q1 A1A4V4 A2A3U5 A2RUS0 A4D1Q0 A8K1F6 A8K249 A8K7N8 A8KAF4 A8KAG8 B0ZBE0 B2R7Y7 B2RXH2 B4DN15 B7Z1L9 B8K2Q5 C1ID52 E5KQF5 F1D8N3 F1D8P8 F5H1T4 G5E9C5 H6UYS5 H6VQ59 K9J958 L7RSL3 L7RXH5 O94782 P00533 P00918 P02545 P05177 P05181 P06239 P06241 P07550 P08173 P08246 P08311 P08588 P08684 P08913 P11229 P11509 P11712 P14780 P15428 P17252 P18825 P21397 P21452 P21554 P21728 P21917 P22303 P23219 P25021 P25024 P25025 P25101 P25103 P25929 P28223 P28482 P30411 P32238 P32245 P33032 P35354 P35367 P37288 P41143 P41595 P41968 P49146 P50052 P50406 P51681 Q01453 Q01959 Q08209 Q16236 Q38Q88 Q99549
CID 4616: oxazepam
A0A024R9X6 A8K177 A8K496 A8MPY1 B2RCW8 B4DTP4 B7ZW53 O60656 P02545 P02768 P06133 P16662 P18505 P18507 P19224 P22309 P24046 P28476 P31644 P34903 P36537 P47870 P48169 P78334 Q16445 Q8N1C3 Q92887 Q99928 Q9UN88
CID 4634: oxybutynin
A0A024QZY7 A0A024R2N2 A0A024R2Q0 A0A024R3C5 A0A024R3S2 A0A024R5Z9 A0A024R6T9 A0A024R9I2 A0A024RAP2 A0A024RAV2 A0A024RCN9 A0A024RD15 A0A024RDJ4 A0A087WU84 A0A090N7W1 A0A090N8Z1 A0A0A0MRG0 A0A0A0MSK3 A0A0A0MT22 A0N0Q1 A1A4V4 A2A3U5 A2RUS0 A4D1Q0 A8K1F6 A8K249 A8K7N8 A8KAF4 A8KAG8 B0ZBE0 B2R7Y7 B4DN15 B7Z1L9 B8K2Q5 C1ID52 E5KQF5 F1D8N3 F5H1T4 F8W6L1 G5E9C5 H6VQ59 K9J958 L7RSL3 L7RXH5 O15245 O15296 O75874 P00533 P00918 P05177 P05181 P06239 P06241 P07550 P08172 P08173 P08246 P08311 P08588 P08684 P08913 P11229 P11509 P11712 P14780 P17252 P17405 P18825 P20309 P21397 P21452 P21554 P21728 P21917 P22303 P25021 P25024 P25025 P25101 P25103 P25929 P27695 P28223 P28482 P30411 P32238 P32245 P33032 P35354 P35367 P37288 P39748 P41143 P41595 P41968 P43220 P49146 P50052 P50406 P51681 Q01453 Q01959 Q08209 Q38Q88 Q99700 Q9UNA4
CID 4649: para-aminosalicylic acid
A0A024R2N2 A0A024R2Q0 A0A024R3C5 A0A024R3S2 A0A024R5Z3 A0A024R6L5 A0A024R6R4 A0A024R6T9 A0A024R9I2 A0A024R9Y0 A0A024RAP2 A0A024RCN9 A0A024RD15 A0A087WU84 A0A090N7W1 A0A0A0MQX8 A0A0A0MRG0 A0A0A0MSK3 A0A0A0MT22 A0N0Q1 A1A4V4 A2A3U5 A2RUS0 A4D1Q0 A8K1F6 A8K249 A8K7N8 A8KAF4 A8KAG8 B0ZBE0 B2R7Y7 B2RXH2 B4DN15 B7Z1L9 B7Z1W5 B8K2Q5 C1ID52 E5KQF5 F1D8N3 F5H1T4 G5E9C5 H6VQ59 K9J958 L7RSL3 L7RXH5 O15111 O60656 O94925 O95467 P00352 P00533 P00915 P00918 P05177 P05181 P06239 P06241 P07550 P08173 P08246 P08254 P08311 P08588 P08684 P08913 P09917 P10253 P11229 P11509 P11712 P14780 P17252 P18825 P21397 P21452 P21554 P21728 P21917 P22303 P22894 P25021 P25024 P25025 P25101 P25103 P25929 P27695 P28223 P28482 P30411 P32238 P32245 P33032 P35354 P35367 P37288 P41143 P41595 P41968 P49146 P50052 P50406 P51681 P83916 Q01959 Q08209 Q38Q88 Q9NZK7
CID 4678: panthenol
A0A024QZY7 A0A024R2N2 A0A024R2Q0 A0A024R3C5 A0A024R3S2 A0A024R6T9 A0A024R9I2 A0A024RAP2 A0A024RD15 A0A087WU84 A0A090N7W1 A0A0A0MRG0 A0A0A0MSK3 A0A0A0MT22 A0N0Q1 A1A4V4 A2A3U5 A2RUS0 A4D1Q0 A8K1F6 A8K249 A8K7N8 A8KAF4 A8KAG8 B0ZBE0 B2R7Y7 B4DN15 B7Z1L9 B8K2Q5 C1ID52 E5KQF5 F1D8N3 F5H1T4 G5E9C5 H6VQ59 K9J958 L7RSL3 L7RXH5 O75874 P00533 P00918 P05177 P05181 P06239 P06241 P07550 P08173 P08246 P08311 P08588 P08684 P08913 P11229 P11509 P11712 P14780 P17252 P18825 P21397 P21452 P21554 P21728 P21917 P22303 P25021 P25024 P25025 P25101 P25103 P25929 P28223 P28482 P30411 P32238 P32245 P33032 P35354 P35367 P37288 P41143 P41595 P41968 P49146 P50052 P50406 P51681 Q01959 Q08209 Q38Q88
CID 4679: pantoprazole
A0A024R2N2 A0A024R2Q0 A0A024R3C5 A0A024R3S2 A0A024R5I4 A0A024R6T9 A0A024R9I2 A0A024R9Y0 A0A024RAP2 A0A024RAU7 A0A024RD15 A0A024RDD4 A0A087WU84 A0A090N7W1 A0A0A0MRG0 A0A0A0MSK3 A0A0A0MT22 A0N0Q1 A1A4V4 A2A3U5 A2RUS0 A4D1D2 A4D1Q0 A8K1F6 A8K249 A8K7N8 A8KAF4 A8KAG8 B0ZBE0 B2R7Y7 B2RXH2 B3KP78 B4DN15 B4E0R9 B7Z1L9 B8K2Q5 C1ID52 E5KQF5 F1D8N3 F1D8P8 F5H1T4 G5E9C5 H6VQ59 K9J958 L7RSL3 L7RXH5 O15244 O15245 O75751 P00352 P00533 P00918 P02545 P05023 P05177 P05181 P06239 P06241 P07550 P08173 P08246 P08311 P08588 P08684 P08913 P11229 P11509 P11712 P14780 P15428 P16050 P17252 P18825 P20648 P21397 P21452 P21554 P21728 P21917 P22303 P25021 P25024 P25025 P25101 P25103 P25929 P27695 P28223 P28482 P30411 P32238 P32245 P33032 P35354 P35367 P37288 P41143 P41595 P41968 P49146 P50052 P50406 P51681 Q01959 Q08209 Q38Q88 Q86VL8 Q92830 Q96FL8
CID 4680: papaverine
A0A024QZY7 A0A024R2N2 A0A024R2Q0 A0A024R3C5 A0A024R3S2 A0A024R6T9 A0A024R909 A0A024R9I2 A0A024R9Y0 A0A024RAP2 A0A024RAP4 A0A024RBV5 A0A024RCN9 A0A024RD15 A0A024RD62 A0A024RDJ4 A0A087WU84 A0A090N7W1 A0A090N8Z1 A0A0A0MQX8 A0A0A0MRG0 A0A0A0MSK3 A0A0A0MT22 A0A0A0MTJ0 A0N0Q1 A1A4V4 A2A3U5 A2RUS0 A4D1Q0 A7E2E5 A8K1F6 A8K249 A8K7N8 A8KAF4 A8KAG8 B0ZBE0 B2R7Y7 B2RXH2 B4DN15 B7Z1L9 B7ZKN7 B8K2Q5 C1ID52 D0VY79 E5KQF5 F1D8N3 F5H1T4 F8W6L1 G5E9C5 H6VQ59 K9J958 L7RSL3 L7RXH5 O15245 O75604 O75874 O76074 O94782 P00352 P00533 P00918 P02545 P05177 P05181 P06239 P06241 P06280 P07550 P08173 P08246 P08311 P08588 P08684 P08913 P11229 P11509 P11712 P14780 P15428 P16050 P17252 P17405 P18054 P18825 P21397 P21452 P21554 P21728 P21917 P22303 P25021 P25024 P25025 P25101 P25103 P25929 P27695 P28223 P28482 P30411 P32238 P32245 P33032 P35354 P35367 P37288 P41143 P41595 P41968 P43220 P47989 P49146 P50052 P50406 P51681 P83916 Q01453 Q01959 Q07343 Q08209 Q14432 Q38Q88 Q96QE3 Q99549 Q9UIF8 Q9UM07 Q9UNA4 Q9Y233

CID 4723: pemoline
A0A024R2N2 A0A024R2Q0 A0A024R3C5 A0A024R3S2 A0A024R6T9 A0A024R9I2 A0A024RAP2 A0A024RBV5 A0A024RD15 A0A087WU84 A0A090N7W1 A0A0A0MRG0 A0A0A0MSK3 A0A0A0MT22 A0N0Q1 A1A4V4 A2A3U5 A2RUS0 A4D1Q0 A8K1F6 A8K249 A8K7N8 A8KAF4 A8KAG8 B0ZBE0 B2R7Y7 B4DN15 B7Z1L9 B8K2Q5 C1ID52 E5KQF5 F1D8N3 F5H1T4 G5E9C5 H6VQ59 K9J958 L7RSL3 L7RXH5 P00533 P00918 P05177 P05181 P06239 P06241 P07550 P08173 P08246 P08311 P08588 P08684 P08913 P11229 P11509 P11712 P14780 P17252 P18825 P21397 P21452 P21554 P21728 P21917 P22303 P25021 P25024 P25025 P25101 P25103 P25929 P28223 P28482 P30411 P32238 P32245 P33032 P35354 P35367 P37288 P41143 P41595 P41968 P49146 P50052 P50406 P51681 Q01959 Q08209 Q38Q88
CID 4725: penciclovir
A0A024R2N2 A0A024R2Q0 A0A024R3C5 A0A024R3S2 A0A024R6T9 A0A024R9I2 A0A024RAP2 A0A024RD15 A0A087WU84 A0A090N7W1 A0A0A0MRG0 A0A0A0MSK3 A0A0A0MT22 A0N0Q1 A1A4V4 A2A3U5 A2RUS0 A4D1Q0 A8K1F6 A8K249 A8K7N8 A8KAF4 A8KAG8 B0ZBE0 B2R7Y7 B4DN15 B7Z1L9 B8K2Q5 C1ID52 E5KQF5 F1D8N3 F5H1T4 G5E9C5 H6VQ59 K9J958 L7RSL3 L7RXH5 P00533 P00918 P05177 P05181 P06239 P06241 P07550 P08173 P08246 P08311 P08588 P08684 P08913 P11229 P11509 P11712 P14780 P17252 P18825 P21397 P21452 P21554 P21728 P21917 P22303 P25021 P25024 P25025 P25101 P25103 P25929 P28223 P28482 P30411 P32238 P32245 P33032 P35354 P35367 P37288 P41143 P41595 P41968 P49146 P50052 P50406 P51681 Q01959 Q06278 Q08209 Q38Q88
CID 4737: pentobarbital
A0A024R9X6 A0A090N7W1 A0A0A6YYA8 A8K177 B2RCW8 B2RXH2 B4DK78 P00352 P08684 P14867 P31644 P34903 P42262 P48169 Q16445
CID 4740: pentoxifylline
A0A024R2N2 A0A024R2Q0 A0A024R3C5 A0A024R3S2 A0A024R6T9 A0A024R909 A0A024R9I2 A0A024RAP2 A0A024RCN9 A0A024RD15 A0A024RDJ4 A0A087WU84 A0A087WWV0 A0A090N7W1 A0A0A0MRG0 A0A0A0MSK3 A0A0A0MT22 A0A0A0MTJ0 A0N0Q1 A1A4V4 A2A3U5 A2RUS0 A4D1Q0 A8K1F6 A8K249 A8K7N8 A8KAF4 A8KAG8 B0ZBE0 B2R7Y7 B4DN15 B7Z1L9 B8K2Q5 C1ID52 D3DNN4 E5KQF5 F1D8N3 F5H1T4 G5E9C5 H6VQ59 K9J958 L7RSL3 L7RXH5 O75604 P00533 P00918 P01375 P02545 P05177 P05181 P06239 P06241 P07550 P08173 P08246 P08311 P08588 P08684 P08913 P11229 P11509 P11712 P14780 P17252 P18089 P18825 P21397 P21452 P21554 P21589 P21728 P21917 P22303 P25021 P25024 P25025 P25101 P25103 P25929 P27815 P28223 P28482 P30411 P32238 P32245 P33032 P35354 P35367 P37288 P41143 P41595 P41968 P47901 P49146 P50052 P50406 P51681 Q01453 Q01959 Q07343 Q08209 Q38Q88 Q92830 Q96QE3 Q9UNA4
CID 4748: perphenazine
A0A024QZY7 A0A024R2N2 A0A024R2Q0 A0A024R3C5 A0A024R3S2 A0A024R5Z3 A0A024R6L5 A0A024R6T9 A0A024R909 A0A024R9I2 A0A024R9Y0 A0A024RAP2 A0A024RAV2 A0A024RBV5 A0A024RCN9 A0A024RD15 A0A024RDJ4 A0A068F658 A0A087WT22 A0A087WU84 A0A090N7W1 A0A090N8Z1 A0A0A0MRG0 A0A0A0MSK3 A0A0A0MT22 A0A0A0MTJ0 A0N0Q1 A1A4V4 A2A3U5 A2RUS0 A4D1Q0 A6NGA6 A8K1F6 A8K249 A8K5W4 A8K7N8 A8KAF4 A8KAG8 B0ZBD3 B0ZBE0 B2R7Y7 B4DN15 B4DN83 B7Z1L9 B7Z2G8 B8K2Q5 C1ID52 E5KQF5 E7ETZ0 F1D8N3 F1D8P8 F5H1T4 F8W6L1 G5E9C5 H6VQ59 K9J958 L7RSL3 L7RXH5 O15118 O15296 O75164 O75604 O75874 P00533 P00918 P02545 P05177 P05181 P06239 P06241 P07550 P08173 P08246 P08311 P08588 P08684 P08913 P11021 P11229 P11509 P11712 P14416 P14780 P17252 P18825 P21397 P21452 P21554 P21728 P21917 P22303 P25021 P25024 P25025 P25101 P25103 P25929 P27695 P28223 P28335 P28482 P30411 P30939 P31388 P32238 P32245 P32305 P33032 P34969 P35354 P35367 P37288 P41143 P41595 P41968 P42345 P43220 P49146 P50052 P50406 P51681 P61088 P83916 Q01453 Q01959 Q06278 Q08209 Q38Q88 Q8NER1 Q99549 Q99700 Q9BRL5 Q9UIF8
CID 4763: phenobarbital
A0A024QZY7 A0A024R2N2 A0A024R2Q0 A0A024R3C5 A0A024R3S2 A0A024R5I4 A0A024R6T9 A0A024R9I2 A0A024R9X6 A0A024RAP2 A0A024RAU7 A0A024RD15 A0A087WU84 A0A090N7W1 A0A0A0MRG0 A0A0A0MSK3 A0A0A0MT22 A0A0A6YYA8 A0N0Q1 A1A4V4 A2A3U5 A2RUS0 A4D1D2 A4D1Q0 A8K177 A8K1F6 A8K249 A8K7N8 A8KAF4 A8KAG8 B0ZBE0 B2R7Y7 B3KP78 B4DK78 B4DN15 B7Z1F5 B7Z1L9 B8K2Q5 C1ID52 E5KQF5 F1D8N3 F1D8P9 F1DAL4 F5H1T4 G5E9C5 H6VQ59 K9J958 L7RSL3 L7RXH5 O15245 O75469 O76068 P00533 P00918 P05177 P05181 P06239 P06241 P07550 P08173 P08246 P08311 P08588 P08684 P08913 P11229 P11509 P11712 P14780 P17252 P18825 P20813 P21397 P21452 P21554 P21728 P21917 P22303 P22309 P25021 P25024 P25025 P25101 P25103 P25929 P28223 P28482 P30411 P31644 P32238 P32245 P33032 P33527 P34903 P35354 P35367 P37288 P41143 P41595 P41968 P42262 P48169 P49146 P50052 P50406 P51681 Q01959 Q08209 Q16445 Q38Q88 Q92887
CID 4768: phenoxybenzamine
A0A024QZY7 A0A024R6L5 A0A024RAP4 A0A024RCN9 A0A024RCW6 A0A024RDA5 A0A024RDJ4 A0A068F658 A0A087WT22 A0A090N7W1 A0A090N8Z1 A0A0A0MTJ0 A2RUS0 A8KAF4 B0ZBD3 B2RXH2 B6ZGS9 C1ID52 D0VY79 D2KUA6 E5KQF5 E7ETZ0 F1D8N5 F1D8N7 F1D8P6 F1D8P8 O15244 O15245 O75751 O94782 P00352 P02545 P05177 P06280 P07550 P08684 P08913 P11021 P11712 P16050 P18089 P18825 P27695 P39748 P83916 Q92830 Q99549 Q9BRL5
CID 4771: phentermine
A0A024R6T9 B2R7Y7 B7Z242 C1ID52 P05177 P08684 P11712 P21397 Q01959 Q96RJ0
CID 4828: pindolol
A0A024R2N2 A0A024R2Q0 A0A024R3C5 A0A024R3S2 A0A024R5I4 A0A024R6T9 A0A024R909 A0A024R9I2 A0A024RAP2 A0A024RAU7 A0A024RCN9 A0A024RD15 A0A024RDJ4 A0A087WT22 A0A087WU84 A0A090N7W1 A0A0A0MRG0 A0A0A0MSK3 A0A0A0MT22 A0A0A0MTJ0 A0N0Q1 A1A4V4 A2A3U5 A2RUS0 A4D1Q0 A8K1F6 A8K249 A8K5W4 A8K7N8 A8KAF4 A8KAG8 B0ZBD3 B0ZBE0 B2R7Y7 B2RXH2 B3KP78 B4DN15 B4E398 B7Z1L9 B7ZKN7 B8K2Q5 C1ID52 E5KQF5 F1D8N3 F1D8N7 F1D8P8 F5H1T4 G5E9C5 H6VQ59 K9J958 L7RSL3 L7RXH5 O15244 O15245 O75604 P00352 P00533 P00918 P02545 P02768 P05177 P05181 P06239 P06241 P06280 P07550 P08173 P08246 P08311 P08588 P08684 P08908 P08913 P11229 P11509 P11712 P14780 P16050 P16066 P17252 P18825 P20594 P21397 P21452 P21554 P21728 P21917 P22303 P25021 P25024 P25025 P25101 P25103 P25929 P28222 P28223 P28482 P30411 P32238 P32245 P33032 P35354 P35367 P35368 P37288 P39748 P41143 P41595 P41968 P49146 P50052 P50406 P51681 P83916 Q01959 Q08209 Q38Q88 Q99549
CID 4829: pioglitazone
A0A024QZY7 A0A024R2N2 A0A024R2Q0 A0A024R3C5 A0A024R3S2 A0A024R5I4 A0A024R6T9 A0A024R9I2 A0A024RAP2 A0A024RAU7 A0A024RCW6 A0A024RD15 A0A087WU84 A0A090N7W1 A0A0A0MRG0 A0A0A0MSK3 A0A0A0MT22 A0N0Q1 A1A4V4 A2A3U5 A2RUS0 A4D1Q0 A8K1F6 A8K249 A8K7N8 A8KAF4 A8KAG8 B0ZBE0 B2R7Y7 B3KP78 B4DN15 B7Z1F5 B7Z1L9 B7Z242 B8K2Q5 C1ID52 D2KUA6 E5KQF5 F1D8N3 F1D8S4 F5H1T4 G5E9C5 H6VQ59 K9J958 L7RSL3 L7RXH5 O60341 P00352 P00533 P00918 P05177 P05181 P06239 P06241 P07550 P08173 P08246 P08311 P08588 P08684 P08913 P11229 P11509 P11712 P14780 P17252 P18825 P21397 P21452 P21554 P21728 P21917 P22303 P25021 P25024 P25025 P25101 P25103 P25929 P28223 P28482 P30411 P32238 P32245 P33032 P35354 P35367 P37231 P37288 P41143 P41595 P41968 P49146 P50052 P50406 P51681 Q01959 Q07869 Q08209 Q38Q88 Q9HCF6
CID 4891: praziquantel
A0A024R2N2 A0A024R2Q0 A0A024R3C5 A0A024R3S2 A0A024R6T9 A0A024R909 A0A024R9I2 A0A024RAP2 A0A024RD15 A0A087WT22 A0A087WU84 A0A090N7W1 A0A090N8Z1 A0A0A0MQX8 A0A0A0MRG0 A0A0A0MSK3 A0A0A0MT22 A0A0A0MTJ0 A0N0Q1 A1A4V4 A2A3U5 A2RUS0 A4D1Q0 A8K1F6 A8K249 A8K7N8 A8K987 A8KAF4 A8KAG8 B0ZBE0 B2R7Y7 B4DN15 B7Z1L9 B7ZKN7 B8K2Q5 C1ID52 E5KQF5 F1D8N3 F5H1T4 G5E9C5 H6VQ59 K9J958 L7RSL3 L7RXH5 O94782 P00352 P00533 P00918 P02545 P05177 P05181 P06239 P06241 P07550 P08173 P08246 P08311 P08588 P08684 P08913 P11229 P11509 P11712 P14780 P17252 P18825 P21397 P21452 P21554 P21728 P21917 P22303 P25021 P25024 P25025 P25100 P25101 P25103 P25929 P28223 P28482 P30411 P32238 P32245 P33032 P34969 P35348 P35354 P35367 P35368 P37288 P39748 P41143 P41595 P41968 P42345 P43140 P49146 P50052 P50406 P51681 Q01453 Q01959 Q08209 Q38Q88 Q86VL8 Q8IUX4 Q92887 Q96FL8 Q96QE3 Q99700 Q99714 Q9NS40 Q9UIF8 Q9UNA4
CID 4893: prazosin
A0A024QZY7 A0A024R2N2 A0A024R2Q0 A0A024R3C5 A0A024R3S2 A0A024R4E2 A0A024R5I4 A0A024R6T9 A0A024R9I2 A0A024R9Y0 A0A024RAP2 A0A024RAP4 A0A024RAU7 A0A024RBV5 A0A024RCN9 A0A024RD15 A0A024RDD4 A0A068F658 A0A087WT22 A0A087WU84 A0A090N7W1 A0A0A0MRG0 A0A0A0MSK3 A0A0A0MT22 A0N0Q1 A1A4V4 A2A3U5 A2RUS0 A4D1D2 A4D1Q0 A8K1F6 A8K249 A8K5W4 A8K7N8 A8K996 A8KAF4 A8KAG8 B0ZBD3 B0ZBE0 B2R7Y7 B2RXH2 B3KP78 B4DKC0 B4DN15 B4E398 B7Z1L9 B7ZKN7 B8K2Q5 C1ID52 D0VY79 E5KQF5 F1D8N3 F5H1T4 G5E9C5 H6VQ59 K9J958 L7RSL3 L7RXH5 O15118 O15244 O15245 O15296 O75751 O75874 O94782 P00352 P00533 P00918 P02545 P05177 P05181 P06239 P06241 P06280 P07550 P08173 P08246 P08311 P08588 P08684 P08913 P10253 P11229 P11509 P11712 P14780 P15428 P17252 P17405 P18089 P18825 P21397 P21452 P21554 P21728 P21917 P22303 P25021 P25024 P25025 P25100 P25101 P25103 P25929 P28223 P28482 P30411 P32238 P32245 P33032 P34969 P35348 P35354 P35367 P35368 P37288 P39748 P41143 P41595 P41968 P42345 P43140 P49146 P50052 P50406 P51681 Q01453 Q01959 Q08209 Q38Q88 Q86VL8 Q8IUX4 Q92887 Q96FL8 Q96QE3 Q99700 Q99714 Q9NS40 Q9UIF8 Q9UNA4
CID 4906: prilocaine
A0A024R2N2 A0A024R2Q0 A0A024R3C5 A0A024R3S2 A0A024R6T9 A0A024R9I2 A0A024R9Y0 A0A024RAP2 A0A024RCN9 A0A024RD15 A0A087WU84 A0A090N7W1 A0A0A0MRG0 A0A0A0MSK3 A0A0A0MT22 A0N0Q1 A1A4V4 A2A3U5 A2RUS0 A4D1Q0 A8K1F6 A8K249 A8K7N8 A8KAF4 A8KAG8 B0ZBE0 B2R7Y7 B4DN15 B7Z1L9 B8K2Q5 C1ID52 E5KQF5 E9PG18 F1D8N3 F5H1T4 G5E9C5 H6VQ59 K9J958 L7RSL3 L7RXH5 O00167 P00533 P00918 P02545 P05177 P05181 P06239 P06241 P07550 P08173 P08246 P08311 P08588 P08684 P08913 P10253 P11229 P11509 P11712 P14780 P15428 P17252 P18825 P21397 P21452 P21554 P21728 P21917 P22303 P25021 P25024 P25025 P25101 P25103 P25929 P27695 P28223 P28482 P30411 P32238 P32245 P33032 P35354 P35367 P37288 P41143 P41595 P41968 P49146 P50052 P50406 P51681 P83916 Q01959 Q08209 Q14524 Q38Q88 Q99700
CID 4908: primaquine
A0A024QZY7 A0A024R2N2 A0A024R2Q0 A0A024R3C5 A0A024R3S2 A0A024R6T9 A0A024R9I2 A0A024RAP2 A0A024RCN9 A0A024RD15 A0A087WT22 A0A087WU84 A0A090N7W1 A0A0A0MRG0 A0A0A0MSK3 A0A0A0MT22 A0N0Q1 A0N0X8 A1A4V4 A2A3U5 A2RUS0 A4D1Q0 A8K1F6 A8K249 A8K7N8 A8KAF4 A8KAG8 B0ZBE0 B2R7Y7 B2RXH2 B3KPX6 B4DN15 B7Z1L9 B7Z242 B8K2Q5 C1ID52 D0VY79 E5KQF5 F1D8N3 F5H1T4 G5E9C5 H6VQ59 K9J958 L7RSL3 L7RXH5 O94782 P00352 P00533 P00918 P02545 P02768 P05177 P05181 P06239 P06241 P07550 P08173 P08246 P08311 P08588 P08684 P08729 P08913 P11021 P11229 P11509 P11712 P14780 P17252 P18825 P21397 P21452 P21554 P21728 P21917 P22303 P25021 P25024 P25025 P25101 P25103 P25929 P28223 P28482 P30411 P32238 P32245 P33032 P35354 P35367 P37288 P41143 P41595 P41968 P49146 P50052 P50406 P51681 Q01959 Q08209 Q38Q88
CID 4909: primidone
A0A024R2N2 A0A024R2Q0 A0A024R3C5 A0A024R3S2 A0A024R4E2 A0A024R6L5 A0A024R6T9 A0A024R909 A0A024R9I2 A0A024R9X6 A0A024RAP2 A0A024RCN9 A0A024RD15 A0A087WU84 A0A090N7W1 A0A0A0MRG0 A0A0A0MSK3 A0A0A0MT22 A0A0A0MTJ0 A0A0A6YYA8 A0N0Q1 A1A4V4 A2A3U5 A2RUS0 A4D1Q0 A8K177 A8K1F6 A8K249 A8K7N8 A8KAF4 A8KAG8 B0ZBE0 B2R7Y7 B4DK78 B4DN15 B7Z1L9 B7Z1W5 B8K2Q5 C1ID52 E5KQF5 F1D8N3 F1D8N5 F5H1T4 G5E9C5 H6VQ59 K9J958 L7RSL3 L7RXH5 O94782 P00533 P00918 P05177 P05181 P06239 P06241 P07550 P08173 P08246 P08311 P08588 P08684 P08913 P11229 P11509 P11712 P14780 P14867 P17252 P18825 P21397 P21452 P21554 P21728 P21917 P22303 P25021 P25024 P25025 P25101 P25103 P25929 P27695 P28223 P28482 P30411 P31644 P32238 P32245 P33032 P34903 P35354 P35367 P37288 P39748 P41143 P41595 P41968 P42262 P48169 P49146 P50052 P50406 P51681 P83916 Q01959 Q08209 Q16236 Q16445 Q38Q88 Q9UNA4
CID 4911: probenecid
A0A024QZY7 A0A024R2N2 A0A024R2Q0 A0A024R397 A0A024R3C5 A0A024R3S2 A0A024R5I4 A0A024R6Q6 A0A024R6T9 A0A024R9I2 A0A024RAP2 A0A024RAU7 A0A024RBV5 A0A024RD15 A0A087WU84 A0A090N7W1 A0A0A0MRG0 A0A0A0MSK3 A0A0A0MT22 A0N0Q1 A1A4V4 A2A3U5 A2RUS0 A4D1D2 A4D1Q0 A8K1F6 A8K249 A8K2Q2 A8K7N8 A8KAF4 A8KAG8 B0ZBE0 B2R7Y7 B2R807 B3KP53 B3KP78 B4DN15 B7Z1L9 B8K2Q5 C1ID52 E5KQF5 F1D8N3 F1D8P8 F5H1T4 G5E9C5 H6VQ59 K9J958 L7RSL3 L7RXH5 O15245 O15440 O60656 O76082 O94782 O95255 P00533 P00915 P00918 P02768 P05177 P05181 P06239 P06241 P06280 P07550 P08173 P08246 P08311 P08588 P08684 P08913 P11229 P11509 P11712 P14780 P17252 P18825 P19224 P21397 P21452 P21554 P21728 P21917 P22303

P22309 P25021 P25024 P25025 P25101 P25103 P25929 P28223 P28482 P30411 P32238 P32245 P33032 P33527 P35354 P35367 P37288 P41143 P41595 P41968 P49146 P50052 P50406 P51681 P83916 Q01959 Q08209 Q38Q88 Q4U2R8 Q5DSZ6 Q5DSZ7 Q5DT02 Q92887 Q9NSA0 Q9NYB5 Q9WUD2 Q9Y694

CID 4913: procainamide

A0A024R2N2 A0A024R2Q0 A0A024R3C5 A0A024R3S2 A0A024R5I4 A0A024R6T9 A0A024R9I2 A0A024RAP2 A0A024RAU7 A0A024RCN9 A0A024RD15 A0A087WU84 A0A090N7W1 A0A0A0MQX8 A0A0A0MRG0 A0A0A0MSK3 A0A0A0MT22 A0A0A0MTJ0 A0N0Q1 A1A4V4 A2A3U5 A2RUS0 A4D1Q0 A8K1F6 A8K249 A8K7N8 A8KAF4 A8KAG8 B0ZBE0 B2R7Y7 B3KP78 B4DN15 B7Z1L9 B7ZKN7 B8K2Q5 C1ID52 D3DNN4 E5KQF5 E9PG18 F1D8N3 F5H1T4 G5E9C5 H6VQ59 I6L9H2 K9J958 L7RSL3 L7RXH5 O15244 O15245 O75751 O76082 O94782 P00352 P00533 P00918 P02545 P05177 P05181 P06239 P06241 P07550 P08173 P08246 P08311 P08588 P08684 P08913 P11229 P11509 P11712 P14780 P17252 P18825 P21397 P21452 P21554 P21728 P21917 P22303 P25021 P25024 P25025 P25101 P25103 P25929 P28223 P28482 P30411 P32238 P32245 P33032 P35354 P35367 P37288 P39748 P41143 P41595 P41968 P49146 P50052 P50406 P51681 Q01453 Q01959 Q08209 Q13526 Q14524 Q38Q88 Q96FL8 Q9H015

CID 4914: procaine

A0A024QZY7 A0A024R2N2 A0A024R2Q0 A0A024R3C5 A0A024R3S2 A0A024R4E2 A0A024R6T9 A0A024R9I2 A0A024RAP2 A0A024RCN9 A0A024RD15 A0A087WU84 A0A090N7W1 A0A090N8Z1 A0A0A0MRG0 A0A0A0MSK3 A0A0A0MT22 A0A0A0MTJ0 A0N0Q1 A1A4V4 A2A3U5 A2RUS0 A4D1Q0 A8K1F6 A8K249 A8K7N8 A8KAF4 A8KAG8 B0ZBE0 B2R7Y7 B4DN15 B4E398 B7Z1L9 B7ZKN7 B8K2Q5 C1ID52 C4IXS7 E5KQF5 F1D8N3 F5H1T4 F7VJQ1 G5E9C5 H6VQ59 I6L9H2 K9J958 L7RSL3 L7RXH5 P00533 P00918 P05177 P05181 P06239 P06241 P07550 P08173 P08246 P08311 P08588 P08684 P08913 P11229 P11509 P11712 P14780 P17252 P18825 P21397 P21452 P21554 P21728 P21817 P21917 P22303 P25021 P25024 P25025 P25101 P25103 P25929 P28223 P28482 P30411 P32238 P32245 P33032 P35354 P35367 P37288 P41143 P41595 P41968 P46098 P49146 P50052 P50406 P51681 Q01959 Q08209 Q15822 Q38Q88 Q8TCU5 Q92736 Q92830 Q9Y5Y9

CID 4915: procarbazine

A0A024QZY7 A0A024R2N2 A0A024R2Q0 A0A024R3C5 A0A024R3S2 A0A024R6T9 A0A024R9I2 A0A024RAP2 A0A024RD15 A0A087WU84 A0A090N7W1 A0A0A0MRG0 A0A0A0MSK3 A0A0A0MT22 A0N0Q1 A1A4V4 A2A3U5 A2RUS0 A4D1Q0 A8K1F6 A8K249 A8K7N8 A8KAF4 A8KAG8 B0ZBE0 B2R7Y7 B4DN15 B7Z1L9 B8K2Q5 C1ID52 E5KQF5 F1D8N3 F5H1T4 G5E9C5 H6VQ59 K9J958 L7RSL3 L7RXH5 O75164 O94782 P00352 P00533 P00918 P02545 P05177 P05181 P06239 P06241 P07550 P08173 P08246 P08311 P08588 P08684 P08913 P11229 P11509 P11712 P14780 P16050 P17252 P18825 P21397 P21452 P21554 P21728 P21917 P22303 P25021 P25024 P25025 P25101 P25103 P25929 P28223 P28482 P30411 P32238 P32245 P33032 P35354 P35367 P37288 P41143 P41595 P41968 P47989 P49146 P50052 P50406 P51681 P83916 Q01959 Q08209 Q38Q88

CID 4917: prochlorperazine

A0A024QZY7 A0A024R2N2 A0A024R2Q0 A0A024R3C5 A0A024R3S2 A0A024R5Z3 A0A024R6T9 A0A024R909 A0A024R9I2 A0A024R9Y0 A0A024RAP2 A0A024RCN9 A0A024RD15 A0A024RDJ4 A0A068F658 A0A087WT22 A0A087WT64 A0A087WU84 A0A090N7W1 A0A090N8Z1 A0A0A0MRG0 A0A0A0MSK3 A0A0A0MT22 A0A0A0MTJ0 A0N0Q1 A1A4V4 A2A3U5 A2RUS0 A4D1D2 A4D1Q0 A8K1F6 A8K249 A8K7N8 A8KAF4 A8KAG8 B0ZBD3 B0ZBE0 B2R7Y7 B4DN15 B7Z1L9 B8K2Q5 C1ID52 D0VY79 E5KQF5 F1D8N3 F5H1T4 F8W6L1 G5E9C5 H6VQ59 K9J958 L7RSL3 L7RXH5 O15245 O15296 O75164 O75874 O94782 O94925 P00533 P00918 P02545 P05177 P05181 P06239 P06241 P07550 P08173 P08246 P08311 P08588 P08684 P08913 P11229 P11509 P11712 P14416 P14780 P17252 P18825 P21397 P21452 P21554 P21728 P21917 P22303 P25021 P25024 P25025 P25101 P25103 P25929 P27695 P28223 P28482 P30411 P30939 P32238 P32245 P33032 P35354 P35367 P35462 P37288 P39748 P41143 P41595 P41968 P42345 P43220 P49146 P50052 P50406 P51681 P83916 Q01959 Q08209 Q38Q88 Q96QE3 Q99549 Q99700 Q9UIF8 Q9UNA4

CID 4927: promethazine

A0A024QZY7 A0A024R2N2 A0A024R2Q0 A0A024R3C5 A0A024R3S2 A0A024R4E2 A0A024R6T9 A0A024R909 A0A024R9I2 A0A024R9Y0 A0A024RAP2 A0A024RCN9 A0A024RCW6 A0A024RD15 A0A024RDJ4 A0A068F658 A0A087WU84 A0A090N7W1 A0A0A0MRG0 A0A0A0MSK3 A0A0A0MT22 A0N0Q1 A1A4V4 A2A3U5 A2RUS0 A4D1D2 A4D1Q0 A8K1F6 A8K249 A8K7N8 A8KAF4 A8KAG8 B0ZBD3 B0ZBE0 B2KJ49 B2R7Y7 B4DN15 B7Z1L9 B7ZKN7 B8K2Q5 C1ID52 D0VY79 D2KUA6 E5KQF5 E7ETZ0 F1D8N3 F1D8P8 F5H1T4 G5E9C5 H6VQ59 K9J958 L7RSL3 L7RXH5 O15245 O15296 O60656 O75164 O94782 P00352 P00533 P00918 P02545 P05177 P05181 P06239 P06241 P07550 P08173 P08246 P08311 P08588 P08684 P08913 P11229 P11509 P11712 P14780 P16050 P17252 P18825 P19224 P21397 P21452 P21554 P21728 P21917 P22303 P22310 P25021 P25024 P25025 P25101 P25103 P25929 P27695 P28223 P28482 P30411 P30939 P32238 P32245 P33032 P35354 P35367 P37288 P39748 P41143 P41595 P41968 P42345 P42858 P49146 P50052 P50406 P51681 P83916 Q01453 Q01959 Q03164 Q08209 Q16236 Q38Q88 Q8NER1 Q99549 Q99700 Q99714 Q9BRL5 Q9UIF8

CID 4932: propafenone

A0A024QZY7 A0A024R2N2 A0A024R2Q0 A0A024R3C5 A0A024R3S2 A0A024R4E2 A0A024R6T9 A0A024R909 A0A024R9I2 A0A024RAP2 A0A024RCN9 A0A024RD15 A0A087WT22 A0A087WU84 A0A090N7W1 A0A090N8Z1 A0A0A0MRG0 A0A0A0MSK3 A0A0A0MT22 A0A0A0MTJ0 A0N0Q1 A1A4V4 A2A3U5 A2RUS0 A4D1D2 A4D1Q0 A8K1F6 A8K249 A8K7N8 A8KAF4 A8KAG8 B0ZBE0 B2R7Y7 B4DN15 B7Z1L9 B8K2Q5 C1ID52 D0VY79 E5KQF5 E9PG18 F1D8N3 F5H1T4 F8W6L1 G5E9C5 H6VQ59 K9J958 L7RSL3 L7RXH5 O15245 O15296 P00533 P00918 P02545 P05177 P05181 P06239 P06241 P07550 P08173 P08246 P08311 P08588 P08684 P08913 P11229 P11509 P11712 P14780 P17252 P18825 P21397 P21452 P21554 P21728 P21917 P22303 P22460 P25021 P25024 P25025 P25101 P25103 P25929 P28223 P28482 P30411 P32238 P32245 P33032 P35354 P35367 P37288 P41143 P41595 P41968 P42345 P43220 P49146 P50052 P50406 P51681 P83916 Q01453 Q01959 Q08209 Q12809 Q16850 Q38Q88 Q92887 Q99549 Q99700

CID 4934: propantheline

A0A024R6L5 A0A024R9Y0 A0A024RAV2 A0A024RCN9 A0A024RDJ4 A0A090N7W1 A0A0A0MTJ0 B4DN83 C1ID52 O75874 P02545 P08172 P08173 P08684 P11229 P20309 P27695 Q01453 Q96QE3

CID 4935: proparacaine

A0A024R2N2 A0A024R2Q0 A0A024R3C5 A0A024R3S2 A0A024R6T9 A0A024R9I2 A0A024RAP2 A0A024RAP4 A0A024RD15 A0A024RD62 A0A087WU84 A0A090N7W1 A0A0A0MRG0 A0A0A0MSK3 A0A0A0MT22 A0N0Q1 A1A4V4 A2A3U5 A2RUS0 A4D1Q0 A8K1F6 A8K249 A8K7N8 A8KAF4 A8KAG8 B0ZBE0 B2R7Y7 B4DN15 B7Z1L9 B8K2Q5 C1ID52 E5KQF5 F1D8N3 F5H1T4 G5E9C5 H6VQ59 K9J958 L7RSL3 L7RXH5 O94782 O94925 P00533 P00918 P05177 P05181 P06239 P06241 P07550 P08173 P08246 P08311 P08588 P08684 P08913 P11229 P11509 P11712 P14780 P17252 P18825 P21397 P21452 P21554 P21728 P21917 P22303 P25021 P25024 P25025 P25101 P25103 P25929 P28223 P28482 P30411 P32238 P32245 P33032 P35354 P35367 P37288 P41143 P41595 P41968 P43220 P49146 P50052 P50406 P51681 P83916 Q01959 Q08209 Q14524 Q38Q88 Q9UNA4 Q9Y5Y9

CID 4943: propofol

A0A024R2N2 A0A024R2Q0 A0A024R3C5 A0A024R3S2 A0A024R6T9 A0A024R9I2 A0A024RAP2 A0A024RCN9 A0A024RD15 A0A087WU84 A0A090N7W1 A0A0A0MRG0 A0A0A0MSK3 A0A0A0MT22 A0A0A0MTJ0 A0N0Q1 A1A4V4 A2A3U5 A2RUS0 A4D1Q0 A8K177 A8K1F6 A8K249 A8K7N8 A8KAF4 A8KAG8 B0ZBE0 B2R7Y7 B2RCW8 B4DN15 B7Z1L9 B7ZKN7 B7ZW53 B8K2Q5 C1ID52 D0VY79 E5KQF5 F1D8N3 F5H1T4 G5E9C5 H6VQ59 K9J958 L7RSL3 L7RXH5 O00519 O15245 O60656 O88704 O94782 P00533 P00915 P00918 P02545 P02768 P05177 P05181 P06239 P06241 P07550 P08173 P08246 P08311 P08588 P08684 P08913 P11229 P11509 P11712 P14780 P15428 P16662 P17252 P18825 P19224 P20813 P21397 P21452 P21554 P21728 P21917 P22303 P22309 P22310 P25021 P25024 P25025 P25101 P25103 P25929 P28223 P28482 P30411 P32238 P32245 P33032 P35354 P35367 P35499 P37288 P41143 P41595 P41968 P47870 P49146 P50052 P50406 P51681 Q01959 Q08209 Q38Q88 Q5DSZ6 Q5DT02 Q99250 Q9UNA4

CID 4946: propranolol

A0A024QZY7 A0A024R2N2 A0A024R2Q0 A0A024R3C5 A0A024R3S2 A0A024R5I4 A0A024R6L5 A0A024R6T9 A0A024R9I2 A0A024RAP2 A0A024RAU7 A0A024RCN9 A0A024RD15 A0A024RD62 A0A024RDJ4 A0A087WT22 A0A087WU84 A0A090N7W1 A0A0A0MRG0 A0A0A0MSK3 A0A0A0MT22 A0A0A0MTJ0 A0N0Q1 A1A4V4 A2A3U5 A2RUS0 A4D1D2 A4D1Q0 A8K1F6 A8K249 A8K5W4 A8K7N8 A8KAF4 A8KAG8 B0ZBE0 B2R7Y7 B2RA41 B3KP78 B4DN15 B4E398 B6ZGS9 B7Z1L9 B7ZKN7 B8K2Q5 C1ID52 D2KUA6 E5KQF5 F1D8N3 F5H1T4 F8W6L1 G5E9C5 H6VQ59 K9J958 L7RSL3 L7RXH5 O15244 O15245 O15296 O60656 O94782 P00352 P00533 P00918 P02545 P02768 P05177 P05181 P06133 P06239 P06241 P07550 P08173 P08246 P08311 P08588 P08684 P08913 P11229 P11509 P11712 P13945 P14780 P16662 P17252 P18825 P21397 P21452 P21554 P21728 P21917 P22303 P22309 P25021 P25024 P25025 P25101 P25103 P25929 P25962 P26255 P27695 P28221 P28223 P28482 P30411 P30939 P32238 P32245 P33032 P35354 P35367 P36537 P37288 P39748 P41143 P41595 P41968 P43220 P49146 P50052 P50406 P51681 P83916 Q01453 Q01959 Q08209 Q38Q88 Q5DSZ6 Q5DT02 Q8NER1 Q92887 Q99549 Q99700 Q99714

CID 4976: protriptyline

A0A024QZY7 A0A024R6T9 A0A024RCN9 A0A024RDJ4 A0A087WT22 A0A090N7W1 A4D1D2 A4D1Q0 B2R7Y7 B2RXH2 B7Z1L9 B7Z242 C1ID52 F8W6L1 H6VQ59 O15296 O43526 O75874 P02545 P02768 P05177 P07550 P08588 P08684 P08913 P11229 P11712 P17405 P21397 P21728 P22310 P23975 P25021 P28223 P31645 P35367 P43220 Q01453 Q01959 Q16696 Q99700 Q99714

CID 4991: pyridostigmine

A0A024QZY7 A0A024RCN9 A0A0A0MTJ0 A4D1D2 C1ID52 D3DNN4 P02545 P05177 P06280 P08684 P11712 P22303 P27695 P28482 P83916 Q96QE3 Q99549

CID 4993: pyrimethamine

A0A024QZY7 A0A024R5Z3 A0A024R6L5 A0A024RCW6 A0A087WT22 A0A090N7W1 A8KAF4 B0YJ76 B4DZW8 B6ZGS9 C1ID52 D2KUA6 F1D8P6 K9J958 O75874 P00352 P02545 P05181 P08684 P11229 P11712 P24666 P43220 Q16236 Q3V050 Q96FL8 Q99700 Q9HBH1

CID 5002: quetiapine

A0A024QZY7 A0A024R2N2 A0A024R2Q0 A0A024R3C5 A0A024R3S2 A0A024R6T9 A0A024R9I2 A0A024RAP2 A0A024RD15 A0A087WU84 A0A090N7W1 A0A0A0MRG0 A0A0A0MSK3 A0A0A0MT22 A0N0Q1 A0PJF5 A1A4V4 A2A3U5 A2RUS0 A4D1D2 A4D1Q0 A4D2N2 A8K1F6 A8K249 A8K5W4 A8K7N8 A8KAF4 A8KAG8 B0ZBD3 B0ZBE0 B2KJ49 B2R7Y7 B4DN15 B4DN83 B4E398 B7Z1L9 B8K2Q5 C1ID52 E5KQF5 F1D8N3 F5H1T4 G5E9C5 H6VQ59 K9J958 L7RSL3 L7RXH5 O00325 P00533 P00918 P02545 P05177 P05181 P06239 P06241 P08173 P08246 P08311 P08684 P08908 P08913 P11229 P11509 P11712 P14416 P14780 P17252 P18825 P21397 P21452 P21554 P21728 P21731 P21917 P21918 P22303 P23975 P25024 P25025 P25101 P25103 P25929 P28222 P28223 P28482 P28566 P30411 P30939 P32238 P32245 P32297 P33032 P34969 P35354 P35367 P35368 P37288 P41143 P41595 P41968 P49146 P50052 P50406 P51681 Q08209 Q15822 Q38Q88 Q92830 Q96QE3

CID 5029: rabeprazole

A0A024R2N2 A0A024R2Q0 A0A024R3C5 A0A024R3S2 A0A024R6T9 A0A024R9I2 A0A024RAP2 A0A024RD15 A0A087WU84 A0A090N7W1 A0A0A0MRG0 A0A0A0MSK3 A0A0A0MT22 A0N0Q1 A1A4V4 A2A3U5 A2RUS0 A4D1Q0 A8K1F6 A8K249 A8K7N8 A8KAF4 A8KAG8 B0ZBE0 B2R7Y7 B4DN15 B7Z1L9 B8K2Q5 C1ID52 E5KQF5 F1D8N3 F5H1T4 G5E9C5 H6VQ59 K9J958 L7RSL3 L7RXH5 P00533 P00918 P05177 P05181 P06239 P06241 P07550 P08173 P08246 P08311 P08588 P08684 P08913 P11229 P11509 P11712 P14780 P17252 P18825 P20648 P21397 P21452 P21554 P21728 P21917 P22303 P25021 P25024 P25025 P25101 P25103 P25929 P28223 P28482 P30411 P32238 P32245 P33032 P35354 P35367 P37288 P41143 P41595 P41968 P49146 P50052 P50406 P51164 P51681 Q01959 Q08209 Q38Q88

CID 5035: raloxifene

A0A024QYX0 A0A024QZY7 A0A024R136 A0A024R2N2 A0A024R2Q0 A0A024R3C5 A0A024R3S2 A0A024R5Z3 A0A024R6L5 A0A024R6T9 A0A024R9I2 A0A024R9Y0 A0A024RAP2 A0A024RAV2 A0A024RCN9 A0A024RCW6 A0A024RD15 A0A024RDJ4 A0A068F658 A0A087WT22 A0A087WU84 A0A090N7W1 A0A090N8Z1 A0A0A0MRG0 A0A0A0MSK3 A0A0A0MT22 A0A0A0MTJ0 A0A0A0N0L2 A0N0Q1 A1A4V4 A2A3U5 A2RUS0 A4D1Q0 A8K1F6 A8K249 A8K7N8 A8KAF4 A8KAG8 B0ZBE0 B2R7Y7 B4DN15 B6ZGS9 B7Z1L9 B7ZKN7 B8K2Q5 C1ID52 D2KUA6 E5KQF5 F1D8N3 F1D8N7 F1D8P8 F1D8P9 F1D8Q5 F5H1T4 F8W6L1 G5E9C5 H6VQ59 K9J958 L7RSL3 L7RXH5 O14939 O15296 O75164 O75604 O75874 O94782 P00352 P00533 P00918 P02545 P03372 P05177 P05181 P06239 P06241 P07550 P08173 P08246

P08311 P08588 P08684 P08913 P11229 P11509 P11712 P14780 P16050 P17252 P18825 P21397 P21452 P21554 P21728 P21917 P22303 P22309 P25021
P25024 P25025 P25101 P25103 P25929 P28223 P28482 P30411 P32238 P32245 P33032 P35354 P35367 P37288 P41143 P41595 P41968 P42345 P42858
P43220 P49146 P50052 P50406 P51681 P61088 P83916 Q01453 Q01959 Q03164 Q06278 Q08209 Q13393 Q13526 Q16236 Q38Q88 Q5DSZ6 Q5DT02 Q8IUX4
Q92731 Q96QE3 Q99549 Q99700 Q99714 Q9HC16 Q9UIF8 Q9UNA4

CID 5039: ranitidine

A0A024R2N2 A0A024R2Q0 A0A024R3C5 A0A024R3S2 A0A024R6T9 A0A024R9I2 A0A024R9Y0 A0A024RAP2 A0A024RCN9 A0A024RD15 A0A024RDJ4 A0A087WU84
A0A090N7W1 A0A0A0MR48 A0A0A0MRG0 A0A0A0MSK3 A0A0A0MT22 A0A0A0MTJ0 A0N0Q1 A1A4V4 A2A3U5 A2RUS0 A4D1D2 A4D1Q0 A8K1F6 A8K249 A8K7N8
A8KAF4 A8KAG8 B0ZBE0 B2KJ49 B2R7Y7 B2R807 B4DN15 B4E398 B7Z1L9 B7Z2G8 B7ZKN7 B8K2Q5 C1ID52 D0VY79 E5KQF5 F1D8N3 F5H1T4 G5E9C5 H6VQ59
K9J958 L7RSL3 L7RXH5 O15244 O15245 O75874 O94782 P00533 P00918 P02545 P05177 P05181 P06239 P06241 P07550 P08173 P08246 P08311 P08588
P08684 P08913 P11229 P11509 P11712 P14780 P17252 P18825 P21397 P21452 P21554 P21728 P21917 P22303 P25021 P25024 P25025 P25101 P25103
P25929 P28223 P28482 P30411 P32238 P32245 P33032 P35354 P35367 P37288 P41143 P41595 P41968 P49146 P50052 P50406 P51681 P83916 Q01959
Q08209 Q38Q88 Q92830 Q92887 Q96FL8 Q96QE3 Q99549 Q99714 Q9UNA4

CID 5070: riluzole

A0A024QZY7 A0A024R2N2 A0A024R2Q0 A0A024R3C5 A0A024R3S2 A0A024R4E2 A0A024R5Z9 A0A024R6T9 A0A024R909 A0A024R9I2 A0A024RAP2 A0A024RBV5
A0A024RCN9 A0A024RD15 A0A024RDJ4 A0A087WT22 A0A087WU84 A0A090N7W1 A0A0A0MRG0 A0A0A0MSK3 A0A0A0MT22 A0N0Q1 A1A4V4 A2A3U5 A2RUS0
A4D1Q0 A8K1F6 A8K249 A8K7N8 A8KAF4 A8KAG8 B0YJ76 B0ZBE0 B2R7Y7 B4DN15 B7Z1L9 B7ZKN7 B8K2Q5 C1ID52 E5KQF5 E9PG18 F1D8N3 F5H1T4 G5E9C5
H6UYS5 H6VQ59 K9J958 L7RSL3 L7RXH5 O15118 O15554 O75604 O75874 O94782 O95069 P00533 P00918 P02545 P05177 P05181 P06239 P06241 P07550
P08173 P08246 P08311 P08588 P08684 P08913 P10253 P11229 P11509 P11712 P14780 P16050 P17252 P18825 P21397 P21452 P21554 P21728 P21917
P22303 P25021 P25024 P25025 P25101 P25103 P25929 P28223 P28482 P30411 P32238 P32245 P33032 P35354 P35367 P37288 P39748 P41143 P41595
P41968 P49146 P50052 P50406 P51681 P57789 P70604 P70605 P83916 Q01453 Q01959 Q08209 Q16236 Q38Q88 Q62897 Q8NDX3 Q8TCU5 Q96QE3 Q99700
Q99714 Q9NYG8 Q9UPY5

CID 5071: rimantadine

A0A024R2N2 A0A024R2Q0 A0A024R3C5 A0A024R3S2 A0A024R6T9 A0A024R9I2 A0A024R9Y0 A0A024RAP2 A0A024RAP4 A0A024RD15 A0A087WU84 A0A090N7W1
A0A0A0MRG0 A0A0A0MSK3 A0A0A0MT22 A0N0Q1 A1A4V4 A2A3U5 A2RUS0 A4D1Q0 A8K1F6 A8K249 A8K7N8 A8KAF4 A8KAG8 B0ZBE0 B2R7Y7 B4DN15 B4DN83
B7Z1L9 B8K2Q5 C1ID52 E5KQF5 F1D8N3 F5H1T4 G5E9C5 H6VQ59 K9J958 L7RSL3 L7RXH5 O15244 P00533 P00918 P05177 P05181 P06239 P06241 P07550
P08173 P08246 P08311 P08588 P08684 P08913 P11229 P11509 P11712 P14780 P17252 P18825 P21397 P21452 P21554 P21728 P21917 P22303 P25021
P25024 P25025 P25101 P25103 P25929 P28223 P28482 P30411 P32238 P32245 P33032 P35354 P35367 P37288 P41143 P41595 P41968 P49146 P50052
P50406 P51681 Q01959 Q08209 Q38Q88 Q86VL8 Q96FL8 Q99700

CID 5073: risperidone

A0A024R2N2 A0A024R2Q0 A0A024R3C5 A0A024R3S2 A0A024R5Z3 A0A024R6T9 A0A024R9I2 A0A024RAP2 A0A024RD15 A0A087WU84 A0A090N7W1 A0A0A0MRG0
A0A0A0MSK3 A0A0A0MT22 A0A0A0MTJ0 A0N0Q1 A0PJF5 A1A4V4 A2A3U5 A2RUS0 A4D1D2 A4D1Q0 A4D2N2 A8K1F6 A8K249 A8K5W4 A8K7N8 A8KAF4 A8KAG8
B0ZBD3 B0ZBE0 B2KJ49 B2R7Y7 B4DN15 B4DN83 B4E398 B7Z1L9 B8K2Q5 C1ID52 E5KQF5 F1D8N3 F5H1T4 G5E9C5 H6VQ59 K9J958 L7RSL3 L7RXH5 O00325
O15244 O15245 O75164 P00533 P00918 P05177 P05181 P06239 P06241 P08246 P08311 P08684 P08908 P08913 P11509 P11712 P14416 P14780 P14842
P17252 P18825 P19327 P21397 P21452 P21554 P21728 P21731 P21917 P21918 P22303 P25021 P25024 P25025 P25100 P25101 P25103 P25929 P28221
P28222 P28223 P28335 P28482 P30411 P30939 P31388 P32238 P32245 P32297 P32305 P33032 P34969 P35348 P35354 P35367 P35368 P35462 P37288
P41143 P41595 P41968 P49146 P50052 P50406 P51681 Q01453 Q08209 Q15822 Q38Q88 Q86VL8 Q96FL8

CID 5078: rizatriptan

A8K5W4 P08908 P21397 P28221 P28222 P28566 P30939 Q13639

CID 5090: rofecoxib

A0A024R2N2 A0A024R2Q0 A0A024R3C5 A0A024R3S2 A0A024R6T9 A0A024R9I2 A0A024RAH7 A0A024RAP2 A0A024RD15 A0A087WU84 A0A090N7W1 A0A0A0MRG0
A0A0A0MSK3 A0A0A0MT22 A0N0Q1 A1A4V4 A2A3U5 A2RUS0 A4D1Q0 A8K1F6 A8K249 A8K2Q2 A8K5W4 A8K7N8 A8KAF4 A8KAG8 B0ZBD3 B0ZBE0 B2R7Y7
B3KRT8 B4DN15 B4E398 B7Z1L9 B8K2Q5 C1ID52 E5KQF5 F1D8N3 F5H1T4 G5E9C5 H6VQ59 K9J958 L7RSL3 L7RXH5 P00352 P00533 P00918 P05177 P05181
P06239 P06241 P07550 P08173 P08246 P08311 P08588 P08684 P08913 P09917 P11229 P11509 P11712 P14780 P17252 P18054 P18825 P21397 P21452
P21554 P21728 P21917 P21918 P22303 P25021 P25024 P25025 P25101 P25103 P25929 P28221 P28222 P28223 P28482 P28566 P30411 P32238 P32245
P33032 P34913 P34969 P35354 P35367 P35368 P37288 P41143 P41595 P41968 P43116 P49146 P50052 P50406 P51681 P83916 Q01959 Q08209 Q15722
Q38Q88

CID 5095: ropinirole

A0A024QZY7 A0A024R3C5 A0A024RCN9 A0A090N7W1 A1A4V4 A2RUS0 A4D2N2 A8K5W4 B0ZBD3 B0ZBE0 B2RXH2 B7ZKN7 C1ID52 K9J958 P02545 P05177
P08684 P08913 P11712 P14416 P18825 P21917 P27695 P28221 P28482 P34969 P35462 P39748 P41595 P83916

CID 5152: salmeterol

A0A024R5Z3 A0A068F658 A0A087WT22 A0A0A0MTJ0 A8KAG8 B2RXH2 C1ID52 P02768 P07550 P08588 P08684 P11712 P16050 P28482

CID 5161: salsalate

A0A024R2N2 A0A024R2Q0 A0A024R3C5 A0A024R3S2 A0A024R6T9 A0A024R9I2 A0A024RAP2 A0A024RD15 A0A087WU84 A0A090N7W1 A0A0A0MRG0 A0A0A0MSK3
A0A0A0MT22 A0N0Q1 A1A4V4 A2A3U5 A2RUS0 A4D1Q0 A8K1F6 A8K249 A8K7N8 A8KAF4 A8KAG8 B0ZBE0 B2R7Y7 B2RXH2 B4DN15 B7Z1L9 B8K2Q5 C1ID52
E5KQF5 F1D8N3 F5H1T4 G5E9C5 H6VQ59 K9J958 L7RSL3 L7RXH5 P00352 P00533 P00918 P05177 P05181 P06239 P06241 P07550 P08173 P08246 P08311
P08588 P08684 P08913 P11229 P11509 P11712 P14780 P15428 P17252 P18825 P21397 P21452 P21554 P21728 P21917 P22303 P23219 P25021 P25024
P25025 P25101 P25103 P25929 P28223 P28482 P30411 P32238 P32245 P33032 P35354 P35367 P37288 P41143 P41595 P41968 P49146 P50052 P50406
P51681 Q01959 Q08209 Q38Q88 Q99714

CID 5193: secobarbital

A0A024QZY7 A0A024R2N2 A0A024R2Q0 A0A024R3C5 A0A024R3S2 A0A024R6T9 A0A024R9I2 A0A024R9X6 A0A024RAP2 A0A024RD15 A0A087WU84 A0A090N7W1
A0A0A0MRG0 A0A0A0MSK3 A0A0A0MT22 A0A0A6YYA8 A0N0Q1 A1A4V4 A2A3U5 A2RUS0 A4D1Q0 A8K177 A8K1F6 A8K249 A8K7N8 A8KAF4 A8KAG8 B0ZBE0
B2R7Y7 B4DK78 B4DN15 B7Z1L9 B8K2Q5 C1ID52 E5KQF5 F1D8N3 F5H1T4 G5E9C5 H6VQ59 K9J958 L7RSL3 L7RXH5 P00533 P00918 P05177 P05181 P06239
P06241 P07550 P08173 P08246 P08311 P08588 P08684 P08913 P11229 P11509 P11712 P14780 P14867 P17252 P18825 P21397 P21452 P21554 P21728
P21917 P22303 P25021 P25024 P25025 P25101 P25103 P25929 P28223 P28482 P30411 P31644 P32238 P32245 P33032 P34903 P35354 P35367 P37288
P41143 P41595 P41968 P42262 P48169 P49146 P50052 P50406 P51681 Q01959 Q08209 Q16445 Q38Q88

CID 5206: sevoflurane

A8K177 B4E295 P03886 P05181 P23415 P30049 P42261 Q09470

CID 5210: sibutramine

A0A024QZY7 A0A024R2N2 A0A024R2Q0 A0A024R3C5 A0A024R3S2 A0A024R6T9 A0A024R9I2 A0A024R9Y0 A0A024RAP2 A0A024RD15 A0A087WU84 A0A090N7W1
A0A0A0MRG0 A0A0A0MSK3 A0A0A0MT22 A0A0A0MTJ0 A0N0Q1 A1A4V4 A2A3U5 A2RUS0 A4D1Q0 A8K1F6 A8K249 A8K7N8 A8KAF4 A8KAG8 B0ZBE0 B2R7Y7
B4DN15 B7Z1L9 B8K2Q5 C1ID52 E5KQF5 F1D8N3 F5H1T4 G5E9C5 H6VQ59 K9J958 L7RSL3 L7RXH5 O15296 O75874 P00352 P00533 P00918 P02545 P05177
P05181 P06239 P06241 P07550 P08173 P08246 P08311 P08588 P08684 P08913 P11229 P11509 P11712 P14780 P16050 P17252 P17405 P18825 P21397
P21452 P21554 P21728 P21917 P22303 P23975 P25021 P25024 P25025 P25101 P25103 P25929 P28482 P30411 P31645 P32238 P32245 P33032 P35354
P35367 P37288 P41143 P41968 P43220 P49146 P50052 P50406 P51681 P83916 Q01959 Q08209 Q38Q88 Q62897

CID 5212: sildenafil

A0A024QZY7 A0A024R2N2 A0A024R2Q0 A0A024R3C5 A0A024R3S2 A0A024R5I4 A0A024R6Q6 A0A024R6T9 A0A024R9I2 A0A024RAP2 A0A024RAU7 A0A024RC53
A0A024RD15 A0A024RD21 A0A087WU84 A0A090N7W1 A0A0A0MRG0 A0A0A0MSK3 A0A0A0MT22 A0N0Q1 A1A4V4 A2A3U5 A2RUS0 A4D1Q0 A8K1F6 A8K249 A8K2Q2
A8K7N8 A8KAF4 A8KAG8 B0ZBE0 B2R7Y7 B3KP78 B4DN15 B7Z1L9 B8K2Q5 C1ID52 E5KQF5 F1D8N3 F1D8P8 F5H1T4 G5E9C5 H6VQ59 K9J958 L7RSL3 L7RXH5
O00408 O15440 O76074 O76083 P00533 P00918 P05177 P05181 P06239 P06241 P07550 P08173 P08246 P08311 P08588 P08684 P08913 P09871 P11229
P11509 P11712 P14780 P17252 P18545 P18825 P21397 P21452 P21554 P21728 P21917 P22303 P25021 P25024 P25025 P25101 P25103 P25929 P28223
P28482 P30411 P32238 P32245 P33032 P35354 P35367 P37288 P41143 P41595 P41968 P49146 P50052 P50406 P51160 P51681 Q01959 Q08209 Q08499
Q13946 Q13956 Q38Q88 Q9NPD5 Q9Y233 Q9Y6L6

CID 5215: sulfadiazine

A0A024QZY7 A0A024R2N2 A0A024R2Q0 A0A024R3C5 A0A024R3S2 A0A024R6T9 A0A024R9I2 A0A024RAP2 A0A024RD15 A0A087WU84 A0A090N7W1 A0A0A0MRG0
A0A0A0MSK3 A0A0A0MT22 A0A0A0MTJ0 A0N0Q1 A1A4V4 A2A3U5 A2RUS0 A4D1Q0 A8K1F6 A8K249 A8K7N8 A8KAF4 A8KAG8 B0ZBE0 B2R7Y7 B4DN15 B4DN83
B7Z1L9 B8K2Q5 C1ID52 E5KQF5 F1D8N3 F5H1T4 G5E9C5 H6VQ59 K9J958 L7RSL3 L7RXH5 O15296 P00533 P00918 P02545 P05177 P05181 P06239 P06241
P07550 P08173 P08246 P08311 P08588 P08684 P08913 P11229 P11509 P11712 P14780 P16050 P17252 P18054 P18825 P21397 P21452 P21554 P21728
P21917 P22303 P25021 P25024 P25025 P25101 P25103 P25929 P28223 P28482 P30411 P32238 P32245 P33032 P35354 P35367 P37288 P41143 P41595
P41968 P43220 P49146 P50052 P50406 P51681 P83916 Q01959 Q08209 Q38Q88 Q99714

CID 5245: risedronate

A0A024R2N2 A0A024R2Q0 A0A024R3C5 A0A024R3S2 A0A024R3W4 A0A024R6T9 A0A024R9I2 A0A024RAP2 A0A024RCN9 A0A024RD15 A0A087WU84 A0A087X090
A0A090N7W1 A0A0A0MRG0 A0A0A0MSK3 A0A0A0MT22 A0N0Q1 A1A4V4 A2A3U5 A2RUS0 A4D1Q0 A8K1F6 A8K249 A8K7N8 A8KAF4 A8KAG8 B0ZBE0 B2R7Y7
B4DN15 B7Z1L9 B8K2Q5 C1ID52 E5KQF5 F1D8N3 F5H1T4 G5E9C5 H6VQ59 K9J958 L7RSL3 L7RXH5 P00533 P00918 P05177 P05181 P06239 P06241 P07550
P08173 P08246 P08311 P08588 P08684 P08913 P11229 P11509 P11712 P14324 P14780 P17252 P18825 P21397 P21452 P21554 P21728 P21917 P22303
P25021 P25024 P25025 P25101 P25103 P25929 P28223 P28482 P30411 P32238 P32245 P33032 P35354 P35367 P37288 P41143 P41595 P41968 P49146
P50052 P50406 P51681 Q01959 Q08209 Q38Q88

CID 5253: sotalol

A0A024QZY7 A0A024R2N2 A0A024R2Q0 A0A024R3C5 A0A024R3S2 A0A024R5I4 A0A024R6T9 A0A024R9I2 A0A024RAP2 A0A024RAU7 A0A024RD15 A0A087WU84
A0A090N7W1 A0A0A0MRG0 A0A0A0MSK3 A0A0A0MT22 A0N0Q1 A1A4V4 A2A3U5 A2RUS0 A4D1Q0 A8K1F6 A8K249 A8K7N8 A8KAF4 A8KAG8 B0ZBE0 B2R7Y7
B2RXH2 B3KP78 B4DN15 B4DN83 B7Z1L9 B7ZKN7 B8K2Q5 C1ID52 E5KQF5 F1D8N3 F5H1T4 G5E9C5 H6VQ59 K9J958 L7RSL3 L7RXH5 O15245 O94925 P00533
P00918 P02545 P02768 P05177 P05181 P06239 P06241 P07550 P08173 P08246 P08311 P08588 P08684 P08913 P11229 P11509 P11712 P14780 P17252
P18825 P21397 P21452 P21554 P21728 P21917 P22303 P25021 P25024 P25025 P25101 P25103 P25929 P28223 P28482 P30411 P32238 P32245 P33032
P35354 P35367 P37288 P41143 P41595 P41968 P49146 P50052 P50406 P51681 P83916 Q01959 Q08209 Q38Q88 Q92887

CID 5291: imatinib

A0A024QYW7 A0A024QZ12 A0A024QZ20 A0A024QZ26 A0A024QZ70 A0A024QZA8 A0A024QZU0 A0A024QZU1 A0A024QZV1 A0A024QZY5 A0A024QZY7 A0A024R049
A0A024R0H9 A0A024R0I0 A0A024R0J1 A0A024R0L5 A0A024R0Q9 A0A024R183 A0A024R1H6 A0A024R230 A0A024R244 A0A024R2M7 A0A024R2N2 A0A024R2Q0
A0A024R2Y6 A0A024R328 A0A024R3C5 A0A024R3G7 A0A024R3S2 A0A024R3S3 A0A024R440 A0A024R452 A0A024R4B2 A0A024R567 A0A024R5E6 A0A024R5P0
A0A024R5W3 A0A024R5X5 A0A024R5Z3 A0A024R603 A0A024R6N2 A0A024R6T9 A0A024R704 A0A024R720 A0A024R728 A0A024R7E4 A0A024R7J0 A0A024R7M7

A0A024R7T2 A0A024R880 A0A024R8A6 A0A024R8E2 A0A024R8K3 A0A024R906 A0A024R964 A0A024R980 A0A024R9I2 A0A024R9Q4 A0A024R9Q5 A0A024RA66
A0A024RAH0 A0A024RAP2 A0A024RAP4 A0A024RAY5 A0A024RB10 A0A024RBB6 A0A024RBH0 A0A024RBL3 A0A024RBP6 A0A024RBU5 A0A024RBW9 A0A024RC92
A0A024RCE9 A0A024RCJ0 A0A024RD04 A0A024RD15 A0A024RD18 A0A024RD25 A0A024RD59 A0A024RD88 A0A024RDA0 A0A024RDD4 A0A024RDK3 A0A024RDL4
A0A024RDM3 A0A075B7B4 A0A087WSY1 A0A087WU84 A0A087WVC4 A0A087WW79 A0A087WZ06 A0A087X0I6 A0A090N7W1 A0A090N7W4 A0A0A0MQR8 A0A0A0MRG0
A0A0A0MS52 A0A0A0MSK3 A0A0A0MT22 A0N0Q1 A0PJF8 A0ZT98 A1A4V4 A1A5A9 A1L4K2 A2A3U5 A2RUF7 A2RUS0 A2VDG3 A3QNQ0 A4D1D2 A4D1Q0 A4D2J9
A4QPA9 A6PW57 A7E2E0 A8K161 A8K1F6 A8K249 A8K2S4 A8K341 A8K379 A8K3B6 A8K3J4 A8K4G3 A8K5M4 A8K602 A8K7I0 A8K7N8 A8K9L2 A8KAE3 A8KAE4
A8KAF4 A8KAG8 A8MWW6 B0AZM9 B0LPE5 B0YIY3 B0YJ89 B0ZBE0 B2R7Y7 B2RAP9 B2RCU6 B3KNJ3 B3KPX6 B3KQV3 B3KRI8 B3KRP1 B3KRV2 B3KS07 B3KS12
B3KS39 B3KUB4 B3KVM3 B3KWC4 B3KXJ4 B4DDG2 B4DER4 B4DER9 B4DEW2 B4DG22 B4DG79 B4DHI4 B4DII1 B4DK59 B4DLF9 B4DM55 B4DM56 B4DN15 B4DR80
B4DS37 B4DT73 B4DTW8 B4DUB1 B4DUC2 B4DUH8 B4DV95 B4DVP5 B4DX41 B4E058 B4E0X2 B4E0Y5 B6D4Y2 B7Z1G6 B7Z1L9 B7Z274 B7Z325 B7Z3V5 B7Z5K4
B7Z9H7 B7ZKJ3 B7ZLY6 B7ZM71 B8K2Q5 C1ID52 C9J5X1 C9JXA2 D2CGD1 D3DPA4 D3YTB5 D4Q8H0 E5KQF5 E7ESA6 E9PER6 E9PJX5 F1D8N3 F1T0G6 F2Z2J1
F5H1T4 F6U4U2 F8VBW7 F8WBA3 F8WCM8 G5E9C5 H6VQ59 H7BYT1 J3KMW1 J3KNB8 J3KNE8 J3KNN3 J3KRN4 K9J958 L7RSL3 L7RTI5 L7RXH5 M0R0W6 O00444
O14578 O14920 O14936 O14965 O15111 O15244 O15245 O15296 O43283 O43318 O43353 O60331 O60674 O75116 O75385 O75460 O75582 O75751 O76039
O94768 O94804 O94806 O95382 O95835 O96017 P00519 P00533 P00915 P00918 P02545 P02768 P04629 P05177 P05181 P06213 P06239 P06241 P07451
P07550 P07947 P08173 P08246 P08311 P08588 P08684 P08913 P08922 P09619 P09769 P0C1S8 P0C264 P10721 P11229 P11362 P11509 P11712 P12931
P14616 P14780 P15056 P16234 P16591 P17252 P18825 P19525 P19784 P21397 P21452 P21554 P21709 P21728 P21860 P21917 P22303 P22607 P22748
P23443 P23458 P24723 P25021 P25024 P25025 P25101 P25103 P25929 P27037 P28223 P28482 P29322 P29323 P30291 P30411 P31947 P32238 P32245
P32298 P33032 P33981 P35218 P35354 P35367 P35916 P36507 P36888 P36894 P36896 P36897 P37023 P37288 P39748 P41143 P41595 P41743 P41968
P42336 P42345 P42681 P42684 P42685 P43166 P43403 P45984 P45985 P46734 P49137 P49146 P49336 P49759 P49841 P50052 P50406 P50613 P51681
P51813 P51956 P51957 P53350 P53667 P54646 P54753 P54760 P54762 P57058 P68400 P78356 P78368 Q00526 Q01538 Q01959 Q02763 Q02779 Q04759
Q06187 Q06418 Q08209 Q08881 Q0IJ49 Q12866 Q13043 Q13131 Q13233 Q13464 Q13470 Q13547 Q13563 Q13627 Q13705 Q13873 Q13882 Q13976 Q14289
Q15303 Q15375 Q15418 Q15569 Q15746 Q15759 Q15831 Q15835 Q16288 Q16512 Q16513 Q16566 Q16659 Q16790 Q17RV3 Q2M2I8 Q32MK0 Q38Q88 Q4LE27
Q4VBY6 Q52WX2 Q53EW6 Q56UN5 Q5JXL9 Q5SQQ7 Q5VT25 Q6DT37 Q6P3R8 Q6PKF2 Q6XUX3 Q6ZN16 Q86UX6 Q86V86 Q86VL8 Q86YV6 Q8IW41 Q8IYT8 Q8N4C8
Q8N568 Q8N5S9 Q8N752 Q8NE63 Q8NEV4 Q8NFD2 Q8TD08 Q8TDC3 Q8TDR2 Q8WTQ7 Q92630 Q92918 Q96FL8 Q96GD4 Q96L34 Q96NX5 Q96Q40 Q96SB4 Q99683
Q9BRS2 Q9BVS4 Q9BX84 Q9BZL6 Q9H1R3 Q9H2G2 Q9H2K8 Q9H2X6 Q9H3Y6 Q9H4B4 Q9HAZ1 Q9NRP7 Q9NSY1 Q9NY57 Q9P289 Q9P2K8 Q9UBF8 Q9UEE5 Q9UEW8
Q9UHD2 Q9UK32 Q9UKE5 Q9UL54 Q9UPE1 Q9UQB9 Q9Y2H1 Q9Y2H9 Q9Y616 Q9Y6M4 V9GXZ4

CID 5314: succinylcholine

A0A024QZ30 A0A024QZY7 A0A024R040 A0A024R2N2 A0A024R2Q0 A0A024R325 A0A024R3C5 A0A024R3S2 A0A024R4H0 A0A024R6T9 A0A024R9I2 A0A024R9Y0
A0A024RAP2 A0A024RB43 A0A024RCN9 A0A024RD15 A0A087WU84 A0A090N7W1 A0A0A0MRG0 A0A0A0MSK3 A0A0A0MSK8 A0A0A0MT22 A0A0A6YYA8 A0N0Q1
A1A4V4 A2A3U5 A2RUS0 A4D0X1 A4D1Q0 A8K1F6 A8K249 A8K7N8 A8KAF4 A8KAG8 B0ZBE0 B2R7Y7 B4DF27 B4DK78 B4DN15 B4E1E9 B7Z1L9 B7ZKN7 B8K2Q5
C1ID52 C4IXS7 D3DNN4 E5KQF5 E5KS60 F1D8N3 F5H1T4 G5E9C5 H6VQ59 K9J958 L7RSL3 L7RXH5 O14521 O15460 O60568 O75874 O75936 P00533 P00918
P02708 P05177 P05181 P06239 P06241 P07550 P08173 P08246 P08311 P08588 P08684 P08913 P11229 P11509 P11712 P14780 P17252 P18825 P20309
P21397 P21452 P21554 P21728 P21912 P21917 P22303 P25021 P25024 P25025 P25101 P25103 P25929 P28223 P28482 P30411 P32238 P32245 P33032
P35354 P35367 P37288 P41143 P41595 P41968 P49146 P50052 P50406 P51681 P53597 Q01959 Q08209 Q13183 Q32P28 Q38Q88 Q8IVL5 Q8IVL6 Q99643
Q9BXA5 Q9BYC2 Q9NVH6

CID 5318: sulconazole

A0A024QZY7 A0A024R2N2 A0A024R2Q0 A0A024R3C5 A0A024R3S2 A0A024R6L5 A0A024R6T9 A0A024R9I2 A0A024RAP2 A0A024RD15 A0A087WU84 A0A090N7W1
A0A0A0MRG0 A0A0A0MSK3 A0A0A0MT22 A0N0Q1 A1A4V4 A2A3U5 A2RUS0 A4D1Q0 A8K1F6 A8K249 A8K7N8 A8KAF4 A8KAG8 B0ZBE0 B2R7Y7 B4DN15 B6ZGS9
B7Z1L9 B8K2Q5 C1ID52 E5KQF5 F1D8N3 F1D8P8 F1D8P9 F5H1T4 G5E9C5 H6VQ59 K9J958 L7RSL3 L7RXH5 O15296 O75604 O94782 P00533 P00918 P02545
P05177 P05181 P06239 P06241 P07550 P08173 P08246 P08311 P08588 P08684 P08913 P11229 P11509 P11712 P14780 P16050 P17252 P18825 P21397
P21452 P21554 P21728 P21917 P22303 P25021 P25024 P25025 P25101 P25103 P25929 P27695 P28223 P28482 P30411 P32238 P32245 P33032 P35354
P35367 P37288 P41143 P41595 P41968 P49146 P50052 P50406 P51681 Q01959 Q08209 Q38Q88 Q92830

CID 5320: sulfacetamide

A0A024QZY7 A0A024R4E2 A0A024R6L5 A0A024RDA5 A0A0A0MTJ0 B0YJ76 F1D8N5 O75874 P34949 P83916 Q92830 Q96FL8

CID 5344: sulfisoxazole

A0A024QZY7 A0A024R2N2 A0A024R2Q0 A0A024R3C5 A0A024R3S2 A0A024R6T9 A0A024R9I2 A0A024RAP2 A0A024RD15 A0A024RDA5 A0A087WU84 A0A090N7W1
A0A0A0MRG0 A0A0A0MSK3 A0A0A0MT22 A0A0A0MTJ0 A0N0Q1 A1A4V4 A2A3U5 A2RUS0 A4D1Q0 A8K1F6 A8K249 A8K7N8 A8KAF4 A8KAG8 B0ZBE0 B2R7Y7
B4DN15 B6ZGS9 B7Z1L9 B7Z242 B8K2Q5 C1ID52 E5KQF5 F1D8N3 F1D8N5 F1D8N7 F5H1T4 G5E9C5 H6VQ59 K9J958 L7RSL3 L7RXH5 P00533 P00918 P05177
P05181 P06239 P06241 P07550 P08173 P08246 P08311 P08588 P08684 P08913 P11229 P11509 P11712 P14780 P17252 P18825 P21397 P21452 P21554
P21728 P21917 P22303 P25021 P25024 P25025 P25101 P25103 P25929 P28223 P28482 P30411 P32238 P32245 P33032 P35354 P35367 P37288 P41143
P41595 P41968 P49146 P50052 P50406 P51681 Q01959 Q08209 Q38Q88

CID 5358: sumatriptan

A0A024R2N2 A0A024R2Q0 A0A024R3C5 A0A024R3S2 A0A024R6T9 A0A024R9I2 A0A024RAP2 A0A024RD15 A0A087WU84 A0A090N7W1 A0A0A0MRG0 A0A0A0MSK3
A0A0A0MT22 A0N0Q1 A1A4V4 A2A3U5 A2RUS0 A4D1D2 A4D1Q0 A8K1F6 A8K249 A8K5W4 A8K7N8 A8KAF4 A8KAG8 B0FWH2 B0ZBE0 B2R7Y7 B4DN15 B7Z1L9
B8K2Q5 C1ID52 E5KQF5 F1D8N3 F1D8P9 F5H1T4 G5E9C5 H6VQ59 K9J958 L7RSL3 L7RXH5 O15244 O15245 P00533 P00918 P05177 P05181 P06239 P06241
P07550 P08173 P08246 P08311 P08588 P08684 P08908 P08913 P11229 P11509 P11712 P14780 P17252 P18825 P21397 P21452 P21554 P21728 P21917
P22303 P22309 P25021 P25024 P25025 P25101 P25103 P25929 P28221 P28222 P28482 P28566 P30411 P30939 P30966 P31388 P32238 P32245 P32305
P33032 P34969 P35354 P35367 P37288 P41143 P41968 P47898 P49146 P50052 P51681 P83916 Q01959 Q08209 Q38Q88 Q96FL8

CID 5359: suprofen

A0A024R6T9 A0A087WU84 A0A087WWV0 B2R7Y7 B2RXH2 B8K2Q5 K9J958 P00352 P02545 P02768 P11712 P15428 P22309 P23219 P35354 P83916 Q92830

CID 5379: gatifloxacin

A0A024QZY7 A0A024R2N2 A0A024R2Q0 A0A024R3C5 A0A024R3S2 A0A024R6L5 A0A024R6T9 A0A024R9I2 A0A024RAP2 A0A024RD15 A0A087WU84 A0A090N7W1
A0A0A0MQX8 A0A0A0MRG0 A0A0A0MSK3 A0A0A0MT22 A0N0Q1 A1A4V4 A2A3U5 A2RUS0 A4D1Q0 A8K1F6 A8K249 A8K7N8 A8KAF4 A8KAG8 B0ZBE0 B2R7Y7
B2RXH2 B4DN15 B7Z1L9 B7Z1W5 B8K2Q5 C1ID52 E5KQF5 F1D8N3 F1D8P8 F5H1T4 G5E9C5 H6VQ59 K9J958 L7RSL3 L7RXH5 P00352 P00533 P00918 P02768
P05177 P05181 P06239 P06241 P07550 P08173 P08246 P08311 P08588 P08684 P08913 P11229 P11388 P11509 P11712 P14780 P15428 P16050 P17252
P18825 P21397 P21452 P21554 P21728 P21917 P22303 P25021 P25024 P25025 P25101 P25103 P25929 P27695 P28223 P28482 P30411 P32238 P32245
P33032 P35354 P35367 P37288 P39748 P41143 P41595 P41968 P49146 P50052 P50406 P51681 Q01959 Q02880 Q08209 Q38Q88 Q99714

CID 5381: tazarotene

A0A024QZY7 A0A024RCN9 A8K3H3 A8K840 B7Z7J5 F1D8S6 O94782 P10276 P10826 P13631 Q03164

CID 5391: temazepam

A0A024R9X6 A8K177 A8K496 A8MPY1 B2RCW8 B4DTP4 O60656 O76068 P02545 P06133 P16662 P18505 P18507 P19224 P22309 P24046 P28476 P31644
P34903 P36537 P47870 P48169 P78334 Q16445 Q8N1C3 Q99928 Q9UN88

CID 5401: terazosin

A0A024QZY7 A0A024R2N2 A0A024R2Q0 A0A024R3C5 A0A024R3S2 A0A024R6T9 A0A024R9I2 A0A024RAP2 A0A024RCN9 A0A024RD15 A0A068F658 A0A087WT22
A0A087WU84 A0A090N7W1 A0A0A0MRG0 A0A0A0MSK3 A0A0A0MT22 A0A0A0MTJ0 A0N0Q1 A1A4V4 A2A3U5 A2RUS0 A4D1Q0 A8K1F6 A8K249 A8K7N8 A8KAF4
A8KAG8 B0ZBD3 B0ZBE0 B2R7Y7 B2RXH2 B4DKC0 B4DN15 B4DN83 B7Z1L9 B8K2Q5 C1ID52 E5KQF5 F1D8N3 F5H1T4 G5E9C5 H6VQ59 K9J958 L7RSL3 L7RXH5
O15245 O75164 O75874 P00352 P00533 P00918 P02545 P05177 P05181 P06239 P06241 P06280 P07550 P08173 P08246 P08311 P08588 P08684 P08913
P10253 P11229 P11509 P11712 P14780 P15428 P17252 P17405 P18825 P21397 P21452 P21554 P21728 P21917 P22303 P25021 P25024 P25025 P25100
P25101 P25103 P25929 P27695 P28223 P28482 P30411 P32238 P32245 P33032 P35348 P35354 P35367 P35368 P37288 P41143 P41595 P41968 P42858
P49146 P50052 P50406 P51681 Q01959 Q08209 Q38Q88 Q92887 Q96QE3 Q99714 Q9NS40 Q9UIF8

CID 5403: terbutaline

A0A024R2N2 A0A024R2Q0 A0A024R3C5 A0A024R3S2 A0A024R6T9 A0A024R9I2 A0A024RAP2 A0A024RD15 A0A087WU84 A0A090N7W1 A0A0A0MRG0 A0A0A0MRL7
A0A0A0MSK3 A0A0A0MT22 A0A0A0MTJ0 A0N0Q1 A1A4V4 A2A3U5 A2RUS0 A4D1Q0 A8K1F6 A8K249 A8K7N8 A8KAF4 A8KAG8 B0ZBE0 B2R7Y7 B4DN15 B7Z1L9
B8K2Q5 C1ID52 D0VY79 D3DNN4 E5KQF5 F1D8N3 F5H1T4 G5E9C5 H6VQ59 K9J958 L7RSL3 L7RXH5 O15245 O94782 P00533 P00918 P02545 P05177 P05181
P06239 P06241 P08173 P08246 P08311 P08684 P08913 P11229 P11509 P11712 P14780 P17252 P18825 P21397 P21452 P21554 P21728 P21917 P22303
P25021 P25024 P25025 P25101 P25103 P25929 P28223 P28482 P30411 P32238 P32245 P33032 P35354 P35367 P35368 P37288 P41143 P41595 P41968 P49146
P50052 P50406 P51681 Q01959 Q03164 Q08209 Q38Q88

CID 5411: tetracaine

A0A024QZY7 A0A024R2N2 A0A024R2Q0 A0A024R3C5 A0A024R3S2 A0A024R6T9 A0A024R909 A0A024R9I2 A0A024RAP2 A0A024RBV5 A0A024RCN9 A0A024RD15
A0A068F658 A0A087WU84 A0A090N7W1 A0A0A0MRG0 A0A0A0MSK3 A0A0A0MT22 A0N0Q1 A1A4V4 A2A3U5 A2RUS0 A4D1D2 A4D1Q0 A8K1F6 A8K249 A8K7N8
A8KAF4 A8KAG8 B0ZBE0 B2R7Y7 B2RXH2 B4DN15 B7Z1L9 B7Z242 B7ZKN7 B8K2Q5 C1ID52 E5KQF5 E9PG18 F1D8N3 F5H1T4 G5E9C5 H6VQ59 K9J958 L7RSL3
L7RXH5 O15296 P00533 P00918 P02545 P05177 P05181 P06239 P06241 P07550 P08173 P08246 P08311 P08588 P08684 P08913 P11021 P11229 P11509
P11712 P14780 P17252 P17405 P18825 P21397 P21452 P21554 P21728 P21917 P22303 P25024 P25025 P25101 P25103 P25929 P28223 P28482
P30411 P32238 P32245 P33032 P35354 P35367 P37288 P41143 P41595 P41968 P49146 P50052 P50406 P51681 Q01453 Q01959 Q08209 Q15858 Q38Q88
Q92830 Q99250 Q99700 Q9UIF8 Q9Y5Y9

CID 5419: tetrahydrozoline

A0A024QZY7 A0A024R909 A0A024RAP4 B7ZKN7 C1ID52 O75874 P00352 P21728 P43220 P83916 Q96RJ0

CID 5426: thalidomide

A0A024QZY7 A0A024R2H8 A0A024R2N2 A0A024R2Q0 A0A024R3C5 A0A024R3S2 A0A024R6L5 A0A024R6T9 A0A024R9I2 A0A024RAP2 A0A024RCN9 A0A024RD15
A0A024RDJ4 A0A087WU84 A0A090N7W1 A0A0A0MRG0 A0A0A0MSK3 A0A0A0MT22 A0A0A0MTJ0 A0N0Q1 A1A4V4 A2A3U5 A2RUS0 A4D1Q0 A8K1F6 A8K249 A8K7N8
A8KAF4 A8KAG8 B0ZBE0 B2R7Y7 B4DN15 B7Z1L9 B7ZKN7 B8K2Q5 C1ID52 D2CGD1 E5KQF5 F1D8N3 F1D8N7 F5H1T4 G5E9C5 H6VQ59 K9J958 L7RSL3 L7RXH5
O00519 P00352 P00533 P00918 P01375 P05177 P05181 P06239 P06241 P06401 P07550 P08173 P08246 P08311 P08588 P08684 P08913 P11229 P11509
P11712 P14780 P17252 P18825 P21397 P21452 P21554 P21728 P21917 P22303 P25021 P25024 P25025 P25101 P25103 P25929 P28223 P28482 P30411
P32238 P32245 P33032 P35354 P35367 P37288 P41143 P41595 P41968 P49146 P50052 P50406 P51681 Q01959 Q08209 Q38Q88

CID 5430: thiabendazole

A0A024R1V0 A0A024R2N2 A0A024R2Q0 A0A024R3C5 A0A024R3S2 A0A024R6L5 A0A024R6T9 A0A024R9I2 A0A024R9Z8 A0A024RAP2 A0A024RBV5 A0A024RD15
A0A087WT22 A0A087WTS4 A0A087WU84 A0A090N7W1 A0A0A0MRG0 A0A0A0MSK3 A0A0A0MT22 A0A0A0MTJ0 A0N0Q1 A0N0X8 A1A4V4 A2A3U5 A2RUS0 A4D1Q0
A8K1F6 A8K249 A8K7N8 A8KAF4 A8KAG8 B0ZBE0 B2R7Y7 B2RXH2 B4DN15 B7Z1L9 B8K2Q5 C1ID52 D0VY79 E5KQF5 F1D8N3 F1D8N7 F1D8P6 F5H1T4 F8VQZ7
G5E9C5 H6VQ59 K9J958 L7RSL3 L7RXH5 O15118 P00533 P00918 P05177 P05181 P06239 P06241 P07550 P08173 P08246 P08311 P08588 P08684 P08913

P11229 P11509 P11712 P14780 P17252 P18825 P21397 P21452 P21554 P21728 P21917 P22303 P25021 P25024 P25025 P25101 P25103 P25929 P28223 P28482 P30411 P32238 P32245 P33032 P35354 P35367 P37288 P41143 P41595 P41968 P49146 P50052 P50406 P51681 P53582 Q01959 Q08209 Q38Q88 Q96FL8 Q96QE3 Q99700

CID 5452: thioridazine

A0A024QZY7 A0A024R2N2 A0A024R2Q0 A0A024R3C5 A0A024R3S2 A0A024R5I4 A0A024R5Z3 A0A024R6L5 A0A024R6T9 A0A024R909 A0A024R9I2 A0A024R9Y0 A0A024RAP2 A0A024RAU7 A0A024RBV5 A0A024RCN9 A0A024RD15 A0A024RD25 A0A087WT22 A0A087WU84 A0A090N7W1 A0A090N8Z1 A0A0A0MRG0 A0A0A0MSK3 A0A0A0MT22 A0A0A0MTJ0 A0N0Q1 A0PJF5 A1A4V4 A2A3U5 A2RUS0 A4D1Q0 A4D2N2 A8K1F6 A8K249 A8K4S9 A8K5W4 A8K7N8 A8KAF4 A8KAG8 B0ZBD3 B0ZBE0 B2KJ49 B2R7Y7 B2RXH2 B3KP78 B4DN15 B4E398 B7Z1L9 B7Z2G8 B8K2Q5 C1ID52 E5KQF5 F1D8N3 F5H1T4 F8W6L1 G5E9C5 H6VQ59 K9J958 L7RSL3 L7RXH5 O00325 O15118 O75164 O75874 O94782 P00352 P00533 P00918 P02545 P05177 P05181 P06239 P06241 P08173 P08246 P08311 P08684 P08908 P08913 P11229 P11509 P11712 P14780 P16050 P17252 P17405 P18825 P21397 P21452 P21554 P21728 P21917 P21918 P22303 P25021 P25024 P25025 P25101 P25103 P25929 P28221 P28222 P28223 P28335 P28482 P28566 P30411 P30939 P31388 P32238 P32245 P32297 P32305 P33032 P34969 P35354 P35367 P35368 P37288 P39748 P41143 P41595 P41968 P42345 P42858 P43220 P48542 P49146 P50052 P50406 P51681 P83916 Q01453 Q01959 Q03164 Q08209 Q15822 Q38Q88 Q92887 Q96QE3 Q99549 Q99700 Q99714 Q9UIF8 Q9UNA4

CID 5453: thiotepa

A0A024QZY7 A0A024R5I4 A0A024R6L5 A0A024R909 A0A024RAU7 A0A024RCN9 B3KP78 D9YZU5 F1D8P8 P02545 P08684 P09211 P15428 P20813 P83916 Q9UNA4

CID 5472: ticlopidine

A0A024R2N2 A0A024R2Q0 A0A024R3C5 A0A024R3C7 A0A024R3S2 A0A024R5I4 A0A024R6T9 A0A024R9I2 A0A024RAP2 A0A024RAP4 A0A024RAU7 A0A024RAV2 A0A024RCN9 A0A024RD15 A0A087WU84 A0A090N7W1 A0A090N8Z1 A0A0A0MRG0 A0A0A0MSK3 A0A0A0MT22 A0A0A0MTJ0 A0N0Q1 A1A4V4 A2A3U5 A2RUS0 A4D1Q0 A8K1F6 A8K249 A8K7N8 A8K7T1 A8KAF4 A8KAG8 B0ZBE0 B2R7Y7 B2RXH2 B3KP78 B4DN15 B7Z1L9 B8K2Q5 C1ID52 E5KQF5 F1D8N3 F5H1T4 G5E9C5 H6VQ59 K9J958 L7RSL3 L7RXH5 O75164 O75604 O75874 O95467 P00352 P00533 P00918 P02545 P05177 P05181 P06239 P06241 P07550 P08173 P08246 P08311 P08588 P08684 P08913 P11229 P11509 P11712 P14780 P17252 P18825 P20813 P21397 P21452 P21554 P21728 P21917 P22303 P25021 P25024 P25025 P25101 P25103 P25929 P28223 P28482 P30411 P32238 P32245 P33032 P35354 P35367 P37288 P41143 P41595 P41968 P43220 P49146 P50052 P50406 P51681 P83916 Q01959 Q08209 Q38Q88 Q96QE3 Q99700 Q9H244 Q9UIF8 Q9UNA4

CID 5479: tinidazole

A0A024R2N2 A0A024R2Q0 A0A024R3C5 A0A024R3S2 A0A024R4E2 A0A024R6T9 A0A024R9I2 A0A024RAP2 A0A024RD15 A0A087WU84 A0A090N7W1 A0A0A0MQX8 A0A0A0MRG0 A0A0A0MSK3 A0A0A0MT22 A0N0Q1 A1A4V4 A2A3U5 A2RUS0 A4D1Q0 A8K1F6 A8K249 A8K7N8 A8KAF4 A8KAG8 B0ZBE0 B2R7Y7 B4DN15 B7Z1L9 B8K2Q5 C1ID52 E5KQF5 F1D8N3 F5H1T4 G5E9C5 H6VQ59 K9J958 L7RSL3 L7RXH5 O15245 P00533 P00918 P02545 P05177 P05181 P06239 P06241 P07550 P08173 P08246 P08311 P08588 P08684 P08913 P11229 P11509 P11712 P14780 P17252 P18825 P21397 P21452 P21554 P21728 P21917 P22303 P25021 P25024 P25025 P25101 P25103 P25929 P28223 P28482 P30411 P32238 P32245 P33032 P35354 P35367 P37288 P41143 P41595 P41968 P49146 P50052 P50406 P51681 P83916 Q01959 Q08209 Q38Q88 Q92887

CID 5487: tizanidine

A0A024QZY7 A0A024R909 A0A024RCN9 A2RUS0 O00519 P02545 P05177 P08913 P18825 P83916 Q96QE3 Q9UIF8 Q9UNA4 Q9Y2I1

CID 5503: tolazamide

A0A024QZY7 A0A024R2N2 A0A024R2Q0 A0A024R3C5 A0A024R3K6 A0A024R3S2 A0A024R6T9 A0A024R9I2 A0A024R9Y0 A0A024RAP2 A0A024RCN9 A0A024RD15 A0A024RDJ4 A0A087WT22 A0A087WU84 A0A090N7W1 A0A0A0MRG0 A0A0A0MSK3 A0A0A0MT22 A0N0Q1 A1A4V4 A2A3U5 A2RUS0 A4D1Q0 A8K1F6 A8K249 A8K7N8 A8KAF4 A8KAG8 B0ZBE0 B2R7Y7 B2RXH2 B4DN15 B7Z1L9 B8K2Q5 C1ID52 E5KQF5 F1D8N3 F5H1T4 G5E9C5 H6VQ59 K9J958 L7RSL3 L7RXH5 O75164 O94782 O94925 P00352 P00533 P00918 P02768 P05177 P05181 P06239 P06241 P06280 P07550 P08173 P08246 P08311 P08588 P08684 P08913 P10253 P11229 P11509 P11712 P14780 P17252 P18054 P18825 P21397 P21452 P21554 P21728 P21917 P22303 P25021 P25024 P25025 P25101 P25103 P25929 P27695 P28223 P28482 P30411 P32238 P32245 P33032 P35354 P35367 P37288 P41143 P41595 P41968 P49146 P50052 P50406 P51681 P78508 Q01959 Q08209 Q38Q88 Q92830 Q9UIF8

CID 5523: tramadol

A0A024R2N2 A0A024R2Q0 A0A024R3C5 A0A024R3S2 A0A024R6T9 A0A024R9I2 A0A024RAP2 A0A024RAP4 A0A024RD15 A0A087WU84 A0A090N7W1 A0A0A0MRG0 A0A0A0MSK3 A0A0A0MT22 A0A0A6YYA8 A0N0Q1 A1A4V4 A2A3U5 A2RUS0 A4D1Q0 A8K1F6 A8K249 A8K7N8 A8KAF4 A8KAG8 B0ZBE0 B2R7Y7 B4DN15 B7Z1L9 B8K2Q5 C1ID52 E5KQF5 F1D8N3 F5H1T4 G5E9C5 H6VQ59 K9J958 L7RSL3 L7RXH5 O15245 P00533 P00918 P05177 P05181 P06239 P06241 P07550 P08173 P08246 P08311 P08588 P08684 P08913 P11229 P11509 P11712 P14780 P17252 P18825 P21397 P21452 P21554 P21728 P21917 P22303 P25021 P25024 P25025 P25101 P25103 P25929 P28223 P28482 P30411 P32238 P32245 P33032 P35354 P35367 P37288 P41143 P41595 P41968 P49146 P50052 P50406 P51681 Q01959 Q08209 Q38Q88 Q8TCU5 Q92887

CID 5533: trazodone

A0A024QZY7 A0A024R2N2 A0A024R2Q0 A0A024R3C5 A0A024R3S2 A0A024R6T9 A0A024R9I2 A0A024RAH7 A0A024RAP2 A0A024RCN9 A0A024RD15 A0A087WU84 A0A090N7W1 A0A0A0MRG0 A0A0A0MSK3 A0A0A0MT22 A0N0Q1 A0PJF5 A1A4V4 A2A3U5 A2RUS0 A4D1D2 A4D1Q0 A4D2N2 A8K1F6 A8K249 A8K5W4 A8K7N8 A8KAF4 A8KAG8 B0ZBD3 B0ZBE0 B2KJ49 B2R7Y7 B2RXH2 B4DK78 B4DN15 B4E398 B7Z1L9 B8K2Q5 C1ID52 D0VY79 E5KQF5 F1D8N3 F5H1T4 G5E9C5 H6VQ59 K9J958 L7RSL3 L7RXH5 O00325 O00519 O94782 P00352 P00533 P00918 P02545 P05177 P05181 P06239 P06241 P08246 P08311 P08684 P08909 P08913 P11509 P11712 P14780 P14842 P15428 P17252 P17405 P18825 P21397 P21452 P21728 P21917 P22303 P25021 P25024 P25025 P25101 P25103 P25929 P28221 P28223 P28335 P28482 P30411 P32238 P32245 P32297 P33032 P34969 P35354 P35367 P35368 P37288 P41595 P41968 P49146 P50052 P51681 P83916 Q08209 Q15822 Q38Q88 Q92830 Q99714

CID 5546: triamterene

A0A024QZY7 A0A024R2N2 A0A024R2Q0 A0A024R3C5 A0A024R3S2 A0A024R5Z3 A0A024R5Z9 A0A024R6L5 A0A024R6T9 A0A024R9I2 A0A024RAP2 A0A024RCN9 A0A024RCW6 A0A024RD15 A0A024RDA5 A0A024RDJ4 A0A068F658 A0A087WT22 A0A087WU84 A0A090N7W1 A0A0A0MQX8 A0A0A0MRG0 A0A0A0MRL7 A0A0A0MSK3 A0A0A0MT22 A0A0A0MTJ0 A0N0Q1 A1A4V4 A2A3U5 A2RUS0 A4D1D2 A4D1Q0 A5X2V1 A6NNF7 A8K1F6 A8K249 A8K7N8 A8KAF4 A8KAG8 B0ZBE0 B2R7Y7 B2R812 B2RXH2 B4DN15 B6ZGS9 B7Z1L9 B8K2Q5 C1ID52 D0VY79 D2KUA6 E5KQF5 F1D8N3 F1D8N5 F1D8N7 F1D8P8 F1D8Q5 F5H1T4 G5E9C5 H6VQ59 K9J958 L7RSL3 L7RXH5 O60674 O75874 P00352 P00533 P00918 P01375 P02545 P05177 P05181 P06239 P06241 P06280 P07550 P08173 P08246 P08311 P08588 P08684 P08913 P10253 P11229 P11509 P11712 P14780 P15428 P17252 P18054 P18825 P21397 P21452 P21554 P21728 P21917 P22303 P25021 P25024 P25025 P25101 P25103 P25929 P27695 P28223 P28482 P30411 P32238 P32245 P33032 P34969 P35354 P35367 P37288 P41143 P41595 P41968 P42345 P49146 P50052 P50406 P51168 P51170 P51681 P83916 Q01453 Q01959 Q08209 Q13526 Q38Q88 Q92830 Q96QE3 Q99700 Q99714

CID 5556: triazolam

A0A024R5I4 A0A024R9X6 A0A024RAU7 A8K177 A8K496 A8K7N8 A8MPY1 B2RCW8 B3KP78 B4DTP4 O76068 P08684 P14867 P18505 P18507 P24046 P28476 P31644 P34903 P47869 P47870 P48169 P78334 Q16445 Q8N1C3 Q99928 Q9UN88

CID 5566: trifluoperazine

A0A024QYX0 A0A024QZY7 A0A024R2N2 A0A024R2Q0 A0A024R3C5 A0A024R3S2 A0A024R5Z3 A0A024R6L5 A0A024R6T9 A0A024R909 A0A024R9I2 A0A024R9Y0 A0A024RAP2 A0A024RAP4 A0A024RBV5 A0A024RCN9 A0A024RD15 A0A024RDJ4 A0A068F658 A0A087WT22 A0A087WU84 A0A087WYZ4 A0A090N7W1 A0A090N8Z1 A0A0A0MQX8 A0A0A0MRG0 A0A0A0MRV2 A0A0A0MSK3 A0A0A0MT22 A0A0A0MTJ0 A0N0Q1 A1A4V4 A2A3U5 A2RUS0 A4D1D2 A4D1Q0 A6NGA6 A8K1F6 A8K249 A8K5W4 A8K7N8 A8KAF4 A8KAG8 B0ZBD3 B0ZBE0 B2R7Y7 B2RXH2 B4DN15 B7Z1L9 B7Z1W5 B7Z2G8 B8K2Q5 C1ID52 E5KQF5 E7ETZ0 F1D8N3 F1D8P8 F5H1T4 F8W6L1 G5E9C5 H6VQ59 K9J958 L7RSL3 L7RXH5 O15118 O15296 O75164 O75604 O75874 O94782 O95467 P00352 P00533 P00918 P02545 P02593 P05177 P05181 P06239 P06241 P07550 P08173 P08246 P08311 P08588 P08684 P08913 P11021 P11229 P11509 P11712 P14416 P14780 P16050 P17252 P18825 P20648 P21397 P21452 P21554 P21728 P21917 P22303 P22310 P25021 P25024 P25025 P25101 P25103 P25929 P26447 P28223 P28335 P28482 P30411 P30939 P32238 P32245 P33032 P34969 P35354 P35367 P37288 P41143 P41595 P41968 P42345 P42858 P43220 P47989 P49146 P50052 P50406 P51681 P61088 P63316 P78527 P83916 Q01453 Q01959 Q08209 Q16236 Q38Q88 Q92830 Q96QE3 Q99549 Q99700 Q99714 Q9BRL5 Q9HC16 Q9NYX4 Q9UIF8 Q9UNA4

CID 5572: trihexyphenidyl

A0A024R2N2 A0A024R2Q0 A0A024R3C5 A0A024R3S2 A0A024R6L5 A0A024R6T9 A0A024R909 A0A024R9I2 A0A024R9Y0 A0A024RAP2 A0A024RD15 A0A024RDJ4 A0A087WU84 A0A090N7W1 A0A0A0MRG0 A0A0A0MSK3 A0A0A0MT22 A0A0A0MTJ0 A0N0Q1 A1A4V4 A2A3U5 A2RUS0 A4D1Q0 A8K1F6 A8K249 A8K7N8 A8KAF4 A8KAG8 B0ZBE0 B2R7Y7 B4DN15 B7Z1L9 B7ZKN7 B8K2Q5 C1ID52 E5KQF5 F1D8N3 F5H1T4 G5E9C5 H6VQ59 K9J958 L7RSL3 L7RXH5 O15245 O15296 O75874 O94782 P00533 P00918 P05177 P05181 P06239 P06241 P07550 P08173 P08246 P08311 P08588 P08684 P08913 P11229 P11509 P11712 P14780 P17252 P17405 P18825 P21397 P21452 P21554 P21728 P21917 P22303 P25021 P25024 P25025 P25101 P25103 P25929 P27695 P28223 P28482 P30411 P32238 P32245 P33032 P35354 P35367 P37288 P41143 P41595 P41968 P49146 P50052 P50406 P51681 Q01453 Q01959 Q08209 Q38Q88 Q99700

CID 5578: trimethoprim

A0A024QZY7 A0A024R5I4 A0A024RAU7 A0A024RCN9 A0A024RDA5 A0A024RDJ4 A0A090N7W1 A0A0A0MTJ0 A4D1D2 B0YJ76 B3KP78 B7Z1F5 B7Z242 B7ZKN7 C1ID52 O15245 P00352 P04818 P05177 P08684 P11712 P21397 P21728 P83916 Q92887 Q96QE3 Q99714 Q9HBH1

CID 5591: troglitazone

A0A024QYT5 A0A024QZY7 A0A024R2N2 A0A024R2Q0 A0A024R3C5 A0A024R3S2 A0A024R6L5 A0A024R6T9 A0A024R909 A0A024R9I2 A0A024R9Y0 A0A024RAP2 A0A024RAU7 A0A024RAV2 A0A024RCN9 A0A024RCW6 A0A024RD15 A0A087WT22 A0A087WU84 A0A090N7W1 A0A0A0MRG0 A0A0A0MSK3 A0A0A0MT22 A0N0Q1 A1A4V4 A2A3U5 A2RUS0 A4D1Q0 A8K1F6 A8K249 A8K7N8 A8KAF4 A8KAG8 B0ZBE0 B2R7Y7 B4DN15 B6ZGS9 B7Z1F5 B7Z1L9 B7Z242 B7Z5E9 B8K2Q5 C1ID52 D2KUA6 E5KQF5 F1D8N3 F1D8N5 F1D8N7 F1D8P8 F1D8Q5 F1D8S4 F5H1T4 G5E9C5 H6VQ59 K9J958 L7RSL3 L7RXH5 O15245 O15296 O60341 O94782 O95342 P00533 P00918 P05177 P05181 P06239 P06241 P07550 P08173 P08246 P08311 P08588 P08684 P08913 P11229 P11474 P11509 P11712 P14780 P17252 P18825 P19224 P21397 P21452 P21554 P21728 P21917 P22303 P22309 P25021 P25024 P25025 P25101 P25103 P25929 P28223 P28482 P30411 P32238 P32245 P33032 P35354 P35367 P37231 P37288 P41143 P41595 P41968 P49146 P50052 P50225 P50406 P51681 Q01959 Q08209 Q38Q88 Q5DSZ6 Q5DT02 Q92830 Q99808 Q9HCF6

CID 5593: tropicamide

A0A024R2N2 A0A024R2Q0 A0A024R3C5 A0A024R3S2 A0A024R6L5 A0A024R6T9 A0A024R9I2 A0A024R9Y0 A0A024RAP2 A0A024RCN9 A0A024RD15 A0A024RDJ4 A0A087WU84 A0A090N7W1 A0A0A0MRG0 A0A0A0MSK3 A0A0A0MT22 A0A0A0MTJ0 A0N0Q1 A1A4V4 A2A3U5 A2RUS0 A4D1Q0 A8K1F6 A8K249 A8K7N8 A8KAF4 A8KAG8 B0ZBE0 B2R7Y7 B4DN15 B4DN83 B7Z1L9 B7ZKN7 B8K2Q5 C1ID52 E5KQF5 F1D8N3 F5H1T4 G5E9C5 H6VQ59 K9J958 L7RSL3 L7RXH5 P00533 P00918 P02545 P05177 P05181 P06239 P06241 P07550 P08173 P08246 P08311 P08588 P08684 P08913 P11229 P11509 P11712 P14780 P17252 P18825 P20309 P21397 P21452 P21554 P21728 P21917 P22303 P25021 P25024 P25025 P25101 P25103 P25929 P28223 P28482 P30411 P32238 P32245 P33032 P35354 P35367 P37288 P41143 P41595 P41968 P49146 P50052 P50406 P51681 Q01959 Q08209 Q38Q88 Q99714

CID 5625: delavirdine

C1ID52 O00519 O15438 P08684 P11712 P33527 Q92887

CID 5656: venlafaxine

A0A024QZY7 A0A024R2N2 A0A024R2Q0 A0A024R3C5 A0A024R3S2 A0A024R6T9 A0A024R9I2 A0A024RAP2 A0A024RCN9 A0A024RD15 A0A087WU84 A0A090N7W1
A0A0A0MRG0 A0A0A0MSK3 A0A0A0MT22 A0N0Q1 A1A4V4 A2A3U5 A2RUS0 A4D1D2 A4D1Q0 A8K1F6 A8K249 A8K5W4 A8K7N8 A8KAF4 A8KAG8 B0ZBD3 B0ZBE0
B2R7Y7 B4DN15 B7Z1L9 B8K2Q5 C1ID52 E5KQF5 F1D8N3 F5H1T4 G5E9C5 H6VQ59 K9J958 L7RSL3 L7RXH5 P00533 P00918 P02545 P05177 P05181 P06239
P06241 P07550 P08246 P08311 P08588 P08684 P11509 P11712 P14780 P17252 P18825 P21397 P21452 P21554 P21728 P21917 P22303 P23975 P25021
P25024 P25025 P25101 P25103 P25929 P28482 P30411 P31645 P32238 P32245 P33032 P35354 P37288 P41143 P41968 P49146 P50052 P50406 P51681
Q08209 Q38Q88

CID 5665: vigabatrin

A0A024RCN9 A0A024RDJ4 A0A0A0MTJ0 B7ZKN7 C1ID52 O94782 P21728 P80404 P83916 Q5SUJ9 Q92830 Q9H598

CID 5717: zafirlukast

A0A024QZY7 A0A024R2N2 A0A024R2Q0 A0A024R3C5 A0A024R3S2 A0A024R6L5 A0A024R6T9 A0A024R9I2 A0A024R9Y0 A0A024RAP2 A0A024RAP4 A0A024RAV2
A0A024RCN9 A0A024RD15 A0A087WU84 A0A090N7W1 A0A090N8Z1 A0A0A0MRG0 A0A0A0MSK3 A0A0A0MT22 A0N0Q1 A1A4V4 A2A3U5 A2RUS0 A4D1Q0 A8K1F6
A8K249 A8K7N8 A8KAF4 A8KAG8 B0ZBE0 B2R7Y7 B4DN15 B4E292 B7Z1F5 B7Z1L9 B7Z1W5 B8K2Q5 C1ID52 E5KQF5 F1D8N3 F1D8P8 F5H1T4 G5E9C5 H6VQ59
K9J958 L7RSL3 L7RXH5 O15244 O94782 P00533 P00918 P05177 P05181 P06239 P06241 P07550 P08173 P08246 P08311 P08588 P08684 P08913 P11229
P11509 P11712 P14780 P17252 P18825 P21397 P21452 P21554 P21728 P21917 P22303 P25021 P25024 P25025 P25101 P25103 P25929 P28223 P28482
P30411 P32238 P32245 P33032 P35354 P35367 P37288 P41143 P41595 P41968 P49146 P50052 P50406 P51681 Q01959 Q08209 Q15722 Q38Q88 Q5KU17
Q86VL8 Q92830 Q96FL8 Q9NS75 Q9UIF8 Q9Y271

CID 5719: zaleplon

A0A024R2N2 A0A024R2Q0 A0A024R3C5 A0A024R3S2 A0A024R6T9 A0A024R9I2 A0A024RAP2 A0A024RD15 A0A087WU84 A0A090N7W1 A0A0A0MRG0 A0A0A0MSK3
A0A0A0MT22 A0N0Q1 A1A4V4 A2A3U5 A2RUS0 A4D1Q0 A8K177 A8K1F6 A8K249 A8K7N8 A8KAF4 A8KAG8 B0ZBE0 B2R7Y7 B2RXH2 B4DN15 B7Z1L9 B8K2Q5
C1ID52 E5KQF5 F1D8N3 F5H1T4 G5E9C5 H6VQ59 K9J958 L7RSL3 L7RXH5 O76068 P00533 P00918 P05177 P05181 P06239 P06241 P07550 P08173 P08246
P08311 P08588 P08684 P08913 P11229 P11509 P11712 P14780 P17252 P18825 P21397 P21452 P21554 P21728 P21917 P22303 P25021 P25024 P25025
P25101 P25103 P25929 P28223 P28482 P30411 P32238 P32245 P33032 P35354 P35367 P37288 P41143 P41595 P41968 P49146 P50052 P50406 P51681
Q01959 Q06278 Q08209 Q38Q88 Q92830

CID 5732: zolpidem

A0A024R9X6 A8K177 B2RXH2 C1ID52 O76068 P02545 P05177 P08684 P11712 P14867 P15428 P31644 P34903 P47869 P48169 Q16445 Q99714

CID 5734: zonisamide

A0A024QZY7 A0A024R3H7 A0A024RBW9 A0A090N7W1 A8K3J4 B0YJ93 B3KQH9 B3KUB4 B4DUH8 B7Z1F5 B7Z242 B7ZKN7 E9PG18 O00519 O43497 O43570
O60939 O76068 P00915 P00918 P07451 P08684 P21397 P22748 P35218 P35219 P35498 P35499 P43166 Q06278 Q07699 Q15858 Q16790 Q8N1Q1 Q99250
Q9C007 Q9NS85 Q9P0X4 Q9UI33

CID 5735: zopiclone

A0A024R9X6 A0A024R9Y0 A0A024RAV2 A0A024RCN9 A0A0A0MQX8 A0A0A0MTJ0 A8K177 B7Z1F5 C1ID52 O00519 O76068 O94782 P05181 P08684 P31644
P34903

CID 5746: mitomycin C

A0A024QZY7 A0A024R2N2 A0A024R2Q0 A0A024R3C5 A0A024R3S2 A0A024R5Z3 A0A024R6L5 A0A024R6T9 A0A024R9I2 A0A024R9Y0 A0A024RAP2 A0A024RAP4
A0A024RD15 A0A087WT22 A0A087WU84 A0A087WYZ4 A0A090N7W1 A0A0A0MRG0 A0A0A0MSK3 A0A0A0MT22 A0N0Q1 A1A4V4 A2A3U5 A2RUS0 A4D1D2 A4D1Q0
A8K1F6 A8K249 A8K7N8 A8KAF4 A8KAG8 B0ZBE0 B2R7Y7 B2RXH2 B4DN15 B7Z1L9 B8K2Q5 C1ID52 E5KQF5 F1D8N3 F5H1T4 G5E9C5 H6VQ59 K9J958 L7RSL3
L7RXH5 O75874 O94782 O95467 P00352 P00533 P00918 P05177 P05181 P06239 P06241 P07550 P08173 P08246 P08311 P08588 P08684 P08913 P11229
P11509 P11712 P14780 P14902 P16435 P17252 P18825 P21397 P21452 P21554 P21728 P21917 P22303 P25021 P25024 P25025 P25101 P25103 P25929
P27695 P28223 P28482 P30411 P32238 P32245 P33032 P35354 P35367 P37288 P41143 P41595 P41968 P42858 P49146 P50052 P50406 P51681 Q01959
Q08209 Q38Q88 Q99700 Q9UNA4

CID 5775: phentolamine

A0A024R2N2 A0A024R2Q0 A0A024R3C5 A0A024R3S2 A0A024R6T9 A0A024R909 A0A024R9I2 A0A024R9Y0 A0A024RAP2 A0A024RCN9 A0A024RD15 A0A087WU84
A0A090N7W1 A0A0A0MRG0 A0A0A0MSK3 A0A0A0MT22 A0N0Q1 A1A4V4 A2A3U5 A2RUS0 A4D1Q0 A8K1F6 A8K249 A8K7N8 A8KAF4 A8KAG8 B0ZBD3 B0ZBE0
B2R7Y7 B4DN15 B7Z1L9 B8K2Q5 C1ID52 E5KQF5 F1D8N3 F5H1T4 G5E9C5 H6VQ59 K9J958 L7RSL3 L7RXH5 O75164 O94925 P00533 P00918 P01258 P01275
P02545 P05177 P05181 P06239 P06241 P07550 P08173 P08246 P08311 P08588 P08684 P08913 P11229 P11509 P11712 P14780 P17252 P18089 P18825
P21397 P21452 P21554 P21917 P22303 P25021 P25024 P25025 P25100 P25101 P25103 P25929 P27815 P28223 P28482 P30411 P32238 P32245 P33032
P35348 P35354 P35367 P35368 P37288 P41143 P41595 P41968 P43140 P43220 P49146 P50052 P50406 P51681 P83916 Q01959 Q08209 Q38Q88 Q96QE3
Q99700 Q9UIF8 Q9UNA4 Q9Y2I1

CID 5978: vincristine

A0A024QZY7 A0A024R2N2 A0A024R2Q0 A0A024R3C5 A0A024R3S2 A0A024R5I4 A0A024R5Z3 A0A024R6T9 A0A024R909 A0A024R9I2 A0A024RAP2 A0A024RAU7
A0A024RCN9 A0A024RD15 A0A024RD21 A0A087WT22 A0A087WU84 A0A090N7W1 A0A0A0MRG0 A0A0A0MSK3 A0A0A0MT22 A0N0Q1 A1A4V4 A2A3U5 A2RUS0
A4D1D2 A4D1Q0 A8K1F6 A8K249 A8K7N8 A8KAF4 A8KAG8 B0ZBE0 B2R7Y7 B3KP78 B4DMJ5 B4DN15 B4DXF8 B7Z1L9 B7Z3P6 B8K2Q5 C1ID52 D0VY79 E5KQF5
F1D8N3 F5H1T4 F8W6L1 G5E9C5 H6VQ59 K9J958 L7RSL3 L7RXH5 O15296 P00533 P00918 P02545 P05177 P05181 P06239 P06241 P07437 P07550 P08173
P08246 P08311 P08588 P08684 P08913 P11229 P11509 P11712 P14780 P16050 P17252 P18825 P21397 P21452 P21554 P21728 P21917 P22303 P25021
P25024 P25025 P25101 P25103 P25929 P28223 P28482 P30411 P32238 P32245 P33032 P33527 P35354 P35367 P37288 P41143 P41595 P41968 P42345
P42858 P49146 P50052 P50406 P51681 P68366 P83916 Q01959 Q08209 Q16236 Q38Q88 Q92887 Q96QE3 Q99700

CID 6018: tetrabenazine

A0A024R3C5 A0A024R9Y0 A0A0A0MTJ0 B2RXH2 B7Z1W5 F1D8P8 O15296 O75164 O94925 P00352 P15428 P28482 P39748 P42345 P43220 P54219 Q05940
Q96QE3 Q99714 Q9UNA4

CID 6049: EDTA

A0A024R6L5 A0A024RCN9 E5KQF5 O15296 Q16236

CID 6256: trifluorothymidine

A0A024QZY7 O75874 P02545 P04818 P18054 P43220 P83916 Q96QE3 Q99700 Q9UNA4

CID 6476: methsuximide

A0A024R9X6 A8K177 O43497 P31644 P32239 P34903 Q16445 Q9P0X4

CID 6503: Tris-HCl

A0A024R2N2 A0A024R2Q0 A0A024R3C5 A0A024R3S2 A0A024R6T9 A0A024R8U8 A0A024R9I2 A0A024R9I5 A0A024RAP2 A0A024RAP4 A0A024RBG6 A0A024RD15
A0A024RD33 A0A087WU84 A0A088AWN0 A0A090N7W1 A0A0A0MRG0 A0A0A0MSK3 A0A0A0MT22 A0N0Q1 A1A4V4 A2A3U5 A2RUS0 A4D1Q0 A8K1F6 A8K249 A8K7N8
A8KAF4 A8KAG8 B0ZBE0 B2R7Y7 B4DF30 B4DN15 B4DPF4 B7Z1L9 B7ZM24 B8K2Q5 C1ID52 E5KQF5 F1D8N3 F5H1T4 G5E9C5 H6VQ59 K9J958 L7RSL3 L7RXH5
P00533 P00918 P02545 P05177 P05181 P06239 P06241 P07550 P08173 P08246 P08311 P08588 P08684 P08913 P11229 P11509 P11712 P14780 P17252
P18825 P21397 P21452 P21554 P21728 P21917 P22303 P25021 P25024 P25025 P25101 P25103 P25929 P28223 P28482 P30411 P32238 P32245 P33032
P35354 P35367 P37288 P41143 P41595 P41968 P49146 P50052 P50406 P51681 Q01959 Q08209 Q38Q88 Q96FI4 Q9H2X9 Q9Y666

CID 6834: brompheniramine

A0A024R3S2 A0A024R9I2 A0A024RCN9 A0A024RDJ4 A0A090N7W1 A4D1Q0 A8K1F6 B7Z1L9 C1ID52 D0VY79 F5GWI4 F8W6L1 G5E9C5 P02545 P05177 P05181
P08173 P11229 P21728 P27815 P29275 P35367 P83916 Q07343 Q14432 Q16236 Q99700

CID 7638: 4-benzyloxyphenol

A0A024R2N2 A0A024R2Q0 A0A024R3C5 A0A024R3S2 A0A024R6T9 A0A024R9I2 A0A024RAP2 A0A024RD15 A0A087WU84 A0A090N7W1 A0A0A0MRG0 A0A0A0MSK3
A0A0A0MT22 A0N0Q1 A1A4V4 A2A3U5 A2RUS0 A4D1Q0 A8K1F6 A8K249 A8K7N8 A8KAF4 A8KAG8 B0ZBE0 B2R7Y7 B4DN15 B7Z1L9 B8K2Q5 C1ID52 D0VY79
E5KQF5 F1D8N3 F5H1T4 G5E9C5 H6VQ59 K9J958 L7RSL3 L7RXH5 L8B082 P00533 P00918 P02545 P05177 P05181 P06239 P06241 P07550 P08173 P08246
P08311 P08588 P08684 P08913 P11229 P11509 P11712 P14679 P14780 P17252 P18825 P21397 P21452 P21554 P21728 P21917 P22303 P25021 P25024
P25025 P25101 P25103 P25929 P28223 P28482 P30411 P32238 P32245 P33032 P35354 P35367 P37288 P41143 P41595 P41968 P49146 P50052 P50406
P51681 Q01959 Q08209 Q38Q88

CID 7699: benzonatate

A0A024QZY7 E9PG18 O75874 P08684 P83916 Q14524 Q92830 Q96QE3

CID 8271: mephobarbital

A0A024R9X6 A0A024RCN9 A0A0A6YYA8 A8K177 B4DK78 P02545 P14867 P20813 P31644 P34903 P42262 P48169 Q16445

CID 8612: chloroprocaine

B4E398 C4IXS7 P05023 Q01959 Q8TCU5 Q9Y5Y9

CID 10100: propoxyphene

A0A087WU84 A0A090N7W1 A4D2N2 B8K2Q5 C1ID52 P41143 P83916

CID 10413: gamma-hydroxybutyrate

A0A024R8U1 A0A024RBB2 P18505 Q9BXC0 Q9HAB3

CID 12555: benzydamine

B2RXH2 B7Z1W5 C1ID52 O15296 O75874 P43220 P83916

CID 16362: pimozide

A0A024QZY7 A0A024R3C5 A0A024R3S2 A0A024R4E2 A0A024R6L5 A0A024R9Y0 A0A024RAP4 A0A024RBV5 A0A024RCN9 A0A024RCW6 A0A024RDJ4 A0A087WT22
A0A087WV24 A0A090N7W1 A0A090N8Z1 A0A0A0MTJ0 A1A4V4 A2RUS0 A4D1D2 A8K5W4 A8KAF4 B0ZBD3 B2R7Y7 B2RXH2 B6ZGS9 B7Z1F5 B7ZKN7 B8K2Q5
C1ID52 D0VY79 D2KUA6 E7ETZ0 F1D8N5 F1D8N7 F1D8P8 F1D8Q5 F8W6L1 K9J958 O15244 O15296 O43497 O54898 O75164 O75604 O75874 O94782 P00352
P02545 P05177 P08684 P08908 P08913 P11021 P11229 P11712 P14416 P16050 P17405 P18825 P19020 P20813 P21917 P27695 P28221 P28223 P28482
P31388 P32305 P34969 P35367 P35462 P41143 P42345 P42858 P43220 P48542 P50406 P61169 P83916 Q01453 Q16322 Q86VL8 Q96FL8 Q96QE3 Q99549
Q99700 Q9BRL5 Q9EQ60 Q9P0X4 Q9UIF8 Q9UNA4

CID 23897: molindone

A0A024R3C5 A0A024R3S2 A0A024R909 A0A024RCN9 A1A4V4 A2RUS0 A8K5W4 B0ZBD3 B7ZKN7 K9J958 O94782 P02545 P08684 P08913 P11229 P14416
P18825 P21728 P21917 P28223 P30939 P34969 P50406 P83916 Q99549

CID 25419: clodronate

A0A024R6R4 A0A024RCN9 A8K3M3 B2RXH2 O15245 P05141 P08254 P12235 P12236 P14780 P39900 P83916 Q03164 Q13526 Q99549

CID 27400: pizotifen

A0A024R3C5 A8K5W4 K9J958 P02545 P08908 P11229 P28223 P34969 P41595

CID 27661: isosorbide-5-mononitrate
B7Z242 P00915 P00918 P08684 P16066 P22748 P33402 Q02108 Q02153
CID 30623: dexrazoxane
A0A024RCN9 F1D8P8 P02545 P11388 P39748 Q02880 Q9UNA4
CID 34312: oxcarbazepine
A0A024QZY7 A0A024R2N2 A0A024R2Q0 A0A024R3C5 A0A024R3S2 A0A024R6T9 A0A024R9C1 A0A024R9I2 A0A024R9Y0 A0A024RAP2 A0A024RAP4 A0A024RCN9
A0A024RD15 A0A087WU84 A0A090N7W1 A0A0A0MRG0 A0A0A0MSK3 A0A0A0MT22 A0N0Q1 A1A4V4 A2A3U5 A2RUS0 A4D1Q0 A8K1F6 A8K249 A8K7N8 A8KAF4
A8KAG8 B0ZBE0 B2R7Y7 B2RXH2 B4DN15 B7Z1L9 B7ZKN7 B8K2Q5 C1ID52 E5KQF5 E9PG18 F1D8N3 F1D8P8 F5H1T4 G5E9C5 H6VQ59 K9J958 L7RSL3 L7RXH5
O94782 P00352 P00533 P00918 P05177 P05181 P06239 P06241 P07550 P08173 P08246 P08311 P08588 P08684 P08913 P11229 P11509 P11712 P14780
P17252 P18825 P21397 P21452 P21554 P21728 P21917 P22303 P25021 P25024 P25025 P25101 P25103 P25929 P28223 P28482 P30411 P32238 P32245
P33032 P35354 P35367 P37288 P41143 P41595 P41968 P49146 P50052 P50406 P51681 Q01959 Q03164 Q08209 Q38Q88 Q8NDX3 Q99571
CID 36811: dobutamine
A0A024QZY7 A0A024R2N2 A0A024R2Q0 A0A024R3C5 A0A024R3S2 A0A024R6T9 A0A024R9I2 A0A024R9Y0 A0A024RAP2 A0A024RBW9 A0A024RCN9 A0A024RD15
A0A024RDJ4 A0A087WU84 A0A090N7W1 A0A0A0MRG0 A0A0A0MSK3 A0A0A0MT22 A0A0A0MTJ0 A0N0Q1 A1A4V4 A2A3U5 A2RUS0 A4D1Q0 A8K1F6 A8K249 A8K3J4
A8K7N8 A8KAF4 A8KAG8 B0ZBE0 B2R7Y7 B2RXH2 B3KUB4 B4DN15 B4DUH8 B7Z1L9 B8K2Q5 C1ID52 D0VY79 E5KQF5 F1D8N3 F5H1T4 F8W6L1 G5E9C5 H6VQ59
K9J958 L7RSL3 L7RXH5 O75874 O94925 P00533 P00915 P00918 P02545 P05177 P05181 P06239 P06241 P07451 P07550 P08173 P08246 P08311 P08588
P08684 P08913 P11021 P11229 P11509 P11712 P14780 P17252 P18825 P21397 P21452 P21554 P21728 P21917 P21964 P22303 P22748 P25021 P25024
P25025 P25101 P25103 P25929 P28223 P28482 P30411 P32238 P32245 P33032 P35218 P35354 P35367 P37288 P41143 P41595 P41968 P42858 P43166
P49146 P50052 P50406 P51681 P83916 Q01453 Q01959 Q08209 Q16790 Q38Q88 Q8N1Q1 Q99549 Q99700 Q99714 Q9GZV3
CID 39042: bezafibrate
A0A024R2N2 A0A024R2Q0 A0A024R3C5 A0A024R3S2 A0A024R6T9 A0A024R9I2 A0A024RAP2 A0A024RCW6 A0A024RD15 A0A087WU84 A0A090N7W1 A0A0A0MRG0
A0A0A0MSK3 A0A0A0MT22 A0N0Q1 A1A4V4 A2A3U5 A2RUS0 A4D1Q0 A8K1F6 A8K249 A8K7N8 A8KAF4 A8KAG8 B0ZBE0 B2R7Y7 B4DN15 B6ZGS9 B7Z1L9
B8K2Q5 C1ID52 D2KUA6 E5KQF5 F1D8N3 F1D8S4 F5H1T4 G5E9C5 H6VQ59 K9J958 L7RSL3 L7RXH5 P00352 P00533 P00918 P02741 P05177 P05181 P06239
P06241 P07550 P08173 P08246 P08311 P08588 P08684 P08913 P11229 P11509 P11712 P14780 P17252 P18825 P21397 P21452 P21554 P21728 P21917
P22303 P23141 P25021 P25024 P25025 P25101 P25103 P25929 P28223 P28482 P30411 P32238 P32245 P33032 P35354 P35367 P37288 P39748 P41143
P41595 P41968 P49146 P50052 P50406 P51681 P83916 Q01959 Q07869 Q08209 Q38Q88 Q8TE04
CID 41684: nitazoxanide
A0A024QZY7 A0A024R5Z9 A0A024R9Y0 A0A024R9Z8 A0A024RAP4 A0A024RBV5 A0A024RCN9 A0A024RCW6 A0A087WT22 A0A090N8Z1 A0A0A0MQX8 A0A0A0MTJ0
A8KAF4 B6ZGS9 D2KUA6 E5KQF5 F1D8N5 F1D8P6 F1D8P8 F1D8Q5 O15118 P00352 P02545 P08684 P28482 P42858 Q92830 Q99714 Q9UIF8
CID 41693: sufentanil
A0A087WU84 A4D1D2 B8K2Q5 P33535 P35372 P41143
CID 41781: torasemide
A0A024R2N2 A0A024R2Q0 A0A024R3C5 A0A024R3S2 A0A024R4E2 A0A024R6T9 A0A024R9I2 A0A024RAP2 A0A024RD15 A0A087WU84 A0A090N7W1 A0A0A0MRG0
A0A0A0MSK3 A0A0A0MT22 A0N0Q1 A1A4V4 A2A3U5 A2RUS0 A4D1Q0 A8K1F6 A8K249 A8K7N8 A8KAF4 A8KAG8 B0ZBE0 B2R7Y7 B2RXH2 B4DN15 B4DPF4
B7Z1F5 B7Z1L9 B8K2Q5 C1ID52 D0VY79 E5KQF5 F1D8N3 F5H1T4 G5E9C5 H6VQ59 K9J958 L7RSL3 L7RXH5 P00533 P00918 P05177 P05181 P06239 P06241
P07550 P08173 P08246 P08311 P08588 P08684 P08913 P11229 P11509 P11712 P14780 P17252 P18825 P21397 P21452 P21554 P21728 P21917 P22303
P25021 P25024 P25025 P25101 P25103 P25929 P28223 P28482 P30411 P32238 P32245 P33032 P35354 P35367 P37288 P41143 P41595 P41968 P49146
P50052 P50406 P51681 Q01959 Q08209 Q13621 Q38Q88
CID 42113: desflurane
A8K177 B4E295 P03886 P23415 P30049 P42261 P47989 Q09470
CID 47641: naftifine
A0A024QYX0 A0A024R3C7 A0A0A0MTJ0 C1ID52 D0VY79 O15296 O75874 P02545 P42858 P43220 P83916 Q14534 Q16236 Q9UIF8 Q9Y468
CID 50294: nedocromil sodium
K9JA46 P21462 P35367 Q13258 Q38Q88 Q5KU17
CID 51263: alfentanil
A4D1D2 A4D2N2 B7Z242 B7Z3P6 B8K2Q5 P02763 P02768 P08684 P21397 P35372 P41143 P83916
CID 51634: miglustat
A0A024R157 A0A068F658 B4DIW2 P02545 P10253 P28482 Q16739 Q9HCG7 Q9UNA4
CID 54454: simvastatin
A0A024QYT5 A0A024QZY7 A0A024R2N2 A0A024R2Q0 A0A024R324 A0A024R3C5 A0A024R3S2 A0A024R4E2 A0A024R5I4 A0A024R5Z3 A0A024R6T9 A0A024R909
A0A024R9I2 A0A024R9Y0 A0A024RAP2 A0A024RAU7 A0A024RD15 A0A024RD33 A0A024RDA5 A0A087WT22 A0A087WU84 A0A090N7W1 A0A0A0MRG0 A0A0A0MSK3
A0A0A0MT22 A0A0A0MTJ0 A0N0Q1 A1A4V4 A2A3U5 A2RUS0 A4D1D2 A4D1Q0 A4D2P0 A8K1F6 A8K249 A8K7N8 A8KAF4 A8KAG8 B0ZBE0 B0ZBE2 B2R7Y7
B2RXH2 B3KP78 B4DN15 B4DNQ5 B4E0R1 B7Z1F5 B7Z1L9 B8K2Q5 C1ID52 C8C060 E5KQF5 F1D8N3 F1D8P8 F1D8S4 F5H1T4 G5E9C5 H6VQ59 K9J958 L7RSL3
L7RXH5 O15245 O75164 O75604 O75874 O94782 P00352 P00533 P00734 P00918 P01375 P01579 P02545 P04035 P05177 P05181 P05362 P06239 P06241
P06280 P07550 P08173 P08246 P08254 P08311 P08588 P08684 P08913 P11229 P11509 P11712 P13500 P14780 P16050 P17252 P18825 P21397 P21452
P21554 P21728 P21917 P22303 P25021 P25024 P25025 P25101 P25103 P25929 P27695 P28223 P28482 P30411 P32238 P32245 P33032 P35354 P35367
P37288 P41143 P41595 P41968 P42574 P49146 P50052 P50406 P51639 P51681 Q01959 Q06643 Q08209 Q38Q88 Q5TAT6 Q92887 Q9HC16 Q9UIF8
CID 56959: ranolazine
A0A024R5I4 A0A024RAU7 A0A024RCN9 A0A024RDJ4 A0A090N8Z1 A0A0A0MTJ0 A4D1D2 B3KP78 B4DN83 B7ZKN7 C1ID52 E9PG18 O75164 P02545 P08684
P83916 Q01453 Q15858 Q16236 Q9UNA4 Q9Y5Y9
CID 57469: imiquimod
A0A024QZY7 A0A024R2N2 A0A024R2Q0 A0A024R3C5 A0A024R3S2 A0A024R6T9 A0A024R9I2 A0A024RAP2 A0A024RD15 A0A087WU84 A0A090N7W1 A0A0A0MRG0
A0A0A0MSK3 A0A0A0MT22 A0N0Q1 A1A4V4 A2A3U5 A2RUS0 A4D1Q0 A8K1F6 A8K249 A8K7N8 A8KAF4 A8KAG8 B0ZBE0 B2R7Y7 B2R9N9 B4DN15 B7Z1L9
B7Z1W5 B8K2Q5 C1ID52 E5KQF5 F1D8N3 F5H1T4 G5E9C5 H6VQ59 K9J958 L7RSL3 L7RXH5 P00533 P00918 P02545 P05177 P05181 P06239 P06241 P07550
P08173 P08246 P08311 P08588 P08684 P08913 P11229 P11509 P11712 P14780 P17252 P18825 P21397 P21452 P21554 P21728 P21917 P22303 P25021
P25024 P25025 P25101 P25103 P25929 P28223 P28482 P30411 P32238 P32245 P33032 P35354 P35367 P37288 P41143 P41595 P41968 P49146 P50052
P50406 P51681 Q01959 Q08209 Q38Q88 Q9NR97 Q9NYK1
CID 59708: levetiracetam
A0A024RCN9 A4D1D2 B4E000 O43497 P00915 P02545 P35498 P39748 Q00975 Q92830 Q92887
CID 59768: esmolol
A0A024QZY7 A0A024R2N2 A0A024R2Q0 A0A024R3C5 A0A024R3S2 A0A024R6T9 A0A024R9I2 A0A024RAP2 A0A024RD15 A0A087WU84 A0A090N7W1 A0A0A0MRG0
A0A0A0MSK3 A0A0A0MT22 A0N0Q1 A1A4V4 A2A3U5 A2RUS0 A4D1Q0 A8K1F6 A8K249 A8K7N8 A8KAF4 A8KAG8 B0ZBE0 B2R7Y7 B4DN15 B7Z1L9 B8K2Q5
C1ID52 E5KQF5 F1D8N3 F5H1T4 G5E9C5 H6VQ59 K9J958 L7RSL3 L7RXH5 O15245 P00533 P00918 P05177 P05181 P06239 P06241 P07550 P08173 P08246
P08311 P08588 P08684 P08913 P11229 P11509 P11712 P14780 P17252 P18825 P21397 P21452 P21554 P21728 P21917 P22303 P25021 P25024 P25025
P25101 P25103 P25929 P28223 P28482 P30411 P32238 P32245 P33032 P35354 P35367 P37288 P41143 P41595 P41968 P49146 P50052 P50406 P51681
Q01959 Q08209 Q38Q88
CID 60164: adapalene
A0A024QZY7 A0A024R6L5 A0A087WZ88 A8K3H3 A8K840 B7Z7J5 B7ZKN7 F1D8Q5 F1D8S6 O94782 P02545 P10276 P10826 P13631
CID 60198: exemestane
A0A024R5S8 A0A024RCN9 B2RXH2 P00352 P08684 P11511
CID 60726: bromfenac
A0A024R2N2 A0A024R2Q0 A0A024R3C5 A0A024R3S2 A0A024R6T9 A0A024R9I2 A0A024RAP2 A0A024RD15 A0A087WU84 A0A090N7W1 A0A0A0MRG0 A0A0A0MSK3
A0A0A0MT22 A0N0Q1 A1A4V4 A2A3U5 A2RUS0 A4D1Q0 A8K1F6 A8K249 A8K5Z0 A8K7N8 A8KAF4 A8KAG8 B0ZBE0 B2R7Y7 B2RAZ5 B4DN15 B7Z1L9 B8K2Q5
C1ID52 C9JEV6 E5KQF5 F1D8N3 F5H1T4 G5E9C5 H6VQ59 K9J958 L7RSL3 L7RXH5 O60909 P00533 P00918 P02545 P05177 P05181 P06239 P06241 P07550
P08173 P08246 P08311 P08588 P08684 P08913 P11229 P11509 P11712 P14780 P15291 P17252 P18825 P21397 P21452 P21554 P21728 P21917 P22303
P23219 P25021 P25024 P25025 P25101 P25103 P25929 P28223 P28482 P30411 P32238 P32245 P33032 P35354 P35367 P37288 P41143 P41595 P41968
P49146 P50052 P50406 P51606 P51681 P54802 Q01959 Q08209 Q38Q88 Q9UK23
CID 60753: ibutilide
A0A024R3T2 A0A090N7W1 A0A0A0MR67 B2RC52 B2RDS2 B4DKC0 E7ERK3 Q02641 Q06432 Q12809 Q13936 Q9NS40
CID 60795: aripiprazole
A0A024QZY7 A0A024R3C5 A0A024R3S2 A0A024R6L5 A0A024R6T9 A0A024R9I2 A0A024R9Y0 A0A024RCN9 A0A087WU84 A0A090N7W1 A0A090N8Z1 A0PJF5
A1A4V4 A2RUS0 A4D1D2 A4D1Q0 A4D2N2 A8K5W4 B0ZBD3 B2KJ49 B2R7Y7 B4DN83 B4E398 B8K2Q5 C1ID52 K9J958 O00325 O15244 O75164 O94782 P07550
P08173 P08588 P08684 P08908 P08913 P10253 P11021 P11229 P14416 P14842 P17252 P18825 P21728 P21917 P21918 P28221 P28222 P28223 P28335
P28566 P30729 P31388 P32297 P32305 P34969 P35367 P35368 P41595 P50406 P61169 Q01959 Q15822 Q86VL8 Q92830 Q96FL8
CID 60843: pemetrexed
A0A024QZ15 A0A024R5H1 A0A024RAP4 B0YJ76 F5CTF3 O94782 P00374 P04818 P14207 P22102 P31939 P34896 P41440 Q64737
CID 60852: ibandronate
A0A024R3W4 A0A087X090 P05369 P14324 P39748 Q02769
CID 60877: emtricitabine
A0A024R5I4 A0A024RAU7 B3KP78 O15438 P33527 Q92887
CID 60953: capecitabine
B2RBL3 O00519 P02545 P04818 P11712 P23141 P32320 Q12882
CID 65863: sertaconazole
A0A024R6L5 C1ID52 F1D8P8 O15296 P02545 P08684 P11712
CID 65999: telmisartan
A0A024R4E2 A0A024R5I4 A0A024RAU7 A0A024RCN9 A0A024RCW6 A0A090N8Z1 A0A0A0MSE3 B2RXH2 B3KP78 B4DKH4 D2KUA6 F1D8P8 F1D8S4 O00167 O75604
O75874 O94782 O95467 P00352 P02545 P08684 P28482 P30556 Q96FL8 Q99714
CID 68740: zoledronic acid

A0A024R3W4 A0A024R6R4 A0A087X090 P02545 P05369 P14324 P14780 P22894 P33527 P50281
CID 68844: brinzolamide
A0A024RBW9 A8K3J4 B3KUB4 B4DUH8 O43570 P00915 P00918 P02545 P07451 P22748 P35218 P43166 P83916 Q16790 Q8N1Q1 Q9UIF8 Q9ULX7
CID 71158: acamprosate
A4D1D0 A8K177 A8K5P7 Q05586 Q13255 Q8TCU5
CID 71329: dofetilide
A0A024R5I4 A0A024RAU7 A0A090N7W1 B3KP78 C1ID52 O94925 O95069 O95259 P05177 P08684 P11712 Q12809 Q14500
CID 71616: voriconazole
A0A087X0W8 B7Z1F5 C1ID52 P02545 P05177 P08684 P11509 P11712 P20813 P28482 P43220
CID 71771: aceclofenac
A0A024QZY7 A0A024R2N2 A0A024R2Q0 A0A024R3C5 A0A024R3S2 A0A024R6T9 A0A024R9I2 A0A024RAP2 A0A024RD15 A0A087WU84 A0A090N7W1 A0A0A0MRG0
A0A0A0MSK3 A0A0A0MT22 A0N0Q1 A1A4V4 A2A3U5 A2RUS0 A4D1Q0 A8K1F6 A8K249 A8K7N8 A8KAF4 A8KAG8 B0ZBE0 B2R7Y7 B4DN15 B7Z1L9 B8K2Q5
C1ID52 E5KQF5 F1D8N3 F5H1T4 G5E9C5 H6VQ59 K9J958 L7RSL3 L7RXH5 O75604 O94925 P00533 P00918 P02545 P05177 P05181 P06239 P06241 P07550
P08173 P08246 P08311 P08588 P08684 P08913 P11229 P11509 P11712 P14780 P17252 P18825 P21397 P21452 P21554 P21728 P21917 P22303 P25021
P25024 P25025 P25101 P25103 P25929 P28223 P28482 P30411 P32238 P32245 P33032 P35354 P35367 P37288 P41143 P41595 P41968 P49146 P50052
P50406 P51681 P83916 Q01959 Q03164 Q08209 Q38Q88
CID 77993: eletriptan
A0A024R5I4 A0A024RAU7 A4D1D2 A8K5W4 B3KP78 O94925 P08684 P08908 P28221 P28222 P28566 P30939 P34969 P41595
CID 77999: rosiglitazone
A0A024QZY7 A0A024R2N2 A0A024R2Q0 A0A024R3C5 A0A024R3S2 A0A024R5I4 A0A024R6T9 A0A024R7C0 A0A024R9I2 A0A024RAP2 A0A024RAU7 A0A024RCW6
A0A024RD15 A0A087WU84 A0A090N7W1 A0A0A0MRG0 A0A0A0MSK3 A0A0A0MT22 A0N0Q1 A1A4V4 A2A3U5 A2RUS0 A4D1Q0 A8K1F6 A8K249 A8K7N8 A8KAF4
A8KAG8 B0ZBE0 B2R7Y7 B2RXH2 B3KP78 B4DN15 B7Z1F5 B7Z1L9 B7Z242 B8K2Q5 C1ID52 E5KQF5 F1D8N3 F1D8S4 F5H1T4 G5E9C5 H6VQ59 K9J958 L7RSL3
L7RXH5 O14842 O60341 O75164 O94782 P00533 P00918 P02545 P05177 P05181 P06239 P06241 P07550 P08173 P08246 P08311 P08588 P08684 P08913
P11229 P11509 P11712 P14780 P15428 P17252 P18825 P21397 P21452 P21554 P21728 P21917 P22303 P25021 P25024 P25025 P25101 P25103 P25929
P28223 P28482 P30411 P32238 P32245 P33032 P35354 P35367 P37231 P37288 P41143 P41595 P41968 P49146 P50052 P50406 P51681 Q01959 Q08209
Q38Q88 Q99714 Q9HCF6 Q9NZQ8 Q9UL62
CID 82146: bexarotene
A0A024RAV2 A0A087WZ88 A8K840 B7Z7J5 B7ZKN7 F1D8P8 F1D8Q5 O94782 P08684 P11021 P19793 P28702 P48443 Q92830
CID 104741: ICI 182,780
A0A024R913 A0A024RAP4 A0A024RCN9 A8KAF4 B6ZGS9 F1D8N3 F1D8P9 O94782 P03372 P06401 P08684 P11474 P16050 P34913 Q16236 Q92731 Q92830
Q96QE3 Q99527
CID 104758: raltitrexed
B0YJ76 P04818 P07607 P41440 P42898 Q05932
CID 104865: bosentan
A0A024R638 O95342 P08684 P11712 P21451 P24530 P25101 P26684
CID 110634: vardenafil
G5E9C5 O00408 O76074 P08684 P18545 Q13956
CID 110635: tadalafil
A0A024RCN9 A0A090N7W1 A7E2E5 G5E9C5 O00408 O76074 P08684 P27815 P28482 Q07343 Q9HCR9
CID 115237: paliperidone
A0A024R3C5 A0A024R3S2 A0A024R6T9 A0A024R9I2 A0A024RAH7 A0A024RCN9 A0A087WU84 A0A090N7W1 A0PJF5 A1A4V4 A2RUS0 A4D1Q0 A4D2N2 A8K5W4
B0ZBD3 B2KJ49 B2R7Y7 B4E398 B7Z3P6 B8K2Q5 C1ID52 K9J958 O00325 P08684 P08913 P14416 P18825 P21728 P21731 P21917 P21918 P25021 P25103
P28221 P28222 P28223 P32297 P34969 P35367 P35368 P41595 P50406 Q15822 Q92830
CID 119182: clofarabine
A0A024QZY7 A6NMQ1 F5CTF3 P02545 P23921 P31350
CID 119607: valdecoxib
A0A024R2N2 A0A024R2Q0 A0A024R3C5 A0A024R3S2 A0A024R6T9 A0A024R9I2 A0A024RAH7 A0A024RAP2 A0A024RBW9 A0A024RD15 A0A087WU84 A0A090N7W1
A0A0A0MRG0 A0A0A0MSK3 A0A0A0MT22 A0N0Q1 A1A4V4 A2A3U5 A2RUS0 A4D1Q0 A8K1F6 A8K249 A8K3J4 A8K5W4 A8K7N8 A8KAF4 A8KAG8 B0ZBD3 B0ZBE0
B2R7Y7 B3KUB4 B4DN15 B4DUH8 B4E398 B7Z1L9 B8K2Q5 C1ID52 E5KQF5 F1D8N3 F5H1T4 G5E9C5 H6VQ59 K9J958 L7RSL3 L7RXH5 O43570 P00403 P00533
P00915 P00918 P02545 P05177 P05181 P06239 P06241 P07451 P07550 P08173 P08246 P08311 P08588 P08684 P08913 P11229 P11509 P11712 P14780
P17252 P18825 P21397 P21452 P21554 P21728 P21917 P21918 P22303 P22748 P25021 P25024 P25025 P25101 P25103 P25929 P28221 P28222 P28223
P28482 P28566 P30411 P32238 P32245 P33032 P34969 P35218 P35354 P35367 P35368 P37288 P41143 P41595 P41968 P43166 P49146 P50052 P50406
P51681 P83916 Q01959 Q08209 Q16790 Q38Q88 Q8N1Q1
CID 123606: almotriptan
C1ID52 P02545 P08684 P21397 P28221 P28222 P43220
CID 123631: gefitinib
A0A024QYW7 A0A024QZ12 A0A024QZ20 A0A024QZ70 A0A024QZA8 A0A024QZU0 A0A024QZU1 A0A024QZV1 A0A024QZY5 A0A024QZY7 A0A024R049 A0A024R0H9
A0A024R0I0 A0A024R0J1 A0A024R0L5 A0A024R0Q9 A0A024R183 A0A024R1H6 A0A024R230 A0A024R244 A0A024R2M7 A0A024R2Y6 A0A024R328 A0A024R3G7
A0A024R3S3 A0A024R440 A0A024R452 A0A024R4B2 A0A024R567 A0A024R5E6 A0A024R5P0 A0A024R5W3 A0A024R5X5 A0A024R603 A0A024R6N2 A0A024R704
A0A024R720 A0A024R728 A0A024R7E4 A0A024R7J0 A0A024R7M7 A0A024R7T2 A0A024R880 A0A024R8A6 A0A024R8E2 A0A024R8K3 A0A024R906 A0A024R964
A0A024R980 A0A024R9Q4 A0A024R9Q5 A0A024R9Y0 A0A024RA66 A0A024RAH0 A0A024RAY5 A0A024RB10 A0A024RBB6 A0A024RBH0 A0A024RBL3 A0A024RBP6
A0A024RBU5 A0A024RC92 A0A024RCE9 A0A024RCJ0 A0A024RD04 A0A024RD15 A0A024RD18 A0A024RD25 A0A024RD59 A0A024RD88 A0A024RDA0 A0A024RDD4
A0A024RDK3 A0A024RDL4 A0A024RDM3 A0A075B7B4 A0A087WSY1 A0A087WVC4 A0A087WW79 A0A087WZ06 A0A087X0I6 A0A090N7W4 A0A0A0MQR8 A0A0A0MS52
A0PJF8 A0ZT98 A1A5A9 A1L4K2 A2RUF7 A2VDG3 A3QNQ0 A4D2J9 A4QPA9 A6PW57 A7E2E0 A8K161 A8K2S4 A8K341 A8K379 A8K3B6 A8K4G3 A8K5M4 A8K602
A8K7I0 A8K9L2 A8KAE3 A8KAE4 A8MWW6 B0AZM9 B0LPE5 B0YIY3 B0YJ89 B2RAP9 B2RCU6 B3KNJ3 B3KQV3 B3KRI8 B3KRP1 B3KRV2 B3KS07 B3KS12 B3KS39
B3KVM3 B3KWC4 B3KXJ4 B4DDG2 B4DER4 B4DER9 B4DEW2 B4DG22 B4DG79 B4DHI4 B4DII1 B4DK59 B4DLF9 B4DM55 B4DM56 B4DR80 B4DS37 B4DT73 B4DTW8
B4DUB1 B4DUC2 B4DV95 B4DVP5 B4DX41 B4E058 B4E0X2 B4E0Y5 B6D4Y2 B7Z1G6 B7Z274 B7Z3V5 B7Z5K4 B7Z9H7 B7ZKJ3 B7ZLY6 B7ZM71 C1ID52 C9J5X1
C9JXA2 D2CGD1 D3DPA4 D3YTB5 D4Q8H0 E7ESA6 E9PER6 E9PJX5 F1D8P8 F1T0G6 F2Z2J1 F5H1T4 F6U4U2 F8VBW7 F8WBA3 F8WCM8 H7BYT1 J3KMW1 J3KNB8
J3KNE8 J3KNN3 J3KRN4 L7RSL3 L7RTI5 L7RXH5 M0R0W6 O00444 O14578 O14920 O14936 O14965 O15111 O15296 O43283 O43318 O43353 O60331 O75116
O75385 O75460 O76039 O94768 O94804 O94806 O95382 O95835 O96017 P00533 P02545 P06239 P08684 P08922 P0C1S8 P0C264 P12931 P14616 P15056
P16234 P17252 P19525 P19784 P21709 P21860 P23443 P24723 P27037 P28482 P29323 P30291 P32298 P36507 P36894 P36896 P36897 P37023 P41743
P42336 P42345 P42681 P43403 P45984 P45985 P46734 P49137 P49336 P49841 P50613 P51956 P51957 P53350 P54646 P54753 P54762 P57058 P68400
P78356 Q00526 Q01538 Q02779 Q04759 Q06418 Q08881 Q0IJ49 Q12866 Q13233 Q13464 Q13470 Q13627 Q13705 Q13873 Q13976 Q14289 Q15303 Q15418
Q15569 Q15746 Q15831 Q15835 Q16288 Q16512 Q16513 Q16566 Q16659 Q17RV3 Q32MK0 Q4VBY6 Q52WX2 Q53EW6 Q56UN5 Q5JXL9 Q5SQQ7 Q5VT25 Q6DT37
Q6P3R8 Q6PKF2 Q6XUX3 Q6ZN16 Q86UX6 Q86V86 Q86YV6 Q8IW41 Q8IYT8 Q8N4C8 Q8N568 Q8N752 Q8NE63 Q8NEV4 Q8NFD2 Q8TD08 Q8TDC3 Q8TDR2 Q8WTQ7
Q92630 Q92887 Q92918 Q96GD4 Q96L34 Q96Q40 Q96SB4 Q9BRS2 Q9BVS4 Q9BX84 Q9BZL6 Q9H2G2 Q9H2K8 Q9H2X6 Q9H3Y6 Q9H4B4 Q9NY57 Q9P289 Q9P2K8
Q9UBF8 Q9UEE5 Q9UEW8 Q9UHD2 Q9UK32 Q9UKE5 Q9UL54 Q9UPE1 Q9Y2H9 Q9Y616 Q9Y6M4 V9GXZ4
CID 124087: desloratadine
A0A024R2N2 A0A024R2Q0 A0A024R3C5 A0A024R3S2 A0A024R6T9 A0A024R9I2 A0A024RAP2 A0A024RCN9 A0A024RD15 A0A087WU84 A0A090N7W1 A0A0A0MRG0
A0A0A0MSK3 A0A0A0MT22 A0N0Q1 A1A4V4 A2A3U5 A2RUS0 A4D1D2 A4D1Q0 A8K1F6 A8K249 A8K7N8 A8KAF4 A8KAG8 B0ZBE0 B2R7Y7 B4DN15 B7Z1L9
B8K2Q5 C1ID52 E5KQF5 F1D8N3 F1D8P8 F5H1T4 G5E9C5 H6VQ59 K9J958 L7RSL3 L7RXH5 O15296 P00533 P00918 P02545 P05177 P05181 P06239 P06241
P07550 P08173 P08246 P08311 P08588 P08684 P08913 P11229 P11509 P11712 P14780 P17252 P18825 P21397 P21452 P21554 P21728 P21917
P22303 P25021 P25024 P25025 P25101 P25103 P25929 P28223 P28482 P30411 P32238 P32245 P33032 P35354 P35367 P37288 P41143 P41595 P41968
P49146 P50052 P50406 P51681 Q01959 Q08209 Q38Q88 Q9UIF8
CID 125017: desvenlafaxine
A0A024R6T9 A4D1D2 B2R7Y7 P23975 P31645 Q01959
CID 129228: rufinamide
A0A024R4E2 A0A024R5Z3 A8K5P7 P27695 P83916 Q15858
CID 130881: olmesartan medoxomil
A0A024R5I4 A0A024R6L5 A0A024RAU7 B3KP78 P08684 P30556
CID 148192: atazanavir
A0A024R5I4 A0A024RAU7 A4D1D2 B3KP78 P02768 P08684
CID 150311: ezetimibe
A0A024QZY7 A0A024R5I4 A0A024RAH7 A0A024RAU7 A0A024RC61 A0A090N8Z1 B3KP78 B6ZGS9 F1D8P8 P02545 P04054 P08684 P16662 P21554 P22309
P22310 P35610 P43220 Q9H221 Q9H222 Q9UHC9
CID 151171: conivaptan
A0A024R720 A7E2E0 B4DER4 P08684 P30518 P37288 P42336 P42345
CID 166548: anidulafungin
B7Z1F5 C1ID52 P05177 P08684 P11712 P20813
CID 170361: varenicline
A0A024R5I4 A0A024RAU7 A0A0A6YYA8 B3KP78 B4DK78 B4E000 O15244 O43497 P00915 P32297 P35498 P43681 Q15825
CID 176870: erlotinib
A0A024QYW7 A0A024QZ12 A0A024QZ20 A0A024QZ70 A0A024QZA8 A0A024QZU0 A0A024QZU1 A0A024QZV1 A0A024QZY5 A0A024QZY7 A0A024R049 A0A024R0H9
A0A024R0I0 A0A024R0J1 A0A024R0L5 A0A024R0Q9 A0A024R183 A0A024R1H6 A0A024R230 A0A024R244 A0A024R2M7 A0A024R2Y6 A0A024R328 A0A024R3G7
A0A024R3S3 A0A024R440 A0A024R452 A0A024R4B2 A0A024R567 A0A024R5E6 A0A024R5I4 A0A024R5P0 A0A024R5W3 A0A024R5X5 A0A024R603 A0A024R6N2
A0A024R704 A0A024R720 A0A024R728 A0A024R7E4 A0A024R7J0 A0A024R7M7 A0A024R7T2 A0A024R880 A0A024R8A6 A0A024R8E2 A0A024R8K3 A0A024R906
A0A024R964 A0A024R980 A0A024R9Q4 A0A024R9Q5 A0A024RA66 A0A024RAH0 A0A024RAU7 A0A024RAY5 A0A024RB10 A0A024RBB6 A0A024RBH0 A0A024RBL3
A0A024RBP6 A0A024RBU5 A0A024RC92 A0A024RCE9 A0A024RCJ0 A0A024RCN9 A0A024RD04 A0A024RD15 A0A024RD18 A0A024RD25 A0A024RD59 A0A024RD88

A0A024RDA0 A0A024RDD4 A0A024RDK3 A0A024RDL4 A0A024RDM3 A0A075B7B4 A0A087WSY1 A0A087WVC4 A0A087WW79 A0A087WZ06 A0A087X0I6 A0A090N7W4
A0A0A0MQR8 A0A0A0MS52 A0PJF8 A0ZT98 A1A5A9 A1L4K2 A2RUF7 A2VDG3 A3QNQ0 A4D1D2 A4D2J9 A4QPA9 A6PW57 A7E2E0 A8K161 A8K2S4 A8K341
A8K379 A8K3B6 A8K4G3 A8K5M4 A8K602 A8K7I0 A8K9L2 A8KAE3 A8KAE4 A8MWW6 B0AZM9 B0LPE5 B0YIY3 B0YJ89 B2RAP9 B2RCU6 B3KNJ3 B3KP78 B3KQV3
B3KRI8 B3KRP1 B3KRV2 B3KS07 B3KS12 B3KS39 B3KVM3 B3KWC4 B3KXJ4 B4DDG2 B4DER4 B4DER9 B4DEW2 B4DG22 B4DG79 B4DHI4 B4DII1 B4DK59 B4DLF9
B4DM55 B4DM56 B4DR80 B4DS37 B4DT73 B4DTW8 B4DUB1 B4DUC2 B4DV95 B4DVP5 B4DX41 B4E058 B4E0X2 B4E0Y5 B6D4Y2 B7Z1G6 B7Z274 B7Z3V5 B7Z5K4
B7Z9H7 B7ZKJ3 B7ZLY6 B7ZM71 C9J5X1 C9JXA2 D2CGD1 D3DPA4 D3YTB5 D4Q8H0 E7ESA6 E9PER6 E9PJX5 F1D8P9 F1T0G6 F2Z2J1 F5H1T4 F6U4U2 F8VBW7
F8WBA3 F8WCM8 H7BYT1 J3KMW1 J3KNB8 J3KNE8 J3KNN3 J3KRN4 L7RSL3 L7RTI5 L7RXH5 M0R0W6 O00444 O14578 O14920 O14936 O14965 O15111 O43283
O43318 O43353 O60331 O60674 O75116 O75385 O75460 O75582 O76039 O94768 O94804 O94806 O95382 O95835 O96017 P00533 P02545 P04629 P06213
P06239 P06241 P07947 P08684 P08922 P09619 P09769 P0C1S8 P0C264 P11362 P12931 P14616 P15056 P16234 P16591 P17252 P19525 P19784 P21709
P21860 P22607 P23443 P23458 P24723 P27037 P28482 P29322 P29323 P30291 P32298 P33981 P35916 P36507 P36888 P36894 P36896 P36897 P37023
P41743 P42336 P42345 P42681 P42684 P42685 P43403 P45984 P45985 P46734 P49137 P49336 P49759 P49841 P50613 P51813 P51956 P51957 P53350
P53667 P54646 P54753 P54760 P54762 P57058 P68400 P78356 P78368 Q00526 Q01538 Q02763 Q02779 Q04759 Q06187 Q06418 Q08881 Q0IJ49 Q12866
Q13043 Q13131 Q13233 Q13464 Q13470 Q13627 Q13705 Q13873 Q13882 Q13976 Q14289 Q15303 Q15375 Q15418 Q15569 Q15746 Q15759 Q15831 Q15835
Q16288 Q16512 Q16513 Q16566 Q16659 Q17RV3 Q2M2I8 Q32MK0 Q4VBY6 Q52WX2 Q53EW6 Q56UN5 Q5JXL9 Q5SQQ7 Q5VT25 Q6DT37 Q6P3R8 Q6PKF2 Q6XUX3
Q6ZN16 Q86UX6 Q86V86 Q86YV6 Q8IW41 Q8IYT8 Q8N4C8 Q8N568 Q8N5S9 Q8N752 Q8NE63 Q8NEV4 Q8NFD2 Q8TD08 Q8TDC3 Q8TDR2 Q8WTQ7 Q92630 Q92887
Q92918 Q96GD4 Q96L34 Q96NX5 Q96Q40 Q96SB4 Q99683 Q9BRS2 Q9BVS4 Q9BX84 Q9BZL6 Q9H1R3 Q9H2G2 Q9H2K8 Q9H2X6 Q9H3Y6 Q9H4B4 Q9HAZ1 Q9NRP7
Q9NSY1 Q9NY57 Q9P289 Q9P2K8 Q9UBF8 Q9UEE5 Q9UEW8 Q9UHD2 Q9UK32 Q9UKE5 Q9UL54 Q9UPE1 Q9UQB9 Q9Y2H1 Q9Y2H9 Q9Y616 Q9Y6M4 V9GXZ4

CID 216237: tolvaptan

A0A024R9X9 P30518 P30560 P37288 Q00788

CID 216239: sorafenib

A0A024QYW7 A0A024QZ12 A0A024QZ20 A0A024QZ70 A0A024QZA8 A0A024QZU0 A0A024QZU1 A0A024QZV1 A0A024QZY5 A0A024QZY7 A0A024R049 A0A024R0H9
A0A024R0I0 A0A024R0J1 A0A024R0L5 A0A024R0Q9 A0A024R183 A0A024R1H6 A0A024R230 A0A024R244 A0A024R2M7 A0A024R2W7 A0A024R2Y6 A0A024R328
A0A024R3G7 A0A024R3S3 A0A024R440 A0A024R452 A0A024R4B2 A0A024R567 A0A024R5E6 A0A024R5P0 A0A024R5W3 A0A024R5X5 A0A024R5Z3 A0A024R603
A0A024R6N2 A0A024R704 A0A024R720 A0A024R728 A0A024R7E4 A0A024R7J0 A0A024R7M7 A0A024R7T2 A0A024R880 A0A024R8A6 A0A024R8E2 A0A024R8K3
A0A024R906 A0A024R964 A0A024R980 A0A024R9Q4 A0A024R9Q5 A0A024RA66 A0A024RAH0 A0A024RAY5 A0A024RB10 A0A024RBB6 A0A024RBH0 A0A024RBL3
A0A024RBP6 A0A024RBU5 A0A024RC92 A0A024RCE9 A0A024RCJ0 A0A024RD04 A0A024RD15 A0A024RD18 A0A024RD25 A0A024RD59 A0A024RD88 A0A024RDA0
A0A024RDK3 A0A024RDL4 A0A024RDM3 A0A075B7B4 A0A087WSY1 A0A087WVC4 A0A087WW79 A0A087WZ06 A0A087X0I6 A0A090N7W4 A0A0A0MQR8 A0A0A0MS52
A0PJF8 A0ZT98 A1A5A9 A1L4K2 A2RUF7 A2VDG3 A3QNQ0 A4D2J9 A4QPA9 A6PW57 A7E2E0 A8K161 A8K2S4 A8K341 A8K379 A8K3B6 A8K4G3 A8K5M4 A8K602
A8K7I0 A8K9L2 A8KAE3 A8KAE4 A8MWW6 B0AZM9 B0LPE5 B0YIY3 B0YJ89 B2RAP9 B2RCU6 B3KNJ3 B3KQV3 B3KRI8 B3KRP1 B3KRV2 B3KS07 B3KS12 B3KS39
B3KVM3 B3KWC4 B3KXJ4 B4DDG2 B4DER4 B4DER9 B4DEW2 B4DG22 B4DG79 B4DHI4 B4DII1 B4DK59 B4DLF9 B4DM55 B4DM56 B4DR80 B4DS37 B4DT73
B4DTW8 B4DUB1 B4DUC2 B4DUH8 B4DV95 B4DVP5 B4DX41 B4E058 B4E0X2 B4E0Y5 B6D4Y2 B7Z1G6 B7Z274 B7Z3V5 B7Z5K4 B7Z9H7 B7ZKJ3 B7ZLY6 B7ZM71
C9J5X1 C9JXA2 D2CGD1 D3DPA4 D3YTB5 D4Q8H0 E7ESA6 E9PER6 E9PJX5 F1T0G6 F2Z2J1 F5H1T4 F6U4U2 F8VBW7 F8WBA3 F8WCM8 H7BYT1 J3KMW1 J3KNB8
J3KNE8 J3KNN3 J3KRN4 L7RSL3 L7RTI5 L7RXH5 M0R0W6 O00444 O14578 O14920 O14936 O14965 O15111 O43283 O43318 O43353 O60331 O60674 O75116
O75385 O75460 O75582 O76039 O94768 O94804 O94806 O95382 O95835 O96017 P00519 P00533 P00915 P00918 P04629 P06213 P06239 P06241 P07451
P07947 P08922 P09619 P09769 P0C1S8 P0C264 P10721 P11362 P12931 P14616 P15056 P16234 P16591 P19525 P19784 P21709 P21860 P22607 P22748
P23443 P24723 P27037 P28482 P29322 P29323 P30291 P32298 P33981 P35218 P35916 P36507 P36888 P36894 P36896 P36897 P37023 P41743 P42336
P42345 P42681 P42684 P42685 P43166 P43403 P45984 P45985 P46734 P49137 P49336 P49759 P49841 P50613 P51813 P51956 P51957 P53350 P53667
P54646 P54753 P54760 P54762 P57058 P68400 P78356 P78368 Q00526 Q02763 Q02779 Q04759 Q06187 Q06418 Q08881 Q0IJ49 Q12866 Q13043 Q13131
Q13233 Q13464 Q13470 Q13627 Q13705 Q13873 Q13882 Q13976 Q14289 Q15303 Q15375 Q15418 Q15569 Q15746 Q15759 Q15831 Q15835 Q16288 Q16512
Q16513 Q16566 Q16659 Q16790 Q17RV3 Q2M2I8 Q32MK0 Q4VBY6 Q52WX2 Q53EW6 Q56UN5 Q5JXL9 Q5SQQ7 Q5VT25 Q6DT37 Q6P3R8 Q6PKF2 Q6XUX3 Q6ZN16
Q86UX6 Q86V86 Q86YV6 Q8IW41 Q8IYT8 Q8N4C8 Q8N568 Q8N5S9 Q8N752 Q8NE63 Q8NEV4 Q8NFD2 Q8TD08 Q8TDC3 Q8TDR2 Q8WTQ7 Q92630 Q92918 Q96GD4
Q96L34 Q96NX5 Q96Q40 Q96SB4 Q99683 Q9BRS2 Q9BVS4 Q9BX84 Q9BZL6 Q9H1R3 Q9H2G2 Q9H2K8 Q9H2X6 Q9H3Y6 Q9H4B4 Q9HAZ1 Q9NRP7 Q9NSY1 Q9NY57
Q9P289 Q9P2K8 Q9UBF8 Q9UEE5 Q9UEW8 Q9UHD2 Q9UK32 Q9UKE5 Q9UL54 Q9UPE1 Q9UQB9 Q9Y2H1 Q9Y2H9 Q9Y616 Q9Y6M4 V9GXZ4

CID 657298: propylthiouracil

A0A024QZY7 A0A024R2N2 A0A024R2Q0 A0A024R3C5 A0A024R3S2 A0A024R6T9 A0A024R9I2 A0A024RAP2 A0A024RCN9 A0A024RD15 A0A024RDA5 A0A087WU84
A0A090N7W1 A0A0A0MRG0 A0A0A0MSK3 A0A0A0MT22 A0A0A0MTJ0 A0N0Q1 A1A4V4 A2A3U5 A2RUS0 A4D1Q0 A8K1F6 A8K249 A8K7N8 A8KAF4 A8KAG8 B0ZBE0
B2R7Y7 B4DN15 B7Z1L9 B8K2Q5 C1ID52 D2KUA6 E5KQF5 F1D8N3 F1D8P8 F5H1T4 G5E9C5 H6VQ59 K9J958 L7RSL3 L7RXH5 P00533 P00918 P02545 P05177
P05181 P06239 P06241 P07202 P07550 P08173 P08246 P08311 P08588 P08684 P08913 P11229 P11509 P11712 P14780 P17252 P18825 P21397 P21452
P21554 P21728 P21917 P22303 P25021 P25024 P25025 P25101 P25103 P25929 P28223 P28482 P30411 P32238 P32245 P33032 P35354 P35367 P37288
P41143 P41595 P41968 P49146 P49895 P50052 P50406 P51681 P83916 Q01959 Q08209 Q13526 Q16236 Q38Q88

CID 667490: 6-mercaptopurine

A0A024QZY7 A0A024R2N2 A0A024R2Q0 A0A024R3C5 A0A024R3S2 A0A024R6L5 A0A024R6T9 A0A024R909 A0A024R9I2 A0A024RAP2 A0A024RCN9 A0A024RD15
A0A087WT22 A0A087WU84 A0A090N7W1 A0A0A0MRG0 A0A0A0MSK3 A0A0A0MT22 A0N0Q1 A1A4V4 A2A3U5 A2RUS0 A4D1Q0 A8K1F6 A8K249 A8K2Q2 A8K7N8
A8K987 A8KAF4 A8KAG8 B0ZBE0 B2R7Y7 B2RXH2 B4DN15 B4DN83 B7Z1L9 B8K2Q5 C1ID52 D9YZU5 E5KQF5 F1D8N3 F5H1T4 G5E9C5 H6VQ59 K9J958 L7RSL3
L7RXH5 O15440 O75164 O75874 P00352 P00491 P00492 P00533 P00918 P05177 P05181 P06239 P06241 P07550 P08173 P08246 P08311 P08588 P08684
P08913 P11229 P11509 P11712 P14780 P15428 P17252 P18825 P21397 P21452 P21554 P21728 P21917 P22303 P25021 P25024 P25025 P25101 P25103
P25929 P28223 P28482 P30411 P32238 P32245 P33032 P35354 P35367 P37288 P41143 P41595 P41968 P47989 P49146 P50052 P50406 P51681 Q01959
Q08209 Q38Q88 Q92830 Q99700 Q9UIF8

CID 1349907: methimazole

A0A024QZW0 A0A024R2N2 A0A024R2Q0 A0A024R3C5 A0A024R3S2 A0A024R6T9 A0A024R9I2 A0A024RAP2 A0A024RCN9 A0A024RD15 A0A087WU84 A0A090N7W1
A0A0A0MRG0 A0A0A0MSK3 A0A0A0MT22 A0N0Q1 A1A4V4 A2A3U5 A2RUS0 A4D1Q0 A8K1F6 A8K249 A8K7N8 A8KAF4 A8KAG8 B0ZBE0 B2R7Y7 B4DN15 B7Z1L9
B8K2Q5 C1ID52 E5KQF5 F1D8N3 F5H1T4 G5E9C5 H6VQ59 K9J958 L7RSL3 L7RXH5 O15245 O75164 P00352 P00491 P00492 P00533 P00918 P02545 P05177
P05181 P06239 P06241 P07202 P07550 P08173 P08246 P08311 P08588 P08684 P08913 P11229 P11509 P11712 P14780 P17252 P18825 P20813 P21397
P21452 P21554 P21728 P21917 P22303 P25021 P25024 P25025 P25101 P25103 P25929 P28223 P28482 P30411 P32238 P32245 P33032 P35354 P35367
P37288 P41143 P41595 P41968 P47989 P49146 P50052 P50406 P51681 Q01959 Q08209 Q16850 Q38Q88

CID 2723601: 6-thioguanine

A0A024QZY7 A0A024R2N2 A0A024R2Q0 A0A024R3C5 A0A024R3S2 A0A024R4X8 A0A024R5Z3 A0A024R6T9 A0A024R909 A0A024R9I2 A0A024RAP2 A0A024RCN9
A0A024RD15 A0A087WT22 A0A087WU84 A0A090N7W1 A0A0A0MRG0 A0A0A0MSK3 A0A0A0MT22 A0N0Q1 A1A4V4 A2A3U5 A2RUS0 A4D1Q0 A8K1F6 A8K249 A8K2Q2
A8K4H7 A8K7N8 A8KAF4 A8KAG8 B0ZBE0 B2R7Y7 B3KRZ3 B4DN15 B4DN83 B7Z1L9 B8K2Q5 C1ID52 D9YZU5 E5KQF5 F1D8N3 F5H1T4 G5E9C5 H6VQ59 K9J958
L7RSL3 L7RXH5 O75164 O75874 O94925 P00352 P00492 P00533 P00918 P05177 P05181 P06239 P06241 P07550 P08173 P08246 P08311 P08588 P08684
P08913 P11229 P11509 P11712 P12268 P14780 P15428 P17252 P18825 P20839 P21397 P21452 P21554 P21728 P21917 P22303 P25021 P25024 P25025
P25101 P25103 P25929 P28223 P28482 P30411 P32238 P32245 P33032 P35354 P35367 P37288 P41143 P41595 P41968 P47989 P49146 P50052 P50406
P51681 Q01959 Q08209 Q38Q88 Q99700

CID 2761171: ethionamide

A0A024R5Z3 B7Z1W5 B7Z242 E5KQF5 F1D8P6 Q16236

CID 3062316: dasatinib
A0A024QYW7 A0A024QZ12 A0A024QZ20 A0A024QZ70 A0A024QZA8 A0A024QZU0 A0A024QZU1 A0A024QZV1 A0A024QZY5 A0A024QZY7 A0A024R049 A0A024R0H9
A0A024R0I0 A0A024R0J1 A0A024R0L5 A0A024R0Q9 A0A024R183 A0A024R1H6 A0A024R230 A0A024R244 A0A024R2M7 A0A024R2Y6 A0A024R328 A0A024R3G7
A0A024R3S3 A0A024R440 A0A024R452 A0A024R4B2 A0A024R567 A0A024R5E6 A0A024R5P0 A0A024R5W3 A0A024R5X5 A0A024R5Z3 A0A024R603 A0A024R6N2
A0A024R704 A0A024R720 A0A024R728 A0A024R7E4 A0A024R7J0 A0A024R7M7 A0A024R7T2 A0A024R880 A0A024R8A6 A0A024R8E2 A0A024R8K3 A0A024R906
A0A024R964 A0A024R980 A0A024R9Q4 A0A024R9Q5 A0A024RA66 A0A024RAH0 A0A024RAY5 A0A024RB10 A0A024RBB6 A0A024RBH0 A0A024RBL3 A0A024RBP6
A0A024RBU5 A0A024RC92 A0A024RCE9 A0A024RCJ0 A0A024RD04 A0A024RD15 A0A024RD18 A0A024RD25 A0A024RD59 A0A024RD88 A0A024RDA0 A0A024RDD4
A0A024RDK3 A0A024RDL4 A0A024RDM3 A0A075B7B4 A0A087WSY1 A0A087WVC4 A0A087WW79 A0A087WZ06 A0A087X0I6 A0A090N7W4 A0A0A0MQR8 A0A0A0MS52
A0PJF8 A0ZT98 A1A5A9 A1L4K2 A2RUF7 A2VDG3 A3QNQ0 A4D1D2 A4D2J9 A4QPA9 A6PW57 A7E2E0 A8K161 A8K2S4 A8K341 A8K379 A8K3B6 A8K4G3 A8K5M4
A8K602 A8K7I0 A8K9L2 A8KAE3 A8KAE4 A8MWW6 B0AZM9 B0LPE5 B0YIY3 B0YJ89 B2RAP9 B2RCU6 B3KNJ3 B3KQV3 B3KRI8 B3KRP1 B3KRV2 B3KS07 B3KS12
B3KS39 B3KVM3 B3KWC4 B3KXJ4 B4DDG2 B4DER4 B4DER9 B4DEW2 B4DG22 B4DG79 B4DHI4 B4DII1 B4DK59 B4DKH4 B4DLF9 B4DM55 B4DM56 B4DR80 B4DS37
B4DT73 B4DTW8 B4DUB1 B4DUC2 B4DV95 B4DVP5 B4DX41 B4E058 B4E0X2 B4E0Y5 B6D4Y2 B7Z1G6 B7Z274 B7Z3V5 B7Z5K4 B7Z9H7 B7ZKJ3 B7ZLY6 B7ZM71
C9J5X1 C9JXA2 D2CGD1 D3DPA4 D3YTB5 D4Q8H0 E7ESA6 E9PER6 E9PJX5 F1T0G6 F2Z2J1 F5H1T4 F6U4U2 F8VBW7 F8WBA3 F8WCM8 H7BYT1 J3KMW1 J3KNB8
J3KNE8 J3KNN3 J3KRN4 L7RSL3 L7RTI5 L7RXH5 M0R0W6 O00444 O14578 O14920 O14936 O14965 O15111 O43283 O43318 O43353 O60331 O60674 O75116
O75385 O75460 O75582 O76039 O94768 O94804 O94806 O94925 O95382 O95835 O96017 P00519 P00533 P04629 P06213 P06239 P06241 P07947 P08684
P08922 P09619 P09769 P0C1S8 P0C264 P11362 P12931 P14616 P15056 P16234 P16591 P19525 P19784 P21709 P21860 P22607 P23443 P23458 P24723
P27037 P28482 P29322 P29323 P30291 P32298 P33981 P35916 P36507 P36888 P36894 P36896 P36897 P37023 P41743 P42336 P42345 P42681 P42684
P42685 P42858 P43403 P45984 P45985 P46734 P49137 P49336 P49759 P49841 P50613 P51692 P51813 P51956 P51957 P53350 P53667 P54646 P54753
P54760 P54762 P57058 P68400 P78356 P78368 Q00526 Q01538 Q02763 Q02779 Q04759 Q05513 Q06187 Q06418 Q08881 Q0IJ49 Q12866 Q13043 Q13131
Q13233 Q13464 Q13470 Q13627 Q13705 Q13873 Q13882 Q13976 Q14289 Q15303 Q15375 Q15418 Q15569 Q15746 Q15759 Q15831 Q15835 Q16288 Q16512
Q16513 Q16566 Q16659 Q17RV3 Q2M2I8 Q32MK0 Q4VBY6 Q52WX2 Q53EW6 Q56UN5 Q5JXL9 Q5SQQ7 Q5VT25 Q6DT37 Q6P3R8 Q6PKF2 Q6XUX3 Q6ZN16 Q86UX6
Q86V86 Q86YV6 Q8IW41 Q8IYT8 Q8N4C8 Q8N568 Q8N5S9 Q8N752 Q8NE63 Q8NEV4 Q8NFD2 Q8TD08 Q8TDC3 Q8TDR2 Q8WTQ7 Q92630 Q92918 Q96GD4 Q96L34
Q96NX5 Q96Q40 Q96SB4 Q99683 Q9BRS2 Q9BVS4 Q9BX84 Q9BZL6 Q9H1R3 Q9H2G2 Q9H2K8 Q9H2X6 Q9H3Y6 Q9H4B4 Q9HAZ1 Q9NRP7 Q9NSY1 Q9NY57 Q9P289
Q9P2K8 Q9UBF8 Q9UEE5 Q9UEW8 Q9UHD2 Q9UK32 Q9UKE5 Q9UL54 Q9UPE1 Q9UQB9 Q9Y2H1 Q9Y2H9 Q9Y616 Q9Y6M4 V9GXZ4
CID 4369359: sitagliptin
A0A024R5Z6 B2RAH7 B4DLR2 B7Z1F5 P08684 P27487 Q86TI2 Q9UHL4
CID 5311181: iloprost
A0PJF5 O00325 P00750 P27815 P34995 P43088 P43116 P43119 Q13258 Q92959 Q9UIG8
CID 5312125: silodosin
B0ZBD3 B0ZBE0 P21439 P25100 P35348 P35368
CID 5493444: aliskiren
A0A024R3D5 B0ZBE2 B7ZW66 P00797 P07339 P08684 P14091
CID 6918558: fesoterodine
A0A024R3S2 A0A024R9I2 A4D1Q0 P08173 P11229